United States
Environmental Protection
Agency

Office of Air and Radiation
Washington D.C. 20460

EPA 400/1-87/001C
December 1987

EPA

Assessing the Risks of Trace Gases That Can Modify the Stratosphere

Volume III:
Chapters 6 - 18

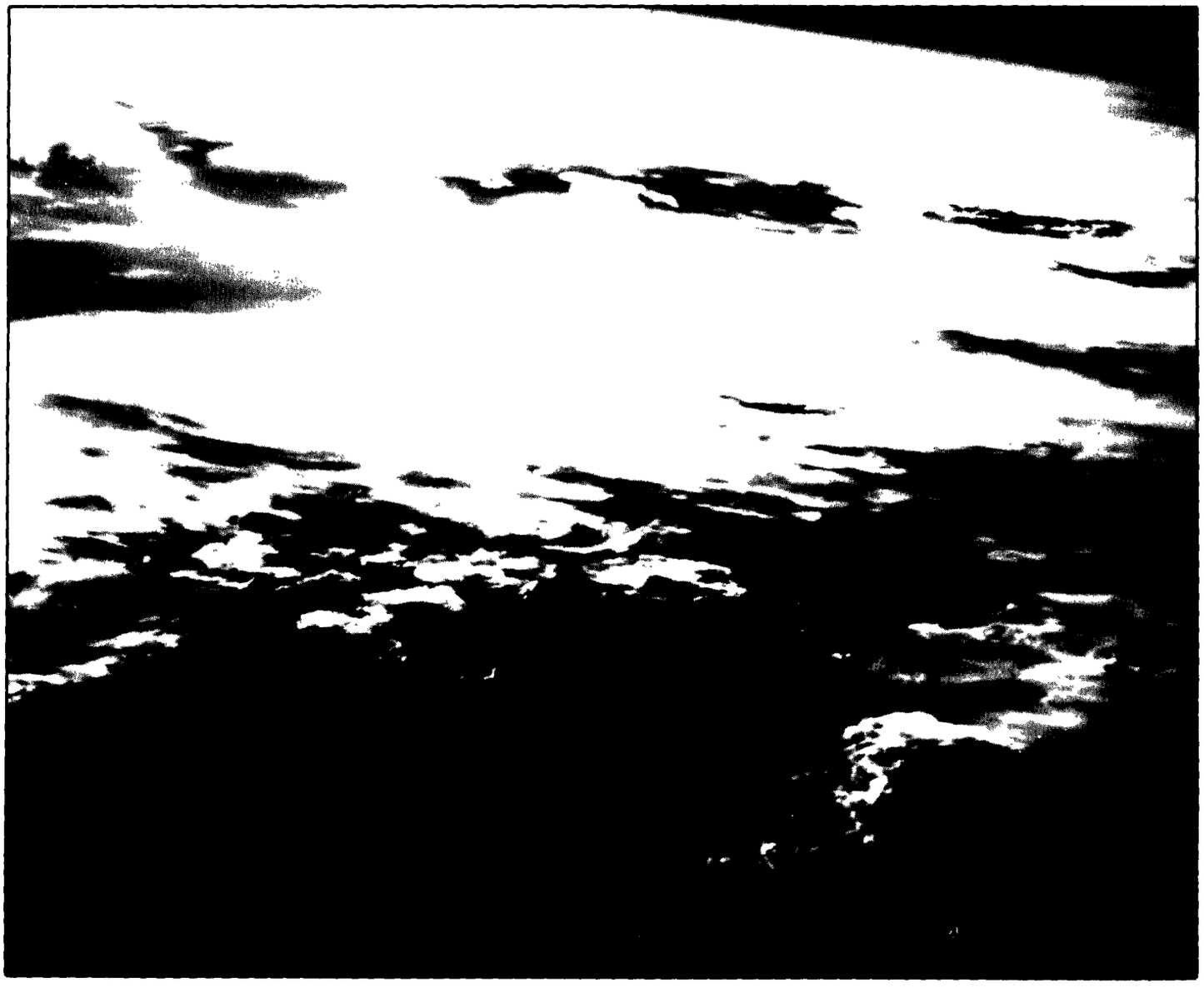

Assessing The Risks of Trace Gases That Can Modify The Stratosphere

Volume III: Chapters 6-18

Senior Editor and Author: John S. Hoffman

Office of Air and Radiation
U.S. Environmental Protection Agency
Washington, D.C. 20460

December 1987

U.S. Environmental Protection Agency
Region 5, Library (PL-12J)
77 West Jackson Boulevard, 12th Floor
Chicago, IL 60604-3590

ACKNOWLEDGEMENTS

Many people made this document possible.

A Science Advisory Board (SAB) panel chaired by Dr. Margaret Kripke and co-chaired by Dr. Warner North conducted an extensive and constructive review of this document. Members of the panel provided important insights and assistance in the assessments development. Members of the panel are:

Dr. Martyn Caldwell (Utah State University)
Dr. Leo T. Chylack, Jr. (Center for Clinical Cataract Research)
Dr. Nien Dak Sze (A.E.R., Inc.)
Dr. Robert Dean
Dr. Thomas Fitzpatrick (Massachusetts General Hospital)
Dr. James Friend (Drexel University)
Dr. Donald Hunten (University of Arizona)
Dr. Warren Johnson (National Center for Atmospheric Research)
Dr. Margaret Kripke (Anderson Hospital and Tumor Institute)
Dr. Lester Lave (Carnegie-Melon University)
Dr. Irving Mintzer (World Resources Institute)
Dr. Warner North (Decision Focus, Inc.)
Dr. Robert Watson (National Aeronautics and Space Administration)
Dr. Charles Yentsch (Bigelow Laboratory)
Dr. Terry F. Yosie (U.S. Environmental Protection Agency)

The panel's contribution to the process of protecting stratospheric ozone has been critical. We also want to thank Terry Yosie, Director of the Science Advisory Board, for setting up and helping to run the panels, and Joanna Foellmer for helping to organize meetings.

Other scientists and analysts, too numerous to name, provided reviews of early drafts of the chapters.

Production assistance, including editing, typing, and graphics, was provided by the staff of ICF Incorporated, including:

Bonita Bailey
Susan MacMillan
Mary O'Connor

Maria Tikoff of the U.S. Environmental Protection Agency, coordinated logistical parts of this document.

The cover photograph was supplied by the National Aeronautics and Space Administration.

Technical support documents (Volumes VI, VII, and VIII) have been published along with the first five volumes of the Risk Assessment. These documents are not part of the official Risk Assessment, and have not been reviewed by the SAB. Their publication is simply to assist readers who wish more background than available in the Risk Assessment.

List of Contributors

Craig Ebert
ICF Incorporated,
9300 Lee Highway,
Fairfax, VA 22031

Sarah Foster
ICF-Clement,
9300 Lee Highway,
Fairfax, VA 22031

Michael J. Gibbs
ICF Incorporated,
9300 Lee Highway,
Fairfax, VA 22031

Kevin Hearle
ICF Incorporated,
9300 Lee Highway,
Fairfax, VA 22031

Brian Hicks
ICF Incorporated,
9300 Lee Highway,
Fairfax, VA 22031

Patsy H. Lill
Department of Pathology,
University of South Carolina School of Medicine,
VA Bldg No. 1, Garnet Ferry Rd,
Columbia, SC 29208

Janice Longstreth
ICF-Clement,
9300 Lee Highway,
Fairfax, VA 22031

Neil Patel
U.S. Environmental Protection Agency,
401 M Street, S.W.,
Washington, DC 20460

Hugh M. Pitcher
U.S. Environmental Protection Agency,
401 M Street, S.W.,
Washington, DC 20460

Alan F. Teramura
Department of Botany,
University of Maryland,
College Park, MD 20742

Dennis Tirpak
U.S. Environmental Protection Agency,
401 M Street, S.W.,
Washington, DC 20460

Jim Titus
U.S. Environmental Protection Agency,
401 M Street, S.W.,
Washington, DC 20460

John B. Wells
The Bruce Company,
Suite 410, 3701 Massachusetts Ave., N.W.,
Washington, DC 20016

G. Z. Whitten
Systems Applications, Inc.,
101 Lucus Valley Road,
San Rafael, CA 94903

Robert Worrest
Corvallis Environmental Research Laboratory,
200 Southwest 35th Street,
Corvallis, OR 97333

TABLE OF CONTENTS

PAGE

VOLUME I

ACKNOWLEDGMENTS i

ORGANIZATION ES-1

INTRODUCTION ES-2

SUMMARY FINDINGS ES-5

CHANGES IN ATMOSPHERIC COMPOSITION ES-15

POTENTIAL CHANGES IN OZONE AND CLIMATE ES-23

HUMAN HEALTH, WELFARE, AND ENVIRONMENTAL EFFECTS ES-32

QUANTITATIVE ASSESSMENT OF RISKS WITH INTEGRATED MODEL ES-54

VOLUME II

ACKNOWLEDGEMENTS i

INTRODUCTION 1

The Rise of Concern About Stratospheric Change 1
Concern About Public Health and Welfare Effects of Global Atmospheric Change 1
Need for Assessments 2

1. GOALS AND APPROACH OF THIS RISK ASSESSMENT 1-1

Analytic Framework 1-1
Supporting Documents and Analysis for this Review 1-2
Chapter Outlines 1-2

2. STRATOSPHERIC PERTURBANTS: PAST CHANGES IN CONCENTRATIONS AND FACTORS THAT DETERMINE CONCENTRATIONS 2-1

Summary 2-1
Findings 2-3
Measured Increases in Tropospheric Concentrations of Potential Ozone Depleters 2-4
Measured Increases in Tropospheric Concentrations of Potential Ozone Increasers 2-13
Factors that Influence Trace Gas Lifetimes 2-21
Long-Lived Trace Gases 2-22
Trace Gases with Shorter Lifetimes 2-26
Carbon Dioxide and the Carbon Cycle 2-26
Source Gases for Stratospheric Sulfate Aerosol (OCS, CS2) 2-26
Appendix A: CFC Emissions-Concentrations Model 2-28
References 2-30

TABLE OF CONTENTS
(Continued)

		PAGE
3.	EMISSIONS OF INDUSTRIALLY PRODUCED POTENTIAL OZONE MODIFIERS	3-1
	Summary	3-1
	Findings	3-3
	Introduction	3-6
	Chlorofluorocarbons	3-6
	Chlorocarbons	3-58
	Halons	3-59
	References	3-66
	Appendix A: Chemical Use Estimate Made Available Since Publication of the Risk Assessment	A-1
	Appendix A: References	A-10
4.	FUTURE EMISSIONS AND CONCENTRATIONS OF TRACE GASES WITH PARTLY BIOGENIC SOURCES	4-1
	Summary	4-1
	Findings	4-2
	The Influence of Trace Gases on the Stratosphere and Troposphere	4-4
	Trace Gas Scenarios	4-4
	Effects of Possible Future Limits on Global Warming	4-23
	Conclusion	4-23
	References	4-25
5.	ASSESSMENT OF THE RISK OF OZONE MODIFICATION	5-1
	Summary	5-1
	Findings	5-3
	Introduction	5-6
	Equilibrium Predictions for Two-Dimensional Models	5-18
	Time Dependent Predictions for One-Dimensional Models for Different Scenarios of Trace Gases	5-32
	Time Dependent Predictions for Two-Dimensional Models with Different Scenarios of Trace Gases	5-40
	Models Fail to Represent All Processes That Govern Stratospheric Change in a Complete and Accurate Manner	5-61
	The Implications of Ozone Monitoring for Assessing Risks of Ozone Modification	5-80
	References	5-104
VOLUME III		
6.	CLIMATE	6-1
	Summary	6-1
	Findings	6-2
	The Greenhouse Theory	6-7
	Radiative Forcing by Increases in Greenhouse Gases	6-8
	Ultimate Temperature Sensitivity	6-15
	The Timing of Global Warming	6-18
	Regional Changes in Climate Due to Global Warming	6-22

TABLE OF CONTENTS
(Continued)

PAGE

Effects on the Stratosphere of Possible Control of Greenhouse Gases 6-26
Attachment A: Description of Model to be Used in Integrating Chapter 6-28
Attachment B: Trace Gas Scenarios 6-32
References 6-33

7. NONMELANOMA SKIN TUMORS 7-1

Summary 7-1
Findings 7-2
Background on Solar Radiation and the Concept of Dose 7-5
Introduction 7-5
Biology of Nonmelanoma Skin Tumors: Links to UV-B 7-11
Epidemiological Evidence 7-27
Dose-Response Relationships 7-40
Attachment A 7-49
References 7-58

8. CUTANEOUS MALIGNANT MELANOMA 8-1

Summary 8-1
Findings 8-3
Introduction 8-7
Epidemiologic Evidence 8-11
Experimental Evidence 8-28
Dose-Response Relationships 8-29
References 8-41

9. UVR-INDUCED IMMUNOSUPPRESSION: CHARACTERISTICS AND POTENTIAL IMPACTS 9-1

Summary 9-1
Findings 9-3
Introduction 9-5
Basic Concepts in Immunology 9-5
Salt: Skin-Associated Lymphoid Tissues 9-7
Effects of Ultraviolet Radiation on Immunological Reactions 9-8
Human Studies 9-14
Effects of Ultraviolet Radiation on Infectious Diseases 9-15
References 9-18

10. CATARACTS AND OTHER EYE DISORDERS 10-1

Summary 10-1
Findings 10-2
Cataracts 10-3
Potential Changes in Senile Cataract Prevalence for Changes in UV-B 10-29
Other Eye Disorders 10-33
References 10-37

TABLE OF CONTENTS
(Continued)

PAGE

11. RISKS TO CROPS AND TERRESTRIAL ECOSYSTEMS FROM ENHANCED UV-B RADIATION 11-1

Summary 11-1
Findings 11-2
Introduction 11-5
Issues and Uncertainties in Assessing the Effects of UV-B Radiation on Plants 11-5
Issues Concerning UV Dose and Current Action Spectra for UV-B Impact Assessment 11-5
Issues Concerning Natural Plant Adaptations to UV Radiation 11-7
Issues Associated with the Extrapolation of Data from Controlled Environments to the Field 11-10
Uncertainties in Our Current Knowledge of UV-B Effects on Terrestrial Ecosystems and Plant Growth Forms 11-11
Uncertainties with the Ability to Extrapolate Knowledge to Higher Ambient CO2 Environment and Other Atmospheric Pollutants 11-13
Risks to Crop Yield Resulting from an Increase in Solar UV-B Radiation 11-15
Risks to Yield Due to a Decrease in Quality 11-20
Risks to Yield Due to Possible Increases in Disease or Pest Attack 11-20
Risks to Yield Due to Competition with Other Plants 11-22
Risks to Yield Due to Changes in Pollination and Flowering 11-23
References 11-25

12. AN ASSESSMENT OF THE EFFECTS OF ULTRAVIOLET-B RADIATION ON AQUATIC ORGANISMS 12-1

Summary 12-1
Findings 12-2
Introduction 12-4
Background on Marine Organisms and Solar Ultraviolet Radiation 12-4
Effects of UV-B Radiation in Phytoplankton 12-9
Effects on Invertebrate Zooplankton 12-11
Effects on Ichthyoplankton (Fisheries) 12-23
Conclusions 12-28
References 12-29

TABLE OF CONTENTS
(Continued)

PAGE

13. EFFECTS OF UV-B ON POLYMERS 13-1

Summary 13-1
Findings 13-2
Photodegradation of Polymers 13-4
Polymers in Outdoor Uses and the Potential for Degradation 13-7
Damage Functions and Response to Damage 13-16
Effect of Temperature and Humidity on Photodegradation 13-29
Future Research 13-31
References 13-32

14. POTENTIAL EFFECTS OF STRATOSPHERIC OZONE DEPLETION ON TROPOSPHERIC OZONE 14-1

Summary 14-1
Findings 14-2
Introduction 14-3
Potential Effects of Ultraviolet Radiation and Increased Temperatures on Urban Smog 14-5
Conclusions and Future Research Directions 14-9
References 14-14

15. CAUSES AND EFFECTS OF SEA LEVEL RISE 15-1

Summary 15-1
Findings 15-2
Causes of Sea Level Rise 15-5
Effects of Sea Level Rise 15-15
Conclusion 15-32
Notes 15-33
References 15-34

16. POTENTIAL EFFECTS OF FUTURE CLIMATE CHANGES ON FORESTS AND VEGETATION, AGRICULTURE, WATER RESOURCES AND HUMAN HEALTH 16-1

Summary 16-1
Findings 16-5
References 16-10

TABLE OF CONTENTS
(Continued)

PAGE

17. MODELS FOR INTEGRATING THE ANALYSES OF HEALTH AND ENVIRONMENTAL RISKS ASSOCIATED WITH OZONE MODIFICATION 17-1

Summary 17-1
Introduction 17-2
The Model as a Framework 17-2
Analysis Procedure 17-4
Model Limitations 17-9
References 17-11
Appendix A: Model Design and Model Flow A-1
Appendix B: Scenarios of Chemical Production, Population, and GNP B-1
Appendix C: Evaluation of Policy Alternatives C-1
Appendix D: Emissions of Potential Ozone-Depleting Compounds D-1
Appendix E: Atmospheric Science Module E-1
Appendix F: Health and Environmental Impacts of Ozone Depletion F-1

18. HUMAN HELATH AND ENVIRONMENTAL EFFECTS 18-1

Summary 18-1
Findings 18-2
Introduction 18-6
Methods for Estimating Health and Environmental Risks 18-11
Description of Range of Production, Emissions, and Concentrations Scenarios for Evaluating Risks 18-12
Sensitivity of Health and Environmental Effects to Differences in Emissions of Ozone Depleters 18-18
Sensitivity of Results to Alternative Atmospheric Assumptions 18-23
Sensitivity of Effects to Uncertainty in Dose Response 18-54
Relative Importance of Key Uncertainties 18-61
Summary 18-62
References 18-65

VOLUME IV

Appendix A

Ultraviolet Radiation and Melanoma

VOLUME V

Appendix B

Potential Effects of Future Climate Changes on Forests and Vegetation, Agriculture, Water Resources, and Human Health

VOLUME VI

Technical Support Documents

Appendix C

Projecting Production of Ozone Depleting Substances

TABLE OF CONTENTS
(Continued)

VOLUME VII

Technical Support Document

Appendix D

Scientific Papers

VOLUME VIII

Technical Support Document

Appendix E

Current Risks and Uncertainties of Stratospheric Ozone Depletion Upon Plants

LIST OF EXHIBITS

		Page
1-1	Relationships Among the Chapters	1-3
2-1	Measured Increases in Tropospheric Concentrations of CFC-11 (CFC-13)	2-5
2-2	Measured Increases in Tropospheric Concentrations of CFC-12 (CF2CL2)	2-6
2-3	Measured Increases in Tropospheric Concentrations of HCFC-22 (CHClF2)	2-7
2-4	Measured Increases in Tropospheric Concentrations of CFC-113 (C2CL3F3)	2-7
2-5	Measured Increased in Tropospheric Concentrations of Carbon Tetrachloride (CCl4)	2-9
2-6	Measured Increases in Tropospheric Concentrations of Methyl Chloroform (CH3CCl3)	2-10
2-7	Measured Increases in Tropospheric Concentrations of Halon-1211 (CF2ClBr)	2-11
2-8	Measured Increases in Tropospheric Concentrations of Nitrous Oxide (N2O)	2-12
2-9	Measured Increases in Tropospheric Concentrations of Nitrous Oxide (N2O)	2-14
2-10	Ice Core Measurements of Historical Nitrous Oxide (N2O) Concentrations	2-15
2-11	Measured Increases in Tropospheric Concentrations of Carbon Dioxide (CO2)	2-16
2-12	Ice Core Measurements of Historical Carbon Dioxide (CO2) Concentrations	2-17
2-13	Measured Increases in Tropospheric Concentrations of Methane (CH4)	2-19
2-14	Ice Core Measurements of Historical Methane (CH4) Concentrations	2-20
2-15a	CFC-12: Constant Emissions	2-23
2-15b	CFC-12: Atmospheric Concentrations	2-23
2-16a	CFC-12: Emissions	2-24

LIST OF EXHIBITS
(Continued)

		Page
2-16b	CFC-12: Atmospheric Concentrations	2-24
2-17	CFC-12: Atmospheric Concentrations from Different Emission Trajectories	2-25
A-1	Concentrations of Fluorocarbons	2-29
A-2	Locations of Stations	2-29
3-1	Selected Properties of CFCS	3-8
3-2	CFC Characteristics and Substitutes	3-10
3-3	Companies Reporting Data to CMA	3-11
3-4	Production of CFC-11 and CFC-12 Reported to CMA	3-13
3-5	Historical Production of CFC-11 and CFC-12	3-15
3-6	CFC-11 and CFC-12 Used in Aerosol and Nonaerosol Applications in the EEC	3-16
3-7	Comparison of Estimated CFC-11 Use: 1985	3-18
3-8	Comparison of Estimated CFC-12 Use: 1985	3-19
3-9	Estimates of Production and Emissions of CFC-11 and CFC-12	3-21
3-10	Published Estimates of U.S.S.R. Production of CFC-11 and CFC-12	3-22
3-11	Historical Production of CFC-11 and CFC-12 in the U.S.	3-24
3-12	EEC Production and Sales Data	3-25
3-13	The Bottom Up Approach	3-27
3-14	Range of Population and GNP Per Capita Projections	3-30
3-15	Summary of Demand Projection Estimates	3-32
3-16	Summary of Demand Projection Estimates (Average annual rate of growth in percent)	3-34
3-17	Long Term Projections CFC-11 and CFC-12 World Production (2000-2050)	3-35

LIST OF EXHIBITS
(Continued)

		Page
3-18	Bevington's Projections for Use of CFCs in the EEC	3-38
3-19	Camm Projections of World Use	3-40
3-20	Summary of EFCTC Projections	3-42
3-21	Global Population and GNP Scenarios Used in Gibbs' Analysis	3-43
3-22	Gibbs Scenarios of World CFC Use	3-45
3-23	Hammitt Projections of World CFC Use	3-47
3-24	Summary of Hedenstrom Projections for Sweden	3-49
3-25	Knollys Projections	3-51
3-26	Summary of Kurosawa Projections for Japan	3-53
3-27	Nordhaus Scenarios of World Nonaerosol CFC Consumption	3-55
3-28	Summary of Sheffield Projections for Canada ..... (1984-2005)	3-57
3-29	Global Halon Projections for Quinn	3-62
3-30	Hammitt and Camm Global Halon Projections	3-64
A-1a	Global Annual Production in Millions of Kilograms	A-4
A-1b	U.S. Annual Production in Millions of Kilograms	A-4
A-2	Assumptions for IEc Halon Projections	A-5
A-3	IEc Projections of Sales and Emissions for Halon-1301 and Halon-1211	A-6
A-4	Global Halon-1301 and Halon-1211 Growth Rates	A-7
A-5	Dupont Estimates of CFC per Capita Use	A-8
4-1	Effects of Changes in Composition of Atmosphere	4-5
4-2	Historical Carbon Dioxide Emissions from Fossil Fuels and Cement	4-7
4-3	A Schematic of the Carbon Cycle	4-8

LIST OF EXHIBITS
(Continued)

		Page
4-4	Projected Carbon Dioxide Emissions and Doubling Time of Concentrations	4-10
4-5	Estimated CH4 Emission Sources (10^{12} grams per year)	4-12
4-6	Two Ways That CH4 Concentrations Could Have Changed	4-14
4-7	Possible Changes in CH4 Sources and in Emission Factors	4-15
4-8	Current Sources and Sinks of Carbon Monoxide (1984 concentration of CO: 30-200 ppb)	4-17
4-9	Scenarios of Carbon Monoxide (CO) Emissions from Combustion	4-18
4-10	Preliminary Scenario of Future Growth in N2O Emissions by Source	4-21
4-11	Projected Nitrous Oxide (N2O) Concentrations	4-22
4-12	Summary of Standard Scenarios Proposed for Assessment	4-24
5-1	Temperature Profile and Ozone Distribution in the Atmosphere	5-7
5-2	Steady-State Scenarios Used in International Assessment	5-10
5-3	Change in Total Ozone from Representative One-Dimensional Models for Steady-State Scenarios Containing Clx Perturbations	5-12
5-4	Change in Total Ozone at 40 Kilometers for Steady-State Scenarios Containing Clx Perturbations	5-13
5-5	Change in Total Ozone for Steady-State Scenarios	5-14
5-6	Effect of Stratospheric Nitrogen (NOy) on Chlorine-Induced Ozone Depletion	5-15
5-7	Effect of Doubled CO2 Concentrations on Ozone Temperature	5-16
5-8	Calculated Changes in Ozone Versus Altitude	5-17
5-9	Two-Dimensional Model Scenarios Used in International Assessment	5-19

LIST OF EXHIBITS
(Continued)

		Page
5-10	2-Dimensional Model Results: Globally and Seasonally-Averaged Ozone Depletion	5-20
5-11	Ozone Depletion by Latitude, Altitude, and Season for Clx Increase of 6.8 ppbv (MPIC 2-D Model)	5-21
5-12	Ozone Depletion by Latitude, Altitude, and Month for Clx Increase of 6.8 ppbv (AER 2-D Model)	5-22
5-13	Ozone Depletion by Latitude, Altitude, and Month for Clx Increase of 14.2 ppbv (AER 2-D Model)	5-23
5-14	Ozone Depletion of Latitude, Altitude, and Month for Clx Increase of 6.8 ppbv (GS 2-D Model)	5-24
5-15	Ozone Depletion by Latitude and Season for Clx Increase of 6.0 ppbv (IS 2-D Model) (AER 2-D Model)	5-25
5-16	Change in Ozone by Latitude and Season for Clx Perturbations (MPIC 2-D Model)	5-26
5-17	Change in Ozone by Latitude and Season for Clx Perturbations (AER 2-D Model)	5-27
5-18	Latitudinal Dependence of AER and MPIC 2-D Models	5-28
5-19	Change in Ozone by Latitude, Altitude, and Month for Coupled Perturbations (GS 2-D Model)	5-29
5-20	Changes in Ozone by Latitude, Altitude, and Season for Coupled Perturbations (MPIC 2-D Model)	5-30
5-21	Changes in Ozone by Latitude and Altitude in Winter for Coupled Perturbations (MPIC 2-D Model)	5-31
5-22	Models With Reported Time Dependent Runs	5-33
5-23	LLNL 1-D Model Versus Parameterization Fit	5-34
5-24	Trace Gas Assumptions for Results in Exhibit 5-25 (Brasseur and DeRudder 1-D Model, 1986)	5-35
5-25	Time-Dependent Change in Ozone for CFC Growth and Coupled Perturbations (Brasseur and DeRudder 1-D Model)	5-36
5-26	Time-Dependent Change in Ozone for Constant CFC Emissions and Growth in Other Trace Gases (Brasseur and DeRudder 1-D Model)	5-37

LIST OF EXHIBITS
(Continued)

		Page
5-27	Sensitivity of 1-D Models to Representation of Radiative Processes (Brasseur and DeRudder 1-D Model)	5-38
5-28	Model Comparison: Time-Dependent Change in Ozone for CFC Growth and Coupled Perturbations	5-39
5-29	Trace Gas Assumptions for Results in Exhibit 5-30 (AER 1-D Model, 1986)	5-41
5-30	Time-Dependent Change in Ozone for Various Scenarios of Coupled Perturbations (AER 1-D Model)	5-42
5-31	Trace Gas Scenarios Tested in LLNL 1-D Model	5-43
5-32	Time-Dependent, Globally Averaged Change in Ozone for Coupled Perturbations (LLNL 1-D Model) "Reference Case" ...	5-45
5-33	Time Dependent, Globally Averaged Change in Ozone for Coupled Perturbations (LLNL 1-D Model)	5-46
5-34	Effect of Potential Greenhouse Gas Controls on Ozone Depletion (Results from 1-D Parameterization)	5-47
5-35	Calculated Ozone Depletion for 1970 to 1980 Versus Umkehr Measurements	5-49
5-36	Time-Dependent Globally and Seasonally Averaged Changes in Ozone for Coupled Perturbations (IS 2-D Model)	5-50
5-37	Time-Dependent Globally and Seasonally Averaged Changes in Ozone for Coupled Perturbations (IS 2-D Model)	5-51
5-38	Time-Dependent Seasonally Averaged Change in Ozone for 1980 CFC Emissions and Coupled Perturbations (IS 2-D Model)	5-52
5-39	Time-Dependent Seasonally Averaged Change in Ozone for 1.2% Growth in CFC Emissions and Coupled Perturbations (IS 2-D Model)	5-53
5-40	Time-Dependent Seasonally Averaged Change in Ozone for 3% Growth in CFC Emissions and Coupled Perturbations (IS 2-D Model)	5-54
5-41	Time-Dependent Seasonally Averaged Change in Ozone for 3.8% Growth in CFC Emissions and Coupled Perturbations (IS 2-D Model)	5-55

LIST OF EXHIBITS
(Continued)

		Page
5-42	Temperature Feedback Experiment: Time-Dependent, Globally and Seasonally Averaged Change in Ozone for 3% Growth in CFC Emissions and Coupled Perturbations (IS 2-D Model)	5-57
5-43a	Two-Dimensional, Time-Dependent Simulation for Constant CFC Emissions (AER 2-D Model)	5-58
5-43b	Two-Dimensional, Time-Dependent Simulation for CFC Growth of 62 Percent Per Year (AER 2-D Model)	5-59
5-44	Model Comparison for Coupled Perturbations Scenario	5-60
5-45	Calcualted Ozone -- Column Change to Steady-State for Two Standard Assumed Perturbations	5-63
5-46	Latitudinal Gradients in Odd Nitrogen: Models vs Measurements	5-65
5-47	Logical Flow Diagram for Monte Carlo Calculations	5-67
5-48	Histogram of Measurements for a Rate Constant	5-68
5-49	Recommended Rate Constants and Uncertainties Used in Monte Carlo Analyses	5-70
5-50	Monte Carlo Results: Change in Ozone Versus Fluorocarbon Flux	5-71
5-51	Monte Carlo Results: Change in Ozone Versus Fluorocarbon Flux	5-72
5-52	Monte Carlo Results: Ozone Depletion for Coupled Pertubations	5-73
5-53	A Monte Carlo Distribution of Column Ozone Changes for Changes in CFC Production	5-74
5-54	Monte Carlo Results: Changes in Ozone by Altitude	5-76
5-55	Monte Carlo Results: Changes in Ozone by Column and Altitude, Unscreen Data	5-77
5-56	Monte Carlo Analysis With the LLNL 1-D Model	5-78
5-57	Monte Carlo Results: Changes in Ozone by Altitude	5-79
5-58	Ozone Trend Estimates by Latitude	5-83

LIST OF EXHIBITS
(Continued)

		Page
5-59	Changes in Ozone from 1970 to 1980: Umkehr Measurements and Model Calculations	5-85
5-60	SBUV Zonal Trends Estimates Versus "Umkehr Station Blocks"	5-86
5-61	Ozone Trend Estimates and 95% Confidence Intervals	5-88
5-62	Ozone Balloonsonde Stations	5-90
5-63	Correction Factors for Balloonsonde Measurements	5-91
5-64	Ozone Trend Emissions (% per year) As Determined from Balloon Ozonesondes Versus Those Determined from Dodson Measurements (Tiao, et al., personal communication)	5-93
5-65	Monthly Means of Total Ozone at Halley Bay	5-96
5-66	Nimbus 7 Antarctic Ozone Measurements: 12-Day Sequence	5-97
5-67	Nimbus 7 Antarctic Ozone Measurements: Mean Total Ozone in October	5-98
5-68	Global (60°N-60°S) Monthly Ozone Determined from NOAA TOVS System	5-100
5-69	Preliminary Ozone Trend Data (Health versus 2-D Model Results) (Isaksen)	5-102
6-1	Stratospheric Perturbants and Their Effects	6-9
6-2	Absorption Characteristics of Trace Gases	6-10
6-3	Radiative Forcing for a Uniform Increase in Trace Gases	6-11
6-4	Effects of Vertical Ozone Distribution on Surface Temperature	6-13
6-5	Water Vapor, Altitude, and Radiative Forcing	6-14
6-6	Temperature Sensitivity to Climatic Feedback Mechanisms	6-16
6-7	Empirical Estimates of Climate Sensitivity are Sensitive to Estimates of Historical Temperature Increases and Trace Gas Concentrations	6-17
6-8	Relationship of Radiative Forcing, Ocean Heat Uptake, and Realized and Unrealized Warming	6-20

LIST OF EXHIBITS
(Continued)

		Page
6-9	Transient Estimates of Global Warming	6-21
6-10	Expected Temperature Increases	6-23
6-11	Results of Transient Analysis Using a General Circulation Model	6-24
6-12	Regions of U.S.: Change in Runoff	6-25
7-1	Variation in UV Radiation by Latitude as Percent of Levels at the Equator on March 21 at Noon	7-6
7-2	UV Radiation by Month in Washington, D.C.	7-8
7-3	Ratio of Instantaneous Flux Throughout the Day to Flux at 5:15 a.m. in Washington on June 21 (Assumes a Clear Day)	7-9
7-4	Average DNA-Damage Action Spectrum	7-10
7-5	Organization of the Adult Skin	7-12
7-6	Ultraviolet Absorption Spectra of Major Epidermal Chromophores	7-14
7-7	Skin Types and Skin Tanning Responses	7-16
7-8	Ultraviolet Action Spectra for DNA Dimer Induction, Lethality and Mutagenicity	7-19
7-9	Effectiveness of UVR at Inducing Pyrimidine Dimers and Transformation	7-21
7-10	Action Spectrum for the Induction of Single-Strand Breaks in DNA	7-24
7-11	Action Spectrum of Mouse Edema (MEE48) as Compared to that of DNA Damage and the Robertson-Berger Meter	7-26
7-12	Comparison of Age-Adjusted Incidence Rates Per 100,000 Persons for Squamous Cell Carcinoma (SCC) and Basal Cell Carcinoma (BCC) Among White Males and Females in the United States	7-29
7-13	Percentage of Tumors by Anatomic Site for Nonmelanoma Skin Cancer Among White Males and Females in the United States (1977-1978 NCI Survey Data)	7-31

LIST OF EXHIBITS
(Continued)

		Page
7-14	Distribution by Sex and Anatomic Site of Nonmelanoma Skin Tumors: Canton of Vaud, Switzerland (1974-1978)	7-32
7-15	Annual Age Adjusted Incidence Rates for Basal and Squamous Cell Carcinoma (1977-1978 NCI Survey Data) and Melanoma (1973-1976 SEER Data) Among White Males	7-35
7-16	Annual Age Adjusted Incidence Rates for Basal and Squamous Cell Carcinomas (1977-1978 NCI Survey Data) and Melanoma (1973-1976 SEER Data) Among White Females	7-36
7-17	Estimated of Relative Risks of Basal and Squamous Cell Carcinomas for 32 Combinations of Risk Factors	7-38
7-18	Relative Mutagenicity of UV-B as a Function of Wavelength .	7-46
A-1	Correlation of Alternative Measurements of UV-B Radiation for Ten Locations in the United States	7-51
A-2	Population Weights for Ten Locations in the United States	7-52
A-3	Estimated Dose-Response Coefficeints (and t-Statistics) for Basal and Squamous Cell Skin Cancers (UV-B Dose-Skin Cancer Incidence)	7-53
A-4	Estimated Percentage Changes in UV-B Radiation in San Francisco for a Two and Ten Percent Depletion in Ozone	7-55
A-5	Percentage Change in Incidence of Basal and Squamous Cell Skin Cancers for a Two Percent Depletion in Ozone for San Francisco	7-56
A-6	Percentage Change in Incidence of Basal and Squamous Cell Skin Cancers for a Ten Percent Depletion in Ozone for San Francisco	7-57
8-1	Location of Melanocyte in the Epidermis	8-8
8-2	Comparative Transmittance of UV Radiation	8-9
8-3	Increases in Incidence and Mortality Rates from Malignant Melanoma in Different Countries	8-17
8-4	Anatomic Site Distribution of Cutaneous Malignant Melanoma	8-19

LIST OF EXHIBITS
(Continued)

		Page
8-5	Anatomic Site Distribution of Cutaneous Malignant Melanoma by Gender	8-20
8-6	Malignant Melanoma Risk Factors by Measures of Skin Pigmentation Within the Caucasian Population	8-26
8-7	Multiple Ways in which UVR can Play a Role in Melanoma Development	8-30
8-8	Summary Statistics for Regressions of Skin Cancer Incidence and Mortality on Latitude	8-32
8-9	Estimated Relative Increases in Melanoma Skin Cancer Incidence and Mortality Associated with Changes in Erythema Dose	8-33
8-10	Summary of Fears, Scotto, and Schneiderman (1977) Regression Analyses of Melanoma Incidence Dose-Response	8-35
8-11	Biological Amplification Factors for Skin Melanoma by Sex and Anatomical Site Groups, Adjusting for Age and Selected Constitutional and Exposure Variables	8-35
8-12	Biological Amplification Factors for Melanoma Incidence by Sex and Anatomical Site Groups, Adjusting for Age and Combinations of Selected Constitutional and Exposure Variables	8-36
8-13	Percentage Increase in Melanoma Death Rates for a One Percent Decline in Ozone	8-39
9-1	Action Spectra for Local Suppression of Contact Hypersensitivity Assuming Either One-Hit or Multi-Hit Mechanisms	9-11
9-2	Action Spectrum For Systemic Suppression of Contact Hypersensivity	9-12
10-1	Cataract Prevalence by UV Zone	10-7
10-2	Comparison of Cataract Prevalence for Aborigines and Non-Aborigines	10-7
10-3	Composite Transmittance Curves for the Rabbit	10-9
10-4	Calculated Total Transmittance of the Human Eye	10-10
10-5	Percent Transmissivity Through the Entire Rhesus Eye	10-11

LIST OF EXHIBITS
(Continued)

		Page
10-6	Transmittance of the Total Rabbit Cornea, the Total Human Cornea, and the Rabbit Corneal Epithalium	10-12
10-7	Transmittance of the Anterior Ocular Structures of the Human and Rabbit Eyes	10-13
10-8	UV Radiant Exposure Threshold Data for the Cornea H_C, Lens HL Cataracts, and Retina H_R for the Rabbit and Primate	10-14
10-9	The Action Spectra for Photokeratitis and Cataracts for the Primate and Rabbit	10-15
10-10	Free Radicals and Oxidation: Reduction Systems	10-17
10-11	Enzyme Systems Involved in Oxidation: Reduction	10-18
10-12	Standardized Regression Coefficients for Cataract	10-31
10-13	Estimated Relationship Between Risk of Cataract and UV-B Flux	10-32
11-1	A Summary of Studies Examining the Sensitivity of Cultivars to UV-B Radiation	11-8
11-2	Survey of UV Studies by Major Terrestrial Plant Ecosystems (after Whittaker 1975)	11-12
11-3	Summary of UV-B and CO2 Effects on Plants	11-14
11-4	Summary of Field Studies Examining the Effects of UV-B Radiation on Crop Yields	11-16
11-5	Details of Field Study by Teramura (1981-1985)	11-17
11-6	Summary of Changes in Yield Quality in Soybean Between the 1982 and 1985 Growing Seasons (Teramura 1982-1985)	11-21
12-1	Solar Irradiance Outside the Earth's Atmosphere and at the Surface of the Earth for a Solar Zenith Angle of 60°	12-5
12-2	Relationship Between Ozone Depletion and Biological Effectiveness of Increased UV-B Radiation	12-6
12-3	Solar Spectral Irradiance at the Surface of the Ocean and at Four Depths	12-7

LIST OF EXHIBITS
(Continued)

		Page
12-4	Lethal Effects on Shrimp Larvae for Various Combinations of UV-R, Dose-Rate, and Total Dose	12-13
12-5	Estimated Effective UV-B Solar Daily Dose at Various Atmospheric Ozone Concentrations Based on a 4-Year Mean of Medians, Manchester, Washington, 1977-1980	12-14
12-6	Estimated Biologically Effective UV-B Doses Leading to Significant Effects in Major Marine Zooplankton Groups	12-17
12-7	Percentage of Total Dose Limit to be Reached on Any Particular Day: Lethal Doses Accumulated Only After Dose-Rate Threshold is Exceeded	12-20
12-8	Effect of Increased Levels of Solar UV-B Radiation on the Predicted Loss of Larval Northern Anchovy from Annual Populations, Considering the Dose/Dose-Rate Threshold and Three Vertical Mixing Models	12-27
13-1	Wavelengths of UV Radiation and Polymers with Maximum Sensitivity and Corresponding Photon Energies	13-4
13-2	Plastics Used in Applications Where Exposure of the Material to Sunlight Might Be Expected	13-8
13-3	Modes of Damage Experienced by Polymers Used in Outdoor Application	13-11
13-4	PVC Siding Compound Composition	13-13
13-5	UV Screening Effectiveness of Selected Pigments	13-14
13-6	Domestic Consumption of Light Stabilizers, 1984-85	13-15
13-7	Increased Stabilization Market (1970-2020)	13-18
13-8	Ozone Depletion Estimates	13-19
13-9	Cumulative Added Cost	13-20
13-10	Diagrammatic Representation of the Effect of Pigment/Fillers as Light Shielders (Monodisperse Spherical Filler)	13-22
13-11	Relative Damage Indices for Yellowing of PVC Under Miami (March 22nd) Conditions, at Different Extents of Ozone Layer Deterioration	13-25
13-12	Estimated Ranges of Factor Increase in Damage and the Factor Increase in Stabilizer Needed to Counter the Change of Yellowing of Rigid PVC Compositions	13-28

LIST OF EXHIBITS
(Continued)

		Page
13-13	PVC Damage with Ozone Depletion	13-29
13-14	Projections of Future Demand for Selected Years (Thousands of Metric Tons)	13-30
14-1	Ozone Concentrations for Short-Term Exposure That Produce 5% to 20% Injury to Vegetation Growth Under Sensitive Conditions	14-6
14-2	Ozone Concentrations at Which Significant Yield Losses Have Been Noted for a Variety of Plant Species Exposed Under Various Experimental Conditions	14-7
14-3	Ozone Concentrations Predicted for Changes in Dobson Number and Temperature for Three Cities (ppm)	14-10
14-4	Global Warming Would Exacerbate Effects of Depletion on Ground-Based Ozone in Nashville	14-11
15-1	Snow and Ice Components	15-6
15-2	Worldwide Sea Level in the Last Century	15-8
15-3	Temperature Increase At Various Depths and Latitudes	15-10
15-4	Estimates of Future Sea Level Rise	15-13
15-5	Local Sea Level Rise	15-14
15-6	Evolution of Marsh as Sea Level Rises	15-17
15-7	Composite Transect -- Charleston, S.C.	15-18
15-8	Louisiana Shoreline in the Year 2030	15-20
15-9	Distribution of Population in Bangladesh	15-21
15-10	The Bruun Rule	15-23
15-11	Percent of Tidal Cycles in Which Specified Concentration is Exceeded at Torresdale During a Recurrence of the 1960's Drought for Three Sea Level Scenarios	15-28
15-12	Estimates of Flood Damages for Charleston and Galveston Resulting From Sea Level Rise	15-30
16-1	Summary of Findings from the WMO/UNEP/ICSU Conference on Global Climate Held in Villach, Austria, October 1985	16-1
17-1	Modular Structure	17-3

LIST OF EXHIBITS
(Continued)

		Page
17-2	Major Model Input Choices	17-5
17-3	Effects Not Quantified	17-10
A-1	Flow of Analysis Program	A-4
A-2	Files Required to Specify a Run	A-6
B-1	Future Global Production Scenarios: Middle Scenario	B-3
B-2	Regional Use Shares for CFC-11	B-4
B-3	U.S. End Use Shares for CFC-11	B-6
B-4	Middle U.S. Population Scenario	B-7
B-5	Middle U.S. GNP Scenario	B-7
B-6	User-Modified Scenario Specifying a Growth Rate of 2 Percent Annually for CFC-11 in the U.S.	B-9
B-7	A User-Modified Scenario: Production as a Function of Population	B-9
D-1	Release Tables for CFC-11	D-2
D-2	Emissions from a Hypothetical 100 Million Kilograms of Production in 1985	D-4
D-3	Emissions from Production Over a Series of Years (Millions of Kilograms)	D-5
D-4	Sample Table of Exogenously Specified Emissions	D-6
E-1	Trace Gas Assumptions Used to Develop the Ozone Depletion Relationship	E-2
E-2	Comparison of Total Column Ozone Depletion Results from the 1-D Model and the Parameterized Numerical Fit	E-3
E-3	Hypothetical Table of User-Specified Ozone Depletion	E-6
E-4	Example Ozone Depletion Scaling Factors	E-7
F-1	Cities Used to Evaluate Changes in UV Flux for the Three Regions of the U.S.	F-3
F-2	States Included in the Three Regions of the U.S.	F-5
F-3	Percent Change in UV as a Function of Change in Ozone Abundance for Three U.S. Regions	F-6

LIST OF EXHIBITS
(Continued)

		Page
F-4	Age Distribution of the U.S. Population Over Time in the North Region	F-8
F-5	Baseline Incidence for Nonmelanoma Skin Cancers	F-10
F-6	Basal Incidence for Melanoma Skin Cancers	F-12
F-7	Mortality Rates for Melanoma Skin Cancers	F-14
F-8	Standardized Regression Coefficients for Cataract	F-16
F-9	Estimated Relationship Between Risk of Cataract and UV-B Flux	F-17
F-10	Sample Table for Specifying Relative Weights for Exposure During a Person's Lifetime	F-19
F-11	Coefficients Relating Percent Change in UV to Percent Change in Skin Cancer Incidence	F-22
F-12	Coefficients Relating Percent Change in UV to Percent Change in Melanoma Mortality	F-23
F-13	Dose-Response Coefficients	F-25
F-14	Damage Index and Increase in Stabilizer for Ranges of Ozone Depletion	F-29
18-1	Types of Human Health and Environmental Effects Estimated	18-8
18-2A	Real World Equivalent to the No-Growth Scenario in Risk Assessment	18-15
18-2B	Real World Equivalent to the 1.2% Growth Scenario in Risk Risk Assessment	18-16
18-3	Global Average Ozone Depletion: Central Case	18-20
18-4	Additional Cases of Nonmelanoma Skin Cancer by Type of Nonmelanoma	18-21
18-5	Additional Mortality From Nonmelanoma Skin Cancer by Type of Nonmelanoma	18-22
18-6	Additional Cases of Melanoma Skin Cancer by Cohort	18-23
18-7	Additional Mortality From Melanoma Skin Cancer by Cohort	18-24
18-8	Additional Senile Cataract Cases by Cohort	18-25
18-9	Environmental Effects Estimated Quantitatively for the U.S.	18-26

LIST OF EXHIBITS
(Continued)

Page

18-10 Environmental Effects Based on Case Studies and Research in Early Stages 18-27

18-11 Equilibrium Temperature Change for the Emissions Scenarios Assuming 3°C Warming for Doubled CO2 18-28

18-12 Global Average Ozone Depletion: Comparison to Results with a 2-D Dimensional Atmospheric Model 18-30

18-13 Climate, and Other Effects: Sensitivity to Relationship Between Climate Change and CO2 Emissions 18-31

18-14 Summary of Effects of Greenhouse Gases on Ozone Depletion and Global Equilibrium Temperature 18-33

18-15 Global Average Ozone Depletion: Scenario of Limits to Future Global Warming 18-34

18-16 Human Health Effects: Scenarios of Limits to Future Global Warming. Additional Cumulative Cases and Deaths Over Lifetimes of People Alive Today 18-36

18-17 Human Health Effects: Scenarios of Limits to Future Global Warming. Additional Cumulative Cases and Deaths Over Lifetimes of People Born 1986-2029 18-37

18-18 Human Health Effects: Scenarios of Limits to Future Global Warming. Additional Cumulative Cases and Deaths Over Lifetimes of People Born 2030-2074 18-38

18-19 Materials, Climate, and Other Effects: Scenarios of Limits to Future Global Warming 18-39

18-20 Global Average Ozone Depletion: Methane Scenarios 18-41

18-21 Human Health Effects: Methane Scenarios Additional Cumulative Cases and Deaths Over Lifetimes of People Alive Today 18-42

18-22 Human Health Effects: Methane Scenarios Additional Cumulative Cases and Deaths Over Lifetimes of People Born 1986-2029 18-43

18-23 Human Health Effects: Methane Emissions Cases Additional Cumulative Cases and Deaths Over Lifetimes of People Born 2030-2074 18-44

18-24 Materials, Climate and Other Effects: Methane Scenarios .. 18-45

18-25 Global Average Ozone Depletion: Sensitivity to Relationship Between Ozone Depletion and Emissions 18-46

LIST OF EXHIBITS
(Continued)

Page

18-26 Human Health Effects: Sensitivity to Relationship Between Ozone Depletion and Emissions. Additional Cumulative Cases and Deaths Over Lifetimes of People Alive Today 18-48

18-27 Human Health Effects: Sensitivity to Relationship Between Ozone Depletion and Emissions. Additional Cumulative Cases and Deaths Over Lifetimes of People Born 1985-2029 18-49

18-28 Human Health Effects: Sensitivity to Relationship Between Ozone Depletion and Emissions. Additional Cumulative Cases and Deaths Over Lifetimes of People Born 2030-2074 18-50

18-29 Human Health Effects: Maximum Depletion of 95 Percent. Additional Cumulative Cases and Deaths Over Lifetimes of People Alive Today 18-51

18-30 Human Health Effects: Maximum Depletion of 95 Percent. Additional Cumulative Cases and Deaths Over Lifetimes of People Born 1986-2029 18-52

18-31 Human Health Effects: Maximum Depletion of 95 Percent. Additional Cumulative Cases and Deaths Over Lifetimes of People Born 2030-2074 18-53

18-32 Human Health Effects: Sensitivity to Dose-Response Relationship. Additional Cumulative Cases and Deaths Over Lifetimes of People Alive Today 18-55

18-33 Human Health Effects: Sensitivity to Dose-Response Relationship Additional Cumulative Cases and Deaths Over Lifetimes of People Born 1986-2029 18-56

18-34 Human Health Effects: Sensitivity to Dose-Response Relationship Additional Cumulative Cases and Deaths Over Lifetimes of People Born 2030-2074 18-57

18-35 Human Health Effects: Sensitivity to Relationship Between Ozone Depletion and Action Spectrum. Additional Cumulative Cases and Deaths Over Lifetimes of People Alive Today 18-58

18-36 Human Health Effects: Sensitivity to Relationship Between Ozone Depletion and Action Spectrum. Additional Cumulative Cases and Deaths Over Lifetimes of People Born 1986-2029 18-59

18-37 Human Health Effects: Sensitivity to Relationship Between Ozone Depletion and Action Spectrum. Additional Cases and Deaths Over Liftimes of People Born 2030-2074 18-60

LIST OF EXHIBITS
(Continued)

Page

18-38 Comparative Sensitivity of Mortality From Skin Cancer to Various Factors 18-63

CHAPTER 6

CLIMATE

SUMMARY

Stratospheric perturbants are trace gases that are emitted by industrial or biogenic processes that can change the amount and location of ozone or water vapor in the stratosphere. Increases in these trace gases can be expected to warm the earth directly by reducing the escape of infrared radiation to space. As stratospheric perturbants, they will indirectly warm the earth by altering the vertical distribution of ozone[1] and the abundance of water vapor in the stratosphere.

The magnitude of warming anticipated from the expected increases in greenhouse gases is quite large compared to past natural variations in global temperature. The anticipated speed of the warming is more rapid than has occurred before. The temperature increase from the Wisconsin Ice Age, 18,000 years before present (B.P.), is believed to be 4°C. Global average temperature increase in the next 100 years, without curtailment of the growth in the concentration of greenhouse gases, is likely to be somewhat comparable.

The major uncertainty in predicting the magnitude of global warming is the extent to which clouds will amplify or possibly reduce the warming. The major uncertainty in predicting the timing is the rate at which the oceans will absorb heat. Despite the numerous uncertainties, the realized global temperature rise would be expected to exceed 1.6°C by 2075 and be as high as 4.5°C if no steps are taken to limit the rise in the concentrations of greenhouse gases.

Major weather and climatic changes would be expected to accompany global warming, although it is impossible to specify details of how the changes will occur in different regions of the world. In addition to temperature increases, changes can be expected in precipitation, storms, and weather patterns. Current evidence suggests that significant changes will occur in the dryness or wetness of many regions and in the frequency and location of extreme weather.

Policies aimed at reducing chlorofluorocarbons (CFCs) in order to limit ozone depletion would also reduce global warming. Increases in other stratospheric perturbants (e.g., methane and carbon dioxide), while also contributing to the greenhouse effect, are expected to buffer the earth from ozone depletion. Reducing emissions of these gases to limit global warming would make the stratosphere more vulnerable to depletion from CFCs.

---

[1] If ozone depletion grows to a sufficient magnitude that there is a decrease in ozone at altitudes below 28 kilometers, something that occurs in models only in cases where depletion is large, the net effect of the ozone change would, from that point on, produce a cooling effect.

FINDINGS

1. INCREASES IN THE ABUNDANCE OF CFCs AND OTHER TRACE GASES CAN INCREASE GLOBAL TROPOSPHERIC SURFACE TEMPERATURES. THESE GASES CAN ALTER THE VERTICAL DISTRIBUTION OF OZONE AND INCREASE STRATOSPHERIC WATER VAPOR, THEREBY INFLUENCING GLOBAL WARMING.

   1a. Trace gases that act as stratospheric perturbants also are greenhouse gases--as their concentrations increase in the troposphere they will retard the escape of infrared radiation from earth, causing global warming.

   1b. Increases in methane (CH4) will also add water vapor to the stratosphere, thereby enhancing global warming. Methane increases will also add ozone to the troposphere, where it acts as a strong greenhouse gas that will further increase global warming.

   1c. In all model-generated scenarios of ozone depletion, ozone decreases in the stratosphere above 28 km. This allows more ultraviolet radiation to penetrate to lower altitudes where the "self-healing effect" increases ozone to partially compensate for the ozone loss above. In some scenarios sufficient depletion occurs so that ozone eventually decreases at all altitudes.

   1d. Decreases in ozone at approximately 28 km or above will have a warming effect on the Earth. There is a small net gain in energy because the increase in ultraviolet radiation (UV-B) allowed to reach the earth's surface more than compensates for the infrared radiation that is allowed to escape due to depletion of ozone above that altitude.

   1e. Below approximately 28 km, increases in ozone are more effective as absorbers of infrared radiation. Consequently, increases in ozone below 28 km also will produce a net warming. In this case, the additional UV blocked by more ozone is less than the additional infrared that is blocked from escaping the earth. Conversely, a decrease in ozone below 28 km will tend to cool the Earth's surface.

   1f. The direct effect of column depletion of ozone on global temperatures will depend on the magnitude of the depletion. Until the depletion is of sufficient magnitude that it occurs at the lower part of the column, ozone depletion will be a net contributor to global warming. If the stratosphere continues to deplete so that ozone is depleted below 28 km, this depletion will cause a cooling. One-dimensional models differ from two-dimensional models in the vertical distribution of ozone change, with depletion occurring at all altitudes in the higher latitudes in two-dimensional models, rather than just at high altitudes. Thus, according to 2-D models, the changes in radiative balance will be latitude dependent. At the current time, no studies have been undertaken to determine the net radiative forcing of changes projected by 2-D models.

   1g. Radiative forcing may vary strongly with changes in ozone at different altitudes and latitudes. Consequently, until comparisons are made between the models in terms of their global impact, estimates of the effects of changes in the vertical column of ozone on global warming made with 1-D models must be viewed cautiously. In addition, changed

vertical distribution of ozone could influence stratospheric dynamics.

2. INCREASES IN TRACE GAS CONCENTRATIONS ASSOCIATED WITH STRATOSPHERIC MODIFICATION ARE LIKELY TO WARM THE EARTH SIGNIFICANTLY.

2a. Two National Academy of Sciences panels have concluded that the equilibrium warming for doubling atmospheric concentrations of CO2, or for an equivalent increase in the radiative forcing of other trace gases, will most likely be between 1.5° and 4.5°C.

2b. The magnitude of warming that would be directly associated with radiative forcing from increases in trace gases without feedback enhancement would increase temperature by approximately 1.2°C for a doubling of CO2, and approximately an additional 0.45°C for a simultaneous doubling of N2O and CH4. Direct radiative forcing from a uniform 1 ppb increase in both CFC-11 and CFC-12 would increase temperature by about 0.15°C.

2c. The initial warming from direct radiative forcing would change some of the geophysical factors that determine the earth's radiative balance (i.e., feedbacks will occur) and these changes would amplify the initial warming. Increased water vapor and altered albedo effects (snow and ice melting, reducing the reflection of radiation back to space) have been projected by several modeling groups to increase the warming by as much as 2.5°C for doubled CO2 or its radiative equivalent. Large uncertainties exist about the feedbacks between global warming and clouds, which could further amplify, or possibly reduce, the magnitude of warming.

2d. The three major general circulation modeling groups in the U.S. estimate an average global warming of around 4°C for doubled CO2 or its radiative equivalent. However, because of uncertainties in the representation of the cloud contributions, greater or lesser amplifications, including a negative feedback that would reduce the warming to 2°C or an even lower value, cannot be ruled out.

2e. Global average temperature has been estimated as having risen about 0.6°C over the last century. This increase is consistent with general predictions of climate models. Attempts to use these data to derive empirically the temperature sensitivity of the earth to a greenhouse forcing are not likely to succeed. Uncertainty about the past concentrations of trace gases in the atmosphere, other exogenous factors that affect the climate (such as aerosols or solar input), and oscillation and instabilities in the internal dynamics of the climate system (such as ocean circulation), currently prevent the derivation of the earth's temperature sensitivity from examination of the historic rise of temperature. This limitation is likely to remain for more than another decade.

2f. The global warming associated with increases in ozone-modifying gases varies with scenarios of future growth in these gases. If the use of CFCs grows at 2.5 percent per year through 2050, CO2 concentrations grow at the 50th percentile rate defined by the NAS (approximately 0.6 percent per year from 1985 to 2050), N2O concentrations grow at 0.20 percent per year, and CH4 concentrations grow at 0.017 ppm per year (approximately 1.0 percent of current concentrations), then equilibrium

temperatures would rise by about 5.6°C by 2075 (relative to observed temperature in 1985), based on a temperature sensitivity of 3°C for doubled CO2. Values would be about 50 percent higher for a 4.5°C-based temperature sensitivity and about 50 percent lower for 1.5°C. If CFC use remains constant through 2050, the projected warming would be about 4.3°C by 2075 (± 50%), and if use were phased out by 2010, projected warming would be about 4.0°C (± 50%).

2g. Efforts to gather worldwide time series data for clouds have begun. If adequate, these data may narrow estimates of the cloud contribution to temperature sensitivity within the next decade. However, because of the complexity of this issue, this effort may fail to resolve the large uncertainties affecting this aspect of climate.

3. THE TIMING OF GLOBAL WARMING DEPENDS ON THE RATES AT WHICH GREENHOUSE GASES INCREASE, THE RATES AT WHICH OTHER FORCINGS SUCH AS VOLCANOES AND SOLAR RADIATION CHANGE, AND THE RATE AT WHICH OCEANS TAKE UP HEAT AND PARTIALLY DELAY TEMPERATURE EFFECTS. A GLOBAL WARMING GREATER THAN VARIATIONS THAT OCCURRED THIS PAST CENTURY IS EXPECTED IN THE NEXT TEN YEARS IF VOLCANIC AND SOLAR FACTORS DO NOT SUBSTANTIALLY CHANGE.

3a. The delay in temperature rise introduced by absorption of heat by the oceans can only be roughly estimated. The simple one-dimensional models of oceans that have been used for this purpose do not realistically portray the mechanisms for heat transport into the oceans. Instead, these models use eddy diffusion to treat heat in a parameterized manner so that heat absorption is consistent with data from the paths of transient tracers. These models indicate that the earth will experience substantial delays (on the order of several decades) in experiencing the full warming from greenhouse gases.

3b. The earth's current average temperature is not in equilibrium with the radiative forcing from current concentrations of greenhouse gases. Consequently, global average temperature would increase in the future even if concentrations of gases did not rise any further. For example, if 2°C is the actual sensitivity of the earth's climate system to a CO2 doubling, simple models estimate the current "unrealized warming" to be approximately 0.34°C; for a 4°C temperature sensitivity, the current unrealized warming would be approximately 1.0°C.

3c. Only one three-dimensional general circulation model has been used to simulate changes in temperature as concentrations of greenhouse gases increase over time. This simulation shows a faster warming than predicted by simpler one-dimensional models that use ocean box models to simulate time-dependent warming.

3d. Future uptake of heat by the oceans may change as global warming alters ocean circulation, possibly altering the delaying effect of the oceans as well as reducing their uptake of CO2.

3e. Inadequate information exists to predict how volcanic or solar forcings may change over time. Analyses done of transient warming assume that past levels of volcanic aerosols will continue into the future and that solar forcing changes will average out over relatively short periods of time.

4. WITH A FEW GENERALIZED EXCEPTIONS, THE CLIMATIC CHANGE ASSOCIATED WITH GLOBAL WARMING CANNOT BE RELIABLY PREDICTED ON A REGIONAL BASIS.

   4a. In general, as the earth warms, temperature increases will be greater with increasing distance from the equator.

   4b. Global warming also can be expected to increase precipitation and evaporation, intensifying the hydrological cycle. While models lack sufficient reliability to make projections for any single region, all perturbation studies with three-dimensional models (general circulation models) show significant regional shifts in dryness and wetness, which suggests that shifts in hydrologic conditions will occur throughout the world.

   4c. Current general circulation models represent oceanic, biospheric, and cloud processes with insufficient realism to determine how extreme weather events and climatic norms are likely to change on a regional basis. For example, one analysis of general circulation model outputs suggests that the frequency of extreme climatic conditions will change in many regions of the world. Another model projects increased summer drying in mid-latitudes for perturbation studies, utilizing either of two different representations of clouds. Still another analysis suggests changes in latitudinal gradients of sea surface temperature will play a critical role in determining regional climatic effects.

5. LIMITING GLOBAL WARMING BY REDUCING EMISSIONS OF STRATOSPHERIC PERTURBANTS THAT TEND TO INCREASE OZONE WOULD INCREASE THE STRATOSPHERE'S VULNERABILITY TO OZONE DEPLETION. UNDER SCENARIOS IN WHICH CONTINUED BUFFERING OF OZONE DEPLETION BY OTHER TRACE GASES IS ASSUMED, SUBSTANTIAL GLOBAL WARMING RESULTS.

   5a. Decreases in substances with the potential to deplete stratospheric ozone--that is, chlorofluorocarbons and nitrous oxides--would decrease the rate and magnitude of global warming.

   5b. Decreases in methane emissions, which have the potential to increase stratospheric and tropospheric ozone and thereby buffer ozone depletion, would decrease warming in three ways: by reducing direct radiative effects from its presence in the troposphere; by lowering water vapor in the stratosphere; and by reducing ozone build-up below 28 km.

   5c. Decreases in CO2 emissions would decrease global warming, but would also have the effect of increasing the stratosphere's vulnerability to ozone depletion.

   5d. Decreases in carbon monoxide concentrations, which may occur as energy production practices change, could result in decreases in methane concentrations by increasing OH-radical abundance which, in turn, would shorten the lifetime of methane and could shorten the lifetime of methyl chloroform and CFC-22.

6. ADDITIONAL RESEARCH IS NEEDED ON CLIMATE TO REDUCE UNCERTAINTIES ABOUT GLOBAL WARMING ASSOCIATED WITH TRACE GAS GROWTH.

6a. The key to improving the accuracy of estimates of global temperature sensitivity is to acquire a better understanding of the effect of clouds. This recommendation has been made by numerous groups over the last decade; yet research devoted to this issue remains relatively small.

6b. An increased understanding of ocean circulation is critical to improving estimates of timing and regional projections.

6c. The effect of climate on biological systems and soils and their impact on climate must be modeled if regional estimates of climate change are to be developed.

6d. A better understanding of the radiative properties of CFC-113 and other compounds is needed for estimating the effects of this compound on climate.

6e. Experiments with three-dimensional models that have altered scenarios of vertical ozone need to be undertaken to assess the possible impacts on the magnitude of global warming and on general circulation.

THE GREENHOUSE THEORY

The earth is heated by solar radiation that penetrates the atmosphere in a variety of wavelengths; the greatest quantity of energy that reaches the earth is in the visible part of the spectrum. In turn, the earth is cooled by the infrared radiation given off to space. The average surface temperature that results is a balance of this heating and cooling.

Since Tyndall discovered in 1861 that water vapcr can absorb infrared radiation (Tyndall 1861), it has been understood that increases in the abundance of infrared absorbing gases (the "greenhouse" gases) in the atmosphere can raise the earth's temperature by reducing the escape of this energy to space. It has also long been known that other aspects of atmospheric composition, including ozone and aerosol abundance, can influence the quantity of radiation (ultraviolet and visible) that reaches the earth's surface.

A variety of studies and international assessments (NAS 1979; NAS 1982; WMO 1986a) have been conducted over the last two decades concerning the potential for increasing concentrations of trace gases to raise global temperature and alter weather and climate. All of the reviews conducted have come to general agreement that increases in greenhouse gases will lead to a global warming.

This chapter reviews studies on how the gases that can alter the stratosphere create a greenhouse effect and how the alterations in the stratosphere itself can add to or reduce the magnitude of the greenhouse warming. The chapter is divided into five sections:

The section on radiative forcing examines evidence that gases that could perturb the stratosphere are also gases that could retard the escape of infrared radiation, thereby forcing an increase in the earth's surface temperature. In particular, this section analyzes potential indirect greenhouse effects of these gases by reviewing how changes they cause in the stratosphere can add to or subtract from the direct radiative forcing of any of the gases. This section also reviews studies that estimate the magnitude of warming that would directly result from radiative forcing in the absence of feedbacks (that is, changes in the earth's surface or atmosphere that could alter the warming).

A section on the earth's ultimate temperature sensitivity to radiative forcing reviews evidence that bears on the magnitude of feedbacks that would amplify or dampen the initial radiative warming. Uncertainties in current knowledge about the magnitude of the feedbacks is highlighted.

A section on timing reviews those factors in the earth's geophysical system that will delay the full experience of the temperature equilibrium associated with specific increases in greenhouse gases. In particular, this section reviews evidence on the uncertainties associated with oceanic heat absorbtion.

A section on regional climate changes associated with global warming focuses on changes in regional weather and climatic patterns which could alter the basic environmental conditions of the planet.

The final section on the effects of possible control of greenhouse gases, analyzes the possible impact that curtailing emissions of various greenhouse gases (CO_2 and CH_4) to limit global warming would have on stratospheric ozone.

Together the five sections cover the major issues that will determine how

the greenhouse effect will unfold with time and how that evolution is interrelated to risks to the stratosphere.

RADIATIVE FORCING BY INCREASES IN GREENHOUSE GASES

By their influence on chemical or physical processes, a large number of gases can influence the structure and composition of the stratosphere. During their residence in the troposphere, these gases, alternatively called stratospheric perturbants, trace species, radiatively important trace species, or greenhouse gases, retard the flux of infrared radiation from the earth's surface to space. Exhibit 6-1 shows the multiple effects that these gases have on atmospheric processes. Carbon dioxide (CO2), the most important greenhouse gas, cools the stratosphere and, in most models, increases ozone (NAS 1984 and WMO 1986b). Methane (CH4) has three major effects on warming: its direct radiative effect in the troposphere; its effect in adding ozone to the atmosphere below 28 kilometers; and its effect in adding water vapor to the stratosphere (NAS 1984). Nitrous oxide (NO2) warms the surface by its presence in the stratosphere and depletes ozone in the stratosphere unless interfered with by high chlorine levels (Ramanathan et al. 1985 and Stolarski, personal communication).

While small uncertainties still exist in our understanding of the radiation that is absorbed by each gas, with a few exceptions (CFC-113, for instance), the absorption feature of these gases are well characterized, as shown in Exhibit 6-2 (WMO 1986b; Luther and Ellingson 1985; and Ramanathan et al. 1985 for discussion). Consequently, increases in the concentrations of these gases will reduce the escape of infrared radiation from earth, providing a radiative forcing of the earth's climate system. When computing the magnitude of that forcing for multiple perturbants, care must be taken in considering possible overlaps that would reduce net forcing (Wang, Wuebbles, and Washington 1985; Luther and Ellingson 1985).

Studies of the direct radiative effects of increases in infrared-absorbing gases all produce approximately the same result -- that a doubling of CO2 (or equivalent) eventually will raise global temperatures 1.26°C if no other factors in the geosystem are changed (Ramanathan et al. 1985; Schlesinger and Mitchell 1985; Hansen et al. 1984).

Exhibit 6-3 shows the relative effectiveness of a 1 ppm increase in such greenhouse gases. Notice that chlorofluorocarbons and methane have much greater impact per molecule than CO2. The reason is that they 'cover' a part of the infrared spectrum that is 'open' or 'transparent' to much of the infrared radiation given off by earth, whereas the region of CO2 absorption is already somewhat 'opaque' or 'closed' to part of the infrared spectrum.

Changes In Stratospheric Structure and Composition Can Change Radiative Forcing

In photochemical models, the structure and composition of the stratosphere changes as gases such as CFC and methane increase in the atmosphere. These changes can influence the radiative forcing of the earth by altering fluxes of infrared or ultraviolet radiation from or to its surface. The critical factors of the stratosphere's organization that influence radiative balance are the

EXHIBIT 6-1

Stratospheric Perturbants and Their Effects

	Direct Effect on Global Temperature from Tropospheric Presence	Physical Effect on Stratosphere	Effect on Column Ozone
Carbon Dioxide	Increases[1]	Cools[2]	Increases differently at different latitudes[3]
Methane	Increases[1]	Adds water vapor, hydrogen[4]	Increases at some latitudes[5]
Nitrous oxide	Increases[1]	Adds nitrogen[4]	Decreases[6]
Chlorofluorocarbons	Increases[1]	Adds chlorine[4]	Decreases[4]
Other Trace Gases (methyl chloroform, carbon tetrachloride, Halons)	Increases[1]	Adds catalytic species to stratosphere[4]	Decreases[4]

[1] Ramanathan et al. 1985.

[2] Connell and Wuebbles 1986.

[3] Isaksen, personal communication.

[4] NAS 1984.

[5] Isaksen and Stordal 1986.

[6] NAS (1984) notes the direct effect of N2O on column ozone. In the presence of high levels of chlorine, N2O may interfere with the catalytic cycle of chlorine, reducing net depletion (Stolarski, personal communication).

EXHIBIT 6-2

Absorption Characteristics of Trace Gases

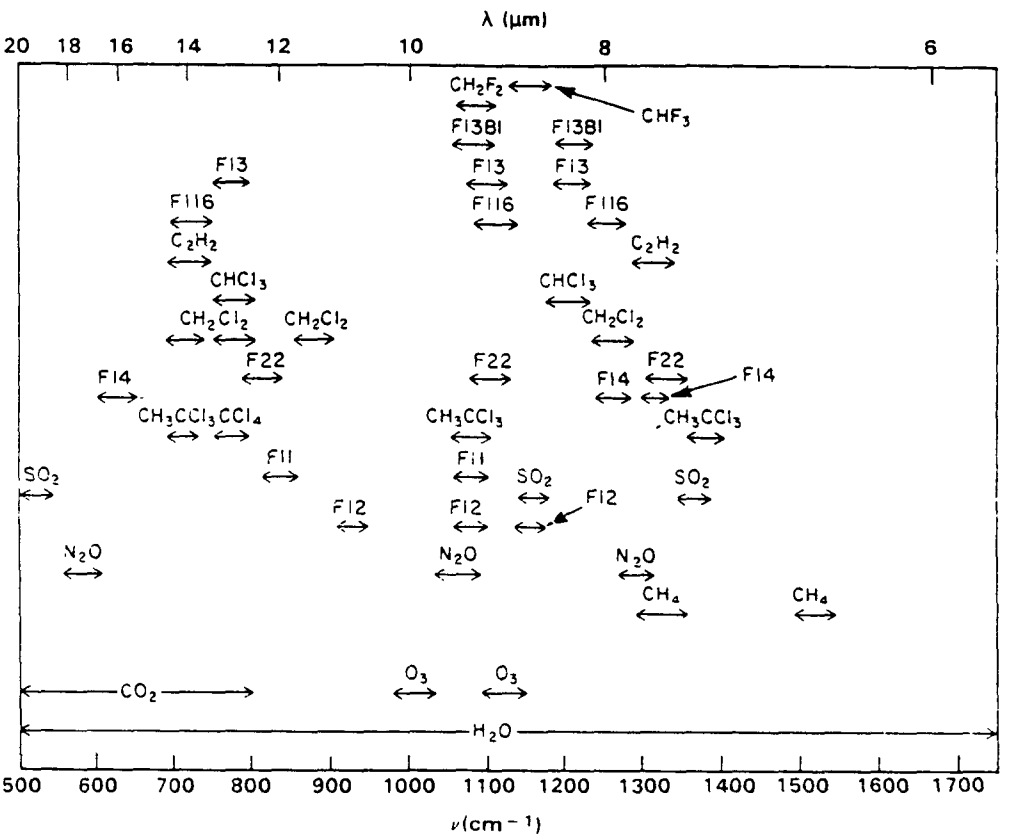

Atmospheric trace gases absorb outgoing infrared radiation of various wavelengths. Carbon dioxide absorbs much of the radiation in the spectral region between 13μ m and 20μ m. Several trace gases, including chlorofluorocarbons 11 and 12 (F11 and F12) have strong absorption features in the spectral region of 7μ m to 13μ m. This spectral region is called the atmospheric "window," since in this region the atmosphere is relatively transparent.

Source: WMO 1986.

EXHIBIT 6-3

Radiative Forcing for a Uniform Increase in Trace Gases

Compound	Temperature Sensitivity (^{o}C/ppb)
CO_2	.000004
CH_4	.0001
N_2O	.001
CFC-11	.07
CFC-12	.08
CFC-13	.10
Halon 1301	.10
F-116	.08
CCl_4	.05
$CHCl_3$	.04
F-14	.04
HCFC-22	.03
CH_2Cl_2	.02
CH_3CCl_3	.01
C_2H_2	.01
SO_2	.01

Source: Adapted from Ramanathan et al. 1985.

amount and vertical distribution of water vapor located in the stratosphere and the vertical distribution of ozone. One-dimensional and two-dimensional models of the stratosphere project changes in the vertical organization of ozone in response to increasing concentrations of CFCs and other gases (Connell and Wuebbles 1986; Stordal and Isaksen 1986). These changes are significant. Two-dimensional models also show that the changes are latitude dependent (Stordal and Isaksen 1986). Increases in water vapor (due to increasing methane) are also projected for most scenarios of trace gas growth (Connell and Wuebbles 1986).

Changes in ozone abundance can have two effects on radiation. They can alter the penetration of UV-B and visible radiation from space and the escape of infrared from the surface. Ozone decreases anywhere in the column will always allow more UV-B and visible radiation (in the Hartley-Huggins and Chanpuis bands) to reach the earth's surface. Ozone increases will decrease UV-B penetration. Ozone decreases will allow more infrared to escape, but the effect of ozone changes on infrared escape varies substantially with altitude. Ozone increments added near the troposphere produce the largest increases in surface temperature. This is because greenhouse efficiency is proportional to the difference in the temperature of the radiation that is absorbed by the ozone (essentially the ground temperature) and the radiation that is emitted by the ozone (the local atmospheric temperature) (Lacis, Wuebbles, and Logan 1986). As a result, a net column depletion that consists of depletion of ozone in the upper atmosphere and of increases of ozone in the lower atmosphere, will increase the infrared radiation that is blocked from escaping from earth.

Exhibit 6-4 shows the relationship of ozone and altitude to increases in temperature (Lacis, Wuebbles and Logan 1986). At 12 km, the net sensitivity of the surface warming to a given increase in ozone is approximately 15 times greater than at 20 km. Above 28 km an ozone decrease actually would produce a small net temperature decrease. Exhibit 6-5 shows the relationship between water vapor, altitude, and radiative forcing. However, increases in water vapor always produce a warming, with maximum effect for water vapor increases at 14 km (Lacis and Wuebbles 1986).

Scenarios in which total column ozone depletion is small combine two effects: a large decrease above 28 km and a smaller increase in the lower stratosphere (self-healing effect and methane) and troposphere (from methane increases). In these cases, the total net radiative forcing of the planet will be increased (Lacis and Wuebbles 1986).

In scenarios in which total depletion becomes large enough that ozone decreases at altitudes below 28 kilometers, the total radiative forcing from changes in vertical ozone will begin to favor cooling.

Care must be taken in estimating vertical changes in ozone from one-dimensional models; the forcing may be different than predicted. The reason is that, as two-dimensional chemical models show, depletion levels will vary with latitude. At higher latitudes, there may be less ozone increase at low altitudes. At mid-latitudes, where industrial pollution is important, ozone increases are already evident. Nearer the equator, tropospheric increases in ozone from CH_4 will be more important and help balance depletion more. Consequently, the radiative forcing is not likely to be equal at all latitudes.

EXHIBIT 6-4

Effects of Vertical Ozone Distribution on Surface Temperature

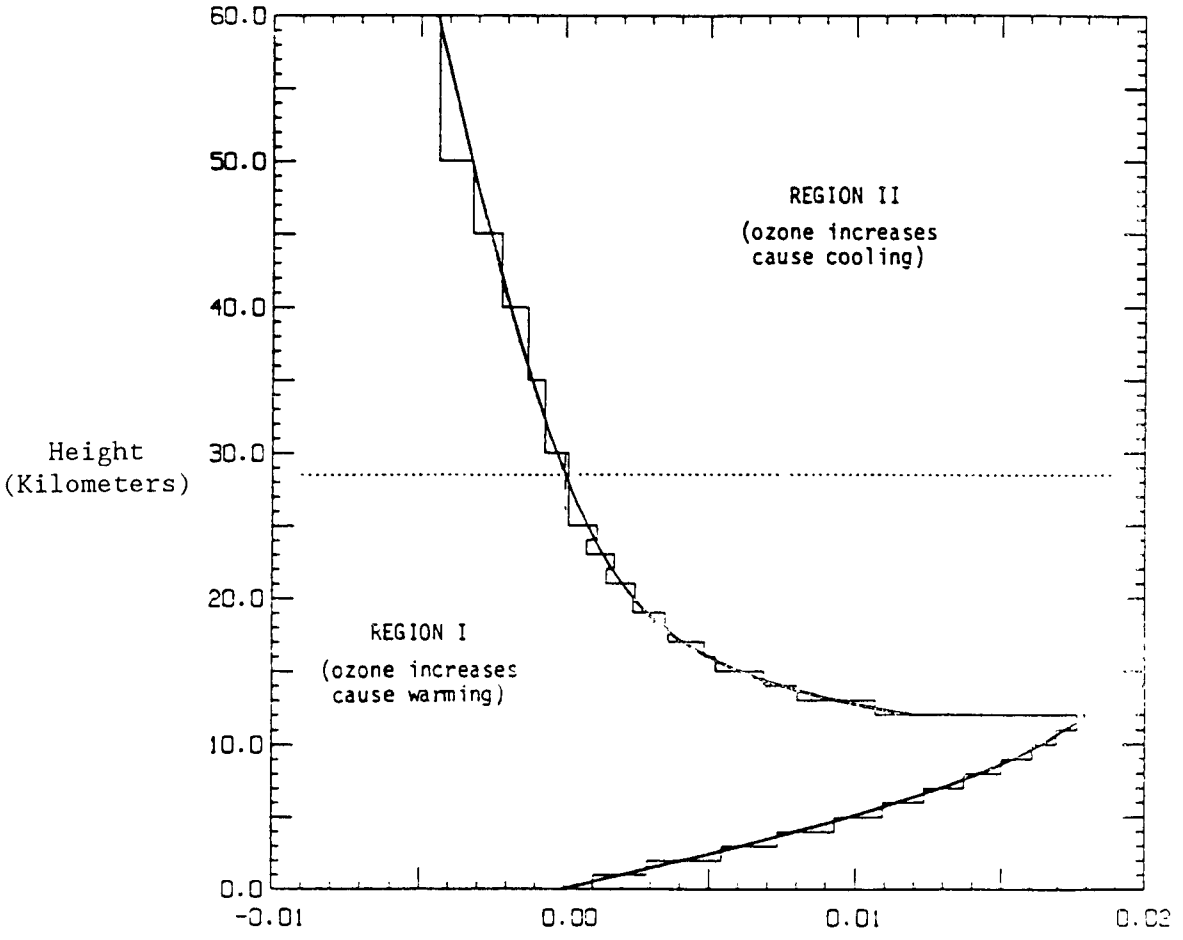

Sensitivity of global surface temperature to changes in vertical ozone distribution. The heavy solid line is a least square fit to model results for an increase in ozone of 10 Dobson units (approximately 3%) added to each vertical layer. Above 28 kilometers, increases in ozone cause a net cooling of the surface. Below 28 kilometers, increases in ozone cause a net warming of the surface.

Source: Lacis, Wuebbles, and Logan 1986.

EXHIBIT 6-5

Water Vapor, Altitude, and Radiative Forcing

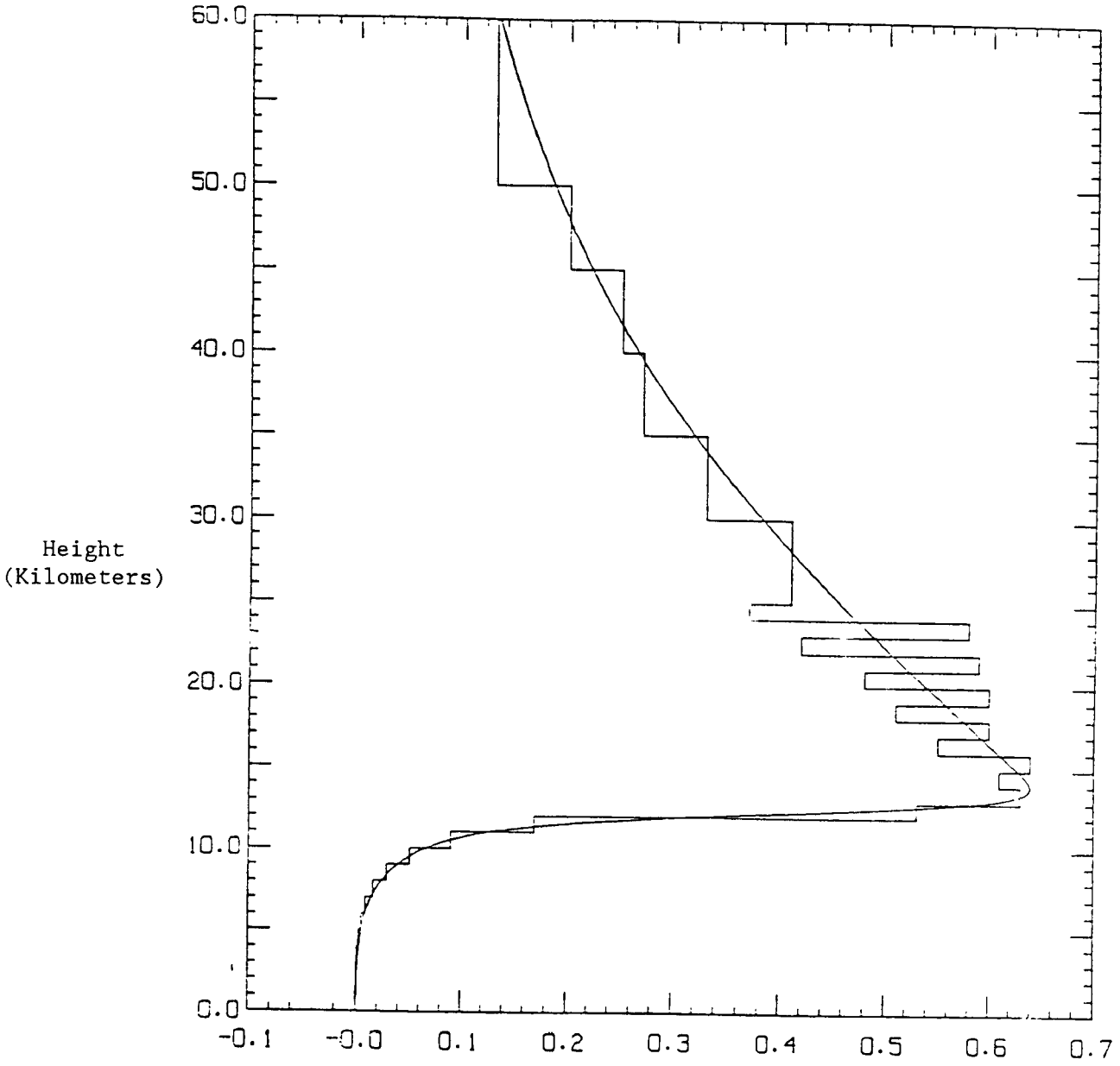

Increases in water vapor at all altitudes will warm the surface. The maximum warming occurs for increases at 14 kilometers.

Source: Lacis, personal communication.

As a consequence, the positive feedbacks from albedo changes (snow and ice melting) may be different (Lacis and Wuebbles 1986).

ULTIMATE TEMPERATURE SENSITIVITY

To understand the possible role of feedbacks on the warming caused solely by the initial radiative forcing, one must model the effects of that warming on the earth. A number of modeling analyses have been used to examine the earth's responses to radiative forcing and how those responses can increase or decrease the global temperature rise (Hansen et al. 1984; Washington and Meehl 1983; Manabe and Wetherald 1975). Exhibit 6-6 shows an analysis by Hansen et al. (1984) of the changes that would occur with the initial warming. While the exact responses are peculiar to their model, they are representative of the feedbacks found by other modeling groups. Thus, as Exhibit 6-6 shows, increases in water vapor due to an initial warming and snow and ice melting will enhance the warming significantly. Water vapor has a warming effect because it is a greenhouse gas. The melting of snow and ice enhances warming because snow and ice reflect more visible radiation back to space than do land and water -- so snow and ice melting will reduce the amount of visible radiation reflected back to space (Hansen et al. 1984).

Consistency between models is quite strong. In Hansen's model (Hansen et al. 1984), the magnitude of the global warming is 2.0°C without cloud or snow and ice feedback. Manabe and Wetherald (1975) obtain a 2°C warming for perturbation experiments in which their model assumes fixed clouds. When Manabe allows clouds to vary, his model shows that the warming is amplified to 4°C (Manabe and Wetherald 1986). Washington and Meehl (1984), who also allow clouds to vary, obtain a global temperature sensitivity of 3.5°C.

Despite this apparent consensus, however, care should be taken in interpreting this agreement. The exact nature of future cloud changes remain uncertain. Somerville and Remer (1984) propose a mechanism by which clouds might dampen the warming. Manabe, Washington, and Hansen all counsel caution (personal communications), and each is uncertain of his model's portrayal of cloud feedback processes. The uncertainty associated with clouds is, of course, completely consistent with the National Academy of Sciences (NAS) estimate of temperature sensitivity. Instead of using the range of temperature responses produced by models, 2° to 4°C, the NAS has recommended a range of 1.5°C to 4.5°C, which characterizes their judgment about the possible range of temperature sensitivity. Unfortunately, the possibility that the earth's temperature sensitivity lies outside this range cannot be excluded (NAS 1982).

Past and Near-Term Rises in Temperature Cannot be Expected to Resolve Uncertainties about Actual Climate Sensitivity

A different approach other than modeling has been suggested as a means for estimating the temperature sensitivity of the earth to a given radiative forcing -- to compare historical temperature rises to past increases in greenhouse gases (Webb and Wigley 1985; Broecker 1986). Unfortunately, this approach cannot provide precise estimates of temperature sensitivity because many of the factors that may have contributed to past temperature changes are themselves uncertain. Exhibit 6-7 from Hansen et al. (1984) shows the extent to which the derived temperature sensitivity would depend on knowing initial trace gas concentrations and the rise in temperature. Uncertainty exists about both past temperature

EXHIBIT 6-6

Temperature Sensitivity to Climatic Feedback Mechanisms

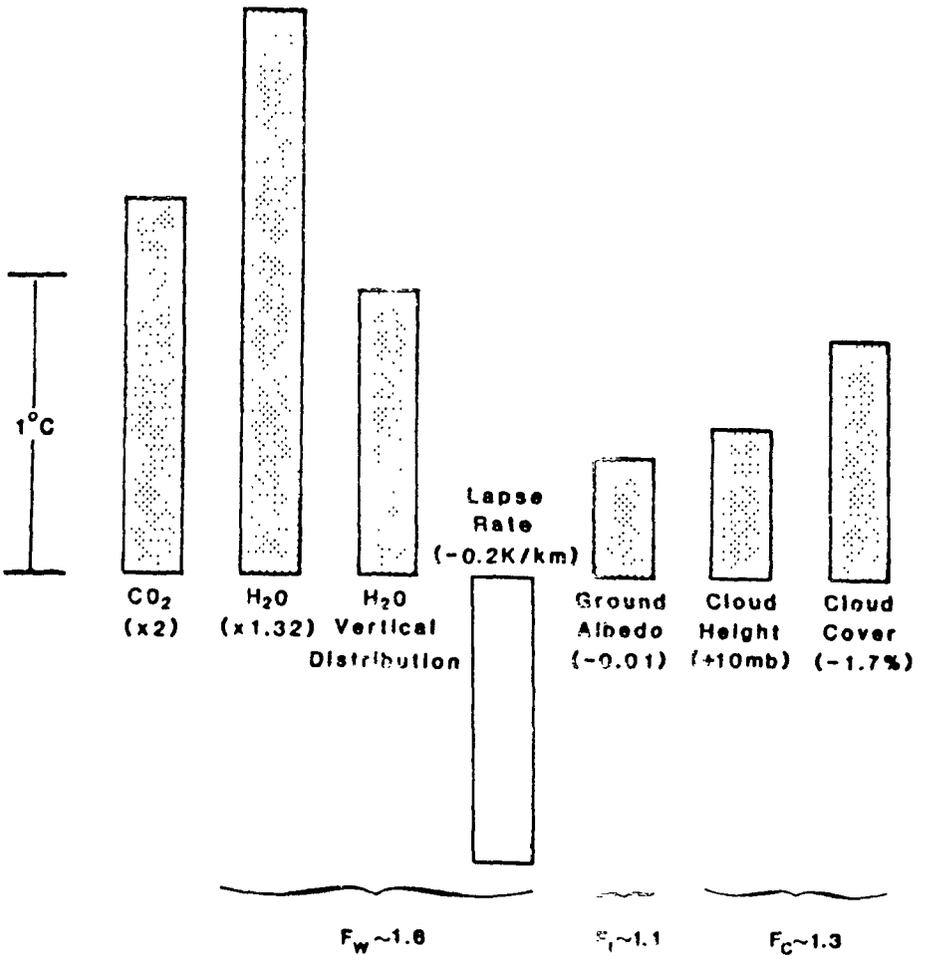

The earth's responses to an initial radiative forcing will determine the final temperature change. The direct radiative forcing of doubled CO2 would increase the global average temperature by 1.26°C. Subsequent melting of snow and ice would affect water vapor (H2O) concentrations and distributions, amplifying the initial warming by approximately 1.6°C. The effect of melting on the earth's reflectivity, or ground albedo, would amplify the warming by 0.4°C. Changes in cloud cover would add 0.8°C. Total warming would thus equal approximately 4°C.

Source: Hansen et al. 1984.

EXHIBIT 6-7

Empirical Estimates of Climate Sensitivity are Sensitive to Estimates of Historical Temperature Increases and Trace Gas Concentrations

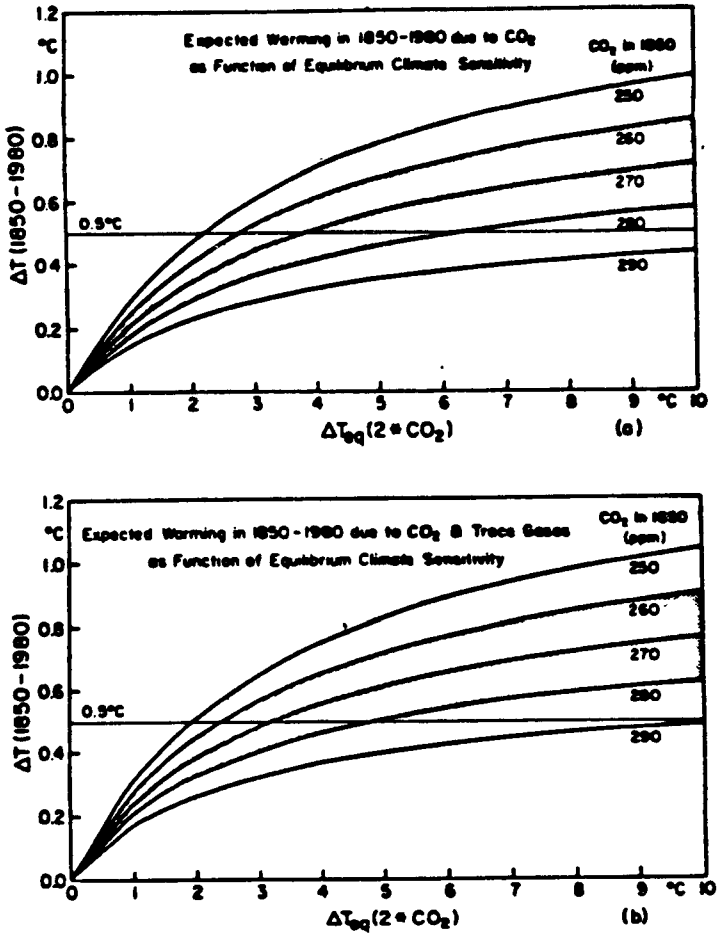

The vertical axis measures the increase in global average temperature that occurred from 1850 to 1980. The horizontal axis indicates the earth's temperature sensitivity to doubled CO2 concentrations. The curves represent temperature changes consistent with different historical changes in trace gas concentrations. Panel "a" shows the uncertainty for CO2 alone. Panel "b" incorporates other trace gases. If one assumes a historical temperature rise of 0.5°C, Panel "b" shows that temperature sensitivity could vary from approximately 2.3°C to 4.5°C, within a reasonably accepted range of 260 ppm to 280 ppm for pre-industrial CO2 concentrations.

Source: Hansen et al. 1984.

change and past concentrations of CO2 and trace gases. Estimates of pre-industrial values of CO2 based on ice core and other data range from 260 to 290 ppm (Oeschger et al. 1982; Neftel et al. 1982; Pearman et al. 1986; and Peng et al. 1983). To complicate matters further, uncertainty also exists about changes in other kinds of forcing that can influence radiative balance, such as changes in solar radiation and aerosols from volcanoes (Bradley and Jones 1985). Failure to include these possible changes in forcing could bias estimates of temperature sensitivity. In addition, uncertainties about instabilities and oscillations in the internal dynamics of the climate/ocean system are also unknown, and could produce variation in observed temperatures (Hoffert and Flannery 1985). For example, in a recent run of the Goddard Institute for Space Studies (GISS) general circulation model, without any change for radiative forcing, global average temperature varied 0.2°C from the 100-year mean in a period of 100 years (Hansen et al. 1986). Based on this estimate of "natural variation which is entirely expected according to model runs (Hansen et al. 1986b)," an accurate assessment of temperature sensitivity will not be possible even after the temperature has risen another 0.5°C.

Clouds are the Major Uncertainty

The International Satellite Cloud Climatology Project is seeking to collect a global database of radiation information that can be used to improve our understanding of clouds and their response to global warming (WMO 1984). Several research obstacles including insufficient satellite coverage, difficulties in converting radiation data to accurate representation of clouds, and the complexity of modeling cloud systems and their effects, must be overcome for this endeavor to be successful. The goal of this effort is to provide data that allows us to narrow considerably our uncertainty about clouds. However, the possibility exists that the data from this international project will provide a useful beginning for resolving our questions about this important climate feedback (Luther and MacCracken 1985).

THE TIMING OF GLOBAL WARMING

The timing of global warming is of particular importance to assessing the associated risks. Knowing the radiative forcing and the temperature sensitivity of earth to that forcing are insufficient for assessing the time-dependent evolution of the climate system. To determine timing, oceanic heat absorption must be considered.

In this section, we review the results of two research teams that have considered all three components of climate change: changes in greenhouse gases, temperature sensitivity, and oceanic heat absorption.

The timing estimates represented here can be broken down into efforts that utilized one-dimensional and three-dimensional models. Hansen et al. (1981) used a one-dimensional model to estimate the rise of temperatures from historic levels. Details of the model, a parameterized version of which was also used by Hoffman, Wells, and Titus (1985), are presented in Attachment A. Before proceeding, however, a brief discussion of the radiative forcings and how the model deals with oceanic heat uptake is warranted.

The rate at which infrared-absorbing gases are expected to increase has been presented elsewhere in this document (Chapters 2, 3, and 4). While changes in volcanic aerosols and solar radiation could accelerate or retard the increase in net radiative forcing, changes in these factors will not be examined here,

except to say that the radiation output of the sun has been measured since early 1980 by the NASA Solar Maximum Mission Satellite, and unpublished data show a decrease in the last four years. Previous studies have speculated on various cycles for changes in solar radiation (Newkirk Jr. 1983; Hoyt 1979; and Gilliland and Schneider 1984). At this time, there is no basis for predicting future trends (Hoffert and Flannery 1985).

Aerosols from volcanoes depend on the rate and nature of volcanic eruptions. In general, the eruptions must propel aerosols into the stratosphere in order to produce a climatic effect. For example, despite its magnitude the Mt. St. Helens eruption had negligible effects on climate because of the lack of sulfur in the explosion and because of its sideways ballistics. The 1982 El Chichon eruption had a very large climatic effect, possibly placing more aerosols into the stratosphere than any eruption since Krakatoa (MacCracken and Luther 1984; NASA 1982; and Pollack 1983). Future eruptions cannot yet be predicted, but volcanic aerosols from single eruptions are unlikely to have more than a two- to three-year influence on radiative forcing (Hoffert and Flannery 1985).

Oceanic heat absorption is the major factor that could influence the timing of the warming (NAS 1979). At this time, it is impossible to describe accurately all the processes that will influence the ocean system's ability to take up or give off heat. Data and knowledge are both lacking. The ocean is a complex three-dimensional system in which heat-exchange processes operate by many means, including both convection and diffusion. The specific topography of ocean floors is important, as is the salt and water density. Initial attempts are now being made to model the ocean in more of its complexity (Hoffert and Flannery 1985; Sarmiento and Bryan 1982; and Woods 1985). However, an adequate ocean general circulation model does not yet exist.

In the absence of an adequate three-dimensional representation of oceanic processes and heat uptake, representation of the oceans has been relegated to simple parametric models of oceanic heat uptake that use diffusion as a surrogate for other mechanisms to absorb heat. Such models, while clearly not portraying mechanisms, have the advantage of allowing different assumptions to be used about the quantity of heat uptake in perturbation studies, thereby providing some understanding of the variation in estimates of warming that is attributable to uncertainties in oceanic heat absorption. One-dimensional (1-D) ocean models that use eddy diffusion to transport heat have been developed for this purpose. The models have been calibrated to reproduce the behavior of transient tracers (Broecker and Peng 1982). Such models have allowed experiments to be conducted that allow for changes in the rate of heat absorption. Exhibit 6-8 shows the logical flow of how these models can be used for estimating transient atmospheric temperatures. Note the parameter "k," which can be exogenously manipulated to test differing rates of heat absorption.

Hansen et al. (1984) used a one-dimensional radiative convective model coupled to an ocean box model to estimate future realized and unrealized warming through time (Exhibit 6-9). The scenarios used for trace gas growth are approximately the same as those discussed in Chapters 2 and 4. (see Attachment B for details). The distance between the dotted and solid lines represents the

EXHIBIT 6-8

Relationship of Radiative Forcing, Ocean Heat Uptake, and Realized and Unrealized Warming

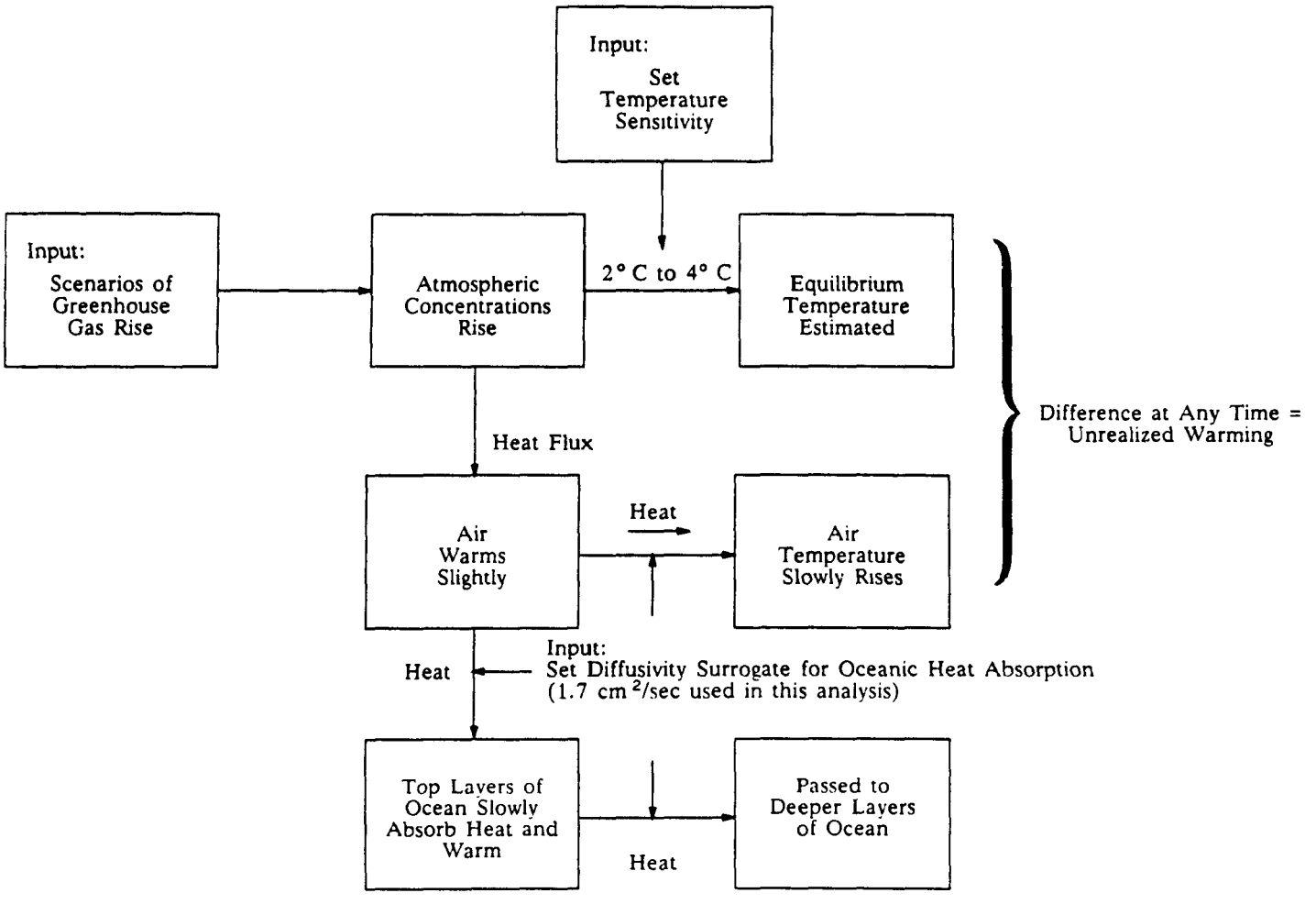

The model allows input parameters to be set and then consistently simulates time-dependent evolution of the system.

EXHIBIT 6-9

Transient Estimates of Global Warming

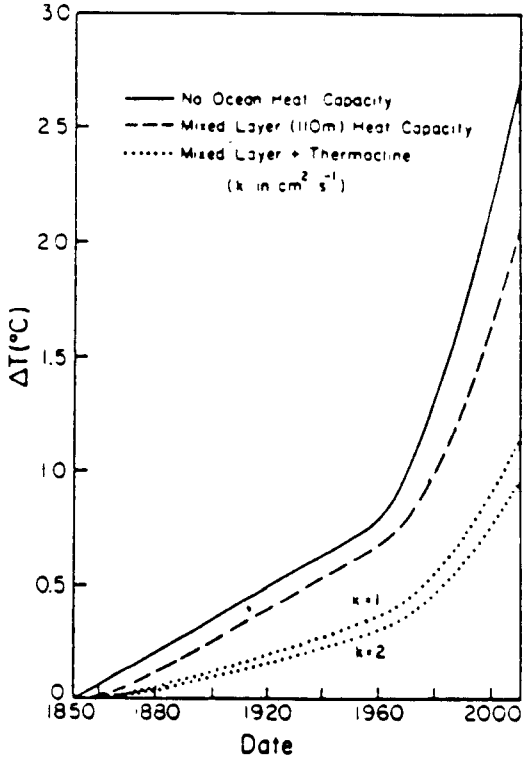

Change in global average surface temperature due to increases in CO2 and other trace gases from 1850 to 2007. The solid line shows the warming that would occur if oceanic heat absorption did not delay global warming. The dashed line represents oceanic heat absorption by only the top layers of the ocean. The dotted lines represent heat absorption by the lower layers of the ocean, and test two assumptions about the rate of heat uptake, "k". The distance between the solid line, which shows "equilibrium" temperature, and the dotted lines, which show "transient" temperature, equals the "unrealized" warming. Note that changes in this exhibit are relative to 1850.

Source: Hansen et al. 1984.

unrealized warming for two different assumptions about heat uptake. Note that in the time period examined, that is, until the year 2007, the projected temperatures are quite similar for different heat absorption. Hoffman, Wells, and Titus (1985) also use a modified version of this model to make estimates of temperature change farther into the future (see Exhibit 6-10). They simulated a similar scenario, using 2°C and 4°C as the earth's temperature sensitivities to doubled CO2.

Only two time-dependent simulations have been conducted using a general circulation model (Hansen et al. 1986). The representation of the oceans in that model, while still unrealistic, does use three-dimensional heat absorption based on transient tracers. Exhibit 6-11 shows their results, which predict a faster warming than do their 1-D models. Since the results are from the same modeling group, the question arises of whether 1-D time-dependent representations underestimate the actual rate of global warming. Another question that deserves close attention is whether other parameterizations, such as upwelling diffusion, should be used; these would give smaller results (Hoffert and Flannery 1985).

REGIONAL CHANGES IN CLIMATE DUE TO GLOBAL WARMING

Only one change in regional climate can be projected with a high degree of confidence. Temperatures will rise more for latitude bands as distance from the equator increases. For model runs in which the atmospheric CO2 concentration is doubled, Hansen et al. (1986) and Washington and Meehl (1983) find a ratio of approximately two to one between warming near the poles and near the equator. Manabe and Wetherald (1975) show a larger gradient of up to seven to one. Almost as certain as the latitudinal gradient is that global warming can be expected to intensify the hydrological cycle, increasing global mean precipitation and evaporation (Schlesinger and Mitchell 1985). In response to a quadrupling of CO2 (with a model with a 2°C sensitivity; no cloud feedback allowed), Manabe and Wetherald (1985) find a 7% increase in both precipitation and evaporation. In a similar experiment Washington and Meehl (1984) showed an increase of 6% in precipitation. For a doubled CO2 experiment, which yields a temperature increase of approximately 4°C, the Goddard Institute for Space Studies model predicts an 11% increase in precipitation and evaporation (Rind and Lebedeff 1984).

All three-dimensional models predict significant shifts in dryness and wetness throughout the world. For the U.S., the Goddard Institute for Space Studies model (Rind and Lebedeff 1984) predicts an average increase in runoff of 18%. Exhibit 6-12 shows the distribution of changes predicted by that model. Estimates of the distribution of runoff change from the general circulation model of Princeton's Geophysical Fluid Dynamics Laboratory and National Center for Atmospheric Research are similar to the Goddard Institute for Space Studies run, even though they vary greatly in regional detail (Manabe and Wetherald 1985; Washington and Meehl 1984).

The reliability of regional projections from general circulation models is weak, however. Current general circulation models lack realism in representing important ocean, biospheric, and cloud processes that are critical to establishing precise estimates of hydrological change for particular regions. At this time, no interactive climate/ocean model has been successfully developed and published. Yet we know from events such as the 1983 El Nino that changes in

EXHIBIT 6-10

Expected Temperature Increases

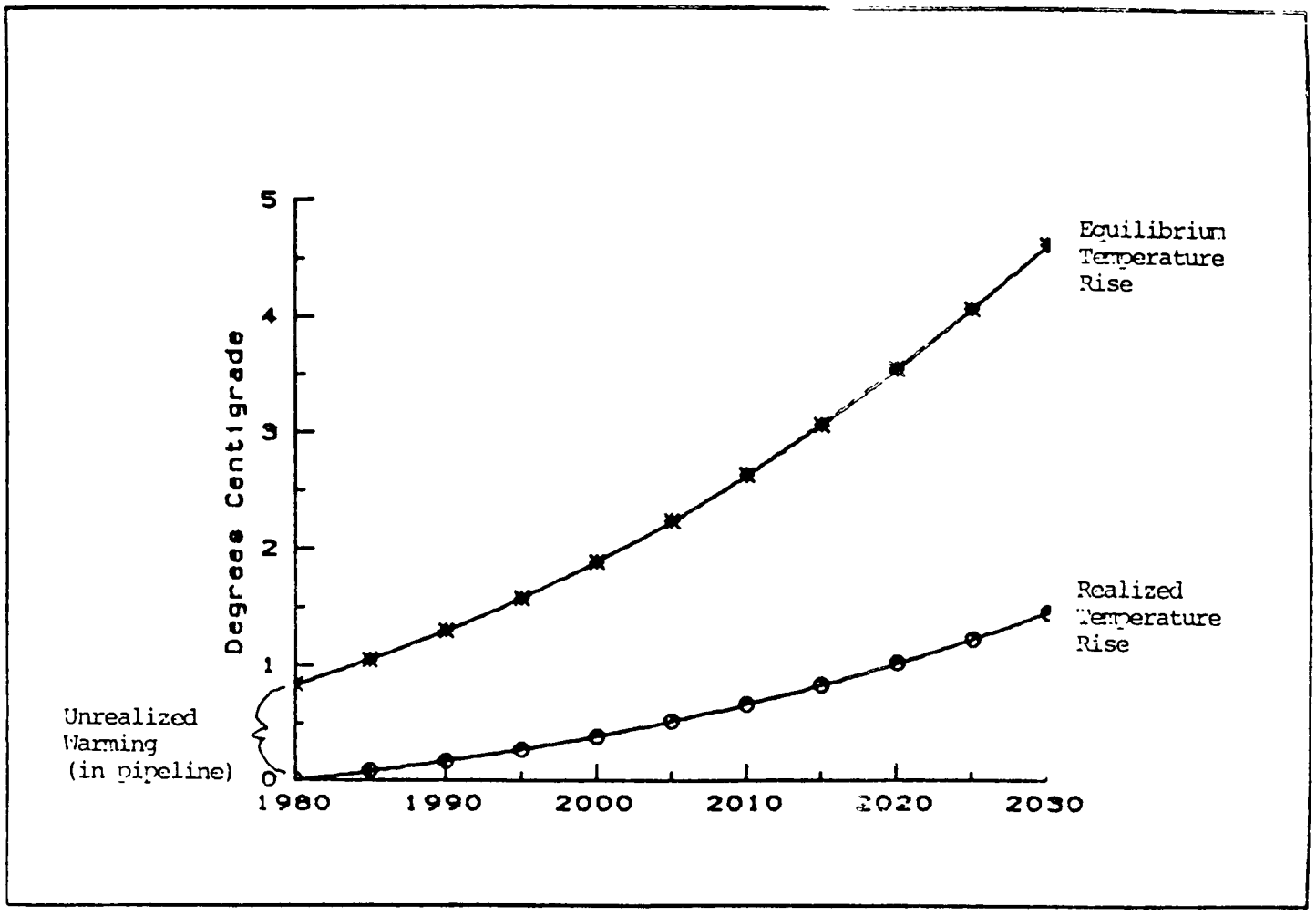

Change in global average surface temperature due to increases in CO2 and trace gases from 1980 to 2030. A modified version of the Goddard Institute for Space Studies model (Hansen et al. 1981) was used. The model's thermal sensitivity is 4°C for doubled CO2 concentrations. Note that changes in this figure are relative to 1980.

Source: Hoffman, Wells, and Titus 1985.

EXHIBIT 6-11

Results of Transient Analysis Using a General Circulation Model

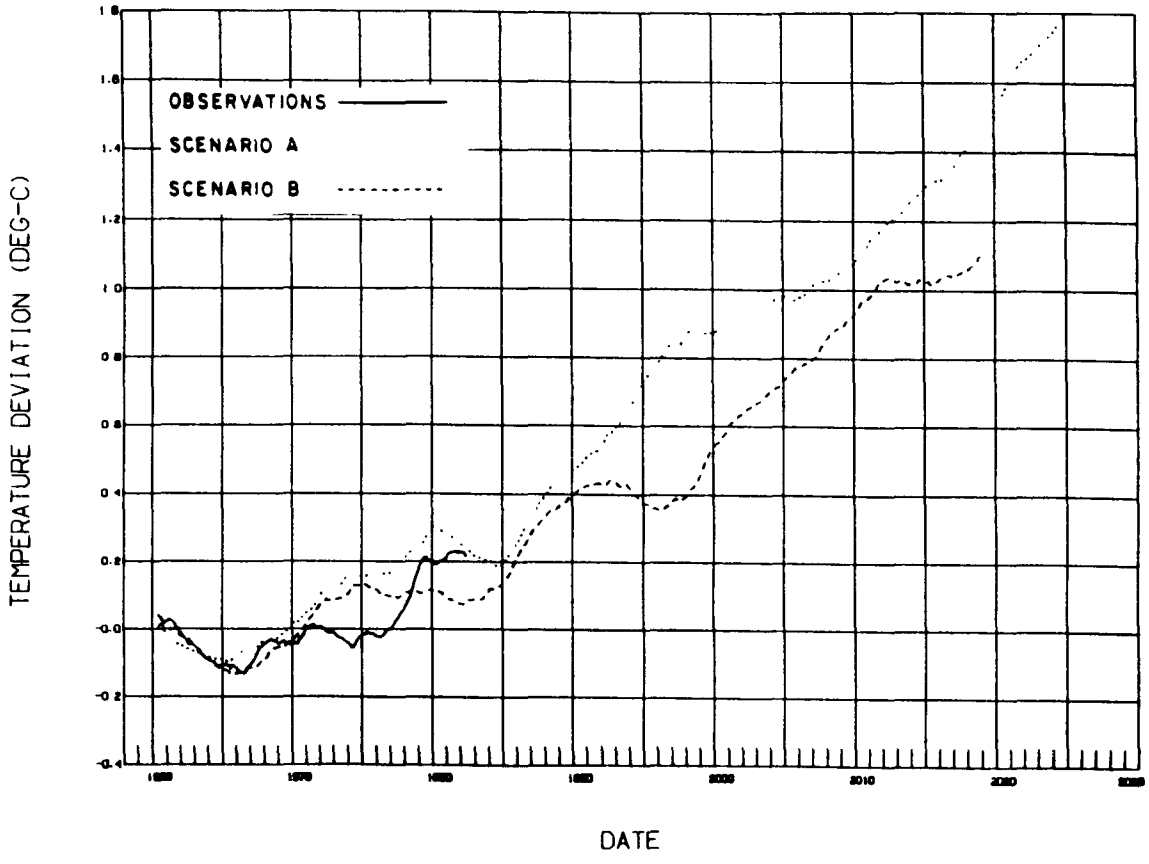

Only two time-dependent simulations have been conducted using a general circulation model. The results, shown above, indicate an increase in global average temperature of approximately 0.9°C by the year 2000 for Scenario A (which is a continuation of current rates of growth in trace gases). Scenario B (which reflects reduced rates of trace gas growth) indicates a warming of about 0.5°C by 2000. Scenario A achieves a radiative forcing equivalent to that of doubled CO2 about 40 years from now; Scenario B requires 75 years.

Source: Hansen et al. 1986.

EXHIBIT 6-12

Regions of U.S.: Change in Runoff

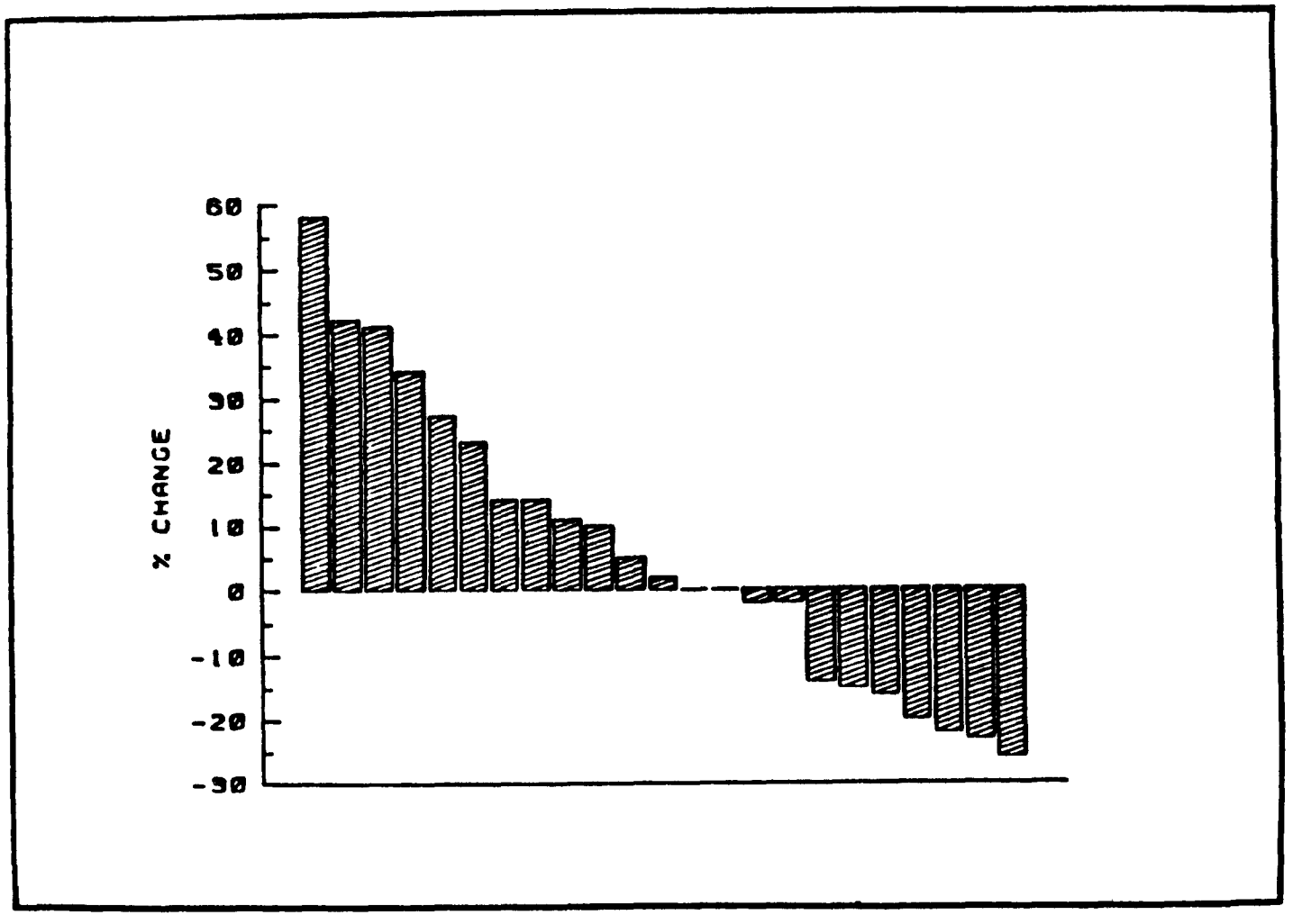

The general circulation model of the Goddard Institute for Space Studies was used to simulate changes in hydrology due to increases in CO2 and other trace gases. Estimates were made for 23 gridded regions of the United States. The graph above shows the distribution of changes in precipitation runoff: increases in 14 regions and decreases in 9 regions.

Source: Rind and Lebedeff 1984.

oceanic circulation can influence regional climates (Wigley, Angell, and Jones 1985). None of the models adequately represents the hydrological process, especially the role of the biosystem. In fact, in all models the biosystem remains constant as climate changes and CO2 increases. In reality we can expect large alterations in ecosystems in response to the effects of climate change and the response to the direct physiological effects of CO2 on photosynthesis (Strain 1985). These changes would alter hydrological processes in important ways.

The possibility still exists, however, that for large enough areas, some robust projections can be made. The general circulation model at Princeton's Geophysical Fluid Dynamics Laboratory has been run using two very different cloud regimes -- one in which clouds are prescribed and one in which they change. Manabe and Wetherald (1986) find that in both simulations summer drying occurs at mid-latitudes: "... it seems significant that all the experiments discussed in this report indicate CO2-induced summer reduction and winter enhancement of soil wetness over extensive, mid-continental regions in middle and high latitudes ... it is likely that the basic conclusion is valid despite the imperfections of the model." If Manabe is correct, it means that, while regional changes are difficult to state with confidence, some can be projected.

EFFECTS ON THE STRATOSPHERE OF POSSIBLE CONTROL OF GREENHOUSE GASES

Stratospheric perturbants that are greenhouse gases may also alter stratospheric structure and composition. Limiting chlorofluorocarbon emissions in the future would decrease both stratospheric ozone depletion and global warming. This relationship is straightforward. For other perturbants, however, the situation is more ambiguous.

Miller and Mintzer (1986) point out that emissions of some stratospheric perturbants may eventually be reduced by governments in an effort to limit global warming. Targets could include nitrous oxide (N2O), carbon dioxide (CO2), or methane (CH4). Decreases in nitrous oxide would lower global temperatures (Ramanathan et al. 1985). The net effect on ozone depends on chlorine concentrations (Stolarski, personal communication). In many scenarios considered plausible, lowering N2O to reduce global warming might actually exacerbate ozone depletion. Decreases in methane would reduce global warming in three ways: by reducing its direct radiative effects while it's in the troposphere (Ramanathan et al. 1985); by altering its indirect effects on increasing tropospheric and lower stratospheric ozone (NAS 1984); and by reducing the amount of water vapor added to the stratosphere (NAS 1984). Methane emissions might be limited by altering rice cropping practices, by altering livestock rearing practices (and through biotechnology to reduce livestock methaneogenis), by reducing forest burning, or by controlling pipeline leaks. Methane emissions might also be limited through indirect means, that is by controlling carbon monoxide emissions that would reduce the lifetime of methane molecules (Miller and Mintzer 1986). As a consequence, however, a decrease in methane would allow increasing CFC concentrations to deplete column ozone more effectively.

Carbon dioxide cools the stratosphere, thus slowing the process of ozone loss. Consequently, model scenarios that include CO2 growth show reductions in ozone depletion (Connell and Wuebbles 1986). Efforts to limit the growth of CO2 could include altering energy mixes (e.g., using more nuclear or solar energy), conservation (less energy to do the same work), and altering land clearing practices (Seidel and Keyes 1983). Such actions to limit CO2 could

inadvertently increase the vulnerability of the stratospheric ozone layer.

Decreases in carbon monoxide (CO) emissions from combustion are projected to occur (Kavanaugh 1986). Decreases in CO emissions may also be possible if forest burning decreases (Hoffman and Wells 1986). Since carbon monoxide plays a large role in OH concentrations, which, in turn, influence the lifetime of methane, changes in carbon monoxide emissions could alter methane concentrations (Khalil and Rasmussen 1985). If CO concentrations decrease, the lifetime of methane (CH4) would decrease, and there would be a tendency to lower concentrations (Thompson and Cicerone 1986). Decreasing CH4 concentrations would not only decrease global warming but would also make the ozone layer more vulnerable to depletion.

ATTACHMENT A

DESCRIPTION OF MODEL TO BE USED IN INTEGRATING CHAPTER

The model used in the integrated assessment chapter at the end of this document was adapted from a one-dimensional radiative-convective model developed by the Goddard Institute for Space Studies for estimating temperature increases associated with atmospheric CO2 rises (Hansen et al. 1981).

The model computes vertical temperature profiles over time from net radiative and convective energy fluxes. Radiative fluxes, in turn, depend on changes in atmospheric gases, and on the associated feedback effects. The parameterized equation used here is based on an empirical fit to the radiative-convective model.

The fitted equation, described in Hansen et al. (1981), was developed for CO2 only. It was later modified by Lacis (personal communication) to incorporate CFC-11, CFC-12, CH4, and N2O. Other minor trace gases were incorporated based on the work of Ramanthan et al. (1985).

Radiative Forcing Equations

The equations in the model are:

CO2: $FCO2 = \ln [1 + .942*CO2/(1+.00062*CO2) + .0088*CO2^2 + 3.26*10^{-6}*CO2^3 + .156*CO2^{1.3} \exp (-CO2/760)]$

CH4: $FCH4 = [.394*CH4^{.66} + .16*CH4 \exp (-1.6*CH4] / (1 + .169*CH4^{.62})$

N2O: $FN2O = 1.556 \ln [1 + 1.098 (1+.032*N2O)*N2O^{.77} / (1+.0014*N2O^2)]$

Overlap: $FOVL = .14 \ln [1 + .636 (CH4*N2O)^{.75} + (.007*CH4 (CH4*N2O)^{1.52}]$

F11: $FF11 = .066*F11$

F12: $FF12 = .084*F12$

$\Delta Trad = FCO2(now)-FCO2(ref) = FCH4(now)-FCH4(ref) + FN2O(now)-FN2O(ref) - FOVL(now)+FOVL(ref) = FF11(now)-FF11(ref) + FF12(now)-FF12(ref)$

For CO2 from 300 to 600: $\Delta Trad = FCO2(600) - FCO2(300) = 1.26°$

Where: $\Delta Trad$ is the radiative forcing in year t, expressed in degrees centigrade (C). The model is initialized to the year 1880 ("ref" = 1880).

CO2 is the CO2 concentration in year t, in parts per million (ppm). CO2(ref) = 270.

CH4 is the CH4 concentration in year t, in ppm. CH4(ref) = 1.02.

N2O is the N2O concentration in year t, in ppm. N2O(ref) = 0.2853.

F11 is the CFC-11 concentration in year t, in parts per billion (ppb). F11(ref) = 0.0

F12(t) is the CFC-12 concentration in year t, in ppb. F12(ref) = 0.0

For the other trace gases incorporated in the model, the radiative forcing in any year is computed in the same fashion as CFC-11 and CFC-12:

$$\Delta Trad_{(j)} = a_j * X_{jt}$$

where: $\Delta Trad_{(j)}$ = radiative forcing in degrees C in year t for compound "j".

a_j = sensitivity to a uniform 1 ppb increase in the trace gas concentration (0 to 1 ppb) for compound "j".

x_{jt} = the concentration in ppb in year t for compound "j".

The sensitivities were extracted from the work of Ramanathan et al. (1985) and are:

Trace Gas	"a" Direct radiative forcing for a 0 to 1 ppb increase (degrees C)
SO2	0.01
F14	0.06
F116	0.13
HCFC-22	0.05
CFC-13	0.22
CH2C12	0.03
CHC13	0.06
CC14	0.08
CH3CC13	0.02
Halon 1301	0.17
C2H2	0.02

The total radiative forcing (the sum of the radiative forcing from each trace gas) is the basis for estimating heat flux into the earth's surface. The following equations, from Hansen et al. (1984), are used:

$\Delta Teq = f.\Delta Trad$

$$F\ (W/m^2) = \frac{Fo(2*CO2)}{\Delta Teq(2*CO2)}\ (\Delta Teq - \Delta T) = \text{global flux into the ocean}$$

ΔT = is the current global temperature change from initial reference state

We use the flux conversion efficiency of Model II for global flux into the ocean as determined by the 2*CO2 experiment.

$F\ (W/m^2) = 3.58.(\Delta Trad - \Delta T/f)*(0.7)$

$F\ (W/m^2)/697.4 = F\ (cal*min^{-1}*cm^{-2})$

The heat flux is estimated for time periods ranging from each month to each year (a semimonthly time step was used in this study). The appropriate ΔT value for calculating F(t) in each time period (t=n) is the value estimated for the previous period (t=n-1). For a simple one-layer ocean model, ΔT is obtained by solving the following differential equation:

$$\frac{d\ \Delta\ T}{dt} = \frac{F(t)}{C_o}$$

Where: C_o is the heat capacity of the mixed layer of the ocean per unit area ($cal\ cm^{-2}$).

Diffusion of Heat in the Ocean

The ocean model consists of a mixed layer of depth H_m = 100m and a thermocline with 63 layers and depth H = 900m. The mixed layer temperature is assumed to be independent of depth, while the thermocline temperature is defined by a diffusion equation with constant thermal diffusivity.

The temperature change in the mixed layer (ΔT_m) is a solution of the equation:

$$CH_m \frac{d\ \Delta\ T_m}{dt} = F(t) + F_D(t)$$

where C is the heat capacity of water, H_m is the depth of the mixed layer, F(t) is the heat flux from the atmosphere into the ocean, and

$$F_D(t) = - \lambda \frac{\partial \Delta\ T}{\partial z} \Big|_{z=H_m}$$

is the heat flux from the thermocline into the mixed layer. Note that our z-axis is directed toward the bottom of the ocean. Also, we use g, cm, sec and cal, so the heat conductivity lamda is numerically equal to the heat diffusivity K. Different values for diffusivity may be chosen.

The temperature change in the thermocline (Δ T) is determined by the diffusion equation:

$$c \frac{\partial \Delta\ T(z,t)}{\delta A} = \lambda \frac{\partial^2 \Delta T(z,t)}{\delta z^2}$$

The boundary conditions for ΔT are:

$$\Delta T = \Delta T_m \quad \text{at } z = H_m$$

and zero heat flux at the bottom of the thermocline:

$$\frac{\lambda \partial \Delta T}{\partial z} = 0 \text{ at } z = H + H_m.$$

Thus it is assumed that no energy escapes through the lower boundary of the thermocline. Note that ΔT_m and ΔT are temperature changes of the mixed layer and the thermocline between the initial time (1880) and time t. It is assumed that in the year 1880 $\Delta T_m = \Delta T = 0$ and thus that the ocean temperature was in a state of equilibrium with the atmosphere at that time.

The use of diffusivity coefficients as a surrogate for all circulation processes that transport heat may fail to describe the time paths well, with the downward heat transport in the latter period probably being overestimated because of increasing oceanic stability. Nevertheless this method simplified the problem substantially, and a range of different possible coefficients can be used to investigate the sensitivity of the overall estimate to the rate of downward heat transport.

Using transient tracers, Broecker and Peng (1982) developed an average eddy diffusion coefficient for the ocean of 1.7 cm^2/sec. This value, accepted by many as a reasonable surrogate measure for estimating heat absorption, is the reference value in our model. To test the sensitivity of the results to this choice, other values may be chosen.

The range of coefficients tested, from 0.85 to 3.4 cm^2/sec, covers the range of mean ocean-wide mixing rates as determined by the National Science Foundation-sponsored transient tracer experiment and others. Variation in estimates of the exact value of the data depend on the tracer used and the statistical method of computing the global mean. The values of 0.2 and 4.0 cm^2/sec were tested in earlier work to account for the possibility of dramatic changes in ocean transports due to deglaciation and climate change (Hoffman et al. 1983).

ATTACHMENT B

Trace Gas Scenarios Used in Hansen et al. 1984; Exhibit 6-9

YEAR	CO2 (ppm)	CFC-11 (ppt)	CFC-12 (ppt)	CH4 (ppb)	N2O (ppb)
1850	270	0	0	1400	295
1900	291	0	0	1400	295
1950	312	7	1	1400	295
1960	317	33	11	1416	295
1970	326	126	62	1500	295
1980	338	308	178	1650	301
1990	353	479	280	1815	307
2000	372	638	369	1996	313
2010	396	787	447	2196	320

Trace Gas Scenarios Used in Hoffman, Wells, and Titus 1985; Exhibit 6-10

YEAR	CO2 (ppm)	CFC-11 (ppt)	CFC-12 (ppt)	CH4 (ppb)	N2O (ppb)
1880	280	0	0	1402	295
1900	288	0	0	1448	296
1950	311	1	8	1568	298
1960	316	11	36	1593	299
1970	326	64	137	1619	299
1980	339	185	337	1645	300
1990	355	341	577	1822	307
2000	373	599	903	2093	313
2010	398	992	1371	2406	320
2020	431	1500	2023	2764	328
2030	470	2116	2863	3177	338

REFERENCES

Bradley, R.S., and P.D. Jones (1985). "Data Bases for Isolating the Effects of the Increasing Carbon Dioxide Concentration." In MacCracken, M.C., and F.M. Luther (eds.), Protecting the Climatic Effects of Increasing Carbon Dioxide, DOE/ER-0235, U.S. Department of Energy, Washington, D.C.

Broecker, W.S., (1986). "Statement for Ozone Depletion, the Greenhouse Effect, and Climate Change," Hearings before the Subcommittee on Environmental Pollution of the Committee on Environment and Public Works, United States Senate, Ninety-Ninth Congress, Second Session, June 10 and 11, 1986.

Broecker, W.S., and T. Peng (1982). Tracers in the Sea. Palisades, NY: Lamont-Doherty Geophysical Observatory. Columbia University.

Connell, P.S., and O.J. Wuebbles (1986). Ozone Perturbations in the LLNL One-Dimensional Model -- Calculated Effects of Projected Trends in CFC's, CH4, CO2, N2O, and Halons Over 90 Years, Lawrence Livermore National Laboratory, Livermore, CA.

Dickinson, R.E., and R.J. Cicerone (1986). "Future Global Warming from Atmospheric Trace Gases," Nature 319:109-115.

Gilliland, R.L., and S.H. Schneider (1984). "Volcanic, CO2 and Solar Forcing of Recent Climatic Changes," Nature 310:38-41.

Hansen, J.E. (1986). "Statement for Ozone Depletion, the Greenhouse Effect, and Climate Change," Hearings before the Subcommittee on Environmental Pollution of the Committee on Environment and Public Works, United States Senate, Ninety-Ninth Congress, Second Session, June 10 and 11, 1986.

Hansen, J., D. Johnson, A. Lacis, S. Lebedeff, P. Lee, D. Rind, and G. Russell (1981). "Climate Impacts of Increasing Atmospheric CO2, Science 213:957-966.

Hansen, J., A. Lacis, D. Rind, G. Russell, I. Fung, and S. Lebedeff (1986). "Evidence for Future Warming: How Large and When," presented at the CO2 Conference of the National Forest Products Association, June 25-27, 1984, Boulder, Colorado, in press.

Hansen, J., A. Lacis, D. Rind, G. Russell, P. Stone, I. Fung, R. Ruedy, and J. Lerner (1984). "Climate Sensitivity: Analysis of Feedback Mechanisms." In Hansen, J.E., and T. Takahashi (eds.), Climate Processes and Climate Sensitivity, Geophysical Monograph 29, Maurice Ewing Volume 5, American Geophysical Union, Washington, D.C.

Hoffert, M.I., and B.P. Flannery (1985). "Model Projections of the Equilibrium Climatic Response to Increased Carbon Dioxide." In MacCracken, M.C., and F.M. Luther (eds.), Projecting the Climatic Effects of Increasing Carbon Dioxide, DOE/ER-0237, U.S. Department of Energy, Washington, D.C.

Hoffman, J.S., and J.B. Wells (1986). "Trace Gas Scenarios," presented at the UNEP Economic Workshop on Protection of the Ozone Layer, May 26-30, 1986, Rome, Italy.

Hoffman, J.S., J.B. Wells, and J.G. Titus (1985). "Future Global Warming and Sea Level Rise." In G. Sigbjarnarson (ed.), Iceland Coastal and River Symposium, Proceedings, Library of the National Energy Authority, Reykjavik, Iceland.

Hoyt, D.V. (1979). "Variations in Sunspot Structure and Climate," Climatic Change 21:79-92.

Isaksen, I.S.A., and F. Stordal (1986). "Ozone Perturbations by Enhanced Levels of CFCs, N2O, and CH4: A Two-Dimensional Diabatic Circulation Study Including Uncertainty Estimates," Journal of Geophysical Research, 91(D4): 5249-5263.

Kavanaugh, M. (1986). "Estimates of Future CO, N2O, and NOx Emissions from Energy Combustion," to appear in Atmospheric Environment (in press).

Khalil, M.A.K., and R.A. Rasmussen (1985). "Causes of Increasing Atmospheric Methane: Depletion of Hydroxyl Radicals and the Rise of Emissions," Atmospheric Environment 19(3): 397-407.

Lacis, A.A. and D.J. Wuebbles (1986). "Radiative Forcing of Global Climate Changes in Stratospheric Water Vapor," to be submitted to Geophysical Research Letters.

Lacis, A.A., D.J. Wuebbles, and J.A. Logan (1986). "Radiative Forcing of Global Climate by Changes in the Vertical Distribution of Atmospheric Ozone," to be submitted to Geophysical Research Letters.

Luther, F.M., and R.G. Ellingson (1985). "Carbon Dioxide and the Radiation Budget." In MacCracken, M.C., and F.M. Luther (eds.), Projecting the Climatic Effects of Increasing Carbon Dioxide, DOE/ER-0237, U.S. Department of Energy, Washington, D.C.

Luther, F.M., and M.C. MacCracken (1985). "Recommendations for Research and Modeling Activities for Projecting the Climatic Effects of Increasing Carbon Dioxide." In MacCracken, M.C., and F.M. Luther (eds.), Projecting the Climatic Effects of Increasing Carbon Dioxide, DOE/ER-0237, U.S. Department of Energy, Washington, D.C.

MacCracken, M.C. and F.M. Luther (1984). "Radiative and Climatic Effects of the El Chichon Eruption," Geofisica International 23(3): 385-401.

Manabe, S., and R.T. Wetherald (1975). "The Effect of Doubling the CO2 Concentration in the Climate of a General Circulation Model," Journal of Atmospheric Sciences 32:3-15.

Manabe, S., and R.T. Wetherald (1986). "Reduction in Summer Soil Wetness Induced by an Increase in Atmospheric Carbon Dioxide," Science 232:626-628.

Miller, A.S., and I.M. Mintzer (1986). "'Draining the Sink' Policy Implications of CFC Growth Trajectories," discussion draft prepared for the U.S. Environmental Protection Agency Workshop, "'Protecting the Ozone Layer' Workshop of Demand and Control Technologies", March 6-7, 1986, Washington, D.C.

National Academy of Sciences (NAS) (1979). Carbon Dioxide and Climate: A Scientific Assessment, National Academy Press, Washington, D.C.

National Academy of Sciences (NAS) (1982). Carbon Dioxide and Climate: A Second Assessment, National Academy Press, Washington, D.C.

National Academy of Sciences (NAS) (1984). Causes and Effects of Changes in Stratospheric Ozone and Update 1983, National Academy Press, Washington, D.C.

National Aeronautics and Space Administration (NASA) (1982). "Radiative Effect of the El Chichon Volcanic Eruption: Preliminary Results Concerning Remote Sensing" (NASA TM 84959), NASA, Washington, D.C.

Neftel, A., H. Oeschger, J. Schwander, B. Stauffer, and R. Zumbrunn (1982). "Ice Core Sample Measurements Give Atmospheric CO2 Content During the Past 40,000 Yr.," Nature 295:220-223.

Newkirk, G., Jr. (1983). "Variations in Solar Luminosity," Annual Reviews of Astronomy and Astrophysics 21:429-467.

Oeschger, H., B. Stauffer, A. Neftel, J. Schwander, and R. Zumbrunn (1982). "Atmospheric CO2 Content in the Past Deduced from Ice-Core Analyses," Annals of Glaciology 3:227-232.

Pearman, G.I., D. Etheridge, F. deSilva, and P.J. Fraser (1986). "Evidence of Changing Concentrations of Atmospheric CO2, N2O, and CH4 from Air Bubbles in Antarctic Ice," Nature, 320:248-250.

Peng, T.H., W.S. Broecker, H.D. Freyer, and S. Trumbore (1983). "A Deconvolution of the Tree Ring Based d13C Record," Journal of Geophysical Research 88:3609-3620.

Pollack, J.B., O.B. Toon, E.F. Hoffman, O.J. Rosen, and J.M. Rosen (1983). "The El Chichon Volcanic Cloud: An Introduction," Geophysical Research Letters 10:989-992.

Ramanathan, V., R.J. Cicerone, H.B. Singh, and J.T. Kiehl (1985). "Trace Gas Trends and their Potential Role in Climate Change," Journal of Geophysical Research, 90(D3): 5557-5566.

Rind, D., and S. Lebedeff (1984). Potential Climatic Impacts of Increasing Atmospheric CO2 with Emphasis on Water Availability and Hydrology in the United States, U.S. Environmental Protection Agency, Washington, D.C.

Sarmiento, J., and K. Bryan (1982). "An Ocean Transport Model for the North Atlantic," Journal of Geophysical Research 87:9694-9698.

Schlesinger, M.E., and J.F.B. Mitchell (1985). "Model Projections of the Equilibrium Climatic Response to Increased Carbon Dioxide." In MacCracken, M.C., and F.M. Luther (eds.), Projecting the Climatic Effects of Increasing Carbon Dioxide, DOE/ER-0237, U.S. Department of Energy, Washington, D.C.

Seidel, S. and D. Keyes (1983). Can We Delay a Greenhouse Warming?, U.S. Environmental Protection Agency, Washington, D.C.

Somerville, R.C.J., and L.A. Remer (1984). "Cloud Optical Thickness Feedbacks in the CO2 Climate Problem," Journal of Geophysical Research 89(d6): 9668-9672.

Stordal, F., and I.S.A. Isaksen (1986). "Ozone Perturbations Due to Increases in N2O, CH4, and Chlorocarbons: Two-Dimensional Time Dependent Calculations," prepared for UNEP Economic Workshop on the Ozone Layer, Rome, Italy, May 26-30, 1986.

Strain, B.R. (1985). "Background on the Response of Vegetation to Atmospheric Carbon Dioxide Enrichment." In Strain, B.R., and J.D. Cure (eds.), Direct Effects of Increasing Carbon Dioxide on Vegetation, DOE/ER-0238, U.S. Department of Energy, Washington, D.C.

Thompson, A.M., and R.J. Cicerone (1986). "Atmospheric CH4, CO and OH from 1860 to 1985," Nature, in press.

Tyndall, J. (1861). "On the Absorption and Radiation of Heat by Gases and Vapours, and on the Physical Coxection of Radiation, Absorption, and Conduction," Philosophical Magazine and Journal of Science 22(146): 169-194.

Wang, W.C., D.J. Wuebbles, and W.M. Washington (1985). "Potential Effects of Perturbations Other than Carbon Dioxide." In MacCracken, M.C., and F.M. Luther (eds.), Projecting the Climatic Effects of Increasing Carbon Dioxide, DOE/ER-0237, U.S. Department of Energy, Washington, D.C.

Washington, W.M., and G.A. Meehl (1984). "Seasonal Cycle Experiment on the Climate Sensitivity Due to a Doubling of CO2 With an Atmospheric General Circulation Model Coupled to a Simple Mixed-Layer Ocean Model," Journal of Geophysical Research 89(D6): 9475-9503.

Webb, T., III and T.M.L. Wigley (1985). "What Past Climates Can Indicate about a Warmer World." In MacCracken, M.C., and F.M. Luther (eds.), Projecting the Climatic Effects of Increasing Carbon Dioxide, DOE/ER-0237, U.S. Department of Energy, Washington, D.C.

Wigley, T.M.L., J. Angell, and P.D. Jones (1985). "Analysis of the Temperature Record." In MacCracken, M.C., and F.M. Luther (eds.), Projecting the Climatic Effects of Increasing Carbon Dioxide, DOE/ER-0237, U.S. Department of Energy, Washington, D.C.

Woods, J.D. (1985). "The World Ocean Circulation Experiment," Nature 314:501-511.

World Meteorological Organization (WMO) (1984). The International Satellite Cloud Climatology Project (ISCCP)," report of the Third Session of the International Working Group on Data Management, March 6-8, 1984, Tokyo. World Climate Programme Report WCP-82, WMO, Geneva, Switzerland.

World Meteorological Organization (WMO) (1986a). Report of the International Conference on the Assessment of the Role of Carbon Dioxide and of other Greenhouse Gases in Climate Variations and Associated Impacts, Villach, Austria, 9-15 October 1984, WMO-No. 661, International Council of Scientific Unions, United Nations Environment Programme, and World Meteorological Organization.

World Meteorological Organization (WMO) (1986b). Atmospheric Ozone 1985. Assessment of Our Understanding of the Processes Controlling its Present Distribution and Change, Global Ozone Research and Monitoring Project -- Report No. 16, WMO, Geneva, Switzerland.

CHAPTER 7

NONMELANOMA SKIN TUMORS

SUMMARY

Nonmelanoma skin tumors are the most common cancers occurring in white populations. The two major forms of nonmelanoma skin tumors are basal cell carcinoma (BCC) and squamous cell carcinoma (SCC). Although the incidence of BCC is generally several times greater than the incidence of SCC, SCCs account for as much as four-fifths of all nonmelanoma skin cancer deaths. Prolonged sunlight exposure is considered to be the dominant (but not only) risk factor for nonmelanoma skin tumors. As a result, it is believed that increased exposure to solar ultra-violet (UV) radiation (due to the depletion of the ozone layer) will increase the incidence of nonmelanoma skin tumors among susceptible populations. SCC would have a much larger percentage increase than BCC.

Individuals with predisposing genetic traits such as albinism and xeroderma pigmentosum (a genetically inherited inability to repair UV-induced DNA damage) are at the highest risk of developing nonmelanoma skin tumors. The much larger population consisting of light-skinned individuals (skin phenotypes I and II) is considered to be at high risk, especially those with a susceptibility to sunburn, poor tanning ability, red or blond hair, blue or green eyes, and a Celtic heritage. Populations with pigmented skin, such as blacks, are at significantly lower (but not zero) risk.

FINDINGS

1. BASED ON SURVEYS (PARTICULARLY IN THE UNITED STATES AND IN AUSTRALIA), PROLONGED SUN EXPOSURE IS CONSIDERED TO BE THE DOMINANT RISK FACTOR FOR NONMELANOMA SKIN TUMORS.

   1a. Nonmelanoma skin tumors tend to develop in sun-exposed sites (e.g., the head, face, and neck).

   1b. Higher incidence rates occur among groups subject to greater exposure to the sun's rays because of occupations that necessitate their working outdoors.

   1c. A latitudinal gradient exists for UV-B radiation, and higher incidence rates of nonmelanoma skin tumors generally occur in geographic areas of relatively high UV radiation exposure.

   1d. Skin pigmentation provides a protective barrier that reduces the risk of developing nonmelanoma skin tumors.

   1e. The risk of nonmelanoma skin tumors is highest among genetically predisposed individuals (e.g., those with xeroderma pigmentosum).

   1f. A predisposition to develop nonmelanoma skin tumors exists among light-skinned individuals (skin phenotypes I and II) who are susceptible to sunburn and who have red/blond hair, blue/green eyes, and a Celtic heritage.

2. AVAILABLE EPIDEMIOLOGICAL EVIDENCE INDICATES THAT THE TWO MAJOR TYPES OF NONMELANOMA SKIN TUMORS, SQUAMOUS CELL CARCINOMA (SCC) AND BASAL CELL CARCINOMA (BCC), RESPOND DIFFERENTLY TO SOLAR EXPOSURE. IT HAS BEEN SUGGESTED THAT CUMULATIVE UV RADIATION HAS A GREATER EFFECT ON THE DEVELOPMENT OF SCC THAN ON BCC.

   2a. The BCC/SCC incidence ratio decreases with decreasing latitude and therefore, increasing UV levels.

   2b. BCC is more likely to develop on normally unexposed sites (e.g., the trunk) compared to SCC.

   2c. SCC is more likely than BCC to develop on sites receiving the highest cumulative UV radiation doses (e.g., the nose).

   2d. For a given cumulative level of sunlight exposure, the risk of developing SCC may be greater than the risk of developing BCC.

3. THE RESULTS FROM SEVERAL EXPERIMENTAL STUDIES SUGGEST THAT UV-B MAY BE THE MOST IMPORTANT COMPONENT OF SOLAR RADIATION THAT CAUSES VARIATIONS IN THE INCIDENCE OF NONMELANOMA SKIN TUMORS.

   3a. UV radiation produces nonmelanoma skin tumors in animals. UV-B wavelengths have been shown to be most effective in producing these tumors.

   3b. UV-B has been shown to cause a variety of DNA lesions, to induce neoplastic transformation in cells, and to be a mutagen in both animal and bacterial cells.

4. SEVERAL RESEARCHERS HAVE INVESTIGATED THE CHANGES IN THE INCIDENCE OF NONMELANOMA SKIN TUMORS THAT MAY RESULT FROM INCREASES IN EXPOSURE TO SOLAR UV RADIATION. GIVEN UNCERTAINTIES, RANGES OF ESTIMATES OF INCREASED INCIDENCE THAT COULD OCCUR WITH DEPLETION ARE ESTIMATED.

   4a. The action spectra for initiation and promotion of basal cell and squamous cell skin cancer have not been precisely determined. Photocarcinogenic studies indicate that the erythema and DNA action spectra span a range likely to encompass that of squamous cell and basal cell skin cancer. The Robertson-Berger (R-B) meter, while providing useful data for describing ambient UV radiation, does not relate as closely to those wavelengths thought to promote sunburn and skin cancer.

   4b. Several studies have provided estimates of a biological amplification factor (BAF), which is defined as the percent change in tumor incidence that results from a 1 percent change in UV-B radiation. The results from six studies produced an overall BAF range that is 1.8-2.85 for all nonmelanoma skin tumors.

   4c. BAF estimates are generally higher for males than for females and generally increase with decreasing latitude. In addition, the BAF estimates for SCC are higher than the BAF estimates for BCC. This finding is consistent with observations that the BCC/SCC ratio decreases with decreasing latitude and that BCC is more likely to develop on unexposed sites.

   4d. Optical amplification (the change in UV-B radiation related to ozone depletion) increases the response of these cancers to ozone depletion, because the relevant action spectra increase more than 1 percent for a 1 percent depletion. For example, a 1 percent depletion has an optical amplification of over 2 for the DNA action spectrum.

   4e. Uncertainty exists in the actual doses of solar UV radiation received by populations and in the statistical estimates of the dose-response coefficients. Therefore, a range of estimates must be developed for changes in incidence associated with changes in dose.

4f. Currently available nonmelanoma mortality data are of uncertain accuracy because of the discrepancy of reporting between death certificates and hospital diagnoses and the low proportion of deaths reported on both hospital diagnoses and death certificates. Based on published studies, the rates of metastasis among SCCs and BCCs have been estimated to be 2-20% and 0.0028-0.55%, respectively. The overall case fatality rate for nonmelanoma skin tumors is approximately 1-2% with three-fourths to four-fifths of the deaths attributable to SCC.

4g. Changes in behavior have tended to increase skin cancer incidence and mortality. While some evidence exists that this is reaching a limit, skin cancer rates, even in the absence of ozone depletion, would be likely to rise. Future rates of skin cancer could be reduced if people changed their behavior. Care should be taken, however, in interpreting such a change as a cost-free response.

INTRODUCTION

There are two major types of nonmelanoma skin tumors: basal cell carcinoma (BCC) and squamous cell carcinoma (SCC). These tumors are among the most common cancers occurring in white populations. In the United States alone, nonmelanoma skin cancers develop in more than 400,000 white Americans each year and represent over half of all cancers occurring in U.S. whites.

Prolonged sunlight exposure is considered to be the dominant, but not the only, risk factor for these tumors based on several observations. Nonmelanoma skin tumors tend to develop in sun-exposed sites (e.g., head and face) and occur at a higher rate among outdoor workers compared to indoor workers. Nonmelanoma incidence rates are higher in areas with high ultraviolet radiation (UVR) exposure (e.g., closer to the equator) than in areas with low UVR exposure. Light-skinned individuals who are susceptible to sunburn and who have red or blond hair, blue or green eyes, and a Celtic heritage are at high risk of developing nonmelanoma skin tumors.

To evaluate the role of solar radiation, and UV-B in particular, in the development of nonmelanoma skin tumors, this chapter presents background information on solar radiation as it relates to the concept of dose. Then reviews the biology of the skin and nonmelanoma skin cancers (NMSC), focusing on how skin responses to solar radiation can result in NMSC. Evidence from molecular and animal studies relating nonmelanoma skin tumors to UVR is discussed. Epidemiologic evidence linking exposure to solar radiation and development of nonmelanoma skin tumors among human populations is also reviewed. Finally, the available dose-response relationships that estimate potential changes in the incidence of nonmelanoma skin tumors due to changes in exposures to UVR are presented.

BACKGROUND ON SOLAR RADIATION AND THE CONCEPT OF DOSE

The total amount of energy from UVR that any target receives in a given amount of time will depend, in part, on variations in ambient radiation that occur in the natural environment. One effect of the ozone layer and the earth's rotation and revolution is the modification of the quality and quantity of solar energy delivered from place to place over time. Ambient solar radiation incident on various sites on the earth's surface varies significantly with latitude, altitude, season (day of the year), time of day, cloudiness, reflectiveness of surfaces (albedo), and atmospheric aerosols. More importantly, these variations differ quantitatively for different wavelengths of UVR.

The latitude of a particular location on the Earth's surface determines the average angle between the location and the sun. This angle, in turn, determines the thickness of the atmosphere that photons must pass through before reaching the Earth's surface. The lower the angle, the longer the path through the ozone-containing stratosphere that photons must travel and the greater the amount of UVR absorption that can occur. A longer path also allows longer exposure to aerosols and, thus, more scatter -- thereby additionally reducing the amount of energy reaching a location. Because ozone absorbs different wavebands differently, however, all photons are not retarded equally; instead differential gradients for various wavelengths occur. Exhibit 7-1 shows

EXHIBIT 7-1

Variation in UV Radiation by Latitude as Percent of Levels at the Equator on March 21 at Noon

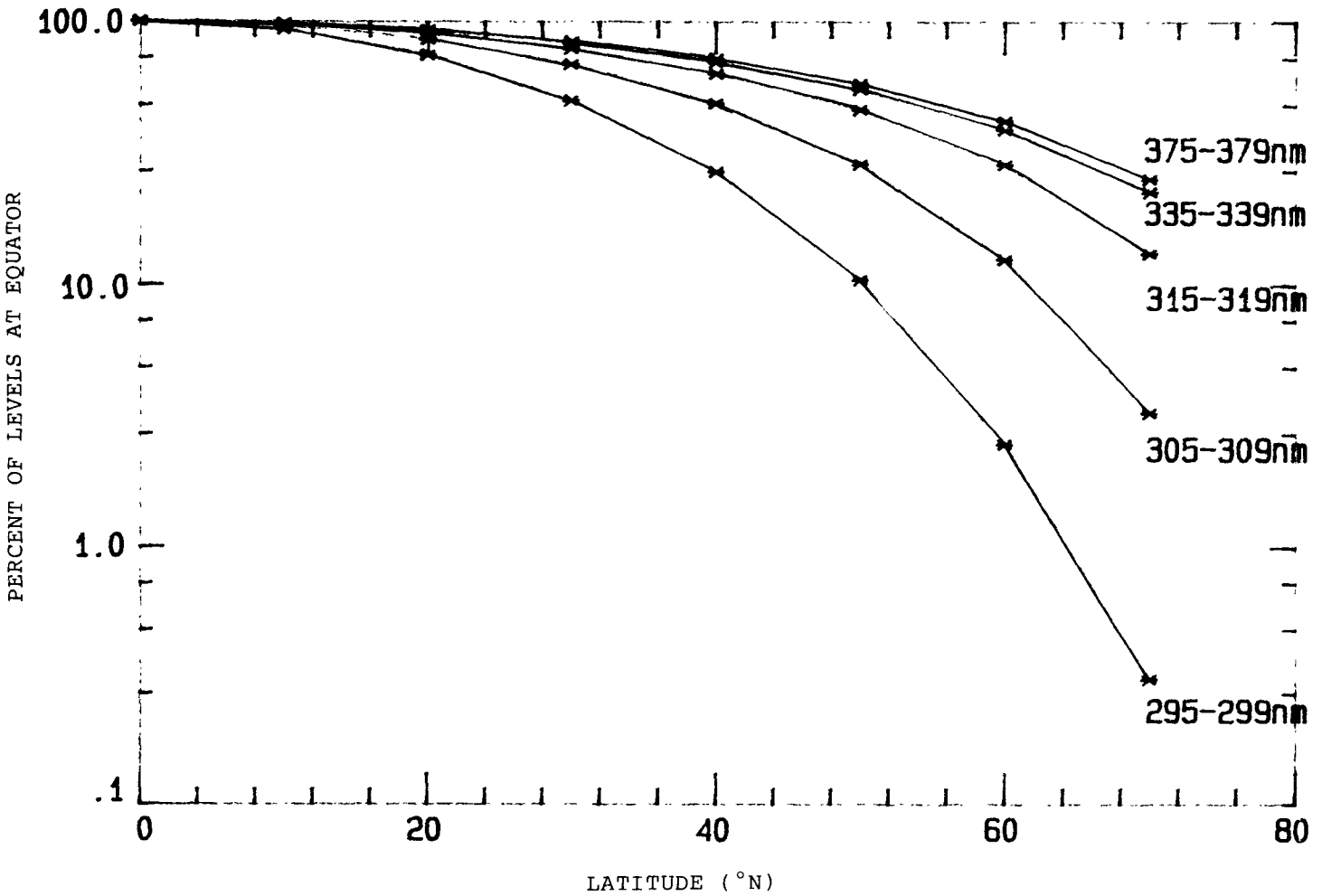

This graph shows the variation estimated by the NASA model for five wavebands of ultraviolet radiation for a single day, high noon, in March. The variation would be different for other days.

estimates from the NASA UV Model, developed by Serafino and Frederick (1986), which predict that at 12 noon on March 21, the flux of UV-B at 295-299 nm can be expected to vary from the equator to 70°N by a factor of over 100, while UV-A at 335-339 nm can be expected to vary by a factor of 5.

Season also has a tremendous impact on the flux of solar radiation at a given location. Again, this occurs because the relationship of a location to the sun changes with season. Exhibit 7-2 shows model estimates of how the various wavelengths vary by month for Washington, D.C. Energy at 295 nm increases by about a factor of 10 from winter (December) to Spring (March) and by about another factor of 10 by midsummer (July). UV-B at 305 nm shows much less variation and UV-A very little, if any, variation.

Exhibit 7-3 shows the impact that varying time of day has on estimates of UV-B. Clearly, the time of day of exposure is a very important factor in determining the amount of UV energy received at the various wavelengths. Variations in cloud cover and surface albedo also cause variations in ambient solar energy levels, however, there is not much differential variation by wavelength (for additional details, see Chapter 2 of Appendix A of the Risk Assessment).

In addition to factors that modify the ambient levels of UVR in the environment, there are a number of factors that can influence the biologically effective dose (i.e., the amount of energy received by a target in the skin that results in the development of skin cancer). These include an individual's clothing and sun-exposure behavioral habits, the degree of skin pigmentation and thickening, and the action spectrum for the biologically important effect.

The amount of energy that is actually effective is determined by the action spectrum of the effect of concern. If, for instance, damage to DNA is the underlying effect linking solar radiation to skin cancer, then not all of the photons delivered to the target molecules will be effective. Instead, the absolute amounts of energy delivered in the various wavelengths need to be weighted according to the action spectrum presented in Exhibit 7-4. There are a number of different effects that might underlie the relationship between solar radiation and skin cancer (details of which are presented in Chapters 2 and 3 of Appendix A); a key characteristic of the effects is that energy in the UV-B wavelengths (295-320 nm) tends to be much more biologically effective.

How much energy target cells can potentially receive depends on the time a person spends outside during certain periods of the day and certain days of the year. The total amount of energy delivered at a given location provides an upper bound of exposure, not the actual exposure. Few individuals are out in the sun during all daylight hours, therefore actual exposure is correspondingly reduced. As indicated above, the seasonal and hourly variations in incident energy from solar radiation can be considerable, particularly in those wavelengths that are the most biologically effective (295-299 nm), so all hours of the day cannot be considered equally. In addition, people living in areas having the same number of daylight hours may have additional behavioral differences that modify the amount of radiation reaching the skin (the actual exposure). For example, some people wear lots of clothing, others do not. Some people wear sunscreens, while others use sun reflectors to gather more solar radiation.

EXHIBIT 7-2

UV Radiation by Month in Washington, D.C.

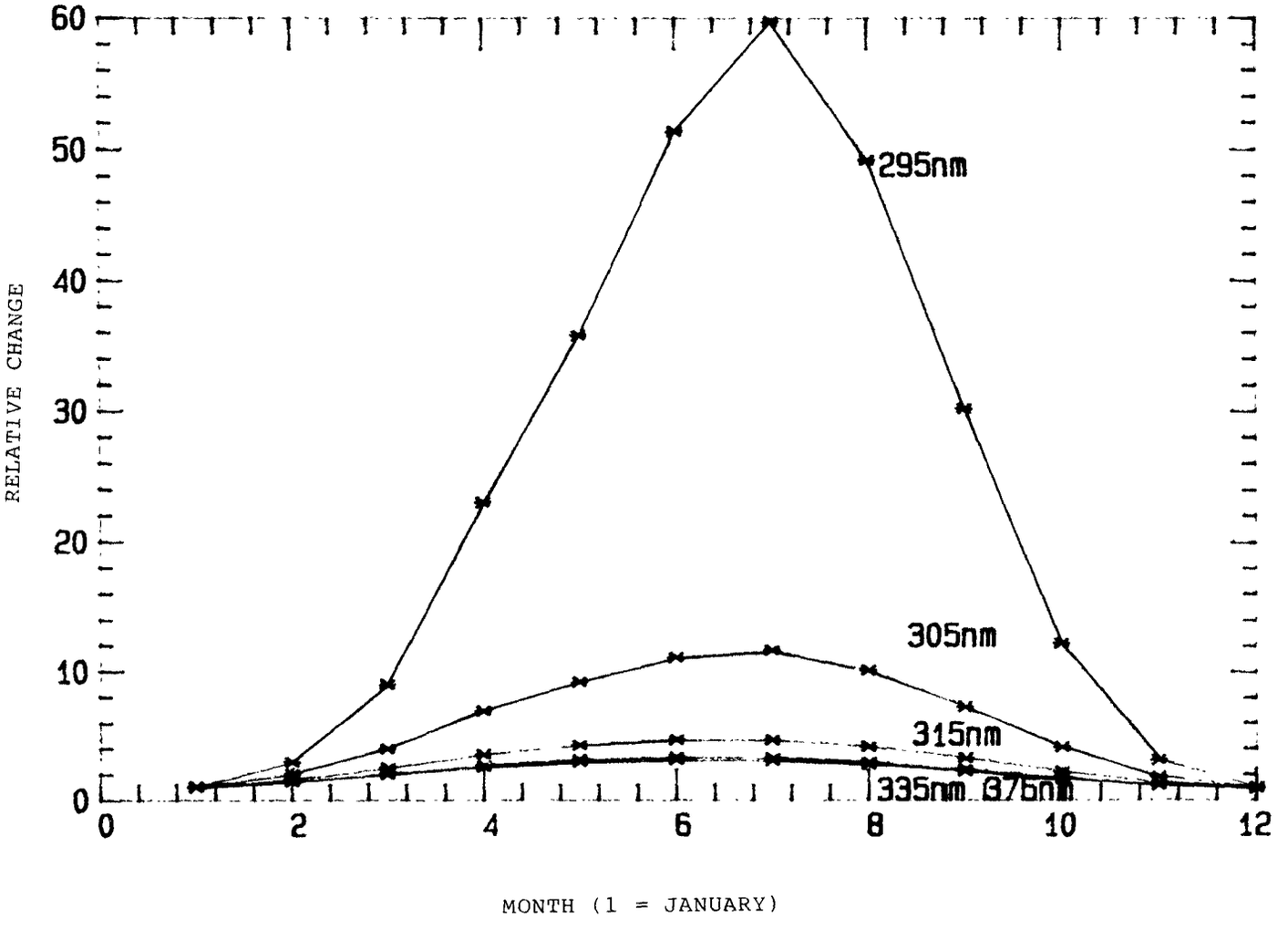

This graph shows that the NASA model estimates that radiation at 295 nm has a much larger proportional gain than at 305 nm or higher wavelengths. Note that the 335 nm line is almost coincident with the x axis, indicating low monthly variation in Washington, D.C.

EXHIBIT 7-3

Ratio of Instantaneous Flux Throughout the Day to Flux at 5:15 am in Washington on June 21 (Assumes a Clear Day)

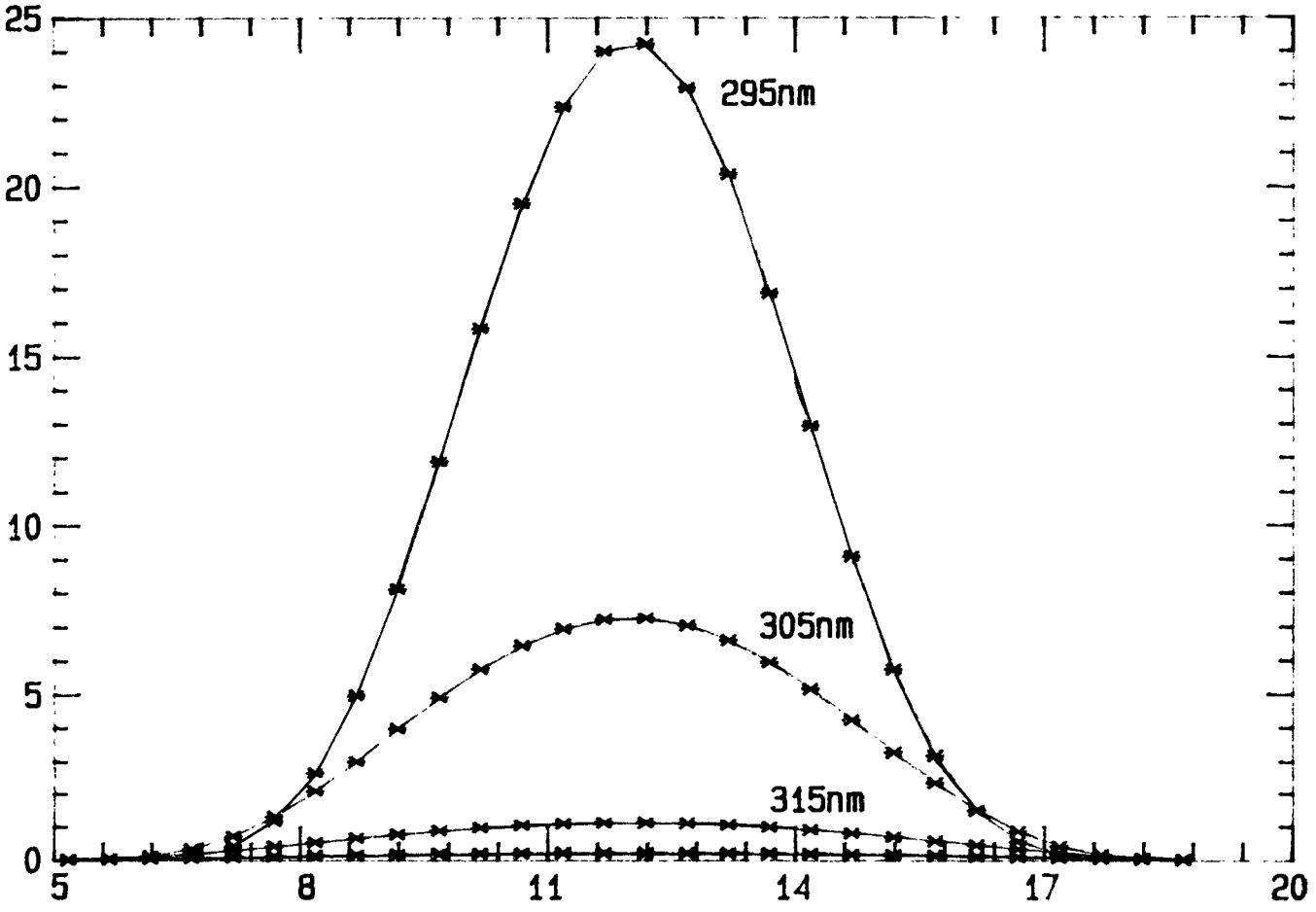

EXHIBIT 7-4

Average DNA-Damage Action Spectrum

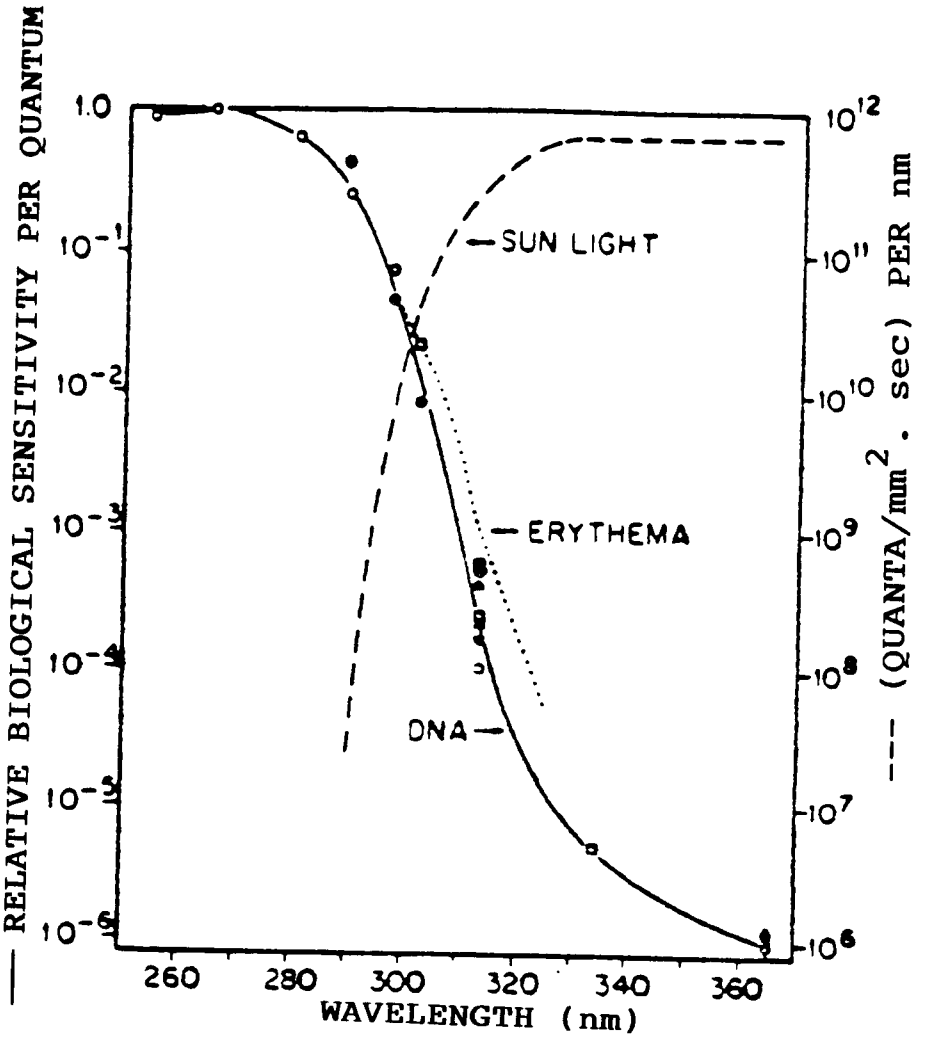

Source: Adapted from Setlow (1974).

Finally, the transition from the amount of energy to which an individual is exposed to the amount of energy that is delivered to a target molecule (the biologically effective dose), involves the interplay of factors such as skin thickness and pigmentation. The greater the skin thickness and degree of pigmentation, the smaller the amount of energy penetrating to the potential targets.

BIOLOGY OF NONMELANOMA SKIN TUMORS: LINKS TO UV-B

A general understanding of the biology and photobiology of the skin provides a useful background against which to examine the association between solar radiation and nonmelanoma skin tumors.

Biology of the Skin

There are three principal layers of skin: the epidermis, the dermis, and the panniculus adiposus (Exhibit 7-5). These layers vary in thickness depending on their location. The epidermis normally consists of about 6-10 cell layers and is typically 60 -100 mm thick. The thinner epidermis is found on the head, trunk, and upper limbs and the thicker epidermis is found on the lower limbs. The epidermis on the palms and soles is as much as ten times thicker than that on the head and trunk. The stratum corneum is the outermost, more dense layer of the epidermis and generally comprises between 8 :m and 15 :m of the epidermis' thickness (Pearl 1984; Fitzpatrick and Soter 1985). The dermis is typically between 1700 :m and 2000 :m thick and the subcutaneous layer, the panniculus adiposus, is typically 4000-9000 :m thick (Fitzpatrick and Soter 1985).

The epidermis is principally a mixture of three cell types of different embryonic origin and function; these are (in order of percent composition) the keratinocyte (80 percent), the melanocyte (5-10 percent), and the Langerhans cell (5-10 percent). The dermis is composed mainly of connective tissue fibers. These fibers, which are secreted by cells called fibroblasts, are responsible for the skin's resilience and elasticity. Many skin changes associated with aging are caused by the impact of solar radiation on these dermal fibers. The subcutaneous layer is a specialized layer of connective tissue that functions as a cushion between the bone and the epidermis and dermis. It consists primarily of fat cells.

The major cell type of the epidermis is the keratinocyte. In the epidermis, keratinocytes are organized vertically by various stages of differentiation. In its first differentiation state, the keratinocyte is termed a basal cell. Basal cells are organized in layers along a basement membrane that marks the interface of the dermis and the epidermis. There are structurally and functionally distinct populations of basal cells; some may represent the epidermal stem cell population, whereas others may serve as an anchoring function (Fitzpatrick and Soter 1985).

Both basal cell and squamous cell carcinomas are of keratinocyte origin. It is currently believed that BCC is derived from undifferentiated pluripotent stem cells; ultrastructural studies indicate that BCC cells are very similar to primitive ectodermal cells and can simulate both epidermal and adnexal development. In contrast, SCC consists of cells that are differentiated to the point of producing keratin (Laerum and Iversen 1981).

EXHIBIT 7-5

Organization of the Adult Skin

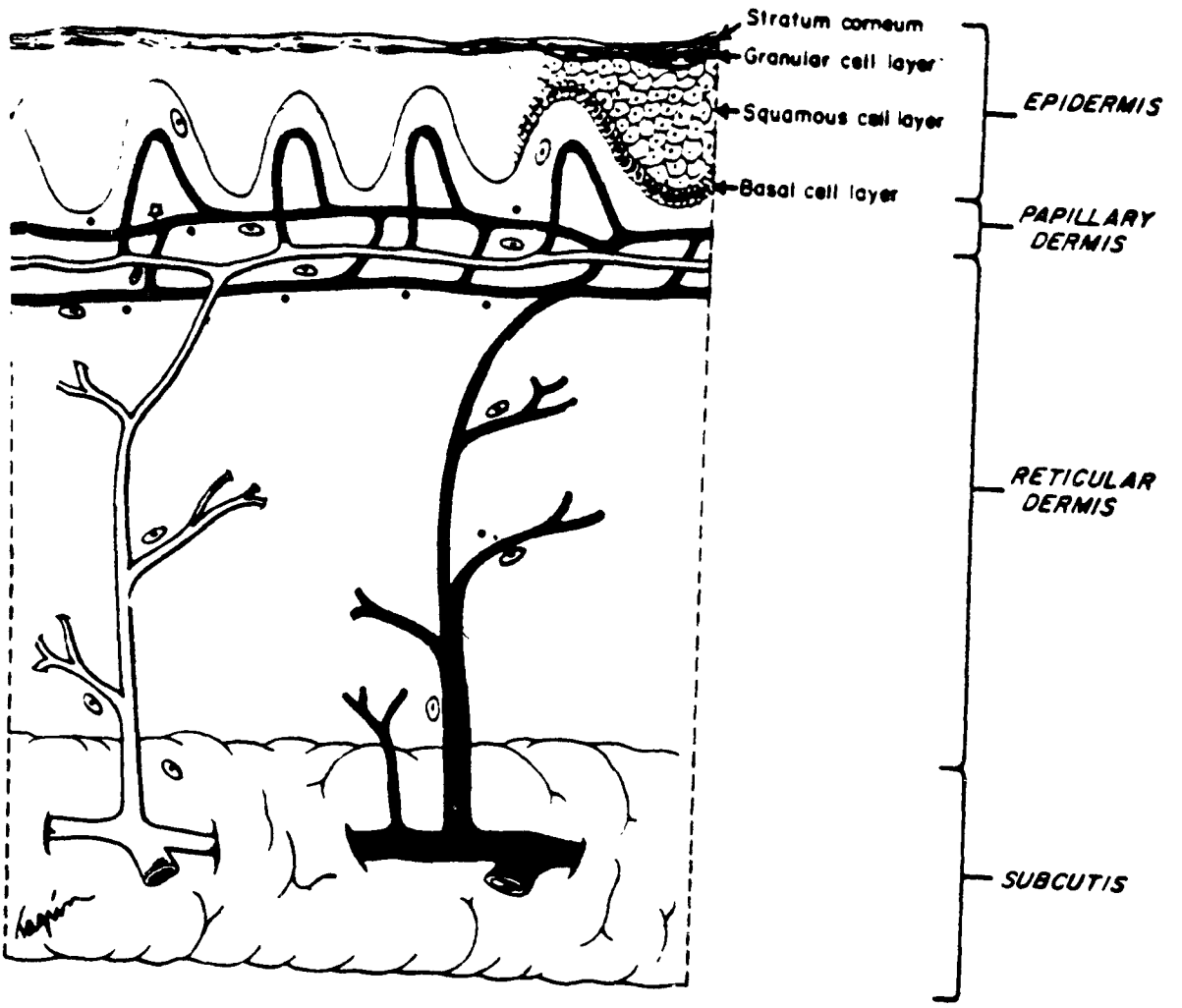

Source: Fitzpatrick and Soter (1985).

Keratinocytes produce at least three biologically important proteins: keratin, histidine-rich proteins, and interleukin 1 (IL-1, also known as epidermal-derived thymocyte activation factor [ETAF]). Keratins, the primary structural proteins of the epidermis, consist of a family of polypeptides that have strong absorption properties in the UV-C and UV-B range (Harber and Bickers 1981). Histidine-rich proteins (HRPs) are produced by keratinocytes and sequestered with keratin into keratohyalin granules. As keratinocytes terminally differentiate into corneocytes (enucleated keratinocytes that comprise the major component of the stratum corneum), the HRPs break down and release free histidine, which is converted into urocanic acid (Scott et al. 1982). IL-1/ETAF functions as a major mediator in both immune and inflammatory responses and may play a role in the immunosuppression induced by sunlight. Once thought to be solely a macrophage-produced lymphokine, it is now known to be produced by other cells (e.g., keratinocytes). Investigation into its biologic properties indicates that it is a potent inducer of lymphocyte activation and chemotaxis, that it enhances the production of acute phase proteins by the liver, increases the number of circulating macrophages, and can result in elevated temperatures (fevers) (Daynes et al. 1986).

Photobiology of the Skin

The interaction of sunlight with the skin is a complex process. It involves the transfer of energy from sunlight to various molecules in the skin layers and the subsequent cellular responses to this energy transfer. About 95 percent of incident radiation penetrates the skin, while the remaining 5 percent is reflected by the stratum corneum. Two processes, scatter and absorption, determine the penetration of radiation into the skin. Measurements of the transmission of UVR through isolated epidermis tissue from medium-complexion Caucasian skin (Bruls et al. 1984; Kaidbey et al. 1979) indicate that between 1 percent and 20 percent of 295 nm UV-B radiation would reach the basal layer. For 340 nm UV-A radiation, as much as 20 to 60 percent may penetrate to the basal layer (Kubitschek et al. n.d.). Above 400 nm (in the visible range), transmission approaches 90 percent (Anderson 1983). The amount of radiation reaching the basal layer is a function of the thickness of the epidermis and stratum corneum as well as their content of radiation-absorbing molecules called chromophores. There are a large number of chromophore types in the skin, one of which is melanin. Most of the optical absorbance within the skin, however, is attributable to melanin, as graphically shown in Exhibit 7-6.

The skin has three response mechanisms for dealing with exposure to solar radiation: (1) dose-reduction through the production of increased melanin (tanning) or through keratinocyte hyperplasia; (2) damage repair in which the cell's DNA repair mechanisms remove photoinduced damage; and (3) cell removal.

Solar Radiation Dose Reduction

Dose-reduction may occur via one of two mechanisms: tanning or skin thickening. Tanning involves the de novo synthesis of new melanosomes that are subsequently transported to keratinocytes where they produce a tan within about 10 hours after exposure. This response may continue for several days, with the maximal tan being achieved in about one week. With time the tan wears off as the keratinocytes containing the extra pigment are sloughed off. In addition to the increased production of melanosomes, the number of active melanocytes in the

EXHIBIT 7-6

Ultraviolet Absorption Spectra of Major Epidermal Chromophores

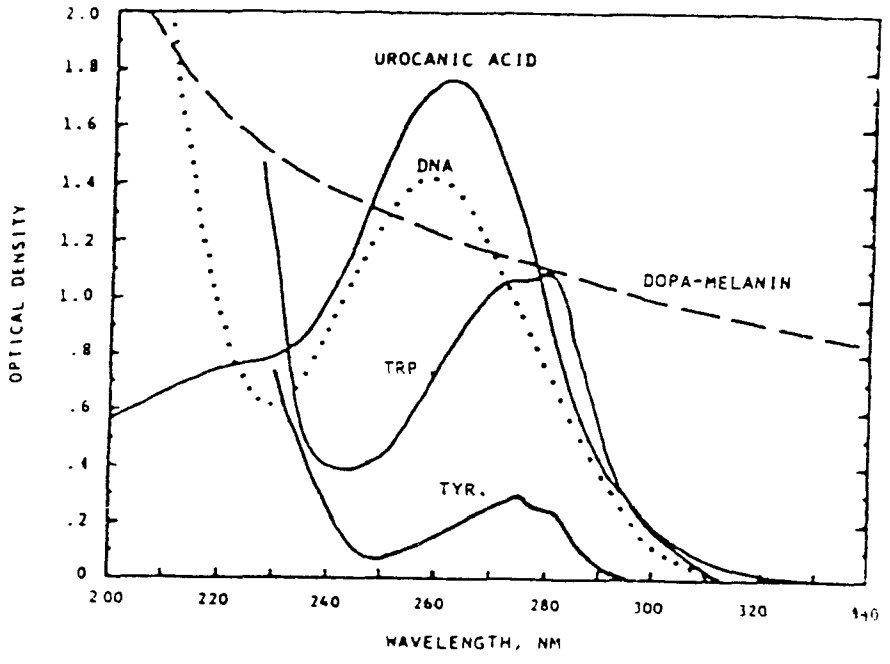

Experimental Conditions:

DOPA-melanin, 1.5 mg% in H_2O;

urocanic acid, 10^{-4} M in H_2O;

calf thymus DNA, 10 mg% in H_2O (pH 4.5);

tryptophan (TRP), 2×10^{-4} M (pH 7);

tyrosine (TYR), 2×10^{-10} M (pH 7).

Source: Anderson (1983).

skin also increases, probably as a result of increased mitosis and recruitment of dormant melanocytes. The delayed tanning response is induced predominantly by wavelengths in the UV-B range, although UV-C, UV-A, and visible light can also induce the response. There is a wide variation in the actual tanning response of individuals to sunlight exposure. Skin tanning responses have been generally classified into six skin type categories as outlined in Exhibit 7-7 (Fitzpatrick 1986).

The other dose-reduction response involves the increased production of keratinocytes and a subsequent thickening of the epidermis (keratinocyte hyperplasia). Studies in humans have shown that after a single exposure to UV-B, a sustained increase in epidermal mitoses occurs, which leads to a 1.5- to 3-fold increase in the thickness of the epidermis and stratum corneum over the course of one to three weeks. The UV dose first induces a transient depression in macromolecular synthesis in which DNA, RNA, and protein synthesis are markedly reduced and then elevated. The response is maximal within 24 to 48 hours after irradiation but may continue for as long as one week. UV-B and UV-C are the most effective wavelengths for inducing this response. Keratinocyte hyperplasia protects individuals with a poor tanning ability because the disulfide-rich keratin synthesized by the keratinocytes absorbs photons in the UV-C and UV-B ranges. Among lightly pigmented individuals, this skin thickening is probably the most important dose-reducing response, whereas among dark-skinned individuals, tanning is the more important response (Gange and Parrish 1983).

DNA Repair Mechanisms

A different response mechanism for dealing with exposure to solar radiation is DNA repair. UVR can either directly or indirectly damage DNA. Direct damage results from the absorption of UVR by DNA and the subsequent formation of DNA lesions. The most studied form of direct damage is the development of cyclobutyl pyrimidine dimers (Spikes 1983). These dimers are formed between adjacent pyrimidines on the same DNA strand, and their presence renders the phosphodiester bond joining the deoxyribose moieties resistant to nuclease digestion. Indirect DNA damage is mediated by a reactive oxygen species, such as a superoxide radical, which absorbs radiative energy and transfers it to the DNA. UV-B principally inflicts direct damage on DNA but can also cause indirect damage at some wavelengths. UV-A and UV-C can inflict direct or indirect DNA damage on cells. DNA has an absorption maximum at 265 nm (UV-C range).

When DNA is damaged, the lesions may cause cell death or may merely disturb DNA transcription and replication. Based on the somatic mutation theory of carcinogenesis, these lesions may also result in mutations that subsequently result in neoplastic transformation. Alternatively, damage to the DNA may result in oncogene activation. DNA damage that adversely affects cell function and survival needs to be repaired in order to assure continuation of a species.

The cell possesses three DNA repair mechanisms to respond to UV-induced damage: photoreactivation, excision repair, and postreplication gap repair. Repair mechanisms that result in unchanged DNA are called "error-free," whereas mechanisms that generate altered segments of DNA are generally called "error-prone." The inaccuracy of a repair mechanism is likely to result in secondary structural changes in DNA, some of which may lead to mutations.

EXHIBIT 7-7

Skin Types and Skin Tanning Responses[a/]

Skin Color (unexposed skin)	Skin Types	'Sunburn'	'Tan'
White	I	yes	no
	II	yes	minimal
	III	yes	yes
	IV	no	yes
Brown	V	no	yes
Black	VI	no	yes

[a/] Sun-reactive skin types: based on verbal response regarding first, moderate 45- to 60-min. (3 MED)1 unprotected sun exposure. MED = Minimal erythema dose.

Source: Fitzpatrick (1986).

Photoreactivation repair of pyrimidine dimers occurs when an enzyme binds to the dimer, forming an enzyme-substrate complex. The enzyme-substrate complex absorbs photons of UV-A light and the dimer is then monomerized (Spikes 1983). Photoreactivation is an error-free, nonmutagenic repair pathway, which offers a number of advantages to the cell: It uses UV-A photons as an energy source, there is no incision into the DNA phosphodiester backbone, and therefore no risk of DNA degradation; and there is no polymerization, and thus, no chance for the introduction of coding errors (Spikes 1983).

Another efficient DNA repair mechanism is called excision repair. Excision repair works more slowly than photoreactivation but may repair not only dimers but also other kinds of damage, such as, methylations. In the case of dimers, excision repair involves the activity of three enzymes, an endonuclease specific for dimers, a polymerase, and a ligase. The endonuclease attacks the DNA at or adjacent to the dimer and introduces a nick in the DNA. The DNA polymerase removes the damaged DNA segments while utilizing the opposite strand as a template for new synthesis, and finally, a ligase joins the newly synthesized DNA to the preexisting strand. Other kinds of DNA damage, such as methylations, require different first enzymes, but the activities of the polymerase and the ligase remain the same (Spikes 1983).

The third cell repair mechanism is termed postreplication gap repair. This mechanism is invoked when, following DNA replication, there are gaps left in the DNA opposite the dimer. The cell invokes a DNA recombinational mechanism, which provides a good copy of the DNA needed to repair the damage. Using this information, the cell can repair the damage with an excision repair mechanism (Spikes 1983). This mechanism is, however, fairly error prone.

Biology of Nonmelanoma Skin Tumors

Although most skin cancer statistics combine both BCC and SCC cell types, the limited data available from the U.S. and several other countries indicate differences in a number of characteristics. Basal cell carcinomas are neoplasms of the germinal layers of the epidermis and the appendages that differentiate toward glandular structures (Scotto and Fraumeni 1982). As a rule, these tumors are slow growing and follow a relatively benign course, although on rare occasions they may result in extreme morbidity, mutilation, or, if they metastasize, death (Pollack et al. 1982).

Basal cell carcinomas are believed to arise from a pluripotent epithelial cell present in the epidermis. It has been hypothesized that basal cell carcinomas arise because an abnormal interaction between these pluripotent stem cells and the surrounding connective tissue induces the cells to differentiate neoplastically (Pollack et al. 1982; Kent 1976). These tumors appear to be very stromal dependent, however, and it has been suggested that they will rarely metastasize to a foreign tissue bed unless they take along a portion of their stroma (Pinkus 1953). This hypothesis has been confirmed in part by studies that have shown that basal cell tumor cells cultured <u>in vitro</u> in the absence of accompanying connective tissue convert to a keratinizing epithelium (Flaxman 1972; Kubilus et al. 1980). It has also been shown that autotransplants fail if the cells are transferred without stroma (Epstein et al. 1984).

Squamous cell carcinomas are neoplasms of the epidermis that differentiate towards keratin formation (Scotto and Fraumeni 1982). SCCs are far less

fastidious in their growth requirements in vitro and will grow under a variety of conditions. They are generally more aggressive than BCCs and account for about three-fourths to four-fifths of the deaths attributable to nonmelanoma skin cancer (Dunn et al. 1965).

The most prevalent precursor skin lesions for solar-radiation-induced BCC or SCC are actinic hypertrophy and keratoses (Urbach 1981, Schwartz and Stoll 1987). Actinic keratosis affects nearly 100 percent of the elderly white population and may be found among younger light-skinned individuals living in sunny areas (Schwartz and Stoll 1987). Both epidemiologic and experimental evidence indicate that BCC and SCC may develop at sites of actinic keratosis (Carter 1987; Schwartz and Stoll 1987). Stoll and Schwartz (1987), in a review of SCC, reported that approximately 12 percent of untreated actinic keratoses may develop into SCC, but they noted that this figure may be as high as 25 percent. The likelihood of metastasis from SCC arising in actinic keratoses (excluding SCCs of the lip) appears to be low, with 0.1 percent to 2.6 percent of the SCCs potentially becoming metastatic (Stoll and Schwartz 1987).

EXPERIMENTAL EVIDENCE

Cellular Studies

Solar radiation and its component UV and visible wavelengths have been observed to cause cellular changes, such as the induction of cell division and/or differentiation, the loss of specialized functions (e.g., antigen presentation), mutation, transformation, and death. Evidence from cellular and molecular studies clearly indicate that UVR can cause transformation in mammalian cells in the absence of any confounding immunological, hormonal, or physiological effects encountered in vivo. Shorter UV-B wavelengths are generally more effective in transforming mammalian cells.

As already described, a single in vivo exposure of human skin to UV-B radiation can cause the epidermis to thicken, thereby increasing the tolerance of skin to subsequent radiation. UV-B exposure also induces melanocyte division (Rosdahl and Szabo 1978). Some investigators studying the response of melanocytes in trunk epidermis of black mice to UVR have concluded, however, that the increased number of active melanocytes results from both the proliferation and recruitment of amelanogenic melanocytes (Miyazaki et al. 1974).

Ultraviolet light is mutagenic in both bacterial and mammalian cells. In UVR-treated bacteria, researchers have concluded that pyrimidine dimers are responsible for much of the observed mutagenesis (Hall and Mount 1981). UVR-treated cells, if subsequently treated with photoreactivating light, show a substantially decreased frequency of mutants per survivor compared to UVR-treated cells without subsequent photoreactivation treatment. Peak et al. (1984) derived action spectra for DNA dimer induction, lethality, and mutagenicity in E. coli over wavelengths from 254 nm to 405 nm (Exhibit 7-8) and found that all three endpoints decreased in efficiency in a similar fashion as the wavelengths of radiation increased. From 300 nm to 320 nm, all characteristics showed differences of about 2.5 orders of magnitude. Furthermore between about 250 nm and 320 nm, the values for the three endpoints either coincided with or closely paralleled Setlow's (1974) proposed average DNA action spectrum.

EXHIBIT 7-8

Ultraviolet Action Spectra for DNA Dimer Induction: Lethality and Mutagenicity

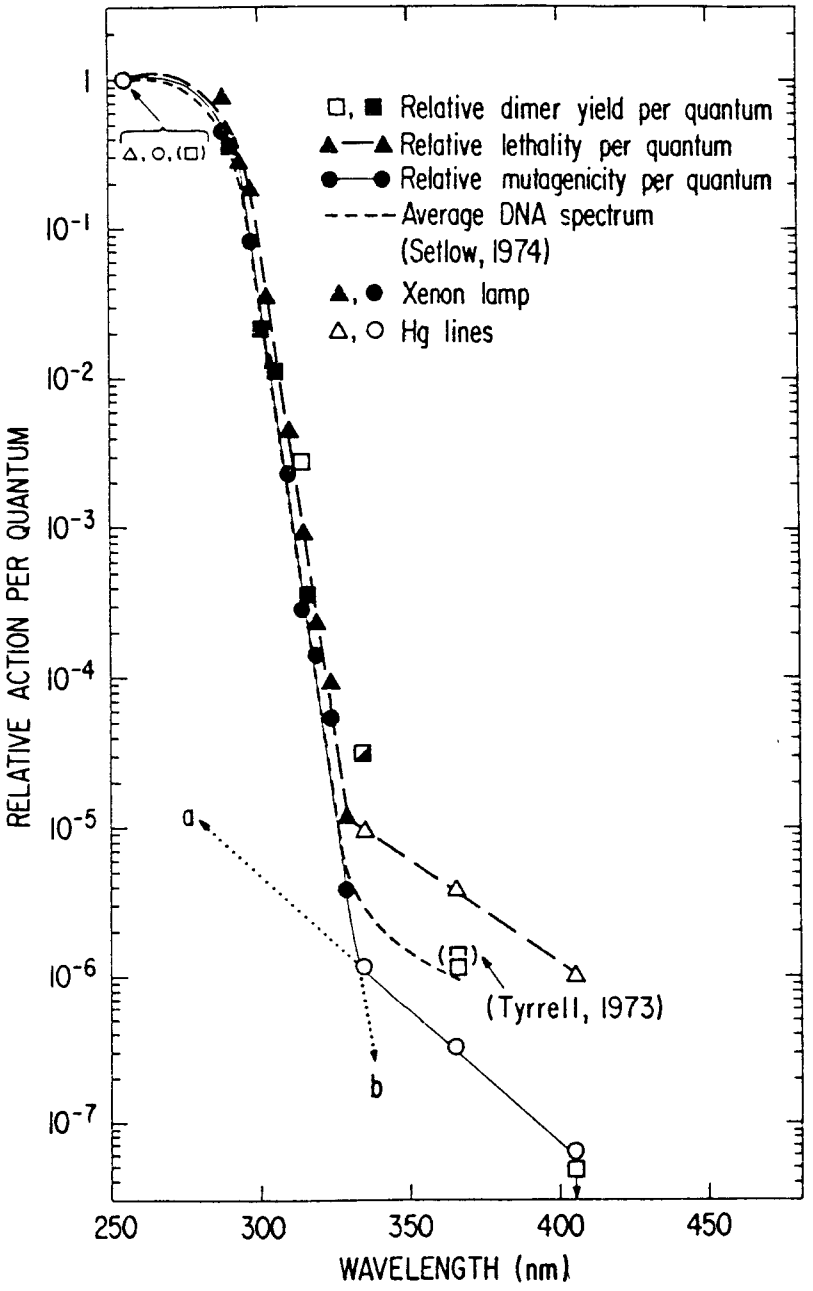

Source: Peak et al. (1984).

Experiments have also been performed using fibroblasts from xeroderma pigmentosum (XP) patients. These patients have a genetic inability to repair UV-induced pyrimidine dimers. Setlow et al. (1969) compared the responses of XP fibroblasts to normal human fibroblasts upon irradiation to UVR. They observed that normal human fibroblasts that were UVR irradiated, then stimulated to undergo cell division by immediate replating, showed much higher numbers of mutations than similarly irradiated normal cells that were incubated for seven days as nondividing monolayer cultures. These results indicated that normal human cells can repair the damage induced by UVR (presumably by excision repair). XP cells, by comparison, produced a comparable number of mutants whether replated immediately or given seven days of incubation. Since XP cells are unable to excise pyrimidine dimers, these experiments suggest that unexcised dimers present at the time of cell division may have been responsible for the production of mutations.

In vitro transformation is thought to be correlated, albeit imperfectly, to in vivo tumorigenesis (Heidelberg 1977). As such, it has been used extensively to characterize the potential carcinogenicity of a wide variety of chemicals and physical agents. Cells that have been induced in vitro to lose certain normal growth controls are frequently, although not always, tumorigenic in mice. A hierarchy of transformational changes is recognized, and the ability of cells to grow without attachment to a solid substrate (loss of anchorage dependence) is generally accepted as the best correlate to tumorigenicity (Freedman and Shin 1974).

Doniger et al. (1981) developed action spectra for transformation and thymine dimer formation using a monochromatic light source (Exhibit 7-9). In dose-response studies comparing pyrimidine dimer formation and transformation of Syrian hamster embryo cells, the slopes of the dose-response curves were not always parallel. The discordance was greatest at 290 nm. The lowest exposure required for equivalent cell transformation, lethality, and pyrimidine dimer formation was at 270 nm. Comparing results at 290 nm, 297 nm, and 302 nm, the respective doses required were 2.3 J/m^2, 8.7 J/m^2, and 25 J/m^2 for dimer formation and 7.4 J/m^2, 47 J/m^2, and 97 J/m^2 for transformation. A similar spectrum was found for induction of anchorage independent growth in human fibroblasts (Sutherland et al. 1981). These authors also found a maximum effectiveness at 265 nm and that transformation at 290 nm was six times more effective per photon than that at 297 nm.

Molecular Studies: DNA and UV Radiation

Chemical changes and biological damage induced by ultraviolet light require the absorption of light energy (photons) by molecules within the target. Each type of molecule is capable of absorbing radiation only in specific wavelength ranges. Examination of the absorption spectra of molecules in biological systems indicates that a number of biomolecules can absorb radiation in the 220- to 400-nm region and thus may be critical targets for detrimental UV effects (Spikes 1983). This section will review information only on the most important molecule, DNA, because of its putative role in mutagenesis, transformation, and carcinogenesis.

As already mentioned, two possible types of mechanisms can induce DNA damage -- a direct mechanism resulting from absorption of energy by DNA and an indirect mechanism involving reactive oxygen species. A number of different lesions may

EXHIBIT 7-9

Effectiveness of 297, 302 and 313+ NM UVR
at Inducing Pyrimidine Dimers (□) and Transformation (■)

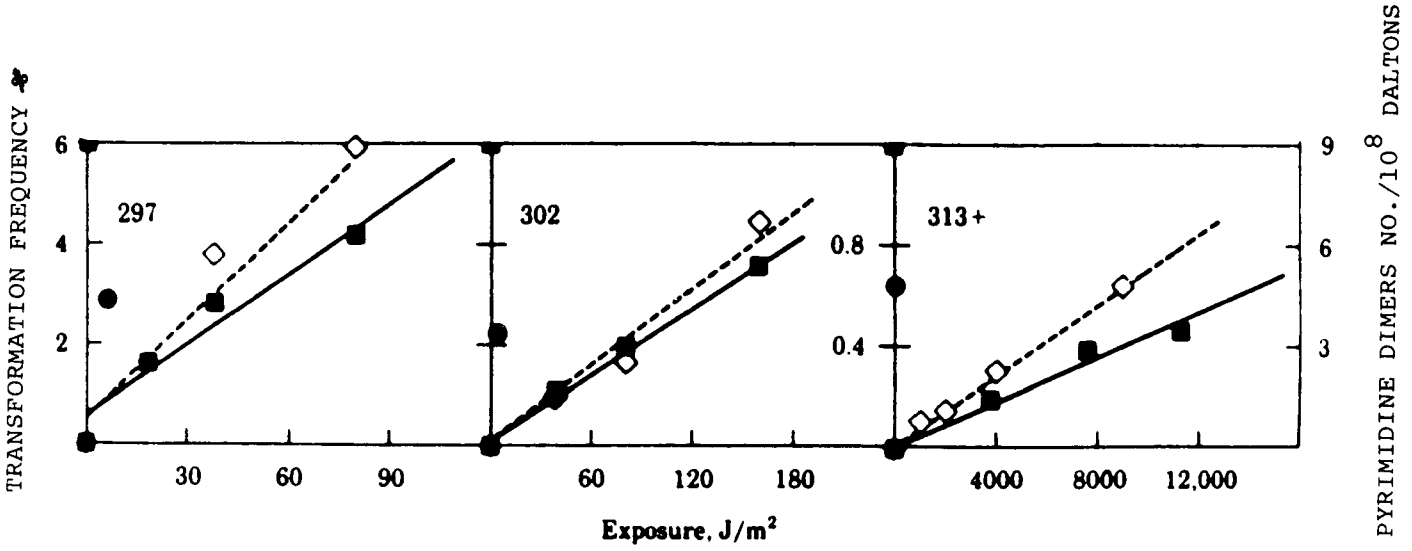

Source: Adapted from Doniger et al. (1981).

be induced in DNA by UV irradiation. These include (1) pyrimidine dimers, (2) pyrimidine adducts, (3) single-strand breaks, (4) double-strand breaks, and (5) protein-DNA crosslinks. Different wavelengths have different efficiencies for the production of these lesions.

Pyrimidine Dimers and Adducts

As described in an earlier section, pyrimidine dimers may be formed by direct absorption of photons in the UV-B wavelength range. Adjacent pyrimidine molecules on the same strand of DNA become linked together by a cyclobutane ring between the 5 and 6 carbon atoms of each residue. Thymine dimers are the most likely pyrimidine dimers because the excited state of thymine is a much lower energy state than that of cytosine. Cytosine co-dimers are also possible, as are heterodimers between thymine and cytosine or uracil (Spikes 1983).

Action spectra for four-membered ring pyrimidine adduct formation between two consecutive bases on the same strand of DNA resemble the action spectra for pyrimidine dimer formation (Patrick and Rahn 1976). The efficiency of formation of these photoproducts is about two to ten times lower than for cytosine-cytosine and thymine-thymine dimers. The proportion of these adducts varies according to the base content of DNA and becomes much higher when the ratio of guanine-cytosine/adenine-thymine is greater than or equal to one.

Thymine glycols, another form of pyrimidine adduct, are defined as a group of ring-saturated lesions of the 5,6-dihydroxydihydrothymine type and have been detected in the DNA of human cells after irradiation at 254 nm and 313 nm (Hariharan and Cerruti 1977). The formation of these lesions is probably caused by the action of hydroxyl radicals on the 5-6 double bond of thymine. In both the UV-B and UV-A range, thymine glycols may result from the action of reactive oxygen species produced by endogenous sensitizers.

Thymine glycol lesions occur with almost the same frequency as thymine dimers at 313 nm, indicating their possible significance in the UV-B range (Cerutti and Netrawali 1979). Glycol lesions may undergo spontaneous decay to form apyrimidinic sites in a fashion similar to that described for gamma-radiation produced saturated thymine glycols (Dunlap and Cerutti 1975). Only about one-third of the thymine glycols are released from the DNA backbone, but there is little evidence to suggest that either the ring-saturated thymine or the apyrimidinic decay products are lethal lesions in UV-irradiated DNA.

Brash and Haseltine (1982) have shown that there is a linear relationship between base damage incidence and mutation incidence. For shorter wavelengths (UV-B) it seems clear that pyrimidine dimers and 6-4 photoadducts are involved in mutagenesis, but at 365 nm the correlation between dimers or adducts and mutagenesis is not known (Peak et al. 1984).

DNA Single-Strand Breaks

DNA single-strand breaks can be induced directly by UV-B radiation or indirectly by UV-A and visible light. Analysis of the relative efficiencies for the induction of single-strand breaks reveals an action spectrum that corresponds with nucleic acid absorption at or below 313 nm (Peak and Peak 1986). Above 313 nm to wavelengths as long as 546 nm, single-strand breaks have been detected in human fibroblasts with an action spectrum in the visible range

resembling that of riboflavin (Rosenstein and Ducore 1983) (Exhibit 7-10). There is, however, some suggestion that this latter observation may be an artifact of bilirubin photosensitization (Peak and Peak 1986). Relative to thymine dimers, single-strand breaks are induced only to a small extent by 254-nm radiation, but as the wavelength is increased, the proportion of single-strand breaks to thymine dimers increases. At 313 nm in E. coli, one single-strand break is induced for every nine thymine dimers (Cerutti and Netrawalli 1979). Some single-strand breaks induced at 313 nm may be due to indirect effects from photosensitizers and oxygen-dependent mechanisms (Miguel and Tyrell 1983), but the spectral analysis indicates that the majority of single- strand breaks induced at this wavelength are due to direct effects (Peak and Peak 1986).

DNA Double-Strand Breaks

DNA double-strand breaks occur about 80 times less frequently than single-strand breaks at 313 nm in bacteria (Tyrrell 1984). Both single- and double-strand breaks are resealed within one hour in both prokaryotes and eukaryotes. Two repair processes, one slow and the other fast, repair damage induced in E. coli by ionizing radiation. There is some evidence that repair of breaks induced at 313 nm may proceed in a similar fashion (Tyrell 1984).

DNA-Protein Crosslinks

DNA-protein crosslinks can be induced in human cellular DNA following borderline UV-B radiation (290 nm) via a direct photon-absorbing mechanism. Below 320 nm, there are approximately 40 DNA-protein crosslinks per lethal event. As cells can survive 2 x 10^3 DNA-protein crosslinks induced at longer wavelengths (405 nm), it appears that such a small number of DNA-protein crosslinks is not important in UV-induced cell lethality. This assumes, however, that there are no interactions between dimers and DNA-protein crosslinks (Peak et al. 1985).

DNA-protein crosslinking is demonstrable in normal human fibroblasts immediately after UV irradiation, but this crosslinking is partially reversed after about 12 hours. In fibroblasts from XP patients, crosslinking after UV-exposure was not reversed and actually progressed with time. This is possibly a secondary change due to severe cell damage (Fornace and Kohn 1976). The abnormal sensitivity of XP cells to UVR has generally been attributed to be a defective capacity to repair cyclobutylpyrimidine dimers in cellular DNA (Smith and Paterson 1981). The inability of XP cells to repair DNA crosslinks suggests, however, that the lethality of UVR to XP cells may not be fully explained by their inability to excise dimers but may also relate to the persistence of DNA-protein crosslinks.

Although the biological significance of DNA-protein crosslinks is not clear, it would seem that these lesions are not lethal to the cell. In normal cells, the number of DNA-protein crosslinks per genome per lethal hit is greater than 900 (Peak and Peak 1986). It can reasonably be concluded, however, that normal cells possess an ability to repair these lesions.

EXHIBIT 7-10

Action Spectrum for the Induction of Single-Strand Breaks in DNA

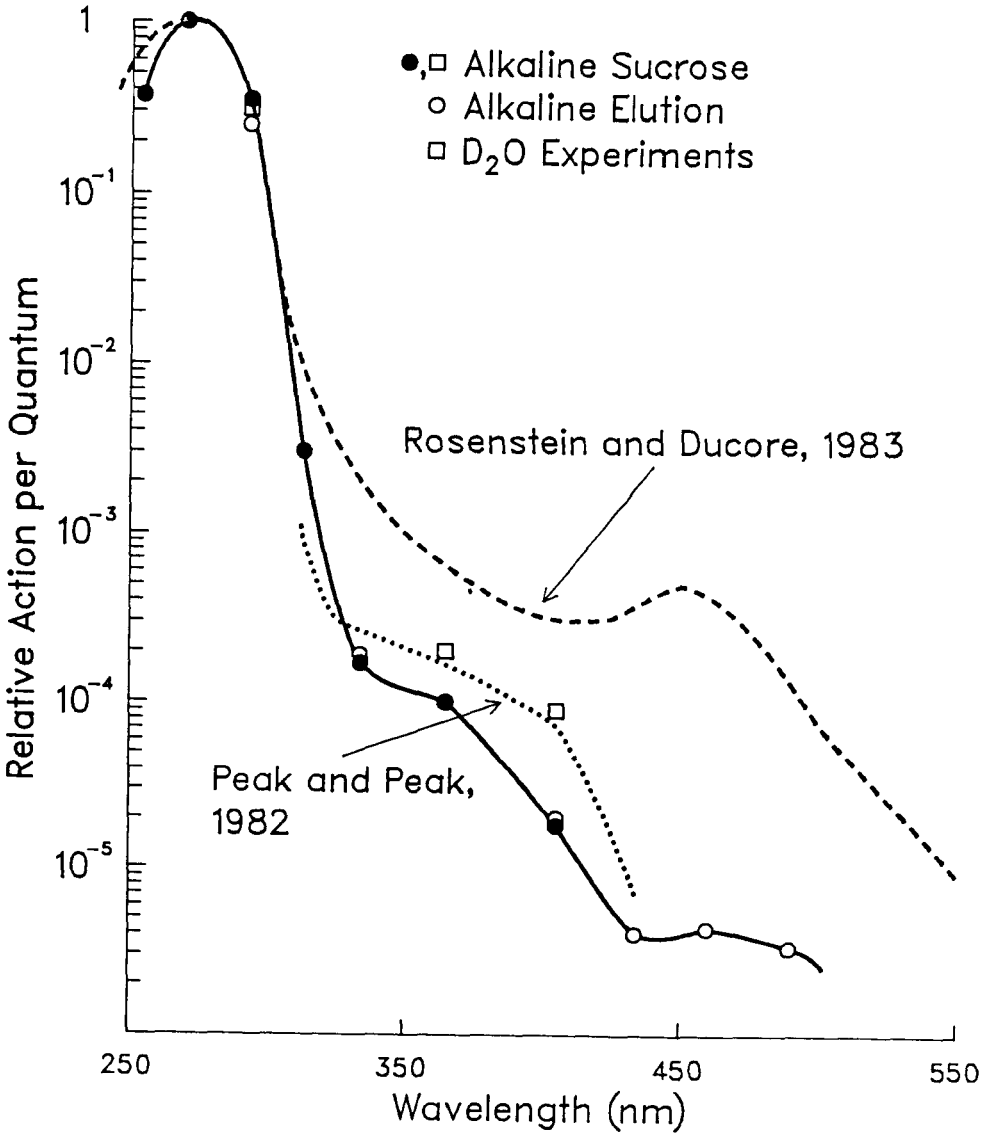

Source: Peak and Peak (1986).

Animal Studies

Observations that outdoor workers had a greater tendency to develop skin cancer promoted Findlay (1928) to examine UV-induced carcinogenesis in mice. Findlay reported that not only did UVR alone induce skin tumors in mice, but tumors induced by topically applied tar appeared more rapidly if those mice were subsequently exposed to UVR. Since Findlay's early works, researchers have found that tumors induced in mice by UVR are primarily squamous cell carcinomas and fibrosarcomas (Epstein and Epstein 1962; Hsu et al. 1975; Kligman and Kligman 1981; Kripke 1977; Spikes et al. 1977; Stenback 1975; Strickland et al. 1979; Winkelman et al. 1963) and are mostly monoclonal in origin (Burnham et al. 1986). There is no animal model for basal cell carcinomas.

A number of studies have attempted to identify specifically those UV wavelengths responsible for the observed carcinogenicity with varying results. In early studies filters were used to remove shorter wavelengths from broadband UVR so that the effect of different wavelengths could be studied. In some of the original studies on the carcinogenic action spectrum of UVR, Rusch et al. (1941) reported that the carcinogenic wavelengths were between 290 nm and 334 nm; wavelengths greater than 334 nm and those at 254 nm were not found to be carcinogenic. Blum (1943), in contrast, concluded from his experiments that the most effective wavelengths for producing tumors in mice were between 260 nm and 300 nm.

Freeman (1975), using monochromatic UVR, exposed the ears of albino mice to a weekly dose of 420 J/m^2 at 290 nm, 600 J/m^2 at 300 nm, 7500 J/m^2 at 310 nm, and 49,500 J/m^2 at 320 nm. Mice exposed to 290 nm developed no tumors, those exposed to 300 nm and 310 nm developed tumors with the same median latent period, and those exposed to 320 nm developed fewer tumors. When the mice were exposed to the same incident radiation at 300 nm and 310 nm, only the mice given radiation at 300 nm developed tumors. This result indicated that UVR at 300 nm is a more potent carcinogen than UVR at 310 nm.

In a more recent study, Cole et al. (1986) investigated the ability of wavelength weighting schemes based on three different action spectra to predict the tumorigenicity of UVR (Exhibit 7-11). Use of a weighting scheme for an averaged spectrum based on DNA damage overestimated the importance of the shorter wavelengths in inducing tumors. Use of an action spectrum based on the sensitivity of the Robertson-Berger (R-B) meter underestimated the contribution of the shorter wavelengths. These authors found that the best predictor of UVR effectiveness at inducing tumorigenesis in hairless mice was an action spectrum based on the induction of "cutaneous edema" 48 hours after a single acute dose (MEE 48).

There has been a great deal of experimentation to determine if there is dose-rate reciprocity in UV carcinogenesis. Blum et al. (1942) studied the effect of the intensity of the dose on the tumor latency period and reported that for a 10-fold dose range of between 4.3 J/m^2/sec and 0.42 J/m^2/sec, no significant differences were found. In a second study in which a wider range of intensities and greater numbers of animals were used, he reported that above 0.4 J/m^2/sec the effectiveness of UVR in inducing tumors was almost independent of dose-rate, but below 0.4 J/m^2/sec the effectiveness fell off rapidly with intensity.

EXHIBIT 7-11

**Action Spectrum of Mouse Edema (MEE48)
as Compared to that of DNA Damage and the Robertson-Berger Meter**

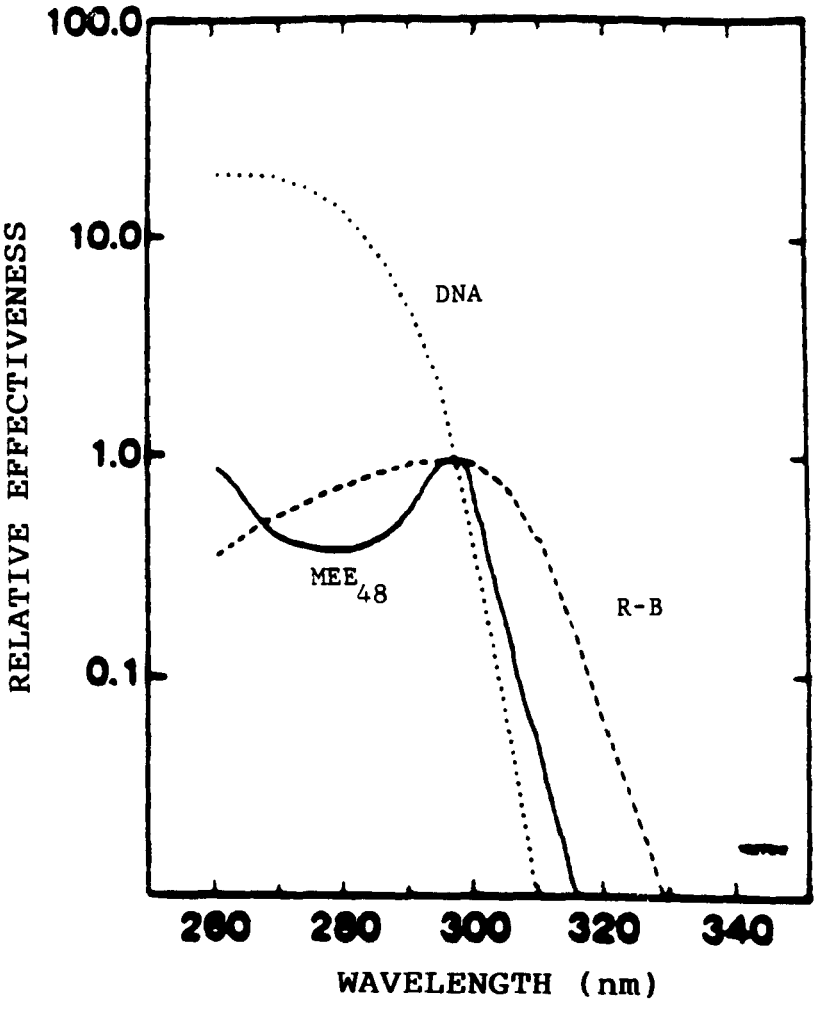

Source: Cole et al. (1986).

To determine if the dose-rate affects tumor development, the amount of energy necessary to produce tumors in 50 percent of the tested animals can also be calculated. De Gruijl et al. (1983) stated that the total dose delivered to hairless mice to induce tumors must be greater if a high daily dose is given than if a low daily dose is given. The greater dose given to the mice was 9.4×10^3 J/m^2/wk. This same trend was reported by Spikes et al. (1977) in C3H mice.

Experiments on photocarcinogenesis in laboratory animals may shed light on the role of UVR in the development of human nonmelanoma skin tumors. Results from animal studies clearly show that UVR is carcinogenic and that UV-B wavelengths (290-320 nm) are most effective in inducing a response.

Immunosuppression

The risk of developing nonmelanoma skin tumors may be influenced by the immune status of a UVR-exposed animal or human. For example, immunosuppressed mice were observed to be less able to reject skin treated with the carcinogen 3-methylcholanthrene than normal mice. In addition, mice exposed to UV light and treated with immunosuppressive drugs developed more tumors than animals exposed to UV light alone or treated only with immunosuppressants (Smith and Brysk 1981). UVR itself is selectively immunosuppressive (Kripke et al. 1977; Spellman and Daynes 1977), inducing the production of a class of lymphocytes, T-suppressor cells, which depress the host's ability to respond to UVR-induced tumor antigens (Fisher and Kripke 1977, 1978; Spellman and Daynes 1977, 1978; Daynes et al. 1979). Exposure to UVR has also been found to result in the impairment of antigen presenting cell function in the mouse (Greene et al. 1979). In animals with primary UVR induced tumors, this impairment is associated with the appearance of UV-tumor antigen-specific suppressor lymphocytes (Kripke et al. 1977; Daynes et al. 1977).

The T-suppressor cell is thought to prevent the generation of the cytotoxic ("T-killer") lymphocytes (Romerdahl and Kripke 1986), which would normally kill UVR-induced tumor cells, having recognized them as foreign by the new antigens present on their surfaces (Kripke 1977). Other forms of immunosuppression (e.g., via administration of an antilymphocyte serum or 6-mercaptopurine) give conflicting results, sometimes enhancing and sometimes depressing photocarcinogenesis (Nathanson et al. 1976). (A more detailed discussion of this subject is presented in Chapter 9.)

EPIDEMIOLOGIC EVIDENCE

Occurrence and Trends

Nonmelanoma skin tumors are among the most common neoplasms occurring in white populations. Based on a one-year survey (1977-1978) conducted by the National Cancer Institute (NCI), it was determined that nonmelanoma skin cancers developed in approximately 400,000 white Americans each year (Scotto and Fraumeni 1982). The annual age-adjusted incidence rate for this survey period was estimated to be $232.6/10^5$ among whites. For comparison, the estimated incidence rate for all other cancers among whites in the United States based on 1973-1976 data from the Surveillance, Epidemiology and End Results (SEER) Program was $318.9/10^5$ (NCI 1985). Among blacks, the annual age-adjusted

incidence rates for nonmelanoma skin tumors and all other cancers (NCI 1985) were $3.4/10^5$ and $347.3/10^5$, respectively.

The incidence of BCC is generally several times greater than the incidence of SCC. For example, based on data collected for 62 skin cancer cases registered from 1956-1960 in three public hospitals in New Zealand, Eastcott (1963) observed that 73 percent of the cases had BCC, 15 percent had SCC, and 7 percent had cutaneous malignant melanoma (CMM). Lee (1982) presented data on 2,019 skin cancer cases in Switzerland for 1974-1978 and showed that approximately 69 percent of the cases had BCC, 20 percent had SCC, and 11 percent had CMM. Among 2,000 individuals whose head, neck, forearms, and dorsa of hands were examined in a survey in Alfred Hospital in Victoria from 1982-1983, 71 percent of the histologically confirmed skin tumors were BCC and 29 percent were SCC (Goodman et al. 1984). A similar distribution of SCC and BCC was observed in a one-week study of 2,113 adults in 1982 in Maryborough, Australia, whose heads, necks, forearms, and dorsa of hands were examined (Marks et al. 1983).

These relative differences in BCC and SCC persist when males and females are examined separately even though the incidence in males generally exceeds that in females. Exhibit 7-12 presents age-adjusted BCC and SCC incidence data for white American males and females (Scotto and Fraumeni 1982). The incidence of BCC was approximately four to six times greater than the incidence of SCC.

The overall case fatality rate for nonmelanoma skin tumors is approximately 1-2 percent (Epstein et al. 1984). SCCs are, however, generally more aggressive than BCCs, accounting for about three-fourths to four-fifths of the deaths attributable to nonmelanoma skin cancer (Dunn et al. 1965; NAS 1982). SCCs may metastasize shortly after their appearance or even at the time of diagnosis (Epstein 1983). The rate of metastasis among SCC patients has been estimated by several researchers to range between 2 percent and 20 percent. Epstein (1983) reported that 25 percent of SCC patients with metastasis were alive 5 years after diagnosis, 13 percent were alive 10 years after diagnosis, and only 8 percent were alive after 15 years. Approximately two-thirds of metastasizing SCCs were observed to occur on the face and dorsa of the hands. BCCs, in contrast, rarely metastasize even when present for many years (Pollack et al. 1982). Their aggressiveness may be correlated with the site of tumor origin. The rate of metastasis among BCC cases in the United States has been reported to be 0.1%, 9 of 9,050 cases (Cotran 1961); 0.4%, 2 of 499 cases (Hughes 1973); and 0.55%, 1 of 183 cases (Cade 1940). In an Australian study (Paver et al. 1973), the rate of metastasis was estimated at 0.0028% (total number of cases not given). The time between primary tumor onset and metastasis has been estimated to range from 0 to 43 years with a mean time of approximately 10-11 years (Blewitt 1980; Farmer and Helwig 1980; Cotran 1961). Once metastasis occurs, the patient's prognosis is poor, with the time to death ranging from 0.8 to 1.6 years (Farmer and Helwig 1980; Coker et al. 1983). As of 1977, only about 109 cases of metastatic BCC had been reported in the United States (Safai and Good 1977).

Two sources of mortality data are available for nonmelanoma skin cancer, hospital records and death certificates. Hospital record data have been obtained, for example, as part of the Third National Cancer Survey (TNCS) which was conducted in two states and seven metropolitan areas from 1969-1971. Death certificates may be obtained from the National Center for Health Statistics

EXHIBIT 7-12

Comparison of Age-Adjusted Incidence Rates Per 100,000 Persons for Squamous Cell Carcinoma (SCC) and Basal Cell Carcinoma (BCC) Among White Males and Females in the United States

Skin Tumor Type	Age-Adjusted Incidence Rate/10^5	
	Males	Females
SCC	65.4	23.6
BCC	246.6	150.1

Source: Scotto and Fraumeni (1982).

(NCHS) or from state health departments. The validity of these mortality data, however, is uncertain (Dunn et al. 1965). The reporting of deaths due to nonmelanoma skin cancer may be biased due to the common perception that nonmelanoma skin cancer is not a lethal disease. Also, since nonmelanoma tends to be a more prevalent disease among older persons, the mortality due to nonmelanoma skin cancer may be underreported due to competing risks of death (Scott and Straf 1977). The reporting of nonmelanoma deaths in hospital records may also be biased downwards because affected patients are often not treated in hospitals.

Time Trends

Several researchers have observed that the incidence of BCC and SCC have been increasing over the past several decades (Lee 1982; NAS 1982). Epstein et al. (1984) have pointed out that the rate of increase of SCC is greater than that of BCC. Scotto and Fraumeni (1982), however, noted when comparing the NCI 1971-1972 and 1977-1978 survey data that the observed incidence increases applied mainly to BCC. The authors noted that the incidence of BCC among United States whites increased by approximately 15-20 percent over the six-year period between surveys.

In general, older individuals (e.g., over 60 years of age) are at higher risk of developing nonmelanoma skin tumors than are younger individuals. Vitaliano and Urbach (1980) observed that only three percent of a total 424 BCC and SCC cases from the Tumor Clinic of the Skin and Cancer Hospital in Philadelphia were under 40 years of age. However, Emmett (1982) and Harris (1982) have observed that SCC and BCC are no longer only diseases of old age since an increasing number of younger individuals have been presenting with nonmelanoma skin tumors. Harris (1982) suggested that these occurrences were consistent with increased sunlight exposure among these age groups.

The age-specific incidence patterns for SCC and BCC are not identical, suggesting that different etiological mechanisms may exist. Although incidence rates for SCC and BCC have been reported to rise with age and level off at the oldest age groups (Scotto and Fraumeni 1982), the increase with age has been observed to be sharper for SCC than BCC. Laerum and Iversen (1981) summarized study results indicating that among a group of BCC cases, 15 percent were less than 50 years of age and 65 percent were less than 70 years of age. Among a group of SCC cases, in contrast, Laerum and Iversen (1981) observed that 70 percent were over 70 years of age.

Anatomical Distribution

The predominant anatomical sites for both SCC and BCC and for both males and females are generally the face, head, and neck. Exhibit 7-13 presents the distribution of BCC and SCC by sex for tumors occurring in whites in the United States (Scotto and Fraumeni 1982). The data were collected as part of the 1977-1978 NCI survey. The face, head, and neck accounted for 60 percent or more of the total nonmelanoma skin tumors. Most of the remaining BCCs occurred on the trunk, whereas most of the remaining SCCs occurred on the upper extremities. Skin tumor data from 1974-1978 from Switzerland (Exhibit 7-14) shows similar tumor site distributions (Lee 1982). Scotto and Fraumeni (1982) noted that the tendency for nonmelanoma skin tumors to develop in exposed areas was consistent with the belief that solar radiation is a dominant risk factor for nonmelanoma.

EXHIBIT 7-13

Percentage of Tumors by Anatomic Site for Nonmelanoma Skin Cancer Among White Males and Females in the United States (1977-1978 NCI Survey Data)

Anatomic Site	BCC		SCC	
	Male	Female	Male	Female
Face, Head and Neck	81.2	84.1	74.8	60.1
Trunk	12.0	8.9	4.5	5.3
Upper Extremities	4.9	3.4	18.1	25.8
Lower Extremities	1.3	2.9	1.3	5.7
Other Sites	0.5	0.7	1.4	3.2

Source: Scotto and Fraumeni (1982).

EXHIBIT 7-14

Distribution by Sex and Anatomic Site of Nonmelanoma Skin Tumors: Canton of Vaud, Switzerland (1974-1978)

Anatomic Site	BCC		SCC	
	Male	Female	Male	Female
Head and Neck	540 (71.2)	505 (78.7)	202 (80.5)	103 (72.5)
Trunk	130 (17.1)	76 (11.9)	8 (3.2)	11 (7.7)
Upper Limbs	14 (1.8)	17 (2.6)	26 (10.3)	19 (13.4)
Lower Limbs	15 (2.1)	18 (2.8)	5 (2.0)	7 (4.9)
Other	58 (7.6)	26 (4.0)	10 (4.0)	2 (1.4)
Total	758 (100.0)	642 (100.0)	251 (100.0)	142 (100.0)

Source: Levi and Chapallaz (1981) as cited in Lee (1982).

There are, again, some general differences in the distributions of SCC and BCC, which suggests that these nonmelanoma skin tumors may respond differently to different dosages of sun exposure. The available epidemiologic data generally show that BCC is more likely than SCC to develop on regularly unexposed sites. Pollack et al. (1982) noted that although it is well established that sun-exposed areas are more prone to BCC, in at least one study (Urbach et al. 1972), approximately one-third of the BCCs occurred in light-protected regions. Laerum and Iversen (1981) observed that among a group of SCC and BCC cases, 90 percent of the BCCs and approximately 50 percent of the SCCs occurred on the head and neck. They estimated that of these tumors, two-thirds of the BCCs occurred on sites of the head and neck receiving the highest UV radiation doses (e.g., the nose) whereas all the SCCs occurred at these sites. Hillstrom and Swanbeck (1970) examined only SCC cases and observed that about 80 percent of the SCCs occurred on the head. Facial SCCs occurred relatively equally between males and females, but of the SCCs on the external ear, 90 percent occurred among males and only 10 percent among females. Emmett (1982) examined only BCC cases and observed that 75.5 percent occurred on the head and neck, 16 percent on the limbs, and 8.4 percent on the trunk. Lee (1982) noted that although BCC and SCC tend to be concentrated on exposed sites, the distribution of BCC did not precisely correspond with sun-exposed areas.

Exposure Factors

Several exposure factors considered to be associated with nonmelanoma skin tumors have been identified in epidemiologic studies, including latitudinal gradient, prolonged exposure to sunlight, and treatment with UVR.

Prolonged sun exposure is considered to be the dominant risk factor for nonmelanoma skin tumors among light-skinned populations (NAS 1982; Scotto and Fraumeni 1982; Greene and O'Rourke 1985; Lee 1982; Beral and Robinson 1981). In its 1982 report, the National Academy of Sciences (NAS) wrote that experts agree that exposure to sunlight causes 90 percent or more of the BCCs and SCCs in the United States. Several observations supporting this hypothesis were cited in the NAS report (NAS 1982) and by other researchers (Scotto and Fraumeni 1982; Urbach 1981; Beral and Robinson 1981; Scotto et al. 1981; Laerum and Iversen 1982; Emmett 1982). These observations include:

- the tendency for nonmelanoma skin tumors to develop in sun-exposed sites (e.g., head, face, and neck);
- the higher incidence rates among occupational groups with outdoor exposures compared to those with indoor exposures;
- the latitudinal and UVR gradient showing the highest incidence rates in geographic areas of relatively high UVR exposure;
- the increase in incidence rates with increasing age;
- the inverse correlation between nonmelanoma skin tumor incidence and degree of skin pigmentation;
- the high risk among genetically predisposed individuals (e.g., those with xeroderma pigmentosum);

- o the predisposition for nonmelanoma skin tumors to develop among light-skinned individuals who are susceptible to sunburn and who have red or blond hair, blue or light eyes, and a Celtic heritage;

- o the increased incidence of SCC in individuals treated with high intensity UV-B sources and oral methoxsalen or topical coal tar; and

- o the capacity of UVR to induce nonmelanoma skin tumors in experimental animals.

The observed variations in nonmelanoma incidence by latitude in particular support an association with sun exposure. For example, Scotto and Fraumeni (1982) observed, based on the 1977-1978 NCI survey data, that the incidence of SCC and BCC in the United States showed a latitudinal gradient with higher rates in the south. These results are displayed in Exhibits 7-15 and 7-16 for white males and white females, respectively. (Also shown in these figures are 1973-1976 CMM data from the SEER program. The latitudinal gradients for CMM were least pronounced.) It should be noted, however, that only a small number of data points (as shown in Exhibits 7-15 and 7-16) were used to examine the latitudinal gradients of BCC and SCC.

Variations in the incidence ratio of BCC to SCC by latitude further suggest that the two forms of nonmelanoma skin tumors respond differently to solar exposure. The results of MacDonald and Bubendorf (1964, as cited in Vitaliano and Urbach 1980) showed that the BCC:SCC ratio decreased from approximately 10:1 in northern United States cities to approximately 2:1 or 3:1 in southern rural areas. Similarly, Scotto and Fraumeni (1982) noted that the ratio of SCC incidence to BCC incidence increased with decreasing latitude and increasing sunlight exposure (see Exhibits 7-15 and 7-16). Pollack et al. (1982) commented that dosimetry studies revealed a poor correlation between BCC density in a site and UVR dose. They suggested that etiological factors for BCC, other than UVR, such as the presence of areas of scarring or epidermal nevi, may exist. Among blacks, in whom nonmelanoma skin tumors occur rarely compared to whites, areas of trauma or scarring may be important sites for the development of SCC (Scotto and Fraumeni 1982).

Vitaliano and Urbach (1980) examined several risk factors for SCC and BCC in a case-control study. The study included 366 BCC and 58 SCC cases seen at the Tumor Clinic of the Skin and Cancer Hospital in Philadelphia (dates were not specified). A group of 294 white controls without carcinoma were selected from the skin and cancer outpatient department. Information compiled on each case and control included cumulative solar exposure based on vocational and military history, time spent sunbathing, and participation in outdoor sports (as a spectator or participant). Exposure was divided into four categories: E1 = 0-9,999 hours, E2 = 10,000-19,999 hours, E3 = 20,000-29,999 hours, and E4 = 30,000 or more hours. The host factors that were examined included complexion (pale or mild-dark), age (0-59 years or 60 and over), and ability to tan (tans or burns-sensitive).

EXHIBIT 7-15

Annual Age-Adjusted Incidence Rates for Basal Cell and Squamous Cell Carcinomas (1977-1978 NCI Survey Data) and Melanoma (1973-1976 SEER Data) Among White Males[a/]

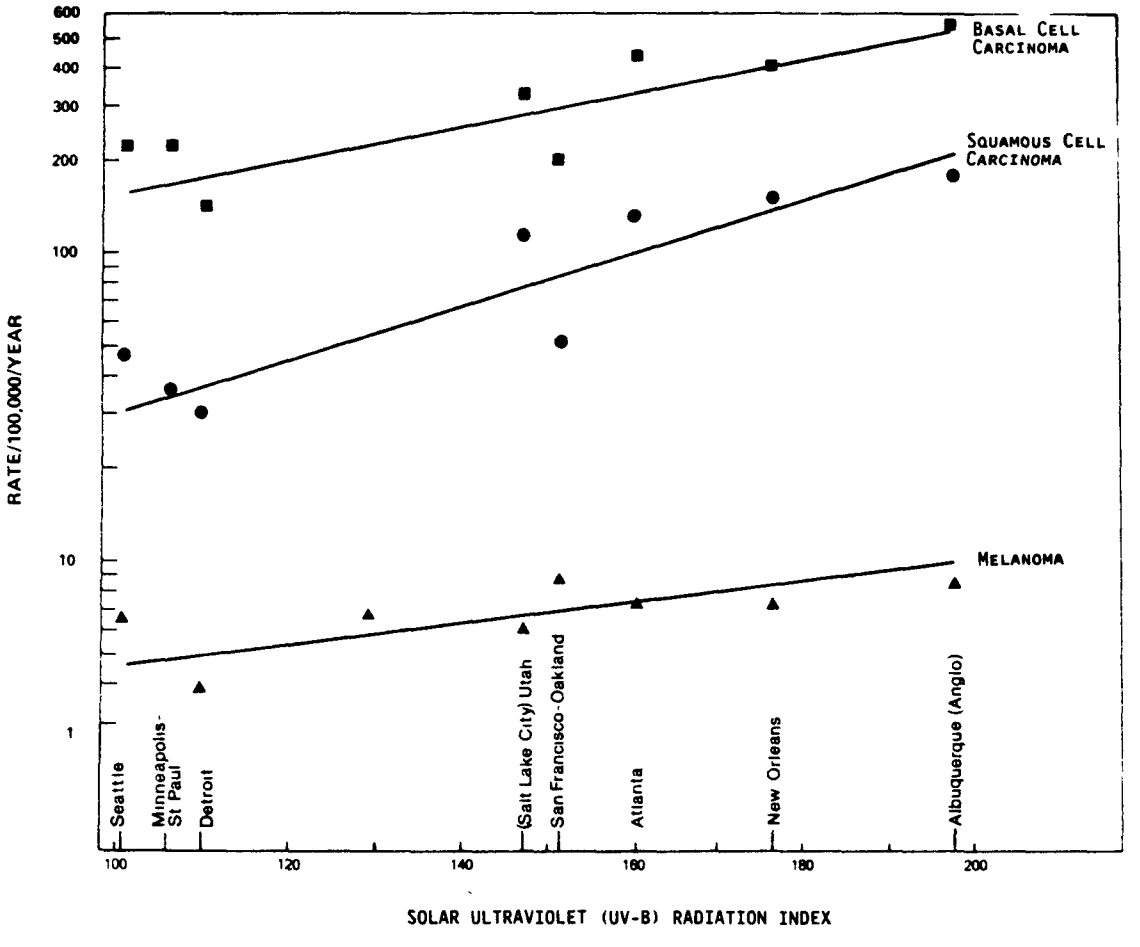

[a/] According to annual UV-B measurements at selected areas of the United States, with regression lines based on an exponential model.

Source: Scotto and Fraumeni (1982).

EXHIBIT 7-16

Annual Age-Adjusted Incidence Rates for Basal Cell and Squamous Cell Carcinomas (1977-1978 NCI Survey Data) and Melanoma (1973-1976 SEER Data) Among White Females[a/]

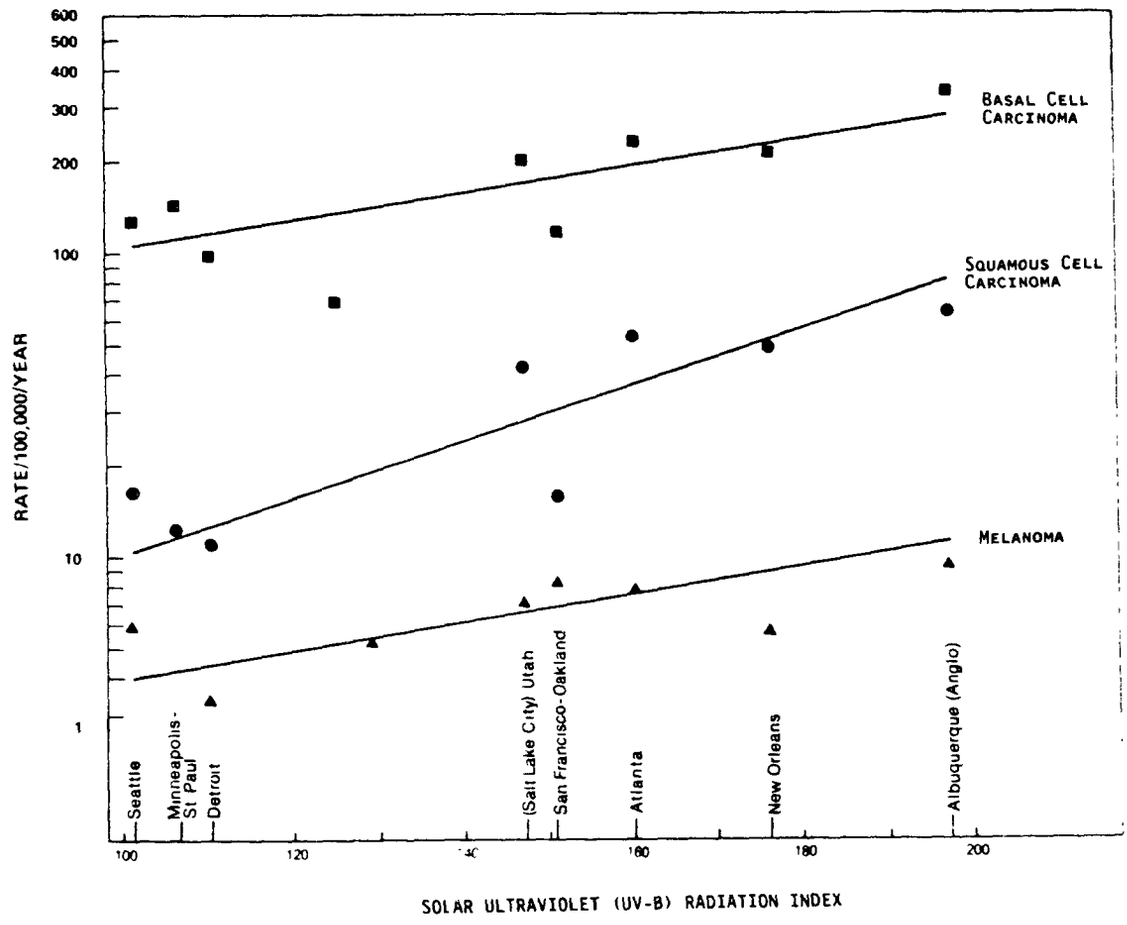

[a/] According to annual UV-B measurements at selected areas of the United States, with regression lines based on an exponential model.

Source: Scotto and Fraumeni (1982).

Based on a statistical logistic regression of the case-control data, Vitaliano and Urbach (1980) identified the most important risk factors for BCC and SCC as follows:

BCC: cumulative solar exposure ($p < 0.001$) >> ability to tan ($p < 0.001$) >> age ($p < 0.005$) >> complexion ($p < 0.025$)

SCC: cumulative solar exposure ($p < 0.001$) >> age ($p < 0.001$) >> ability to tan ($p < 0.005$).

Cumulative solar exposure was the most important risk factor for both SCC and BCC. Ability to tan was also important even at low levels of exposure. Complexion was a less important risk factor for SCC than for BCC.

Exhibit 7-17 presents the estimated relative risks (RRs) of BCC and SCC for the combinations of risk factors considered in the Vitaliano and Urbach (1980) study. Vitaliano and Urbach (1980) concluded that the most important difference between SCC and BCC was their relationship with cumulative exposure. As shown in Exhibit 7-17, a higher exposure level was required for BCC than for SCC to reach similar RRs. The authors noted that the maximum response of BCC to solar exposure occurred in exposure category E4 (30,000 or more hours), whereas for SCC it occurred in exposure category E3 (20,000-29,999 hours). They observed that the results were consistent with the belief that exposure to UVR has a greater effect on the development of SCC than on BCC, although an association between BCC and sunlight does exist.

Additional evidence of an association between UVR and nonmelanoma skin tumors is provided by cohort studies of psoriasis patients treated with high-intensity UV-B radiation. High-intensity UV-B sources would be expected to damage DNA in the same way as 290-300 nm solar wavelengths. The NAS (1982) report noted that in one cohort study, elevated risks were associated with UV-B exposure and topical crude coal tar. Although treatment with photochemotherapy (oral methoxsalen and UV-A) damages DNA in a different way than solar radiation, BCC and SCC rates in 1,373 patients were three times higher than expected (NAS 1982). In a more recent study by Stern et al. (1984) of 1,286 psoriasis patients followed-up for an average of 5.7 years, the risk of SCC 22 months after the first exposure to psoralen and UV-A (PUV-A) among those exposed to a high dose was 12.8 times that for those exposed to a low dose, even after adjustment for exposure to ionizing radiation and topical tar preparations. No substantial dose-related increase was observed for BCC. Stern et al. (1984) concluded that the results showed a substantial dose-dependent increase in the risk of SCC, even in those with neither a prior history of skin cancer nor substantial exposure to cutaneous carcinogens. The authors suggested that PUV-A may act as both a co-carcinogen and an independent carcinogen in the development of SCC. In two European trials (Finland and Vienna-Innsbruck) no increased risk of skin cancer was observed among patients treated with PUV-A (Stern 1984). The absence of a relationship may, however, have been due to different study methods, shorter follow-up periods, less sun or occupational exposure, and lower PUV-A doses in the European patients.

EXHIBIT 7-17

Estimated Relative Risks of Basal Cell and Squamous Cell Carcinomas for 32 Combinations of Risk Factors

Exposure Grade (Total Exposure, hr)	Tans				Burns-Sensitive			
	0-59 yrs		60+ yrs		0-59 yrs		60+ yrs	
	Dark	Pale	Dark	Pale	Dark	Pale	Dark	Pale
Basal Cell Carcinoma								
E4 (30,000 or more)	3.19	4.94	4.99	7.76	6.10	9.43	9.57	14.80
E3 (20,000-29,999)	2.86	4.43	4.49	6.95	5.47	8.47	8.58	13.29
E2 (10,000-19,999)	1.77	2.75	2.79	4.32	3.39	5.26	5.32	8.25
E1 (0-9,999)	1.00	1.55	1.57	2.43	1.91	2.96	3.00	4.65
Squamous Cell Carcinoma								
E4	7.09	22.79	28.61	90.12	26.61	84.66	107.70	347.08
E3	7.09	22.79	28.61	90.12	26.61	84.66	107.17	347.08
E2	4.42	5.72	17.94	23.08	16.60	21.41	66.99	86.52
E1	1.92	1.00	7.76	4.03	7.19	3.74	29.19	15.06

Source: Vitaliano and Urbach (1980).

Host Factors

As already mentioned, in addition to exposure factors, host factors play an important role in the risk of nonmelanoma skin tumors. Characteristics associated with pigmentation, including eye, hair, and skin color, ability to tan, tendency to sunburn, and ethnic origin are particularly important. Evidence presented in the 1982 NAS report and by numerous other researchers has identified those with fair skin, blue or green eyes, red or blond hair, a tendency to burn and to rarely tan, and a Celtic heritage as being at high risk of developing nonmelanoma skin tumors (NAS 1982).

Immunosuppression

One of the first reports of cancer occurring de novo in immunosuppressed transplant patients was published in 1968 (Doak et al. 1968). Since that time, a substantial body of evidence has accumulated showing that impairment of an individual's immune defense system may permit or facilitate the development of skin cancers (Smith and Brysk 1981; Penn 1981; Blohme and Larko 1984). In fact, the most common malignancies developing in immunosuppressed individuals are cancers of the skin, with the greatest frequency occurring, as in the general population, in sun-exposed areas (Sheil 1986). Those at risk include organ transplant patients and others receiving immunosuppressive drugs, patients with lymphoma, leukemia, and other diseases who have defective immune responses, and even those with age- or dietary-related decreases in immune responsiveness (Penn 1981; McMurray 1984; Smith and Brysk 1981). Gupta et al. (1986) estimate that over 7,000 individuals will receive renal transplants each year in North America alone.

The epidemiologic studies in this area have predominantly focused on individuals receiving immunosuppressive treatment, particularly organ transplant patients. The risk of developing skin cancer has been observed to be greater among transplant recipients than in the general population, and the risks appear to also be greater in geographical areas receiving higher amounts of UVR (Smith and Brysk 1981; Blohme and Larko 1984; Gupta et al. 1986; Sheil 1986; Penn 1981; Kinlen 1985). Skin cancer incidence rates among organ transplant recipients have been observed to be approximately 3-8 times greater than in the general population in low sun exposure areas (e.g., the United States, United Kingdom, Canada, and Sweden) and approximately 16-21 times greater in high sun exposure areas (e.g., Australia and South Africa) (Hoxtell et al. 1977; Hardie et al. 1980; Gupta et al. 1986; Penn 1981; Blohme and Larko 1984; Smith and Brysk 1981).

Most of the skin cancers that develop in immunosuppressed individuals are SCCs, in contrast to the observed predominance of BCC over SCC (approximately 4-6 BCC:1 SCC) in the general population. The ratio of SCC:BCC among renal transplant patients has been observed to range from 1.33 (Minnesota) and 2.3 (Toronto) to 11 (Sydney, Australia, and Denver, Colorado) and 16 (New South Wales) (Gupta et al. 1986). Only one Swedish study has reported an SCC:BCC ratio of less than one (Blohme and Larko 1984). In a study of 523 white renal transplant patients in Toronto, Gupta et al. (1986) estimated that the risks of developing all skin cancers, SCC, and BCC were 3.2, 18.4, and 1.4 times higher, respectively, than in the general population. The elevated risks for all skin cancers and SCC were statistically significant. Sheil (1986) observed that SCC occurs about 40 times more frequently among transplant patients than among the

general population, whereas CMM occurs about five times more frequently. Sheil (1986) noted that it was not clear whether BCC occurs more frequently among transplant patients. Among 1,349 British transplant recipients given immunosuppressive therapy, the incidence of SCC was observed to be five times that in the general population (Penn 1981).

The SCCs that develop in immunosuppressed individuals tend to metastasize more frequently and be more aggressive than the SCCs observed in the general population (Sheil 1986; Penn 1981). Furthermore, the average age at which immunosuppressed patients develop skin cancer is about 30 years less than the average age among skin cancer cases in the general population (Penn 1981; Gupta et al. 1986). Sheil (1986) has reported that malignancies occur within a few months following transplant, with the average presentation occurring in two to three years post-transplant and the increased risk persisting indefinitely. Gupta et al. (1986) observed a mean time to development of skin cancer among 523 renal transplant patients of 86.6 months (24 to 181-month range).

The available epidemiologic evidence on the incidence of skin cancer among immunosuppressed individuals clearly indicates that immune mechanisms play an important role in limiting the development of malignant skin tumors. However, the different patterns of disease among immune depressed populations compared with the general population, e.g. (the disproportionate increase in SCC over BCC, the abbreviated time to tumor development, the increased tumor aggressiveness, and the increased tendency for tumor metastasis) indicate that other more complex factors may be involved. One potential factor may involve viruses of human papilloma and herpes types. It has been observed that at least one-third of SCC patients among immunosuppressed transplant recipients carry the genome of the papilloma virus (Sheil 1986). Gupta et al. (1986) suggest that immunosuppression, UV light, and the papilloma virus may act synergistically in the production of skin cancer.

DOSE-RESPONSE RELATIONSHIPS

This section reviews the results of several important studies that have examined the quantitative relationship between exposure to UVR and the incidence of nonmelanoma skin cancer. The methodological issues that add uncertainty to these estimates are also discussed. Much of the discussion in this section is based on review papers by the National Research Council (NAS 1982), van der Leun (1984), and Zeger et al. (1986).

The available evidence from experimental and epidemiologic studies clearly indicates that UVR exposure is associated with the development of nonmelanoma skin tumors. In an effort to evaluate the potential impacts on nonmelanoma of increased UVR exposures due to depletion of the ozone layer, several researchers have attempted to quantify the relationship between UVR dose and the incidence of nonmelanoma skin tumors. Dose-response relationships between UVR and the incidence of nonmelanoma skin tumors can then be combined with estimates of the effects of changing ozone levels on UVR to predict the potential effects of ozone changes on the incidence of nonmelanoma skin tumors.

Previous Analyses

Dose-response relationships for exposure to UVR and nonmelanoma skin tumors have been developed in both epidemiologic and experimental studies. Six major

dose-response analyses are reviewed below; three are based on epidemiologic (ecological) studies, two are based on animal experiments, and the last is based on a molecular experiment. In each of these studies, UV-B exposure is estimated by weighting individual wavelengths in the UV-B spectrum according to biological effectiveness. A single weighting approach is referred to as an action spectrum. Several action spectra based on the UV-B measurement approach are available including Robinson-Berger (R-B) meter, human erythema, and Setlow DNA. The erythema and DNA action spectra weight those wavelengths thought to promote sunburn and damage to DNA more heavily than other wavelengths.

Early epidemiologic research in dose-response of UVR exposure and nonmelanoma skin cancer was conducted by the National Research Council (NRC 1975), Scott and Straf (1977) and Scotto et al. (1974). These studies all used nonmelanoma skin cancer incidence data from the 1971-1972 National Cancer Institute (NCI) survey and UV doses measured by R-B meters at four locations in the United States. The NRC considered these early studies to provide only crude estimates of the dose-response relationship (NAS 1982).

Since these early works, additional epidemiologic data were made available by NCl. A new survey of skin cancer incidence was conducted by NCI in 1977-1978 for eight locations across the U.S. These data consist of newly diagnosed cases of nonmelanoma skin cancer, and are age-, sex-, and cell type-specific for whites only. In addition, new readings from R-B meters at five locations in the U.S. were provided. These readings combined with the earlier R-B meter readings provided UV-B data for all eight locations included in the 1977-1978 NCI survey.

All three epidemiologic studies reviewed below use the 1977-1978 NCI survey data for nonmelanoma cancer incidence. The studies differ, however, in their choice of an action spectrum and in their specification of the model used to estimate the dose-response relationship.

The relationship between UV-B and nonmelanoma skin tumors in the epidemiologic studies is expressed as a biological amplification factor (BAF), which is defined as the percent change in tumor incidence that results from a one percent change in exposure to UV-B radiation. Estimated BAF values can be combined with predictions of the changes in UV-B radiation due to changes in ozone to obtain estimates of the effects of ozone changes on nonmelanoma skin tumor incidence rates.

Scotto et al. (1981) and Fears and Scotto (1983)

Scotto et al. (1981) estimated values for the BAF by correlating the incidence of nonmelanoma skin cancer with UV-B dosage for eight locations in the U.S. Separate estimates were presented by location, sex, and cell type. The functional form of the model used was:

$$\ln(R) = \ln(a) + bU + e$$

where R is nonmelanoma skin cancer incidence rate, U is UV-B radiation dosage, a and b are constants, and e is an error term. The constant b is the BAF that describes the UV-B dose-skin cancer incidence relationship. Incidence rates were obtained from the 1977-1978 NCI survey. Age-adjusted incidence rates were used for all estimates. UV-B dosages were obtained from R-B meters located at major metropolitan airports at each location. The coefficients were estimated

using ordinary least squares regression.

Scotto et al. (1981) found that although incidence rates varied by age, BAFs did not vary significantly by age. Their estimates of the BAFs for BCC ranged from 1.32 to 2.59 for males and from 1.06 to 2.07 for females. The estimates of the BAFs for SCC were slightly greater, from 2.08 to 4.09 for males and from 2.18 to 4.30 for females. In both cases, higher estimates were obtained for locations at lower latitudes.

In a later study, Fears and Scotto (1983) again estimated BAFs by correlating nonmelanoma skin cancer incidence with UV-B radiation dosage. The data used were the same as those used in the earlier study. In this study Fears and Scotto (1983) used two functional forms of the model. The first is the log-linear form used by Scotto et al. (1981) as described above. The second is the log-log form:

$$\ln(R) = \ln(a) + b\ln(U) + e$$

Separate estimates were presented by sex, location, and percent increase in UV-B dosage but not by cell type. The BAF estimates presented in this study ranged from 1.4 to 3.2 for males and from 1.1 to 2.3 for females. Higher estimates were obtained for locations at lower latitudes and for higher percent changes in UV-B dosage.

Fears and Scotto (1983) concluded that the relationship between UV-B radiation and nonmelannoma skin cancer incidence could be modeled using either the log-linear or the log-log form. They noted that there was no strong reason to prefer one form of the model over the other.

Scott (1981)

Scott used the log-linear equation as specified in the Scotto et al. (1981) study discussed above. Incidence data were also obtained from the 1977-1978 NCI survey. However, rather than using the R-B meter data for UV-B dosage, Scott (1981) used the Setlow (1974) action spectrum for DNA damage.

Scott (1981) concluded that the values of UV-B dose obtained from the DNA damage weighting method were approximately linear with those obtained from the R-B meter. Therefore, the estimates for the BAFs were approximately the same as the estimates made by Scotto et al. (1981) using the R-B meter data. Estimates of the change in UV-B dosage associated with changes in ozone concentration, however, were found to be sensitive to the method used. Thus, even though the estimate of the BAFs were insensitive to the method used to measure UV-B dosage, the estimated effect of changes in ozone concentration on nonmelanoma skin cancer is sensitive to the choice of action spectrum.

For example, using the DNA action spectrum, Scott (1981) estimated that a 5 percent ozone reduction would lead to an increase in BCC in Minneapolis-St. Paul of 7.7 percent for males and 5.8 percent for females. Using the R-B meter, with the same functional model and cancer incidence data, Scotto et al. (1981) estimated corresponding increases to be 5.6 percent for males and 4.4 percent for females. The reason for this difference lies in the differential sensitivity of different weighting functions for ozone depletion -- the optical amplification factor. The energy delivered in wavelengths from 295-300 nm

increases much more with ozone depletion than energy in wavelengths from 315-320 nm. Thus the shape of the action spectrum significantly influences the effects of a given ozone depletion.

In an earlier paper, Scott and Straf (1977), using pooled data, pointed out that estimates of the BAF will be biased because actual doses vary by individual. Using survey data from one location only, they estimated that to correct this bias, the BAF's should be increased by 30 percent. More recent estimates of the bias indicate that BAF estimates should be increased by 70 percent (NRC 1982).

Rundel (1983)

The Rundel study is the third epidemiologic study to use the 1977-1978 NCI survey data. Measurements from the R-B meter were used to estimate UV-B exposure. However, Rundel used a different dose-response model than that used by Fears and Scotto (1983) or Scott (1981) to estimate the BAFs. The Rundel model used age as a proxy for cumulative sun exposure and estimated skin cancer incidence at a single location as a function of this proxy variable. Separate BAF estimates were made by sex, cell type, and location.

The Rundel model was based on the assumption of reciprocity; that is, the probability of developing nonmelanoma skin cancer depends only on the cumulative dose received and not on the time course of that dose. The assumption of reciprocity tends to bias the estimates of the BAFs upward. It should be recognized, however, that there is evidence that reciprocity may not be a valid assumption (Fears et al. 1977; Green 1978; de Gruijl 1983).

Rundel (1983) concluded that the probability of a nonmelanoma skin tumor becoming observable in an individual was well described by a log-normal distribution. Estimates of the BAF for males ranged from 1.8 to 2.2 for BCC and from 2.4 to 2.8 for SCC. The corresponding ranges for females were 1.1 to 1.5 for BCC and 1.6 to 2.1 for SCC. The higher values were again obtained for lower latitudes.

Rundel (1983) estimated that a 1 percent depletion in ozone would lead to a 1.78 percent increase in BCC and a 2.3 percent increase in SCC. He concluded that these estimates were insensitive to the choice of action spectrum. Comparing dosage weighted by the R-B meter with dosage weighted by the DNA damage spectrum, Rundel (1983) showed that with the R-B meter the effect of ozone changes on UV-B radiation would be small and the effect of UV-B dosage on skin cancer incidence would be larger. Thus, the total effect of ozone changes on skin cancer incidence would be approximately the same.

Forbes et al. (1982)

In this study, hairless (Skh:HR) mice were exposed 5 days/week to UVR from a xenon arc lamp attenuated by five different filter thicknesses (0.64, 1.0, 1.3, 2.0, and 3.0 mm). The thinner filters transmit increasing amounts of UVR at wavelengths less than 295 nm. For each filter thickness, four different exposure periods were tested (43.6, 61.2, 85.5, and 120 minutes/day). Forbes et al. observed that the proportion of affected animals, the mean number of tumors per affected animal, and the size of individual tumors all tended to increase with time exposed.

The effects of varying filter thicknesses and action spectra were determined by examining the median time to the appearance of the first tumor on each animal (T50 or latent period). When the reciprocal of T50 was compared to the daily UVR dose expressed as R-B meter counts for all filter groups combined, a high correlation was observed ($r = 0.957$). However, when the reciprocal of T50 was compared to dose (R-B meter counts) for each filter thickness separately, different slopes were observed. The latent period was observed to decrease at a faster rate with increasing exposure for thinner filters than for thicker filters. These results indicated that incremental additions of shorter wavelength UVR had a relatively greater carcinogenic effect than the R-B meter predicted. The authors concluded that, although the R-B meter is a reasonably good model for the UV wavelength dependence of UV photocarcinogenesis, it may underestimate the consequences of some environmental changes.

A similar evaluation of the T50 data was carried out using the MEE48 action spectrum (based on the acute "delayed" edema response in hairless mice). For all filter thicknesses combined, a better correlation between latent period and daily effective dose ($r = 0.995$) was observed for the MEE48 action spectrum than for the R-B meter spectrum. When the filters were analyzed separately, significant differences between separate filters and the combined filter data were not observed, in contrast to the R-B meter analysis. The authors noted that these results suggested that the MEE48 action spectrum is a better model for mouse photocarcinogenesis for simulated solar spectra at wavelengths greater than 295 nm.

de Gruijl et al. (1983)

The dose-response analysis presented by de Gruijl et al. (1983) was also based on data from an animal experiment. Mice were exposed to radiation from a sunlamp for 3.25 hours per day at seven different levels ranging from 0 mJ/cm^2 to 190 mJ/cm^2. The response was measured by observing the initiation and growth of tumors on the mice. The results of this study showed that the initiation of tumors was dependent on the dose, but that the growth and yield of tumors were independent of dose. These authors also concluded that reciprocity was not supported, except at high dosage levels.

Kubitschek et al. (1986)

This study presented a method for calculating the effects of a reduction in atmospheric ozone upon the incidence of nonmelanoma skin tumors by calculating the incidence of mutations in *E. coli*. The model that was applied had the following form:

$$Sm = \int E(\Theta,\lambda,W)\ T(\lambda)\ \epsilon(\lambda)\ d\lambda$$

where

Sm	= Rate of induction of mutation
Θ	= Solar zenith angle
λ	= Wavelength
W	= Amount of stratospheric ozone
$E(\Theta,\lambda,W)$	= irradiation at earth's surface
$T(\lambda)$	= rate of transmission through skin

$\epsilon(\lambda)$ = action spectrum from E. coli

The Kubitschek et al. (1986) study predicted that a one percent reduction in atmospheric ozone would lead to a 1.7 percent increase in mutation rate. This estimate was constant for solar zenith angles up to 70 degrees, a range that includes most heavily populated areas of the globe. Their conclusions were based on the action spectrum for mutagenesis in E. coli (Exhibit 7-18), unpublished information in similar studies in mammalian cells, information on the epidermal transmission rate of the various UV wavelengths, and consideration of a BAF taken from van der Leun (1984). They estimated that a 3-5 percent depletion of stratospheric ozone would lead to an increase in nonmelanoma skin cancer rates of about 10-20 percent.

Uncertainties in Estimates of Dose-Response

There are a number of issues related to the studies described above that add uncertainty to dose-response estimates. The degree of uncertainty that is added has not been fully quantified.

A major factor contributing uncertainty to dose-response estimates is the limited availability of epidemiologic data. All of the epidemiologic studies described above use the 1977-1978 NCI survey for nonmelanoma-tumor incidence data. These researchers, thus, used a single measure of UV-B dosage for all individuals in a given location. Actual dosages received by individuals will, however, vary because of behavioral factors such as time spent outdoors. Unfortunately, data on individual UV-B exposures are not currently available. The incidence of nonmelanoma skin cancer will also vary by individual because of genetic characteristics such as skin color. If these factors are correlated with location, the estimates could be biased.

The issue of peak versus cumulative dose has not been addressed in these studies. The failure to consider this factor may be important since BCC and SCC are believed to respond differently to solar exposure. As described earlier in this chapter, exposure to UVR is believed to have a greater effect on the development of SCC than on BCC.

Furthermore, the three epidemiologic studies discussed above cannot be considered independent because they are all based on the same skin cancer incidence database. As more comprehensive data are collected for more locations, across longer time periods, and for individuals, estimates of dose-response will hopefully become more precise.

Another important issue is the choice of action spectrum for measuring UV-B dosage. The estimate of the effect of ozone depletion on skin cancer incidence is sensitive to the choice of action spectrum. There is, however, no current consensus on what is the best action spectrum to use to estimate the dose-response relationship.

EXHIBIT 7-18

Relative Mutagenicity of UV-B as a Function of Wavelength

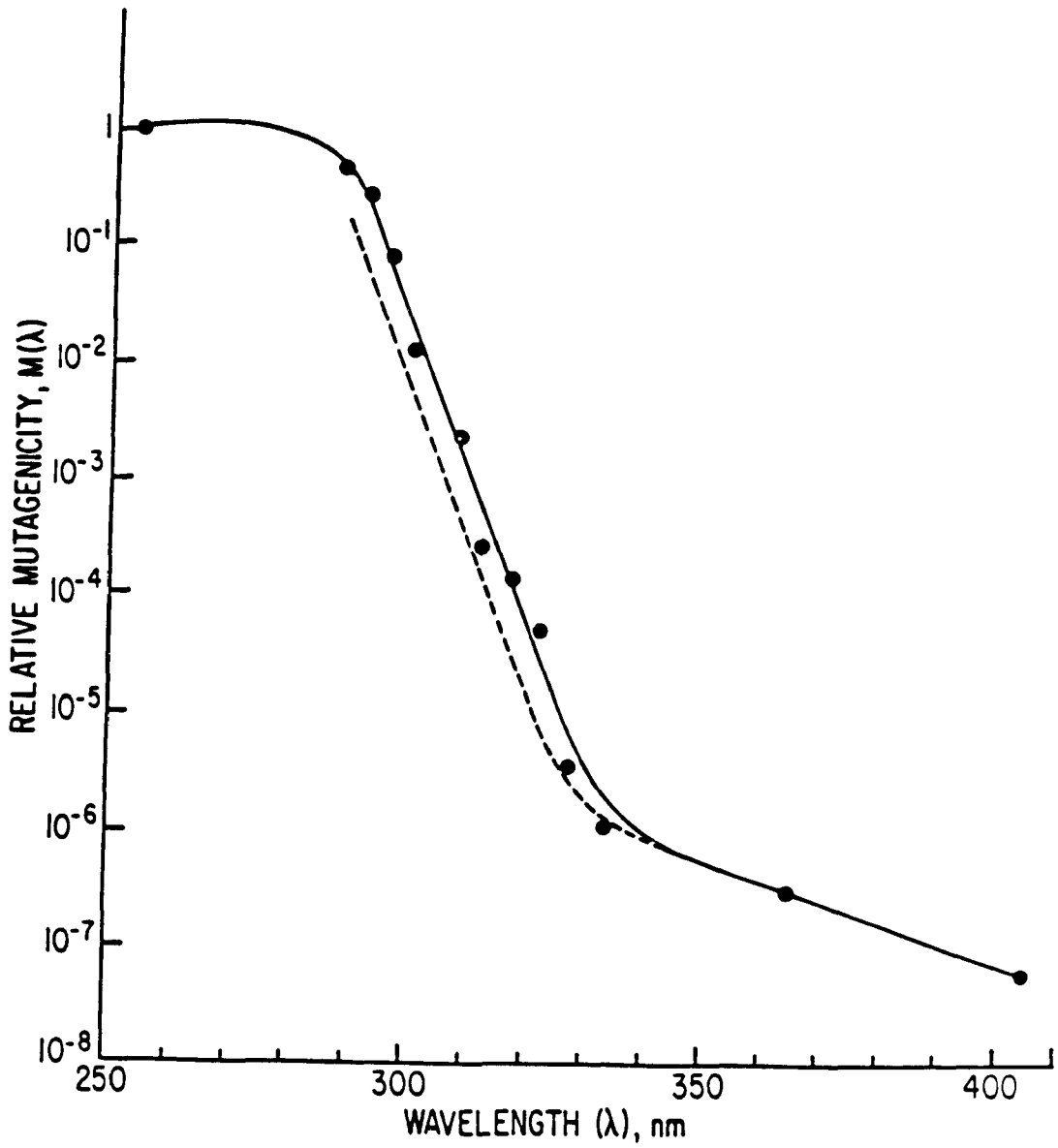

The smooth line shows the fit to these data by the sum of two exponentials at wavelengths above 293 nm, as described in the text. The broken line is the fit after correction for spectrophotometer slit width.

Source: Kubitschek et al. (1986).

There is also statistical uncertainty in the measurement of UV-B flux. This uncertainty is not captured in regression analysis, which considers the UV-B values as certain. As a result, dose-response coefficients are subject to a greater degree of statistical uncertainty than is indicated in the regressions. Incorporating statistical uncertainty in the estimates of UV-B would probably result in different dose-response coefficients, but the direction and magnitude of this difference is not known (Zeger 1986).

Another issue is whether the models used are valid for all scenarios of ozone change. For large levels of ozone depletion, for example, the amount of UV-B radiation reaching the Earth's surface may be outside the range of UV-B data used to estimate the dose-response relationship in the models, or may occur in a different pattern.

Because it is impossible to experiment on humans, experimental (e.g., animal) studies may be used to examine the association between UV-B and nonmelanoma skin cancer. The extent to which the animal response to UV-B resembles the human response is not well known. Furthermore, the intensity, duration, schedule, and range of the doses applied in an animal experiment is likely to differ from the exposures received by humans in the ambient environment.

In conclusion, while quantified dose-response estimates provide critical information relating skin cancer incidence rates to changes in the ozone level, they should be regarded with caution. As briefly described above, there are numerous uncertainties associated with such dose-response estimates.

Sensitivity of Dose-Response Estimates to Choice of Action Spectrum

As noted above, one important methodological issue that adds uncertainty to the estimates of dose-response is the choice of action spectrum. In comparing the DNA damage weighting method with the R-B meter method used by Scotto et al. (1981), Scott (1981) found that estimates of the BAFs were approximately the same but that estimates of the effect of ozone depletion on UV-B dosages were different. On the other hand, Rundel (1983) concluded that the effect of ozone depletion on skin cancer incidence was insensitive to the choice of action spectrum.

An independent analysis of the sensitivity of dose-response estimates to the choice of action spectrum was conducted and is summarized in Attachment A. The methodology used in this analysis follows that used by Fears and Scotto (1983). The dose-response is estimated using three alternative action spectra -- R-B meter, human erythema, and Setlow DNA.

The major result of this analysis was that the estimated BAF is not sensitive to the choice of action spectrum. The estimated coefficient using the human erythema and Setlow DNA action spectra all fell well within one standard error of the coefficients estimated for the R-B meter action spectrum (see Exhibit A-3 in Attachment A).

However, because the optical amplification factor is sensitive to ozone depletion, (that is, because UV-B at 295-300 nm increases more than at 315-320 nm) estimates of the effect of ozone depletion on UV-B dosage were found to differ significantly by choice of action spectrum. Use of an action spectrum

based on the effects to a biological target, of course, makes sense. Nevertheless, an issue still exists about whether DNA, erythema, cutaneous edema, or some other biological action spectrum should be used. The Setlow DNA action spectrum was found to give the highest estimates of the effect of ozone depletion on UV-B dosage of the three examined (see Exhibit A-4 in Attachment A). Thus, the choice of an action spectrum will influence estimates of the effect of ozone depletion on skin cancer incidence.

ATTACHMENT A

Sensitivity Analysis of the Selection of Action Spectra on Dose-Response Estimates Relating UVR Exposures to Nonmelanoma Skin Tumors

This attachment presents the results of an analysis of the relationship between changes in ozone levels and incidence rates of nonmelanoma skin tumors. Estimating the impact of ozone change on tumor incidence requires two pieces of information: (1) the response of UV-B radiation to changes in ozone, and (2) the dose-response relationship between UV-B exposure and the incidence of nonmelanoma skin tumors. This analysis focuses on the sensitivity of the selection of an action spectrum used to describe the relationship between UV exposure and the incidence of nonmelanoma skin cancer.

UV-B Exposure and Nonmelanoma Skin Cancer

The relationship between UV-B exposure and the incidence of nonmelanoma skin tumors was estimated from the power model used by Fears and Scotto (1983):

$$\ln(R) = a + b\ln(UV) + e$$

where R is age-adjusted incidence, e is an error term, and a and b are constants. The constant b is the BAF that describes the UV-B dose-skin cancer incidence relationship.

The coefficients a and b were estimated using weighted ordinary least squares regression. Two sets of data were required to develop these estimates: (1) incidence rates for nonmelanoma skin tumors, and (2) measurements of UV-B exposure for individuals developing these tumors. The sources of each data set are discussed below.

Incidence of Nonmelanoma Skin Cancer

Age-specific incidence rates (new cases per 100,000 population) for nonmelanoma skin cancer among whites were obtained from Scotto et al. (1981) for eight locations in the United States (1977-1978 NCI survey data).

UV-B Radiation

Although there is substantial agreement that wavelengths within the UV-B band are primarily involved in the development of nonmelanoma skin cancers, there is uncertainty about which individual wavelengths are most important. In this analysis, the relative effect of using three alternative action spectra in regressions to quantify the coefficients relating UV-B dose to skin cancer incidence relationship were: Robertson-Berger (R-B) meter, human erythema, and Setlow DNA. The erythema and DNA action spectra weight those wavelengths thought to promote sunburn and damage to DNA more heavily than other wavelengths.

Data on UV-B radiation were obtained from the NASA UV-B model (Serafino and Frederick 1986). This model uses mathematical relationships to estimate UV solar flux along different wavelengths (UV-A and UV-B) reaching the Earth's

surface at any time of year and location on the globe. To estimate UV flux, the model uses information about global ozone abundance, terrain height, cloud cover, cloud transmission, and surface characteristics.

The NASA model provided estimates of UV-B radiation for each of the eight U.S. locations. The data were provided for all three action spectra, and for each action spectrum, data were presented for three different time periods -- annual, a day in the month of June, and a clear day. In addition to UV-B data at current ozone levels, the NASA model provided estimates of radiation reaching the Earth's surface at different ozone levels.

To analyze the significance of measuring UV-B radiation using different action spectra and time periods, Exhibit A-1 shows correlations among the NASA UV-B data for the three action spectra and for annual, month of June, and clear day time periods. The exhibit also shows correlations among actual UV-B measurements (Scotto et al. 1981) and the modeled data. The strong correlation among these UV-B data suggests that dose-response coefficients are not highly sensitive to the different measures. Nonetheless, a regression analysis was performed using dose-response coefficients for the annual time period for all three action spectra. Before performing the regression analysis, two weights were applied to the data. First, the data were weighted by the population of each respective location. Exhibit A-2 shows the populations of these locations. Second, as a correction for heteroskedasticity, the data were weighted by the inverse of the estimated variance of the logarithm of the age-adjusted incidence rates.

Exhibit A-3 presents regression estimates of dose-response coefficients for basal cell and squamous cell skin cancers by sex. Separate estimates are given for all three action spectra (annual only). The exhibit shows a low, middle, and high estimate. The low value represents the estimated coefficient minus one standard error. The high coefficient adds one standard error. The dose-response coefficients for SCC are higher than those for BCC for each of the action spectra. In addition, the coefficients for SCC were found to be of greater statistical significance. These findings are consistent with the belief that cumulative UV-B radiation has a greater effect on the development of SCC than on the development of BCC. As already mentioned, epidemiologic observations indicate that the ratio of basal cell to squamous cell skin cancer decreases with decreasing latitude and that BCC is more likely to develop on regularly unexposed sites. In addition, the sensitivity of basal cell cancer incidence rates to UV-B was higher for males than for females. The relative sensitivity by sex is reversed for SCC.

It is important to recognize that the NASA model's UV-B flux values are subject to statistical uncertainty. This uncertainty is not captured in the regression analysis, which treats the UV-B values as certain. As a result, the dose-response coefficients are subject to a greater degree of statistical uncertainty than is indicated in the regressions. Incorporating statistical uncertainty into the estimates of UV-B would probably result in different dose-response coefficients, but the direction and magnitude of this difference is not known.

EXHIBIT A-1

Correlation of Alternative Measurements of UV-B Radiation for Ten Locations in the United States[a/]

	Annual[b/]				Clear Day[b/]			Month of June[b/]		
	R-B Actual	R-B	Erythema	DNA	R-B	Erythema	DNA	R-B	Erythema	DNA
Annual[c/]										
R-B Actual	1.00	0.979	0.988	0.987	0.940	0.977	0.977	0.882	0.955	0.967
R-B Meter		1.00	0.990	0.984	0.964	0.975	0.970	0.935	0.975	0.989
Erythema			1.00	0.999	0.941	0.985	0.986	0.883	0.959	0.971
DNA				1.00	0.932	0.984	0.987	0.866	0.949	0.963
Clear Day										
R-B Meter					1.00	0.986	0.955	0.938	0.967	0.968
Erythema						1.00	0.999	0.869	0.947	0.960
DNA							1.00	0.850	0.936	0.951
June										
R-B Meter								1.00	0.978	0.967
Erythema									1.00	0.999
DNA										1.00

a/ The ten locations include: Seattle, Washington; Minneapolis, Minnesota; Detroit, Michigan; Des Moines, Iowa; Salt Lake City, Utah; San Francisco-Oakland, California; Atlanta, Georgia; Dallas-Ft. Worth, Texas; New Orleans, Louisiana; Albuquerque, New Mexico. Data for Des Moines and Dallas-Ft. Worth were included in the correlations; however, because nonmelanoma skin cancer rates were available only for 1971-1972, these locations were excluded from the dose-response regression analysis.

b/ Model data from the NASA UV model.

c/ Annual UV-B data from Scotto, Fears and Fraumeni (1981). These data are actual UV-B measurements taken at National Weather Service stations.

EXHIBIT A-2

Population Weights for Ten Locations in the United States

Location	Weight
Seattle (King County)	1,000,000
Minneapolis-St. Paul	2,113,533
Detroit	4,353,413
Salt Lake City [a/]	1,461,000
San Francisco-Oakland [b/]	3,250,630
Atlanta	2,029,710
New Orleans	1,076,204
Albuquerque [c/]	1,303,000

a/ State of Utah.

b/ San Francisco.

c/ State of New Mexico.

Source: State and Metropolitan Area Data Book, 1982, U.S. Department of Commerce, Bureau of the Census, U.S. Government Printing Office, August 1982.

EXHIBIT A-3

**Estimated Dose-Response Coefficients (and t-Statistics)
for Basal Cell and Squamous Cell Skin Cancers
(UV-B Dose-Skin Cancer Incidence)**

	R-B Meter			Human Erythema			Setlow DNA		
	a/ Low	Mid	b/ High	a/ Low	Mid	b/ High	a/ Low	Mid	b/ High
Basal Cell									
Male	1.300	1.810 (3.53)	2.330	1.020	1.410 (3.60)	1.800	0.932	1.290 (3.60)	1.650
Female	0.443	1.050 (1.73)	1.670	0.346	0.809 (1.75)	1.270	0.316	0.739 (1.75)	1.160
Squamous Cell									
Male	1.940	2.840 (3.20)	3.730	1.540	2.210 (3.31)	2.880	1.420	2.030 (3.33)	2.640
Female	1.880	3.060 (2.60)	4.230	1.570	2.420 (2.87)	3.260	1.470	2.220 (2.94)	2.980

a/
Estimated coefficient minus one standard error.

b/
Estimated coefficient plus one standard error.

Ozone Levels and Changes in UV-B Exposure

The NASA UV-B model was used to estimate changes in UV-B radiation associated with changes in ozone levels. Exhibit A-4 shows representative estimates for San Francisco. In the exhibit, a 2 percent reduction in ozone resulted in an estimated 1.6 percent increase in UV-B radiation as measured on an R-B meter. The estimated percentage increase is greater using the human erythema or Setlow DNA action spectra.

Relationship Between Ozone Changes and the Incidence of Nonmelanoma Skin Tumors

The NASA estimates of the sensitivity of UV-B radiation to changes in ozone were combined with the UV-B dose-skin cancer incidence coefficients. Exhibits A-5 and A-6 present the results of this analysis for an estimated 2 percent and 10 percent depletion in the ozone layer for San Francisco. For example, Exhibit A-5 indicates that the steady-state incidence rate of basal cell skin cancer could increase by 2.98 percent for males and 1.72 percent for females in response to a 2 percent depletion in ozone.

EXHIBIT A-4

Estimated Percentage Changes in UV-B Radiation in San Francisco For a Two Percent and Ten Percent Depletion in Ozone

Weighting Function	Ozone Depletion	
	2 percent	10 percent
R-B Meter	1.6	8.6
Human Erythema	3.5	19.0
Setlow DNA	4.3	23.0

EXHIBIT A-5

Percentage Change in Incidence of Basal Cell and Squamous Cell Skin Cancers for a Two Percent Depletion in Ozone for San Francisco

	R-B Meter			Human Erythema			Setlow DNA		
	Low	Mid	High	Low	Mid	High	Low	Mid	High
Basal									
Male	2.13	2.98	3.86	3.55	4.95	6.36	3.99	5.56	7.17
Female	0.72	1.72	2.75	1.19	2.81	4.44	1.33	3.15	4.99
Squamous									
Male	3.20	4.72	6.24	5.41	7.86	10.36	6.14	8.89	11.72
Female	3.10	5.09	7.11	5.52	8.64	11.81	6.36	9.76	13.32

EXHIBIT A-6

Percentage Change in Incidence of Basal Cell and Squamous Cell Skin Cancers for a Ten Percent Depletion in Ozone for San Francisco

	R-B Meter			Human Erythema			Setlow DNA		
	Low	Mid	High	Low	Mid	High	Low	Mid	High
Basal									
Male	11.34	16.14	21.24	19.10	27.34	36.14	21.15	30.41	40.45
Female	3.73	9.07	14.80	6.11	14.87	24.32	6.72	16.43	26.97
Squamous									
Male	17.39	26.46	36.12	30.20	46.05	63.82	33.95	51.87	72.19
Female	16.81	28.78	41.86	30.88	51.40	74.84	35.34	57.93	84.68

REFERENCES

Anderson, R.R. Tissue optics and photoimmunology. In: Photoimmunology, J.A. Parrish, M.L. Kripke, and W.L. Morison, (eds). New York: Plenum Medical Book Co. pp 61-76 (1983).

Beral, V., and N. Robinson. The relationship of malignant melanoma, basal and squamous skin cancers to indoor and outdoor work. Br J Cancer 44:886-891 (1981).

Blewitt, R.W. Why does basal cell carcinoma metastasize so rarely? Int J Dermatol 19:144-146 (1980).

Blohme, I. and O. Larko. Premalignant and malignant skin lesions in renal transplant patients. Transpl 37:165-167 (1984).

Blum, H.F. Wavelength dependence of tumor induction by ultraviolet radiation. JNCI 3:533-537 (1943).

Blum, H.F., H.G. Grady, and J.S. Kirby-Smith. Relationships between dosage and rate of tumor induction by ultraviolet radiation. JNCI 3:91-97 (1942).

Brash, D.E., and W.A. Haseltine. UV induced mutation hotspots occur at DNA damage hotspots. Nature 298:189-192 (1982).

Briele, H.A. and T.K. das Gupta. Natural history of cutaneous malignant melanoma. World J Surg 3:255-270 (1979).

Bruls, W.A.G., H. Slaper, J.C. van der Leun, and L. Berrens. Transmission of human epidermis and stratum corneum as a function of thickness in the ultraviolet and visible wavelengths. Photochem Photobiol 40(4):485-494 (1984).

Burnham, D.K., L.C. Gahring, and R.A. Daynes. Clonal origin of tumors induced by ultraviolet radiation. JNCI 76:151-158 (1986).

Cade, S. Malignant Disease and Its Treatment By Radium. John Wright & Sons, Ltd., Bristol, England, (1940). As cited in Safai and Good (1977).

Carter, D.M. Basal cell carcinoma. In: Dermatology in General Medicine, 3rd ed., Fitzpatrick, T.B., A.Z. Eisen, K. Wolf, I.M. Freedberg, and K.F. Austen, (eds.), New York: McGraw-Hill Book Co. pp. 759-772 (1987).

Cerutti, P.A. and M. Netrawali. Formation and repair of DNA damage induced by indirect action of ultraviolet light in normal and xeroderma pigmentosum skin fibroblasts. Proc 6th Int'l Long Rad Res: 424-432 (1979).

Coker, D.D., E.G. Elias, T. Viravathana, E. McCrea, and M. Hafiz. Chemotherapy for metastatic basal cell carcinoma. Arch Dermatol 119:44-50 (1983).

Cole, C.A., D. Forbes, and R.E. Davies. An action spectrum for UV photocarcinogenesis. Photochem Photobiol 43:275-284 (1986).

Cotran, R.S. Metastasizing basal cell carcinoma. Cancer 14:1036-1040 (1961).

Daynes, R.A., and C.W Spellman. Evidence for the generation of suppressor cells by ultraviolet light. Cell Immunol 31:182-___ (1977).

Daynes, R.A., M.K. Schmitt, L.K. Roberts, and C.W. Spellman. Phenotypic and physical characteristics of the lymphoid cells involved in the immunity to syngeneic UV-induced tumors. J Immunol 122:2458-2464 (1979).

Daynes, R.A., W.E. Samlowski, D.K. Burnham, L.C. Gahring, and L.K. Roberts. Immunobiological consequences of acute and chronic UV exposure. Curr Probl Derm 15:176-194 (1986).

Doak, P.B., J.Z. Montgomerie, J.D.K. North, and F. Smith. Reticulum cell sarcoma after renal homotransplantation and azothioprine and prednisone therapy. Brit Med J 4:746 (1968). As cited in Sheil (1986).

Doniger, J., E.D. Jacobson, K. Krell, and J.A. DiPaolo. Ultraviolet light action spectrum for neoplastic transformation and lethality of Syrian hamster embryo cells correlate with spectrum for pyrimidine dimer formation in cellular DNA. Proc Natl Acad Sci USA 78:2378-2382 (1981).

Dunlap, B., and P. Cerutti. Apyrimidinic sites in gamma-irradiated DNA. FEBS Letters 51:188-190 (1975).

Dunn, J.E., Jr., E.A. Levin, G. Linden, and L. Harzfeld. Skin cancer as a cause of death. Calif Med 102:361-363 (1965).

Eastcott, D.F. Epidemiology of skin cancer in New Zealand. NCI Monograph No. 10:141-151 (1963).

Emmett, A.J. Basal cell carcinoma. In: Malignant Skin Tumors. A.J. Emmett, and M.G.E. O'Rourke (eds). Churchill Livingston, New York (1982).

Epstein, J.H., and W.L. Epstein. Cocarcinogenic effects of ultraviolet light on DMBA tumor initiation in albino mice. J Invest Dermatol 39:455-460 (1962).

Epstein, W.L. Malignant sun induced squamous cell carcinoma of the skin. J Dermatol Surg Oncl 9:505-506 (1983).

Epstein, W.L., J.C. Bystryn, R. Edelson, P.M. Elias, D.R. Lowy, and S. Yuspa. Nonmelanoma skin cancer melanomas, warts and viral oncogenesis. J Amer Acad Dermatol 5(2):960-970 (1984).

Farmer, E.R., and E.B. Helwig. Metastatic basal cell carcinoma: A clinicopathologic study of seventeen cases. Cancer 46:748-757 (1980).

Fears, T.R., and J. Scotto. Estimating increases in skin cancer morbidity due to increased in ultraviolet radiation exposure. Cancer Investig 1(2):119-26 (1983).

Fears, T.R., J. Scotto, and M.A. Schneiderman. Mathematical models of age and ultraviolet effects on the incidence of skin cancer among whites in the United States. Am J Epidemiol 105(5):420-27 (1977).

Findlay, G.M. Ultraviolet light and skin cancer. Lancet (ii):1070-1073 (1928).

Fisher, M.S., and M.L. Kripke. Systemic alteration induced in mice by ultraviolet radiation and its relationship to ultraviolet carcinogenesis. Proc Natl Acad Sci 74:1688-1692 (1977).

Fisher, M.S., and M.L. Kripke. Further studies on the tumor-specific suppressor cells induced by ultraviolet radiation. J Immunol 121:1139-1144 (1978).

Fitzpatrick, T.B., and N.A. Soter. Pathophysiology of the skin. In: Pathophysiology: The Biological Principles of Disease. L.H. Smith, Jr., and S.O. Thier (eds), Philadelphia: W.B. Saunders Co. pp. 1297-1330 (1985).

Fitzpatrick, T.B. Ultraviolet-induced pigmentary changes: Benefits and hazards In: Therapeutic Photomedicine, Honigsmann H. and Stingl G. (eds.) Vienna, KARGER, Basel (1986).

Flaxman, B.A. Growth in vitro and induction of differentiation in cells of basal cell cancer. Cancer Res 32:462-469 (1972).

Forbes, P.D., R.E. Davies, F. Urbach, D. Berger, and C. Cole. Simulated stratospheric ozone depletion and increased ultraviolet radiation: Effects on photocarcinogenesis in hairless mice. Cancer Res 42:2796-2803 (1982).

Fornace, A.J. and K.W. Kohn. DNA-protein cross-linking by ultraviolet radiation in normal human and xeroderma pigmentosum fibroblasts. Biochim Biophys Acta 435:95-103 (1976).

Freedman, V.H., and S. Shin. Cellular tumorigenicity in nude mice: correlation with cell growth in a sensi-solid medium. Cell 3:355-359 (1974).

Freeman, R.G. Data on the action spectrum for ultraviolet carcinogenesis JNCI 55:1119-1122 (1975).

Gange, R.W., and J.A. Parrish. Acute effects of ultraviolet radiation upon the skin. In: Photoimmunology. J.A. Parrish, M.L. Kripke, and W.L. Morison (eds). New York: Plenum Medical Book Co. pp. 77-94 (1983).

Goodman, G.J., R. Marks, T.S. Selwood, M.W. Ponsford, and W. Pakes. Nonmelanotic skin cancer and solar keratoses in Victoria -- clinical studies II. Aust J Dermatol 25:103-106 (1984).

Green, A.C. and M.G.E. O'Rourke. Cutaneous malignant melanoma in association with other skin cancers. JNCI 74(5):977-980 (1985).

Green, A.C.. Ultraviolet exposure and skin cancer: Response. Am J Epidemiol 107:277-80 (1978).

Greene, M.I., M.S. Sy, M. Kripke, and B. Benacerraf. Impairment of antigen-presenting cell function by ultraviolet radiation. Proc Natl Acad Sci USA 76(12):6591-6595 (1979).

Gupta, A.K., C.J. Cardella, and H.F. Haberman. Cutaneous malignant neoplasms in patients with renal transplants. Arch Dermatol 122:1288-1293 (1986).

Hall, J.D,. and D.W. Mount. Mechanisms of DNA replication and mutagenesis in ultraviolet irradiated bacterial and mammalian cells. Prog Nucleic Acid Res Mol Biol 25:53-126 (1981).

Harber, L.C., and D.R. Bickers. Photoprotection. In: Photosensitivity Diseases: Principles of Diagnosis and Treatment, Harber, L.C., and D.R. Bickers, (eds). Philadelphia: W.B. Saunders Co. (1981).

Hardie, I.R., R.W. Strong, L.C.J. Hartley, P.W.H. Woodruff, and G.J.A. Clurie. Skin cancer in Caucasian renal allograft recipients living in a subtropical climate. Surg 87:177-183 (1980).

Hariharan, P.V., and P.A. Cerutti. Excision of ultraviolet and gamma ray products of the 5,6-dihydrothymine type by nuclear preparations of xeroderma pigmentosum cells. Biochim Biophys Acta 447:375-378 (1976).

Hariharan, P.C., and Cerutti, P.A. Formation of products of the 5,6-dihydroxydihydrothymine type by ultraviolet light in HeLa cells. Biochemistry 16(12):2791-2795 (1977).

Harris, T.J. Squamous cell carcinoma. In: Malignant Skin Tumors. A.J. Emmett and M.G.E. O'Rourke (eds.). New York: Churchill Livingston (1982).

Heidelberg, C. Oncogene transformation of rodent cell lines by chemical carcinogens. In: Origins of Human Cancer. H.H. Hiatt, T.D. Watson, and J.A. Winster. (eds). New York: Cold Spring Harbor Laboratory (1977).

Hillstrom, L., and G. Swanbeck. Analysis of etiological factors of squamous cell skin cancer of different locations. Acta Derm Venereol 50:129-133 (1970).

Hoxtell, E.O., J.S. Mandel, S.S. Murray, L.M. Schuman, and R.W. Goltz. Incidence of skin carcinoma after renal transplantation. Arch Dermatol 113:436-438 (1977).

Hughes, J.M. Metastatic basal cell carcinoma: A report of two cases and a review of literature. Clin Radiol 34:392-393 (1973).

Hsu, J., P.D. Forbes, L.C., Harber, and E. Lakow. Induction of skin tumors in hairless mice by a single exposure to UVR. Photochem Photobiol 21:185-288 (1975).

Hu, F. Melanocyte cytology in normal skin, melanocytic nevi and malignant melanomas: A review. In: The Pathology of Malignant Melanoma, A.B. Ackerman, (ed.), New York: Masson Publishing, pp. 1-22 (1981).

Kaidbey, K.H., P.P. Agin, M.M. Sayre, and A.H. Kligman. Photoprotection by melanin -- A comparison of black and caucasian skin. J Am Acad Dermatol 1:249-260 (1979).

Kent, A. Pathology of basal cell carcinoma. In: Cancer of the Skin, R. Andrade, S.L. Gumport, and G.L. Popkin (eds.). Philadelphia: W.B. Sanders Co., pp. 845-882 (1976).

Kinlen, L.J. Incidence of cancer in rheumatoid arthritis and other disorders after immunosuppressive treatment. Am J Med 78 (Suppl 1A):44-49 (1985).

Kligman, L.H., and A.M. Kligman. Histogenesis and progression of ultraviolet light-induced tumors in hairless mice. JNCI 67:1289-1297 (1981).

Kripke, M.L. Latency, histology, and antigenicity of tumors induced by ultraviolet light in three inbred mouse strains. Cancer Res 37:1395-1400 (1977).

Kripke, M.L., J.S. Lofgreen, J. Beard, J.M. Jessup, M.S. Fisher. In vivo immune responses of mice during carcinogenesis by ultraviolet irradiation. J Natl Cancer Inst, 1977, Oct:59(4):1227-30.

Kubilus, J., H.P. Baden, and N. McGilvray. Filamentous protein of basal cell epithelioma: Characteristics in vivo and in vitro. JNCI, 65:869-875 (1980).

Kubitschek, H.E., K.S. Baker, and M.J. Peak. Enhancement of mutagenesis and human skin cancer rates resulting from increased fluences of solar ultraviolet radiation. Photochem Photobiol (in press).

Laerum, O.D., and O.H. Iversen (eds.). Biology of Skin Cancer (Excluding Melanomas): A series of workshops on the biology of human cancer. Report No. 15, International Union Against Cancer, UICC Technical Report Series, Volume 63, Geneva (1981).

Lee, J.H. Melanoma and Exposure to Sunlight. Epidemiol Rev 4:110-136 (1982).

Marks, R., M.W. Ponsford, T.S. Selwood, G. Goodman, and G., Mason Non-melanotic skin cancer and solar keratoses in Victoria. Med J Aust 2:619-622 (1983).

McMurray, D.N. Cell-mediated immunity in nutritional deficiency. Prog Food Nut Sci 8:193-228 (1984).

Miguel, A.G., and R.M. Tyrell. Induction of oxygen dependent lethal damage by monochromatic UV-B (313 nm) radiation: Strand breakage, repair, and cell death. Carcinogenesis 4:375-380 (1983).

Miyazaki H., A. Kawada, Y. Tahaki, T Sato, and M. Matsutani. Effects of ultraviolet light on epidermal dendritic cells of hairless mice. In: Sunlight and Man: M. Pathak, L Harber, M. Seiji, and A. Kukita, (eds.), Tokyo: University of Tokyo Press, pp. 217-229 (1974).

Nathanson, R.B., P.D. Forbes, and F. Urbach. Modification of photocarcinogenesis by two immunosuppressive agents. Cancer Lett 1:243-247 (1976).

National Academy of Sciences (NAS). Causes and Effects of Stratospheric Ozone Reduction: An Update. Washington, D.C.: National Academy Press (1982).

National Cancer Institute (NCI). 1985 Annual Cancer Statistics Review. Presented to the National Cancer Advisory Board, National Institutes of Health, Bethesda, Maryland. (1985).

National Research Council (NRC). Environmental Impact of Stratospheric Flight: Biological and Climatic Effects of Aircraft Emissions in the Stratosphere. Washington, D.C.: National Academy of Sciences (1975).

Nordlund, J.J. Genetic basis of pigmentation and the disorders of pigmentation. In: Pathology of Malignant Melanoma, A.B. Ackerman (ed.), New York: Masson Publishing, pp. 23-45 (1981).

Pathak, M.A. Activation of the melanocyte system by ultraviolet radiation and cell transformation. Ann NY Acad Sci 453:328-339 (1985).

Patrick, M.H., and R.O. Rahn. In: Photochemistry and Photobiology of Nucleic Acids, Vol II, Chap 2. S.Y. Wang (ed.). New York: Academic Press (1976).

Paver, K., K. Poyzer, N. Burry, and M. Deakin. The incidence of basal cell carcinoma and their metastases in Australia and New Zealand. Aust J Dermatol 14:53 (1973).

Peak, M.J., J.G. Peak, M.P. Moehring, and R.B. Webb. Ultraviolet action spectra for DNA dimer induction, lethality, and mutagenesis in Escherichia coli with emphasis on the UV-B region. Photochem Photobiol 40(5):613-620 (1984).

Peak, M.J., and J.G. Peak. Induction of single-strand breaks in human cell DNA by far-ultraviolet, near-ultraviolet, and visible radiations: Action spectrum and mechanisms. (unpublished manuscript).

Peak, M.J., J.G. Peak, and C.A. Jones. Different (direct and indirect) mechanisms for the induction of DNA-protein crosslinks in human cells by far- and near-ultraviolet radiation (290 and 405 nm). Photochem Photobiol 42:141-146 (1985).

Pearl, D.H. A stochastic cancer model involving the environment of transforming cells with application to skin cancer. Ph.D. Thesis, University of California, Berkeley (1984).

Penn, I. Depressed immunity and the development of cancer. Clin Exp Immunol 46:459-474 (1981).

Percy, C., E. Stanek, and L. Gloeckler. Accuracy of cancer death certificates and its effect on cancer mortality statistics. Am J Publ Health 71:242-250 (1981).

Pinkus, H. Premalignant fibroepithelial tumors of skin. Arch Dermatol Syphilol 67:98-615 (1953).

Pollack, S.V., J.B. Gaslen, E.F. Sherertz, and B.V. Jegasothy. The biology of basal cell carcinoma: A review. J Amer Acad Dermatol 7:569-577 (1982).

Romerdahl, C.A., and M.L. Kripke. Regulation of the immune response against UV-induced skin cancers: Specificity of helper cells and their susceptibility to UV-induced suppressor cells. J Immunol 137:3031-3035 (1986).

Romsdahl, M.M., and I.S. Cox. Biological aspects of pigment cells and malignant melanoma. In: Neoplasms of the Skin and Malignant Melanoma, from the 20th Annual Clinical Conference on Cancer, New York: Year Book Medical Publishers, Inc., pp. 251-277 (1976).

Rosdahl, I.K., and G. Szabo. Mitotic activity of epidermal melanocytes in UV irradiated mouse skin. J Invest Dermatol 70: 143-148 (1978).

Rosenstein, B.S., and J.M. Ducore. Induction of DNA strand breaks in normal human fibroblasts exposed to monochromatic ultraviolet and visible wavelengths in the 260-546 nm range. Photochem Photobiol 38:51-56 (1983).

Rundel, R.D. Action spectra and estimation of biologically effective UV radiation. Physiol Plant 58: 360-366 (1983).

Rusch, H.P., B.E. Kline, and C.A. Baumann. Carcinogenesis by ultraviolet rays with reference to wavelength and energy. Arch Pathol 31:135-146 (1941).

Safai, B., and R.A. Good. Basal cell carcinoma with metastasis. Arch Pathol Lab Med 101:327-331 (1977).

Schwartz, R.A., and H.L. Stoll, Jr. Epithelial precancerous lesions. In: Dermatology in General Medicine, 3rd ed. T.B. Fitzpatrick, A.Z. Eisen, K. Wolff, I.M. Freedberg, K.F. Austen (eds.). New York: McGraw-Hill Book Co. pp. 733-796 (1987).

Scott, E.L. Summary of studies made since December 1979: Estimating the increase in skin cancer that will result from the depletion of stratospheric ozone. University of California, Berkeley (1981) (transmitted to J.R. Hibbs, U.S. Environmental Protection Agency, Washington, D.C.) (unpublished).

Scott, E.L., and M.L. Straf. Ultraviolet radiation as a cause of cancer. In: Origins of Human Cancer, Book A, Incidence of Cancer in Humans, Vol. 4. H.H. Hiatt, J.D. Watson, and J.A. Winsten, (eds.). New York: The Cold Spring Harbor Laboratory, pp. 529-549 (1977).

Scott, I.R., Harding, C.R., and Barrett, J.G. Histidine-rich protein of the keratohyalin granules source of the free amino acids, urocanic acid and pyrrolidone carboxylic acid in the stratum corneum. Biochem Biophys Acta 719:110-117 (1982).

Scotto, J., and J.F. Fraumeni, Jr. Skin (other than melanoma). In: Cancer Epidemiology and Prevention. D. Schottenfeld and J.F. Fraumeni, Jr., (eds.), Philadelphia: W.B. Saunders Co., pp. 996-1011 (1982).

Scotto, J., T.R. Fears, and J.F. Fraumeni, Jr. Incidence of Nonmelanoma Skin Cancer in the United States. National Cancer Institute, U.S. Department of Health and Human Services, (NIH) 82-2433 (1981).

Scotto, J., A.W. Kopf, and F. Urbach. Nonmelanoma skin cancer among Caucasians in four areas of the United States. Cancer 34:1333-1338 (1974).

Setlow, R.B., J.D. Regan, J. German, and W.L. Carrier. Evidence that xeroderma pigmentosum cells do not perform the first step in the repair of ultraviolet damage to DNA. Proc Natl Acad Sci USA 64: 1035-1041 (1969).

Setlow, R.B. The wavelengths in sunlight effective in producing skin cancer: A theoretical analysis. Proc Natl Acad Sci USA 69: 3363-3366 (1974).

Sheil, A.G.R. Cancer after transplantation. World J Surg 10:389-396 (1986).

Smith, E.B., and M.M. Brysk. Immunity and skin cancer. South Med J 74:44-46 (1981).

Smith, P.J., and M.C. Patterson. Abnormal responses to mid-ultraviolet light of cultured fibroblasts from patients with disorders featuring sunlight sensitivity. Cancer Res 41: 511-518 (1981).

Spellman, C.W., and R.A. Daynes. Modification of immunologic potential by ultraviolet radiation. II. Generation of suppressor cells in short term UV-irradiated mice. Transplantation 24:120-126 (1977).

Spellman, C.W., and R.A. Daynes. Properties of ultraviolet light-induced suppressor lymphocytes within a syngeneic tumor system. Cell Immunol 36:383-387 (1978).

Spikes, J.D. UV-damage in biological systems. In: Experimental and Clinical Photoimmunology, Daynes, R.A., and Spikes, J.D. (eds.). Boca Raton: CRC Press Inc. pp. 28-41 (1983).

Spikes, J.D., M.L. Kripke, R.J. Conner, and E.J. Eichwald. Time of appearance and histology of tumors induced in the dorsal skin of C3Hf mice by ultraviolet radiation from a mercury arc lamp. JNCI 59:1637-1643 (1977).

Stenback, F. Species-specific neoplastic progression by ultraviolet light on the skin of rats, guinea pigs, hamsters and mice. Oncology 31:309-225 (1975).

Stern, R.S., N. Laird, J. Melski, J.A. Parrish, T.B. Fitzpatrick, and H.L. Bleich. Cutaneous squamous-cell carcinoma in patients treated with PUVA. N Engl J Med 310(18):1156-1161 (1984).

Stoll, H.L., R.A. Schwartz. Squamous cell carcinoma. In: Dermatology in General Medicine, 3rd, T.B. Fitzpatrick, A.Z. Eisen, K. Wolf, I.M. Freedberg, and K.F. Austen. New York: McGraw-Hill Book Co., pp. 746-758 (1987).

Strickland, P.T., F.J. Burns, and R.E. Albert. Induction of skin tumors in the rat by single exposure to ultraviolet radiation. Photochem Photobiol 30:683-688 (1979).

Sutherland, B.M., N.C. Delihas, R.P. Oliver, and J.C. Sutherland. Action spectra for ultraviolet light-induced transformation of human cells to anchorage independent growth. Cancer Res 41:2211-2214 (1981).

Tyrrell. Damage and repair from non-ionizing radiation, In: Repairable Lesions in Microorganisms, A. Hurst, and A. Nasim (eds). London: Academic Press (1984).

Urbach, F., D.B. Rose, and M. Bonnem. Genetic and environmental interactions in skin carcinogenesis. In: Environment and Cancer, (eds). Baltimore: Williams and Wilkins Co., pp. 355-371 (1972).

Urbach, F., C.J. Witcop, and O.D. Laerum. Skin cancer in man. In: Biology of Skin Cancer (Excluding Melanomas), O.D. Laerum and O.H. Iverson (eds.), Geneva: International Union Against Cancer, pp. 58-86 (1981).

van der Leun, J.C. Yearly Review: UV-Carcinogensis. Photochem Photobiol 39(6):861-868 (1984).

Vitaliano, P.P., and F. Urbach. The relative importance of risk factors in nonmelanoma carcinoma. Arch Dermatol 116:454-456 (1980).

Winkelman, R.K., P.E. Zollman, and E.J. Baldes. Squamous cell carcinoma produced by ultraviolet light in hairless mice. J Invest Derm 40:217-224 (1963).

Zeger, S.L., L. Cameron, E. Gold, and E. Emmett. Nonmelanoma skin cancer and ultraviolet radiation. Johns Hopkins School of Hygiene and Public Health (1986), (unpublished).

CHAPTER 8

CUTANEOUS MALIGNANT MELANOMA

SUMMARY

In 1987, it is estimated that there will be 25,800 cases and 5,800 deaths from cutaneous malignant melanoma (CMM) in the United States. For more than a decade, there has been serious concern that CMM is at least partially caused by ultraviolet-B (UV-B) radiation. However, several aspects of the scientific information about CMM have puzzled researchers and have contributed to uncertainty about the relationship of CMM to solar radiation, in particular UV-B. In the past several years, some progress has been made in understanding CMM and its possible relationship to solar radiation, and there now exists an array of evidence that indicates that exposure to solar radiation, and to UV-B in particular, is a likely cause of CMM.

Supporting evidence includes (1) for this relationship the fact that people who lack the protection of pigmentation which blocks penetration of ultraviolet radiation (UVR) in the skin have higher CMM incidence rates; (2) a correlation, in well-designed ecological studies, of higher CMM rates with decreasing latitude and increasing UV-B levels; (3) the discovery of an association between freckling and nevus formation (risk factors for CMM) and solar exposure; (4) differences in CMM rates found between natives and immigrants to sunny climates; (5) high rates of CMM in patients who are genetically deficient at repairing DNA damage induced by UV-B; and (6) the indication, in controlled studies, that sun exposure at early ages and of an intermittent nature results in higher CMM risks.

The results of some studies have created uncertainty about the relationship between solar radiation and CMM: several econological studies failed to find latitude gradients for CMM; outdoor workers have been found to have lower CMM rates than indoor workers (but higher non-melanoma skin cancer rates); and anatomic sites with lower sun exposure have high CMM rates.

The latter evidence has made it clear that the relationship between solar radiation and CMM is not a simple one. Indeed other information indicates that the relationship is a complex one. Part of the complexity lies in the nature of CMM. It is a multifactorial disease which includes several histologically different types of tumors with different biologic behavior and clearly different relationships to solar exposure. Additional complexity is contributed by the nature of the relationship of UV exposure to CMM; not only is there likely to be a direct relationship via an initiating (DNA damaging) step, but an indirect relationship via promotional events such as immunosuppression, is also likely. Indeed the information contributing to the uncertainty about the relationship indicates that cumulative dose based on total number of hours in the sun may not be the appropriate dose parameter to correlate with CMM development. This has led to the emergence of hypotheses that postulate the importance of intermittent exposure to high fluxes of UV-B (resulting in large UV-B doses) in the causation and/or promotion of CMM.

Unfortunately, at this time, there have been no studies which have examined the correlation between CMM and actual measured UV-B doses received by individuals, thus making it impossible to prove various hypotheses concerning CMM. The balance of available evidence appears to support the conclusion that solar radiation is at least a major cause of CMM. Other evidence appears to indicate that cumulative sun-exposed hours is not an appropriate measure of dose for CMM, and that CMM has a complicated etiology.

A variety of different kinds of evidence supports the hypothesis that UV-B is a component of solar radiation that causes CMM. Most important is the fact that xeroderma pigmentosum patients, who are genetically deficient in repairing UV-B-induced DNA damage, have significantly higher rates of CMM than the general population. Another fact that supports this hypothesis is that, in experimental studies, UV-B is the most mutagenic and carcinogenic waveband as well as being the most active at causing immunosuppression. All of this information suggests that UV-B is the primary component of solar radiation that causes CMM. Together, this evidence does not provide proof that UV-B is the waveband of solar radiation that causes CMM; however, the preponderance of evidence makes UV-B a likely cause of CMM.

Finally, although much remains uncertain about the relationships among solar radiation, UV-B, and CMM, enough information exists to make reasonable estimates of the dose-response relationships that exist between UV-B and CMM. These can then be used to estimate future incidence and mortality of CMM if ozone depletion occurs. The possible relationships based on an improving but still deficient database in the United States indicate that each 1 percent ozone depletion will produce around a 1 to 2 percent increase in incidence and 0.8 to 1.5 percent increase in mortality. At this time, it is impossible to estimate how incidence and mortality of CMM will change in other countries whose populations have unknown skin pigmentation and sun exposure behavior.

FINDINGS

1. CUTANEOUS MALIGNANT MELANOMA (CMM) IS A SERIOUS LIFE-THREATENING DISEASE THAT AFFECTS A LARGE NUMBER OF PEOPLE IN THE UNITED STATES. THERE ARE SEVERAL HISTOLOGICAL FORMS OF MELANOMA THAT ARE LIKELY TO HAVE SOMEWHAT DIFFERENT ETIOLOGIES AND RELATIONSHIPS TO SOLAR AND UV-B RADIATION.

   1a. CMM incidence and mortality is increasing among fair-skinned populations. These increases appear not to be merely the result of improved diagnosis and reporting.

   1b. In 1987, it is estimated that there will be an estimated 25,800 cases of CMM and 5,800 fatalities related to melanoma in the United States. In the absence of ozone depletion, the lifetime risk of CMM in the United States is expected to be about 1 in 150.

2. LIMITATIONS IN THE DATABASE PREVENT ABSOLUTE CERTAINTY ABOUT THE RELATIONSHIP OF SOLAR RADIATION, UV-B, AND CUTANEOUS MALIGNANT MELANOMA (CMM).

   2a. There currently is no animal model in which exposure to UV-B radiation experimentally induces melanomas.

   2b. There is also no experimental *in vitro* model for malignant transformation of melanocytes.

   2c. No epidemiologic studies of CMM have been conducted in which individual human UV-B exposures (and biologically effective doses of solar radiation) have been adequately assessed.

3. EVALUATION OF THE EPIDEMIOLOGICAL AND EXPERIMENTAL DATABASES FOR MELANOMA REQUIRES CLOSE ATTENTION TO THE RELATIONSHIP OF WAVELENGTH AND DOSE AND TO THE VARIATIONS OF SOLAR RADIATION IN THE AMBIENT ENVIRONMENT.

   3a. Ozone differentially removes wavelengths of UV-B between 295 and 320 nm; UV-A (320-400 nm) in wavelengths above 350 nm is not removed, nor is visible light (400-900 nm). Ozone removes all UV-C (i.e., wavelengths less than 295 nm).

   3b. Wavelengths between 295 nm and 300 nm are generally more biologically effective (i.e., damage target molecules in the skin, including DNA) than other wavelengths in UV-B and even more so than UV-A radiation.

   3c. Latitudinal variations exist in solar radiation; model predictions indicate that the greatest variability is seen in cumulative UV-B (e.g., monthly doses) followed by peak UV-B (highest one-day doses) and then cumulative UV-A. Peak UV-A does not vary significantly across latitudes up to 60°N. Greater ambient variation also exists in UV-B than in UV-A by time of day.

   3d. The biologically effective dose of radiation that actually reaches target molecules depends on the duration of exposure at particular locations, time of day, time of year, behavior (i.e., in terms of clothes and sunscreens), pigmentation, and other characteristics of the

skin including temporal variations (e.g., changes in pigmentation due to tanning).

3e. Cloudiness and albedo, although causing large variations in the amount of exposure to UV-B and UV-A, do not greatly change the ratio of UV-B to UV-A.

3f. Ozone depletion is predicted to cause the largest increases in radiation in the 295-299 nm UV-B range, less in the 300-320 nm UV-B range; UV-A is virtually unaffected by ozone depletion.

3g. Cutaneous malignant melanoma has a number of different histologic types that vary in their relationship to sunlight, site, racial preference, and possibly in their precursor lesions. Assessment of incidence by types is not consistent among registries, thus complicating attempts to evaluate the relationship between CMM and solar radiation.

3h. Melanin is the principal pigment in skin that gives it color; melanin effectively absorbs UV radiation; the darker the skin, the more the basal layer is protected from UV radiation.

4. A LARGE ARRAY OF EVIDENCE SUPPORTS THE CONCLUSION THAT SOLAR RADIATION IS ONE OF THE CAUSES OF CUTANEOUS MALIGNANT MELANOMA.

4a. Whites, whose skin contains less protective melanin, have higher incidence and mortality rates from CMM than do blacks.

4b. Light-skinned whites, including those who are unable to tan or who tan poorly, have a higher incidence of CMM than do darker-skinned whites.

4c. Sun exposure leading to sunburn apparently induces melanocytic nevi.

4d. Individuals who have more melanocytic nevi have a higher incidence of CMM; the greatest risk is associated with a particular type of nevus -- the dysplastic nevus.

4e. Sunlight induces freckling, and freckling is an important risk factor for CMM.

4f. Incidence has been increasing in cohorts in a manner consistent with changes in patterns of sun exposure, particularly with respect to increasing intermittent exposure of certain anatomical sites.

4g. Immigrants who move to sunnier climates have higher rates of CMM than populations who remain in their country of origin. Immigrants develop rates approaching those of prior (but native born) immigrants to the adopted country; this is particularly accentuated in individuals arriving before the age of puberty (10-14 years).

4h. It has been suggested that CMM risk may be associated with childhood sunburn; other evidence suggests that childhood sunburn may reflect an individual's pigmentary characteristics or may be related to nevus development, rather than being a separate risk factor.

4i. Most studies that have used latitude as a surrogate for sunlight or UV-B exposure have found an increase in the incidence or mortality of CMM correlated to proximity to the equator. A recent study of incidence using measured UV-B and CMM survey data found a strong relationship between UV-B and incidence of CMM. Another study that used modeled UV-B data and an expanded database on mortality found a strong UV-B/mortality relationship.

4j. One form of CMM, Hutchinson's melanotic freckle, appears almost invariably on the chronically sun-damaged skin of older people.

5. SOME EVIDENCE CREATES UNCERTAINTY ABOUT THE RELATIONSHIP BETWEEN SOLAR RADIATION AND CUTANEOUS MALIGNANT MELANOMA.

5a. Some ecologic epidemiology studies, primarily in Europe or close to the equator, have failed to find a latitudinal gradient for CMM.

5b. Outdoor workers generally have lower incidence and mortality rates for CMM than indoor workers, which appears incompatible with a hypothesis that cumulative dose from solar exposure causes CMM.

5c. Unlike basal cell and squamous cell carcinomas, most CMM occurs on sites that are not habitually exposed to sunlight; this contrast suggests that cumulative exposure to solar radiation or UV-B is not solely responsible for variations in CMM.

6. UV-B RADIATION IS A LIKELY COMPONENT OF SOLAR RADIATION THAT CAUSES CUTANEOUS MALIGNANT MELANOMA (CMM), EITHER THROUGH INITIATION OF TUMORS OR THROUGH SUPPRESSION OF THE IMMUNE SYSTEM.

6a. Xeroderma pigmentosum patients who fail to repair UV-B-induced pyrimidine dimers in their DNA have a 2,000-fold excess rate of CMM by the time they are 20.

6b. UV-B is the most active part of the solar spectrum in the induction of mutagenesis and transformation in vitro.

6c. UV-B is the most active part of the solar spectrum in the induction of carcinogenesis in experimental animals and is considered by most to be a causative agent of nonmelanoma skin cancer in humans.

6d. UV-B is the most active portion of the solar spectrum in inducing immunosuppression, which may have a role in melanoma development.

6e. The limitations in the epidemologic and experimental database leave some doubt as to the effectiveness of UV-B wavelengths in causing CMM.

7. WHILE UNCERTAINTY EXISTS, INCREASES IN THE INCIDENCE AND MORTALITY OF CUTANEOUS MALIGNANT MELANOMA ARE LIKELY AS A RESULT OF OZONE DEPLETION. WHILE MANY UNCERTAINTIES EXIST (E.G., REGARDING ACTION SPECTRA, PEAK VERSUS CUMULATIVE DOSE, ETC.) ABOUT THE NATURE OF THE RELATIONSHIP BETWEEN UV-B AND MELANOMA, THE FACT THAT UV-B RADIATION VARIES ACROSS THE ENVIRONMENT IN THE RANGE OF VARIATION EXPECTED FROM DEPLETION PROVIDES INFORMATION USUALLY

UNAVAILABLE TO RESEARCHERS MAKING QUANTITATIVE RISK ESTIMATES. THUS ALTHOUGH IMPERFECT, EPIDEMIOLOGIC INFORMATION EXISTS TO ESTIMATE A RANGE OF CHANGES IN INCIDENCE AND MORTALITY IF THE OZONE LAYER IS DEPLETED.

7a. Uncertainty exists about the appropriate action spectrum to be used in estimating dose, the best functional form for dose-response, and the best way to characterize dose (peak value, cumulative summer exposure, etc.). Histologically different CMMs (or possibly CMM located at different anatomical sites) are likely to have different dose-response relationships. Most estimates of CMM dose-response relationships fail to consider these histological or site differences. Nonetheless, by encompassing a range of possibilities, it is possible to estimate dose-response because of the systematic variations in UV-B.

7b. A recent study by the NIH presents a well-designed ecological study of melanoma and UV-B using survey data and measured UV-B at ground level. While uncertainties exist, this dose-response relationship, when used with different action spectra and assumptions about the importance of peak versus cumulative exposure, can be utilized to estimate a range of values for cases. The relationship estimates that a 1 percent change in ozone is likely to increase incidence by between slightly less than 1 to 2 percent, depending on the choice of action spectrum. The appropriate action spectrum is likely to be encompassed in the range of erythema and DNA.

7c. Melanoma mortality is estimated at about 25 percent of all cases. This result is consistent with the projections of a dose-response model of mortality developed by EPA/NCI. It is estimated that a 1 percent change in ozone would result in between a 0.3 and a 2.0 percent change in CMM mortality depending on the assumptions about the appropriate dose and UV weighting functions used in the model.

7d. Additional uncertainties for projecting future incidence and mortality of CMM in the U.S. include the lack of an adequate database describing variations in skin pigmentation and human sun-exposure behavior among different populations and estimates of how these relationships may change in the future.

INTRODUCTION

This chapter is designed to examine the current state of knowledge with regard to the relationship between human cutaneous malignant melanoma and solar radiation, in particular UV-B. Two previous reviews examining this question came to the following somewhat contradictory conclusions:

> "The NCI [National Cancer Institute] is collecting skin melanoma incidence from ten locations in the United States. Earlier data analyses indicate that skin melanomas, which predominate in Caucasians, are related to UV-B exposure. A preliminary finding is that the incidence is increasing and that the rate of increase may be greater than expected from earlier surveys. The dose-response relationship between skin melanoma and UV-B appears to be more complicated than that observed for nonmelanomas of the skin." (NAS 1979)

> "...since 1976, the case for an association between UV-B and melanoma has been weakened rather than strengthened by the results of additional clinical, pathological and epidemiological studies. Furthermore (with the exception of a single animal), it has not been possible to use UV-B alone to induce melanomas in experimental animals." (NAS 1982)

These contrasting conclusions require that a closer examination be made of the relationship between melanoma and UV-B.

Since publication of the second NAS document in 1982, more information has been gathered; this chapter reviews briefly both the old and the new information in order to ascertain what can be said at the current time about the relationship of UV-B to melanoma. A much more detailed review of the relevant information is presented in Appendix A.

Background on Melanoma and the Concept of Response

Malignant melanoma is a rare tumor that arises as the result of the neoplastic transformation of a melanocyte. Melanocytes are pigment-producing cells. Exhibit 8-1 shows the relationship of the melanocyte to other cells in the epidermis and other skin layers.

The major function of the melanocyte is the production and distribution of melanin to keratinocytes -- the major cell population of the skin. Melanin is a pigment that absorbs UV light over a broad range of wavelengths (25 nm to 1200 nm); it is the principal chromophore responsible for the difference between black and white skin in the transmittance of UV light (shown in Exhibit 8-2).

Melanin is a pigment that absorbs light in the broad range of 250-1200 nm; however, its absorption increases steadily towards the shorter wavelengths (Anderson 1983). It is synthesized in melanocytes from tyrosine and deposited in a protein matrix in organelles termed melanosomes (Romsdahl and Cox 1976). Melanosomes, in turn, are eventually destributed to keratinocytes which are vertically arranged in the skin. In humans and other mammals there are two predominant forms of melanin: eumelanin, which is brown or black, and phaeomelanin, which is yellow or auburn (the pigment responsible for red hair).

EXHIBIT 8-1

Location of Melanocyte in the Epidermis

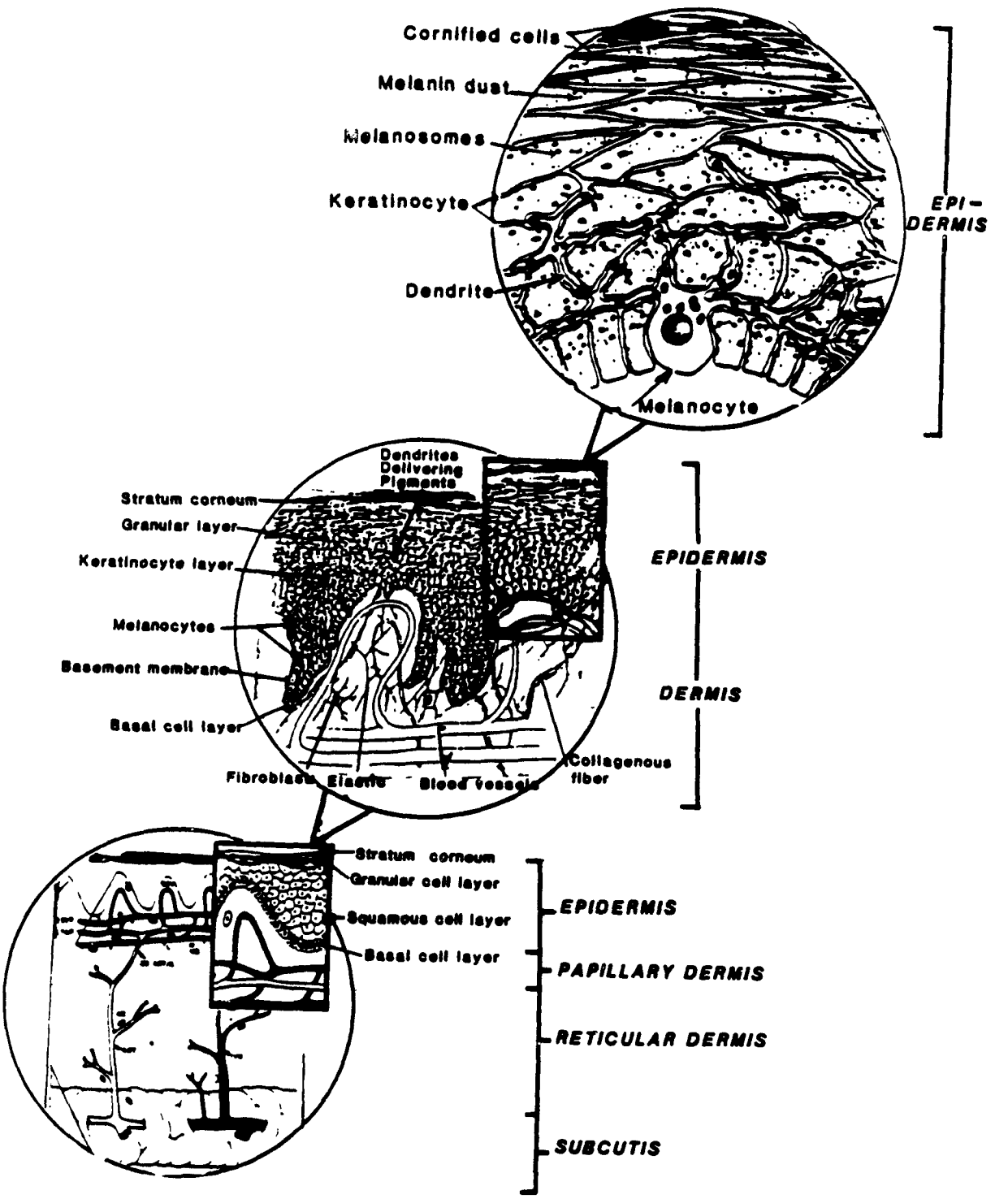

EXHIBIT 8-2

Comparative Transmittance of UV Radiation

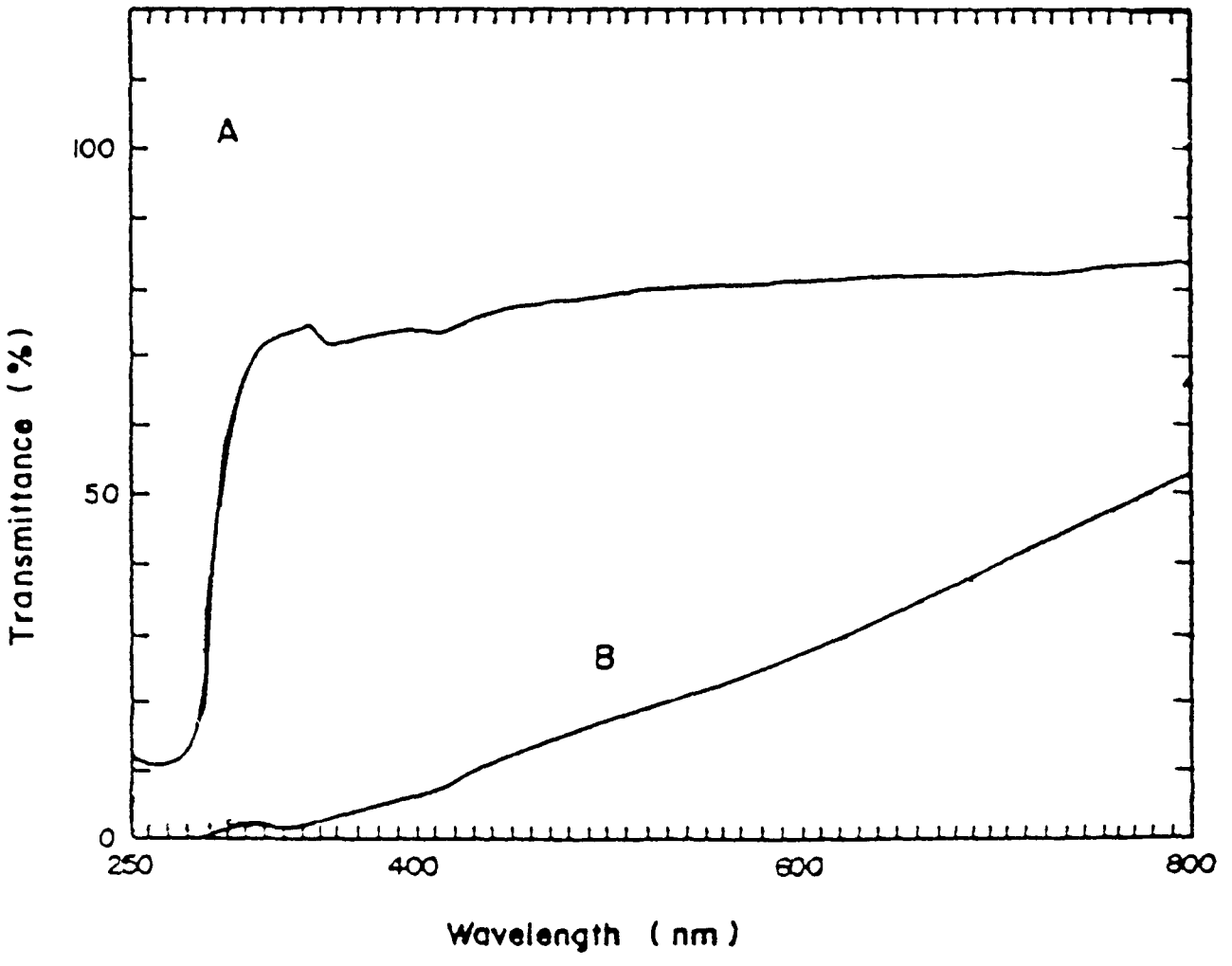

A: Caucasians; B: dark blacks.

Source: Wan et al. 1981.

The melanosomes containing these two types of melanin differ structurally in that those with phaeomelanin are round and have a protein matrix with a "tangled" appearance, whereas eumelanin-containing melanosomes are round and have a characteristic lamellar structure (Norlund 1981).

It is the degree of melanosome aggregation and their number which determine skin color. Melanosomes in keratinocytes from light-skinned individuals are characteristically found as aggregates, whereas melanosomes in keratinocytes from dark-skinned individuals, because they are larger, generally occur singly. Extensive studies have indicated nonsignificant differences in the number of melanocytes in various racial groups, although there are variations by anatomic region. The highest concentration of melanocytes is in the cheek (2,310 + 150 melanocytes/mm^2) and the lowest is in the back and thigh (890 $\pm$ 70/mm^2 and 1,000 $\pm$ 70/mm^2, respectively) (Briele and das Gupta 1979).

The biology of cutaneous malignant melanoma is complex; there are several morphologic types of tumor that may have different pathways of histogenesis; they tend to behave differently in terms of age at appearance and characteristic location, and yet have common elements in their progression. The majority $\geq$85% of melanomas are superficial spreading and nodular; these are located on the habitually or intermittantly exposed (trunk) areas, while the melanomas on the feet and hands, etc. are $\leq$10% in whites (Fitzpatrick 1986). Brief information is presented below; more detailed information is found in Appendix A.

Terminology for the four principal classes of melanomas was proposed by McGovern et al. (1973) and has been subsequently modified (Smith 1976; Elder et al. 1980). The four principal types of melanoma are given below:

(1) Melanoma arising in Hutchinson's melanotic freckle (HMF); it occurs predominantly on sites receiving the greatest cumulative exposure and is thought to have the strongest relationship to cumulative solar exposure.

(2) Superficial spreading melanoma (SSM); it shows the strongest preference for sites that are intermittently exposed (trunks in males, lower extremities in females). It also shows a stronger association with nevi-possible precursor lesion.

(3) Nodular melanoma (NM); it has growth characteristics that differ from those of SSM and HMFM, although these types may progress to NM.

(4) Unclassifiable melanoma (UCM).

A fifth type of melanoma -- acral lentiginous melanoma (ALM) -- has been distinguished with a site preference for soles, palms, and subungual surfaces. It is virtually the only form observed in blacks and in people who have never lived south of the Artic Circle (Clarke et al. 1986). Thus in characterizing response to dose, aggregation of all types of melanoma will tend to obfuscate real relationships.

EPIDEMIOLOGIC EVIDENCE

With the above background, the remainder of this chapter will review the epidemiologic and experimental evidence relevant to assessing the role of solar radiation and UV-B in the development of CMM. Since the National Academy of Sciences published its latest document (NAS 1983) evaluating the impact of UV-B on skin cancer, several major epidemiologic studies have been completed by Green, Holman, Elwood, Dubin, and their colleagues. These authors' results have provided valuable insights into the potential relationships between sunlight and melanoma. At the same time, these results have illustrated the extremely complex nature of CMM. In this section, the major findings presented in these recent studies will be briefly reviewed. Then, because of the extensive quantity of epidemiologic information available, five areas of evidence--time trends, anatomical site distribution, exposure factors, host factors, and miscellaneous factors--will each be reviewed. This discussion is followed by a brief review of the experimental evidence and a discussion of possible dose-response relationships.

Recent Epidemiologic Studies

The epidemiologic data described below were based on information obtained from four different parts of the world. Green and her colleagues examined epidemiologic data from Queensland in Northeast Australia, while Holman and his colleagues focused on data from Western Australia. Elwood and his colleagues analyzed data from Western Canada. Data obtained from three New York City hospitals were evaluated by Dubin and his colleagues.

Green and Colleagues - Queensland Melanoma Data

The Queensland patient series consists of 633 cases of first primary CMM diagnosed at the 24 Queensland pathology laboratories between 1 July 1979 and 30 June 1980, directly age-standardized to 1979 Australian Bureau of Statistics population estimates. Patient information included age, sex, residential address at time of diagnosis, and histologically classified lesion according to the Clark method. In a series of seven publications to date, Green and her colleagues have examined several subsets of the Queensland patient series. The four major studies present case-control comparisons for randomly selected patient subsets and age-, sex-, and residence- matched controls randomly selected from the Queensland electoral roll. Information obtained on each subject included lifetime sun exposure (occupational or recreational), acute and chronic response to sun exposure, episodes of severe sunburn, complexion (skin, eye, and hair color), number of nevi (2 mm or more in diameter) on the left arm, family melanoma history, social class (based on occupation), ethnic origin, and nonmelanotic facial skin cancers.

In the first study of 183 matched case-control pairs (Green 1984), the risk of melanoma was observed to increase as cumulative hours of sun exposure throughout life increased, even after adjusting for the effects of exact age, presence of nevi on the arms, hair color, and sunburn propensity in a multivariate model. For less than 2,000 cumulative hours of sun exposure, the relative risk (RR) was 1.0. For 2,000 to 50,000 hours, the RR was 3.2 (95% C.I. 0.9-12.4) and for more than 50,000 hours, the RR was 5.3 (95% C.I. 0.9-30.8). A subsequent analysis of the same 183 matched case-control pairs (Green et al. 1985) indicated a strong association between the presence of <u>any pigmented nevi</u>

(check) on the arms and CMM. The RR, after adjusting for hair color, propensity to sunburn, and lifetime sun exposure, was 30.1. The authors observed that, among all the phenotypic characteristics evaluated, the major CMM determinants were nevi on the arms, propensity to sunburn upon acute exposure, and hair color.

The third published examination of the 183 matched case-control pairs (Green, et al. 1985b) revealed an association between multiple sunburns and CMM. After controlling for age and the number of nevi on the arms, the relative risk of developing CMM was 1.5 for those with 2-5 sunburns per lifetime and 2.4 for 6 or more sunburns. The dose-response relationship of increasing CMM risk with increasing number of sunburns per lifetime was statistically significant ($p < 0.05$). When the presence of skin cancers, migrant status, and social class were taken into account, the relative risks remained essentially unchanged.

In the fourth case-control study of 232 matched case-control pairs (Green and O'Rourke 1985), increased risks were associated with the presence of facial actinic tumors (RR = 3.6 after adjusting for age and nevi). Risks also increased with increasing lifetime sun exposure. After adjusting for age, nevi, hair color, and sunburn propensity, the relative risks were 3.2 for 2,000-50,000 hours cumulative exposure and 5.3 for 50,000 or more hours exposure.

Based on the results of these studies, Green and her colleagues have made several observations regarding the potential associations between CMM and sunlight. They have indicated that the data

- "strongly suggest that melanoma does have an association with high doses of solar UV radiation" (Green 1984), and

- in conjunction with "similar findings regarding the risk of melanoma in sun sensitive persons... provide excellent circumstantial evidence that sun exposure has a causal association with disease [CMM]" (Green et al. 1985).

Holman and Colleagues - Western Australia Melanoma Data

Holman and his colleagues have presented several important case-control comparisons based on 511 melanoma patients presenting from 1 January 1980 to 5 November 1981 in Western Australia and 511 age-, sex-, and residence-matched controls. In addition to determining histogenic tumor type, level of invasion, and tumor thickness, information corrected on each case and control by interview consisted of skin, hair, and eye color, number of palpable nevi on the arms, history of sun exposure, hormone use, diet, measurements of weight, height, hairiness, and extent of actinic damage in skin (based on cutaneous microtopographs), acute and chronic skin reactions to sunlight, ethnicity of grandparents, family history of melanoma or xeroderma pigmentosum, history of mole excisions, and treatment of nonskin cancers. Skin color was measured at the dorsum of the left hand (continuous sun exposure), tip of left shoulder (intermittently exposed), and left upper inner arm (not usually exposed) and was graded according to ranges of reflectance values (%).

In one analysis of this case-control data (Holman and Armstrong 1984), the strongest risk factor identified was the number of palpable benign nevi on the

arms, with crude RRs of 2.0 for 1-4 nevi, 4.0 for 5-9 nevi, and 11.3 for 10 or more nevi ($p < 0.0001$). The authors noted that nevi are probably important "either as an early stage in the pathogenesis of non-HMF melanomas or as indicators of increased risk." Inability to tan was the most important pigmentary trait associated with the risk of CMM, followed by susceptibility to sunburn, and then hair color. After taking these three factors into account, skin and eye color had no additional effects, leading the authors to conclude "that the ability to tan quickly in response to sunlight is of prime importance in reducing risk of skin cancers and is more important than the base-line skin color."

Another evaluation of the case-control data (Holman and Armstrong 1984a) focused on indicators of total accumulated exposure to the sun and separate histogenic tumor types. Two important factors were positively associated with CMM risk: duration of residence in Australia of migrants and mean annual hours of bright sunlight (averaged over a lifetime) among native-born Australians. For all melanomas combined and SSM alone among migrants, age at arrival was a better predictor of melanoma risk than was duration of residence. The authors suggested that "it is possible that exposure to sunlight in childhood is a factor in the production of benign nevi, which have their strongest relationship with SSM, probably as precursor lesions." Among native Australians, the risk of developing CMM significantly increased with increasing mean annual hours of bright sunlight for all melanomas combined ($p = 0.003$) and for SSM alone ($p = 0.02$). The gradient of increasing risk was steepest, however, for HMFM.

Holman and Armstrong (1984a) also observed that persons with a history of nonmelanotic skin cancer had a threefold higher risk of developing CMM ($p < 0.00001$) and SSM, and a fivefold higher risk of developing HMF ($p = 0.001$). After controlling for the effects of chronic and acute skin reactions to sunlight, hair color, and number of European, African, and Asian grandparents, the risks associated with nonmelanotic skin cancers dropped slightly, suggesting that the association with nonmelanotic skin cancer was explained only partly by constitutional factors. Based on the results of this study, Holman and Armstrong (1984a) concluded that HMF "may be related to the total accumulated dose of sunlight received on exposed body sites." They also suggested that their results generally supported the hypothesis that "an individual's maximum potential to develop SSM would be fixed by the number of initiated nevus cells induced by UV radiation and other agents in childhood and young adulthood." Finally, they concluded that "a role of sunlight in the causation of NM is supported by these results."

A third study of the case-control data focused on the relationship between CMM and individual sunlight-exposure habits (Holman et al. 1986). The authors identified the presence, and absence, of several associations:

- Increased risks of SMM were associated with low total outdoor exposure in early adulthood and frequent participation in boating and fishing. SSM of the trunk was related to the frequency of sunbathing at 15-24 years of age and to exposure of the trunk while working outdoors.

- The risks of developing CMM (except for SSM) were higher in persons if the body site was sometimes exposed rather than usually exposed or usually covered.

- In females, the risks of developing CMM on the trunk were significantly elevated (odds ratio = 12.97) in those who work a bikini or bathed nude at 15-24 years of age compared to those who wore a more conservative one-piece bathing suit.

- After controlling for confounding factors (e.g., hair color, skin reaction to sunlight, ethnic origin, age at arrival in Australia), only HMF showed a relationship to the highest severity of past sunburn. No relationship was observed between childhood sunburn or sunburn in early adulthood and any histologic type of melanoma.

- Little support for the hypothesis that CMM may be related to occasional bursts of recreational sun exposure during early adult life was obtained when recreational sun exposure was expressed as a proportion of total outdoor exposure (a proportion which had been considered, a priori, to be an index of intermittent sunlight exposure).

Holman et al. (1986) noted that "some but not all" of their results supported the hypothesis that intermittent exposure plays an important role in the etiology of SSM. They concluded that their results suggested that "nevi and occasional or recreational sun exposure interact to produce an effect on the rate of SSM greater than the addition of the two independent effects but... less than expected [based on] multiplication of effects."

Holman and his colleagues published one more important study since 1982 on the relationship between CMM and exogenous sex hormones and reproductive factors (Holman et al. 1984d). The case-control study was based on the 276 female CMM patients identified in the West Australia Lions Melanoma Research Project from 1980 to 1981 and 276 age- and residence-matched female controls. No consistent evidence was observed of a relationship between incidence rates of different histogenic tumor types and age at menarche, duration of menstral life, degree of obesity, number of pregnancies of more than 20 weeks' duration, or use of oral contraceptives. However, borderline evidence was shown of an association between SSM and duration of estrogen use.

Elwood and colleagues - Western Canada Melanoma Study

This major case-control study was based on data from four western Canadian provinces (British Columbia, Alberta, Saskatchewan, and Manitoba). The cases consist of 595 histologically confirmed primary CMM patients registered in each province's cancer registry from 1 April 1979 to 31 March 1981 (excluding acral lentiginous melanoma and lentigo maligna). Each patient was matched by sex and age with a control randomly selected from medical insurance plan subscriber lists. Information obtained by interview from each case and control included pigmentation, skin freckling in childhood, sensitivity to sunlight, tanning and sunbathing behavior (both as an adult and as a child), residence, occupational

history, recreational activities with specific reference to sunlight exposure, medical history, chronic drug use, family history, diet, smoking and alcohol consumption. In addition, for women participants, information was gathered on reproductive history and the use of oral contraceptives and menopausal estrogents. Skin and hair color were determined by direct comparison with prosthesis and wigmaker samples made specifically for the project. Eye color was recorded based on direct observation.

In the first published analysis of this data (Elwood et al. 1984), CMM risks were observed to be significantly increased among individuals with increasingly light hair and skin color (pigmentation factors), many freckles in adolescence, and a tendency to burn and rarely tan. The associations with these risk factors did not substantially change after adjustment for ethnic origin or UV exposure during occupational or recreational activities. Elwood et al. (1984) concluded that their results "are consistent with the hypothesis that SSM and NM [which were diagnosed in the majority of the cases] develop from nevi and suggest that SSM and NM have similar relations to characteristics of pigmentation." After observing that the associations between CMM and a history of severe or frequent sunburns became weaker and non-significant by adjusting for pigmentation factors, the authors suggested "that rather than the occurrence of sunburn itself increasing the risk of melanoma, the risk is due to the characteristics of pigmentation associated with poor sun tolerance."

In a subsequent analysis of the case-control data, which focused on intermittent and chronic sun exposure (Elwood et al. 1985a), factors significantly associated with CMM were vacation and recreational activities during which a bathing suit or very light clothing is worn and increasing number of sunny vacations per decade (after adjusting for skin and hair color, freckling in adolescence, and ethnic origin). The risk of developing CMM was also significantly elevated among individuals with mild occupational sun exposure (roughly 8 hours/week) but not among those with higher occupational sun exposures (over 8 hours/week). The authors concluded that their results "suggest that intermittent and continuous exposures have different effects øand! are consistent with the hypothesis that intermittent sun exposure raises the risk of melanoma, while long-term constant exposure may have no effect or may reduce risk."

The third published analysis to date focused on the effects of sunburn and suntan to CMM risk (Elwood et al. 1985b). The results showed that a mild suntan in winter and summer and a history of severe vacation sunburns are both independently associated with elevated CMM risks. However, neither factor is a significant predictor of risk when usual reaction to sun exposure (e.g., tan with no burn or burn, rarely tan) is concurrently evaluated. In a multivariate analysis of history of vacation sunburns, usual degree of suntan, usual reaction to sun, and a host factor score (representing skin and hair color and freckling in childhood), the usual reaction to sun variable and host factor score were the only statistically significant predictors of CMM risk. Individuals with a tendency to burn easily were at nine times greater risk of developing CMM than those with a tendency to tan and not burn. Individuals with light hair and skin color and many freckles in adolescence were at 37 times greater risk than those with dark hair and skin color and few freckles in adolescence. The results indicate that the tendency to burn easily and tan poorly is more strongly associated with CMM than is the history of sunburn or suntan. "The implication," state the authors, "is the factor contributing to the risk of

melanoma is the individual's tendency to burn rather than the history of having had burns."

Dubin Colleagues - New York University Medical Center Data

This large case-control study was based on 1,103 primary CMM patients seen at the New York University Medical Center from 1972 to 1982 and 585 non-matched controls (Dubin et al. 1986). In a multiple logistic regression of the data, Dubin et al. observed elevated risks for those with no ability to tan (relative to average ability), no tendency to burn (relative to tendency for painful burn), a history of freckling, red hair color, blue eyes, and a previous medical history of solar keratosis.

Time Trends

As indicated in Exhibit 8-3, there have been sharp increases in incidence and mortality due to CMM reported in Caucasian populations worldwide (Magnus 1982; Roush et al. 1985b; Osterlind and Jensen 1986). Based on observational and analytical evidence, most experts agree that these trends in CMM incidence and mortality are genuine, and not due to increases in the registration and diagnosis of the disease (Magnus 1975; Pakkenen 1977; Malec et al. 1977). It has been estimated that in 1987 there will be 25,800 cases and 5,800 deaths from CMM (Kopf 1987). At the current rate of increase, the lifetime risk of CMM for individuals born in the United States in the year 2000 has been predicted to be 1 in 150 (Kopf et al. 1984).

Birth cohort analyses of CMM incidence rates across six nations show consistent increases in CMM for cohorts born between 1910 and 1930, whereas later birth cohorts (1940-1950) that show these increases do so to a lesser extent (Muir and Nectoux 1982). Most authors that have conducted cohort analyses of CMM incidence and mortality rates conclude that virtually all secular increases in CMM are due to cohort effects (Magnus 1981a 1981b; Houghton et al. 1980; Muir and Nectoux 1982; Holman et al. 1980a; Cooke et al. 1983).

In most countries, the first signs of increasing rates are seen in cohorts born around 1900, though increases in cohorts born as early as 1865 are observed in Australia and New Zealand (Holman et al. 1980a; Cooke et al. 1983). In Norway and several other countries, there is a slight tendency for a slowing of increase in incidence in cohorts born around and after 1930 (Magnus 1981a). Stabilization of mortality rates is also occurring in cohorts born 1925-1939 and later in countries such as Australia, New Zealand, England, Wales, and Finland (Lee and Carter 1970; Teppo 1978; Holman et al. 1980a; Cooke et al. 1983).

Age-adjusted incidence rates of CMM of the head, neck, and face for birth cohorts born after approximately 1900 have not differed markedly; however, age-adjusted incidence rates of CMM of the lower extremities among females and the trunk among males have increased in successively younger birth cohorts born during the first half of this century (Magnus 1981a; Houghton et al. 1980; Cooke et al. 1984; Stevens and Moolgavkar 1984).

On the basis of the Connecticut Tumor Registry data, modeling of the CMM incidence rates observed in subsequent birth cohorts indicated that the incidence rate of CMM in the 1955 birth cohort will rival those for colon

EXHIBIT 8-3

Increases in Incidence and Mortality Rates From Malignant Melanoma in Different Countries

	Country	Sex	First Period of Observation: Time	First Period of Observation: Rate per 10^6	Second Period of Observation: Time	Second Period of Observation: Rate per 10^6	Percent Increase	Total Number of Years	Average Annual Percent Increase*
Incidence	New York State	M	1941-1943	1.2	1967	3.4	176	25	7.0
		F	1941-1943	1.8	1967	2.9	65	25	2.6
Incidence	Norway	M	1955	1.8	1970	6.3	264	15	17.6
		F	1955	2.6	1970	6.8	195	15	13.0
Mortality	Norway	M	1956-1960	1.6	1966-1970	2.7	69	10	6.9
		F	1956-1960	1.3	1966-1970	1.8	36	10	3.6
Mortality	Canada	M	1951-1955	0.7	1966-1970	1.4	93	15	6.2
		F	1951-1955	0.6	1966-1970	1.2	107	15	7.1
Mortality	United Kingdom	Both	1950	0.5	1967	1.0	100	16	6.3
Mortality	Australia	M	1931-1940	1.0	1961-1970	3.6	267	30	8.9
		F	1931-1940	0.8	1961-1970	2.5	227	30	7.6
Mortality	Denmark	M	1956-1960	1.6	1966-1969	2.4	49	10	4.9
		F	1956-1960	1.6	1966-1969	2.1	32	10	3.2
Mortality	Sweden	M	1956-1960	1.7	1966-1968	2.1	30	9	3.3
		F	1956-1960	1.1	1966-1968	1.5	40	9	4.4
Incidence	Connecticut	M	1935-1939	1.1	1975-1979	8.2	645	40	16.1
		F	1935-1939	0.9	1975-1979	6.8	656	40	16.4
Incidence	U.S.A.	WM	1974	6.7	1983	9.6	43	10	4.3
		WF	1974	6.0	1983	8.3	38	10	3.8
Mortality	U.S.A.	WM	1950	1.0	1977	2.6	160	27	5.9
		WF	1950	0.8	1977	1.6	200	27	7.4

* Computed by dividing total percent increase in incidence or mortality rate by the number of years between the first and second periods of observations. The figures in this column do not represent compounded annual growth rates.

Adapted from: Elwood and Lee (1975); Sondik et al. (1985); Heston et al. 1985.

cancer, currently the third most common cancer in Connecticut (Roush et al. 1985a).

Those anatomical sites that show the greatest amount of increase are not the sites that receive the greatest amount of cumulative solar exposure. This finding tends to lead to a conclusion that cumulative solar exposure is not causally associated with melanoma; as discussed in more detail below, cutaneous melanoma may be related to some other measure of exposure to solar radiation.

Anatomical Site Distribution

Cutaneous malignant melanoma has a unique anatomical distribution that has been the subject of numerous epidemiologic investigations. Research efforts have focused on the site-specific trends in CMM incidence related to sex, age, race, histogenic type, birth cohort, and season. The most pronounced differences have been associated with gender, race, and birth cohort.

The overall site distribution is presented in Exhibit 8-4. There is wide variability among the studies presented in the exhibit, making it difficult to generalize about these data. However, as a rule, among white populations, the upper extremities have the lowest overall proportion of melanomas, while the lower extremities have the highest proportion. The variability is most probably due to differences among the study populations, such as their sex and racial distribution.

Gender is one of the factors associated with the most pronounced differences in CMM site distribution. Exhibit 8-5 lists data from 14 studies that reported CMM site distribution by sex. Data in the table indicate that most of the studies observed higher incidences of CMM on the lower extremities among females and on the trunk among males than on other parts of the body. Most authors have concluded that the observed differences in site distribution by gender are not incompatible with the role of sunlight as a major etiologic factor (Pathak et al. 1982, Crombie 1981; Hinds and Kolonel 1980).

Race and gender also are associated with pronounced effects in site distribution of CMM. The predominant difference is a higher percentage of CMM emphasize that increase occurring on the feet and, in some cases, on the hands of darker-skinned ethnic groups. These groups have a much lower incidence than the light-skinned ethnic groups, so that the higher percentages on feet may not represent a higher incidence. Trauma has been suggested as a possible reason for the increased percentage of melanomas occurring on feet (Lewis 1967; Hinds 1979). Although in a recent review of the subject, Briggs (1984) concluded that there is no unequivocal evidence for a role of trauma in the vast majority of melanomas. One group has concluded that sunlight is not an important risk factor for melanoma (Hinds 1979; Hinds and Kolonel 1980) for any site among non-Caucasians.

There appear to be site-dependent differences in melanoma incidence by age, with melanomas of the face showing one pattern and melanoma of trunks and lower extremities, another. In several instances the differences have been identified as being between continuously exposed sites (e.g., head) and intermittently exposed sites (e.g., trunk and lower extremities). As a general rule the pattern observed for the exposed sites is characteristic of that observed for many other cancers -- a slow increase with age, up to the age of 40 or 50,

EXHIBIT 8-4

Anatomic Site Distribution of Cutaneous Malignant Melanoma
(Percentage of Total Tumors)

Location	Years	Sample Size	Head/Neck	Trunk	Extremities		Source
					Upper	Lower	
United States[a] (Caucasian)	1978-1981	4,864	20	35	23	22	Scotto and Fears 1986
Texas	1944-1966	911	22	25	19	13	MacDonald 1976
Texas	1954-1970	510	25	16	21	37	Smith 1976
Alabama	1955-1980	537	27	28	19	23	Balch et al. 1982
New Mexico	1966-1977	403	27	29	19	25	Pathak et al. 1982
New South Wales	1955-1980	1,110	14	37	14	33	Balch et al. 1982
Queensland	1977	690	21	34	20	24	Little et al. 1980
New Zealand (Maori/Polynesian)	1963-1981	24	13	13	0	54	Moss 1984
Israel	1960-1972	966	16	25	21	38	Anaise et al. 1978
Norway	1955-1970	2,541	22[b]	43[c]	8	18	Magnus 1973
Finland	1953-1973	2,501	19	37	10	26	Teppo et al. 1978
Japan	1961-1982	546	15	20	13	46	Takahashi 1983
Hong Kong	1964-1982	43	7	7	21[d]	63[e]	Collins 1984
Uganda	1963-1966	152	8	11[f]	5	72[g]	Kiryabwire et al. 1968

[a] Based on data from Seattle, Detroit, Iowa, Utah, San Francisco/Oakland, Atlanta, and New Mexico.
[b] Face.
[c] Neck/truck.
[d] 17 percent of the total on the hands.
[e] 56 percent of the total on the feet.
[f] "Skin" and genitals.
[g] Feet and legs.

EXHIBIT 8-5

Anatomic Site Distribution of Cutaneous Malignant Melanoma by Gender
(Percentage of total tumors by gender[a])

Location (Ethnic Group)	Years	Sample Size	Sex	Head/Neck	Trunk	Extremities		Source
						Upper	Lower	
			Predominantly Caucasian Study Populations					
United States	1980	4,545	F	15	31	19	35	Balch et al. 1984
			M	23	53	13	11	
United States[b]	1978-1981	4,864	F	16	25	26	33	Scotto and Fears (in press) 1986
			M	24	45	21	11	
North America (Caucasian)	-	-	F	16	29	18	36	Crombie 1981[c]
			M	27	44	17	12	
Europe (Caucasian)	-	-	F	16	23	13	47	Crombie 1981[c]
			M	23	42	13	23	
Texas (White)	1944-1966	1,252	F	17	18	25	28	MacDonald 1976
			M	23	25	20	11	
Hawaii (Caucasian)	1960-1977	262	F	9	28	28	35	Hinds and Kolonel 1980
			M	24	37	24	15	
New Mexico (Anglos)	1966-1977	403	F	22	20	21	37	Pathak et al. 1982
			M	33	41	16	10	
Israel	1960-1972	966	F	16	19	15	50	Anaise et al. 1978
			M	16	32	21	31	
Scotland	1961-1976	477	F	25	14	14	47	Pondes et al. 1981
			M	32	27	11	30	
Finland	1953-1973	2,501	F	18	28	11	36	Teppo et al. 1978
			M	19	48	9	17	
Denmark	1943-1957	1,204	F	24	19	14	33	Clemmesen 1965
			M	32	25	9	22	(cited in Lee 1982)
Queensland	1977	713	F	19	21	22	35	Little et al. 1980
			M	23	45	17	13	
Texas	1954-1970	510	F	17	10	24	50	Smith 1976
			M	34	23	18	24	

EXHIBIT 8-5 (Continued)

Anatomic Site Distribution of Cutaneous Malignant Melanoma by Gender
(Percentage of total tumors by gender[a])

Location (Ethnic Group)	Years	Sample Size	Sex	Head/Neck	Trunk	Extremities		Source
						Upper	Lower	
Mixed Study Populations								
Israel (Mixed Race)	1961-1967	368	F	15	21	15	42	Movshovitz and Modan 1973
			M	17	35	5	25	
Japan	1961-1982	546	F	20	19	18	42[d]	Takahashi 1983
			M	13	23	11	51[e]	
Texas (Spanish surname)	1944-1966	206	F	22	16	18	30	MacDonald 1976
			M	18	22	11	30	
Texas (Non-White)	1944-1946	30	F	6	6	18	53	MacDonald 1976
			M	31	--	8	54	
New Mexico (Hispanics)	1969-1977	35	F	23	36	32	9	Pathak et al. 1982
			M	23	46	23	8	
Hawaii (Non-Caucasian)	1960-1970	66	F	26	17	13	44	Hinds and Kolonel 1980
			M	16	19	19	47	
Hawaii (Non-Caucasian)	1960-1977	64	F	26	17	13	44[f]	Hinds 1979
			M	16	20	20	44[g]	
Uganda	1963-1966	152	F	6	11[h]	4	78[i]	Lewis 1967
			M	10	11[h]	5	74[j]	

[a] Percentages may not total 100 percent because of rounding errors and exclusion of "other sites" of MM.

[b] Based on data from Seattle, Detroit, Iowa, Utah, San Francisco/Oakland, Atlanta, and New Mexico.

[c] Trunk includes scrotum and "unspecified" melanomas.

[d] 29 percent of the total were on the feet.

[e] 39 percent of the total were on the feet.

[f] 22 percent of the total were on the feet.

[g] 42 percent of the total were on the feet.

[h] "Skin" and genitals.

[i] 63 percent of the total were on the feet.

[j] 64 percent of the total were on the feet.

followed by a rapid increase with age thereafter (Magnus 1981b; Teppo 1982; Holman et al. 1980b). For the intermittently exposed sites, the pattern is quite different a relatively steep increase that peaks between 40 and 60 (depending on the data set) and levels off or decreases thereafter (Magnus 1981a,b; Teppo 1982; Holman et al. 1980b).

There are also differences in the anatomic distribution of melanomas associated with different histologic (histogenetic) types of CMM. HMFM and its precursor lesion, HMF, are observed predominantly on the face and other exposed sites, whereas SSM was most commonly observed on less exposed sites (trunk and lower extremities) (Holman et al. 1980b, Smith 1976, Adler and Gaeta 1979, Pondes et al. 1981).

Very few studies have examined the relationship of geographic area to differences in a anatomic site distribution. In Norway, Magnus (1973) noted that the only site lacking a definite north/south gradient was the foot, and a comparison of Alabama patients to Australian patients revealed that whereas melanomas of the trunk were the most common in both sets of patients, melanomas of the lower extremities were more common in Australians than in the Alabama patients, and head and neck tumors showed the reverse trend (Balch et al. 1982).

A final important parameter that has been associated with differences in site distribution of CMM is the temporal pattern of exposure. This is a complex parameter that is, as indicated earlier, difficult to separate from the observed age effects, but it is fairly clear that there are differences in the anatomic distribution of melanomas, which are associated with the year of diagnosis and/or birth cohort. It is difficult to generalize, however, the conclusion drawn by Boyle et al. (1983) that there were cohort effects of melanoma incidence that differed by site and that the site effects differed by sex. The overall impression from the studies that looked at these cohort effects is, as well, that birth cohort-site differences are greater for sites that are intermittently exposed (e.g., trunk and lower extremities) than for those that are always exposed (e.g., face).

Exposure Factors

A number of studies have examined how various indicators or measures of exposure are related to melanoma incidence or mortality. This section reviews information from ecological studies that have looked at the correlation of melanoma incidence or mortality on the one hand, and geographic location and migration on the other. Studies that have examined the relationship between type of exposure (e.g., early, intermittent) and melanoma incidence are also discussed.

Geographic Location

Within predominantly Caucasian nations, most of the ecological studies of melanoma and latitude show increasing melanoma incidence and/or melanoma mortality with decreasing latitude, leading to the hypothesis that melanoma is associated with ultraviolet radiation because of the strong correlation between UV and latitude. As a general rule, those studies that failed to find this association did not adequately account for pigmentation differences (Crombie 1979b) or had other serious methodological flaws (poor measurement of UV-B) (Baker-Blocker 1980).

In general, melanoma rates (incidence and/or mortality) were found to be higher in areas closer to the equator, in coastal rather than inland areas, and in urban rather than rural areas within various nations (Holman and Armstrong 1984; Green and Siskind 1983; Magnus 1981a, 1981b).

Migrant Behavior

In an Australian study (Holman and Armstrong 1984b), age at arrival in Australia was more important than duration of residence with respect to the risk of SSM, with arrival before age 10 incurring a risk approaching or exceeding the risk of SSM for those born in Australia. The odds ratio decreased when the age at arrival was 10-14 years and stabilized at a significantly lower level for those arriving at or after the age of 15.

Immigrants moving to sunnier climates in which the native CMM incidence rates exceed those of the immigrant's country of origin initially tend to have lower CMM risks than the native population. These risks increase, however, with increasing duration of residence or earlier age of arrival in the adopted homeland (Holman and Armstrong 1984b).

Type of Sun Exposure

Early Exposures. CMM risk is associated with childhood sunburn (Green, et al. 1985b, Elwood et al. 1985b) but this association appears only to reflect an individual's pigmentary characteristics as related to poor sun tolerance. One study that evaluated the risk associated with outdoor work before college found a significantly elevated odds ratio for those who had worked outdoors compared with those who had not (Paffenbarger et al. 1978).

Intermittent ("Summer Sun") Exposure. One commonly examined surrogate for intermittent exposure has been a parameter related to a history of sunny vacations (Eklund and Malec 1978; Klepp and Magnus 1979; Adam et al. 1981). Different studies have used slightly different measures of this type of exposure behavior (e.g., one study evaluated those who "tanned themselves while on holiday abroad" (Adam et al. 1981), another evaluated those with a history of long (30 days or more), sunny vacations as a child (Lew et al. 1983). In general, however, there was a positive association between CMM risk and increasing number of "sunny vactions" taken.

The strongest evidence for an association between a measure of sunny vacation exposure comes from a case-control study conducted in Western Canada (Elwood et al. 1985a, 1985b). Analysis of data from this study of 595 melanoma case-control pairs indicated that there was a significant ($p < 0.001$) trend of increasing risk of CMM with increasing numbers of sunny vacations per decade, with a relative risk of 1.8 associated with four or more sunny vacations per decade. In addition, this relative risk remained significant (RR = 1.7, 95% C.I. 1.2-2.3) even after controlling for significant host factors (hair color, skin color, history of freckles) and ethnic origin.

At least one study that evaluated a different measure of intermittent exposure found no significant association between intermittent exposure and an increased incidence of any histologic type of CMM (Holman et al. 1986). This study of 507 pairs (matched according to sex, age, and residence) used as its surrogate for intermittent exposure a variable based on the ratio of

recreational outdoor sun exposure in summer to total outdoor sun exposure in summer.

In the same study (Holman et al. 1986), an increased SSM risk for some summer sun activities at early ages (from history or estimated) was observed for boating, fishing, and female sunbathing (on trunk). This study also found some increased risks for summer sun exposure by clothing habits. The primary CMM site was more frequently "sometimes exposed to sun" than usually exposed or usually covered, except for SSM, which showed increasing risk with increasing exposure. The risk of developing CMM of the trunk (especially SSM) was found to be greater for women whose bathing suits covered less of their bodies between 15 and 24 years of age.

A seasonal pattern with a summertime peak was found for CMM incidence rates (female in U.S. [Scotto and Nam 1980], both sexes in Hawaii [Hinds et al. 1981]). This seasonal pattern may be related to greater awareness of skin changes in summer months or could indicate promotional effects of UV-B exposures.

Sunburn. A number of case-control studies that have examined the relationship of CMM to history of sunburn have found statistically significant associations. (Beral et al. 1983, Elwood et al. 1984) Most of these studies did not, however, adjust for pigmentary factors. One study that controlled for pigmentary factors found a significant association (Lew et al. 1983); however, in this study, biased selection of controls was likely, leaving this association in doubt. The conclusion drawn from studies that appeared to be subject to the fewest biases was that the presence or absence of factors associated with a tendency to sunburn, rather than the sunburn itself, determine the CMM risk. In a very recent report, Armstrong and his colleagues (1986) observed a significant correlation between number of burns received up to the age of ten and the number of nevi. Thus, the relationship of CMM to sunburn could be via an intermediate risk factor - number of nevi.

A study from Western Australia (Holman, et al. 1980b) found significantly increased total CMM risk, SSM risk, and HMFM risk with increased annual hours of bright sunlight at residence, with increasing actinic skin damage, and with previous nonmelanoma skin cancer.

Assessment of individual exposure through questionnaires. In Western Canada, an analysis of total sun exposure showed some increased risks in higher exposure groups compared with the lowest exposure group but none were statistically significant nor was there a significant trend of increasing risk (Holman et al. 1986).

In Queensland, Australia, elevated CMM risks were associated with increasing estimated total hours of sun exposure at age 10 years and older after adjustment for exact age, presence of nevi on arms, hair color, and sunburn propensity. The confidence intervals for intermediate and higher levels of exposure include unity.

Indirect measures of cumulative sun exposure (i.e., assessment of numbers of hours exposed) show correlations with melanoma risk that were significant, borderline significant, and not significant. Several studies have evaluated a direct measure of received dose (i.e., actinic skin damage), which is also a

measure of the skin's responsiveness to insult. In these studies, melanoma risk increased significantly with the degree of actinic skin damage.

Exposure During Sunspot Activity. Most studies that examined the relationship between CMM incidence rates and sunspot cycles found high correlations (Houghton et al. 1978; Wigle 1978). Different studies have observed differences in the lag time between the period of sunspot activity and changes in CMM incidence rates.

Most of the information presented above tends to support a relationship between melanoma and some function of increased exposure to solar radiation. What the exact function of sunlight exposure may be is unclear. There is some indication that early (childhood) exposure may be important, and other information implicates intensive exposure such as that which occurs during summertime and times of sunspot activity; however, no single kind of exposure clearly stands out. None of these studies considered UV-B, which varies significantly with time of day. Thus, by using sun-exposed hours as a dose variable, such studies may be inaccurately assessing dose, especially when they compare across occupations whose sun-exposure behavior may vary significantly.

Host Factors

There is clear evidence that certain host factors are associated with the risk of developing CMM. It is possible that the factors described below reflect the capability to modify the dose of solar radiation potentially received by a target cell or modify the ability of the cell to respond to insult.

Epidemiologic studies have shown that Caucasian populations have much higher rates of CMM incidence and mortality than other racial groups. Crombie (1979a) analyzed data from the International Agency on Cancer dataset on cancer incidence on five continents and found a statistically significant three-fold increase in CMM incidence in whites over that of non-whites. In South Africa, CMM was approximately six times more frequent in whites than in blacks. Broken down by sex, the ratio of white to black CMM incidence was greater for males (13:1) than for females (4:1) (Rippey and Rippey 1984). Black/white differences in the United States population were even greater, although this may be due to differences in the quality of cancer registry data between South Africa and the United States. Based on 1983 SEER data, white to black ratios were 19:1 and 8:1 in males and females, respectively (Sondik et al. 1985). In addition, whites in New Zealand experience much higher incidence rates than New Zealand Maoris and Polynesians. Likewise, American Indians experience much lower rates of CMM than American whites.

Within white populations, rates of CMM differ according to country of origin. CMM incidence rates for Hispanic whites in New Mexico, for example, are much lower than those for non-Hispanic whites; individuals from the Mediterranean countries in southern Europe tend to have lower rates than Caucasians from northern Europe; individuals of Celtic origin in Australia tend to have higher rates than non-Celtic individuals. Variation in the incidence of CMM within the Caucasian race is commonly thought to be a function of variation in genetically determined pigmentary traits across ethnic groups.

Numerous epidemiologic studies have focused on identification of important pigmentary characteristics in the etiology of CMM. Exhibit 8-6 shows a summary

EXHIBIT 8-6

Malignant Melanoma Risk Factors by Measures of Skin Pigmentation Within the Caucasian Population

Study Reference	Measures of Skin Pigmentation Within Caucasian Population					
	Skin Color	Hair Color	Eye Color	Freckling	Reaction to Sun (Tanning/ Sunburn)	Ethnicity
Lancaster and Nelson 1957	+	+	+		+	
Gellin et al. 1969	+	+	+		+/-	
Lane-Brown et al. 1971						+
IARC 1976						+
MacDonald 1976						+
Klepp and Magnus 1979		-	-	+	+	
Mackie and Atchinson 1982					-	
Beral et al. 1983	+	+	-	+	+	
Hinds and Kolonel 1983						+
Lew et al. 1983		-	-		+	
Elwood et al. 1984	+	+		+	+	+
Holman and Armstrong 1984b	+	+	+	+	+	+
Graham et al. 1985	+	+	+		+	+

NOTE: + = Significant risk factor.
- = Not significant risk factor.
Blank = Not included in study.

of findings from a number of these studies. The following associations between pigmentary traits and CMM risk have been found:

(a) Skin color -- in all studies reviewed, fair complexions were associated with higher risks of CMM than were dark complexions.

(b) Hair and eye color -- in most studies, red and blond hair in childhood were associated with increased risk of CMM relative to dark hair. Blue eyes were an independent risk factor in only one of four well-controlled epidemiologic studies; however, this could be due to the homogeneous nature of most of the study populations.

(c) Freckling -- those who freckled readily were at consistently elevated CMM risk relative to other individuals.

(d) Reaction to sun exposure -- in most studies reviewed, individuals who usually burned and were unable to tan were at significantly higher risk of CMM than those who tanned easily.

Exposure to sunlight appears to encourage the appearance (and possibly the disappearance) of nevi (including dysplastic nevi) from the skin (Kopf et al. 1978, 1985; Armstrong et al. 1986). Dysplastic nevi are clearly a risk factor for melanoma independent of freckling or other pigmentary characteristics; it also appears that the pressure of congenital nevi as well as acquired melanocytic nevi may also be risk factors (Elder et al. 1981).

Information from xeroderma pigmentosum (XP) patients indicates that individuals who have an inability to repair solar-radiation-induced DNA damage also have a high incidence of CMM relative to the normal population (Kraemer et al. 1984). The best characterized defect in XP patients is an inability to excise pyrimidine dimers (Cleaver 1983), which suggests that the repair of such lesions can be important to prevention of CMM development.

Miscellaneous Factors

Although a number of possible etiologic agents for melanoma have been evaluated (e.g., exposure to chemicals or ionizing radiation), no strong candidate has emerged. It has been suggested that the risk of developing CMM may be elevated among individuals exposed to fluorescent lighting at work (Beral et al. 1982); however, several recent well-controlled studies have failed to find such an association (Rigel et al. 1983; Durbin et al. 1986; Elwood et al. 1986). Indeed, one of these studies initially found a positive association based on personal interviews, but a self-administered postal survey of the same study subjects did not confirm the initial findings Pasternack et al. 1983; Durbin et al. 1986).

Total CMM incidence has been found to be higher among professional and administrative indoor office workers, but not among other indoor workers relative to outdoor workers (Lee and Strickland 1980; Holman et al. 1980a);

however, the implications of this finding may be confounded by differences in socioeconomic status, melanoma site, and histologic type. There is a higher risk of indoor office workers developing CMM on an anatomical site that is usually covered (e.g., the trunk) than on a site that is usually exposed (e.g., the face) (Beral and Robinson 1981; Vagero et al. 1986). For usually covered parts of the body, the incidence of CMM among indoor office workers is higher than for outdoor workers. And the reverse is also true; for usually uncovered parts of the body, the incidence of CMM is higher among outdoor workers than among indoor office workers (Beral and Robinson 1981; Vagero et al. 1986).

It is not clear why certain indoor workers are at greater risk for developing CMM than outdoor workers, nor why in these individuals the affected sites are those not normally exposed. One speculation is that indoor workers have more leisure time and that they spend that time under conditions of solar exposure that maximize intensive UV-B exposures of areas that are not protected by a tan; however, there is no information currently available from a published study that would allow this hypothesis to be examined. From current data it is clear that for certain indoor workers, cumulative sun hours of exposure are not associated with melanoma risk. This information does not rule out that some other measure of exposure (e.g., number of high UV-B exposures received at a time of low tan) may be associated with melanoma risk.

Weighing and Balancing the Epidemiologic Evidence

In summary, while there is no single piece of evidence that proves that solar radiation causes CMM, the weight of the available epidemiologic evidence clearly supports the conclusion that solar radiation plays a major role in the development of CMM for susceptible populations. Cumulative dose (i.e., total sun-exposed hours) clearly does not explain important variations in incidence rates. Although from existing evidence it is not possible to determine the most accurate method of calculating dose, the collective evidence does suggest that exposure to solar radiation in some form produces cutaneous malignant melanomas in Caucasian populations.

EXPERIMENTAL EVIDENCE

Much of the experimental evidence relevant to the relationship of CMM and exposure to UV-B has been reviewed on non-melanoma skin cancer. To briefly recapitulate, there are five important points:

(1) UV-B is the most active portion of solar radiation responsible for the induction of adverse effects on mammalian systems; it has been shown in vivo and in vitro to induce transformation of mammalian epidermal cells, (albeit not melanocytes), and to be mutagenic to them as well. All of these effects are thought to occur by a mechanism that involves damage to the DNA (Doniger et al. 1981)

(2) UV-B at 295-300 nm is the most active waveband of UVR for these effects, as well as for the induction of pyrimidine dimers. (See pg 7 of Chapter 7.)

(3) Patients with xeroderma pigmentosum, who cannot repair pyrimidine dimers induced in DNA by UV-B (which are thought to be important to skin cancer development) have a 2000-fold higher rate of CMM by the time they are 20 than normal individuals. (Kraemer et al. 1984)

(4) UVR is carcinogenic in animals and it is the UV-B wavelengths that are the most effective at inducing cancer -- the shorter UV-B wavelenths being more carcinogenic than the longer ones (Forbes et al. 1981). The tumors induced are principally fibrosarcomas and squamous cell carcinomas; melanomas have not yet been experimentally induced with any consistency by UVR. Suppression of the immune response in humans (e.g., in renal transplant patients or those on immunosuppressive drugs) have increased incidence of malignant melanoma.

(5) UVR, and specifically UV-B, can induce the generation of T suppressor cells, which specifically suppress the immune response to UV-induced tumors. The suppressor cells have been shown to be capable of shortening the latent period of tumors induced by UV-B, and UV-B-treated animals also appear to have increased susceptibility to transplanted melanomas. (For detailed discussion see chapter 9.)

Weighing and Balancing the Experimental Evidence

The experimental data indicate that UV-B irradiation damages DNA and induces carcinogenesis and immunosuppression in animals. CMM rates are elevated in patients who cannot repair UVR-induced lesions in DNA. Thus solar ultraviolet radiation has the potential to effect CMM development in multiple ways. A pictorial representation of this, developed by Dr. Thomas Fitzpatrick (1987) of Harvard University, is presented in Exhibit 8-7.

DOSE-RESPONSE RELATIONSHIPS

Empirical relationships between exposure to UV-B and the incidence and mortality of CMM have been estimated in several studies using population-based mortality or incidence information.

Animal studies are inadequate for estimating CMM dose-response because there is no animal model for melanoma induced by UV-B. Because the limitations in animal studies appear insurmountable at this time, epidemiologic studies provide the best candidate dose-response relationships for risk estimation. There are no epidemiologic studies in which individual human UVB exposures have been measured. Instead, population-based estimates of UVB exposure have generally been used to assess dose-response relationships. This section reviews four such studies. Three of the studies -- Fears et al. (1976, 1977) and Scotto and Fears (1986) -- develop dose-response relationships associating UV-B and melanoma incidence. Two studies -- Fears et al. (1976) and Pitcher (1987) -- estimate dose-response relationships for melanoma mortality.

Exhibit 8-7

Multiple Ways in Which UVR
Can Play a Role in Melanoma Development

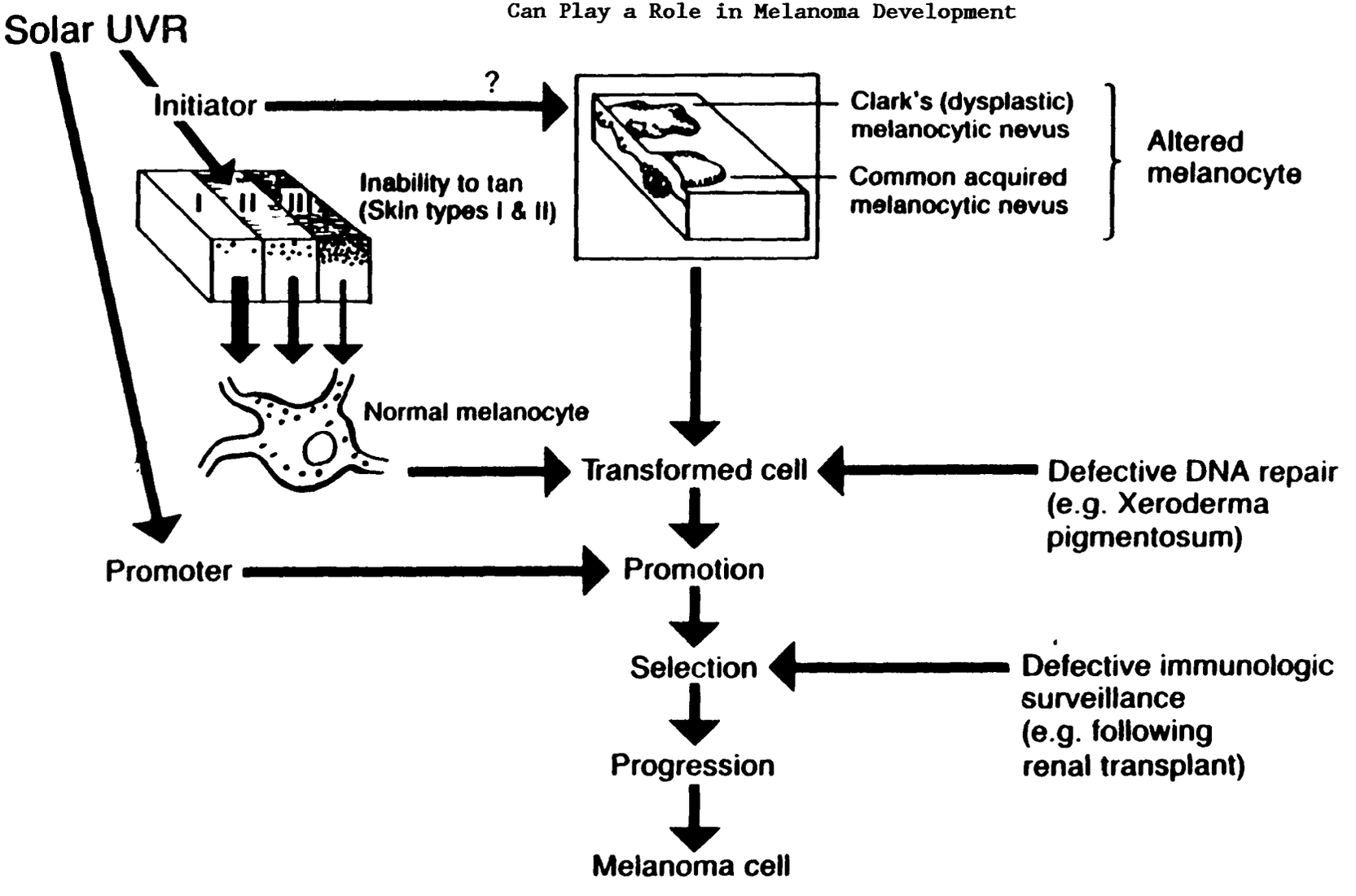

*in the white population

© T.B. Fitzpatrick

Fears et al. (1976) present one epidemiologic analysis that is potentially useful for estimating dose-response. These authors use two types of data to represent UV-B: (1) latitude -- latitude and UV-B radiation weighted for erythema effectiveness correlate at 0.97, and (2) monthly totals of erythema-producing UV radiation expressed as Biologically Effective Units (BEU) and derived from Schultze (1974). Both types of data were correlated with CMM mortality and incidence data. Incidence information for four cities was obtained from the Third National Cancer Survey (TNCS) (1975), and mortality data were obtained from the U.S. Cancer Mortality by County database (Mason and McKay (1973).

Exhibit 8-8 shows the results of a simple correlation model based on latitude:

$$\log R = \alpha + ßL$$

where R is the age-adjusted rate of incidence or mortality, α and ß are constants, and L is latitude. The estimated coefficients were statistically significant at $p \geq 0.01$. Exhibit 8-9 shows the results estimated using BEU's. These estimates were based on an exponential model and represent the percentage changes in incidence and mortality estimated to occur with increases in UV radiation dose of between 10 and 30 percent. Note that the use of an exponential model results in higher dose-response relationships for higher base exposures.

There are several important limitations in this work. In particular, only four cities were used for melanoma incidence. With a sample this small, variations in confounding factors such as behavior, skin pigmentation, and cloud cover may bias dose-response estimates. As a result, caution must be used in evaluating the error of estimate.

In another study, the same authors estimated a dose-response relationship for melanoma incidence using a power model (Fears et al. 1977)

$$P_{ij} = b\ (U_i)^c (A_i)^k$$

where:

P_{ij} = probability of developing melanoma for jth age group at location i;

U_i = annual UV-B count at ith location;

A_j = midrange of jth age group; and

b, c, and k are constants.

This equation was estimated by fitting a log form of the model ($\ln R_{ij} = a + c \ln U_i + kLnA_i + E_{ij}$) to age-specific melanoma incidence rates for both males and females after weighting by the observed number of cases. Annual counts from Robertson-Berger (R-B) meters were used for UV-B; the R-B meter attaches greater

EXHIBIT 8-8

Summary Statistics for Regressions of Skin Cancer Incidence and Mortality on Latitude

	MALES			FEMALES		
	Correlation Coefficient*	Regression Slope ± S.D.	Doubling Latitude	Correlation Coefficient*	Regression Slope ± S.D.	Doubling Latitude
Melanoma Incidence	-.86	-.031 ± .007	- 9.8°	-.83	-.038 ± .007	-10.7°
Melanoma Mortality	-.81	-.017 ± .002	-19.9°	-.71	-.014 ± .002	-22.2°

*Simple correlation coefficient between log of incidence/mortality rate and latitude.

Source: Fears, Scotto, and Schneiderman (1976).

EXHIBIT 8-9

Estimated Relative Increases in Melanoma Skin Cancer Incidence and Mortality Associated with Changes in Erythema Dose a/ (figures in parentheses are 95 percent confidence intervals)

		MALES			FEMALES		
	BASE	Increase in Total Dose			Increase in Total Dose		
	BEU	10%	20%	30%	10%	20%	30%
Melanoma Incidence							
	650	15 (7-24)	32	52	13	29	46
	850	20	44 (18-75)	72	18	39	64
	1050	25	57	96 b/ (37-180)	22	50	84 b/
Melanoma Mortality							
	650	8 (6-10)	16	26	6	13	21
	850	10	22 (16-28)	35	9	18	28
	1050	13	28	45 (33-58)	11	22	36

a/ A sample computation is as follows:

A 10% increase in total dose at 48.25'N, where exposure is 650 biologically effective units (BEU), equals 65 BEU.

A change of 65 BEU is equivalent to a reduction in latitude of 1.93'.

A change of 1.93' at 48.25'N is associated with an 18% increase in nonmelanoma incidence.

b/ These estimates require extrapolation well beyond the range of the data.

Source: Fears, Scotto, and Schneiderman (1976).

weight to longer wavelengths compared to the erythema action spectrum. Incidence data also were from the TNCS (1975).

Exhibit 8-10 presents summary regression coefficients and statistics for this age-specific analysis. Applying the results in this exhibit, a one percent increase in UVR results in an estimated $100*((1.01)^{c}-1)$ percentage increase in melanoma incidence, or 2.47 for females and 2.24 for males. The authors stress, however, that these estimates may be biased by the omission of location-specific demographic and environmental variables.

Scotto and Fears (1986) estimate a dose-response relationship for melanoma incidence using updated information about populations in a greater number of cities. The authors also introduce a new term (VAR) to adjust for the presence of some host or environmental characteristics:

$$\text{Ln } R_{ij} = a + b \text{ ln } (\text{Age}_i) + c \text{ ln UV-B} + dVAR + e$$

Annual counts obtained from Robertson-Berger meters were used for UV-B. Seven areas were included: Detroit, Seattle, Iowa, Utah, San Francisco, Atlanta, and New Mexico. Separate estimates were provided for: (1) anatomical sites of melanoma -- FHN (face, hands, neck), UE (upper extremity), LE (trunk and lower extremity); and (2) age groups -- 20-39, 40-54, 55-64, 65-74.

Scotto and Fears (1986) found that after controlling for confounding variables each 1 percent increase in UV-B causes melanoma incidence to increase by less than 1 percent. Exhibit 8-11 shows results for different anatomical sites. The results are statistically significant ($p < 0.1$). Exhibit 8-12 describes the effects of adding different constitutional and environmental variables derived using step-wise multiple regression. If the DNA action spectrum is used, Scotto's results indicate slightly less than a 2 percent increase in incidence for each 1 percent ozone depletion.

Pitcher (1987) used data on melanoma death rates by county for a 30-year period and exposure data from a satellite-data-based National Air and Space Administration model (the NASA Model; Serafino and Frederick 1986) to estimate the relationship between CMM death rates and several alternative estimates of UV-B doses. These were either peak (a clear day in June) or mean annual dose estimates using weighting functions derived either from the average DNA action spectrum proposed by Setlow (1974) or an erythema action spectrum.

Data on melanoma mortality by county were obtained from an EPA/NCI data base (Riggan et al. 1983) for the period 1950 to 1979. The NASA model estimated UV exposures in these counties by using modeling relationships based on latitude, longitude, altitude, surface albedo, total column ozone, and cloud cover to estimate the amount of UV delivered. Weighting functions derived with various biological action spectra were then applied to these total UV energy estimates to get estimates of "effective" UV energy termed "weighted UV doses." An extensive effort to validate the exposure data obtained from the UV model using ground-based measurements from Robertson-Berger meters has been made and will be reported in a subsequent report (Pitcher 1987b).

An examination of Pitcher's (1987a) data indicated that the relationship between age and melanoma death rates is approximately exponential. Further, the rates of increase for males and females were different. These observations led

EXHIBIT 8-10

Summary of Fears, Scotto, and Schneiderman (1977)
Regression Analyses of Melanoma Incidence Dose-Response*

SEX	R-Squared	t-Statistic (UV Coefficient)	$\alpha \pm$ SD (constant)	$\kappa \pm$ SD (age coefficient)	c $\pm$ SD (UV coefficient
Males	0.74	5.4	-35.6 + 6.5	.80 + .31	2.45 + .45
Females	0.62	4.6	-30.5 + 6.9	.29 + .34	2.23 + .48

* $\ln R\mu = \alpha + c \ln U_i + \kappa \ln A_j + \epsilon\mu_j$

Source: Fears, Scotto, and Schneiderman (1977).

EXHIBIT 8-11

Biological Amplification Factors for[a/] Skin Melanoma by Sex and Anatomical Site Groups, Adjusting for Age and Selected Constitutional and Exposure Variables*

VARIABLE	MALE		FEMALE	
	Trunk/LE	FHN/UE	Trunk/LE	FHN/UE
Age	6%	8%	5%	10%
Sunburn	4	8	5	10
Freckles	5	7	5	10
Scandinavian ancestry	5	9	5	10
Light hair color	5	8	5	10
Scot/Irish ancestry	6	6	4	8
Moles	6	7	5	11
Light eye color	6	8	4	9
Fair skin	6	8	4	9
Sunscreen use	4	7	4	10
Suntan lotion use	5	8	4	10
Radiation protection	5	8	6	10
Protective clothes	8	10	5	10
Hours outdoors during weekdays	7	9	5	10
Hours outdoors during weekends	5	7	8	13

[a/] A biological amplification factor indicates the relative change in melanoma incidence associated with a 10 percent relative increase in UV-B; abbreviations used for anatomical sites are LE: lower extremities; FHN: face, hands, neck; and UE: upper extremities.

Source: Scotto and Fears (1986).

EXHIBIT 8-12

Biological Amplification Factors for[a/] Melanoma Incidence by Sex and Anatomical Site Groups, Adjusting for Age and Combinations of Selected Constitutional and Exposure Variables*

ANATOMICAL SITE	MALE	FEMALE
Trunk/LE	3 Percent	4 Percent
Variables included in model	Suntan lotion use Scandinavian ancestry Light hair color UV-B radiation index Hours outdoors during weekdays	Suntan lotion use Scandinavian ancestry Light hair color UV-B radiation index Hours outdoors during weekends
FHN/UE	5 Percent	6 Percent
Variables included in model	Scot/Irish Suntan lotion use Fair skin UV-B radiation index Hours outdoors during weekends	Scot/Irish suntan lotion use fair skin UV-B radiation index

[a/] A biological amplification factor is a number that indicates the percentage increase in melanoma incidence for a 10 percent relative increase in UV-B; abbreviations used for anatomical sites are LE: lower extremities; FHN: face, hands, neck; and UE: upper extremities.

Source: Scotto and Fears (1986).

Pitcher to fit both a power and an exponential model to data for each sex group. For either model DRM_{ijk} is defined as the death rate for the ith cohort in the jth location in the kth time period. The exponential model then can be expressed as

$$DRM_{ijk} = \exp(a_0 + a_1 AGE_{ik} + a_2 WUV_j) + e_{ijk} \quad \text{(Model 1)}$$

and the power model can be expressed as

$$DRM_{ijk} = \exp\ (b_0 + b_{1i} AGE_{ik} + b_2 \log(WUV_j)) + e_{ijk} \text{ or,}$$

$$DRM_{ijk} = (WUV_j)^{b2} \exp(b_0 + b_{1i} AGE_{ik}) + e_{ijk} \quad \text{(Model 2)}$$

where AGE_{ik} is the age of ith cohort in the kth time period, WUV_j is the UV dose in the jth location (SMA) and e_{ijk} is the error term.

In model 1, the percentage change in melanoma mortality associated with variations in UV flux is higher the greater the baseline exposure. Model 2 differs from the first only in the use of the log of the exposure variable. In it, a 1 percent increase in UV dose generates the same percentage increase in melanoma death rates regardless of the baseline death rate.

Pitcher (1987a) found that many of the birth cohorts had zero deaths in any given 5-year period, especially in smaller cities. Further, because rates differed significantly across cohorts, the variances of the cohort death rates varied under the assumption that the probability of death had a binomial distribution. The different population sizes within cohorts also caused variation in the variance of the cohort death rate. These issues made the use of normal linear regression techniques unfeasible. Normal weighting techniques could not be used because zero rates for some cohorts prevented computation of weights. Therefore, weights were computed using expected rates rather than actual rates.

Using both the power and the exponential models, Pitcher (1987a) estimated the empirical relationships between melanoma mortality and a variety of different estimates of UV dose derived through the combination of two exposure scenarios (peak dose versus annual dose) and two different weighting functions (based on the DNA damage or erythema action spectra). Exhibit 8-13 presents the percentage increase in melanoma death rates predicted for a one percent decline in stratospheric ozone using the two models and four different dose estimates (DNA-weighted peak, DNA weighted annual, erythema-weighted peak and erythema-weighted annual) for males and females. Clearly choice of the dose estimate, particularly between annual or peak exposure durations, will make large differences in the prediction of increases in melanoma death rate. Unfortunately, the strength of the statistical association between any of these dose estimates and melanoma mortality are approximately the same so that a choice cannot be made on that basis. Furthermore, the mechanism of melanoma induction, particularly the role of UV, is sufficiently unclear, that a choice between the various options is difficult. Further investigations are planned in this area (Pitcher 1987b).

EXHIBIT 8-13

PERCENTAGE INCREASE IN MELANOMA DEATH RATES FOR A ONE PERCENT DECLINE IN OZONE

	MALES			
	Peak		Annual	
	Exponential	Power	Exponential	Power
El Paso				
DNA	1.99	1.65	1.18	.82
Erythema	1.90	1.60	1.07	.75
San Francisco				
DNA	1.59	1.64	.82	.82
Erythema	1.54	1.63	.76	.75
Minneapolis				
DNA	1.40	1.72	.52	.86
Erythema	1.34	1.77	.50	.77

	FEMALES			
	Peak		Annual	
	Exponential	Power	Exponential	Power
El Paso				
DNA	1.30	1.11	.76	.56
Erythema	1.27	1.10	.70	.53
San Francisco				
DNA	1.04	1.10	.53	.57
Erythema	1.03	1.09	.50	.53
Minneapolis				
DNA	.92	1.20	.34	.59
Erythema	.90	1.12	.33	.54

Limitations of Epidemiologic Studies

A variety of problems exist in applying the results of the epidemiologic studies to an analysis of melanoma risks associated with ozone depletion; many of these problems have been described in earlier sections. In particular, applying the dose-response relationships requires an assumption that certain key factors will not change. However, the proportion of individuals in the population who are most susceptible to UVR, such as certain ethnic groups, may change over time. Migration was not considered in the studies; if southern states experience large increases in population, then the sensitivity of future populations to UV-B will be underestimated. Individuals might also change their use of sunscreens or their propensity to work outdoors.

The epidemiologic studies do not measure actual ambient UV-B dose. Therefore, UV-B data used to estimate dose-response relationships will differ from the actual potential ambient exposure of individuals at any location. Other factors will also affect actual ambient exposures, such as skin color, patterns of dress, work exposure, recreation, eating, and medical care and intervention. These factors can be expected, in varying degrees, to introduce unexplained variation (i.e., noise) into any analysis of incidence or mortality. Finally, few data are available to assess the significance of the genetic factors that effect melanoma incidence but are not captured in epidemiologic studies.

REFERENCES

Acquavella, J.F., Wilkinson, G.S., Tietjen, G.L., Key, C.R., Stebbings, J.H., and Voelz, G.L. A melanoma case-control study at the Los Alamos National Laboratory. Health Phys 45:587-592 (1983).

Adam, S.A., Sheaves, J.K., Wright, N.H., Mosser, G., Harris, R.W., and Vessey, M.P. A case-control study of the possible association between oral contraceptives and malignant melanoma. Br J Cancer 44:45-50 (1981).

Adler, S., and Gaeta, J.F. Malignant melanoma. In: Cancer Dermatology, Helm, F. (ed). Philadelphia: Lea & Febiger pp. 141-157 (1979).

Anaise, D., Steinitz, R., and Ben Hur, N. Solar radiation: A possible etiological factor in malignant melanoma in Israel: A retrospective study (1960-1972). Cancer 42:299-304 (1978).

Anderson, R.R. Tissue optics and photoimmunology. In: Photoimmunology, Parrish, J.A., Kripke, M.L., and Morison, W.L. (eds). New York: Plenum Medical Book Co. pp. 61-76 (1983).

Armstrong B.K. Melanoma of the skin. Br Med Bull 40:346-350 (1984).

Armstrong, B.K., de Klerk, N.H., and Holman, C.D.J. Etiology of common acquired melanocytic nevi: Constitutional variables, sun exposure, and diet. JNCI 77(2):329-335 (1986).

Armstrong, B.K., Holman, C.D.J., Ford, J.M., and Wooding, T.L. Trends in melanoma incidence and mortality in Australia. In: Trends in Cancer Incidence, Causes and Practical Implications, Magnus, K., ed., Hemisphere Publications (1981).

Austin, D.F., Reynolds, P.J., Snyder, M.A., Biggs, M.W., and Stubbs, H.A. Malignant melanoma among employees of Lawrence Livermore National Laboratory. Lancet 2:712-716 (1981).

Bahr, A.K., Rosewaike, I., Hermann, N., Grover, P., Stellman, J., and O'Leary, K. Letter to the editor: Melanoma after exposures to PCBs. N Engl J Med, August 9, p. 450 (1976).

Baker-Blocker, A. Ultraviolet radiation and melanoma mortality in the United States. Env Res 23:24-28 (1980).

Balch, C.M., Karakousis, C., Mettlin, C., Natarajan, N., Donegan, W.L., Smart, C.R., and Murphy, G.P. Management of cutaneous melanoma in the United States. Surg Gynecol Obstet 158:311-318 (1984).

Balch, C.M., Soong, S., Milton, G.W., Shaw, H.M., McGovern, V.J., McCarthy, W.H., Murad, T.M., and Maddox, W.A. A comparison of prognostic factors and surgical results in 1,786 patients with localized (Stage I) melanoma treated in Alabama, USA, and New South Wales, Australia. Ann Surg 6:677-684 (1982).

Balch, C.M., Soong, S., Milton, G.W., Shaw, H.M., McGovern, V.J., McCarthy, W.H., Murad, T.M., and Maddox, W.A. Changing trends in cutaneous melanoma over a quarter century in Alabama, USA, and New South Wales, Australia. Cancer 52(9): 1748-1753 (1983).

Beral, V., Evans, S., Shaw, H., and Milton, G. Cutaneous factors related to the risk of malignant melanoma. Br J Dermatol 109:165-172 (1983).

Beral, V., Evans, S., Shaw, H. and Milton, G. Milignant melanoma and exposure to fluorescent lighting at work. Lancet 1:290-293 (1982)

Beral, V., Ramcharan, S., and Faris, R. Malignant melanoma and oral contraceptive use among women in California. Br J Cancer 36:804-809 (1977).

Beral, V., and Robinson, N. The relationship of malignant melanoma, basal and squamous skin cancers to indoor and outdoor work. Br J Cancer 44:886-891 (1981).

Boyle, P., Day, N.E., and Magnus, K. Mathematical modeling of malignant melanoma trends in Norway, 1953-1978. Am J Epidemiol 118:887-896 (1983).

Briele, H.A., and Das Gupta, T.K. Natural history of cutaneous malignant melanoma. World J Surg 3:255-270 (1979).

Briggs, J.C. The role of trauma in the aetiology of malignant melanoma: A review article. Br J Plastic Surg 37:517-516 (1984).

Cleaver, J.E. Xeroderma pigmentosum. Chapter 57 in Stanbury, J.B., Wyngarten, J.B., Frederickson, D.S., Goldsteen, J.L. and Brown, M.S. (eds.) The Metabolic Basis of Disease, McGraw-Hill Book Company, New York, pp. 1227-1248 (1983).

Clark, W.H., Jr., Elder, D.E., and van Horn, M. The biologic forms of malignant melanoma. Hum Pathol 17:443-450 (1986).

Collins, R.J. Melanoma in the Chinese of Hong Kong: Emphasis on volar and subungual sites. Cancer 54:1482-1488 (1984).

Cook, P.J., Doll, R., Fellingham, S.A. A mathematical model for the age distribution of cancer in man. Int J Cancer 4:93-112 (1969).

Cooke, K.R., and Fraser, J. Migration and death from malignant melanoma. Int J Cancer 36:175-178 (1985).

Cooke, K.R., Skegg, D.C.G., and Fraser, J. Trends in malignant melanoma of skin in New Zealand. Int J Cancer 31:715-718 (1983).

Cooke, K.R., Skegg, D.C.G., and Fraser, J. Socio-economic status, indoor and outdoor work and malignant melanoma. Int J Cancer 34:57-62 (1984).

Crombie, I.K. Racial differences in melanoma incidence. Br J Cancer 40:185-193 (1979a)

Crombie, I.K. Variation of melanoma incidence with latitude in North America and Europe. Br J Cancer 40:774-781 (1979b).

Crombie, I.K. Distribution of malignant melanoma on the body surface. Br J Cancer 43:842-849 (1981).

Dobson, A.J., and Leeder, S.R. Mortality from malignant melanoma in Australia: Effects due to country of birth. Int J Epidemiol 11(3):207-211 (1982).

Doniger, J., Jacobson, E.D., Krell, K., Di Paolo, J.A. Ultraviolet light action spectra for neoplastic transformation and lethality of syrian hamster embryo cells correlate with spectrum for pyrimidine dimer formation in cellular DNA. Proc Nat Acad Sci (USA) 78(4):2378-2382 (1981).

Durbin, N., Moseson, M., and Pasternack, B.S. Epidemiology of malignant melanoma: Pigmentary traits, ultraviolet radiation, and the identification of high-risk populations. Recent Results in Cancer Research 102:56-75 (1986).

Eklund, G., and Malec, E. Sunlight and incidence of cutaneous malignant melanoma. Scand J Plast Reconstr Surg 12:231-241 (1978).

Elder, D.E., Jucovy, P.M., Tuthill, R.J., and Clark, W.H. The classification of malignant melanoma. Am J Dermatopathol 2:315-320 (1980).

Elder, D.E., Greene, M.H., Bondi, E.E., and Clark, W.H. Acquired melanocytic nevi and melanoma, The dysplatic nevus syndrome, Chap. 11, In: Pathology of Malignant Melanoma, Ackerman, A.B. (ed) New York: Masson Publishing, USA, pp 185-215, (1981).

Elwood, J.M., Gallagher, R.P., Davison, J., and Hill, G.B. Sunburn, suntan and the risk of cutaneous malignant melanoma: The Western Canada melanoma study. Br J Cancer 51:543-549 (1985b).

Elwood, J.M., Gallagher, R.P., Hill, G.B., and Pearson, J.C.G. Cutaneous melanoma in relation to intermittent and constant sun exposure: The Western Canada melanoma study. Int J Cancer 35:427-433 (1985a).

Elwood, J.M., Gallagher, R.P., Hill, G.B., Spinelli, J.J., Pearson, J.C.G., and Threlfall, W. Pigmentation and skin reaction to sun as risk factors for cutaneous melanoma: Western Canada melanoma study. Br Med J 288:99-102 (1984).

Elwood, J.M., and Hislop, T.G. Solar radiation in the etiology of cutaneous malignant melanoma in Caucasians. Natl Cancer Inst Monogr 62:167-171 (1982).

Elwood, J.M., and Lee, J.A.H. Trends in mortality from primary tumors of skin in Canada. CMA Journal 110:913-915 (1974).

Elwood, J.M., and Lee, J.A.H. Recent data on the epidemiology of malignant melanoma. Semin Oncol 2(2):149-154 (1975).

Elwood, J.M., Williamson, C., and Stapleton, P.J. Maligant melanoma in relation to moles, pigmentation and exposure to fluorescent and other lighting sources. Br J Cancer 53:65-74 (1986).

Fears, T.R., Scotto, J., and Schneiderman, M.A. Skin cancer, melanoma and sunlight. Am J Public Health 66:461-464 (1976).

Fears, T.R., Scotto, J., and Schneiderman, M.H. Mathematical models of age and ultraviolet effects on the incidence of skin cancer among whites in the United States. Am J of Epidemiol 105:420-427 (1977).

Fitzpatrick, T.B., personal communication, 1986.

Fitzpatrick, T.B., personal communication, 1987.

Fitzpatrick, T.B., and Soter, N.A. Pathophysiology of the skin. In: Pathophysiology: The Biological Principles of Disease. Smith, L.H., Jr., and Thier, S.O. (eds.), pp. 1297-1330, 1985.

Forbes, P.D., Blum, H.F., Davies, R.E. Photocarcinogenesis in hairless mice: dose-response and the influence of dose-delivery. Photochem Photobiol 34:361-365 (1981).

Gellin, G.A., Kopf, A.W., and Garfinkel, L. Malignant melanoma: a controlled study of possibly associated factors. Arch Derm 99:43-48 (1969).

Gordon, T., Crittenden, M., and Haenszel, W. End results and mortality trends in cancer: II. Cancer mortality trends in the United States. Natl Cancer Inst Monogr 6:133-350 (1961).

Graham, S., Marshall, J., Haughey, B., Stoll, H., Zielezny, M., Brasure, J., and West, D. An inquiry into the epidemiology of melanoma. Am J Epidemiol 122(4):606-619 (1985).

Green, A. Sun exposure and the risk of melanoma. Br J Derm 25:99-102 (1984).

Green, A., MacLennan, R., and Siskind, V. Common acquired naevi and the risk of malignant melanoma. Int J Cancer 35:297-300 (1985a).

Green, A., and O'Rourke, M.G.E. Cutaneous malignant melanoma in association with other skin cancers. JNCI 74(5):977-980 (1985).

Green, A., and Siskind, V. Geographical distribution of cutaneous melanoma in Queensland. Med J Aust 1:407-410 (1983).

Green, A., Siskind, V., Bain, C., and Alexander, J. Sunburn and malignant melanoma. Br J Cancer 51:393-397 (1985b).

Haenszel, W. Variations in skin cancer merdena within the United States. Natl Cancer Inst Monogr 10:225-243 (1963).

Herron, J. The geographical distribution of malignant melanoma in Queensland. Med J Aust 1:892-894 (1969).

Hinds, M.W. Anatomic distribution of malignant melanoma of the skin among non-Caucasians in Hawaii. Br J Cancer 40:497-499 (1979).

Hinds, M.W., and Kolonel, L.B. Malignant melanoma of the skin in Hawaii, 1960-1977. Cancer 45:811-817 (1980).

Heston, J.F., Kelly J.B., Meigs, J.W., and Flannery J.T. Forty-five years of cancer incidence in Connecticut: 1935-1979. NCI Monograph No. 70 (1985).

Hinds, M.W., Lee, J., and Kolonel, L.N. Seasonal patterns of skin melanoma incidence in Hawaii. Am J Public Health 71:496-499 (1981).

Hinds, M.W., and Kolonel, L.B. Cutaneous Malignant Melanoma in Hawaii -- An update. West J Med 138(1):50-54 (1983).

Hoar, S.K., and Pell, S. A retrospective cohort study of mortality and cancer incidence among chemists. J Occup Med 23:483-494 (1981).

Holman, C.D.J., and Armstrong, B.K. Skin melanoma and seasonal patterns. Am J Epidemiol 113:202 (1981).

Holman, C.D.J., and Armstrong, B.K. Cutaneous malignant melanoma and indicators of total accumulated exposure to the sun: An analysis separating histogenetic types. JNCI 73:75-82 (1984a).

Holman, C.D.J., and Armstrong, B.K. Pigmentary traits, ethnic origin, benign nevi, and family history as risk factors for cutaneous malignant melanoma. JNCI 72:257-266 (1984b).

Holman, C.D.J., Armstrong, B.K., Evans, P.R., Lumsden, G.J., Dallimore, K.J., Meehan, C.J., Beagley, J., and Gibson, I.M. Relationship of solar keratosis and history of skin cancer to objective measures of actinic skin damage. Br J Dermatol 110(2):129-38 (1984c).

Holman, C.D.K., Armstrong, B.K., and Heenan, P.J. Guest editorial: A theory of the etiology and pathogenesis of human cutaneous malignant melanoma. JNCI 71:651-656 (1983).

Holman, C.D.J., Armstrong, B.K., and Heenan, P.J. Cutaneous malignant melanoma in women: Exogenous sex hormones and reproductive factors. Br J Cancer 50:673-680 (1984d).

Holman, C.D.J., Armstrong, B.K., and Heenan, P.J. Relationship of cutaneous malignant melanoma to individual sunlight-exposure habits. JNCI 76:403-414 (1986).

Holman, C.D.J., Heenan, P.J., Caruso, V., Glancy, R.J., and Armstrong, B.K. Seasonal variation in the junctional component of pigmented nevi. Int J Cancer 31:213-215 (1983).

Holman, C.D.J., James, I.R., Gattey, P.H., and Armstrong, B.K. An analysis of trends in mortality from malignant melanoma of the skin in Australia. Int J Cancer 26:703-709 (1980a).

Holman, C.D.J., Mulroney, C.D., and Armstrong, B.K. Epidemiology of pre-invasive and invasive malignant melanoma in Western Australia. Br J Cancer 25:317-323 (1980b).

Holmbert, B., Westerholm, P., Massing, R., Kestrup, L., Gumaelius, H., Holmlund, L., and Englund, A. Retrospective cohort study of two plants in the Swedish rubber industry. Scand J Work Environ Health 9(2):59-68 (1983).

Houghton, A., Flannery, J., and Viola, M.V. Malignant melanoma in Connecticut and Denmark. Am J Cancer 25:95-104 (1980).

Houghton, A., Munster, E.W., and Viola, M.V. Increased incidence of malignant melanoma after peaks of sunspot activity. Lancet (April 8):759-760 (1978).

Houghton, A.N., and Viola, M.V. Solar radiation and malignant melanoma of the skin. J Am Acad Dermatol 5:477-483 (1981).

IARC monographs. Biological data relevant to the evaluation of carcinogenic risk to humans. Appendix to Vol 40, in press, (1986).

Katz, L., Ben-Turia, S., and Steinitz, R. Malignant melanoma of the skin in Israel: Effect of migration. In: Trends in Cancer Incidence: Causes and Practical Implications, Magnus, K. (ed), Washington: Hemisphere Pub. Corp. (1982).

Kiryabwire, J.W., Lewis, M.G., Ziegler, J.L., and Loefler, I. Malignant melanoma in Uganda. East Afr Med J 45:498-507 (1968).

Kleinbaum, D.G., Kupper, L.L., and Morgenstern, H. Epidemiologic Research: Principles and Quantitative Methods. New York: Van Nostrand Reinhold (1982).

Klepp, O., and Magnus, K. Some environmental and bodily characteristics of melanoma patients: A case-control study. Int J Cancer 23:482-486 (1979).

Kopf, A.W. Personal communication (1987)

Kopf, A.W., Lazar, M., Bart, R.S., Dubin, N., and Bromberg, J. Prevalence of nevocytic nevi on lateral and medial aspects of arms. J Dermatol Surg Oncol 4124 (1978).

Kopf, A.W., Kripke, M.L., and Stern, R.S. Sun and malignant melanoma . Am Acad Dermatol 11:674-684 (1984).

Kopf, A.W., Lindsay, A.C., Rogers, G.S., Friedman, R.J., Rigel, D.S., and Levenstein, M. Relationship of nevocytic nevi to sun exposure in dyplastic nevus syndrome. J Am Acad Dermatol 12:656-62 (1985).

Kraemer, K.H., Lee, M.M., and Scotto, J. DNA repair protects against cutaneous and internal neoplasia: Evidence from xeroderma pigmentosum. Carcinogenesis 5:511-514 (1984).

Lancaster, H.O., and Nelson, J. Sunlight as a cause of melanoma: A clinical survey. Med J Aust 6:452-456 (1957).

Lane-Brown, M.M., Sharpe, C.A.B., MacMillen, D.S., and McGovern, V.J. Genetic predisposition to melanoma and other skin cancers in Australians. Med J Aust 1:852-853 (1971).

Larsen, T.E., Little, J.H., Orell, S.R., and Prade, M. International pathologists' congruence survey on quantitation of malignant melanoma. Pathology 12:245-253 (1980).

Lee J.A.H. Melanoma. In: Cancer Epidemiology and Prevention, Shottenfeld, D., and Fraumeni, J.F., Jr., (Eds.). Philadelphia: W.B. Saunders Company (1982a).

Lee, J.A.H. Melanoma and exposure to sunlight. Epidemiol Rev 4:110-136 (1982b).

Lee, J.A.H. Epidemiology of malignant melanoma: 10 Years' Progress. Pigment Cell 6:1-21 (1983).

Lee, J.A.H., and Carter A.P. Secular trends in mortality from malignant melanoma. J Natl Cancer Inst 45:19-97 (1970).

Lee, J.A.H., and Issenberg, H.J. A comparison between England and Wales and Sweden in the incidence and mortality of malignant skin tumors. Br J Cancer 26:59-66 (1972).

Lee, J.A.H., Petersen, G.R., Stevens, R.G., and Vesanen, K. The influence of age, year of birth, and date on mortality from malignant melanoma in the populations of England and Wales, Canada, and the white population of the United States. Am J Epidemiol 110:734-739 (1979).

Lee, J.A.H., and Storer, B.E. Further studies on skin melanomas apparently dependent on female sex hormones. Int J Epidemiol 11:127-131 (1982).

Lee, J.A.H., and Strickland, D. Malignant melanoma: Social status and outdoor work. Br J Cancer 41:757-763 (1980).

Lew, R.A., Sober, A.J., Cook, N., Marvell, R., and Fitzpatrick, T.B. Sun exposure habits in patients with cutaneous melanoma: A case control study. J Dermatol Surg Oncol 9:981-986 (1983).

Lewis, M.G. Malignant melanoma in Uganda: The relationship between pigmentation and malignant melanoma on the soles of the feet. Br J Cancer 21:483-495 (1967).

Lilienfeld, A.M., and Lilienfeld, D.E. Foundations of Epidemiology. New York: Oxford University Press (1980).

Little, J.H., Holt, J., and Davis, N. Changing epidemiology of malignant melanoma in Queensland. Med J Aust 1:66-69 (1980)

MacDonald, E.J. Incidence and epidemiology of melanoma in Texas. In: Neoplasms of the Skin and Malignant Melanoma, 20th Annual Clinical Conference on Cancer, 1975. Chicago: Year Book Medical Publishers, Inc. (1976).

Mackie, R.M., and Aitchinson, T. Severe sunburn and subsequent risk of primary cutaneous malignant melanoma in Scotland. Br J Cancer 46:955-950 (1982).

Magnus, K. Incidence of malignant melanoma of the skin in Norway, 1955-1970: Variations in time and space and solar radiation. Cancer 32(5):1275-1286 (1973).

Magnus, K. Epidemiology of malignant melanoma of the skin in Norway with special reference to the effect of solar radiation. In: Biological Characterization of Human Tumors, pp. 249-259, Exerpta Medica International Congress Series No. 375, Amsterdam (1975).

Magnus, K. Incidence of malignant melanoma of the skin in the five Nordic countries: Significance of solar radiation. Int J Cancer 20:477-485 (1977).

Magnus, K. Incidence trends in the Nordic countries: Effects of sun exposure. In: Trends in Cancer Incidence, Causes and Practical Implications (K. Magnus, ed.), Washington: Hemisphere Publication, (1981a).

Magnus, K. Habits of sun exposure and risk of malignant melanoma: An analysis of incidence rates in Norway 1955-1977 by cohort, sex, age, and primary tumor site. Cancer 48:2329-2335 (1981b).

Magnus, K. Incidence Trends in the Nordic countries: effects of sun exposure. In: Trends in cancer incidence causes and practical implications. K. Mangus (ed). Hemisphere Publishing Corp. pp 387-392 (1982).

Malec, E., and Eklund, G. The changing incidence of malignant melanoma of the skin in Sweden, 1959-1968. Scand J Plast Reconstr Surg 12:19-27 (1978).

Malec, E., Eklund, G., and Langerlof, B. Reappraisal of malignant melanoma diagnosis in the Swedish Cancer Registry. Acta Path Microbiol Immunol Scand 85: 707-712 (1977).

Mason, T., and McKay, F. U.S. Cancer Mortality by County, DHEW Publ. No. (NIH) 74-615, Govt. Printing Office, Washington, D.C. (1973).

McCarthy, W.H., Blach, A.L., and Milton, G.W. Melanoma in New South Wales: An epidemiologic survey 1970-76. Cancer 46:427-432 (1980).

McGovern, V.J., Mihm, M.C., Bailly, C., Booth, J.C., Clark, W.H., Jr. Cochran, A.J., Hardy, E.G., Hicks, J.D., Levene, A., Lewis, M.G., Little, J.H., and Milton, G.W. The classification of malignant melanoma and its histologic reporting. Cancer 32:1446-1457 (1973).

McKay, F.W., Hanson, M.R., and Miller, R.W. Cancer mortality in the United States: 1950-1977. Natl Cancer Inst Monog 59 (1982).

Moss, A.L.H. Malignant melanoma in Maoris and Polynesians in New Zealand. Br J Plastic Surg 37:73-75 (1984).

Movshovitz, M., and Modan, B. Role of sun exposure in the etiology of malignant melanoma: Epidemiologic inference. J Natl Cancer Inst 51(3):777-779 (1973).

Muir, C.S., and Nectoux, J. Time trends: Malignant melanoma of the skin. In: Trends in Cancer Incidence, Magnus, K. (ed). Washington: Hemisphere Publishing Corp. pp. 365-385 (1982).

NAS. Protection Against Depletion of Stratospheric Ozone by Chlorofluorocarbons, Washington: National Academy of Sciences (1979).

NAS. Causes and Effects of Stratospheric Ozone Reduction: An Update. National Research Council, Washington: National Academy of Sciences (1982).

National Institute for Occupational Safety and Health (NIOSH). Unpublished data: melanoma after exposure to PCBS (1976).

Nordlund, J.J. Genetic basis of pigmentation and the disorders of pigmentation. In: Pathology of Malignant Melanoma, Ackerman, A.B. (ed). New York: Masson Publishing pp. 23-45 (1981).

Osterlind, A., and Jensen O.M. Trends in incidence of malignant melanoma of the skin in Denmark 1943-1982. Recent Results Cancer Res 102:8-17 (1986).

Paffenbarger, R.S., Wing, A.L., and Hyde, R.T. Characteristics in youth predictive of adult-onset malignant lymphomas, melanomas, and leukemias: Brief communication. J Natl Cancer Inst 60:89-92 (1978).

Pakkanen, M. Clinical appearance and treatment of malignant melanoma of the skin. Ann Chir Gynaecol 66:21-30 (1977).

Pasternack, B.S., Durbin, N., and Moseson, M. Malignant melanoma and exposure to fluorescent lighting at work. Lancet 1:704 (1983).

Pathak, D.R., Samet, J.M., Howard, C.A., and Key, C.R. Malignant melanoma of the skin in New Mexico 1969-1977. Cancer 50:1440-46 (1982).

Pitcher, H.M. Examination of the empirical relationship between melanoma death rates in the United States 1950-1979 and satellite-based estimates of exposure to ultraviolet radiation. In press (1987a).

Pitcher, H.M. Personal communication (1987b).

Pitcher H.M. and Longstreth, J.D. Ultraviolet Radiation.

Pondes, S., Hunter, J.A.A., White, H., McIntyre, M.A., and Prescott, R.J. Cutaneous malignant melanoma in south-east Scotland. Q J Med, New Series L. 197:103-121 (1981).

Riggan, W.B., Briggan, J.B., Acquavella, J.F., Beaubier, J., and Mason, T.J. U.S. Cancer Mortality Rates and Trends, 1950-1979. USEPA (1983).

Rigel, D.S. Fredman, R.J., Bernstein, M. and Greenwald, D.J. Letter to the editor: Malignant melanoma and exposure to fluorescent lighting at work. Lancet 2:704 (1983).

Rippey, J.J., and Rippey, E. Epidemiology of malignant melanoma of the skin in South Africa. SA Med J 65:595-598 (1984)

Romsdahl, M.M., and Cox, I.S. Biological aspects of pigment cells and malignant melanoma. In: Neoplasms of the Skin and Malignant Melanoma, 20th Annual Clinical Conference on Cancer, 1975. Chicago: Year Book Medical Publishers (1976).

Roush, G.C., Schymura, M.J., and Holford, T.R. Risk for cutaneous melanoma in recent Connecticut birth cohorts. Am J Public Health 75:679-682 (1985a).

Roush, G.C., Schymura, M.J., Holford, T.R., White, C., and Flannery, J.T. Time period compared to birth cohort in Connecticut incidence rates for twenty-five malignant neoplasms. JNCI 74:779-788 (1985b).

Rushton, L., Alderson, M.R. An epidemiological survey of eight oil refineries in Britain. Br J Ind Med 38:225-234 (1981).

Scotto, J., and Fears, T.R. The association of solar ultraviolet radiation and skin melanoma among Caucasians in the United States. Cancer Invest (in press 1986).

Scotto, J., and Nam, J. Skin melanoma and seasonal patterns. Am J Epidemiol 111(3):309-314 (1980).

Schultze, R. Increase of carcinogenic ultraviolet radiation due to reduction in ozone concentration in the atmosphere. Proceedings of the International Conference on Structure. Composition and General Circulation of the Upper and Lower Atmospheres and Possible Anthropogenic Perturbations. Atmospheric Environment Service, Ontario, Canda, Volume 1:479-493 (1974).

Serafino, G., and J. Frederick. Global modeling of the ultraviolet solar flux incident on the biosphere, prepared for the U.S. Environmental Protection Agency, Washington, D.C., (1986).

Setlow, R.B. The wavelengths in sunlight effective in producing skin cancer: A theoretical analysis. Proc Natl Acad Sci USA 71(9): 3363-3366 (1974).

Smith, J.L. Histopathology and biologic behavior of malignant melanoma. In: Neoplasms of the Skin and Malignant Melanoma. Chicago: Year Book Medical Publishers, Inc., pp. 293-330 (1976).

Sondik, E., Young, J.L., Horm, J.W., and Ries, L.A.G. 1985 Annual Cancer Statistics Review. National Cancer Institute (1985).

Stevens, R.G., and Moolgavkar, S.H. Malignant melanoma: Dependence of site-specific risk on age. Am J Epidemiol 119:890-895 (1984).

Swerdlow, A.J. Incidence of malignant melanoma of the skin in England and Wales and its relationship to sunshine. Br Med J 2:1324-1327 (1979).

Takahashi, M., and Seiji, M. Acral melanoma in Japan. Pigment cell, 6:150-165 (1983).

Teppo, L. Incidence trends of melanoma of the skin in Finland by histological type. In: Trends in Cancer Incidence: Causes and Practical Implications. K. Magnus (ed.), Hemisphere Publishing Corp., pp. 693-697 (1982).

Teppo, L., Pakkanen, M., and Hakulinen, T. Sunlight as a risk factor of malignant melanoma of the skin. Cancer 41:2018-2027 (1978).

Teppo, L., Pukkala, E., Hakama, M., et al. Way of life and cancer incidence in Finland. Scand J Soc Med (Suppl.) 19:50-54 (1980). As cited in Lee (1982).

TNCS. Third National Cancer Survey: Incidence Data. DHEW Publication No. (NIH) 75-787, Natl Cancer Inst Monogr 41 (1975).

Vagero, D., Ringback, G., and Kiviranta, H. Melanoma and other tumours of the skin among office, other indoor and outdoor workers in Sweden 1961-1979. Br J Cancer 53:507-512 (1986).

Venzon, D.J., and Moolgavkar, S.H. Cohort analysis of malignant melanoma in five countries. Am J Epidemiol 119:62-70 (1984).

Viola, M.V., and Houghton A.N. Solar radiation and cutaneous malignant melanoma. Hosp Pract, June:97-106 (1982).

Wan, S., Anderson, R.R., and Parrish, J.A. Analytical modeling for the optical properties of the skin with in vitro and in vivo applications. Photochem Photobiol 34:493-499 (1981).

Wigle, D.T. Malignant melanoma of skin and sunspot activity. Lancet 2:38 (1978).

CHAPTER 9

UVR-INDUCED IMMUNOSUPPRESSION: CHARACTERISTICS AND POTENTIAL IMPACTS

SUMMARY

Solar radiation has been found to have a detrimental effect on the immune system of both humans and experimental animals. In particular, UV radiation (UVR) reduces the ability of the cell-mediated arm of the immune response to respond adequately to antigens. UV irradiation of the skin predisposes the immune system to form suppressor T cells (Ts) in response to antigens encountered via the skin or injected subcutaneously. These Ts are specific for antigen and prevent the development of immune responses. In a tumor bearing animal, this immunosuppression may result in the out growth of tumor cells which in normal animals would have been destroyed by the immune system.

One cell population in the skin known to be severely damaged are the Langerhans cells. Langerhans cells are skin-resident, antigen-processing cells which are required to induce cell mediated or antibody-based immune responses to antigens which are introduced through the skin. Although it is not certain that the damage to the Langerhans cells is entirely responsible for the immunosuppressive effect of UVR, it is clear that UV irradiation of skin reduces the immune response in that skin. Even more important, it is also clear that it is the UV-B portion of the UV spectrum that is responsible for the depression of the immune response.

One important facet of this UVR-induced immunosuppression is the role it plays in UV-B-induced carcinogenesis; it affects the host's ability to respond to tumor-specific antigens present on the UVR-induced tumor cells thereby increasing the risk for tumor development in animal models, probably by allowing the tumor to escape the normal immune surveillance mechanisms. Thus the tumor cells are allowed to divide and establish a large and growing tumor in the host.

The immunosuppressive effects of UVR also are very likely to have a deleterious effect on the immune response to those infectious diseases that enter through the skin, especially if the initial immune response to the agent takes place in the skin. As yet, little research has been done in this area. Preliminary evidence indicates, however, that UV irradiation during a first cutaneous infection with two very different organisms, the parasite Leishmania sp. and Herpes simplex virus, may result in an impairment of the immune response of the host to subsequent infections. In the case of leishmaniasis, this could lead to the development of the more lethal form of the disease, visceral leishmaniasis.

Although there are no experimental data which specifically address these issues several hypotheses about UVR induced immunosuppression seem reasonable:

1) All populations, black and white may be at risk, particularly if the mechanism of induction for UVR induced immunosuppression lies above the melanin as one theory suggests.

2) Individuals who are already immunosuppressed, e.g., transplant patients or individuals with immunodeficiency diseases, could via additive effects be at greater risk than the normal population, and

3) In developing countries, particularly near the Equator, high solar insulation could result in an immunosuppression which could exacerbate parasitic infections of the skin such as leishmaniasis.

The effects of UV-B and solar radiation on the human immune system have not been studied in sufficient detail to allow estimation of dose-response relationships for these effects. Qualitatively, it is known from animal studies that the doses of UV-B needed to induce immunosuppression are much lower than those required for carcinogenesis. This may mean that exposure to low doses of UVR, even doses that do not cause a sunburn, may decrease the ability of the human immune system to provide an effective defense against neoplastic skin cells or skin infections.

FINDINGS

1. UV-B SUPPRESSES THE IMMUNE SYSTEM IN ANIMAL EXPERIMENTS.

   1a. UV radiation administered at relatively low doses causes a depression in local contact hypersensitivity (a form of cell-mediated immunity) resulting from an inability to respond to an antigen presented through UV-irradiated skin

   1b. High doses of UV radiation cause a depression in systemic contact and delayed type hypersensitivity reactions, that result in an inability of the animal to respond to an antigen which is presented to the animal through unirradiated skin

   1c. Both the local and systemic effects on contact hypersensitivity are mediated by a T suppressor cell which prevents the development of active immunity to the antigen

   1d. The immunosuppressive effects of UVR have been found to reside almost entirely in the UV-B portion of the ground level solar radiation

2. SUPPRESSION OF THE IMMUNE SYSTEM MAY PLAY AN IMPORTANT ROLE IN CARCINOGENESIS.

   2a. Animals which are UV-irradiated develop T suppressor cells which interfere with the immune response to UV-induced tumors in such a way that the animals are more susceptible to the growth of autochthonous UV-induced tumors. The contribution of the suppression of the immune system to cancer incidence that would result from ozone depletion is reflected in the dose-response estimates of photocarcinogenesis assuming that the action spectra for the two phenomena are the same. If these two impacts have different action spectra, the estimates could be either high or low.

3. LIMITED EXPERIMENTAL DATA INDICATE UV-B SUPPRESSES THE HUMAN IMMUNE SYSTEM.

   3a. Although there is limited information about the effects of UV radiation on humans, several studies indicate that the immune response of humans is depressed by UV radiation and is depressed in UV-irradiated skin.

4. UV-B-INDUCED SUPPRESSION OF THE HUMAN IMMUNE SYSTEM COULD HAVE A DELETERIOUS EFFECT WITH REGARD TO MANY HUMAN DISEASES.

   4a. Preliminary studies indicate that UV radiation may prevent an effective immune response to micro-organisms that infect via the skin, thus predisposing to reexpression or chronic infection.

   4b. Two human diseases that may be influenced by UV-B-induced immune suppression are herpes virus infections and leishmaniasis.

   4c. Almost no research has been conducted on the influence of UV-B on other infectious diseases; additional investigation is clearly warranted.

   4d. For at least one theory of the mechanisms of UV-B-induced suppression

of the immune system (that involving urocanic acid), a possibility exists that non-whites, as well as whites, would be vulnerable to increased immune suppression caused by ozone depletion.

4e. Because UV-B can produce systemic immunologic change, the possibility exists that changes in UV-B could have resulted in effects on diseases whose control requires systemic rather than local immunity.

4f. Immunologic studies to date have not assessed the effects of long-term, low-dose UV-B irradiation. Consequently, the magnitude of this risk cannot be assessed.

UVR-INDUCED IMMUNOSUPPRESSION: CHARACTERISTICS AND POTENTIAL IMPACTS

INTRODUCTION

As indicated in Chapter 7, it has been known for years that ultraviolet radiation (UVR) is carcinogenic. In the past decade or so, studies designed to explore the mechanism of UVR-induced carcinogenesis revealed that UVR is a potent but specific immunosuppressive agent which can abrogate the ability of an animal to reject its own or a transplanted syngeneic UV-induced tumor. Subsequent work investigating the mechanism of UVR-induced immunosuppression has indicated that UVR can have a number of effects on the immune system, effects which have the potential to modify a variety of disease processes. This chapter has four goals: 1) to briefly review some of the basic concepts in immunology necessary to understand the effects of UVR on the immune system, 2)to provide an introduction to that portion of the immune system first affected by solar radiation - the skin-associated lymphoid tissues (SALT); 3) to review in some detail what specifically is known about the impact of UVR on immune responses including a discussion of dosimetry and action spectra and 4) to close with a discussion of the potential impacts UVR-induced immunosuppression could have on infectious diseases.

BASIC CONCEPTS IN IMMUNOLOGY

A complete history of immunology is beyond the scope of this review; what follows is a very cursory review which focuses solely on the key concepts required for understanding the impact of ultraviolet radiation on the immune system as it is currently understood. The field is constantly changing however. For entertaining and readable reviews of the immune response in general, the reader is referred to two recent texts by Jan Klein (1982) and Bill Paul (1986). For the most current information on the subject of photoimmunology the reader is referred to the most recent issues of the journals Photoimmunology, and Photobiology and Photochemistry and to recent reviews by Margaret Kripke (1984, 1986), Raymond Daynes and colleagues (1986) and Richard Granstein (1987).

The immune system is a complex network of specialized organs and cells that has evolved to defend the body against "foreign invaders" e.g., infectious agents such as bacteria and viruses. The immune system shows several remarkable characteristics. It is able to distinguish between "self" and "nonself". It is able to remember previous experiences and react accordingly. It displays enormous diversity and extraordinary specificity; not only is it able to recognize many millions of "nonself" molecules, it can produce molecules to match up with and counteract each one of them.

The success of this system in defending the body depends on an incredibly elaborate and dynamic regulatory communications network. Millions and millions of cells organized into sets and subsets pass information back and forth. The result is a sensitive system of checks and balances that produces an immune response which is prompt, appropriate, effective and self-limiting.

By the 1950's, it was generally accepted by immunologists that there were two types of immune responses: those mediated through antibodies (humoral responses) and those mediated by cells (cell-mediated responses). However,

since the antibodies are produced by cells, there was some question as to how the cells involved in producing antibodies differed from those involved in cell mediated responses. Over the decade from mid 1950's to the mid 1960's, this question was answered as the cells important to immune response were characterized. There are certain types of cells and anatomic structures which are critical to the induction and elicitation of the immune response and which are common to immunological phenomena throughout an organism. Given below is a brief introduction to key concepts and terminology.

Antigens

An antigen is any substance that is recognized as foreign ("nonself") by the body's immune system. A molecule is recognized as "self" or "nonself" by virtue of unique structurally-conferred characteristics called epitopes. A substance such as a protein molecule, or an entity such as a bacterium or a virus particle can display many different epitopes all of which can induce unique and specific immune responses. Certain (generally very small) epitopes termed "haptens" will not alone induce an immune response but when displayed on a larger molecules, termed "carriers", are able to induce immune responses specific for themselves and not for the carrier molecule.

Cell Types

The key cell types involved in generating immune responses affected by UVR are lymphocytes and antigen-presenting cells (APC's). Lymphocytes are generally considered to be the ultimate effector cells in the immune response; they comprise a functionally heterogeneous population of two major lineages. B-lymphocytes are important to humoral immune (antibody) responses; their terminal differentiation state is the antibody-exporting plasma cell. T-lymphocytes are important both to cell-mediated and humoral responses. There are several subsets of T-lymphocytes; T-helper/inducer cells provide help to B-lymphocytes in the development of antibody responses, T-killer cells function as effector cells in cytotoxicity (cell killing) responses and T-suppressor cells perform regulatory functions, suppressing both humoral and cell-mediated responses.

Upon exposure to antigen, the first step in the immune response is uptake of antigen by cells capable of processing and/or otherwise focusing the antigen for effective presentation to immunocompetent lymphocytes. Cells which perform this function are termed antigen-presenting cells and there is reason to believe that they comprise a heterogeneous population that at a minimum contains a certain subset of macrophages termed dendritic cells. There is some uncertainty as whether or not all macrophages process antigen; evidence is accumulating to suggest that this function is restricted to the "dendritic" subpopulation, but the final judgement is not yet in (Klein 1982).

Local Versus Systemic Effects

Much of what is known about immunology comes from experiments which characterize systemic immune responses. These are immune response demonstrable throughout the body which occur following antigen processing/presentation by the macrophages, recognition of processed/presented antigen by T-lymphocytes, interaction of the T-lymphocyte antigen complex with B-lymphocytes followed by clonal proliferation and differentiation of T and B lymphocytes. These events are usually considered to take place within the cortical region of lymph nodes

and the equivalent region of the splenic periarteriolar sheath. The cellular and molecular consequences of T cell activation (lymphokines, cytotoxic cells, cells that mediate delayed-type hypersensitivity, and cells that regulate the immune response) and of B cell activation (specific antibodies, memory B cells, regulating anti-antibodies) then disseminate systemically through the lymphatics and the blood.

In contrast to systemic immune responses, there exist immune responses which are localized to a particular microenvironment such as the gut, the respiratory tract, the breast, external eye and the skin. The lymphoid tissues responsible for the immune responses observed in these various tissues have been identified respectively as the gut associated lymphoid tissue (GALT), the bronchial associated lymphoid tissue (BALT), the mammary associated lymphoid tissue (MALT) the conjunctival associated lymphoid tissue (CALT) and the skin associated lymphoid tissue (SALT). In each case, the responses observed in each of these sites are dependent on circuits of lymphocytes specific to the particular milieu provided at these anatomic locations.

SALT: SKIN-ASSOCIATED LYMPHOID TISSUES

Streilein and his colleagues (1983,1984) have proposed that the skin and its component cell types comprise a unique regional sphere of immunologic influence which serves a surveillance function for the skin allowing it to successfully fulfil its role as the main barrier between the organism and the environment. As indicated in chapter 7,the skin has several cell types which function in immune responses including a rather unique version of an antigen-presenting cell (the Langerhans cell), a series of T and probably non-T lymphocytes which can effect immune responses and keratinocytes which produce a substance, epidermal cell derived thymocyte activating factor (ETAF), that may also affect immune responses in the skin.

On virtually a daily basis, the skin protects the body from a plethora of infectious agents such as bacteria, fungi and viruses, as well as to numerous chemical and physical carcinogens the most prevalent one being solar radiation. The daily bombardment by the UVR present in solar radiation poses the risk of neoplastic transformation of epidermal cells; such transformation is generally associated with the expression of unique new antigens on the surface of the neoplastic cells. Streilein and his colleagues (1983, 1984) have proposed that SALT represents the physiologic mechanism created to deal with the special demand this process places upon the skin. The process whereby SALT controls neoplasia might be stated as follows: neoplastic transformation of keratinocyte results in the display of new surface antigens. The ubiquitous Langerhans cells pick up or receive this new antigen, process it and present it in immunogenic form. One of two subsequent events may then transpire: wandering T lymphocytes with predetermined affinity for the epidermis and with immunologic specificity for the new antigen migrate into the epidermis, recognize the new antigen presented on LC, transform into effector cells and directly destroy the adjacent malignant cells, or 2) the Langerhans cell bearing the new antigen migrates via the draining lymph into the regional lymph node, there to attract antigen-specific lymphocytes that transform in response to the antigen, proliferate, and then disseminate systemically albeit returning predominantly to the skin in order to effect destruction of the neoplastic keratinocytes.

Evidence which Streilein and his colleagues (1983) feel support this proposition include: 1) Some, but not all, T lymphocytes display special affinity for skin and draining lymph nodes (Rose et al. 1976). 2) Skin contains immunocompetent lymphocytes (Parker and Billingham 1972) and antigen presenting cells (Stingl et al. 1978) and produces immunoregulatory molecules (Sauder et al. 1981, 1982), 3) Immune recognition of antigen takes place within skin (Streilein 1983); 4) Antigen introduced via the skin which escapes recognition induces specific unresponsiveness (Toews et al. 1980).

EFFECTS OF UVR ON IMMUNOLOGICAL REACTIONS

The effects of UVR on the immune system were first described in investigations of mechanism of carcinogenesis induced by chronic administration of UVR. Subsequent work explored the specific effects of UVR on the immunological reactions - in the absence of carcinogenesis. This section will briefly review the initial work done to characterize the immunologic reactions evaluated during the carcinogenic process (for a detailed review see Chapter __ of Appendix A) and will then focus on the studies designed to explore the exact impact of UVR on the immune response.

Effects of UVR on Tumor Growth

The first indication that UVR might have an impact on the immune system came from studies by Kripke (1974) who reported that most murine tumors induced by UVR were rejected when transplanted into normal syngeneic recipients whereas the same tumors grew progressively in immunosuppressed mice. This phenomenon was originally identified in a C3H mouse system in which tumors were induced using a high intensity mercury arc lamp (Kripke 1974), subsequent studies indicated that it held true for other inbred strains of mice irradiated using FS40 fluorescent sunlamps (Kripke 1977).

Experiments designed to determine if the mechanism of this effect was that UV irradiation of mice led to a generalized immunosuppression, evaluated a variety of immune parameters using a number of different exposure regimens (albeit all involving chronic administration) (Kripke et al. 1977; Spellman et al. 1977; Norbury et al. 1977; Lynch and Daynes 1983). At the doses used to induce carcinogenicity, most of the functions examined (e.g., response to mitogens, allograft rejection, antibody production) remained normal, however, in some instances (e.g., graft-versus-UVR-treated host reactions (Kripke et al. 1977), reactivity to dinitrochlorobenzene (DNCB) (Kripke et al. 1977), and naturally occurring cell-mediated cytotoxicity in UV-irradiated mice (Lynch and Daynes 1983) were found to be transiently suppressed but returned to normal after between 2 and 4 months of UVR treatment.

It is clear from the above information that mice which have been chronically irradiated with UV light are not generally immunosuppressed but have normal immunity when tested over a very wide number of immune functions. Nevertheless they are unable to reject UV-induced tumors. Further experiments revealed that the mechanism for the lack of immune reactivity to UV-induced tumors in UV-irradiated mice was a radiosensitive, Ia positive, Lyt-1+2- (Ullrich and Kripke 1984) T suppressor cell (Fisher and Kripke 1977, 1978, Spellman and Daynes 1977, 1978, Daynes et al. 1979). These cells were specific for an antigen common to UV-induced tumors and did not affect the ability of immune mice to reject tumors as a function of immunity to tumor specific

transplantation antigens (Roberts et al 1980) or to histocompatibility antigens (Kripke and Fisher 1976). Preliminary evidence indicates that UV-irradiated mice immunologically recognize UV-induced tumors (Romerdahl and Kripke, 1986), but that the suppressor cell acts to prevent the development of cytotoxic effector cells.

Other characteristics of this response were 1) that with the exception of a transplantable spontaneous melanoma (B-16), the immunosuppression was specific for the transplantation of UVR induced tumors (Kripke et al 1979); 2)that it can be induced with natural sunlight (as opposed to artificial sources) (Morison and Kelley 1985); 3)that the active wavelengths lie below 315 nm; 4) that there is dose reciprocity (i.e., reducing the dose rate but keeping the total dose constant results in the same carcinogenic impact (De Fabo and Kripke 1979, 1980); 5)that immunosuppression, when transferred via lymphoid cells could result in enhanced UVR-induced tumorigenesis (Fisher and Kripke 1982); and 6) that the effect on tumorigenesis was systemic, i.e., tumor development was enhanced on both exposed and non-exposed skin in irradiated animals (De Gruijl and Van Der Leun 1982, 1983)

Characterization of the Impacts of UVR on the Immune System

In normal mice, application of a contact sensitizing agent such as trinitrochlorobenzene (TNCB) or dinitrofluorobenezene (DNFB) to shaved abdominal skin induces a cell-mediated immune response. A second exposure to the contact sensitizing agent via painting on the ears elicits a contact hypersensitivity (CHS) response characterized by swelling of the ears 24 hours later. The response is specific to the initial sensitizing agent in that TNCB will not sensitize for DNFB and vice versa. A similar phenomenon, delayed type hypersensitivity, differs from CHS only in the way in which the ultimate response is elicited. Whereas in CHS skin painting on the ear elicits the ultimate response, in DTH injection of the sensitizing agent in dimethylsulfoxide into the footpad or injection of haptenated splenic lymphocytes into the footpad or ear elicits the ultimate response.

The specific impacts of UVR on the immune system can generally be characterized one of three ways: 1) suppression of contact hypersensitivity (CHS) at the site of irradiation (also known as local suppression), 2) systemic (generalized) suppression of contact hypersensitivity , and 3) systemic suppression of delayed type hypersensitivity (DHS). These three impacts have different action spectra and dose requirements; what follows is a discussion of the pertinent differences as well as an attempt to relate these differences to possible impacts of UVR in human populations.

<u>Local suppression of contact hypersensitivity</u>. The first description of the impact that ultraviolet radiation could have on contact hypersensitivity was that of Haniszko and Suskind (1963) who demonstrated that, in guinea pigs, prior exposure of skin to UV-B (280-320) resulted in a reduced CHS response. The dose given was approximately a minimum erythemal dose (MED)[1]. Unfortunately, the

---

[1] In humans an MED from exposure to UV-B is generally achieved with about 20 to 70 mjoules/cm^2 (equivalent to 200 to 700 joules/m^2 depending on location and time of year (Pathak 1982); this is the amount that a fair-skinned individual would receive in about 12 to 15 minutes on a clear day in June in

work of Haniszko and Suskind (1963) went unremarked for nearly 20 years until the work of Toews and his colleagues (1980) confirmed the ability of UVR to induce immunological tolerance to skin applied antigens and demonstrated that the defect responsible for this was a local (i.e., occurred at the site of irradiation and antigen administration) impact on the antigen-presenting Langerhans cells. It was considered to be a local impact in that in irradiated animals the effect could only be demonstrated if the sensitizing agent were applied to irradiated skin; application to unirradiated skin in irradiated animals failed to show suppression of the CHS response. Subsequent work showed that the defect in antigen-presenting cell function was accompanied by the development of hapten-specific suppressor T cells (Elmets et al 1983). Further investigation of this phenomenon by Elmets and his colleagues (Elmets et al. 1985) first demonstrated that mice exposed to 700 J/m^2 broad-band UV-B developed a suppressed contact hypersensitivity to dinitrofluorobenzene (DNFB) and then characterized the wavelength dependence of this response. Exhibit 9.1 presents the two action spectra developed in that work; one assumes single hit kinetics and the other assumes multi-hit kinetics. In the single hit case radiation between 260-300 nm was most efficient in inducing immunological unresponsiveness. The dose of 260 nm energy to achieve a 50% inhibition (an ED^{50}) of contact hypersensitivity was about half the dose of 270, 280 and 290 nm energy and at 310 the ED^{50} was more than 30 times the ED50 at 260 nm. Work by Noonan and her colleagues (1984) on the impact of UVR on the number and function of Langerhans cells appears to show a similar wavelength dependency; (and as discussed in some detail below) these authors were able to distinguish a different wavelength dependence for systemic suppression of contact hypersensitivity.

Systemic suppression of contact hypersensitivity. The amounts of broad-band UV-B used to induce local unresponsiveness in the experiments described above were in the range of a human MED (400 to 700 J/m^2) whereas when narrowband energy was used an ED50 could be achieved at doses as low as 200 J/m^2. When much larger doses of broad-band UV-B are used (ED_{50} of around 30 kJ/m^2; Noonan et al 1981a) a systemic suppression of contact hypersensitivity is induced. The action spectrum (Exhibit 9-2) for systemic suppression of CHS is quite different from that found for local suppression (Exhibit 9-1). In the Noonan et al. (1984) study, these authors were able to demonstrate that 320 nm radiation was very much more efficient at systemic suppression as compared to its impact on the number and function of Langerhans cells whereas the converse was true for 270 nm radiation. In an earlier report (from which the action spectrum was derived) De Fabo and Noonan (1983) point out that the action spectrum they derived for systemic suppression of contact hypersensitivity is extremely similar to the absorption spectrum for urocanic acid (UCA), an amino acid found principally in the stratum corneum above most of the skin's protective melanin layer. UCA has some interesting properties in that it is a photoreceptor which when it absorbs a photon undergoes a cis to trans isomerization and concomitantly becomes much more soluble thus allowing its migration out of the stratum corneum. In its cis form it is virtually absolutely restricted (in the skin) to the stratum corneum. The correspondence of the UCA absorption spectrum with that of systemic suppression led De Fabo and Noonan to propose that UCA has a role in the induction of that suppression. At that time they proposed that

---

Philadelphia (Forbes 1987). Note however, that the guinea pig is about 2 to 3 times less sensitive than the human (Forbes 1987).

EXHIBIT 9-1

ACTION SPECTRA FOR LOCAL SUPPRESSION OF CONTACT HYPERSENSITIVITY ASSUMING EITHER ONE-HIT OR MULTI-HIT MECHANISMS

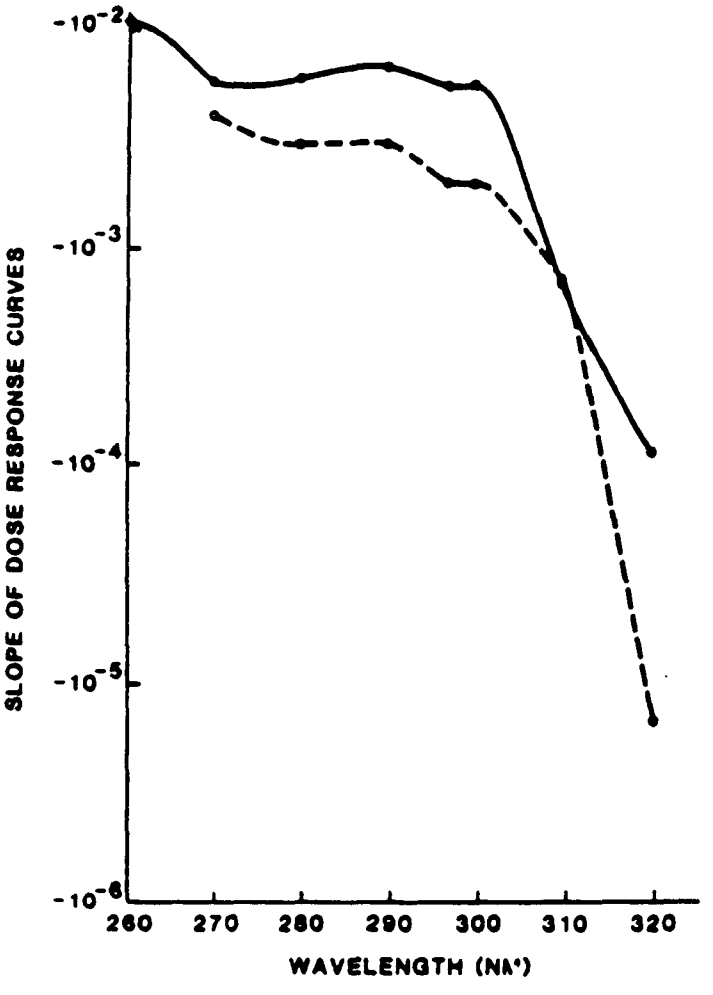

Action spectrum for the induction of unresponsiveness to DNFB in C3H mice by *in vivo* low dose UV radiation. The solid line represents the action spectrum curve if single hit kinetics are observed. The dashed line represents the action spectrum curve if multiple component kinetics are observed.

Source: Elmets et al 1985.

EXHIBIT 9-2

ACTION SPECTRUM FOR SYSTEMIC SUPPRESSION OF CONTACT HYPERSENSITIVITY

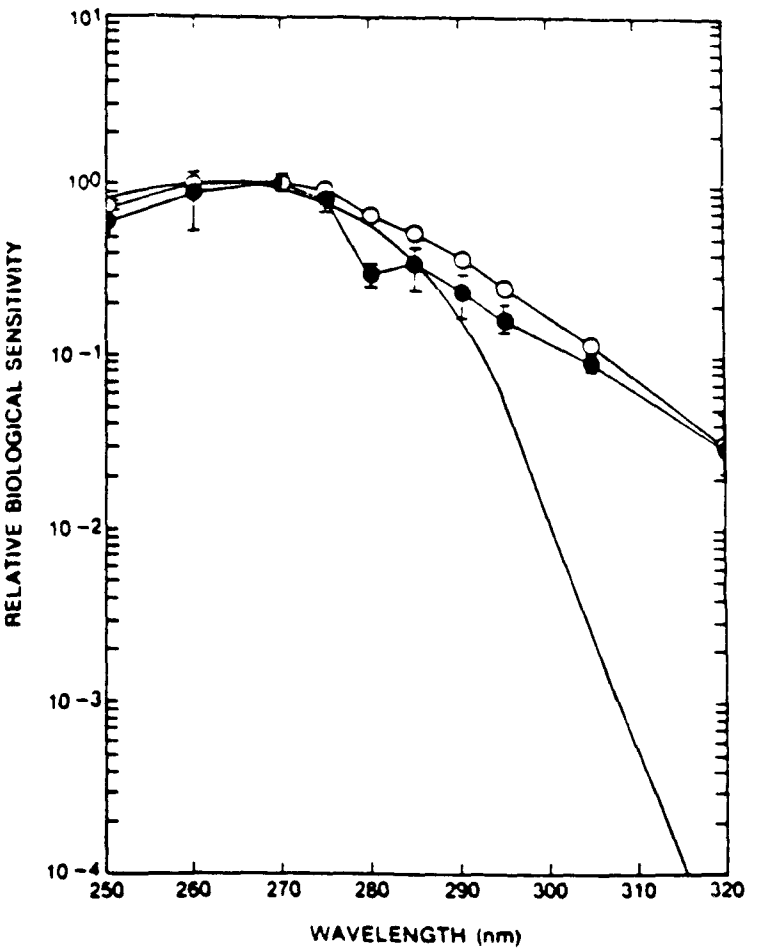

In vivo action spectrum for the induction of systemic suppression of CHS (●). Points on the action spectrum represent the reciprocal of the number of photons (m^2/photon) required to produce 50% suppression, normalized to 270 nm. Bars represent ±1 SEM. For purposes of comparison the DNA action spectrum (—) (34) and the absorption spectrum of urocanic acid (UCA) (○)

Source: De Fabo and Noonan 1983.

UCA was in some way responsible for the antigen presenting cell defect. The fact that they later discovered that the two phenomena had different action spectra led them to discard this notion with regard to the local effect observed on APC; however, this hypothesis is still viable with regard to systemic immunosuppression.

A role for UCA in systemic immunosuppression has as a corollary the fact that UVR-induced immunosuppression may not be restricted to the same fair-skinned individuals who show the greatest sensitivity to UVR-associated skin cancer. This is because UCA's position in the stratum corneum puts it above most of the skin's melanin so that UCA will not be protected from incoming photons by melanin the way that keratinocytes and melanocytes are. In addition, if UCA is important to systemic immunosuppression, then use of sunscreens (which tend to be absorbed into the epidermis rather than staying localized in the stratum corneum) might not be protective against all of the immunosuppressive effects of UV radiation. [As discussed in detail below, there is some evidence that sunscreens may not be protective for the adverse impacts of UVR on cells of the human immune response.]

Systemic suppression of delayed type hypersensitivity. Because of the similarities between DTH and CHS, most authors have assumed that these two reactions are equivalent and thus that the impact of UVR on these responses would be the same. Recently however, work by Kripke and Morison (1986a,b) provides some indication that this is not the case but rather that UVR impacts these two reactions quite differently. Using three one-day exposures (total dose of 48.6 kJ/m^2) these authors found that although suppression of DHS could be overcome by immunizing with hapten-coupled antigen presenting cells from normal donors this was not the case for suppression of CHS, treatment of UV-B irradiated mice with an anti-inflammatory agent (methylprednisolone) before immunization prevented the suppression of delayed hypersensitivity but had no effect on contact hypersensitivity, and that the hyporesponsiveness to CHS in UV-B-irradiated mice could be transferred to x-irradiated mice via the use spleen cells from UV-B irradiated mice, although the induction of hapten specific suppressor cells requires both UV-B irradiation and priming with hapten. Based on their findings, these authors postulated that UV-B irradiation produces a population of suppressor inducer cells with specificity for a modified skin antigen which can serve as a carrier molecule for haptens that induce contact hypersensitivity and for tumor- specific transplantation antigens on UV-B-induced tumors.

Much lower doses have been used by another group to suppress the DTH response to herpes simplex virus (HSV) (Howie et al. 1986a,b). This group used a single dose of 960 J/m^2 to suppress the systemic DTH response to HSV. Timing of the administration was crucial in that maximal suppression occurred if irradiation was given 2 to 3 days prior to sensitization with the virus, was less if given 5 or 7 days prior to sensitization and did not occur if given 14 days before, on the day of, or 3 days after sensitization. These authors further characterized this immunosuppression to show that two types of suppressor cells were involved and that it was the efferent arm (i.e., development of effector cells) of the immune response which was affected. Unfortunately, neither a dose-response nor an action spectrum for this impact on the DTH response has yet been characterized.

In summary there appear to be at least two, and possibly three, distinct ways in which UVR may affect the immune system. There clearly exists a low dose, shorter UV-B waveband-dependent suppression of local hypersensitivity which has an action spectrum consistent with that described for local effects on Langerhans cells and there is as well a high dose, slightly longer wavelength, UV-B-dependent process which induces systemic immunosuppression of contact hypersensitivity and has an action spectrum similar to the absorption spectrum of UCA. In addition, there appears to be a high dose systemic immunosuppression of delayed type hypersensitivity which requires further investigation in order to characterize the dose-response and action spectrum and determine if the DTH impact is a unique phenomenon.

HUMAN STUDIES

There have been fewer studies of the effects of UVR on the immune response in humans. Morison et al (1979) irradiated human volunteers with 1.5 minimal erythemal doses (MED) to produce what they termed asymptomatic erythema or 3 MED to produce what they termed symptomatic erythema. Post irradiation, all subjects showed a significant increase in the proportion of circulating polymorphonuclear leukocytes and a corresponding increase in the proportion of circulating lymphocytes. Subjects who received 3 MED also had a significant decrease in the proportion of circulating E-rosette forming cells, i.e. T cells, and an increase in the proportion of null cells. The changes in the absolute numbers of these cells were not significant. Thirty minutes and 4 hours after UV-irradiation, the response of lymphocytes to PHA was increased, then decreased, reaching a minimum 12 hours after UVR, and returning to normal 72 hours post exposure.

Hersey et al (1983a) reported on the effects of solarium exposure on normal human subjects. Normal volunteers were given a standard course of treatment in a solarium to acquire a suntan; twelve 1/2 hr exposures. The energy delivered was 10 J/m2 for UV-A and about 1% of total irradiation was UV-B (which was not quantitated). Immune functions were analyzed before, on completion, and 2 weeks after the end of irradiation. The test subjects had reduced skin test responses to DNCB and slightly reduced numbers of blood lymphocytes. There was a relative increase in T (OKT3+) cells which was attributable to an increase of OKT8+ (suppressor) cells. There was a significant increase in suppressor T-cell activity against pokeweed mitogen induced IgG production in vitro and a depression of NK activity. The changes were still present in some subjects 2 weeks after solarium exposure. The NK data is a little uncertain since the control subjects had lower levels of NK activity throughout the studies than the UV-irradiated subjects. Some patients had increased NK activity after treatment and some did not change. In a second study (Hersey, 1983b), normal human volunteers were exposed to sunlight for 12 days in a 2 week period. Tests of immune function were made before, on completion and 2 weeks after the end of the UVR. There were 15 UV-irradiated subjects and 13 age- and sex-matched controls. There were no significant changes in hemoglobin levels, total leukocyte count, and lymphocyte, or neutrophil counts. In test subjects there was a small but significant drop in T cell numbers which returned to normal by 2 weeks. There was, however, a marked increase in the ratio of suppressor cells to cytotoxic helper cells which had not returned to normal at 2 weeks after UV-irradiation. After UVR there was an increase in the activity of pokeweed mitogen-induced gamma radiation-sensitive suppressor T cell activity against IgG and IgM production. Although immunoglobulin production in vitro has too wide a range

for statistical analysis of the small numbers of patients to be of value, gamma irradiation of T cells prior to culture increased the amount of immunoglobulin produced in patients exposed to sunlight but not in controls. There were 5 persons who did not show these changes, but they were largely accounted for by persons who did not receive the full dose of UVR. Immunoglobulin levels in vivo did not change nor did NK activity change significantly in this study. In a very recent study, Hersey et al. (1987) confirmed the suppression of NK activity following exposure to radiation from solarium lamps (12 1/2 hr exposures; 18 J/m^2 per exposure equivalent to 185 mJ/m^2 of UV-B and 17.8 J/m^2 of UV-A) with the greatest depression demonstrated against a melanoma target. In the same experiments, designed to evaluate the effectiveness of a sunscreen, these authors were surprised to discover that use of a sunscreen did not prevent depression of NK activity. Although, as the authors point out, this observation could be due to the fact that the dose of UV-A delivered was sufficient to cause the effect, they also suggest that caution should be exercised in the use of such agents. Until the effectiveness of sunscreens in preventing systemic effects of UVR on the immune system is more clearly established, it should be considered that the ability of such agents to prevent erythemal responses may encourage longer exposure to solar radiation and hence lead to greater damage to those elements of the immune system which function in immune surveillance against melanoma.

O'Dell et al (1980) reported that there was a diminished immune response in sun-damaged skin. The concentration of DNCB required to elicit a positive patch test was greater in sun-damaged skin than in skin which was normal. In addition, the delayed-type hypersensitivity to intradermal injection of Candida, mumps, and PPD antigens was decreased in sun-damaged skin so that the differences were not due to a difference in percutaneous absorption of antigen through sun-damaged skin. The response to a primary irritant was the same in both sun-damaged skin and normal skin and there was no difference in the two tested sites (back of the neck and the back) in volunteers without sun-damaged skin at the back of the neck. Therefore, there is apparently a local suppression of contact hypersensitivity in sun damaged skin.

There is also evidence that the inability to repair UV-induced damage may also play a role in impairment of immune function. Patients with xeroderma pigmentosum, who suffer from sun sensitivity and increased numbers of sunlight-induced cancers, also have been shown to have impaired ability to remove and repair lesions in their DNA caused by UVR. Morison et al. (1985) reported that xeroderma pigmentosum patients had impaired ability to develop contact hypersensitivity to DNCB in sun-exposed skin when compared to normal control subjects. The numbers and morphology of Langerhans cells in the skin were the same in both groups. Unfortunately, the study did not include an assessment of ability to develop contact hypersensitivity in skin not usually exposed to sunlight.

EFFECTS OF ULTRAVIOLET RADIATION ON INFECTIOUS DISEASES

Upon the realization that irradiation with UV-B can result in both local and systemic suppression of contact hypersensitivity, concern developed that the immune response to diseases which have a cutaneous phase might be adversely affected by UV irradiation. This was especially true since only low doses of UV irradiation had been found to be necessary to suppress an immune response to antigens applied to UV-irradiated skin. As yet, not a great deal of research

has been published on this problem, although there are at least two infectious diseases, Herpes virus infections and cutaneous leishmaniasis in which research has begun to indicate that UVR-induced immunosuppression may play a role.

It has been reported for some time that exacerbation or recurrences of herpes simplex virus infections can be caused by sun exposure. An exposure of 5 to 6 MED has been reported to cause recurrence of oral herpes (Spruance 1985) and Morison (1984) noted that it is common to report exacerbation following sun exposure or UV-B phototherapy although the mechanism is unknown. In fact, exacerbation of genital herpes has also been reported to occur following exposure to the penis to experimental UVR (Klein and Linnemann, Jr. 1986) and there is a very recent report (Perna et al. 1987) that administration of UV-B at three times an individual's previously determined MED to patients infected with herpes simplex virus can reactivate the infection at sites occurring close to or within the erythema induced by irradiation.

Although, the mechanism of the activation is unknown, recent investigations on the effects of UV radiation on primary herpes infection in mice are yielding very interesting information. Low doses of UVR from sunlamps given 7 days prior to infection of mice with herpes simplex virus suppressed the delayed-type hypersensitivity to the virus (Howie et al. 1986a). Once it was induced, immune suppression to the virus persisted for at least 3 months after the UVR. The suppression has been shown to be due to two different subsets of T lymphocytes (Howie et al. 1986b). Thus in this animal model, exposure to UV radiation at an appropriate time prior to infection, suppressed the immune response made to that organism for some time and may have profound effects on the outcome of the infection.

The observations of Howie et al. (1986a,b) particularly in light of the findings of Perna et al. (1987), are of particular importance in the context of the potential role that UV-B-induced immunosuppression might play in infectious diseases. The dose given by Howie and her colleagues was only slightly in excess of a human MED yet it was sufficient to ensure that rather than developing immunity to HSV, mice became tolerant to the virus. In addition, the dose necessary to induce recurrence in the study by Perna et al. was about equivalent to a moderately severe sunburn and recurrence occurred in 3 to 6 days - a timespan not that difference from the one required in order to ensure immunosuppression (in the Howie study the virus had to be given 3 to 7 days post-irradiation in order to observe any immunosuppression.) Conceivably a moderate sunburn could not only induce recurrences of herpes infections but at the same time induce the development of suppressor cells thus preventing the host from making an efficient immune response. A similar scenario applied to immunization programs might indicate that immunizations given 3 to 7 days post an intense solar exposure could induce tolerance rather than immunity.

In addition to the impact of UVR on herpes infections, there exists another system where preliminary data suggest an impact of UVR on the progression on an infectious disease. Giannini (1986) has reported that suberythematous doses of UV-B blocked the development of the initial skin lesions in experimental leishmaniasis in mice. In addition, much as Howie et al. (1985) showed with herpes, the UV-B irradiation also abrogated the development of delayed type hypersensitivity to the leishmania antigens, so that animals which would normally be immune following primary infection were made tolerant. In a very recent report (Giannini and De Fabo 1987), further investigation of the impact

of UV-B irradiation on leishmaniasis in mice revealed that the waveband which was most active in blocking the development of skin lesions (i.e., in modifying the pathogenesis of a primary infections) was longer length UV-B, 320 nm as compared to 290 nm. What was more interesting, however, was the observation that the waveband which was most effective at affecting immunity was 290 nm (as contrasted to 320 nm) and the effect (albeit looked for in only a small number of animals) was increased parasite dissemination. Thus UV-B irradiation concommitant with an animal's first encounter with Leishmania appears to result in hosts that are non-immune (and possibly even tolerant), heavily parasitized yet free of the skin ulcers which normally announce such infections. Infection of humans through recently UV-irradiated skin might suppress the immune response to leishmanial antigens following a primary infection and thus predispose to a more chronic, or more severe disease in subsequent exposures.

The data reviewed above indicate that UV-B is immunosuppressive both locally and systemically for antigens introduced via the skin either by the epicutaneous or subcutaneous routes. There are as yet no data to indicate that UV-B treatment abrogates immunity to an antigen first introduced by a route other than the skin. The immunosuppression is for cell-mediated rather than humoral responses and is associated with the appearance of suppressor T cells specific for the skin-introduced antigens. UV-B-induced immunosuppression has been demonstrated for tumor, protein, parasite, viral, cellular and contact-sensitizing antigens. In the tumor system, the immunosuppression significantly contributes to tumorigenesis; however, very little is known about the contribution of UV-B-induced immunosuppression to the pathogenesis of infectious disease. In leishmaniasis, irradiation by UV-B results in less severe skin lesions in primary infections; preliminary data suggest that this is at a cost of depressed resistance to subsequent infection.

There are a number of questions which still need to be answered. For instance, is UV-B induced suppression limited to antigens administered via the skin? If an antigen is administered via skin capillaries (e.g., as by mosquito) is that more like being administered via cutaneous administration or intravenous (systemic) administration? Other questions include: 1) Does UV-B induced immunosuppression increase the incidence or severity of infectious diseases? 2) What are the long term consequences of low level UV exposures on the immune system? 3) Does UV-B affect ocular immunity? 4) Are IgE responses suppressed by UV-B irradiation? And, lastly, 5) Can UV-B treatment modify an already established secondary response? If for instance, an individual is immunized as a child, can a subsequent booster shot given after a sizable dose of UV-B convert an immune state to tolerance?

REFERENCES

Barker, C.F. and Billingham, R.E. Immunologically competent passenger cells in mouse skin. Transplantation 14:525-527 (1972)

Daynes, R.A., Samlowski, W.E., Burnham, D.K., Gahring, L.C., and Roberts, L.K. Immunobiological consequences of acute and chronic UV exposure. Curr Probl Derm 15:174-194 (1986)

Daynes, R.A., Schmitt, M.K., Roberts, L.K.,and Spellman, C.W. Phenotypic and physical characteristics of the lymphoid cells involved in the immunity to syngeneic UV-induced tumors. J Immunol 122:2458-2464 (1979)

Daynes, R.A., Spangrude, G.J., Roberts, L.K., and Krueger, G.G. Regulation by the skin of lymphoid cell recirculation and localization properties. J Invest Derm 85:14s-20s (1985)

De Fabo, E.C., and Kripke, M.L. Dose-response characteristics of immunologic unresponsiveness to UV-induced tumors produced by UV-irradiation of mice. Photochem Photobiol 30:385-390 (1979)

De Fabo, E.C., and Kripke, M.L. Wavelength dependence and dose-rate independence of UV radiation-induced immunologic unresponsiveness of mice to a UV-induced fibrosarcoma. Photochem Photobiol 32:183-188 (1980)

De Fabo, E.C., and Noonan, F.P. Mechanism of immune suppression by ultraviolet irradiation in vivo. I. Evidence for the existence of a unique photoreceptor in skin and its role in photoimmunology. J Exp Med 158:84-98 (1983)

De Gruijl, F.R., and Van Der Leun, J.C. Systemic influence of pre-irradiation of a limited skin area on UV-tumorigenesis. Photochem Photobiol 35:379-383 (1982)

De Gruijl, F.R., Van Der Leun, J.C. Follow up on systemic influence of partial pre-irradiation on UV-tumorigenesis. Photochem Photobiol 38:381-383 (1983)

Elmets, C.A., Bergstresser, P.R., Tigelaar, R.E., Wood, P.J., and Streilein, J.W. Analysis of the mechanism of unresponsiveness produced by haptens painted on skin exposed to low dose ultraviolet radiation. J Exp Med 158:781-794 (1983)

Fisher, M.S., and Kripke, M.L. Systemic alteration induced in mice by ultraviolet radiation and its relationship to ultraviolet carcinogenesis. Proc Natl Acad Sci USA. 74:1688-1692 (1977)

Fisher, M.S., and Kripke, M.L. Further studies on the tumor-specific suppressor cells induced by ultraviolet radiation. J Immunol 121:1139-1144 (1978)

Fisher, M.S., and Kripke, M.L. Suppressor T lymphocytes control the development of primary skin cancers in ultraviolet-irradiated mice. Science 216:1133-1134 (1982)

Giannini, M.S.H. Suppression of pathogenesis in cutaneous leishmaniasis by UV-irradiation. Infect Immun 51:838-43 (1986a).

Giannini, S.H., Effects of UV-B on infectious disease in: Effects of Changes-Stratospheric Ozone and Global Climate. Titus, T.G. UNEP/EPA Conference Proceedings, Vol 2, pp 101-112 (1986).

Giannini, S.H., and De Fabo, E.C. Abrogation of skin lesions in cutaneous leishmaniasis by ultraviolet B irradiation. In: Leishmaniasis: The First Centenary (1885-1985) New Strategies for Control. Hart, D.T. (ed.) NATO ASI Series A: Life Sciences, London: Plenum Publishing Company Limited, (1987) in press.

Granstein, R.D. Photoimmunology. In: Dermatology in General Medicine, 3rd ed. Fitzpatrick, T.B., Eisen, A.Z., Wolff, K., Freedberg, I.M., and Austen, K.F. (eds.) New York: McGraw-Hill Book Co., pp 733-796 (1987)

Haniszko, J., and Suskind, R.R. The effect of ultraviolet radiation on experimental cutaneous sensitization in guinea pigs. J Invest Derm 40:183-191 (1963)

Hersey, P., Bradley, M., Hasic, E., Haran, G., Edwards, A., and McCarthy, W.H. Immunological effects of solarium exposure. Lancet 1:545-548 (1983a)

Hersey, P., Haran, G., Hasic, E., and Edwards, A. Alteration of T cell subsets and induction of suppressor T cell activity in normal subjects after exposure to sunlight. J Immunol 131:171-174 (1983b)

Hersey, P., MacDonald, M, Burns, C., Schibeci, S., Matthews, H., and Wilkinson, F.J. Analysis of the effect of a sunscreen agent on the suppression of natural killer cell activity induced in human subjects by radiation from solarium lamps. J Invest Dermatol 88:271-276 (1987)

Howie, S., Norval, M. and Maingay J. Exposure to low-dose ultraviolet radiation suppresses delayed-type hypersensitivity to herpes simplex virus in mice. J Invest Dermatol 86:125-8 (1986a)

Howie, S.E., Norval, M, Maingay, J., and Ross J.A. Two phenotypically distinct T cells (Lyl+2- and Lyl-2+) are involved in ultraviolet-B light-induced suppression of the efferent DTH response to HSV-1 in vivo. Immunology 58:653-8 (1986b)

Kripke, M.L. Antigenicity of murine skin tumors induced by ultraviolet light. J Natl Cancer Inst 53:1333-1336 (1974)

Kripke, M.L. Target organ for a systemic effect of ultraviolet radiation. Photochem Photobiol 24:599-600 (1976)

Kripke, M.L. Latency, histology, and antigenicity of tumors induced by ultraviolet light in three inbred mouse strains. Cancer Res 37:1395-1400 (1977)

Kripke, M.L., Immunological unresponsiveness induced by ultraviolet radiation. Immunol Rev 80:87-102 (1984)

Kripke, M.L. Photoimmunology: The first decade. Curr Probl Derm 15:164-175 (1986)

Kripke, M.L. and Fisher, M.S. Immunologic parameters of ultraviolet carcinogenesis. J Natl Cancer Inst 57:211-215 (1976)

Kripke, M.L. and Morison W.L. Studies on the mechanism of systemic suppression of contact hypersensitivity by UVB radiation. II. Differences in the suppression of delayed and contact hypersensitivity in mice. J Invest Dermatol 86:543-9 (1986)

Kripke, M.L. and Morison W.L. Studies on the mechanism of systemic suppression of contact hypersensitivity by ultraviolet B radiation. Photodermatol 3:4-14 (1985)

Kripke, M.L., Lofgreen, J.S., Beard, J., Jessup, J.M., and Fisher, M.S. In vivo immune responses of mice during carcinogenesis by ultraviolet irradiation. J Natl Cancer Inst 59:1227-1230 (1977)

Kripke, M.L., Thorn, R.M., Lill, P.H., Civin, C.I., Pazmino, N.H., and Fisher, M.S. Further characterization of immunological unresponsiveness induced in mice by ultraviolet radiation. Growth and induction of non-ultraviolet-induced tumors in ultraviolet-irradiated mice. Transplantation 28:212-217 (1979)

Luger, T.A., Stadler, B.M., Katz, S.I. and Oppenheim, J.J. Epidermal (keratinocyte)-derived thymocyte activating factor (ETAF). J Immunol 127:1493-1498 (1981)

Lynch, D.H., and Daynes, R.A. Evaluation of naturally occurring cell-mediated cytotoxic activity in normal and UV-irradiated mice. Transplantation 35:216-223 (1983)

Lynch, D.H., Gurish, M.F., and Daynes, R.A. The effects of high-dose UV exposure on murine Langerhans cell function at exposed and unexposed sites as assessed using in vivo and in vitro assays. J Invest Derm 81:336-341 (1983)

Lynch, D.H., Gurish, M.F., and Daynes, R.A. The effects of ultraviolet irradiation on the generation of antitumor cytotoxic effector cell responses in vitro. J Immunol 127:1163-1168 (1981)

Morison, W.L., and Kelley, S.P. Sunlight suppressing rejection of 280- to 320-nm UV-radiation-induced skin tumors in mice. JNCI 74:525-527 (1985)

Noonan, F.P., Bucana, C., Sauder, D.N., and De Fabo, E.C. Mechanism of systemic immune suppression by UV radiation in vivo. II. The UV effects on number and morphology of epidermal Langerhans cells and the UV-induced suppression of contact hypersensitivity have different wavelengths. J Immunol 132:2408-2416 (1984)

Noonan, F.P., De Fabo, E.C., and Kripke, M.L. Suppression of contact hypersensitivity by UV radiation and its relationship to UV-induced suppression of tumor immunity. Photochem Photobiol 34:683-689 (1981a)

Noonan, F.P., Kripke, M.L., Pedersen, G.M., and Greene, M.I. Suppression of contact hypersensitivity in mice by ultraviolet irradiation is associated with defective antigen presentation. Immunol 43:527-533 (1981b)

Norbury, K.C., Kripke, M.L., and Budmen, M.B. In vitro reactivity of macrophages and lymphocytes from ultraviolet -irradiated mice. J Natl Cancer Inst 59:1231-1235 (1977)

Perna, J.J., Mannix, M.L., Rooney, J.E., Notkins, A.L. and Straus, S.E. Reactivation of latent herpes simplex virus infection by ultraviolet light: A human model (submitted for publication; 1987)

Roberts, L.K., and Daynes, R.A. Modification of the immunologic properties of chemically-induced tumors arising in hosts treated concomitantly with ultraviolet light. J Immunol 125:438-447 (1980)

Roberts, L.K., Spellman, C.W., and Daynes, R.A. Modulation of immunoregulatory responses directed toward various tumor antigens within hosts possessing distinct immunologic potentials. J Immunol 125:663-672 (1980)

Roberts, L.K., Spellman, C.W., and Daynes, R.A. Establishment of a continuous T cell line capable of suppressing anti-tumor immune responses in vivo. J Immunol 131:514-519 (1983)

Romerdahl, C.A., and Kripke, M.L. Detection of UV tumor-specific T helper activity in vitro. J Immunol, In press.

Rose, M.L., Parrot, D.M.V. and Bruce, R.G. Divergent migration of mesenteric and peripheral immunoblasts to sites of inflammation in the mouse. Cell Immunol 27:36-46 (1976)

Sauder, D.N., Carter, C.S., Katz, S.I. and Oppenheim, J.J. Epidermal cell production of thymocyte activating factor (ETAF). J Invest Dermatol 79:34-(1982)

Sauder, D.N., Noonan, F.P., De Fabo, E.C., and Katz, S.I. Ultraviolet radiation inhibits alloantigen presentation by epidermal cells: Partial reversal by the soluble epidermal cell product, epidermal cell-derived thymocyte-activating factor (epidermal T-cell activating factor). J Invest Derm 80:485-489 (1983)

Spellman, C.W., Woodward, C.W., and Daynes, R.A. Modification of immunological potential by ultraviolet radiation. I. Immune status of short-term UV-irradiated mice. Transplantation 24:112-119 (1977)

Spellman, C.W., and Daynes, R.A. Modification of immunologic potential by ultraviolet radiation. II. Generation of suppressor cells in short-term UV-irradiated mice. Transplantation 24:120-126 (1977)

Spellman, C.W., and Daynes, R.A. Properties of ultraviolet light-induced suppressor lymphocytes within a syngeneic tumor system. Cell Immunol 36:383-387 (1978)

Spellman, C.W., and Daynes, R.A. Cross-reactive transplantation antigens between UV-irradiated skin and UV-induced tumors. Photoderm 1:164-169 (1984)

Spikes, J.D. Comments on light, light sources and light measurements. pp. 5-21, In: Experimental and Clinical Photoimmunology, Daynes, R.A., and Spikes, J.D. Eds., CRC Press, Boca Raton, FL, 1983

Spruance, S.L. Pathogenesis of Herpes simplex labialis: Experimental induction of lesions with UV light. J Clin Microbiol 22:366-368 (1985)

Stingl, G., Katz, S.I., Clement, L., Green, I., and Shevach, E.M. Immunologic functions of Ia-bearing epidermal Langerhans cells. J Immunol 121:2005-2013 (1978)

Stingl, L.A., Sauder, D.N., Iijima, M., Wolff, K., Pehamberger, H., and Stingl, G. Mechanism of UV-B-induced impairment of the antigen-presenting capacity of murine epidermal cells. J Immunol 130:1586-1591 (1983)

Streilein, J. W. and Tigelaar, R.E. SALT: Skin-associated lymphoid tissues, In Photoimmunology Kripke, M.L., Parrish, J.A. and Morison W. (eds)

Streilein, J.W. The skin as an immune organ, In The Effect of Ultraviolet Radiation on the Immune System, Parrish, J.A (ed) New Jersey: Johnson and Johnson Baby Products, pp 21-34, (1983)

Streilein, J.W., Toews, G.B., and Bergstresser, P.R. Langerhans cells: Functional aspects revealed by in vivo grafting studies. J Invest Dermatol 75:17-21 (1980)

Toews, G.B., Bergstresser, P.R., Streilein, J.W., and Sullivan, S. Epidermal Langerhans cell density determines whether contact hypersensitivity or unresponsiveness follows skin painting with DNFB. J Immunol 124:445-453 (1980)

Ullrich, S.E., and Kripke, M.L. Mechanisms in the suppression of tumor rejection produced in mice by repeated UV irradiation. J Immunol 133:2786-2790 (1984)

CHAPTER 10

CATARACTS AND OTHER EYE DISORDERS

SUMMARY

Cataracts are opacities that develop in the lens of the eye and impair vision. In the United States and other developed countries, cataract operations prevent most cataracts from causing blindness. However, in the U.S. cataract remains the third leading cause of legal blindness. In developing countries where such operations are not always available, cataracts often result in blindness.

Scientific understanding of the physical mechanisms which cause cataracts is incomplete; it is likely that more than one mechanism operates. Epidemiological studies, laboratory animal studies, and biochemical analysis support the belief that some cataracts are caused by ultraviolet radiation B (UV-B). Ultraviolet radiation A and other causes are also likely. A change in the amount of UV-B radiation is reasonably likely to alter the incidence of cataracts. UV-B may also play a role in causing or exacerbating other eye disorders. Ozone modification that alters the amount of UV-B reaching the earth's surface is likely to change the prevalence (and incidence) of cataracts.

FINDINGS

1. THERE APPEARS TO BE A REASONABLE PROBABILITY THAT CATARACT INCIDENCE WILL CHANGE WITH ALTERATIONS IN THE FLUX OF UV-B CAUSED BY OZONE MODIFICATION.

   1a) Many possible mechanisms exist for formation of cataracts. UV-B may play an important role in some mechanisms.

   1b) Although the cornea and aqueous of the human eye screen out significant amounts of UV-A and UV-B radiation, nearly 50 percent of radiation at 320 nm is transmitted through to the lens. Transmittance declines substantially below 320 nm, so that less than one percent is transmitted below approximately 290 to 300 nm. However, the results of laboratory experiments on animals indicate that short wavelength UV-B (i.e., below 290 nm) is perhaps 250 times more effective than long wavelength UV-B (i.e., 320 nm) in inducing cataract.

   1c) In laboratory animal experiments, the action spectrum for cataracts is weighted heavily in the UV-B range.

   1d) Human cataract prevalence appears to vary with latitude and UV radiation; brunescent nuclear cataracts show the strongest relationship.

2. INCREASES IN THE AMOUNT OF UV-B THAT CAN REACH THE RETINA APPEAR CAPABLE OF CAUSING STABLE RETINAL DISORDERS AND RETINAL DEGENERATION, TWO CAUSES OF BLINDNESS.

3. UV-B MAY PLAY A ROLE IN DISORDERS OF THE EYES AS WELL AS IN DEVELOPMENTAL DISORDERS.

CATARACTS[1]

The longest standing hypothesis which may account for the development of senile cataracts is that radiant energy, particularly sunlight, is a major factor in the etiology of the disease. This concept apparently originated from observations reported by a number of individuals indicating that cataracts occurred more frequently or earlier in persons whose occupations kept them outdoors or that populations living in areas with longer hours of sunshine have a higher frequency of cataract than populations from areas where there is less sunshine. While the early studies were severely flawed by their failure to consider adequately the possible effects of a variety of socioeconomic and other variables, Duke-Elder (1926, 1972) proposed that "the fundamental cause of cataract in all its forms may be traced to the incidence of radiant energy directly on the lens itself."

Definition of Cataract

Cataract is defined as an opacity in the normally transparent lens of the eye which produces an impairment of vision. Cataracts may occur as a result of a wide variety of factors including metabolic disorders, exposure to toxic agents, trauma, exposure to radiation, and hereditary factors. The great majority of cataracts, however, are the so-called senile cataracts which occur in older individuals and for which no specific causative factor can be identified. Cataract is a major cause of visual impairment and blindness particularly in developing countries where access to modern surgical facilities is limited. Even in the United States, cataract is the third leading cause of legal blindness. Some 60 percent of people aged 60 to 74 have at least some cataractous changes in their lenses. The only efficacious treatment for cataract at present is the surgical removal of the opaque lens and nearly 660,000 such operations were performed in 1982 in the U.S.

It is clear therefore that senile cataract is a very significant health problem, both in terms of its impact on the affected individuals and on society at large. While considerable progress has been made in elucidating the biochemical etiology of certain specific cataract types, such as sugar cataracts, there is little conclusive data on the causes of senile cataracts. It is likely that there are a variety of potential risk factors and that, in general, senile cataracts have a multifactorial etiology. This conclusion is supported by the great variability observed clinically in the time of onset, the rate of maturation, and the morphological appearance and location within the lens of these opacities. It appears that many, if not all, of the processes contributing to senile cataractogenesis are normal aging processes which for whatever reason are accelerated in certain individuals.

Cataract Classification

There are now rather sophisticated systems for the classification of cataracts. Chylack et al. (1978, 1983) have devised an in vitro system which is based on photographic documentation of opacification and nuclear color. Almost 2500 cataracts have been studied and classified since the original methods were adopted (Chylack et al., 1983). In addition, Marcantonio et al. (1980) have suggested a system of classification of human senile cataracts by using photography for in vivo and in vitro analysis and determining the sodium and

---

[1] This section in boldface type is taken from Pitts, D.G. et al. (in press).

protein content of the extracted lens. The photographic method gave consistent involvement of the lens nucleus but it was not always possible to relate sodium changes to light scattering. Marcantonio et al. (1980) argue that a dual classification system is necessary because most cataracts are mixed in nature and the osmotic and nuclear mechanisms provide quite different changes in protein distribution.

The present state of knowledge concerning the human senile cataract probably justifies a classification into only two major types in spite of the elegant classification systems mentioned above. The first and most common type of human senile cataract is the cortical cataract. Cortical cataracts are characterized by imbalances in cation levels within the lens cells which produce osmotic swelling and ultimate opacity in the lens cortex. Altered cation balance may result from damage to the Na^+, K^+-ATPase or from compromise of the normal permeability characteristics of the lens membranes. Any of a great variety of potential insults could be the ultimate cause of such cataracts. The second major type of senile cataract is the nuclear cataract which is characterized primarily by very marked modifications to the structural proteins of the lens, the crystalline, in the central region of the lens. These two types of cataracts are not at all mutually exclusive; in many instances, senile cataracts contain both cortical and nuclear opacities. It is advisable for those who are involved in cataract research to become knowledgeable and use a recommended classification system.

Epidemiological Studies

A few general statements should be made relative to the cataract epidemiological studies. Most epidemiological studies have reported an increase in the prevalence of cataracts with an increase in age and at 65 years of age and above there is an acceleration in the prevalence of cataracts. Women have shown a larger prevalence of cataracts than men; however, this difference has not been shown to be statistically significant.

In recent years there have been a number of epidemiological studies reported which have attempted to establish that there is an association between cataract prevalence and exposure to sunlight or the ultraviolet component of sunlight. Hiller, Giacometti and Yuen (1977) utilized data on the populations sampled in two independent health surveys, the Model Reporting Area for Blindness Statistics (MRA) and the National Health and Nutrition Examination Survey (HANES) to compare the prevalence of cataract in geographical areas with varying total annual hours of sunlight. The total annual hours of sunlight was obtained from U.S. Weather Bureau statistics and ranged from 1800 to 3800 hours. For each health survey ocular diseases other than cataract were used as control and the data reported as age-specific ratios of cataract cases to control cases for areas of differing total annual insolation. The findings suggest that in the youngest age group studies (20-44 yrs) there is no greater incidence of cataract in areas of high annual sunlight, but that with increasing age there appears to develop an increasing association of cataract with sunlight exposure. In the 65-74 yr sample population, there was at least a doubling of the ratio of cataract to each control disease between the lowest and highest sunshine area and in persons 75 years and older this trend was even more pronounced. The study did not consider the possible effects of genetic or socioeconomic differences among the populations from different areas nor did it consider the actual sunlight exposure of the individuals (e.g. indoor vs outdoor occupation).

Zigman, Datiles, and Torczynski (1979) have studied populations from three

widely separated areas (Manila, the Philippines; Tampa, Florida; and Rochester, New York) which differ considerably in the yearly levels of ultraviolet radiation in sunlight. This study considered not only the age of the individuals studied, but also considered separately those with indoor and outdoor occupations. The findings which were based on study of extracted cataracts included analysis of the cataract type for each lens. The results indicated that no correlation existed between geographic location and distribution of cataracts except for the brunescent cataracts; i.e., those nuclear cataracts with significantly increased pigmentation levels. In Manila, the area with greatest UV, such cataracts accounted for 43% of total cataracts while in Tampa 20% of cataracts were brunescent and in Rochester, the area of least UV, only 9%. In all three populations, the percentage of brunescent cataracts extracted in persons with outdoor occupations was markedly higher than in those persons working indoors. Thus, both the latitudinal variation and the individual differences within geographic regions suggested a strong relationship between UV exposure and brunescent cataract. These data are consistent with numerous reports that tropical areas have higher cataract incidence than areas at higher latitudes and that the percentage of brunescent cataracts is higher in tropical areas (Pirie 1972 and references in Taylor 1980). The confounding factors which were pointed out by Zigman, Datiles, and Torczynski (1979) as not being controlled in their study included the economic, nutritional and genetic backgrounds of the individuals in the respective populations. While these differences would probably be substantial, particularly between Manila and the two U.S. sites, this study is significant in that it involved some biochemical evaluation of the cataracts as well as the epidemiological data.

Two recent epidemiological studies have concerned cataracts in Australian aborigines, a rural population exposed to relatively intense solar radiation. Taylor (1980) studied 350 individuals from which detailed personal histories were obtained. The possible role of a variety of personal and environmental factors in cataractogenesis were investigated. Among the 350 individuals, all of whom were over 30 years of age, 116 had lens opacities as determined by slit-lamp examination. The major findings relative to the possible influence of radiation exposure to cataractogenesis were a trend toward association of cataracts with increased hours of sunlight and with higher annual mean UV-B levels. These trends were reflected by a strong association of cataract with lower latitudes. No other environmental factors studies appeared to be associated with cataract nor did any personal factors other than age. No correlation would found between occupation and cataract; it is not clear whether this finding is inconsistent with Zigman, Datiles, and Torczynski (1979) since it is not reported whether any of the individuals studied had indoor occupations. Unfortunately, the types of cataracts present were not reported in this study (Taylor 1980).

In a second study involving a much greater geographical area and over 50% (64,307) of the total Aborigine population, Hollows and Moran (1981) also found a statistically significant correlation between environmental UV irradiation and the prevalence of cataract ($p<0.005$). Additionally cataracts occurred much more frequently in the younger age group (40-59 yrs) in geographical zones of high UV radiation than in zones of low UV irradiation. The authors suggest that the Aborigines from remote rural Australia are a suitable population for such studies since their lifestyle tends to be highly uniform throughout the country. In contrast to these results, a large sample of non-Aboriginal people from the same areas showed much lower levels of cataract, particularly at younger ages, and there was no correlation between cataract prevalence and sunlight in this group. This was attributed to the much higher standard of living and the

greater likelihood of indoor occupations in this group.

The data of Hollows and Moran (1981) may be used to estimate the number of senile cataracts which are caused by sunlight if we can accept the confounding factors mentioned above. Exhibit 10-1 presents the prevalence of cataracts found in aborigines by UV zone for three different age groups. Exhibit 10-2 compares the prevalence of cataracts found in non-aborigines and aborigines who live in the same regions.

Exhibit 10-1 shows that 13.6% of the aborigines in the lowest solar region develop cataracts while about 30% in the more solar intense zones develop cataracts. These data appear to indicate that about 15% of the senile cataracts are due to solar exposure. If the aborigine and non-aborigine are compared (Exhibit 10-2) there was about a 13% increase in cataracts which are probably due to solar radiation. More recently, Weale (1982) has presented a method of estimating the risk attributed to light for the incidence of senile cataracts and reported a risk factor of 5. If the risk factor may be expressed in percent form or 20%, the results are not too different from the above. It is interesting that the two sets of diverse data present such interesting results. Incidentally, the 18.3% prevalence for cataracts for the non-aborigine compared quite favorably to the Framingham Study (Kahn et al. 1977a and b) and the Gisborne Study (Martinez et al. 1982).

Thus, there appears to be a consensus from these epidemiological studies in support of the notion that senile cataract or at least a particular segment of the heterogeneous mixture of opacity types which comprise senile cataracts, is associated with higher exposure to sunlight. Substantive questions could certainly be raised concerning each of the studies cited above; however, taken in aggregate they represent a variety of approaches, using different types of populations, different criteria for cataract, different sampling and statistical methods, and different variables to test the same hypothesis. It is striking that the general conclusions of each study are so similar.

Ocular Transmittance

The effect of nonionizing radiation on a cell depends on the specific chemical composition within the cell, that is, on the presence of absorbing molecules or chromophores (Lerman 1980a). This type of radiation must be absorbed in order to cause a change in the molecule since absorbed energy is required to promote a chemical change. Molecules in excited electronic states have different chemical and physical properties than their counterparts in the ground state (prior to absorption of energy). Thus cells that do not contain chemical compounds absorbing at certain wavelengths will transmit these wavelengths. For example, the nucleic acids and most proteins in a cell are essentially transparent to and completely transmit visible light but absorb certain wavelengths in the UV region (between 250 and 295 nm) and can be damaged by this form of radiation, while other macromolecules in a cell such as

EXHIBIT 10-1

Cataract Prevalence by UV Zone

UV Zone	Age 0-39	40-59	60+
1	0	1.7%	13.6%
2	0	2.6%	24.2%
3	0.1%	3.7%	29.5%
4	0.1%	3.8%	30.5%
5	0.2%	5.1%	29.8%

Source: After Hollows and Moran 1981.

EXHIBIT 10-2

Comparison of Cataract Prevalence for Aborigines and Non-Aborigines

Ethnic Group	Age 50-59	60+
Non-aborigine	0.8%	18.3%
Aborigine	4.4%	29.3%

Source: After Hollows and Moran 1981.

rhodopsin, which absorbs at 498 nm, and hemoglobin, which has absorption peaks in the UV and visible region (275, 400, and 540 to 576 nm), appear colored since they absorb visible light. These latter macromolecules can be damaged by high intensities of visible radiation at their specific absorption wavelengths.

The transmittance data for the rabbit, primate and human eye and ocular media for the wavelength range of 200nm to 2500nm are given in Exhibits 10-3, 10-4 and 10-5. Exhibits 10-6 and 10-7 present transmittance data for the 200 to 400 wavelength range (Kinsey 1948; Boettner and Wolter 1962; Maher 1978; Barker 1979).

The Action Spectrum

Since the absorption of nonionizing radiation is determined by the chemical composition of the tissue being exposed, the more radiation that the molecules absorb the greater will be the effect of the radiation. The term "action spectrum" is used as a measure of the relative effect of different wavelengths of radiation on a chemical compound, macromolecule, cell, or entire organism. The action spectrum is a plot of the dose or radiant exposure necessary to produce the defined effect versus the wavelength. For example, the maximum efficiency for experimental photokeratitis has been shown to occur at approximately 300 nm, with a smaller peak at 295 and 320 nm (Pitts 1978 and Pitts and Cullen 1981). The action spectra for photokeratitis, cataracts and retinal lesions for the rabbit, primate and human are presented in Exhibits 10-8 and 10-9.

The eye is the only organ or tissue in the body (aside from the skin) that is particularly sensitive to the non-ionizing wavelengths of radiation (longer than 280 nm) normally present in our environment. In addition to infrared and visible radiation, we are constantly exposed to ultraviolet radiation (solar and man-made) throughout life. It is estimated that approximately 8% (11 mW/cm2) of solar radiation above the atmosphere is in the ultraviolet region (280-400 nm). At sea level this is decreased to 2-5 mW/cm2, depending on geographic location and season (Lerman 1980b).

Nature has provided us with transparent ocular media which are essentially avascular and contain very few visible wavelength absorbing chromophores in order to effectively transmit (as well as refract) the specific wavelengths required to initiate the visual process by photochemical reactions. However, these tissues do have the ability to absorb varying amounts of ultraviolet radiation (particularly the ocular lens). The shorter the wavelengths of radiation absorbed the greater the potential for photic damage since there is an inverse relationship between a wavelength and the photon energy association with it. Thus, UV radiation is the non-ionizing portion of the electromagnetic spectrum which could cause the most damage, provided that it is absorbed. This axiom applies to all the ocular tissues including the retina in the very young eye where the lens has not as yet become as effective UV filter but, in particular, the ocular lens sustains the greatest amount of photochemical change during a lifetime of exposure to ambient UV radiation.

Some Biochemical Mechanisms

There are several mechanisms which are biochemically related to radiation damage to the eye and the lens in particular. These mechanisms include

EXHIBIT 10-3

Composite Transmittance Curves for the Rabbit With Representative Data for Boettner and Wolter (human, 1962), Weisinger (rabbit, 1956) and Kinsey (rabbit, 1948) for Comparison (after Barker, 1979)

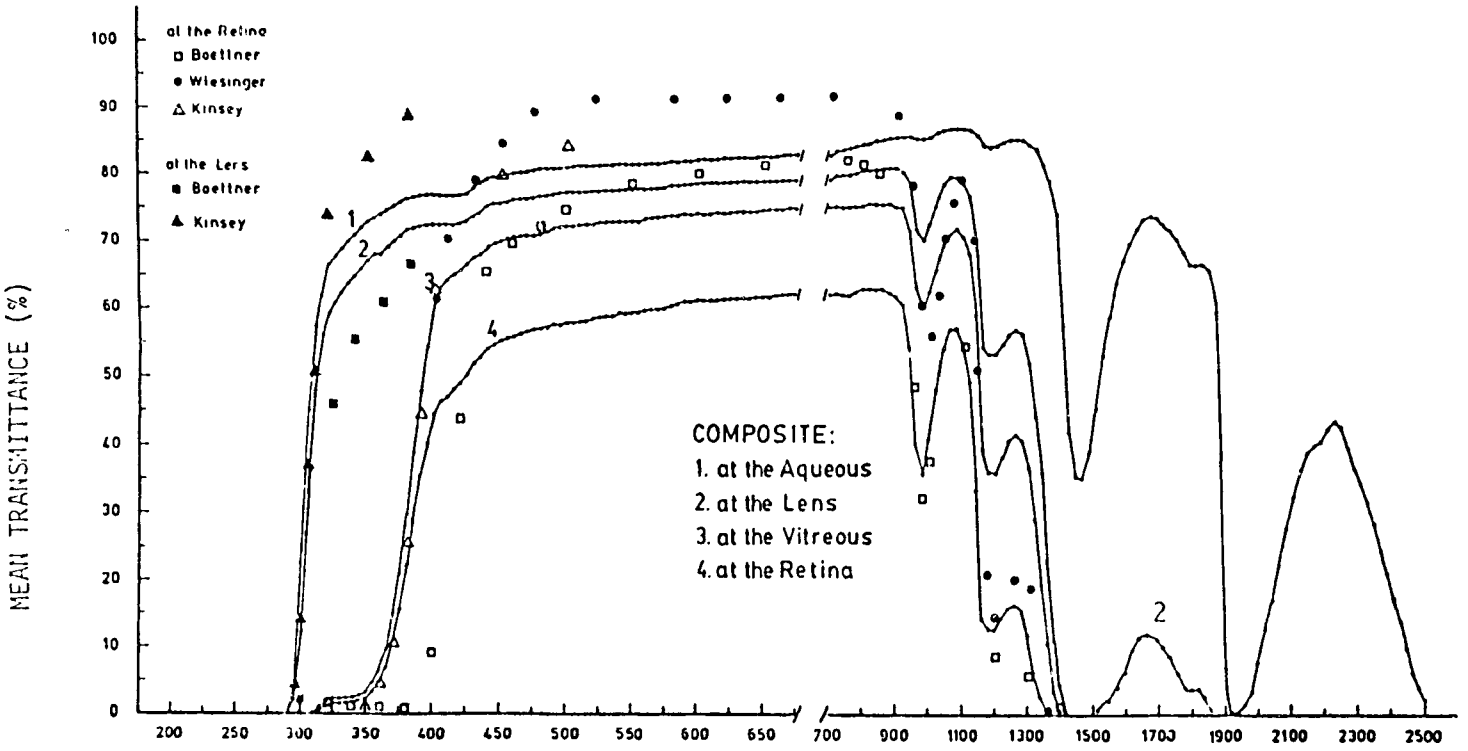

EXHIBIT 10-4

Calculated Total Transmittance of the Human Eye
(after Boettner and Wolter 1962)

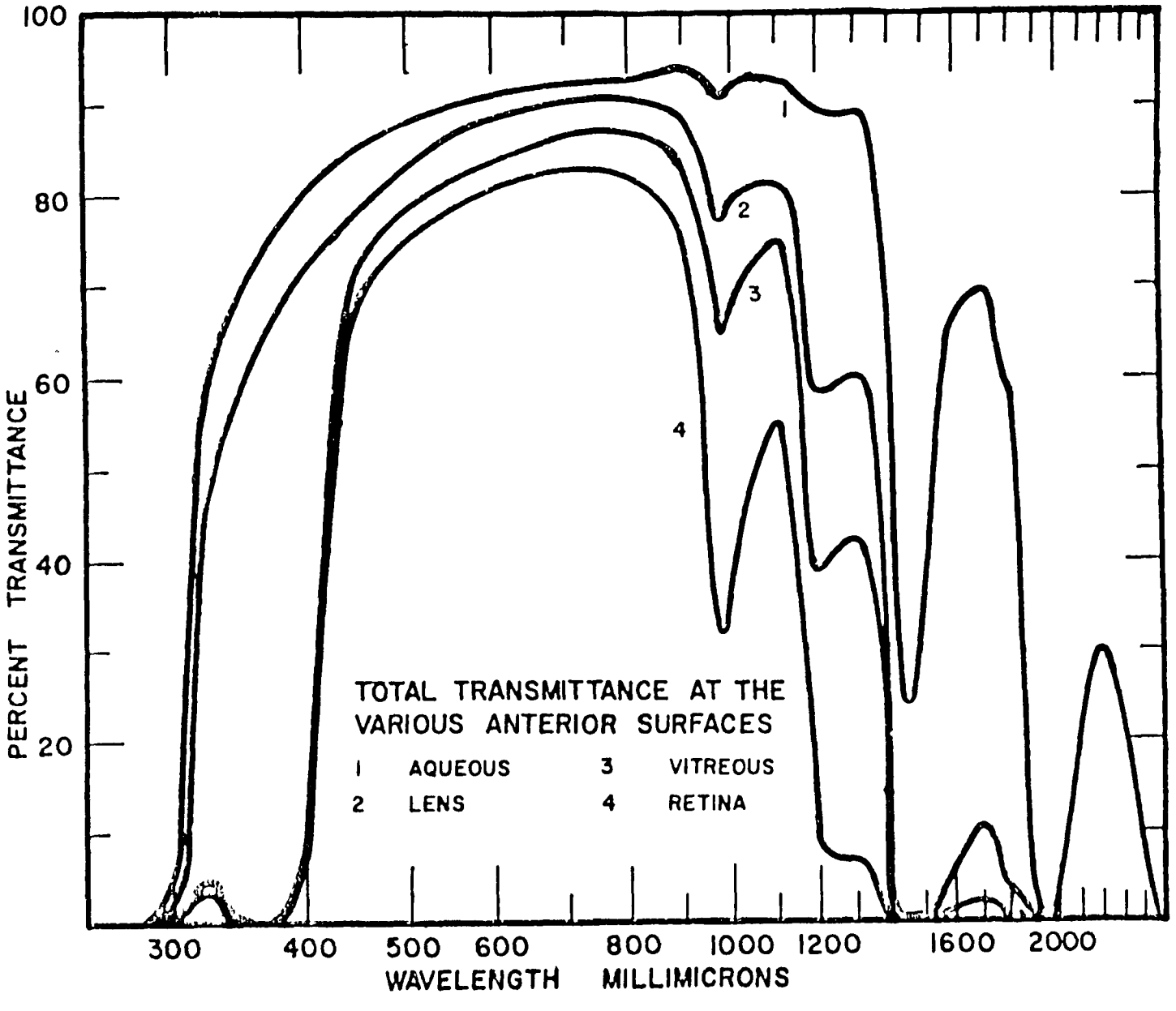

EXHIBIT 10-5

Percent Transmissivity Through the Entire Rhesus Eye
(after Maher 1978)

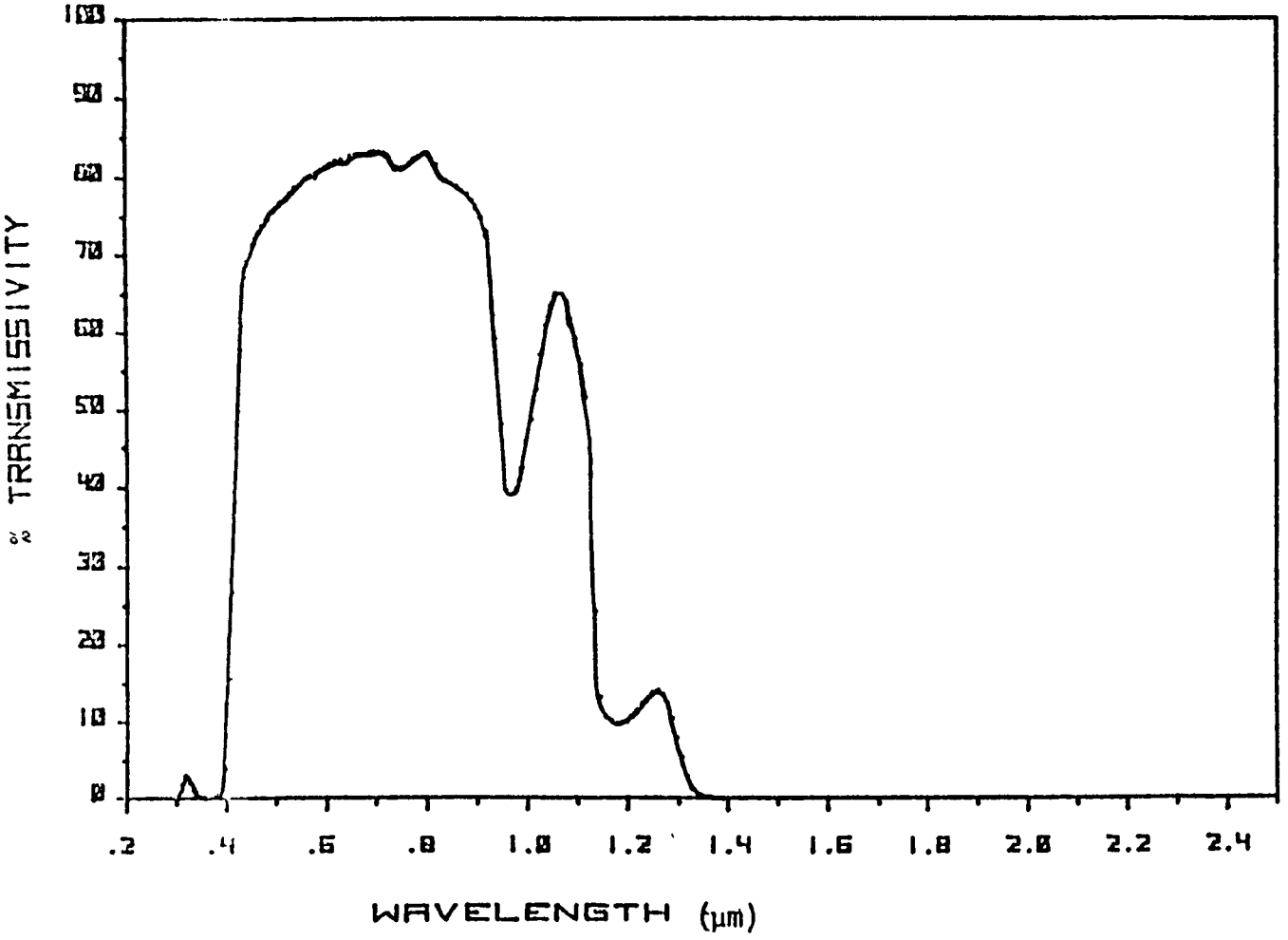

EXHIBIT 10-6

Transmittance of the Total Rabbit Cornea, the Total Human Cornea, and the Rabbit Corneal Epithelium (after Kinsey [1948] and Boettner and Wolter [1962]

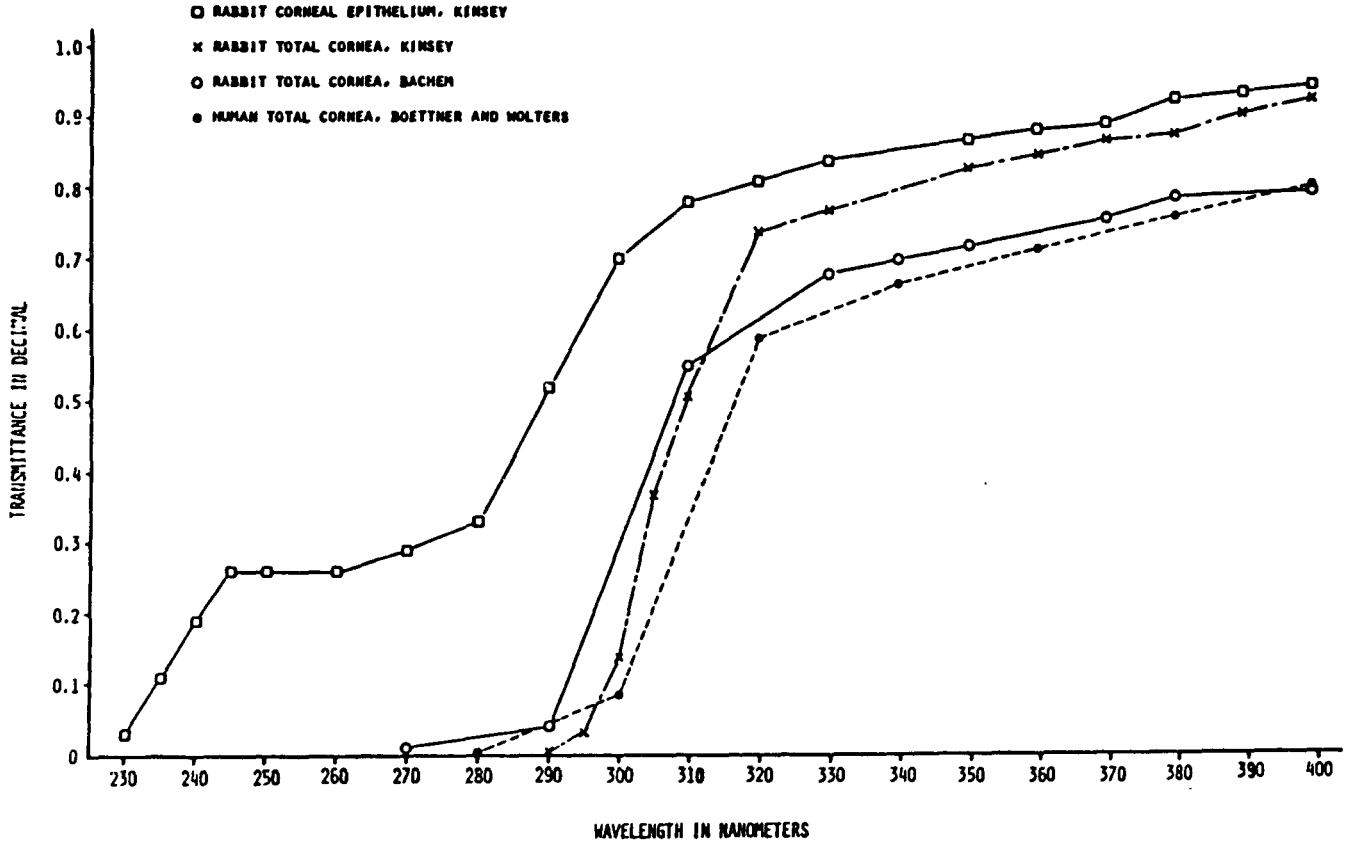

EXHIBIT 10-7

Transmittance of the Anterior Ocular Structures of the Human and Rabbit Eyes. The Symbols Indicate the Percentage of Radiant Energy Incident On a Certain Structure (after Pitts, Hacker, and Parr 1977)

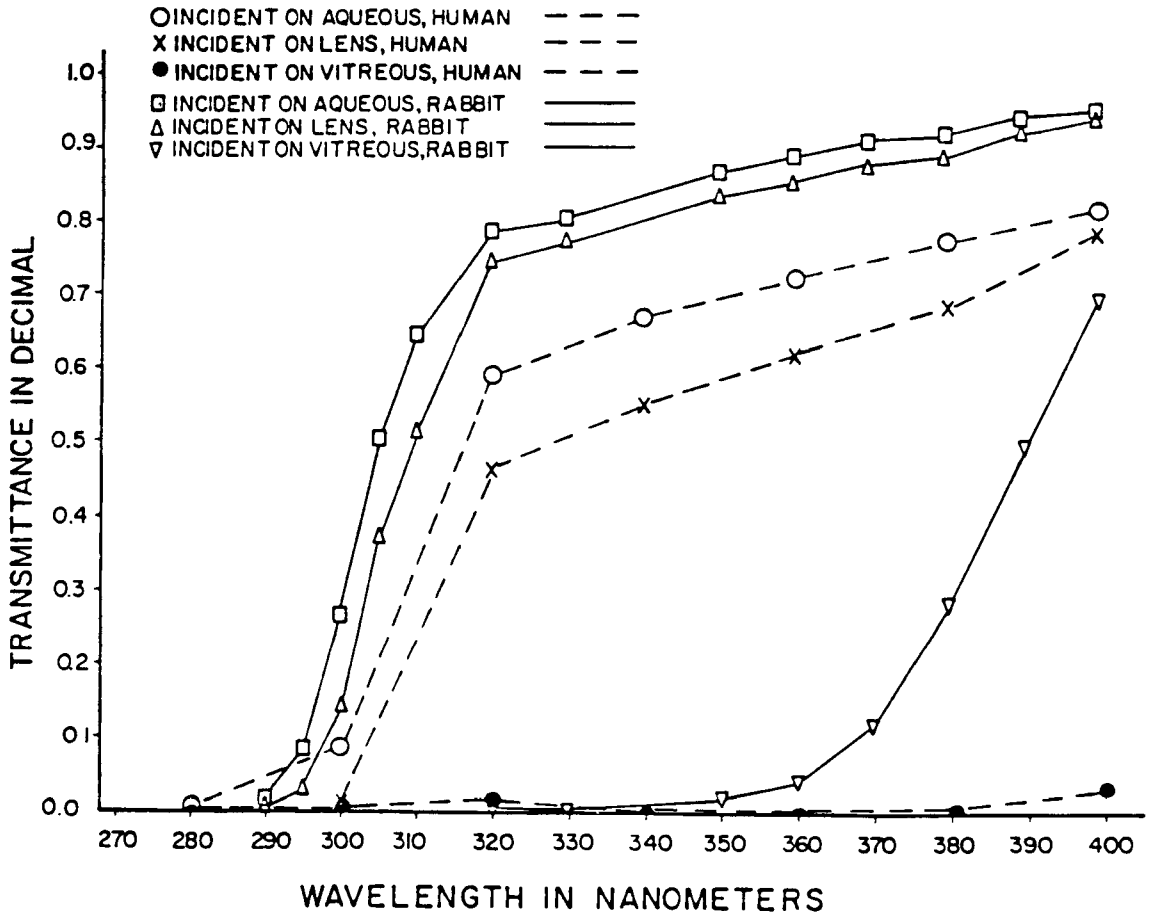

EXHIBIT 10-8

UV Radiant Exposure Threshold Data for the Cornea H_C, Lens H_L Cataracts, and Retina H_R for the Rabbit and Primate

WAVELENGTH nm	CORNEAL Radiant Exposure H_C in J/cm^2		LENS Radiant Exposure H_L in J/cm^2		RETINA Radiant Exposure H_R in J/cm^2	
	Rabbit	Primate	Rabbit	Primate	+Rabbit	*Primate
210	0.17	0.33				
220	0.046	0.021				
230	0.03	0.022				
240	0.033	0.012				
250	0.041	0.020				
260	0.018	0.011				
270	0.005	0.004				
280	0.11	0.006				
290	0.012	0.007	3.00			
295			0.75			
300	0.022	0.01	0.15	0.12	0.225	0.12
305	0.07	--	0.30			
310	0.05	0.02	0.75			
315	7.25	--	4.50			
320	7.5	9.6	12.60			5.0
325	18.0	--	50.00			
330	30.0	41.1				
335	30.0	--				
340	--	58.3				
345	--	--				
350	--	61.5				5.4
355	50.0	--				
360	--	88.4				
365	65.0	--				
370	--	130.				
375	--	--				
380	--	170.				8.1
385	--	--				
390	--	258.				
395	--	--				
405	--	--				15.0
441	--	--				30.0

* for 100s exposure duration in aphakic primate producing retinal lesion.

+ for 650s exposure duration in phakic rabbit eye producing changes in the retina.

EXHIBIT 10-9

The Action Spectra for Photokeratitis and Cataracts for the Primate and Rabbit (after Pitts 1981)

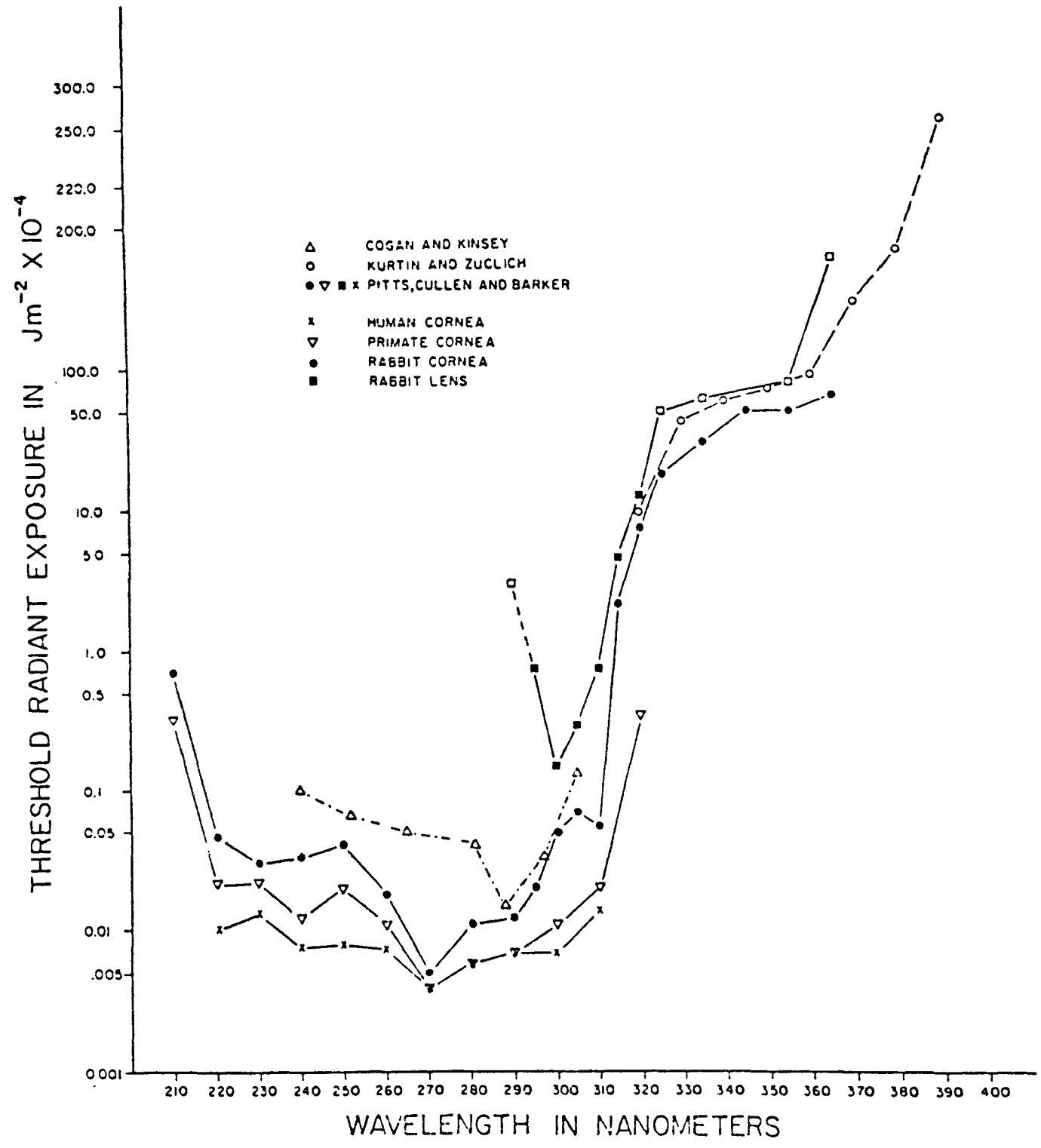

photo-oxidation of free and protein bound tryptophan, photosynthesis processes involving the activated species of oxygen, disruption of the cation transport system and damage to the nucleic acids (DNA) of the lens epithelium. Some of these mechanisms have only been studied only in cultures, some in vitro and others in vivo. It is important to be able to project the mechanism to a "real live" situation in order to be able to evaluate the relative importance of the factors involved in inducing the senile cataract. Prior to discussing these mechanisms it may be desirable to review some of the basic concepts in the biochemical mechanisms of radiation induced damage; therefore, some current interpretations of lens free radicals and oxidation reduction reactions relative to cataract follows. Exposure to UV radiation initiates enzymatic activity involved in cellular protection from oxidative processes which may be due to both light and metabolism (Exhibit 10-10). Catalase destroys hydrogen peroxide, which is produced in all cells by metabolism; superoxide dismutase (SOD) has the responsibility of destroying the superoxide radical, a very toxic radical due to its powerful oxidative nature. In the lens cortex, there is very little SOD or catalase, but they are highly concentrated in the epithelial cells. Of all the ocular tissues, the greatest concentrations of these enzymes are present in the retina. In the lens cortex there are other agents to protect against oxidation such as glutathione (GSH) and ascorbic acid. There is only a small amount of vitamin E in the lens, but attempting to protect animals from ocular tissue oxidative damage by feeding them high levels of vitamin E or other anti-oxidants has not succeeded. The sum total of all of the anti-oxidants that are present in the ocular tissues still does not protect against the formation of free radical oxidative reactions to near-UV radiation. Another toxic oxidant that can form is singlet oxygen.

The content of the stable free radicals previously described is highest in the cortex and seems to decrease in the nucleus, of the lens. The process of aggregation of soluble proteins (TSP) occurs both in the cortex and in the nucleus. Because of the conservative growth process of the lens, much of the aggregated material remains in the nucleus indefinitely and often in a form that is associated with the fiber cell membranes. The lens fraction called the insoluble fraction contains both membranes and the aggregated proteins. There is a chemical reaction between the free radicals and proteins so that the protein binds to free radicals chemically, which quenches the ESR (electron spin resonance) signal. Multiple molecular species of proteins can be associated through new crosslinks leading to aggregation and, therefore, light scattering. In the nucleus of the lens, the free radicals are quenched by their reactions with proteins. Since all enzymes are proteins, this may illustrate a universal process whereby enzyme activity is inhibited by near-UV radiation. These changes would eventually cause malfunction of all cells and tissues.

Exhibit 10-11 shows a scheme of a series of enzymatic oxidation: reduction reactions going on in all cells that are influenced by aging and exposure to near-ultraviolet radiation. These reactions are all linked together. The co-factor NADH/NADP system is linked to the oxidation and reduction of glutathione (GSH). When oxidation occurs, reduced GSH becomes oxidized GSSG, changes which also relate to protein oxidation involving SS-crosslinks. Many enzymes, in order to remain active, must maintain sulfhydryl groups (SH) of cysteine in reduced form in order for the protein portion to maintain its activities as an enzyme. Many enzymes require free-SH groups in their active sites to retain their activity. If these enzymes are oxidized so that

EXHIBIT 10-10

Free Radicals and Oxidation: Reduction Systems

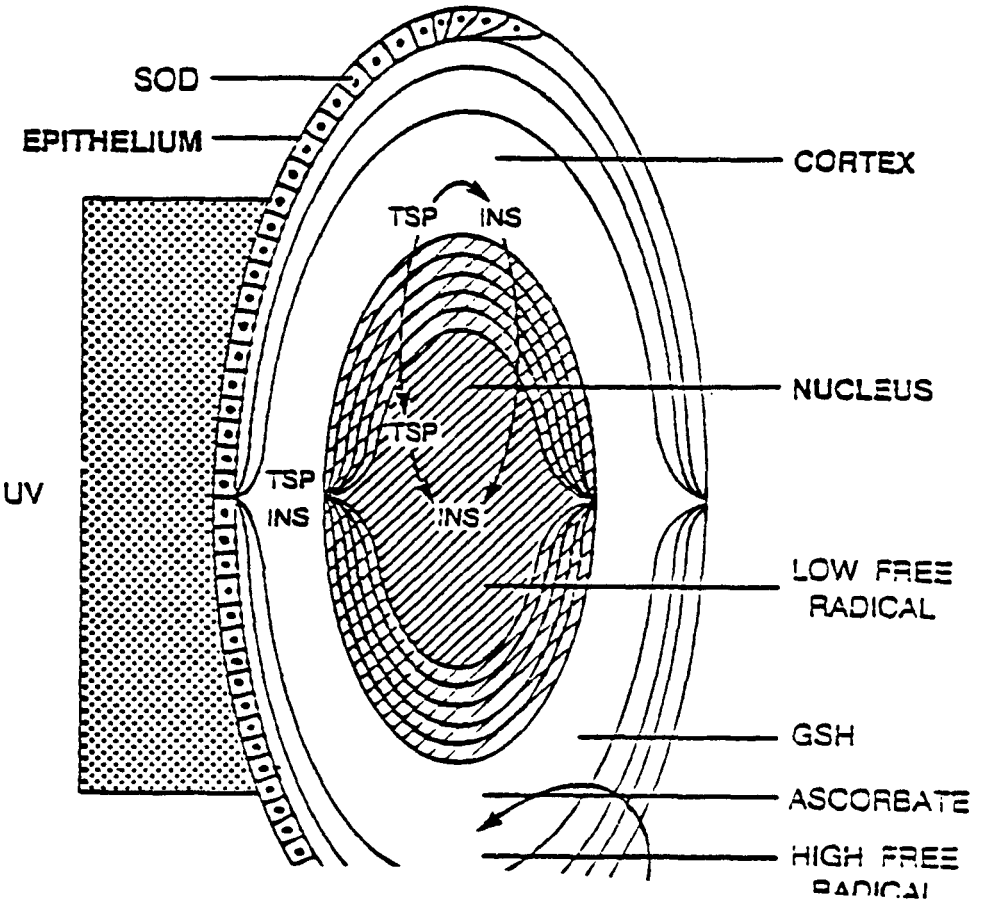

SOD represents superoxide dismutase, GSH represents glutathione. Epithelial SOD and catalase protect these cells against oxidation from excessive hydrogen peroxide and superoxide anion. High levels of ascorbic acid and glutathione protect cortical fibers against oxidation. TSP represents soluble and INS insoluble protein. TSP converts to INS protein both in the cortex and in the nucleus. But INS accumulates more in the nucleus than in the cortex. Free radicals are quenched in nucleus due to binding to proteins.

EXHIBIT 10-11

Enzyme Systems Involved in Oxidation: Reduction

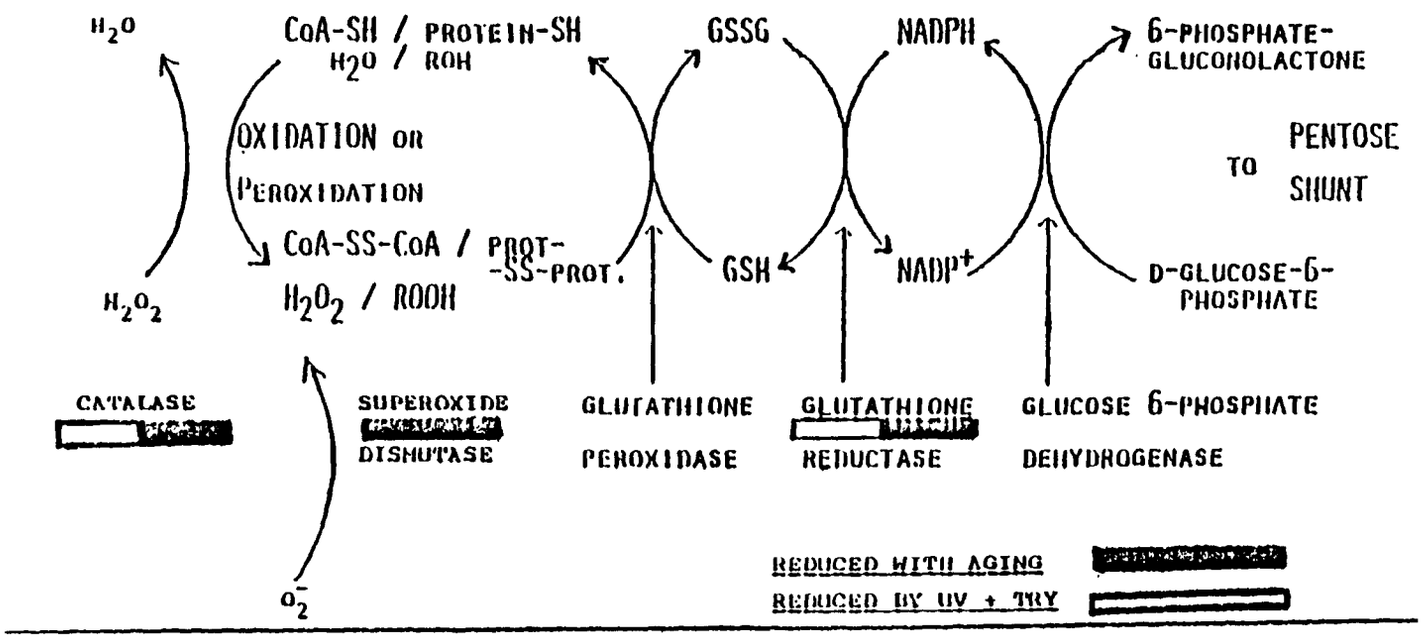

Enzyme activities that are decreased with aging are shown by solid bars and those decreased by light exposure (artificially induced) are shown by the open bars.

disulfides form, they are inactivated. For example, if high concentrations of hydrogen peroxide are generated, protein SH will convert to SS thereby inhibiting the activity. Several of the enzymes referred to in Exhibit 10-11 are known to be reduced with enhanced aging in most living cells. In many cases the cells turn over, so that cells' enzymatic activities are maintained, but where there are populations of cells that do not turn over very actively, a cumulative process can lead to a great loss of enzyme activities. This may occur in the lens.

One enzyme that is diminished with aging is glutathione reductase and it also diminishes under in vitro circumstances in living tissues when near-UV radiation is provided in the presence of excess tryptophan. There has not yet been an aging or photoinactivation study of glutathione peroxidase. The SOD is very important as a protective agent because it destroys the very toxic superoxide radical. SOD activity does diminish with aging, but is not sensitive to destruction from near-UV radiation (with tryptophan as a sensitizer). Because the lens substance contains little oxygen to serve as a superoxide source, the site of lens damage would be the epithelium if SOD activity were to be diminished drastically. Damage to the lens epithelium would certainly lead to both physiological and developmental anomalies in the lens and cataract. The SOD activity must be maintained in the retina, however, due to its high oxygen tension and the potential for oxidation to occur more readily.

Hydrogen peroxide (H2O2) is another very powerful oxidant that is present in ocular tissues and fluids by virtue of the action of SOD on superoxide and other metabolic systems, such as the glutathione and ascorbic acid cycles. Recently, high levels of H2O2 (mM concentrations) have been observed in the human aqueous humor by Garner and Spector (1980). This concentration of H2O2 is suspected of being capable of causing cataracts by poisoning important enzymes and by crosslinking proteins (Spector and Garner 1982). In eyes without lenses, H2O2 from the aqueous humor could more easily diffuse even to the retina (Zigman 1981, Kramer 1980), a highly hazardous circumstance. Ocular tissues utilize the enzyme catalase to destroy and detoxify H2O2. Since this enzyme is diminished with aging and has been shown to be inhibited by near-UV radiation plus tryptophan (Zigman, Yulo, and Griess 1976), its activity loss would allow heightened levels of H2O2 to damage ocular tissues. A large imbalance in favor of H2O2 accumulation would lead to extensively altered ocular tissue proteins and much enzyme inactivation.

Glutathione reductase is another enzyme of great functional importance to the lens and retina, and it is diminished with aging and UV exposure (Kalustian, Sun, and Zigman 1978). Its loss of activity would estimate oxidation of small molecules and proteins in most ocular tissues.

Another enzyme (not involved in oxidation: reduction, but significant with regard to its photoinactivation) is $Na^{+}K^{+}$ ATPase. This enzyme is also sensitive to near-UV radiation in the presence of tryptophan and loses its activity accordingly. In the lens, it maintains the osmotic balance by controlling the sodium and potassium cation exchange and prevents water inhibition and swelling. In some genetic cataracts in mice, it has been found that the cause of cataract is the high concentration of an inhibitor of ATPase in the lens (Kinoshita 1974). It is likely then that a strong inhibition of lens epithelial cell ATPase by light-sensitized action could be a major factor in cataract formation osmotically. In the retina, the ATPase activity is very important in terms of the chemical reactions that support the visual process. Should this enzyme be photochemically inhibited in the retina, the functioning of the visual process

would be markedly reduced. Retinal Na^+K^+ ATPase is also sensitive to inhibition by near-UV plus tryptophan.

Before discussing the biochemical studies which pertain to the possible cataractogenic effects of optical radiation, it may be pertinent to review some contrasts between human lenses and those of the most commonly used laboratory animals. All vertebrate lenses are composed essentially of a single cell type, the lens fiber, which differentiates from a single layer of epithelial cells present only at the bow or equator of the lens. New fibers are continually laid down at the periphery; thus, the oldest tissue is located at the center or nucleus of the lens and the cells become progressively younger as one moves from the center toward the lens capsule in the cortex. Cells are never sloughed from the lens and this makes the cells in the lens nucleus as old as the animal. Furthermore, differentiated lens fibers gradually lose virtually all cell organelles, including nuclei, and lose the capacity to synthesize protein as they age and are forced toward the nucleus. Therefore, the proteins, primarily lens crystallins, present in the aging human lens may be the longest-lived proteins in the organism. This means that unlike most other tissues the central portion of the lens does not have the ability to replace damaged proteins with newly synthesize proteins. This may be an important factor in the presumptive long-term effects of chronic exposure to near UV radiation. There are very clear differences between the lens nucleus and cortex in terms of their biochemistry and the loss of the capacity to repair or replace damaged proteins probably accounts for much of the difference.

There is at least one very significant difference between human lenses and the common laboratory animals and that is the presence of pigmented compounds in the human lens. While the lenses of most non-primate mammals have no pigment, the lenses of diurnal primates and a few other strongly diurnal species are yellow. Cooper and Robson (1969) demonstrated that in the human lens there are two classes of pigmented compounds. One group that is present even before birth is of low molecular weight, is water soluble and absorbs maximally at about 365 nm. A second class of colored compounds appears later, increases with age, is bound to the lens proteins and absorbs maximally near 320 nm. This latter class of chromophores is localized primarily in the lens nucleus and may be responsible for the age-related increase in pigmentation in human lenses. Since these chromophores absorb in the near UV, they may be major determinants of the effects of such radiation on the human lens.

Studies at the Biochemical Level

Studies at the biochemical level have generally been concerned with the structural modifications which crystallins undergo during aging and cataractogenesis and have attempted to explain these reactions in terms of photo-oxidative mechanisms. It is well-documented that crystallins, particularly in the lens nucleus, accumulate a variety of modifications. These include the formation of disulfides and other covalent crosslinks, the development of a novel blue fluorescence, progressive pigmentation, oxidation of methionine, racemization of aspartate residues, polypeptide chain cleavages, deamidations, aggregation and ultimate insolubilization. The lack of turnover of protein in the lens nucleus accounts for the accumulation of these modifications and they have been the subject of several recent reviews (Zigler and Goosey 1981; Hoenders and Bloemendal 1981; Harding 1981). It is clear that most of the protein changes are the result of oxidative stress, and the possible role of radiation in that stress has been the subject of much study over the last 15 years.

Pirie (1968, 1972) studied the effects of sunlight on solutions of lens proteins and of other proteins. The proteins became brown following irradiation and analysis of absorbance changes indicated similarity to those found in lens proteins from cataracts. Pirie also found decreased levels of the oxidation sensitive amino acids, histidine and tryptophan in protein from cataracts relative to normal lenses. Although the data for tryptophan was subsequently retracted as an artifact, Dilley and Pirie (1974) suggested that photooxidation of tryptophan residues, perhaps with formation of N'-formyl kynurenine, was a primary step in cataractogenesis. These studies stimulated a number of other investigators.

Kurzel (1973) performed fluorescence and phosphorescence measurements and Weiter and Finch (1975) ESR studies on human lenses and found signals which they believed to be due to tryptophan free radical species in lens proteins. Van Heyningen (1971) was able to identify several of the components contributing to the color of human lenses as kynurenine derivatives, species which can be derived from tryptophan either metabolically or photooxidatively. These were part of the low molecular weight colored material present in human lenses and Van Heyningen (1973) subsequently showed that lens proteins exposed to sunlight in the presence of these compounds were photo-oxidized more extensively than in their absence. The mechanisms of this accelerated photo-oxidation was not determined.

In addition to oxidation of protein bound tryptophan other possible mechanisms were explored. Zigman et al. (1973) and Zigman and Vaughan (1974) demonstrated that photo-oxidation of free tryptophan yielded pigmented and fluorescent species which would bind to lens crystallins in vitro. This raised the possibility that the target of photo-oxidation could be either free or protein-bound tryptophan. Numerous investigators turned to the study of brunescent nuclear cataracts since these lenses have the greatest concentration of the pigment and of the non-tryptophan fluorescence. The search for clear decreases in the levels of tryptophan in the proteins of such lenses or in their free amino acid pool has not been successful to date (Dilley and Pirie 1974; Pirie and Dilley 1974; Zigler et al. 1976). It should be noted however that tryptophan comprises less than 2% of total amino acid in crystallins and, thus, small changes would be difficult to detect especially in view of the inherent problems of tryptophan analysis.

Lerman (1980b) suggests that in the normal lens less than 20% of the protein tryptophan is susceptible to photo-oxidative damage. Studies on the novel blue fluorescence of aging crystallins, particularly the insoluble fraction from brunescent lens nuclei suggest the presence of a number of related species (Lerman 1980b). The species with emissions in the visible are generally more concentrated in nuclear cataracts. There is some evidence that this fluorescence may be concentrated in certain crystallin polypeptides (Zigman 1981). It has also been demonstrated that the formation of non-disulfide covalent crosslinks between crystallin polypeptides is associated with the heavily pigmented protein fraction and can be generated in vitro by irradiation (Buckingham and Pirie 1972). Additional photoproducts of tryptophan, including B-carbolines (Dillon, Spector and Nakanishi 1976) and anthranilic acid (Truscott, Faull, and Augusteyn 1977) have been identified from the crystallins of nuclear cataracts. Dillon and Spector (1980), Dillion et al. (1982) and Borkman, Tassin, and Lerman (1981) have studied the photolysis of free tryptophan, or tryptophan containing peptides, and of isolated lens crystallins. Analysis of these data suggests that a variety of products are possible and that

the microenvironment of individual tryptophan residues is of paramount importance. Additionally, photolysis is much faster in the presence of oxygen.

Harding and Dilley (1976), however, raised two objections to the idea that sunlight caused brown nuclear cataracts. First, they pointed out that the lens damage is in the nucleus whereas the shortest wavelengths reaching the lens; i.e., those which might be absorbed by tryptophan are probably absorbed in the anterior lens cortex. Indeed as noted above cataracts induced in animals by UV-B are located in the anterior cortex. Secondly, the lack of evidence for loss of tryptophan in brown cataracts was cited. While these arguments are difficult to rebut in terms of mechanisms in which UV oxidation of tryptophan is the central event, there is another mechanism of photo-oxidation for which these objections may be less significant.

Recently, there has been increasing interest in the possible role of photosensitized processes, particularly with the involvement of activated species of oxygen, in the oxidative damage observed in the human lens. This work was spurred by data demonstrating light-mediated lens damage with such photosensitizing drugs as 8-methoxypsoralen, phenothiazines, and tetracycline and by the studies cited above by Pirie and Van Heyningen showing accelerated UV effects on crystallins in the presence of kynurenines and related compounds. Zigler and Goosey (1981) have demonstrated that several of these compounds endogenous to human lenses are capable of generating singlet molecular oxygen, a highly reactive species capable of damaging proteins as well as other biological molecules and structures. The ability of this oxidant to induce the oxidative changes characteristic of human crystallins has been established in vitro. It has also been demonstrated that such photosensitizing activity is present in the heavily altered insoluble lens crystallins from brunescent cataracts and to a lesser extent in the soluble crystallins of normal human lenses as well. Based on experiments in vitro, such a photosensitized process could account for the generation of each of the oxidative modifications presently known to occur in lens crystallins. Furthermore such a process seems consistent with nuclear localization of damage. In the lens nucleus there is no repair or replacement of altered molecules, thus allowing progressive accumulation of crystallins with oxidized residues some of which are photodynamic sensitizers. The UV-A which these species absorb will readily penetrate to the nucleus. Additionally while the lens cortex is protected by a battery of antioxidant defenses it is known that these defenses are markedly reduced in the nucleus (Hata and Hockwin 1977; Fecondo and Augusteyn 1983).

One could envision a system in which there was a slow rate of photo-oxidation ongoing in the lens controlled by antioxidant defenses and by the greatly reduced oxygen tension in the lens nucleus. The oxidative stress might have several components including direct UV oxidation of tryptophan (primarily UV-B), the high levels of H_2O_2 in the aqueous humor (Spector and Gardner 1982) and photosensitized oxidation involving activated species of oxygen. It has been recently demonstrated that even fetal human lenses contain low molecular weight chromophores which can generate singlet oxygen when irradiated with UV-A. The initial photochemical event could be absorption by such chromophores or direct photo-oxidation of tryptophan to produce N-formyl kynurenine (NFK) a known photodynamic sensitizer. In either case, it seems likely that the continued build-up of oxidized products in the nucleus is likely due primarily to a sensitized process, since such a process would not require large-scale tryptophan loss nor would it require penetration of UV-B into the nucleus. A relatively small number of stable sensitizing species such as NFK, bound within the long-lived nuclear crystallins, could continue to generate

singlet oxygen indefinitely with the gradual accumulation of the various oxidative protein changes outlined above culminating in aggregation and insolubilization of much of the nuclear crystallins in advanced brunescent cataracts.

Several suggestions have been made that attempt to reconcile the finding that tryptophan is not reduced in senile cataracts (as compared to normal lenses) with the hypothesis that it acts as an important endogenous photosensitizer. For example, it has been suggested that tryptophan is oxidized to a reactive molecule that simply transfers its energy to some other cell component from the excited state. It then returns to the ground state without being destroyed in the process, yet photosensitizes damage to other lens macromolecules (Weiter and Finch 1975; Weiter and Subramanian 1978). Another explanation is that free tryptophan rather than protein bound tryptophan may be destroyed when it acts as a photosensitizer, whereas tryptophan incorporated within lens proteins is unaffected. The level of free tryptophan may be reduced in cataract (Zigler et al. 1976). The failure of protein-incorporated tryptophans to be photo-oxidized might be explained by the fact that they lie in very different micro-environments that render them less susceptible to photo-oxidation (Lerman, 1980b). A third suggestion to explain the finding that tryptophan is not decreased in cataractous lenses is that only a small percent of the protein-incorporated tryptophan may be susceptible to photo-oxidation and small losses in these susceptible tryptophan might not be detectable with current analytical capabilities. Tryptophan and its photoproducts have become the most frequent culprits implicated in causing photo-oxidative changes in lens proteins, changes that are hypothesized to be responsible for senile cataractogenesis.

Photo-oxidation of lens proteins has become a major topic in lens research and has been shown to be induced by photosensitizers that are either endogenous (Zigler and Goosey 1981) or externally applied (Goosey, Zigler, and Kinoshita 1980) to the lens. One effect frequently found to occur as a direct effect of UV or as an effect of UV plus a photosensitizer is crosslinking of lens proteins (Buckingham and Pirie 1972; Goosey, Zigler, and Kinoshita 1980).

Interest in agents that can cross-link or otherwise aggregate lens proteins has been high since Benedek (1971) first proposed that the mechanisms underlying senile cataract formation was aggregation and insolubilization of lens crystallins. They suggested that aggregated lens proteins would serve as light scattering particles in the lens. The search was then underway for these high molecular weight aggregates, but unfortunately, the research produced very inconsistent and conflicting results. Some research groups found an increase in the amount of high molecular weight proteins in senile cataractous lenses while other groups found no difference in the amount of high molecular weight proteins in cataractous lenses compared to that present in lenses in age matched controls (Harding and Dilley 1976). It was also suggested that aggregation was an artifact resulting from the extraction procedure (Harding 1972). Analogous studies have more recently been carried out on lenses in which the cataracts were separated according to the nature of the changes present in the lens. The results of those studies have suggested that nuclear brunescent, but not cortical cataract, is associated with formation of increasing amounts of water insoluble proteins (Truscott and Augusteyn 1977). Some researchers have attributed this increase to cross-linking of lens proteins induced by photo-oxidation. It has been further suggested that the reason these changes occur more readily in the lens nucleus than in the cortex is that the cortex has a higher concentration of protective anti-oxidants.

If Benedek's (1971) original hypothesis that the mechanism underlying senile cataract formation was aggregation and insolubilization of lens crystallins is correct, then one would expect to find an increase in protein cross-linking and aggregation in lenses that show light scattering. To the contrary, lenses with light scattering opacities in the cortex do not show an increase in high molecular weight proteins or crosslinks (Truscott and Augusteyn 1977; Anderson, Wright, and Spector 1979). Instead, reports in the literature suggest that there may be an increase in protein aggregates in lenses with substantial nuclear brunescence. This is rather a surprise because nuclear brunescence per se is not a light scattering change in the lens; rather, the lens turns a yellow or a brown color that absorbs rather than scatters light, reducing its intensity on the retina (Lerman and Borkman 1976). The effect of brunescence is, therefore, analogous to placing a transparent filter before the eye.

Unfortunately, only man and a very few other diurnal species have been found to develop lens browning so that it has been difficult to find an animal model in which to test the hypothesis that browning can be induced in vivo by exposure to UV radiation. Therefore, those studies that have examined the effects of chronic UV exposure in experimental animals have not demonstrated that UV induces lens browning. They have, however, consistently demonstrated that UV exposure induces light-scattering cortical opacities (Bachem 1956; Zigman and Vaughan 1974; Pitts, Hacker, and Parr 1977). Therefore, though we may lack a suitable model for nuclear brunescence, there are animal models that can be used to study the induction of cortical opacities by UV radiation. These models mimic the common and considerably more visually disturbing senile cortical cataracts in man.

In those studies on UV-induced lens changes in which histology of the lenses were examined, epithelial cell changes were a uniform finding (Zigman and Vaughan 1974; Pitts, Hacker, and Parr 1977). In their study of chronically exposed mice, Zigman and Vaughan (1974) noted the similarity of the lens changes to changes induced by X-irradiation. For example, lens cells appeared to have lost their capacity to differentiate and were found to have migrated to the posterior pole, a situation that has also been found to be associated with senile cortical cataracts (Streeten and Eshaghian 1978).

While biochemical approaches have generally concentrated on nuclear cataracts with respect to UV-mediated effects, there has been recent interest in photosensitized reactions in the aqueous humor as sources of damage to lens membranes and, hence, as a possible initiator of cortical (osmotic) cataracts. Varma, Kumar, and Richards (1979) have been investigating the possibility that a photochemical conversion of molecular oxygen present in the aqueous humor and lens into superoxide and subsequent derivatization of superoxide to other potent oxidants such as hydrogen peroxide, hydroxyl radical and singlet oxygen may be involved in initiating a cascade of toxic biochemical reactions leading to the formation of cataracts. Thus, according to this hypothesis, cataractogenic influence of light is mediated by a photochemical generation of superoxide from the ambient oxygen. Spin restriction offered by the molecular oxygen makes the formation of superoxide a necessary event in most oxidation reactions involving oxygen. It is commonly understood that, like many other free radicals, superoxide and its derivatives, if allowed to remain unscavenged for any length of time in a biological milieu, will initiate many nonspecific and deleterious reactions such as an upsetting of the normal redox chain, oxidation of vitally important protein and nonprotein - SH, peroxidation of membrane and cytosolar lipids, and polymerization and depolymerization of macromolecules such as

proteins and hyaluronic acids. The cataractogenic influence of these oxidants is likely to be modulated by certain endogenous protective mechanisms. Superoxide dismutase (SOD), catalase and perioxidase constitute the first line of defense against the toxic effects of those oxygen species. Jernigan et al. (1981) showed that singlet oxygen generated in the medium had similar effects. Varma, Beachy, and Richards (1982) have demonstrated lipid peroxidation in cultured lenses irradiated with fluorescent light. While such studies are of great interest in terms of the effects of these oxidants on the lens, at the present time there is no real evidence that they are produced insignificant quantities in the ocular humors by light mediated processes.

Considerable effort has been directed at elucidating mechanisms by which UV radiation (alone or in combination with exogenous photosensitizers) might induce cataract formation. As previously mentioned, it has been shown that UV radiation can induce cross-linking and aggregation of proteins. As has also been mentioned, protein aggregation may be associated with nuclear changes but it is not a characteristic associated with cortical cataracts. It may therefore be more relevant to consider the possibility that UV damage to lens proteins induces local perturbations in macromolecular structure and function. This might in turn result in localized changes in lens structure of function. For example, transport systems and ATPase (Varma, Kumar, and Richards 1979) in the lens have been shown to be inhibited by UV radiation. If the lens transport systems are damaged by UV radiation, the osmotic balance will be disrupted which, in turn, would produce major changes in lens morphology.

The UV effects on transport systems may occur due to direct UV absorption by and damage to the related enzymes; however, other mechanisms may also contributed to this inhibition. For example, the activity of transport enzymes could be dramatically altered secondary to UV induced disruption of lipids in lens membranes; and, lipid peroxidation has been proposed as a mechanisms of cataract formation (Goosey, Allison, and Garcia 1983). The resulting alterations in lipid structure could of themselves make the membranes leaky or, as just mentioned, such alterations could disrupt the structure and function of membrane proteins. If one can extrapolate from the large amount of research that has been done on other cell systems, then it may be predicted that fairly long wavelengths of UV will similarly be able to produce membrane damaging effects in the lens (Moss and Smith 1981; Imbrie and Murphy 1982; Sprott, Martin, and Schneider 1976).

If we are to determine the role of lipid peroxidation or inactivation of specific enzyme systems in the development of UV cataracts, it is critically important that lenses be sampled several intervals prior to the onset and during the development of lens opacities. Once the lens is fully opacified, retrospectively, it is difficult to state with any assurance that some observed biochemical change was the specific change that initiated the cataract.

For example, if an ATPase were found to be inactivated after a particular UV-induced cataract was fully developed, one might conclude that this inactivation had caused cell swelling, membrane lysis, and an "osmotic cataract." But it is also possible that the primary cause of the cataract was direct membrane damage or inhibition of protein synthesis and, that, only secondarily was ATPase activity involved. Therefore, to show that ATPase inactivation is of any real significance in the etiology of the cataract, it is necessary to demonstrate that ATPase inactivation precedes development of the lens opacities. In the case of UV-induced cataracts, one also needs to demonstrate that those wavelengths that inactivate the ATPase are those same

wavelengths that most readily induce cataract formation.

It may be misleading to examine effects of UV (with or without added photosensitizers) on lens macromolecules isolated in test tubes because UV effects in vitro may be very different from the effects of UV on the intact lens. For example, it is possible to cause tryptophan destruction in lens proteins irradiated at a concentration of 2.5 mg/ml in a test tube, but the same type of irradiation was not found to produce such effects at the concentration of protein in the lens (Dillon et al. 1982). Also, the action spectrum may differ considerably from the absorption spectrum (Turro and Lamola 1977). The action spectrum shifts markedly in situ in the case of the photosensitizer, psoralen. Psoralen, riboflavin, methylene blue and rose bengal have all been found to induce photo-oxidative changes in isolated lens proteins when these proteins are irradiated with UV. However, each of these photosensitizers requires the presence of oxygen, otherwise lens proteins are not damaged. The amount of oxygen in the lens is not high (Kwan, Ninikoski, and Hunt 1972; Barr and Roetman 1974). Thus, these findings must be extrapolated to the in vivo lens with considerable discretion and it remains to be determined just how much photodynamic damage (that is damage where oxygen is involved as an intermediate) can be produced in the lens in situ. This is a very important research question because any effect that is of significance as a mechanisms of cataract formation must be inducible in a lens that is still in the eye. For example, it might be interesting to use 254 nm radiation as a toll in vitro to demonstrate that the lens epithelium has the capacity to repair damaged DNA (Jose and Yielding 1977). However, 254 nm radiation does not penetrate the cornea, so it will not be hazard for the in vivo lens and it will not cause cataracts. Therefore, it is a far more significant finding that 300 nm radiation can induce DNA repair synthesis in the lens epithelium when the lens is exposed in situ through the intact cornea (Jose, Kock, and Respondek 1982; Brenner and Grabner 1982). This finding shows that 300nm UV radiation penetrates through the cornea and demonstrates that epithelial cell DNA is a target of its effects.

Therefore, if we are to establish mechanisms of UV damage in the lens, we must be able to show that a given damaging reaction can be produced by UV in the in situ lens. An effect that can be produced on lens macromolecules isolated in a test tube may be interesting and stimulate further research, but it must not be taken as sufficient proof that such an effect can occur in vitro. This is especially true for those reactions that require oxygen.

One photosensitizer that may provide important clues as to mechanisms involved in cataract formation is the drug psoralen which in combination with UV radiation is used in treating psoriasis. Two different mechanisms have been proposed to underlie the psoralen cataract. According to one hypothesis, the cataracts occur as a consequence of psoralen binding covalently to lens proteins which results in formation of additional damaging photosensitizers in the lens (Lerman, Megaw, and Willis 1980). The second hypothesis is that the cataracts occur as a consequence of psoralen induced damage to lens nucleic acids (Jose and Yielding 1979).

It has been found that intense exposure to UV radiation will cause psoralen to bind to isolated lens proteins, specifically the tryptophan moieties (Lerman, Megaw, and Willis 1980); however, the reaction requires oxygen (Megaw, Lee, and Lerman 1980). Therefore, it is important to determine whether such protein binding occurs in the intact lens. Although spectra have been presented that demonstrate that UV radiation induces psoralen binding in the in vivo lens, it is not clear that the binding observed represents protein specific binding or

whether the binding is to some other lens macromolecule. Lens protein fractions have been extracted from psoralen-treated humans or laboratory animals and fluorescence spectra taken from these. These spectra were interpreted to demonstrate photobinding of psoralen to lens proteins; however, no effort was made in these studies to extract nucleic acids from these "protein" preparations. It is very possible that a significant amount of the binding that was observed is accounted for by psoralen binding to RNA or DNA present in the degenerating nuclei of the lens cortex. The possibility that the spectra represented binding to nucleic acids in the differentiating fibers was discounted by the researchers because there is such an overwhelming concentration of protein compared to DNA in lens fibers (Lerman, Megaw, and Gardner 1982a). This is a reasonable assumption if a significant percentage of the psoralen were actually bound to the protein. However, the argument would be nullified if the majority of the psoralen were found to be bound to the small amount of nucleic acids in the fibers. Autoradiograms showing psoralen binding in the lens suggest that the latter is in fact the case (Lerman et al, 1981). Examination of those autoradiograms shows pronounced binding of psoralen in the epithelium plus discrete binding to the degenerating fiber nuclei. In comparison, binding to any other portions of the fibers is not distinguishable from background grains.

Autoradiography has also demonstrated psoralen binding in the nucleated layers of the retina and cornea but no binding to the non-nucleated layers of these tissues (Lerman et al, 1981). It is rather difficult to reconcile the failure of psoralen to bind to the non-nucleated regions of the retina and cornea with the suggestion that it binds significantly to cortical fiber proteins. A trivial explanation for this difference is that lens proteins are somehow "different" from corneal and retinal proteins, making the former susceptible to psoralen binding and the latter not. This argument is rather difficult to reconcile with the requirement of oxygen for photo-induction of psoralen linking to proteins, a requirement that would lead one to expect greater binding to the proteins in the highly oxygenated retina and cornea compared to the relatively anoxic lens.

If lens proteins are the major target of psoralen's action on the lens, then one would expect that the cortical fibers would be disrupted as a primary event. In fact, however, histologic observations have shown that the first target of psoralen's effects are the epithelial cells (Jose, Kock, and Respondek 1982). Only after very considerable damage is observable in the epithelium is any damage detectable in the lens cortex which is consistent with DNA as a primary target of psoralen damage. That psoralen plus UVB can induce DNA damage in the lens is shown by the finding that the combination induces DNA repair in lens epithelial cells (Jose and Yielding 1979). It will be interesting to resolve the question as to the relative roles of specific macromolecular targets in development of psoralen-induced cataracts.

As with psoralen, most other studies of UV effects on the lens have directed their major emphasis toward examinations of changes in lens proteins. But, as with the psoralen study, there are compelling reasons to consider other macromolecules a targets of UV damage. Lens lipids have been mentioned previously and interest in lipids peroxidizing effects is of current interest in many laboratories. However, interest in the effect of UV and photosensitizers on lens DNA is currently very limited. The role of DNA damage in development of lens cortical opacities is generally overlooked or rationalized away. Some have assumed that there is so little DNA in the lens that even if it were a target, any effects on it would be overwhelmed by effects on lens proteins. There are,

however, good reasons to consider the lens to be similar to other biological systems in which DNA is a significant target of UV damage.

If one considers the action spectrum that has been determined in those studies in which specific wavelengths of UV were isolated to examine their cataractogenic potential, it is noted that these lie in the range of 290 to 320 nm (Bachem 1956; Pitts, Hacker, and Parr 1977). These are the same wavelengths that most readily produce thymidine dimers in skin (Pathak, Kramer, and Guengerich 1972). Shorter wavelengths are blocked from deeper layers of the skin by the stratum corneum, quite analogous to corneal UV absorption which protects the lens. These are the same wavelengths which most readily induce malignant transformation and skin cancer (Freeman 1975). UV radiation up to 320 nm also can induce DNA repair synthesis in cultured fibroblasts (Ichihashi and Ramsey, 1976). Longer wavelengths of UV do not induce skin cancer, although they may, if applied very intensely, induce strand breaks and other damage in DNA (Webb and Peak 1981, Harm 1978). Endogenous photosensitizers are likely to be involved since DNA itself does not absorb appreciably at that wavelength. Long wave UV may potentiate the action of short wave UV in cancer induction and it can also be noted that 364 nm has been found to inactivate DNA repair mechanisms (Tyrell 1976).

With all the interest in tryptophan as an endogenous photosensitizer of protein damage in the lens, it is interesting to point out parenthetically that photo-oxidation of tryptophan has also been found to induce DNA damage in lower organisms as a consequence of production of H2O2 (Ananthaswamy and Eisenstark, 1976). The possibility that those free radical species that have been found to be generated from UV excitation of tryptophan in the lens may also act on lens DNA as a target should not be overlooked. Furthermore, tryptophan photoproducts have also been found to bind to DNA (Glazer, Rincon, and Eisenstark 1976) and to inhibit strand rejoining in damaged DNA (Yoakum et al. 1974).

Another reason to consider that DNA is a target of UV damage in the lens is the finding that 300 nm radiation can induce DNA repair synthesis in the lens epithelium, even when the irradiation is applied through the intact cornea (Jose, Kock, and Respondek 1982; Brenner and Grabner 1982) and DNA repair synthesis is an indication that DNA was damaged. This point is often misunderstood, repair is not a perfect process and it should not be assumed that lens DNA will be absolutely protected. Mutational and lethal events can occur any time that DNA is damaged and repair is undertaken; thus, anything that can induce DNA repair must be recognized for its primary damaging effects. Errors induced in the genome of lens cells may manifest themselves as mutational events in the target epithelial cell. Such mutational events would be cumulative over an individual's lifetime. Those cells that have undergone mutations might loose their capacity to differentiate into normal lens fibers and, for example, pile up at the posterior pole. The later is seen in the senile cataract (Streeten and Eshaghian 1978) as well as in animals exposed to near UV radiation (Zigman and Vaughan 1974). The cells may also not carry out their normal functions such as maintaining less osmolarity. Then we might develop what appeared to be an "osmotic" cataract, when in fact, the underlying mechanism was genetic.

POTENTIAL CHANGES IN SENILE CATARACT PREVALENCE FOR CHANGES IN UV-B

Epidemiological studies have identified a correlation between the prevalence of various types of cataracts in humans and the flux of sunlight or ultraviolet radiation reaching the earth's surface (Hiller, Giacometti and Yuen 1977, Zigman, Datiler, and Torczynski 1979; Taylor 1980, Hollows and Moran 1981). Hiller, Sperduto and Ederer (1983) developed a multivariate logistic risk

function that describes the correlation found between the prevalence of senile cataracts and the flux of UV-B and other risk factors. The results of this study may indicate the magnitude of change in the prevalence of senile cataracts that could be associated with changes in UV-B flux due to ozone depletion.

Hiller, Sperduto and Ederer based their analysis on the 1971-1972 National Health and Nutrition Examination Survey (HANES) general medical and ophthalmological examinations of over 10,000 persons, ages 1-74 years. Using the HANES data, persons were assigned to one of two mutually exclusive groups: (1) cataract or aphakia (either eye), and (2) neither cataract nor aphakia (either eye). Cataract was defined as "senile lens changes (cortical, nuclear, posterior-subcapsular, or other) consistent with best corrected visual acuity of 20/30 (6/9) or worse" (Hiller, Sperduto and Ederer (1983) p. 240). This definition differs from the HANES survey, which used a visual acuity of 20/25 (6/7.5) or worse. Aphakia was diagnosed when "the lens had been surgically removed and there was no history of congenital, traumatic or secondary cataract" (Hiller, Sperduto and Ederer (1983) p. 240). The study by Hiller, Sperduto and Ederer included HANES data on a total of 2,225 persons between the ages of 45 and 74 years who had resided at least one half of their life in the state where the HANES examination took place. Of these 2,225 people, 413 (18.6 percent) were placed in the cataract or aphakia outcome category.

The UV-B data were developed by NOAA for the 35 HANES locations used in the study based on a statistical analysis of UV-B data collected at 10 locations using Robertson-Berger meters (RB-meters). The statistical analysis incorporates season, latitude, elevation, weather (clouds), and haze. Subsequent validation of the estimates at six locations indicated that the differences between the estimated and observed mean daily flux average about seven percent.

These data on UV-B and outcome (i.e., cataract) were used in conjunction with demographic and medical history data to estimate the following multivariate logistic risk function:

$$P = \frac{1}{1 + \exp(-a - b_i X_i - \ldots - b_k X_k)}$$

where P is the probability (or risk) of having a cataract, and X_i are risk factors. In addition to UV-B, the following risk factors were analyzed: age; race; sex; education; diabetes; systolic blood pressure; and residence (urban, rural).

Exhibit 10-12 displays the standardized regression coefficients estimated for each of the risk factors. Positive coefficients indicate factors that are correlated with increased risk, negative coefficients indicate factors that are correlated with decreased risk. The coefficients presented in the exhibit are "standardized," meaning that they represent the expected change in the logit of P (equal to ln (P/1-P)) for a one standard deviation change in the risk factor. Standardization of the coefficients allows the relative importance of the risk factors to be identified by the relative size of the standardized coefficients.

As shown in Exhibit 10-12, three risk functions were estimated: (1) univariate (outcomes as a function of the risk factor); (2) bivariate (outcome

as a function of the risk factor and age); and (3) outcome as a function of all the risk factors simultaneously. For all three formulations, UV-B is statistically significant, and positively correlated with the increased risk of being in the cataract outcome category.

Using the multivariate risk function coefficients, and the mean values for all the risk factors other than UV-B, the change in the prevalence of cataract for each 1.0 percent change in UV-B is estimated to be approximately 0.5 percent. This relationship holds for changes in UV-B as large as minus 20 percent to plus 30 percent. Outside of this range, reductions in UV-B are associated with less of a reduction in cataract prevalence, and increases in UV-B are associated with larger increases.

Of note is that this estimated relationship between UV-B and cataract prevalence varies with age; UV-B has a larger effect on prevalence (on a percentage basis) among younger individuals. Exhibit 10-13 displays the percent increase in cataract prevalence expected due to increases in UV-B, for peoples of different ages. As shown in the exhibit, the percentage increase in prevalence due to changes in UV-B are estimated to be larger for 50 year olds than for 70 year olds.

Although the effect of UV-B on prevalence is estimated to be larger at younger ages (on a percentage basis) using the multivariate risk function, the prevalence of senile cataracts is known to increase substantially with age. Leske and Sperduto (1983) report the prevalence of senile cataracts in both sexes found in the Framingham Eye Study to be as follows: 52 to 64 years old -- 4.5 percent; 65 to 74 years old -- 18.0 percent; 75 to 85 years old -- 45.9 percent. These prevalence estimates use the same definition of cataracts as used by Hiller, Sperduto, and Ederer. (Larger prevalence rates are reported by Leske and Sperduto based on HANES data. These estimates, however, use a definition of cataract that includes a decrease in vision to 20/25 (6/7.5), instead of the 20/30 (6/9) used in both the Framingham study and the Hiller, Sperduto, and Ederer risk study.) Because cataracts are more prevalent in older individuals, increases in the actual number of cases of cataracts would likely be larger for older individuals, even though the percentage increase in risk has been estimated to be larger for younger individuals.

Using the prevalence data cited above, the prevalence of cataracts in the U.S. population is on the order of 9.3 million. Using the multivariate risk function (with all values set to their means except age and UV-B) the hypothetical increased prevalence for 1985 that would have occurred had the entire population experienced 1.0 percent ozone depletion can be estimated. For a 1.0 percent depletion, the annual UV-B flux measured on the RB-meter has been estimated to increase by approximately 0.83 percent (see Serafino and Frederick (in press) and Chapter 17 for a discussion of the relationship between ozone depletion and UV flux). A 0.83 percent increase in UV-B is associated with increases in cataract prevalence that varies by age. Across all the ages, prevalence would be expected to be about 0.26 percent higher, or about 24,000 cases, had ozone been depleted by 1.0 percent.

Of note is that the RB-meter measure of UV radiation may not be the appropriate action spectrum to use to evaluate the potential biological effects of increased UV-B such as cataract. For example, the DNA action spectrum may be preferred. Even though the RB-meter and DNA action spectra are highly

EXHIBIT 10-12

Standardized Regression Coefficients for Cataract

Risk Factor [a/]	Mean [b/]	Univariate [c/]	Bivariate [d/]	Multivariate [e/]
Age	61.97	1.22[f]	-	1.20[f]
Race	1.22	0.18[f]	0.20[f]	0.13[g]
Sex	1.52	0.07	0.08	0.08
Education	2.87	-0.43[f]	-0.25[f]	-0.14[g]
Diabetes	0.08	0.25[f]	0.23[f]	0.21[f]
Systolic Blood Pressure	146.3	0.33[f]	0.15[g]	0.08
UV-B	3.59	0.19[f]	0.20[f]	0.13[g]
Residence	1.37	0.18[f]	0.21[f]	0.19[f]

a/ Values for categorial risk factors: race: 1 = white, 2 = black; sex: 1 = male, 2 = female; education: 1 = <5 grades; 2 = 5-8 grades; 3 = 9-11 grades; 4 = 12 grades; 5 = college; diabetes: 0= absent, 1 = present; residence: 1 = urban; 2 = rural.

b/ Mean value for the risk factor in the 2,225 persons in the study.

c/ Each risk factor analyzed separately.

d/ Each risk factor analyzed with age only.

e/ All risk factors analyzed simultaneously.

f/ p(two sided) <0.005.

g/ p(two sided) <0.05.

Source: Hiller, R., R. Sperduto and F. Ederer (1983), "Epidemiologic Associations with Cataract in the 1971-1972 National Health and Nutrition Examination Survey," American Journal of Epidemiology, Vol. 118, No. 2, pp. 239-249.

EXHIBIT 10-13

Estimated Relationship Between Risk of Cataract and UV-B Flux

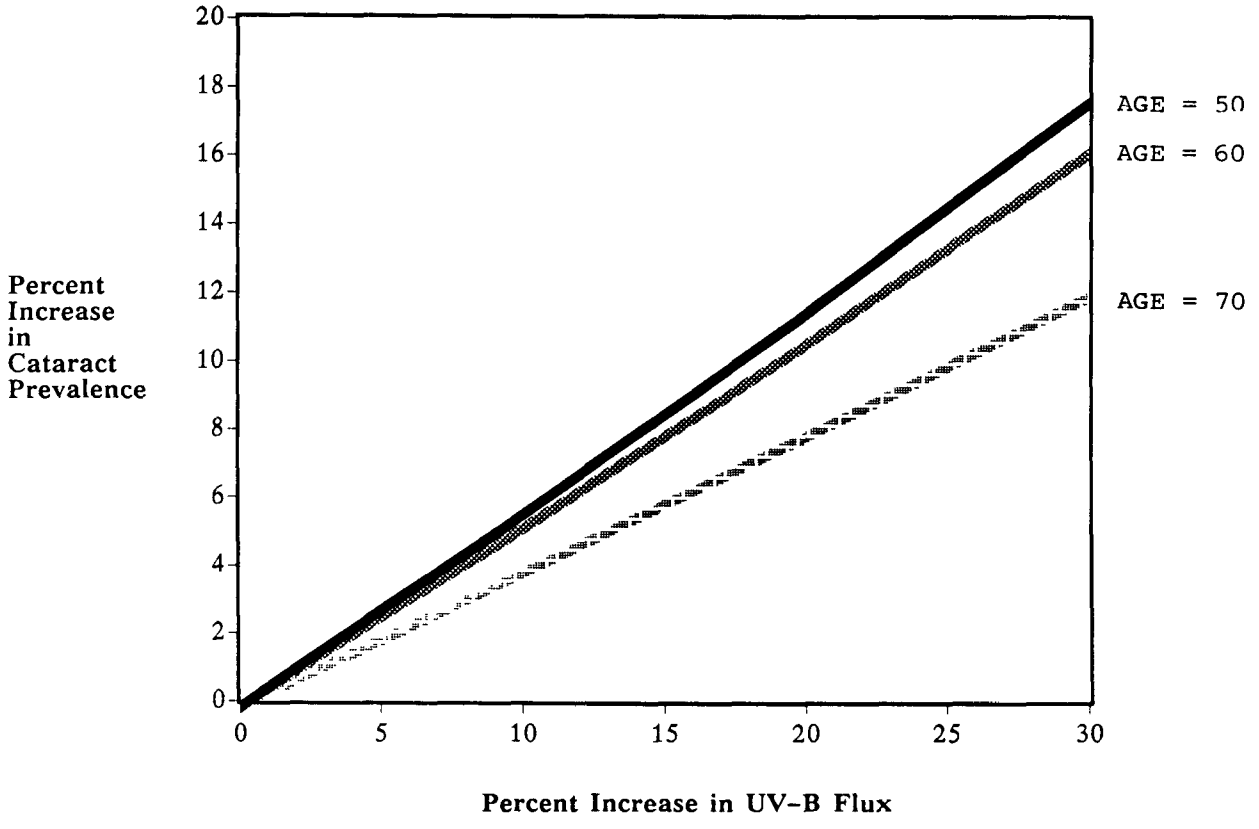

Increased UV-B flux (measured with an RB-meter) is associated with increased prevalence of cataract. The percent change in prevalence varies by age.

Source: Developed from data presented in Hiller R., R. Sperduto, and F. Ederer (1983), "Epidemiologic Associations with Cataract in the 1971-1972 National Health and Nutrition Examination Survey," American Journal of Epidemiology, Vol. 118, No. 2, pp. 239-249.

correlated in the range of current observations, because the DNA action spectrum is more heavily weighted toward shorter wavelengths, it increases more rapidly with decreases in ozone levels; a 1.0 percent depletion would lead to approximately a 2.0 percent increase in UV-B. Using the 2.0 percent increase in UV-B would yield about a 0.6 percent increase in prevalence, or about 57,000 cases.

There are various important limitations in the use of these estimates and data. The correlation between UV-B and cataracts reported by Hiller, Sperduto and Ederer does not prove a causal connection -- other (unknown) factors could be playing a role. These (unknown) factors would have to be correlated with UV-B flux. Also, the study does not have estimates of individual lifetime UV-B exposure, thereby limiting the strength of the evidence for the association between UV-B exposure and cataracts. Additionally, the sample population analyzed may not be representative of the entire U.S. population. Finally, the outcome category used in the study does not differentiate between different types of cataracts, some of which may be more strongly related to UV-B exposure than others.

Confidence in the estimates developed here are strengthened by several considerations. The correlation between UV-B flux and sunlight flux is high, and a correlation between sunlight and cataracts has also been found in Australia (Taylor 1980) and in China (Mao and Hu 1982). An association between UV-B exposure and cataract has also been demonstrated in laboratory animals. Therefore, although considerable investigation remains to be performed, indications are that the association between UV-B and cataract is a reasonable basis for evaluating potential impacts due to increased UV-B flux associated with ozone depletion.

OTHER EYE DISORDERS[2]

Stable Retinal Disorders

Evidence has been adduced which provides a chain of evidence on which to postulate that optical radiation may contribute to human retinal disorders which are not progressive, that is, stable retinal problems. This chain starts with the knowledge that UV-B, UV-A and light are absorbed by various retinal tissues (Wolbarsht 1976; Warner 1982). Moreover, the amount of radiant energy incident on the retina is dependent on the transparency of the cornea and lens, and on pupil diameter. Next a large number of bioeffects of these wavelengths have been identified which are hazardous to the retina (Marshal 1970; Williams and Baker 1980). Further, empirical estimates have been made of the domain of time, intensity, and wavelength which can induce damage to the pigment epithelium, the photoreceptors and the inner retina. These estimates provide sufficient quantitative evidence to establish safety standards to protect people from the short-term retinal damage which could be induced by lasers and other intense sources of optical radiation (Sliney and Wolbarsht 1980; Pitts 1973). There is, moreover, sufficient evidence of additive and persistent changes in the monkey and human retina to hypothesize that some stable long-term visual impairments in humans may be related to optical radiation. There are reports that optical radiation produces retinal damage hours, days, months and years after irradiation. Although sparse, this evidence is instructive. For example, sungazing by humans has been reported to produce persistent, evolving and

---

[2] This section in boldface type is taken from Waxler, M. (in press).

delayed alterations in the visual system. Cavonius, Elgin, and Robbins (1974) reported that aniseikonia may persist for years. Pigmentary patches and blind spots have been reported to evolve in a complicated fashion over many months after solar retinopathy (Lowenstein and Steel 1941). In addition, late complications resulting in reduced visual acuity have been described (McFaul 1969). Furthermore there are several reports in humans of prolonged, and even cumulative, impairments in dark adaptation following extended viewing by humans of skylight (Hecht et al. 1948; Clark, Johnson, and Dreher 1946) or bright blue, violet (Brindley 1953) and ultraviolet (Wolfe 1949) radiation. Also there is at least one report of persistent visual impairment resulting from the accidental exposure to ultraviolet radiation from a welding arc (Naidoff and Sliney 1974). Even more important is the description by Tso and Woodford (1983) of sub-RPE neovascularization and late impairment in fluid transport after several years of evolving changes in retinal pathology following excessive exposure to optical radiation.

Some of these effects are the result of injury to the retina which was ophthalmoscopically visible, some of these effects resulted from exposure to optical radiation which did not produce ophthalmoscopically visible damage. Most important are two demonstrations that the addition of subthreshold exposures separated by several days induces retinal damage (Greiss and Blankenstein 1981; Kuwabara and Okisake 1976). The data strongly suggest that retinal damage induced by optical radiation can cumulate over days. This is especially important since the concern about long-term visual health problems necessarily involves consideration of the intermittent nature of exposure to emissions from multiple sources over an extended period of time.

Retinal Degeneration

There are some reasons to suspect that retinal damage induced by ultraviolet radiation can be unstable, that is, produce progressive damage. The retina of monkeys can be damaged by ultraviolet radiation (Ham 1984; Sykes et al. 1981). This damage to the retinal pigment epithelium, to the photoreceptors and the neurons is dose dependent, photochemically mediated and cumulative over hours and days. Although very few long-term observations have been made on the primate retina following excessive exposure to optical radiation, there are theoretical reasons to suspect that a retina compromised by disease or age would be more vulnerable to any degenerative changes which could be induced by optical radiation (Young 1981). The combination of short-wavelength optical radiation, oxygen, chromophores, and photosensitizers in the retina is potent with possibilities for producing retinal degeneration, although the only direct evidence of the exacerbation of retinal degeneration by optical radiation has been obtained in rodents (LaVail and Batelle 1975). In addition, the higher retinal doses of UV received by aphakes and pseudophakes make these individuals especially vulnerable to cystoid macular edema (Kraff et al. 1985). Fluorescein leakage occurs following exposure of the retina of the aphakic monkey eye to UV-A radiation, but comparable studies using UV-B radiation have not been conducted. Therefore, retinal degeneration should be considered a risk of excessive exposure to ultraviolet radiation.

Very little research has been conducted on primates, on diurnal animal models of human retinal degenerations, or on retinas compromised by chemicals, age or other agents. The striking evidence of long-delayed and persistent changes in the monkey retina following optical radiation, coupled with some clinical evidence in humans, suggests that research on primates needs emphasis.

Aging Disorders

Deterioration of the visual system as individuals age is a fact (Owsley et al. 1986). The likelihood that optical radiation contributes to this deterioration is high for several reasons. First, the cellular pathology observed in older individuals is similar in appearance to radiation induced damage (Kuwabara 1978). Second, the ophthalmoscopic appearance of the aged retina is sometimes similar to that induced by optical radiation (Klein 1958). Third, some of the kinds of vision loss described in the aged are consistent with the losses which could be produced by optical radiation damage (Jaffe, de Monestario, and Podgor 1982; Harweth and Sperling 1975). Fourth, the accumulation of lipofuscin materials in the RPE and other changes in the retina suggest that the aged retina has a lessened capability of repair (Feeney-Burns, Berman, and Rothman 1980).

Optical radiation may have quite different visual health consequences for eyes with and without ocular disease. Optical radiation may accelerate the deterioration of central vision in older individuals with central retinal disease (Hyman et al. 1983), whereas in those free of ocular disease optical radiation may impair paramacular and peripheral vision more than foveal vision. This interpretation is offered to reconcile the facts of visual loss outside the macular in disease-free aged eyes (Owsley et al. 1986) with Young's prediction that the central retina will exhibit the major effects of lifetime retinal exposure to optical radiation (Young 1981). This ad hoc explanation is not very satisfactory but it does indicate the need to temporize theory with data. Other interpretations also are possible, e.g., those individuals with central retinal disease may have had a different exposure history or some genetic vulnerability.

Given these facts and theoretical considerations, exposure of the aged retina to ultraviolet radiation in excess of amounts permitted by the phakic eye probably is hazardous. The retina of the aged individual is exposed to more radiation than phakics receive when the crystalline lens is extracted without placing a comparable filter in front of the retina, even when ordinary sunglasses are used.

Research is needed to determine the extent to which optical radiation is a factor in the deterioration of the vision of the elderly. In the meantime, we should take practical steps to protect our eyes from excessive optical radiation, and thus prolong our visual lifetime.

Development Disorders

While there are several reasons to suspect hazardous effects of optical radiation on visual development, almost no research has been conducted on the developing primate retina. In fact, there is very little experimental exposure data on the developing retina of any species. Glass et al. (1985) have reported that the probability of retinopathy of prematurity (ROP) is highest in infants exposed to more light during their hospital stay. This evidence confirms a prediction by Wolbarsht et al. (1983) about ROP and light and is consistent with the evidence for the interaction of oxygen and light in retinal damage (Ruffolo et al. 1984). The action spectrum for this effect is unknown but UV-B and UV-A probably play a role. Furthermore, there are a large variety of sources and situations in which infants are exposed to optical radiation. Some of the same evidence which gave rise to suspicions about the role of optical radiation in retinal degeneration and visual aging is relevant to the potential hazards to visual development: short-wavelength radiant energy incident on the retina,

short-wavelength chromophores in the retina, dose-dependence of retinal damage, cumulative effects, long duration effects, and delayed effects. In addition, there are special properties of the developing visual system which might decrease injury thresholds, such as more transparent ocular media and different densities of chromophores and screening pigments, or which might increase the vulnerability of infants, such as the long period of post-natal retinal development (especially foveal) and early dependence on non-foveal visual fields. Thus, the long periods required for many visual processes to mature suggests a window-of-vulnerability during which time optical radiation might alter later visual performance, especially if optical radiation alters the spatial and temporal summation properties of the neural retina.

Even though there is little experimental data on the effects of optical radiation on the developing retina, the photobiological and visual science evidence is sufficient to postulate that disorders of visual development are risks of optical radiation.

Retinal Problems

The only human data from which one could derive an estimate of the radiant exposure of UV which could damage the retina is Hecht et al. (1948) and Clark, Johnson, and Dreher (1946). These data showed that staring at skylight for several hours induced an abnormal retardation of dark adaptation. Since rhodopsin has an absorption band in the UVA (Kurzel, Wolbarsht, and Yananashi 1977), this deficit could have been due to the ambient outdoor UVA. If the ambient level of UVA at the cornea was about 9 x 10^{-2} Jcm^{-2}, as suggested by Ham and Mueller (1982), then the retinal radiant exposure might have been about 9 x 10^{-3} Jcm^{-2} in the Hecht and Clark studies. Experimental estimates of UV retinal damage in monkeys have been few. Schmidt and Zuclich (1980) found the threshold at 325 nm to be 10 Jcm^{-2}. Recent evidence in phakic rabbits (Pitts, Bergmanson, and Chu 1983) and rats (Rapp, Jose, and Pitts 1985) suggest that the radiant exposure necessary to damage the retina is even lower at 300 nm. The threshold for 300 nm damage to the monkey retina currently is approximately 0.6 Jcm^{-2}. Ham and Mueller (1982) found the aphakic monkey has thresholds of 5.0 Jcm^{-2} at 325 nm, 5.4 Jcm^{-2} at 350 and 8.1 Jcm^{-2} at 380 nm.

REFERENCES

Ananthaswamy HN and A Eisenstark (1976) "Near-UV-induced breaks in phage DNA: sensitization by hydrogen peroxide (a tryptophan photoproduct)." Photochem. Photobiol. 24:439-442.

Anderson EI, DD Wright and A Spector (1979) "The state of protein sulfhydryl groups in normal and cataractous proteins II cortical and nuclear regions." Exp. Eye Res. 29: 233-243.

Augusteyn RC (1981) In Mechanisms of Cataract Formation in the Human Lens. G. Duncan (ed). Academic Press.

Augusteyne R (1974) "Human lens albuminoid." Jap J. Ophthalmol. 18: 127-134.

Augusteyne RC (1975) "Distribution of fluorescence in the human cataractous lens." Ophthalmic Res. 7: 217-224.

Bachem A (1956) "Ophthalmic ultraviolet action spectrum." Amer. J. Ophthal. 41: 969-980.

Bando M, A Nakauima and K Satoh (1975) "Coloration of human lens protein." Exp. Eye Res. 20: 489-492.

Barker FM II (1979) The transmittance of the EMS from 200nm to 2500nm through the optical tissues of the eye of the pigmented rabbit. MS Thesis University of Houston, Houston, Texas.

Barr RE and EL Roetman (1974) "Oxygen gradients in the anterior chamber of anesthetized rabbits." Invest. Ophthal. 13: 386-392.

Benedek GB (1971) "Theory of transparency of the eye." Applied Optics 10: 459-473.

Berler D and R Peyser (1982) "Light intensity and visual acuity following cataract surgery." Ophthalmology 89 (Suppl.) L 117.

Bhuyan KC and DK Bhuyan (1977) "The relative functions of superoxide dismutase and catalase in the eye." IRCS Medical Science 5: 279.

Boettner EA and JR Wolter (1962) "Transmission of the ocular media." Invest. Ophth. 1(6): 766-783.

Borkman RF (1977) "Ultraviolet action spectrum for tryptophan destruction in aqueous solution." Photochem. Photobiol. 26: 163-166.

Borkman RF and S Lerman (1977) "Evidence for a free radical mechanism in aging and UV irradiated ocular lenses." Ep. Eye Res. 25: 303-309.

Borkman RF, A Dalrymple and S Lerman (1977) "Ultraviolet action spectrum for fluorogen production in the ocular lens." Photochem. Photobiol. 26: 129-132.

Borkman RF, JD Tassin and S Lerman (1981) Exp. Eye. Res. 32: 747-754.

Brenner W and G Grabner (1982) "Unscheduled DNA repair in human lens epithelium following in vivo and in vitro UV irradiation." Ophthal. Res. 14: 160-166.

Brilliant LB, NC Grasset, RP Pokhrel, A Kolstad, JM Lepkowski, GE Brilliant, WN Hawks and B Pararajasegaram (1983) "Associations among cataract prevalence, sunlight hours and altitude in the himalayas." Amer. J. Epidem. 118: 250-264.

Brindley GC (1953) "The effects on colour vision of adaptation to very bright lights." J. Physiol. 122: 332.

Buckingham RH and A Pirie (1972). "The effect of light on lens proteins in vitro." Exp. Eye Res. 14: 297.

Castineiras SG, J Dillon and A Spector (1979) "Effects of reduction on absorption and fluorescence of human lens proteins." Exp. Eye Res. 29: 573-575.

Cavonius, CR, S Elgin, and DO Robbins (1974) "Thresholds for damage to the human retina by white light." Exp. Eye Res. 19: 543-548.

Chand D, HK El-Aguizy, RD Richards and SD Varma (1982) "Sugar cataracts in vitro: implications of oxidative stress and aldose reductase I." Exp. Eye Res. 35: 491-497.

Chand D and SD Varma (1983) "Human lens fatty acids composition." Invest. Ophthal. and Vis. Sci. (ARVO suppl.) 24: 31.

Chand D, SD Varma and RD Richards (1982) "Lens lipid peroxidation. Conjugated acylpolyene and schiff bases in human cataracts." Invest. Ophthal. and Vis. Sci. (ARVO suppl.) 20: 218.

Chylack LT Jr. (1978) "Classification of human cataracts." Arch. Ophthal. 96: 888.

Chylack LT, MR Lee, WH Tung and H-M Cheng (1983) "Classification of human senile cataractous change by the American cooperative Cataract Research Group (CCRG) Method." Invest Ophthalmol. and Vis Sci, 24: 424-431.

Clark, BA, ML Johnson and RE Dreher (1946) "The effect of sunlight on dark adaptation." Am. J. Ophthal. 29: 823-836.

Cooper GF and JG Robson (1969) J. Physiol. 203: 411-17.

Crylin MN, A Pedvis-Leftick and J Sugar (1980) "Cataract formation in association with ultraviolet photosensitivity." Annals of Ophthalmol. 12: 786-790.

Dilley KJ and A Pirie (1974) "Changes to the proteins of the human lens nucleus in cataract." Exp. Eye Res. 19: 59-72.

Dillon J and A Spector (1980) "A comparison of aerobic and anaerobic photolysis of lens proteins." Exp. Eye Res. 31: 591-599.

Dillon J, A Spector and K Nakanishi (1976) Nature 259: 422-433.

Dillon J, M Garner, D Roy and A Spector (1982) "The photolysis of lens protein: molecular changes." Exp. Eye Res. 34: 651-658.

Doniger J, ED Jacobson, K Krell and JAD Paolo (1981) "UV light action spectra for neoplastic transformation and lethality of Syrian hamster embryo cells correlate with spectrum for pyrimidine dimer formation in cellular DNA." PNAS 78: 2378-2382.

Duke-Elder S and PA MacFaul (1972) System of Ophthalmology V xiv pt 929-932.

Duke-Elder WS (1926) Lancet 1: 1188-91.

Fecondo JV and RC Augusteyn (1983) Exp. Eye Res. 36: 15-23.

Feeney-Burns L, ER Berman and H Rothman (1980) "Lipofuscin of human retinal pigment epithelium." Am. J. Ophth. 90: 783-791.

Fraunfelder F, J Megaw and S Lerman (1983) "Further studies on allopurinol in human cataracts." Invest. Ophthalmol. Vis. Sci. 24 (Suppl.): 3.

Freeman RG (1975) "Data on the action spectrum for UV carcinogenesis." J. Nat. Cancer Inst. 55: 1119-1121.

Garner MH and A Spector (1980) "Selective oxidation of cysteine and methionine in normal and senile cataractous lenses." Proc. Natl. Acad. Sci. 77: 1274.

Girgus JS, S Goren and C Porac (1977) "Independence of in vivo human lens pigmentation from UV-light exposure." Vision Res. 17: 749-750.

Glass PA, G Avery, KN Sivasubramanian, M Keys, AN Sostek and DS Friendly (1985) "Effect of bright light in the hospital nursery on the incidence of retinopathy of prematurity." N. Engl. J. Med. 313: 401-

Glazer LD, A Rincon and A Eisenstark (1976) "The binding of near UV light-induced tryptophan photoproducts to DNA." Biochem. Biophys. Acta 418: 137-145.

Goosey JD, JS Zigler and JH Kinoshita (1980) "Cross-linking of lens crystallins in a photodynamic system: a process mediated by a singlet oxygen." Science 208: 1278-1280.

Goosey JD, ME Allison and CA Garcia (1983) "Lipid peroxidative mechanism for posterior subcapsular cataract formation in the rabbit." ARVO Abstracts, Invest. Ophthal. Vis. Sci. 24: 75.

Greiss GA and MF Blakenstein (1981) "Additivity and repair of actinic retinal lesions." Invest. Ophth. and Vis. Sci. 20: 803-807.

Ham WT Jr (1984) "Basic mechanisms underlying the production of photochemical lesions in the mammalian retina." Curr. Eye Res. 3: 165-174.

Ham WT Jr and HA Mueller "Action spectrum for retinal injury from near ultraviolet radiation in the aphakic monkey." Am. J. Ophthalmol. 93:299-

Harding JJ (1972) "The nature and origin of the urea-insoluble protein of human lens." Exp. Eye Res. 13: 33-40.

Harding JJ (1981) In Molecular and Cellular Biology of the Eye Lens. H. Bloemendal (ed). Wiley Interscience.

Harding JJ and KJ Dilley (1976) "Structural proteins of the mammalian lens: a review with emphasis on changes in development, aging and cataract." Exp. Eye Res. 22: 1-73.

Harm, W (1978) "Evidence for photoenzymatically repairable, lethal 'non-dimer' photoproducts formed in E. coli cells by 265 nm radiation or by sunlight 360 nm." Mutat. Res. 51: 301-310.

Harweth RS and HG Sperling (1975) "Effects of intense visible radiation on the increment-threshold spectral sensitivity of the rhesus monkey eye." Vis. Res. 15: 1193-1204.

Hata N and Hockwin O (1977) Ophthal. Res. 9: 256-262.

Hecht S, CD Hendley, S Ross, and PV Richmond (1984) "The effect of exposure to sunlight on night vision." Am. J. Ophthal. 31: 1573-1580.

Hiller R, L Giacometti and K Yuen (1977) "Sunlight and cataract: An epidemiological investigation." Amer. J. Epidemiol. 105: 450-459.

Hiller R, RD Sperduto and F Ederer (1983) "Epidemiologic associations with cataract in the 1971-1972 national health and nutrition examination survey." 118: 239-249.

Hochheimer BF (1981) "A possible cause of chronic cystyc maculopathy the operating microscope." Ann. Ophthalmol. 13: 153-155.

Hockwin O, V Dragomirescu and S Lerman (1983) "In vivo age-related changes in normal and cataractous human lens density." Acta XXIV International Cong. Ophthalmol. In Print.

Hoenders HL and H Bloemendal (1981) In Molecular and Cellular Biology of the Eye Lens. H. Bloemendal (ed). Wiley Intersciences.

Hollows F and D Moran (1981) "Cataract -- The Ultraviolet Risk Factor." Lancet ii: 1249-1251.

Hymen LG, AM Lilienfeld, et al. (1983) "Senile macular degeneraton: A case-control study." Am. J. Epidemiol. 118: 213-227.

Ichihashi M and CA Ramsey (1976) "The action spectrum and dose response studies of unscheduled DNA synthesis in normal human fibroblasts." Photochem. Photobiol. 23: 103-106.

Imbrie CW and TM Murphy (1982) "UV action spectrum (254-405nm) for inhibition of K-stimulated and adenosine triphophosphatase from the pasma membrane of Rosa damascena." Photochem. Photobiol. 36: 537-599.

Jaffe MJ, FM de Monestario and MJ Podgor (1982) "Retinal aging and blue-sensitivity cone functioning." Invest. Ophth. Vis. Sci. 22 (Suppl.): 218.

Jernigan HM, HN Fuki, JD Goosey and JH Kinoshita (1981) "Photodynamic effects of rose bengal or riboflavin on carrier mediated transport systems in rat lens." Exp. Eye Res. 32: 461-466.

Jose JG (1978) "The role of DNA damage, its repair and its misrepair in the etiology of cataract: a review." Ophthal. Res. 10: 52-62.

Jose JG and KL Yielding (1977) "Unscheduled DNA synthesis in lens epithelium following ultraviolet irradiation." Exp. Eye Res. 24: 113-119.

Jose JG and KL Yielding (1979) "Photosensitive cataractogens, chlorpromazine and methoxypsoralen cause DNA repair synthesis in lens epithelial cells." Invest. Opthal. Vis. Sci. 17: 687-691.

Jose JG, HR Kock and A Respondek (1982) "Histological observations of the lenses of psoralem + UV-A treated albino rats and a theory as to the underlying mechanism." Graefe's Arch. Clin. Exp. Ophthalmol. 219-44-

Kahn HA and RC Milton, Revised Framingham eye study prevalence of glaucoma and diabetic retinopathy.

Kahn HA, HM Leibowitz, JP Ganley, MM Kini, T Colton, RS Wickerson and TR Dawaber (1977a) "The Framingham eye study: I. Outline and major prevalence findings." Am. J. Epidemiol. 106: 17-32.

Kahn HA, HM Leibowitz, JP Ganley, MM Kini, T Colton, RS Wickerson and TR Dawaber (1977b) The Framingham eye study: II. Association of ophthalmic pathology with single variables previously measured in the Framingham Heart study." Am. J. Epidemiol. 106: 33-41.

Kalustian A, M Sun and S Zigman (1978) "N-UV light sensitized inactivation of glutathione reductase." Am. Soc. Photobiol. (Abstracts-June) 112-113.

Kinoshita J (1974) "Mechanisms of cataract formation." Invest. Ophth. Vis. Sci. 18: 713-724.

Kinsey VE (1948) "Spectral transmission of the eye to ultraviolet." Arch. Ophth. 39: 508-513.

Klien B (1958) "Diseases of the macula." Arch. Ophthalmol. 60: 175-186.

Kraff MC, DR Sanders, LM Jampol and HL Lieberman (1985) "Effect of an ultraviolet-filtering intraocular lens on cystoid macular edema." Ophthalmology 92:366-

Kramer SG (1980) "Epinephrine distribution after topical administration to phakic and aphakic eyes." Trans-Am Ophthalmol. Soc. 75: 947-982.
Kurtin WE and JA Zuclich (1978) "Action spectrum for oxygen-dependent near-ultraviolet induced corneal damage." Photochem. Photobiol. 27: 329.

Kurzel R, ML Wolbarsht and BS Yamanashi (1977) "UV radiation effects on the human eye." Photochem. Photobiol. Rev. 2: 133-167.

Kurzel RB (1973) "Trypotophan excited states and cataracts in the human lens." Nature 241:132-133.

Kuwabara T and S Okisake (1976) "Effect of electronic strobe flashlight on the monkey retina." Jap. J. Ophthal. 20: 9-18.

Kuwabara T (1978) "Photic and photo-thermal effects on the retinal pigment epithelium." In the Retinal Pigment Epithelium, Harvard University Press, Cambridge.

Kwan M, J Ninikoski and TK Hunt (1972) "In vivo measurements of oxygen tension in the cornea, aqueous human and anterior lens of the open eye." Invest. Ophthal. 11: 108-111.

Lakhanpthal V et al. (1982) Arch Ophthalmol 100: 1068-1070.

LaVail MM and BA Battelle (1975) "Influence of eye pigmentation and light deprivation on inherited retinal dystrophy in the rat." Exp. Eye Res. 21:167.

Lerman S (1980a) "Human ultraviolet light cataracts." Ophth. Res. 12: 303-314.

Lerman S (1980b) "Radiant energy and the eye." MacMillan Publishing Company, New York.

Lerman S (1982) "Ocular photoxicity and PUVA therapy: An experimental and clinical evaluation." FDA Photochemical Toxicity Symp. J. Natl. Cancer Inst. 69: 287-302.

Lerman S (1983) "Psoralens and ocular effects in animals and man: In vivo monitoring of human ocular and cataneous manifestations." Conf. on Photobiologic, Toxicologic and Pharmacologic Aspects of Psoralens, March 1-3, 1982. J. Natl. Cancer Inst., In Print.

Lerman S and R Borkman (1976) "Spectroscopic evaluation and classification of the normal, againing and cataractous lens." Ophthal. Res. 8: 335-353.

Lerman S, J Megaw, and K Gardner (1982a) "Psoralen-long-wave ultraviolet therapy and human cataractogenesis." Invest. Ophthal. Vis. Sci. 23: 801-803.

Lerman S, J Megaw and K Gardner (1982b) "Allopurinol therapy and human cataractogenesis." Amer. J. Ophthalmol. 94: 141-146.

Lerman S, JF Kuck, R Borkman and E Saker (1976) "Acceleration of an aging parameter (Fluorogen) in the ocular lens." Ann. Ophthal. 8: 558-562.

Lerman S, JF Kuck, R Borkman and E Saker (1976) "Induction, acceleration and prevention (in vitro) of an aging parameter in the ocular lens." Ophthal. Res. 8: 213-226.
Lerman S, JM Megaw, K Gardner, Y Takei and I Willis (1981) "Localization of 8-methoxypsoralen in ocular tissues." Opthal. Res. 13: 106-116.

Lerman S, K Gardner, J Megaw and R Borkman (1981) "The prevention of direct and photosensitized UV radiation damage to the ocular lens." Ophthalmic Res. 13: 284-292.

Lerman S, J Megaw and I Willis (1980) "The photreactions of 8-methoxypsoralen with tryptophan and lens proteins." Photochm. Photobiol. 31: 235-242.

Leske MC and RD Sperduto (1983) "The epidemiology of senile cataracts: a review," American Journal of Epidemiology. 118: 152-165.

Lowenstein A and J Steel (1941) "Macular burning and ring scotoma." Glasgow Med. J. 135: 73-85.

Maher EF (1978) "Transmission and absorption coefficients for ocular media of the rhesus monkey." Report SAM-TR-78-32, USAF School of Aerospace Medicine, Brooks AFB, Tx.

Marcantonio JM, G Duncan, PD Davis, and AR Bushell (1980) "Classification of human senile cataracts by nuclear color and sodium content." Exp. Eye Res. 31: 227-237.

Marshal, J (1970) "Thermal and mechanical mechanisms in laser damage to the retina." Invest. Opthalmol. 9: 97-115.

Mao W and T Hu (1982), "An Epidemiologic Survey of Senile Cataract in China," Chinese Medical Journal, 95(11): 813-818.

Martinez GS, AJ Campbell, J Reiken and BC Allan (1982) "Prevalence of ocular disease in a population study of subjects 65 years old and older." Am. J. Ophthalmol. 94: 181.

McCanna, P. et al (1982) Arch Ophthalmol 100: 1071-1073.

McFaul PA (1969) "Visual prognosis after solar retinopathy." Brit. J. Opthalmol. 53: 534-541.

Megaw J, J Lee and S Lerman (1980) "NMR analyses of tryptophan-8-methoxypsoralen photoreaction products formed in the presence of oxygen." Photochem. Photobiol. 32: 265-269.

Moss SH and KC Smith (1981) "Membrane damage can be a significant factor in the inactivation of E. coli by near UV radiation." Photochem. Photobiol. 32: 203-210.

Naidoff MA and DA Sliney (1974) "Ritinal injury from a welding arc." Am. J. Ophthal 77: 663-668.

Owsley C, DW Kline, JS Werner, V Greenstein and J Marshall (1986) "Optical radiation effects on aging and visual perception." In Light Toxicity. M Wahler and VM Hitchens (eds.). CRC Press, Boca Raton, Florida.

Parrish JS, RR Anderson, R Urback and D Pitts (1978) UV-A Biological Effects of Radiation with Emphasis on Human Responses to Longwave Radiation. Plenum Press, New York.

Pathak MA, DM Kraemer and U Guengerich (1972) "Formation of thymine dimers in mammalian skin by UV radiation in vivo" Photochem. Photobiol. 15: 177-185.

Pirie A (1968) Invest. Ophthalmol. 7: 634-649.

Pirie A (1972) "Photo-oxidation of Proteins and Comparisons of Photo-oxidized Proteins with Those of the Cataractous Human Lens." Israeli J. Med Sci. 8: 1567-.

Pirie A and KJ Dilley (1974) "Photooxidation of N-formylkynurenine and tryptophan peptides by sunlight or simulated sunlight." Photochem. Photobiol. 19: 115-118.

Pitts DG (1970) "A comparative study of the effects of ultraviolet radiation on the eye." Am. J. Optom. 47: 535-546.

Pitts DG (1973) "The ocular ultraviolet action spectrum and protection criteria." Health Physics 15: 559-566.

Pitts DG (1974) "The human ultraviolet action spectrum." Am. J. Optom. and Physiol. Optics 51: 946-960.

Pitts DG (1978) "The ocular effects of ultraviolet radiation." Amer. J. Optom. and Physiol. Optics 55: 19.

Pitts DG (1981) "The threat of ultraviolet radiation to the eye - how to protect against it." J.Amer. Optom. Assn., 52: 949-957.

Pitts DG, PD Hacker and WH Parr (1977) "Ocular ultraviolet effects from 295 nm and 400 nm in the rabbit eye." DHEW (NIOSH) Publication no. 77-175.

Pitts DG, JPG Bergmanson and LWF Chu (1983) "Rabbit eye exposure to broad-spectrum fluorescent light." Acta Ophthalmol (Copenhagen) Supp. 159.

Pitts DG and KR Kay (1969) "The photoophthalmic threshold for the rabbit." Am. J. Optom. 46: 561-572.

Pitts DG and AP Cullen (1981) "Determination of infrared radiation levels for acute ocular cataractogenesis." Graefes Arch. Klin. Exp. Ophthalmol. 217:285-.

Pitts DG and TJ Tredici (1971) "The effects of ultraviolet on the eye." Am. Ind. Hyg. Assoc. J. 32: 235-246.

Pitts DG, et al. (in press), "Optical Radiation and Cataracts," in Vicusal Health and Optical Radiation, M. Waxler and V. Hitchens, eds., CRC Press, Inc., Boca Raton, Florida.

Rapp LM, JG Jose and DG Pitts (1985) "DNA reapir synthesis in the rat retina following in vivo exposure to 300 nm radiation." Invest. Ophthalmol. Vis. Sci. 26: 384.

Ruffolo JJ Jr, WT Jr Ham, HA Mueller and JE Miller (1984) "Photochemical lesions in the primate retina under conditions of elevated blood oxygen." Invest. Ophthalmol. Vis. Sci. 25: 893-898.

Satoh K, M Bando and A Nakajima (1973) "Fluorescence in human lens." Exp. Eye Res., 16: 167-172.

Schmidt RE and JA Zuclich (1980) "Retinal lesion due to ultraviolet laser exposure." Invest. Ophthalmol. Vis. Sci. 19: 1166-1175.

Serafino GM and Frederick JE (in press) "Global modeling of the ultraviolet solar flux incident on the biosphere," prepared for the U.S. Environmental Protection Agency, Washington, D.C.

Sliney, D and M Wolbarsht (1980) Safety with Lasers and Other Optical Sources. Plenum Press, New York.

Spector A, D Roy and J Stauffer (1975) "Isolation and characterization of an age-dependent polypeptide from human lens with non-tryptophan fluorescence." Exp. Eye Res. 21: 9-24.

Spector A, O Roy and J Stauffer (1975) "Isolation and characterization of an age-dependent polypeptide from human lens with non-tryptophan fluorescence." Exp. Eye Res. 21: 9-24.

Spector A and WH Gardner (1982) "Hydrogen perioxide and human cataract." Exp. Eye Res. 33: 673-681.

Sprott GD, WG Martin and H Schneider (1976) "Differential effects of near UV and visible light on active transport and other membrane process in E. coli." Photochem. Photobiol. 24: 21-27.

Streeten BW and J Eshaghian (1978) "Human posterior subcapsular cataract: a gross and flat preparation study." Arch. Ophthal. 96: 1653-1658.

Sykes SM, WG Jr Robison, M Waxler and T Kuwabara (1981) "Damage to the monkey retina by broad-spectrum fluorescent light. "Invest. Ophth. Vis. Sci. 20: 425-434.

Taylor HR (1980) "The Environment and the Lens." Brit. J. Ophthal. 64: 303-310.

Thomas DM and KL Schepler (1980) "Raman spectra of normal and ultraviolet-induced cataractous rabbit lens." Invest. Ophthalmol. Vis. Sci. 19: 904-912.

Trevithick JR, MO Creighton and WM Ross (1980) "Vitamin E prevents cataractogenesis in diabetic rats." Invest. Ophth. and VIs. Sci. (Suppl.) 19: 207-208.

Truscott RJW and RC Augusteyn (1977) "Oxidative changes inhuman lens protein during senile nuclear cataract formation." Biochem. Biophys. Acta 492: 43-52.

Truscott RJW, K Faull and RC Augusteyn (1977) Ophthal. Res. 9: 263-8.

Turro NJ and A Lamola (1977) Photochemistry in the Science of Photobiology. KC Smith (ed), Plenum, New York, pp. 63-86.

Tso MOM and BJ Woodford (1983) "Effect of photic injury on the retinal tissues." Ophthalmology 90: 952.

Tyrell RM (1976) Photochem. Photobiol. 23: 13-20.

Van Heyningen R (1971) Nature 230: 393-394.

Van Heyningen R (1973) Exp. Eye Res. 17: 137-147.

Van Heyningen R (1976) "What happens to the human lens in cataract." Sci. Amer. 233: 70-81.

Varma SD (1981) "Superoxide and lens of the eye: a new theory of cataractogenesis." Inter. J. Quantum Chem. XX: 479-484.

Varma SD, A Tina and RD Richards (1977) "Protection against superoxide radicals in rat lens." Ophthal. Res. 9: 421-431.

Varma SD, D Chand, YR Sharma and JF Kuck (1983) "Effect of vitamin E on cataract development in emory mice." Invest. Ophthal. Vis. Sci. (ARVO Suppl.) 24: 31.

Varma SD, D Chand, YR Sharma, JF Kuck and RD Richards (1983) "Oxidative stress on lens and cataract formation: role of light and oxygen." Presented at the 1st International Symposium on Light and Oxygen Effects on the Eye. Current Eye Research, In press.

Varma SD, NA Beachy and RD Richards (1982) "Photoperoxidation of lens lipids: prevention by vitamin E. Photochem. Photobiol. 36: 623-626.

Varma SD, S Kumar and RD Richards (1979) "Light-induced damage to ocular len cation pump: prevention by vitamin C." Proc. Natl. Acad. Sci. 76: 3504-3506.

Varma SD, VK Srivastava and RD Richards (1982) "Photoperoxidation in lens and cataract formation: preventive role of superoxide dismutase, catalase and vitamin C." Ophthal. Res. 14: 167-175.

Warner, JS (1982) "Development of scotopic sensitivity and the absorption spectrum of the human ocular media." J. Optical. Soc. Am. 72: 247-258.

Waxler, M. (in press), "Long-Term Visual Health Problems: Optical Radiation Risks," in Visual Health and Optical Radiation, M. Waxler and V. Hitchens, eds., CRC Press, Inc., Boca Raton, Florida.

Weale RA (1982) "The age variation of senile cataract in various parts of the world." Br. J. Ophthalmol. 66: 31-

Webb RB and MJ Peak (1981) "The effect of stray light in the 300-320 nm range and the role of cyclobutyl pyrimidine dimers in 365 nm lethality." Mutat. Res. 91: 177-182.

Weiter JJ and ED Finch (1975) "Matters arising: UV light and human cataract." Nature 254: 536-537.

Weiter JJ and S Subramanian (1978) "Free radicals produced in human lenses by a biophotonic process." Invest. Ophthal. Vis. Sci. 17: 869-873.

Wiesinger H et al. (1956) "Transmission of light through the ocular media of the rabbit eye." Am. J. Ophthalmol. 42: 907-910.

Williams, TP and BN Baker eds. (1980) The Effects of Constant Light on Visual Processes. Plenum Press, New York.

Wolbarsht, ML (1976) "The function of intraocular color filters." fed. Proc. 35: 44-50.

Wolbarsht ML, GS Goerge, WA Jr. Shearin, JA Klystra and MB III Landers (1983) "Retinopathy of Prematurity: A new look at an old disease." Paper presented at 1st Int. Symp. on Light and Oxygen Toxicity, Baltimore.

Wolfe E (1949) "Effects on visual threshold of exposure to radiation below 4000 angstroms." Trans Am. Acad. Ophthalmol. Otolaryrgol. 53: 400-414.

Yoakum G, W Ferron, A Eisenstark and RB Webb (1974) "Inhibition of replication gap closure in E. coli by near UV photoproducts of L-tryptophan." J. Bacterial 119:62-69.

Young RW (1981) "A theory of central retinal disease." In Future Directions of Ophthalmic Research. ML Sears (ed.). Yale University Press, New Haven, Conn.

Yu N-T, JFR Kuck and CC Askren (1979) "Red fluorescence in older and brunescent human lenses." Invest. Ophthalmol. Vis. Sci. 18: 1278-1280.

Zigler JS and JD Goosey (1981) "Aging of protein molecules: lens crystallins as a model system." Trends in Biochem. Sci. 6: 133-136.

Zigler JS and JD Goosey (1981) "Photosensitized oxidation in the ocular lens: evidence for photosensitizers endogenous to the human lens." Photochem. and Photobiol. 33: 869-874.

Zigler JS, JB Sidbury, BS Yamanashi and M Wohlbarsht (1976) "Studies on brunescent cataract. I. Analysis of free protein-bound amino acids." Ophthal. Res. 8: 379-387.

Zigman S (1970) "Near-UV light and cataracts." Photochem. and Photobiol. 26: 437-441.

Zigman S (1981) "Photochemical mechanisms in cataract formation." In Mechanisms of Cataract Formation in the Human Lens." G. Duncan (ed.). Publ. Acad. Press, Inc. London. Pp. 117-149.

Zigman S and R Vaughan (1974) "Effects of near-UV light on the lenses and retinas of mice." Invest. Ophth. Vis. Sci. 13: 462-465.

Zigman S, Griess, T Yulo and J Schultz (1973) "Ocular protein alterations by near UV light." Exp. Eye Res. 15: 255-264.

Zigman S, M Datiles and E Torczynski (1979) "Sunlight and Human Cataracts." Invest. Ophthal. Vis. Sci. 18: 462-467.

Zigman S, T Yulo and G Griess (1976) "Inactivation of catalase by near-ultraviolet light and tryptophan photoproducts." Mol. Cell. Biochem. 11: 149-154.

Zuclich JA (1977) "Lenticular effects of near-UV laser radiation." In Research on the Ocular Effects of Laser Radiation. Part II. Technology Incorporated, Final Report, Contrast F41609-73-C-0017. USAF School of Aerospace Medicine.

Zuclich JA (1980) "Cumulative effects of near-ultraviolet induced corneal damage." Health Phys. 38: 833.

Zuclich JA and JS Connolly (1976) "Ocular damage induced by near-ultraviolet laser radiation." 15: 760-764.

CHAPTER 11

RISKS TO CROPS AND TERRESTRIAL ECOSYSTEMS FROM ENHANCED UV-B RADIATION

SUMMARY

In making an assessment of the risk to crops and ecosystems of increased ultraviolet-B (UV-B) radiation, it must be recognized that existing knowledge is in many ways deficient. The effects of enhanced levels of UV-B radiation have been studied in only four of the ten major terrestrial plant ecosystems. Most of our knowledge is derived from studies focused upon agricultural crops and conducted at mid-latitudes, not in the tropics or at more poleward latitudes. Trees have not been subject to experimentation. Experimental protocols often have had flaws; too often, single-year studies have been done, rather than long-term ones, and too much of the existing data comes from growth chambers, in which plants grow under unrealistic conditions, rather than from field studies. Therefore, the full extent of the potential impacts of enhanced levels of UV-B radiation on a global basis cannot be adequately assessed.

Despite these limitations, a broad range of experimental results demonstrated that, in nearly half of the plant species examined, UV-B radiation deleteriously affected crop yield and quality. Data exist that indicate that it may be reasonably anticipated that if UV-B radiation increases, crop yield and quality will decline for at least some cultivars. Existing data also suggest that increased UV-B radiation will alter the distribution and abundance of plants and potentially disrupt ecosystems. Unfortunately, a qualitative prediction of how these ecosystems would be altered cannot be determined from the current knowledge base.

FINDINGS

1. LIMITED STUDIES ANALYZING THE EFFECT OF INCREASED UV-B RADIATION ON CROPS GENERALLY SHOW ADVERSE IMPACTS. HOWEVER, CONCLUSIONS ABOUT THE AMOUNT OF YIELD LOSSES ATTRIBUTABLE TO UV-B CANNOT BE DRAWN.

   1a. Difficulties in experimental design, the large number of species and cultivars, and complex interactions between plants and their environment have prevented quantification of total crop loss from increases in UV-B.

   1b. Action spectra for UV damage to higher plants are limited, but indicate a strong weighting toward shorter UV-B wavelengths which are those most affected by ozone reduction.

2. OF PLANT CULTIVARS TESTED IN THE LABORATORY, APPROXIMATELY 70 PERCENT WERE DETERMINED TO BE SENSITIVE TO UV-B; CARE MUST BE TAKEN IN INTERPRETING THIS FINDING.

   2a. Different cultivars within a species have exhibited different degrees of UV-B sensitivity. While this suggests selective breeding could limit damage, neither the basis for selectivity nor the potential effect on other aspects of growth has been studied.

   2b. Laboratory experiments have been shown to inadequately replicate effects in the field, thus the implications of cultivar sensitivity are not certain.

   2c. In some species, mitigation responses more readily apparent in the field (e.g., increased production of UV absorbing flavonoids) have reduced adverse impacts.

3. THE EFFECTS OF UV-B RADIATION HAVE BEEN EXAMINED FOR ONLY FOUR OF THE TEN MAJOR TERRESTRIAL ECOSYSTEMS AND FOR ONLY A THIRD OF THE PLANT GROWTH FORMS.

   3a. Little or no data exist on enhanced UV-B effects on trees, woody shrubs, vines, or lower vascular plants.

4. LARGE UNCERTAINTIES EXIST AS A RESULT OF AN IMPERFECT EXPERIMENTAL DESIGN OR DOSIMETRY. EXISTING EXPERIMENTAL FIELD DATA SUGGEST A POTENTIAL REDUCTION IN CROP YIELD FOR SOME CROPS DUE TO ENHANCED UV-B RADIATION.

   4a. Field experiments in which UV-B radiation has been supplemented are limited. Several of the earlier field experiments are of limited value since UV-B doses or other factors such as soil temperature were not sufficiently controlled or representative of field conditions. Dose-response studies in the field are particularly different.

   4b. The only long-term field studies of a crop involved soybeans. These studies have found that enhanced levels of UV-B, simulating between 16 and 25 percent ozone depletion, caused crop yield reductions of

up to 25 percent in a particular cultivar. Smaller reductions in yield were experienced in years where drought conditions existed.

4c. Soybean (CV Essex) yield could be accurately predicted when total UV-B dose, daily maximum temperature, and number of days of precipitation were included in a regression model.

4d. The lipid and protein content of soybean was reduced up to 10 percent; however, higher UV-B doses alone did not consistently result in the largest reductions.

4e. While only several cultivars have been tested in the field, two out of three soybean cultivars tested under laboratory conditions were sensitive to UV-B. If this relationship holds true in the field, it suggests (when considered in light of yield reduction experiments) that UV-B increases could harm the potential of the world agricultural system to produce soybeans.

5. THE EFFECTS OF UV-B ON FUNGAL OR VIRAL PATHOGENS VARY WITH PATHOGEN, PLANT SPECIES, AND CULTIVAR.

5a. Current evidence on possible interactions with pathogens is very limited.

5b. Reduced vigor in UV-sensitive plants could render the plants more or less susceptible to pest or disease damage and thus result in changes in crop yield.

6. CHANGES IN UV-B LEVELS MAY INDUCE SHIFTS IN INTERSPECIFIC COMPETITION.

6a. If enhanced UV-B favors weeds over crops, agricultural costs (e.g., for increased tilling and herbicide application) could increase. However, insufficient evidence exists to form a basis for evaluating this effect.

6b. Increases in UV-B could alter the results of the competition in natural ecosystems and thus shift community composition. Since UV-B changes would be both global and long term, possible UV-induced alterations of plant species balances could result in large-scale changes in the character and equilibrium of vegetation in nonagricultural areas such as forests and grasslands.

7. UV-B RADIATION INHIBITS AND STIMULATES FLOWERING, DEPENDING ON THE SPECIES AND GROWTH CONDITIONS.

7a. The timing of flowering may also be influenced by UV-B radiation, and there is limited evidence that pollen may be susceptible to UV damage upon germination.

7b. Reproductive structures enclosed within the ovary appear to be well-protected from UV-B radiation.

8. INTERACTIONS BETWEEN UV-B RADIATION AND OTHER ENVIRONMENTAL FACTORS ARE IMPORTANT IN DETERMINING POTENTIAL UV-B EFFECTS ON PLANTS.

   8a. UV-B effects may be worsened under low light regimes or less apparent under conditions of limited nutrients or water.

   8b. Interactions with other environmental effects make extrapolation of data from growth chambers or greenhouses to field conditions difficult and often unreliable.

   8c. The combined effect of higher UV-B and other environmental changes cannot be adequately assessed by current data. Extensive, long-term studies would be required.

INTRODUCTION

This chapter examines the published and unpublished material currently available to assess the likely impact of projected increases in UV-B radiation upon global crop productivity and the distribution and abundance of plants in natural ecosystems. The limitations to this assessment are formidable because of the paucity of experimental data and the slow development of appropriate experimental technology. Therefore, actual risks may be far greater or somewhat less than current knowledge suggests.

ISSUES AND UNCERTAINTIES IN ASSESSING THE EFFECTS OF UV-B RADIATION ON PLANTS

Ideally, experiments should be designed to develop a data base that perfectly simulates future conditions for all plant species. These conditions should include all direct effects of enhanced UV-B radiation, in addition to all of the possible significant combinations with other effects (interactions). Such interactions should include, but not be limited to, the effects of increased atmospheric levels of carbon dioxide (CO2), drought, and mineral deficiency. A perfect simulation of all possible future environments would make it possible to accurately assess the potential impacts of global UV-B radiation increases. Unfortunately, such ideal circumstances do not exist. In reality, we must make assessments based upon imperfect experimental designs, which include only very selective and sometimes unrealistic growing conditions and the testing of only a few representative plant species. Therefore, the existing data base for this assessment will allow us to examine only some of the potential effects of UV-B changes and cannot be regarded as conclusive.

ISSUES CONCERNING UV DOSE AND CURRENT ACTION SPECTRA FOR UV-B IMPACT ASSESSMENT

Total global UV-B irradiance is dependent on a number of factors, including solar angle, latitude and altitude, stratospheric ozone concentration, atmospheric turbidity, and cloud cover. The earth-sun distance and minor solar fluctuations also contribute to annual variations in irradiance (Caldwell 1971). Because of diurnal and seasonal variations in many of these factors, the spectral composition of solar radiation also varies substantially. On a daily basis, solar UV-B irradiance is sinusoidal, peaking at solar noon. Annually, UV-B irradiance is maximum during summer and minimum during winter. Experiments evaluating the effectiveness of UV-B radiation on plants typically do not account for such changes because of practical difficulties in monitoring and supplementing UV-B radiation. Generally, supplemental UV-B radiation is provided using filtered sunlamps as a squarewave function by using timers. This system provides a proportionately greater UV irradiance during morning and late afternoons and under cloudy skies than would be anticipated outdoors. Caldwell et al. (1983) have designed a modulated system to monitor ambient UV-B and provide the desired supplemental UV-B dose. This system provides a more realistic simulation of anticipated ozone depletion because it modulates lamp output in accordance with actual levels of incoming solar UV radiation. Despite substantial expenses, it is highly recommended that such a system be utilized to improve field simulations and sensitivity of validation studies.

The source of UV-B radiation most commonly used in plant effects research is the fluorescent sunlamp, which is a low-pressure mercury vapor lamp containing a phosphor that fluoresces primarily in the UV-B region, and, to a lesser extent, in the UV-C and UV-A regions. Although the energy emitted principally comes from the fluorescing phosphor, some emission from mercury vapor is superimposed upon this, producing distinct lines in the spectrum. A weighting function is absolutely essential to determine the biological effectiveness of the spectral energy emitted from various types of lamps. The biologically effective irradiance (I_{BE}) is given by the following relationship:

$$I_{BE} = I_\lambda \, E_\lambda \, d_\lambda$$

where I_λ is the lamp spectral irradiance and E_λ is the relative effectiveness of the energy to produce a response at wavelength λ. Thus, the biologically effective irradiance is the product of the action spectrum and the spectral irradiance at each wavelength.

Several UV action spectra have been developed that share the common feature of decreasing effectiveness as wavelength increases, but have considerable variation in the rate of this decrease. UV-B effectiveness in an isolated organelle can differ considerably from an intact plant because of the cellular shielding effects in the plant and inherent repair mechanisms. Caldwell (1971) has developed a generalized plant damage spectrum based upon the combined responses of a number of different plant species. Although this represents a step forward in understanding plant responses, an action spectrum developed on intact plants under polychromatic radiation would be preferable. Caldwell et al. (1986) have recently attempted to develop such an action spectrum, and although there are experimental limitations, they were able to show that it is technologically possible.

Another essential reason for developing appropriate action spectra is to evaluate radiation amplification factors (RAF), i.e., the relative increase in biologically effective UV-B radiation associated with a specific ozone reduction. RAF is a complex function taking into consideration initial ozone layer thickness, percent ozone layer reduction, latitude, season, and biological weighting function (NAS 1979). The increase in solar UV-B radiation as a result of ozone reduction becomes appropriate only when the biological effectiveness of this radiation is known. Without an RAF, the absolute increase of total solar UV-B radiation resulting from even an appreciable ozone reduction is insignificant.

Since solar spectral irradiance increases by orders of magnitude with increasing wavelength in the UV-B region, the tails of the action spectra have a profound effect on the net RAF. The RAF values are much higher for those tails with steep slopes than for those with shallow slopes. Thus, the computed biological effectiveness of solar radiation could either be under- or overestimated if the action spectra are not representative of true plant responses.

It is evident from the above discussion that a more realistic action spectrum is needed for a proper assessment of the possible consequences of ozone depletion.

ISSUES CONCERNING NATURAL PLANT ADAPTATIONS TO UV RADIATION

Tremendous variability exists in species' sensitivity to UV-B radiation (Krizek 1978; Van, Gerrard, and West 1976; Hashimoto and Tajima 1980; Tevini, Iwanzik, and Thoma 1981 and 1982; Tevini and Iwanzik 1982; Teramura 1983) (Exhibit 11-1). Some plants show sensitivity to ambient levels of UV-B radiation (Teramura, Biggs, and Kossuth 1980; Bogenrieder and Klein 1978; Sisson and Caldwell 1976), and others are apparently unaffected by rather massive UV enhancements (Becwar, Moore, and Burke 1982; Ambler, Rowland, and Maher 1978). Similarly, large differences have been reported among cultivars of a given species (Biggs, Kossuth, and Teramura 1981; Dumpert and Boscher 1982; Murali and Teramura 1986a,b; Murali, Teramura, and Randall 1986). The mechanisms for these inherent differences have not been well documented.

Three main categories of natural mechanisms that protect against the effects of UV radiation mechanisms may be considered (Beggs, Schneider-Ziebert, and Wellmann 1986). The first includes repair mechanisms such as photoreactivation, a light-activated enzyme-mediated process whereby pyrimidine dimers produced by UV absorption are split (Rupert 1984). Indirect evidence (Beggs, Schneider-Ziebert, and Wellman 1986; Tanada and Hendricks 1953; Bridge and Klarman 1973) suggests that photoreactivation is a widespread phenomenon in plants. Excision repair, the replacement of deleterious photoproducts by new, correct DNA sequences, has also been documented in plant tissues (Howland, Hart, and Yette 1975, Soyfer 1983). Finally, quenching and free radical scavenging of oxygen singlets produced by photo-oxidation also alleviate some types of UV-induced damage.

The second category of protective mechanisms includes those that tend to minimize the damaging effects of UV-B radiation. Probably the most important of these mechanisms in plants is growth delay. If cell division stops or is slowed upon UV irradiation, other repair mechanisms could help ameliorate the damage before it becomes lethal. Although many plants show a growth inhibition upon UV-B radiation exposure (Teramura 1983), it is not clear whether this inhibition is the direct effect of the damage or due to this protective mechanism.

The third category of protective mechanisms involves those that effectively reduce the amount of UV radiation actually reaching sensitive plant targets. Structural attenuation by the cuticle and cell wall may play only a minor role since they offer little UV absorption (Caldwell, Robberecht, and Flint 1983; Steinmueller and Tevini 1985). The principal mechanism is probably the production of UV-absorbing pigments in outer tissue layers. Flavonoids and other related polyphenolic compounds, which occur in epidermal cells and have high UV absorption coefficients (Caldwell, Robberecht, and Flint 1983), are likely candidates. It has been shown that flavonoid concentrations in plant leaves substantially increase upon exposure to UV radiation (Wellman 1982; Murali and Teramura 1985a and 1986a; Robberecht and Caldwell 1978; Tevini, Iwanzik, and Teramura 1981 and 1983; Flint, Jordan, and Caldwell 1985), but it has not been established whether such an increase can

EXHIBIT 11-1

A Summary of Studies Examining The Sensitivity of Cultivar to UV-B Radiation

Crop	Number of Cultivars	Growth Condition [a/]	Conclusion [b/]	Basis of Comparison [c/]	Reference
Glycine max	19	G.C.	20% tolerant 60% intermediate 20% sensitive	d.w.	Biggs et al. 1981
	2	G.H.	Cultivar Altona more sensitive than Bragg	d.w.	Vu et al. 1978
	23	G.H.	8% tolerant 33% unaffected 59% sensitive	d.w.	Teramura and Murali 1986
	5	F	20% sensitive 80% unaffected	seed d.w.	
Phaseolus vulgaris	2	G.H. & G.C.	BBL 290 more sensitive than Astro	leaf resistance	Bennett (1981)
	3	G.H.	Maxidor sensitive Saxa, Favorite tolerant		Dumpert and Boscher (1982)
Brassica oleracea (?)	2	G.H. & G.C. Garrard et al. (1976)	no difference	p.s. & d.w.	Van et al (1976) 2G.C.
Cucumis sativus sensitive	5	G.H. (1986a)	20% tolerant	d.w.	Murali and Teramura 80%
	2	G.H.	Poinsett extremely sensitive, Ashley slightly sensitive	d.w.	Krizek (1978)
Tritium aestivum	4	G.H.	no difference (?)	d.w.	Dumpert and Boscher (1982)
	7	G.C.	no difference	d.w.	Biggs and Kossuth (1978)
	2	F	no difference	d.w.	Biggs et al. (1984)
Zea mays	4	G.C.	25% extremely sensitive 75% sensitive	d.w.	Biggs and Kossuth (1978)
Oryza sativa	5	G.C.	60% tolerant 40% sensitive	d.w.	Biggs and Kossuth (1978)
Hordeum vulgare	4	G.H.	25% tolerant 75% sensitive	d.w.	Dumpert and Boscher (1982)
	3	G.C.	no difference	d.w.	Biggs and Kossuth (1978)

EXHIBIT 11-1

A Summary of Studies Examining The Sensitivity of Cultivar to UV-B Radiation (continued)

Crop	Number of Cultivars	Growth Condition a/	Basis of Conclusion b/	Comparison c/	Reference
Spinacia oleracea	2	G.H	both sensitive	d.w.	Dumpert and Boscher (1982)
Gossypium hirsutum	2	G.H.	no difference	d.w.	Ambler et al. (1978)
Pennisetum glaucum	2	G.C.	no difference	d.w.	Biggs and Kossuth (1978)
Cucurbita pepo	3	G.C.	no difference	d.w.	Biggs and Kossuth (1978)

a/ G.H. = greenhouse; G.C. = growth chamber; F = field

b/ If data presented, sensitive means UV-B radiation reduced d.w. (see footnote c) by at least 10% over control plants. Tolerant indicates that UV-B resulted in less than 10% reduction in growth. In some cases, growth of tolerant plants was even stimulated by UV-B radiation.

c/ d.w. = total plant dry weight; p.s. = net photosynthesis.

completely attenuate the damaging effects of UV radiation. Some studies suggest that despite large increases in flavonoid concentration, metabolic processes, such as photosynthesis, are still affected (Sisson 1981, Teramura et al. 1984, Mirecki and Teramura 1984). Also, total leaf flavonoid concentrations alone do not account for the range of responses observed in species sensitivity. For example, total leaf flavonoid levels found in UV-B irradiated soybeans were less than those found in cucumber, yet cucumber is much more sensitive to UV radiation (Murali and Teramura 1986a,c). Therefore, species sensitivity to UV-B radiation is probably the product of a number of UV-protective mechanisms acting in concert within the plant. We currently need more specific information concerning plant adaptations to UV-B radiation before we can further refine our estimates of the ability of natural plant protective mechanisms to compensate for the projected increases in solar UV-B radiation.

ISSUES ASSOCIATED WITH THE EXTRAPOLATION OF DATA FROM CONTROLLED ENVIRONMENTS TO THE FIELD

Plant responses in growth chambers or greenhouses may neither quantitatively nor qualitatively resemble responses that would occur in the field because the conditions found in controlled environments are unlike those found in nature. Plants grown in growth chambers are more sensitive to a given UV dose than are field-grown plants (Caldwell 1981, Bennett 1981, Teramura 1982, Mirecki and Teramura 1984), because in artificial environments a single factor is generally manipulated, while all other factors are kept constant or are optimized for growth. Plants outdoors commonly experience simultaneous, multiple stresses, including water or nutrient limitation. In addition to these differences in physical factors, artificial environments lack biotic factors such as the interactions between other plants, insects, diseases, etc.

However, enormous complexities are inherent in field studies. Daily changes in the environment are superimposed upon longer-scale seasonal and annual changes. Both temporal and spatial variability often result in inconsistencies in plant responses between one year and the next (for examples see Biggs et al. 1984; Gold and Caldwell 1983; Teramura 1981b; Lydon, Teramura, and Summers 1986).

Therefore, one useful approach in understanding the effects of UV-B radiation on plants under more realistic conditions has been the study of the interactions between UV radiation and other commonly experienced, plant stresses. These studies revealed that exposure to enhanced levels of UV radiation may affect the susceptibility of some plants to water stress, and alter the sensitivity to UV radiation by inducing flavonoid biosynthesis (Teramura, Tevini, and Iwanzik 1983; Tevini, Thoma, and Iwanzik 1983; Teramura et al. 1984a; Teramura, Forseth, and Lydon 1984). The results of field experiments (Murali and Teramura 1986c) revealed no additional deleterious effects of UV-B radiation when radiation was combined with water stress. It was hypothesized that changes in leaf anatomy, increased flavonoid production, and reduced growth induced by water stress masked the UV effects.

Plant productivity (accumulation of dry matter) became more sensitive to UV-B radiation as total mineral supply decreased (Bogenrieder and Doute 1982). Murali and Teramura (1985a,b) found that plant sensitivity to UV-B radiation

decreased as the phosphorus level decreased. This suggests that the greatest impact of UV-B enhancement might appear in well-fertilized (agricultural) regions, rather than in areas of low fertility.

In most growth chambers, visible irradiances range from 10% to 40% of average midday irradiances. This is a cause for concern, since many of the deleterious effects of UV radiation may be ameliorated if plants are exposed to UV radiation in the longer wavelength range. Therefore, growth chamber experiments could overestimate the impact that UV radiation would have in the field. Despite the wide range of plant species and growth conditions, a clear trend emerges: plants grown in higher levels of visible radiation are less sensitive to UV-B radiation. A corollary to this conclusion is that plant sensitivity to UV-B radiation is strongly influenced by the level of visible radiation available during growth and development, and that shaded environments maximize this sensitivity.

Lydon, Teramura, and Summers (1986) and Teramura and Murali (1986) have specifically examined the differences in UV-B radiation response between field- and greenhouse-grown soybean. Six soybean cultivars were grown in an unshaded greenhouse and in the field under a similar UV enhancement regime. Cultivar sensitivity was ranked according to a combined plant response, which included changes in total plant dry weight, in leaf area, and in plant height. The relative ranking for UV-B sensitivity in the greenhouse was quite similar to that found in the field. The major difference was that UV-B radiation produced a substantially larger (2- to 10-fold) effect on greenhouse plants compared with field-grown plants. Also, in specific instances, different conclusions could be drawn from the individual data sets. For example, according to greenhouse data, the James cultivar was sensitive, and the York, cultivar resistant, to UV-B. In the field, however, these cultivars demonstrated the opposite response. Therefore, if controlled environment-to-field extrapolations are necessary, they must be done with the utmost caution. At best, general trends may be implied, but specific or quantitative extrapolations do not yet seem feasible.

Despite a great range of experimental growth conditions and UV doses, most cultivars show large individual variation in response to UV-B radiation (Exhibit 11-1). Therefore, the potential for ameliorating the impacts of projected increases in solar UV radiation may be present in our current crop germ plasm by selecting for UV tolerance. However, we have little understanding of the mechanisms responsible for these cultivar differences and the relationship of genetic factors that provide UV tolerance to other desirable plant characteristics. If tolerance to UV-B radiation were linked (in a genetic sense) to some undesirable characteristics, crop breeding may not ameliorate the impacts of UV-B damage.

UNCERTAINTIES IN OUR CURRENT KNOWLEDGE OF UV-B EFFECTS ON TERRESTRIAL ECOSYSTEMS AND PLANT GROWTH FORMS

Most of our knowledge of the biological effects of increasing solar UV radiation stems from research focused upon agricultural crops. Plants from only four of ten ecosystems, representing only about 27% of global net primary productivity (NPP), have been examined (Exhibit 11-2). In temperate forests and temperate grasslands, only very limited preliminary data are available. Also, of 25 categories of major plant growth forms, the effectiveness of UV-B

EXHIBIT 11-2

Survey of UV Studies by Major Terrestrial Plant Ecosystems (after Whittaker 1975)

Ecosystem	Global NPP (10^9 ton/yr)	Total Area (10^6 km^2)	Included in [a] UV Study
Tropical forest	49.4	24.5	no
Temperate forest	14.9	12.0	yes
Savanna	13.5	15.0	no
Boreal forest	9.6	12.0	no
Agricultural	9.1	14.0	yes
Woodland and scrubland	6.0	8.5	no
Temperate grassland	5.4	9.0	yes
Swamp and marsh	4.0	2.0	no
Desert and semidesert	1.7	42.0	no
Tundra and alpine	1.1	8.0	yes

[a] Only studies examining some aspect of growth.

radiation has only been examined in eight (32%). Only very limited data exist for trees, vines, small woody shrubs, epiphytes, or lower vascular plants. Thus the experimental data base represents only 19 of the 314 plant families in the world (Cronquest 1981). Of those families tested, only seven include representative species in which harvestable yield was examined. Therefore, we have very little information from which to calculate the potential impacts of increasing levels of solar UV radiation on global terrestrial productivity of ecosystem dynamics.

Ecosystem composition and function are dependent upon the influence of numerous biotic and abiotic factors. Within populations, plants may possess mechanisms that protect them from UV-B, but the ability of higher plants to select for those mechanisms within the timeframe of expected changes in UV-B radiation is unclear as to the effect of that selection. Differential sensitivity could result in subtle shifts in species interactions such as competition. These shifts, as well as changes in abiotic factors (soil nutrients, climate, etc.), could produce significant changes in ecosystem composition.

UNCERTAINTIES WITH THE ABILITY TO EXTRAPOLATE KNOWLEDGE TO HIGHER AMBIENT CO2 ENVIRONMENT AND OTHER ATMOSPHERIC POLLUTANTS

Global atmospheric carbon dioxide (CO2) concentration has been gradually increasing from 205 ppm some 20,000 years ago to approximately 340 ppm today (Keelings 1978, Neftel et al. 1982). It is anticipated that sometime between 2075 and 2100, the atmospheric CO2 concentration will reach 600 ppm (Gates 1983).

At present we have no direct experimental evidence on the effects of UV-B radiation under increased levels of atmospheric CO2. However, in general, it is believed that increased CO2 increases photosynthesis and water use efficiency in most plants (both of which are reduced by UV-B radiation), especially in C3 plants. Exhibit 11-3 summarizes some of that research.

Recently, however, some confounding evidence has been found for perennials, in which high levels of CO2 led to a decrease in biomass production (Fried 1986). Furthermore, most CO2 work has been done in growth chambers, in which conditions differ from those that would occur in the field. The net effect of an interaction between UV-B radiation and increased levels of CO2 cannot, at this time, be predicted. Whether the deleterious effects of UV-B will be proportionally higher or lower in a higher CO2 world is uncertain. Similarly, the combined impacts of higher CO2 and UV-B on inter- and intraspecific competitive balance is impossible to ascertain. Other changes in the environment, such as those due to global warming and climatic changes, may also play important roles in determining effects, but cannot be assessed.

Further uncertainty stems from the absence of knowledge on the interactions between increased UV-B levels and that of other pollutants in the lower atmosphere. Primarily anthropogenic in origin, the major pollutants include ozone, sulfur oxides, and nitrogen oxides. According to the National

EXHIBIT 11-3

Summary of UV-B and CO2 Effects on Plants (Lemon 1983; Teramura 1983)

Plant Characteristic	Enhanced UV-B	Doubling of CO2
Photosynthesis	Decreases in many C3 and C4 plants	In C3 plants increases up to 100% but in C4 plant only a small increase
Leaf conductance	No effect in many plants	Decreases both in C3 and C4 plants
Water use efficiency	Decreases in most plants	Increases in both C3 and C4 plants
Dry matter production and yield	Decreases in many plants	In C3 plants almost doubles but in C4 plants only a small increase
Leaf area	Decreases in many plants	Increases more in C3 than in C4 plants
Specific leaf weight	Increases in many plants	Increases
Crop maturity	No effect	Accelerated
Flowering	May inhibit or stimulate flowering in some plants	Flowers produced earlier
Interspecific differences	Species may vary in degree of response	Major differences occur between C3 and C4 plants
Intraspecific differences	Response varies among cultivars	Response may vary among cultivars
Drought stress	Plants become less sensitive to UV-B but not tolerant to drought	Plants become more drought tolerant

Crop Loss Assessment Network, farm crop losses in the United States in 1981 due to air pollution amounted to between $1 billion and $2 billion. Many studies have demonstrated that, in combination, the deleterious effects of air pollutants were additive and, in a few cases, multiplicative (Reinert, Heagle, and Heck 1975).

RISKS TO CROP YIELD RESULTING FROM AN INCREASE IN SOLAR UV-B RADIATION

During the past 10 years, only nine field studies have examined the effects of UV-B radiation on crop yield (Exhibits 11-4 and 11-5). These nine studies included 22 crop species. Corn (Zea mays) was included in six of the nine studies, soybean (Glycine max) in four, and tomato (Lycopersicon esculentum), bean (Phaseolus vulgaris), and potato (Solanum tuberosum) each were found in three of the studies. In about half of these species, UV-B reduced yield.

Ambler, Rowland, and Maher (1978) grew eight species of crops in a field in Beltsville, Maryland (30°N). Plants were grown under a lamp irradiation system maintained 1.6 m above them in a linear arrangement of unfiltered Westinghouse BZS-CLG and FS-40 sunlamps. A two-dimensional gradient was established: one parallel to the lamps and another at right angles. Only broccoli showed a significant UV effect, although the authors suggested that sorghum and corn also were affected. The use of unfiltered lamps, which emit both UV-B and UV-C, make interpretation of the results difficult, since UV-C radiation produces qualitatively and quantitatively different effects from UV-B (Nachtway 1975).

Bartholic, Halsey, and Garrard (1975) conducted field exclusion studies in Gainesville, Florida (29° 36'N), in which ambient UV-B was filtered through plastic films of Mylar Type S or polyethylene. Since plants were grown under panels covered with these films, only the direct beam component of ambient UV was removed (approximately one-half the total ambient UV present). Compared with uncovered plots, total yield decreased in beans and corn growing under both Mylar and polyethylene. Tomato matured significantly earlier under Mylar, resulting in an apparent decrease in fruit weight in plants growing in uncovered plots. There may have been a shading problem associated with the panel framework, or a difference may have been maintained in leaf temperatures or soil moisture as a direct result of the exclosures themselves.

Becwar, Moore, and Burke (1982) also conducted an exclusion study located at 3000 m in the Colorado Rocky Mountains (39° 11'N). Mylar, Aclar, and cellulose acetate filters were used. The only UV effect reported was a decrease in wheat height (between 8% and 19% depending upon plant age), with no corresponding change in total plant dry weight. A second study was conducted using filtered FS-40 sunlamps to supplement ambient levels of solar UV-B. No significant effect on crop yield was produced despite a calculated 52% UV enhancement compared with sea level irradiance, simulating the dose plants received at sea level as control to make actual comparisons.

Biggs and Kossuth (1978) reported yields for seven crops grown in beds filled with a synthetic soil mix in Gainesville, Florida (29° 36'). UV-B

EXHIBIT 11-4

Summary of Field Studies Examining the Effects of UV-B Radiation on Crop Yields
(Values represent percent changes from controls)

	Ambler et al. (1978) (a)	Bartholic et al. (1975) (b)	Becwar et al. (1982) (c)	Biggs and Kossuth (1978) (d)	Biggs et al. (1984) (d)	Eisenstark et al. (1985) (d)	Esser (1980) (e)	Hart et al. (1975) (a)
Cucurbita maxima	0							
Cucurbita pepo				-14 to -90				
Phaseolus vulgaris	0	+12 to +15					+53 to -75	
Triticum aestivum					-5			
Zea mays	0	+29 to +39		0	0	-79 to -87		0
Spinacia oleracea							+11 to -56	
Sorghum bicolor	0							
Capsicum annum								-(?)
Glycine max	0							0
Cynodon dactylon								
Beta vulgaris	0							
Brassica oleracea var. capitata							+19 to -49	
Brassica oleracea var. botrytis	-24 to -45%							
Lycopersicon esculentum		-5 to -26		-11 to -39				0
Nicotiana tobaccum								0
Raphanus sativus			0					
Pennisetum glaucum								0
Solanum tuberosum			0	0			-2 to -41	
Brassica juncea				-9 to -43				
Vigna unguiculata				-18 to -38				
Oryza sativa					0			
Arachis hypogaea				0				0

(a) Unfiltered Westinghouse BZS-CLG and FS-40 sunlamps

(b) Ambient UV filtered with Mylar Type S or poleyethylene

(c) Ambient UV filtered with cellulose acetate, Aclar, or Mylar

(d) Westinghouse FS-40 sunlamps filtered with cellulose acetate or Mylar

(e) Unfiltered Philips TL 40/12 sunlamps and lamps filtered with Schott WG 305 (2 and 3 mm) filters

EXHIBIT 11-5

Details of Field Study by Teramura (1981-1985) a/

	SIMULATED OZONE CHANGE (percent)									
	1981		1982		1983 c/		1984 c/		1985	
CULTIVAR b/	-16	-25	-16	-25	-16	-25	-16	-25	-16	-25
Bay	-10	NE d/	+6	-8						
Essex	-25 e/	NE	-12	-23	+39 e/	+6 e/	+14 e/	-7	+6	-20 e/
James	-14 e/	NE	-22	-25						
Williams	+22 e/	NE	+9	+14	+13 e/	-11 e/	+15 e/	+10 e/	+18 e/	+4 e/
York	-12	NE	-25 e/	-8						
Forrest	NE	NE	-14	+27						

a/ Values reported are percent changes in seed yields for given simulated ozone changes (-16% and -25%) compared to controls (yields measured on a dry weight basis). Irradiance by either Mylar (control) or cellulose acetate (UV-B supplemented) filtered FS-40.

b/ After initially screening 23 cultivars (16 of which were sensitive to UV-B; -10% yield reduction) in the greenhouse, these six were chosen for field experimentation. The six represent the full range of UV sensitivity found in the greenhouse, including very sensitive and very tolerant cultivars. Beginning in 1983 only Essex (very sensitive) and Williams (very tolerant) were planted in the field to increase the experimental sample size to 200. As shown in the table, yields for Essex were generally reduced at the higher UV level (ozone change of -25%) but were mixed (relative to controls) at the other UV level. Yields for Williams were generally enhanced by increased UV. Of note is that Essex is currently replacing other older cultivars (including Williams) and is becoming one of the most widely planted soybeans in the U.S. In a UV-enhanced environment, Essex will be deleteriously affected. Therefore, superior cultivars being developed today by crop breeders may not be suitable for the future should the UV environment change.

c/ Drought year. Low yields for both controls and experimental (i.e., dosed) plants.

d/ NE = Not evaluated.

e/ Significantly different at p = 0.05 level.

radiation was supplemented with a linear arrangement of six FS-40 sunlamps at a 12° angle from horizontal, producing a gradient in UV-B irradiances. Control plants were grown without lamps above them and were adjacent to those receiving the highest UV dose. Although some "significant" UV effects were reported, no indication of statistical tests nor descriptive statistics were given. The greatest reductions in yield were often found in plants receiving the lowest UV irradiance, and the largest UV effects were found in plants growing adjacent to ones showing little or no effect. Although each plant along the gradient received a uniquely different UV dose, plants and treatments were pooled for analysis. These manipulations undoubtedly added a great deal of experimental variability and resulted in interpretation difficulty.

In another field experiment, Biggs et al. (1984) conducted a two-year evaluation of crop yield in rice, wheat, corn, and soybean. Plants were again grown in beds filled with synthetic soils, but UV irradiation was supplied by FS-40 sunlamps filtered with either Mylar or 3-, 5-, or 10-ml cellulose acetate providing 0, 32%, 23% or 16% UV enhancements. The only significant yield reduction reported was for wheat (5% reduction) and only for one of the two experimental years. The data for rice, corn, and soybean were highly variable, and therefore no statistical differences could be detected.

Eisenstark et al. (1985) grew corn in large pots for three growing seasons in Columbia, Missouri (38° 57'N). Two levels of UV radiation were supplied by cellulose acetate-filtered FS-40 sunlamps simulating a 7% and 21% ozone depletion. Controls included lamps filtered with Mylar and no overhead lamps. Plants were found to be particularly susceptible to UV-induced effects during tassel development (Eisenstark and Perrot 1985). Plants irradiated as seedlings produced total grain yield reductions of 23% and 32%, respectively, when compared with Mylar control plants. Even larger differences were found when these plants were compared with those grown without overhead lamps; yield was reduced by 80% in plants filtered by Mylar and 87% in those grown under cellulose acetate. The authors suggested that this large lamp effect could be due to additional UV-A emitted from the sunlamps, but this UV-A supplement was very small relative to UV-A present in midday solar radiation (Caldwell et al. 1986). The implications of this study for field crops (as opposed to potted plants) is doubtful, however, since the pots allowed root structures to reach higher temperatures than they would in fields.

Esser (1980) conducted field studies in Frankfurt, Federal Republic of Germany (50°N), on bean, cabbage, spinach, and potato. He used linearly arranged Philips TL 40/12 sunlamps suspended 3 m above the plants and produced four UV enhancements using a combination of reflectors, Schott WG305 filters, and unfiltered lamps. Significant yield reductions were found only under unfiltered lamps in the four crops tested. Yields for spinach, cabbage, and bean increased under filtered lamps.

Hart et al. (1975) grew plants under linearly arranged unfiltered FS-40 sunlamps in Beltsville, Maryland (39°N). The absence of experimental data and details on this study limit its usefulness. Also, the presence of UV-C radiation from these unfiltered lamps greatly decreases the validity of these data.

Teramura has grown soybeans for five seasons in Beltsville, Maryland (39°N) (Exhibit 11-5). During the first two years, six soybean cultivars were grown and two cultivars were grown in subsequent years under filtered FS-40 sunlamps oriented perpendicularly to the soybean rows. This arrangement avoids the large variation in UV irradiance along the length of the bulb, which is a major problem with linearly arranged (end-to-end) lamps. Control plants were grown under Mylar-filtered lamps. Field experiments simulated 0, 16%, and 25% ozone depletions. Seed yield was consistently reduced at a simulated 25% ozone depletion in cultivar Essex. Yield reductions of up to 20% were reported in three of the five years. The "UV-tolerant" cultivar Williams was less affected but did show an 11% reduction in yield in 1983. Also in 1983, a substantially higher relative yield (6% increase) was found in cultivar Essex, which was opposite to that observed in the previous two years. One critical caveat that must be included with this observation is that 1983 was an extremely dry year. Actual seed weights of control plants during 1983 were only 20%-30% of those harvested in 1981 and 1982. Therefore, it is questionable whether these 1983 data are representative of true (normal) field trends. This graphically illustrates the importance of multi-year studies and emphasizes the need to monitor other environmental variables in addition to UV radiation. If the results on Essex in drought years was repeated, it would indicate that higher UV radiation actually helped plants in severe drought years, reducing the crop loss by a few percent.

Rowe and Adams (1987) reviewed the information developed by Teramura to determine the done-response relationship between UV-B radiation levels and soybean yield. To calculate a representative relationship from the Teramura data, Rowe and Adams limited the data only to those points reported by Teramura as statistically significant at the 0.05 level. This restriction led to the exclusion of data from the "drought" years. With this approach they estimated a yield decline of approximately 0.3 percent for each one percent decrease in stratospheric ozone.

Soybean yield is influenced by other microclimatic factors as well as total UV-B dose. Yield appears to be strongly influenced by the number of days of precipitation and the number of days during which the maximum temperature exceeds 35°C. In general, yield decreases as the number of hot days increases and increases as the number of days with precipitation approaches 25 in the growing season. However, further increases in the number of days with precipitation decreases yield. The relative importance of UV-B dose is a function of the cultivar and other prevailing microclimatic factors. For example, in Essex, total seed yield can be predicted, within 95% confidence intervals, by including total UV-B doses, number of precipitation events, and the number of days where air temperature exceeds 35°C in a regression model.

Despite the broad range of experimental protocols and dosimetry used by various investigators, it appears that increases in solar UV radiation could potentially have a deleterious impact upon global crop yields. Even discounting the data from the three unfiltered lamp studies (Ambler, Rowland, and Maher 1978, Esser 1980, Hart et al. 1975), there are still more instances of significant reductions in yield than reports of no effect. While uncertainty exists, all of these studies were imperfect validations, suffering from one problem or another in experimental design or dosimetry, and only three studies (Biggs et al. 1984, Eisenstark et al. 1984, Teramura 1981-1985)

include multi-year observations in which longer-scale environmental variability has been taken into consideration and only mid-latitude regions have been analyzed. It is reasonably likely that increases in solar UV will decrease global crop yields.

RISKS TO YIELD DUE TO A DECREASE IN QUALITY

Biggs and Kossuth (1978) reported that the number of abnormally shaped tomato fruit decreased between 11% and 41% under enhanced levels of UV-B radiation in the field. They also reported a 6%-23% reduction in the number of culls (rots, cracks, sunscald, etc.) in plants receiving a moderate UV-B dose, while those receiving a low dose produced a 10%-34% increase in culls. Mean potato weight of grade A large potatoes showed an increase of between 3% and 13% under enhanced levels of UV-B radiation, but no other grade of potatoes increased in weight. In neither case was a clear, linear relationship between UV dose and plant response demonstrated.

In a field study conducted in Beltsville, Maryland, Ambler, Rowland, and Maher (1978) reported that the sugar content in sugar beets significantly increased between 17% and 21% with increasing UV-B irradiance. However, the authors observed these significant increases only in plants located directly under the lamp irradiation system and not in plants that received a comparable UV-B dose at some distance away from the light source. Possibly some other uncontrolled factor (perhaps shading) was inadvertently introduced into the experiment.

Teramura (1982-1985) examined the effects of UV-B radiation on seed protein and lipid concentrations of soybean grown in the field at Beltsville, Maryland (Exhibit 11-6). Overall, the effects of UV radiation were relatively small, but some were nonetheless significant. Seed protein concentrations in cultivar Essex declined under elevated levels of UV-B radiation in two of the four years (up to a 5% reduction. Seed lipid concentrations in cultivar Forrest were reduced by 3%-5% in 1982, the only year in which this characteristic was measured in Forrest. Williams showed a slight reduction in seed lipid content, with a maximum reduction of 10% reported in 1984.

The extent of UV-mediated alterations in yield quality cannot presently be estimated with any degree of confidence due to the paucity of experimental data at hand. Furthermore, conclusions drawn from a single growing season may be unreliable because of the annual variation in responses reported. Nonetheless, the consistent reductions in yield quality in soybean suggest that the risk in some crops may be quite high.

RISKS TO YIELD DUE TO POSSIBLE INCREASES IN DISEASE OR PEST ATTACK

Esser (1980) reported a significant decrease in the number of aphids per plant but no significant difference in the spidermite population with increased UV-B radiation. Although the results suggest that UV-B radiation can have potentially beneficial effects on pest control, these conclusions must be judged with caution since the observation period was less than two weeks.

EXHIBIT 11-6

Summary of Changes in Yield Quality in Soybean

Between the 1982 and 1985 Growing Seasons

(Teramura 1982-1985)

Crop	Yield Character	1982 % Change	Signifi-cance%	1983 Change	Signifi-cance%	1984 Change	Signifi-cance%	1985 Change	Signifi-cance
Glycine max									
cv Bay	% protein	0 to -5	ns*						
	% lipid	-1.4 to +3	ns						
Essex	% protein	-3 to -5	P=0.05	+1 to -5	P=0.05	+1 to 0	ns	-0.7 to 0	ns
	% lipid	-2 to +.5	ns	+2 to -2	ns	-2 to 0	ns	0	ns
James	% protein	+.2 to +3	ns						
	% lipid	-1 to -2	ns						
Williams	% protein	0 to -.2	ns	+.4 to -.2	ns	+3 to +5	P=0.05	0.5 to -1	P=0.05
	% lipid	+5 to +8	P=0.05	-1 to +6	ns	-5 to -10	P=0.05	0	ns
Forrest	% protein	+.5 to +2	ns						
	% lipid	-3 to -5	P=0.05						
York	% protein	-2 to -3	ns						
	% lipid	0 to +3	ns						

* ns= Not significant.

Growth chamber and *in vitro* studies of fungal pathogens showed that hyaline spores are more sensitive to UV-B radiation than pigmented spores (Carns, Grahm, and Ravitz 1978). Owens and Krizek (1980), however, found that survival of a pigmented spore (*Cladosporium cucumerinum*) decreased with UV-B radiation due to a delay in germ tube emergence. Other studies (Esser 1980, Biggs et al. 1984) indicate that there is no clear relationship between spore coloration and UV-B radiation.

Three leaf fungal pathogens showed a significant decrease in disease severity with UV-B radiation in a growth chamber study (Esser 1980), whereas a field study by Biggs et al. (1984) showed no significant difference in disease severity on leaves and seeds under increased UV-B radiation. Biggs et al. (1984) and Biggs (1985) found that in a leaf rust-sensitive cultivar of wheat, disease severity increased with UV-B radiation. In a rust-resistant cultivar, however, there were no differences in disease severity.

Semeniuk and Goth (1980) found significant UV-B mediated reductions in potato virus infection on *Chenopodium quinoa*. At irradiances over 86 m^{-2} $UV\text{-}B_{BE}$, no infection occurred. In this study, virus extract was exposed to UV-B radiation immediately upon its application over the leaf surface. Intuitively, viruses should be highly susceptible to UV-B radiation, since they consist of nucleic acids encased in proteins, both of which have high UV absorption properties. However, virus sensitivity must be viewed in light of screening offered by the host tissues.

One of the plant defense mechanisms that inhibits final development is the production of a class of chemicals known as phytoalexins (Bell 1981). Phytoalexin production in plants can be induced artificially through mechanical injury, high temperature, application of fungicides and antibiotics, and by UV radiation (Bridge and Klarman 1973, Reilly 1975). UV-B radiation can induce isoflavonoid phytoalexin synthesis (Bakker et al. 1983), but excess production can be toxic due to free radical formation (Beggs et al. 1984).

At present, it is difficult to forecast the consequences of enhanced UV-B radiation in terms of pest and disease damage. From the limited information available, it appears that in some cases, UV-B radiation might decrease disease severity, while in others it might aggravate disease. The effects vary with pathogen, plant species, and cultivar. Further studies are obviously needed to develop a better understanding of the consequences of increased levels of UV-B radiation on pests and plant diseases.

RISKS TO YIELD DUE TO COMPETITION WITH OTHER PLANTS

Many plants have been shown to exhibit a wide range of sensitivity to enhanced UV-B radiation (Teramura 1983), which could lead to changes in competitive ability within plant communities through differential UV-B resistance (Caldwell 1977). Solar UV exclusion studies (cited in Gold and Caldwell 1983) using natural competing species show large differences in response to present levels of UV radiation. This suggests that current levels of UV radiation may be partly responsible for interspecific competition among various native plant species.

Gold and Caldwell (1983) studied intraspecific competition in wheat (Triticum aestivum L.), wild oats (Avena fatua L.), and goat grass (Aegilops cylindrica Host) at various planting densities in Logan, Utah, under ambient and UV-B levels simulating a 16% ozone reduction. No significant differences in shoot biomass production were observed. Therefore, enhanced levels of UV-B radiation may be of little consequence in terms of intraspecific plant competition. Preliminary results (Caldwell, personal communication; 1985, unpublished manuscript), however, indicate that interspecific competition may be affected. UV-B radiation appeared to alter growth by the inhibition of internode elongation in wild oat, but not in wheat, thus favoring wheat in competition for available light.

Fox and Caldwell (1978) and Gold and Caldwell (1983) examined the effects of UV-B radiation on the competitive interaction of field-grown competing pairs from three plant associations: agricultural crops and associated weeds, montane forage crops, and disturbed weedy associates. To measure competitive ability, relative crowding coefficients (RCCs) were used. RCCs based upon total above-ground biomass indicate that there were significant shifts in the competitive balance of some agricultural crop and weed associations. For example, pigweed (Amaranthus) was more competitive under ambient UV conditions, and alfalfa (Medicago) exhibited the competitive advantage under enhanced UV-B radiation. Under a 40% ozone reduction, wheat (Triticum) had a competitive advantage over wild oats (Avena) and goat grass (Aegilops), but no significant differences were observed with a 16% reduction. In the previous year, the competitive balance was found to be in favor of Avena. It was suggested that this difference was due to a late planting which resulted in large water and temperature stresses during seedling development (Gold and Caldwell 1983). Similarly, the weedy Geum had the competitive advantage over Poa grass under ambient conditions, but the balance was shifted under enhanced UV-B radiation. Preliminary field data suggest that the competitive ability of wheat, based on seed biomass, increased relative to wild oats under enhanced UV-B radiation.

These results demonstrate that enhanced levels of UV-B radiation can alter the competitive interactions of some species. Total harvestable yield, as well as its quality, is altered by the presence of weeds (Bell and Nalewaja 1968, McWhorter and Patterson 1980). Because there are a large number of weeds typically associated with various crop plants, increasing levels of UV-B radiation could potentially have serious consequences if weeds gain a competitive advantage over crops. Even very subtle differences in sensitivity could result in large changes in species composition over time and possibly affect ecosystem function. At this time, however, it is impossible to determine the extent of the risk.

RISK TO YIELD DUE TO CHANGES IN POLLINATION AND FLOWERING

In plants in which pollination and subsequent fertilization take place during the day with flowers fully open, reproductive tissues would seemingly receive an appreciable UV-B dose. However, ovules enclosed in the ovary are well-protected against UV-B radiation. Flint and Caldwell (1983) have shown that the anther wall filters out over 98% of the incident UV-B radiation in six plant species. Therefore, before another dehiscence, pollen is also well protected.

Southworth (1969) found UV-absorbing compounds with a maximum absorbance in the UV-B range in the wall of pollen. Additional studies on the UV absorption profiles of stigmatic surfaces and exudates of many species show one or more peaks in the UV-B region (Martin 1970, Martin and Brewbaker 1971). Therefore, under natural conditions, the effectiveness of UV-B may be minimal because of UV-absorbing pigments in the anther and pollen walls and in stigmatic surface exudate.

Results of numerous studies that were conducted during the early part of this century on the effects of solar UV radiation through window glass filters indicated an inhibition of flowering (see reviews by Popp and Brown 1936 and Caldwell 1971). However, these experiments were generally executed with insufficient sample sizes and failed to isolate UV irradiation as the single contributing factor causing the difference in flowering. For instance, Caldwell (1968) has shown that leaf temperatures increase sufficiently under window glass to alter the induction of flowering (see Zeevaart 1976 for a discussion of the physiology of flowering).

Results of the Kasperbauer and Loomis (1965) study of Melilotus and Caldwell's (1968) study of Trifolium dasyphyllum show an increase in flowering with the exclusion of solar UV radiation. A growth chamber study by Klein, Edsall, and Gentile (1965) which incorporated primarily UV-A radiation, also shows an increase in the number of flowers produced in marigold by the exclusion of UV radiation. Similarly, greenhouse trials on beans and peas also show an inhibition of flowering and decrease in flower number due to UV-B radiation (Biggs and Basiouny 1975). However, field studies in which unfiltered sunlamps (which emit both UV-B and UV-C) were used produced no significant effects on the flowers of marigold and tomato plants, nor on their number or the date on which flowering occurred; neither were significant effects produced in maize tasseling or in sorghum heading (Hart et al. 1975). Biggs and Kossuth (1978), on the other hand, found an increase in flower number but a decrease in the flowering duration in potatoes, and a decrease in flower number in tomatoes at peak flowering in UV-B irradiated plants. Apparently, some changes in flowering suggest a correlation with UV-B radiation, but whether such changes would lead to an appreciable effect in harvestable yield has not been fully investigated.

REFERENCES

Ambler, J.E., R.A. Rowland, and N.K. Maher, 1978. Response of selected vegetable and agronomic crops to increased UV-B irradiation under field conditions. UV-B Biological and Climatic Effects Research (BACER), Final Report EPA-IAG-D6-0168, EPA, Washington, D.C.

Bakker, J., F.J. Grommers, L. Smits, A. Fuchs, and F.W. de Vries, 1983. Photoactvation of isoflavonoid phytoalexins: Involvement of free radicals. Photochem. Photobiol. 38:323-329.

Bartholic, J.F., L.H. Halsey, and L.A. Garrard, 1975. Field trials with filters to test for effects of UV radiation on agricultural productivity. In Climatic Impact Assessment Program (CIAP), Monograph 5 (Nachtwey, D.S., M.M. Caldwell, and R.H. Biggs, eds.), pp. 61-71. U.S. Department of Transportation, Report No. DOT-TST-75-55, National Tech. Infor. Serv., Springfield, Virginia.

Becwar, M.R., F.D. Moore III, and M.J. Burke, 1982. Effects of deletion and enhancement of ultraviolet-B (280-315 nm) radiation on plants grown at 3000 m elevation. J. Amer. Soc. Hort. Sci. 107:771-779.

Beggs, C.J., U. Schneider-Ziebert, and E. Wellmann, 1986. UV-B radiation and adaptive mechanisms in plants. In Stratospheric Ozone Reduction, Solar Ultraviolet Radiation and Plant Life (Worrest, R.C., ed.), Springer-Verlag. ISBN 13875-7.

Bell, A.A., 1981. Biochemical mechanisms of disease resistance. Ann. Rev. Plant Physiol. 32:21-81.

Bell, A.R., and J.D. Nalewaja, 1968. Competition of wild oats in wheat and barley. Weed Sci. 16:505-508.

Bennett, J.H., 1981. Photosynthesis and gas diffusion in leaves of selected crop plants exposed to ultraviolet-B radiation. J. Environ. Qual. 10:271-275.

Biggs, R.H., and F.M. Basiouny, 1975. Plant growth responses to elevated UV-B irradiation under growth chamber, greenhouse, and solarium conditions. In Impacts of Climatic Change on the Biosphere, CIAP Monograph 5 (Nachtway, D.S., M.M. Caldwell, and R.H. Biggs, eds.), pp. 4-197-4-248. U.S. Department of Transportation, Report No. DOT-TST-75-55, National Tech. Info. Serv., Springfield, Virginia.

Biggs, R.H., and S.V. Kossuth, 1978. Effects of ultraviolet-B radiation enhancement under field conditions on potatoes, tomatoes, corn, rice, southern peas, peanuts, squash, mustard and radish. UV-B Biological and Climatic Effects Research (BACER), Final Report, EPA, Washington, D.C.

Biggs, R.H., S.V. Kossuth, and A.H. Teramura, 1981. Response of 19 cultivars of soybeans to ultraviolet-B irradiance. Physiol. Plant. 53:19-26.

Biggs, R.H., P.G. Webb, L.A. Garrard, T.R. Sinclair, and S.H. West, 1984. The effects of enhanced ultraviolet-B on rice, wheat, corn, soybean, citrus, and duckweed. U. S. Evironmental Protection Agency Year 3 Interim Report No. 808075-03, EPA, Washington, D.C.

Bogenrieder, A., and Y. Doute, 1982. The effects of UV on photosynthesis and growth in dependence of mineral nutrition (Lactuca sativa L. and Rumex alpinus L.). In Biological Effects of UV-B Radiation (Bauer, H., M.M. Caldwell, M. Tevini, and R.C. Worrest, eds.), Gesellschaft fur Strahlen-und Umweltforschung mbH Muchen, pp. 164-169.

Bogenrieder, A., and R. Klein, 1978. Die abhangigkeit der UV-empfindlichkeit von der lichtqualitat bel der aufzucht (Lactuca sativa L.). Angew. Botanik 52:283-293.

Bridge, M.A., and W.L. Klarman, 1973. Soybean phytoalexin hydroxyphaseollin, induced by ultraviolet irradiation. Phytopathol. 63:606-608.

Caldwell, M.M., 1968. Solar ultraviolet radiation as an ecological factor for alpine plants. Ecol. Monogr. 38:243-268.

Caldwell, M.M., 1971. Solar UV irradiation and the growth and development of higher plants. Photophysiol. VI (Giese, A.C., ed.), pp. 131-177. Academic Press, New York.

Caldwell, M.M., 1977. The effects of solar UV-B (280-315 nm) on higher plants: Implications of stratospheric ozone reduction. In Research in Photobiology (Castellani, A., ed.), pp. 597-607. Plenum Publ. Corp., New York.

Caldwell, M.M., 1981. Plant response to solar ultraviolet radiation. In Encyclopedia of Plant Physiology New Series, Volume 12A. Physiological Plant Ecology I (Lange, O.L., P.S. Nobel, C.B. Osmond, and H. Ziegler, eds.), pp. 169-197, Springer-Verlag, Berlin, Germany.

Caldwell, M.M., L.B. Camp, C.W. Warner, and S.D. Flint, 1986. Action spectra and their key role in assessing biological consequences of solar UV-B radiation change. In Stratospheric Ozone Reduction, Solar Ultraviolet Radiation and Plant Life (Worrest, R.C., ed.), Springer-Verlag. ISBN 13875-7.

Caldwell, M.M., W.G. Gold, G. Harris, and C.W. Ashurst, 1983. A modulated lamp system for solar UV-B (280-320 nm): Supplementation studies in the field. Photochem. Photobiol. 37:479-485.

Caldwell, M.M., R. Robberecht, and S.D. Flint, 1983. Internal filters: Prospects for UV-allimation in higher plants. Physiol. Plant. 58:445-450.

Carns, H.R., J.H. Grahm, and S.J. Ravitz, 1978. Effects of UV-B radiation on selected leaf pathogenic fungi and on disease severity. EPA-IAG-D6-0168. BACER Program, EPA, Washington, D.C.

Cronquist, A., 1981. An integrated system of classification of flowering plants. Columbia University Press, New York, p. 1262.

Dumpert, K., and J. Boscher, 1982. Response of different crop and vegetable cultivars to UV-B irradiance: Preliminary results. In Biological Effects of UV-B Radiation (Bauer, H., M.M. Caldwell, M. Tevini, and R.C. Worrest, eds.), pp. 102-107. Gesellschaft fur Strahlen-und Umweltforschung mbH, Muchen. ISBN 0721-1694.

Eisenstark, A., and G.H. Perrot 1985. Enhanced UV-B irradiation (290-320 nm) of corn (Zea mays L.), II. Effects of various stages of tassel formation (greenhouse-plants), unpublished manuscript.

Eisenstark, A., G.H. Perrot, G. Ulmer, and C.D. Miles, 1985. Enhanced UV-B irradiation (290-320 nm) of corn (Zea mays L.), I. Effects on growth and yield, unpublished manuscript.

Esser, G., 1980. Einfluss einer nach schadstoffimission vermehrten einstrahlung von UV-B-licht auf kulturpflanzen, 2. Versuchsjahr. Bericht Battelle Institut, E.V. Frankfurt. BF-R-63, 984-I.

Flint, S.D., and M.M. Caldwell, 1983. Influence of floral optical properties on the ultraviolet radiation environment of pollen. Amer. J. Bot. 70:1416-1419.

Flint, S.D., P.W. Jordan, and M.M. Caldwell, 1985. Plant protective response to enhanced UV-B radiation under field conditions: Leaf optical properties and photosynthesis. Photochem. Photobiol. 41(1):95-99.

Fox, F.M., and M.M. Caldwell, 1978. Competitive interaction in plant populations exposed to supplementary ultraviolet-B radiation. Oecologia 36:173-190.

Fried, J.S., K.A. Surano, P.F. Daley, J.H. Shinn, and P. Anderson, 1986. Biomass production and nutrient responses of ponderosa pine to long-term elevated CO2 concentrations. North American Forest Biological Workshop. Lawrence Livermore National Laboratory, UCRL-94281, reprint.

Garrard, L.A., T.K. Van, and S.H. West, 1976. Plant response to middle ultraviolet (UV-B) radiation: Carbohydrate levels and chloroplast reactions. Soil and Crop Sci. Soc. Florida Proc. 36:184-188.

Gates, D.M., 1983. An overview. In CO2 and Plants (Lemon, E.R., ed.), pp. 7-20. Westview Press Inc., Boulder, Colorado.

Gold, W.G., and M.M. Caldwell, 1983. The effects of ultraviolet-B radiation on plant competition in terrestrial ecosystems. Physiol. Plant. 58:435-444.

Hart, R.H., G.E. Carlson, H.H. Klueter, and H.R. Carns, 1975. Response of economically valuable species to ultraviolet radiation. In Climatic Impacts Assessment Program (CIAP), Monograph 5 (Nachtway, D.S., M.M. Caldwell, and R.H. Biggs, eds.), pp. 263-275. U.S. Department of Transportation, Report No. DOT-TST-75-55, National Tech. Info. Serv., Springfield, Virginia.

Hashimoto, T., and M. Tajima, 1980. Effects of ultraviolet irradiation on growth and pigmentation in seedlings. Plant Cell Physiol. 21:1559-1571.

Howland, G.P., R.W. Hart, and M.L. Yette, 1975. Repair of DNA strand breaks after gamma-irradiation of protoplasts isolated from cultured wild carrot cells. Mutat. Res. 27:81-87.

Kasperbauer, M.J., and W.E. Loomis, 1965. Inhibition of flowering by natural daylight on an inbred strain of Mellotus. Crop Sci. 5:193-194.

Keelings, C.D., 1978. Atmospheric carbon dioxide in the 19th century. Sci. 202:1109.

Klein, R.M., P.C. Edsall, and A.C. Gentile, 1965. Effects of near ultraviolet and green radiations on plant growth. Plant Physiol. 40:903-906.

Krizek, D.T., 1978. Differential sensitivity of two cultivars of cucumber (Cucumis sativus L.) to increased UV-B irradiance: I. Dose-response studies. Final Report EPA-IAG-D6-0168, USDA/EPA BACER Prog., EPA, Washington, D.C.

Lemon, E.R., 1983. CO2 and Plants. The Response of Plants to Raising Levels of Atmospheric Carbon Dioxide. Westview Press Inc., Boulder, Colorado.

Lydon, J., A.H. Teramura, and E.G. Summers, 1986. Effects of ultraviolet-B radiation on the growth and productivity of field grown soybeans. In Stratospheric Ozone Reduction, Solar Ultraviolet Radiation and Plant Life (Worrest, R.C., ed.). Springer-Verlag.

Martin, F.W., 1970. The ultraviolet absorption profile of stigmatic extracts. New Phytol. 69:425-430.

Martin, F.W., and J.L. Brewbaker, 1971. The nature of the stigmatic exudate and its role in pollen germination. In Pollen: Development and Physiology (Heslop-Harrison, ed.), pp. 262-266, Appleton-Century-Crofts, New York.

McWhorter, C.G., and D.T. Patterson, 1980. Ecological factors affecting weed competition in soybeans. In World Soybean Res. Conference II: Proceedings (Corgin, F.T., ed.), pp. 371-392. Westview Press, Boulder, Colorado. ISBN 0-89158-158-899-X.

Mirecki, R.M., and A.H. Teramura, 1984. Effects of ultraviolet-B irradiance on soybean. V. The dependence of plant sensitivity on the photosynthetic photon flux density during and after leaf expansion. Plant Physiol. 74:475-480.

Murali, N.S., and A.H. Teramura, 1985a. Effect of UV-B irradiance on soybean. VI. Influence of phosphorus nutrition on growth and flavonoid content. Physiol. Plant. 63:413-416.

Murali, N.S., and A.H. Teramura, 1985b. Effect of UV-B irradiance on soybean. VII. Biomass and concentration and uptake of nutrient at varying P supply. J. Plant Nutrition 8(2):177-192.

Murali, N.S., and A.H. Teramura, 1986a. Intraspecific difference in Cucumis sativa L. sensitivity to ultraviolet-B radiation. Physiol. Plant. In press.

Murali, N.S., and A.H. Teramura, 1986b. Effect of supplemental ultraviolet-B radiation on the growth and physiology of field-grown soybean. Env. Exp. Bot. In press.

Murali, N.S., and A.H. Teramura, 1986c. Effectiveness of UV-B radiation on the growth and physiology of field-grown soybean modified by water stress. Photochem. Photobiol. In press.

Murali, N.S., A.H. Teramura, and S.K. Randall, 1986. A comparative study of ultraviolet-B sensitivity between two soybean cultivars. Env. Exp. Bot. In review.

Nachtway, D.S., 1975. Linking photobiological studies at 254 nm with UV-B. In Climatic Impact Assessment Program (CIAP), Monograph 5 (Nachtway, D.S., M.M. Caldwell and R.H. Biggs, eds.), pp. 3-50 to 3-84. U.S. Department of Transportation, Report No. DOT-TST-75-55, National Tech. Info. Serv., Springfield, Virginia.

National Academy of Sciences (NAS), 1979. Stratospheric ozone depletion by halocarbons: Chemistry and transport. National Academy Press, Washington, D.C.

Neftel, A., H. Oeschger, J. Schwander, B. Stauffer, and R. Zumbrunn. 1982. Ice core sample measurements give atmospheric CO2 content during the past 40,000 years. Nature 295:220-223.

Owens, O.V.H., and D.T. Krizek, 1980. Multiple effects of UV radiation (265-330 nm) on fungal spore emergence. Photochem. Photobiol. 32:41-49.

Popp, H.W., and F. Brown, 1936. The effects of ultra-violet radiation upon seed plants. In Biological Effects of Radiation (Duggar, B.M., ed.), Vol. 2, pp. 853-887, McGraw-Hill, New York.

Reilly, J.J., 1975. The role of thymine dimers in the induction of phytoalexin, hydroxyphaseollin, in ultraviolet irradiated soybean suspension culture. Ph.D. Thesis, University of Maryland, College Park, Maryland.

Reinert, R.A., A.S. Heagle, and W.W. Heck, 1975. Plant responses to pollutant combination. In Response of Plants to Air Pollution (Mudd, J.B., and T.T. Kozlowski, eds.), pp. 159-178. Academic Press, New York. ISBN 0-12-509450-7.

Robberecht, R., and M.M. Caldwell, 1978. Leaf epidermal transmittance of ultraviolet radiation and its implication for plant sensitivity to ultraviolet-radiation induced injury. Oecologia 32:277-287.

Rowe, Robert D. and Richard Adams. Analysis of Economic Impacts of Lower Crop Yields Due to Stratospheric Ozone (Draft Report). Prepared for the U.S. Environmental Protection Agency, August 26, 1987.

Rupert, C.S., 1984. Cellular repair and assessment of UV-B radiation damage. In Stratospheric Ozone Reduction, Solar Ultraviolet Radiation and Plant Life (Worrest, R.C., ed.) Springer-Verlag. ISBN 13875-7.

Semeniuk, P., and R.W. Goth, 1980. Effect of ultraviolet irradiation on local lesion development of potato virus S on Chenopodium quinoa cv. Valdivia leaves. Env. Exp. Bot. 20:95-98.

Sisson, W.B., 1981. Photosynthesis, growth, and ultraviolet irradiance absorbance of Cucurbita pepo L. leaves exposed to ultraviolet-B radiation (280-315 nm). Plant Physiol. 67:120-124.

Sisson, W.B., and M.M. Caldwell, 1976. Photosynthesis, dark respiration, and growth of Rumex patientia L. exposed to ultraviolet irradiance (280 to 315 nanometers) simulating a reduced atmospheric ozone column. Plant Physiol. 58:563-568.

Southworth, D., 1969. Ultraviolet absorption spectra of pollen and spore walls. Grana Palynologia 9(1-3):1-15.

Soyfer, V.N., 1983. Influence of physiological conditions on DNA repair and mutagenesis in higher plants. Physiol. Plant. 58:373-380.

Steinmueller, D., and M. Tevini, 1985. Action of ultraviolet radiation (UV-B) upon cuticular waxes in some crop plants. Planta 164:557-564.

Strain, B.R, and F.A. Bazzaz, 1983. Terrestrial plant communities. In CO2 and Plants (Lemon, E.R., ed.), pp. 177-222. Westview Press Inc., Boulder, Colorado.

Tanada, T., and S.B. Hendricks, 1953. Photoreversal of ultraviolet effects in soybeans. Amer. J. Bot. 40:634-637.

Teramura, A.H., 1981a. Differences in the photosynthetic response to UV-B radiation between mature and immature leaves. Plant Physiol. 67 (Suppl): 93 (Abstract).

Teramura, A.H., 1981b. Cultivar differences in the effects of enhanced UV-B irradiation. Annual Report for EPA. EPA, Washington, D.C.

Teramura, A.H., 1982. The amelioration of UV-B effects on productivity by visible radiation. In The Role of Solar Ultraviolet Radiation in Marine Ecosystems (Calkins, J., ed.), pp. 367-382. Plenum Publ. Corp. New York. ISBN 0-306-40909-7.

Teramura, A.H., 1983. Effects of ultraviolet-B radiation on the growth and yield of crop plants. Physiol. Plant. 58:415-427.

Teramura, A.H., R.H. Biggs, and S. Kossuth, 1980. Effects of ultraviolet-B irradiances on soybean. II. Interaction between ultraviolet-B and photosynthetically active radiation on net photosynthesis, dark respiration, and transpiration. Plant Physiol. 65:483-488.

Teramura, A.H., I.N. Forseth, and J. Lydon, 1984. Effects of ultraviolet-B radiation on plants during mild water stress. IV. The insensitivity of soybean internal water relations to ultraviolet-B radiation. Physiol. Plant 62:384-389.

Teramura, A.H., and N.S. Murali, 1986. Intraspecific differences in growth and yield of soybean exposed to ultraviolet-B radiation under greenhouse and field conditions. Env. Exp. Bot. In press.

Teramura, A.H., M.C. Perry, J. Lydon, M.S. McIntosh, and E.G. Summers, 1984. Effects of ultraviolet-B radiation on plants during mild water stress. III. Effects on photosynthesis recovery and growth in soybean. Physiol. Plant. 60:484-492.

Teramura, A.H., M. Tevini, and W. Iwanzik, 1983. Effects of ultraviolet-B irradiation on plants during mild water stress. I. Effects on diurnal stomatal resistance. Physiol. Plant. 57:175-180.

Tevini, M., W. Iwanzik, and U. Thoma, 1982. The effects of UV-B irradiation on higher plants. In Nato Conference Series, Series IV (Chalkins, J., ed.), pp. 435-448. Plenum Press, New York and London.

Tevini, M., and W. Iwanzik, 1982. The effects of UV-B irradiation on higher plants. In The Role of Solar Ultraviolet Radiation on Marine Ecosystems (Chalkins, J., ed.), pp. 581-615. Plenum Pub. Corp., New York.

Tevini, M., and W. Iwanzik, 1983. Inhibition of photosynthetic activity by UV-B radiation in radish seedlings. Physiol. Plants 58:395-400.

Tevini, M., W. Iwanzik, and A.H. Teramura, 1983. Effects on UV-B radiation on plants during mild water stress. II. Effects on growth, protein and flavonoid content. Z. Pflanzenphysiol 110:459-467.

Tevini, M., W. Iwanzik, and U. Thoma, 1981. Some effects of enhanced UV-B irradiation on the growth and composition of plants. Planta 153:388-394.

Tevini, M., U. Thoma, and W. Iwanzik, 1983. Effects of enhanced UV-B radiation on germination, seedling growth, leaf anatomy, and pigments of some crops. Z. Pflanzenphysiol. 109:435-448.

Van, T.K., L.A. Garrard, and S.H. West, 1976. Effects of UV-B radiation on net photosynthesis of some crop plants. Crop Sci. 16:715-718.

Vu, C.V., L.H. Allen, and L.A. Garrard, 1978. Effects of supplemental ultraviolet radiation (UV-B) on growth of some agronomic crop plants. Soil and Crop Sci. Soc. Florida Proc. 38:59-63.

Wellmann, F., 1982. Phenylpropanoid pigment synthesis and growth reduction as adaptive reactions to increased UV-B radiation. In Biological Effects on UV-B Radiation. (Bauer, H., M.M. Caldwell, M. Tevini, and R.C. Worrest, eds.), pp. 145-149. Gesellschaft fur Strahlen-und Umweltforschung mbH, Muchen.

Whittaker, R.H., 1975. Communities and Ecosystems. MacMillan Publishing Co., Inc., New York.

Zeevaart, J.A.D., 1976. Physiology of flower formation. Ann. Rev. Plant Physiol. 27:321-348.

CHAPTER 12

AN ASSESSMENT OF THE EFFECTS OF ULTRAVIOLET-B RADIATION ON AQUATIC ORGANISMS

SUMMARY

Various experiments have demonstrated that UV-B radiation causes damage to fish larvae and juveniles, shrimp larvae, crab larvae, copepods, and plants essential to the aquatic food web. These damaging effects include decreased fecundity, growth, survival, and other reduced functions in these organisms. In natural marine plant communities a change in species composition rather than a decrease in net production is the probable result of enhanced UV-B exposure. The change in community composition may introduce instabilities to ecosystems and would likely have an influence on higher trophic levels. A decrease in column ozone could diminish the near-surface season of invertebrate zooplankton populations. Whether the population could endure a significant shortening of the surface season is unknown.

The direct effect of UV-B radiation on food-fish larvae closely parallels the effect on invertebrate zooplankton. Information is required on seasonal abundances and vertical distributions of fish larvae, vertical mixing, and penetration of UV-B radiation into appropriate water columns before effects of incident or increased levels of exposure to UV-B radiation can be predicted. However, in one study involving anchovy larvae, a 20% increase in incident UV-B radiation (which would accompany about a 9% decrease in the atmospheric ozone column) would result in the death of all of the larvae within a 10-meter mixed layer in April and August after 15 days. It was calculated that about 8% of the annual larval population throughout the entire water column would be directly killed by a 9% decrease in column ozone.

Effects induced by solar UV-B radiation have been measured to depths of more than 20 m in clear waters and more than 5 m in unclear water. The euphotic zone (i.e, those depths with levels of light sufficient for positive net photosynthesis) is frequently taken as the water column that reaches down to the depth at which photosynthetically active radiation is reduced 99%. In marine ecosystems, UV-B radiation penetrates approximately the upper 10% of the marine euphotic zone before it is reduced to 1% of its surface irradiance. Penetration of UV-B radiation into natural waters is a key variable in assessing the potential impact of this radiation on any aquatic ecosystem.

FINDINGS

1. INITIAL EXPERIMENTS SHOW THAT REDUCTIONS IN STRATOSPHERIC OZONE, WHICH INCREASES SOLAR ULTRAVIOLET RADIATION, HAVE THE POTENTIAL TO HARM AQUATIC LIFE. DIFFICULTIES IN EXPERIMENTAL DESIGNS AND THE LIMITED SCOPE OF THE STUDIES PREVENT THE QUANTIFICATION OF RISKS.

   1a. Increases in energy in the 290-320 nm wavelengths that would occur if the ozone layer were depleted could harm aquatic life.

   1b. Various experiments have shown that UV-B radiation damages fish larvae and juveniles, shrimp larvae, crab larvae, copepods, and plants essential to the marine food web.

   1c. Up to some threshold level of exposure, most zooplankton show no effect due to increased exposure to UV-B radiation. However, exposure above the dose threshold elicits significant and irreversible physiological and behavioral effects.

   1d. While the exact limits of tolerance and current exposure have not been precisely determined, estimates of these two properties for a variety of aquatic organisms show them to be essentially equal.

   1e. The equality of tolerance and exposure suggests that solar UV-B radiation is currently an important limiting ecological factor, and the sunlight-exposed organisms sacrifice potential resources to avoid increased UV-B exposure. Thus, even small increases of UV-B exposure would be likely to further injure species currently under UV-B stress.

   1f. A decrease in column ozone is reasonably likely to diminish the time that zooplankton can survive or breed at or near the surface of waters they inhabit. For some zooplankton, the time they spend at or near the surface is critical for breeding. Whether the population could endure a significant shortening of surface time is unknown.

   1g. Sublethal exposure of copepods produces a reduction in fecundity.

   1h. Of the animals tested, no zooplankton possess a sensory mechanism for directly detecting UV-B radiation; therefore, it would be unlikely that they would actively avoid enhanced levels of exposure resulting from a reduction in column ozone.

   1i. Exposure of a community to UV-B stress in controlled experiments has resulted in a decrease in species diversity, and therefore a possible reduction in ecosystem resilience and flexibility.

   1j. One experiment predicted an 8 percent annual loss of the larval anchovy population from a 9 percent reduction in column ozone in a marine system with a 10-meter mixed layer.

2. IN COMMON WITH ALL OTHER LIVING ORGANISMS, THE AQUATIC BIOTA COPE WITH SOLAR UV-B RADIATION BY AVOIDANCE, SHIELDING, AND REPAIR MECHANISMS. UNCERTAINTY EXISTS AS TO THE EXTENT TO WHICH SUCH MITIGATION MECHANISMS WOULD OCCUR.

3. DETERMINATION OF UV-B EXPOSURE IN AQUATIC SYSTEMS IS COMPLEX BECAUSE OF THE VARIABLE ATTENUATION OF UV-B RADIATION IN THE WATER COLUMN.

   3a. Because aquatic organisms are small and do not usually have fixed locations, it is very difficult to obtain accurate data needed to model the systems and verify results. Current understanding of the life cycle of organisms is very limited.

4. ABOUT ONE HALF OF THE WORLD'S PROTEIN IS DERIVED FROM MARINE SPECIES. IN MANY THIRD WORLD COUNTRIES, THIS PERCENTAGE IS LARGER. RESEARCH IS NEEDED TO IMPROVE OUR UNDERSTANDING OF HOW OZONE DEPLETION COULD INFLUENCE THESE SYSTEMS.

   4a. A comprehensive analysis of sublethal and lethal effects of solar UV on littoral, benthos, and planktonic ecosystems is needed.

   4b. A model of energy flow analysis leading to protein production where solar input is augmented by increased ultraviolet radiation would be required to better evaluate potential effects. Marine organisms responses to projected increases in UV must be considered in the context of the oceans as a dynamic moving fluid.

   4c. Better documentation of the effects of present levels of ultraviolet light on marine organisms is needed.

   4d. Intensive research is needed to identify biochemical indices that reflect UV stress in marine organisms.

INTRODUCTION

As explained in Chapter 2, it is ozone, though in very small concentrations in the atmosphere, that is almost entirely responsible for the absorption of solar ultraviolet (UV) radiation in the 290-320 nm wave band (Exhibit 12-1).

If Exhibit 12-1 were modified to account for a 10% ozone layer reduction, given the scale, one would scarcely notice the difference. The additional UV radiation reaching the earth's surface as a result of a 10% ozone reduction would amount to less than a 0.05% increase in the total sunlight energy. At the very margin of the diagram, however, the percentage increases would be much larger because the base is so small, and it is in those wavelengths that biological responses to the sun's ultraviolet radiation appear substantially greater.

Based on models of depletion, a 10% ozone reduction at 45°N latitude would result in a 28% increase for biologically effective radiation for DNA damage (Setlow 1974). The generalized plant response would increase by 21% (plant damage) (Caldwell 1968). Exhibit 12-2 shows the relationship between ozone depletion and action spectra. Because of the relatively high increases in UV-B at the lower ends of this part of the spectrum and its relative biological effect, ozone depletion constitutes a threat to aquatic life.

BACKGROUND ON MARINE ORGANISMS AND SOLAR ULTRAVIOLET RADIATION

Organisms in fresh water or the oceans are either swimmers (nekton), bottom-dwellers (benthos), or drifters (plankton). Plankton can be either plants (phytoplankton) or animals (zooplankton). An important zooplankton group, the ichthyoplankton, is comprised of the drifting eggs and larvae of many species of fish.

Phytoplankton provide essentially all of the chemical energy required by the marine food web through the photosynthetic process (primary production). Zooplankton are consumers (grazers). Zooplankton are usually less than about 5 cm in diameter or length, most often less than 1-2 mm. Nearly all groups of aquatic animals, at least for some phase in their life history, are considered zooplankton -- for some species, in the egg and/or larval stage, for others, throughout their life cycle. Zooplankton are critical components in typical aquatic feed webs (nutrient pathways) that lead to larger animals, including those comprising the fisheries (finfish and shellfish), and therefore, affect man himself.

In marine ecosystems, UV-B radiation penetrates approximately the upper 10 meters of the marine euphotic zone before it is reduced to 1% of its surface irradiance. Penetration of UV-B radiation into natural waters is a key variable in assessing the potential impact of this radiation on any aquatic ecosystem (Exhibit 12-3).

Photosynthesis requires light, but adequate sunlight seldom penetrates to the bottom of natural waters. Thus, aquatic plants are largely confined to a relatively thin layer at the surface of the water, which is termed the

EXHIBIT 12-1

Solar Irradiance Outside the Earth's Atmosphere and at the Surface of the Earth for a Solar Zenith Angle of 60°

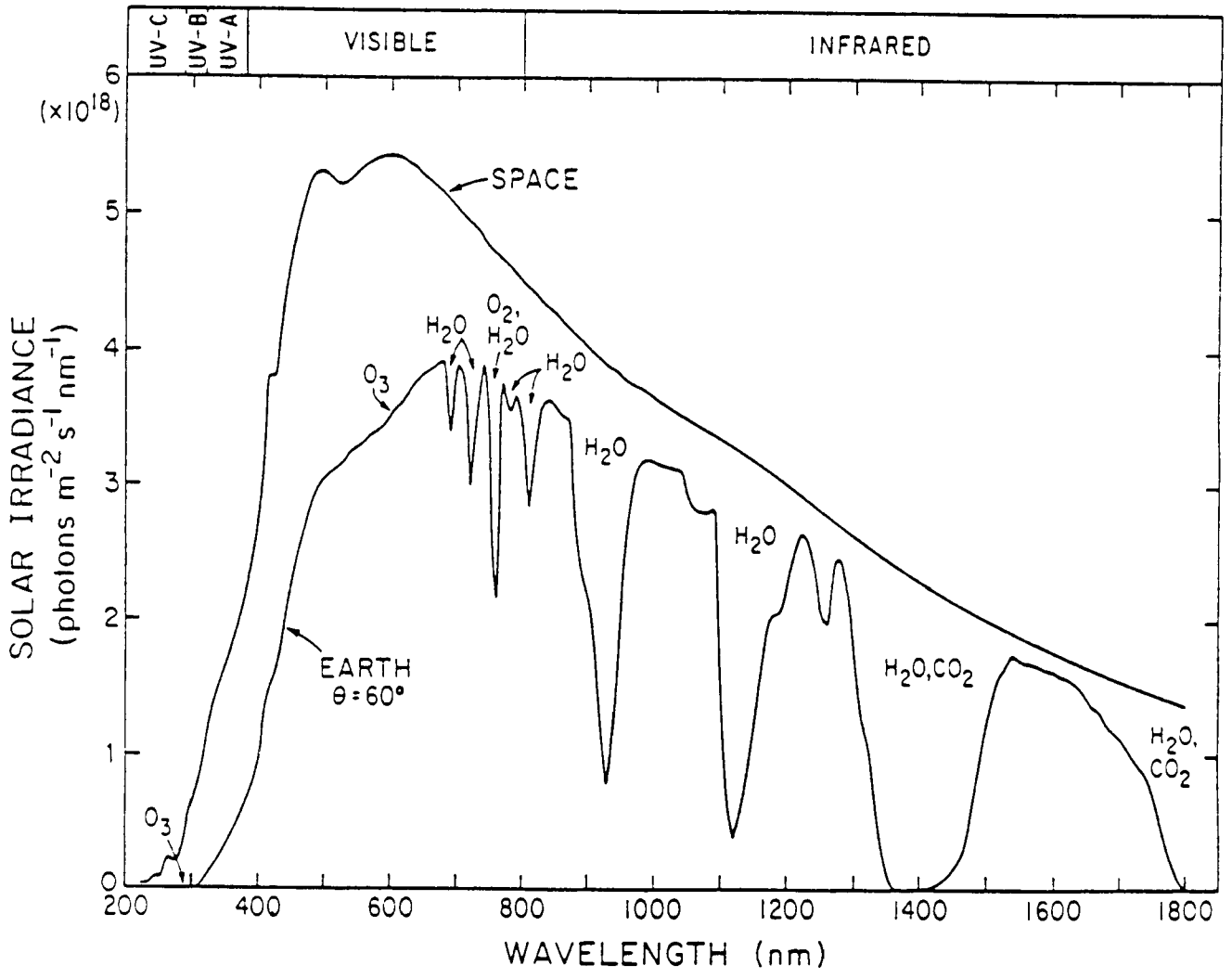

Adapted from Forsythe 1954. Regions of significant absorption by atmospheric ozone, oxygen, water vapor, and carbon dioxide are shown.

EXHIBIT 12-2

Relationship between Ozone Depletion and Biological Effectiveness of Increased UV-B Radiation (Based on model by Green, Cross, and Smith, 1980)

Ozone Decrease	Increase in UV Radiation		Increase in Biological Effectiveness [a]	
	290-320 nm	290-360 nm	DNA	Plant
10%	8%	1.1%	28%	21%
20%	17%	2.4%	67%	49%
30%	27%	3.7%	125%	85%
40%	38%	5.2%	213%	132%

[a] Action spectra are referenced to 300 nm = 1.00.

EXHIBIT 12-3

Solar Spectral Irradiance at the Surface of the Ocean and at Four Depths

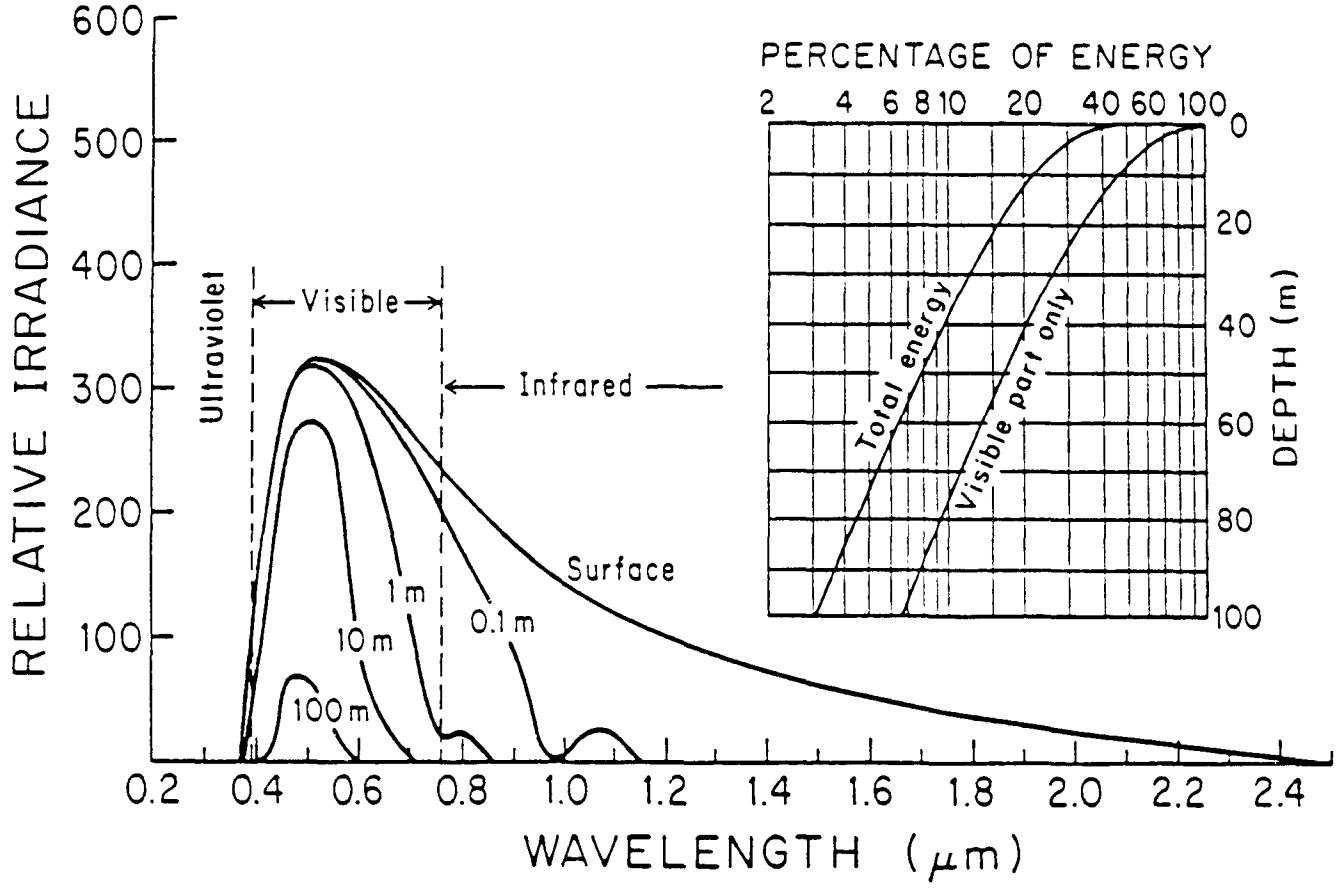

Adapted from Sverdrup, Johnson, and Fleming 1942. Insert illustrates percentage of energy transmitted at depth in oceanic waters.

euphotic zone, the surface layer where plants create more chemical energy by photosynthesis than they use for their own metabolism. This zone is where UV-B can penetrate. Zooplankton are found at all depths, depending on species and season, but are most abundant in the sunlit, upper 100 meters where the bulk of their food, including phytoplankton, is found. Many species normally live very close to the surface, even in daylight, while others occupy the near-surface layer during only part of their life cycle. The near-surface layer is a very important zone in the interactions of the physical/chemical/biological components of aquatic systems.

Zooplankton have apparently evolved mechanisms and behavior by which they have adjusted to current levels of UV radiation (Damkaer 1982), but they may not be able to adjust to relatively rapid increases in total UV exposure. If there are changes in abundance of zooplankton species, those changes would have an impact far beyond any direct effects because of the critical role zooplankton play in energy transfer within the ecosystem.

Limitations of Pioneer Investigations

As early as 1925, scientists were aware of damaging effects from the ultraviolet component of sunlight on aquatic organisms (Huntsman 1925; Klugh 1929, 1930; Harvey 1930; ZoBell and McEwen 1935; Giese 1938; Bell and Hoar 1950; Dunbar 1959; Marinaro and Bernard 1966). These reports are, for the most part, of historical interest only; they cannot be strictly related to present investigations because of a lack of precise or absolute measurements of UV dose-rates and doses. A lack of proper instrumentation for UV irradiance measurements in aquatic research, which included laboratory studies, persisted into at least the late 1960's.

Limitations of Recent Investigations

There are only a few reports that were based on experimental methods appropriate to the problem of enhanced solar UV-B radiation. This meager body of knowledge does not compare well to the enormous literature available on, for example, chemical pollution. Even for chemical pollution there are still great uncertainties in predicting ecosystem responses. It must be recognized that attempts to predict ecosystem responses to enhanced UV-B radiation are in the earliest stages. A number of reports are difficult to apply because the experiments used extraordinarily high UV-B dose-rates and/or doses. Frequently, investigators increased radiation in damaging wavelengths far beyond the amount that can be expected from ozone depletion.

Another problem in predicting UV effects is that we are not yet very close to being able to extrapolate the effects on one species to those on another. Nor can we say with much assurance how the same species might react to UV radiation in a different environment. There are simply too few data of an acceptable quality to make anything other than a general assessment of risk. All that follows must start off with these caveats.

EFFECTS OF UV-B RADIATION ON PHYTOPLANKTON

Direct Impact on Primary Productivity

The amount of UV-B radiation reaching the ocean's surface has long been suspected as a factor influencing primary production. Research shows convincingly that ultraviolet radiation, at levels currently incident at the surface of natural bodies of water, has an influence on phytoplankton productivity (Nielsen 1964; Jitts et al. 1976; Hobson and Hartley 1983). It has been calculated that, near the surface of the ocean, a 25% reduction in ozone concentration would cause a decrease in primary productivity by about 35% (Smith et al. 1980). The estimated reduction in production for the whole euphotic zone would be about 10%. Because these calculations were based on attenuation lengths (i.e., the product of depth in the water column and the diffuse attenuation coefficient of water), waters of various turbidities and absorption characteristics can be compared.

If one assumes that present phytoplankton populations sense and control their average vertical position in such a way as to limit UV-B exposure to a tolerable level, then a 10% increase in solar UV-B radiation would necessitate a downward movement of the average position, thereby reducing the average UV-B exposure by 10%. There would be a corresponding reduction of light for photosynthesis. The loss of photosynthetically active radiation in many locations might not be significant. However, in some very productive areas, especially high latitude ocean areas, photosynthetically active radiation is the primary limiting factor for marine productivity (Russell-Hunter 1970). The loss of photosynthetically active radiation from optical measurements has been estimated to be in the range of 2.5%-5% for a 10% increase in UV-B radiation (Calkins 1982a). If the photosynthetic base of aquatic ecosystems were perturbed, one would expect ramifications to extend up through the food web through predator-prey relationships.

Experiments with marine diatoms have shown significant reductions in biomass, protein, and chlorophyll at UV-B irradiances equivalent to ozone reductions that would occur for a 5%-15% ozone depletion. Laboratory studies on chain-forming diatoms and other phytoplankton show that growth increased when UV-B radiation was filtered out of the incident solar radiation, indicating that existing levels of UV-B radiation depress productivity (Thomson, Worrest, and Van Dyke 1980; Worrest 1982).

Effects Because of Changes in Motility

An additional effect is that UV-B radiation may endanger the survival of microorganisms (Euglena, slime mold, some blue-green algae) by decreasing their motility and by inhibiting phototactic and photophobic responses (Haeder 1986). The inability of a population to move into favorable environments could result in damage that may impair development.

Effects on Photosynthesis

Jones and Kok (1966) observed a direct inhibitory effect of UV radiation on photosynthesis in chloroplasts. This form of inhibition is a short-term response and shows a different UV-B wavelength dependence from most other forms of UV-B injury. Smith et al. (1980) found that the short-term depression of photosynthesis by natural solar UV radiation measured in the ocean resembles the direct photoinhibition described by Jones and Kok. If direct photoinhibition were the only pathway for reduction of photosynthesis by marine phytoplankton, the effect of ozone reduction would be minor; however, Smith and Baker (1980) point out that there could be long-term effects that might show a different action spectrum and be of more consequence.

In Hawaii long-term photoinhibition of the growth of six algal species under natural sunlight has been measured (Jokiel and York 1984). Two strains could not grow at all at the levels of irradiance for full natural surface sunlight. Of the species tested, those collected from tropical surface water showed the greatest adaptive power, but it is reasonable to conclude that resistance to solar UV radiation is achieved through expenditure of resources that can be better applied to other needs in less exposed species.

Worrest et al. (1981) found a short-term (4-5 h) depression of photosynthesis in seven strains of algae upon exposure to enhanced levels of UV radiation. There was a large difference in strain sensitivity. The observed depression appeared to linearly correlate with UV-B dose using the DNA (Setlow 1974) action spectrum. This is in contrast to the results of Smith et al. (1980) who found the Jones and Kok weighting function to be appropriate.

Multi-Day Effects

Measurements of photosynthesis that span only a single day could underestimate the overall action of solar UV exposure by failing to account for effects on the next day's population level. The effects of UV-B radiation could result in delaying growth or direct killing. Thus, subsequent population could fall below the numbers that an unexposed population would attain. Prolonged delays (about two days) in growth of the survivors have been observed in two strains of the diatom Thalassiosira, which had been irradiated with simulated solar UV-B radiation at doses below lethal levels. If unicellular organisms are in a rapid growth phase, a growth delay equalling the time of one growth cycle produces the same effect on the subsequent population as would be produced by a 50% killing (without growth delay).

Shifts in Community Composition and Possible Implications

Shifts in species diversity and community composition of phytoplankton communities have been observed in a simulated marine ecosystem exposed to a UV-B equivalent to ozone decreases of 15% (Worrest et al. 1981). Natural communities appear to show changes in species composition rather than a decreasing net production. Experiments in simulated marine ecosystems seem to indicate that higher UV-B radiation will not decrease biomass and chlorophyll accumulation (Worrest et al. 1981). However, a change in community composition might result in a more unstable ecosystem and might have an impact

on higher trophic levels (Kelly 1986). For example, one effect of enhanced levels of UV-B radiation would be to alter the size distribution of the component producers in a marine ecosystem. Increasing or decreasing the size of the representative primary producers could alter the energy allotment that grazers use for finding and consuming food. This could reduce the feeding efficiency of the consumer, which would have a variety of effects. In addition, the food quality of the producers is altered by exposure to UV-B radiation. It has been demonstrated that the protein content, dry weight, and pigment concentration are all depressed or the composition altered by enhanced levels of UV-B radiation (Doehler 1984, 1985). Consequently, a UV-induced shift in the distribution and abundance of different kinds of aquatic plant organisms could have important ramifications throughout the ecosystem.

EFFECTS ON INVERTEBRATE ZOOPLANKTON

Background

There have been several studies on the effects of UV-B radiation on a variety of zooplankton. Investigators have reported that the effect of increased UV-B radiation on some marine zooplankton (e.g., copepods, shrimp larvae, crab larvae) is increased organism mortality and decreased fecundity in the survivors. Regardless of the species investigated, the potential exists for a disruption of the food web, which would indirectly affect fish populations that are important as food. Of course, studies that consider economically important zooplankton species, such as larvae of certain shrimp, crab, and fish, are important because damage to these species would directly reduce the amount of food for human consumption.

Methodological Issues

How well photorepair mechanisms might mitigate damage is an important issue. It appears that up to some level (daily-dose threshold), photorepair will mitigate damage. However, it also appears that near-surface exposure levels that could accompany a significant reduction in column ozone would exceed threshold levels.

The issue of thresholds is important. It appears that regardless of the cellular-level responses to UV irradiation, it is usually noted that up to some level of UV exposure, the organism appears to suffer no harm. Extrapolating survival curves for different UV exposure levels would indicate that organisms can cope with the damage produced by some levels of additional UV radiation without negative effects. At greater doses, where the survival curve becomes steep, it appears that the repair systems may become inactivated by the radiation, or that the damage to the general tissues has gone beyond the capacity of the repair systems.

A study by Damkaer et al. (1980) illustrates the importance of threshold effect. The authors found no alterations in activity, growth rate, developmental rate, and survival in a number of shrimp and crab larvae exposed to low levels of artificial UV-B radiation. However, when a certain combination of UV dose-rate and total dose was exceeded, negative effects became quite sharply noticeable.

Lethal Effects of Enhanced UV-B Radiation

Damkaer et al. (1980) have done a number of studies in which enhanced UV-B radiation produced irreversible damage and death. UV thresholds, based on the lowest level of irradiance, were statistically significant (exceeding the 95% confidence limits in five replicates). Irreversible effects occurred compared to the controls. Damkaer et al. (1980) have compared the effective UV thresholds with the maximum effective solar daily dose rates at an experimental site in Washington state (Exhibit 12-4). The results indicated that the maximum solar levels are currently exceeded for all tested organisms. Obviously, these animals can survive threshold values for maximum solar UV levels. To be effective, UV thresholds probably must be exceeded during several consecutive days. A more realistic approach would be to compare the threshold levels with median solar UV levels (Exhibit 12-5). The threshold for all groups would then appear to be above the present median solar incident UV levels, at least until late in the time span of natural occurrence near the surface. The data seem to suggest that UV levels have exerted a considerable influence in the long-term adjustments of these populations to those specific seasons. Of course, many other physical as well as biological factors operate concurrently, and the organism's life cycle is a compromise with the total environment. Late in the surface season, it is possible that natural UV levels exert a detrimental effect, particularly on the shrimp larvae, which have a lower total dose tolerance than crab larvae.

Damkaer et al. (1980) compared the estimated effective UV daily dose, simulating various ozone reductions at the experimental site with the UV survival thresholds (Exhibit 12-5). Obviously, the probability that UV thresholds would be exceeded increases with diminishing ozone. With a 40% ozone reduction, there appears only to be a short "window" of safety at the beginning of each group's surface season. Even a 20% ozone reduction significantly shortens the season. Whether or not the populations could endure with a drastically reduced time of near-surface occurrence is not known. Success of any year-class depends on the timing of a great number of other events besides UV level. Under current stress conditions, early larvae may do well one year, whereas only late larvae may survive in a subsequent year. However, an additional stress like enhanced levels of UV-B radiation is not likely to be beneficial. Combined with other stresses that make early year survival impossible, it could devastate populations.

That larval stage development appeared to be unaffected below survival threshold UV levels is an important observation, since the survival of the unharmed larvae is critical to their proper and timely development. Beyond the threshold levels, however, development and survival rapidly declined. The apparent UV thresholds are near-current incident surface UV levels. Nevertheless, the implications of these experiments for zooplankton in nature remains in some doubt because of lack of information on the subsurface UV spectrum, the effects of vertical mixing, unknown in situ behavior of irradiated zooplankton, and unknown sublethal and pre-lethal effects.

EXHIBIT 12-4

Lethal Effects on Shrimp Larvae for Various Combinations of UV-B Dose-Rate and Total Dose

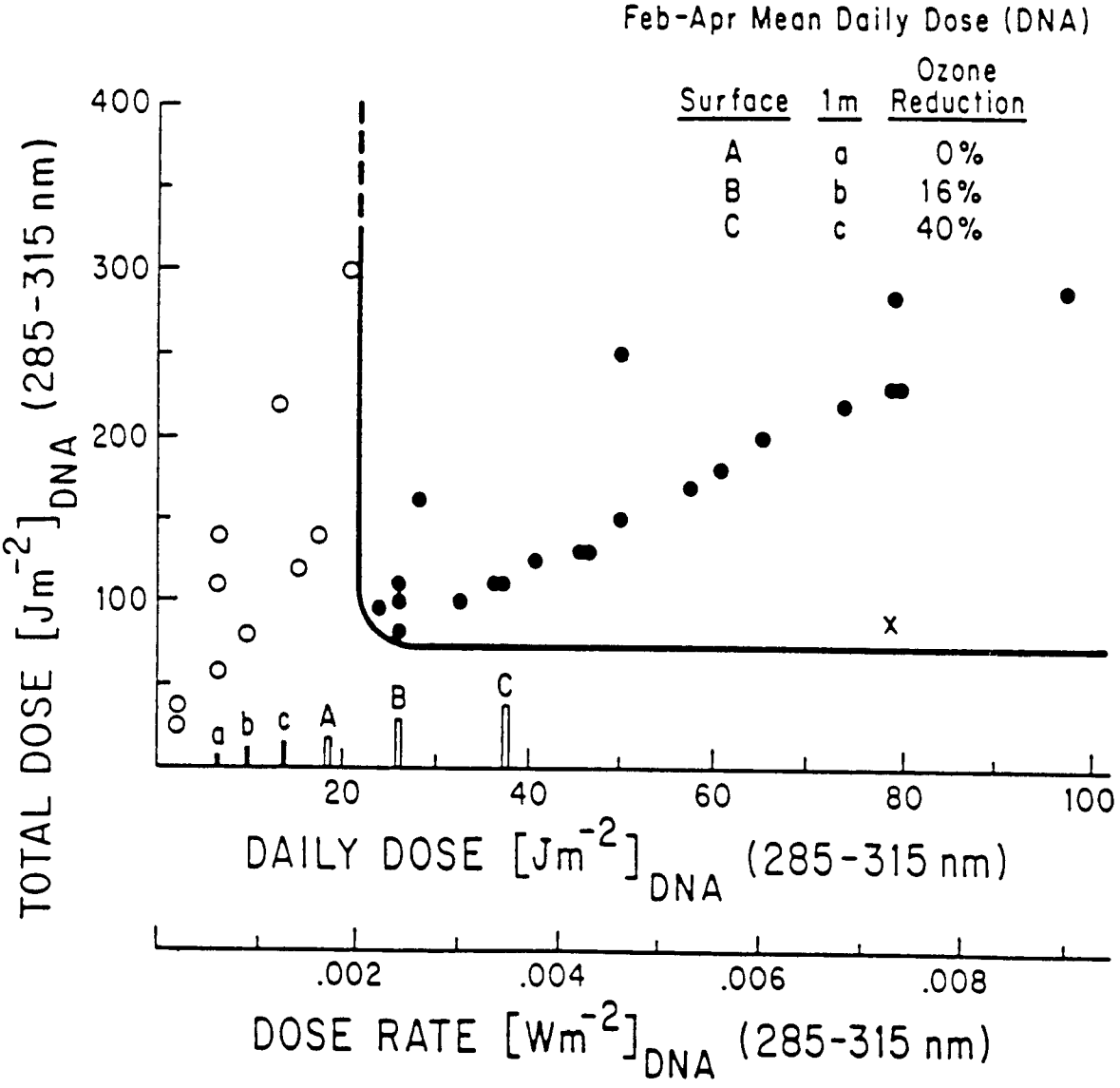

Open circles indicate maximum observed combinations for survival; closed circles indicate minimum observed combinations for mortality. Open vertical bars indicate mean February-April surface solar UV-B daily dose-rates at various atmospheric ozone concentrations; closed vertical bars indicate mean daily dose-rates at 1 m (adapted from Damkaer et al. 1980).

EXHIBIT 12-5

Estimated Effective UV-B Solar Daily Dose at Various Atmospheric Ozone Concentrations Based on 4-Year Mean of Medians Manchester, Washington, 1977-1980

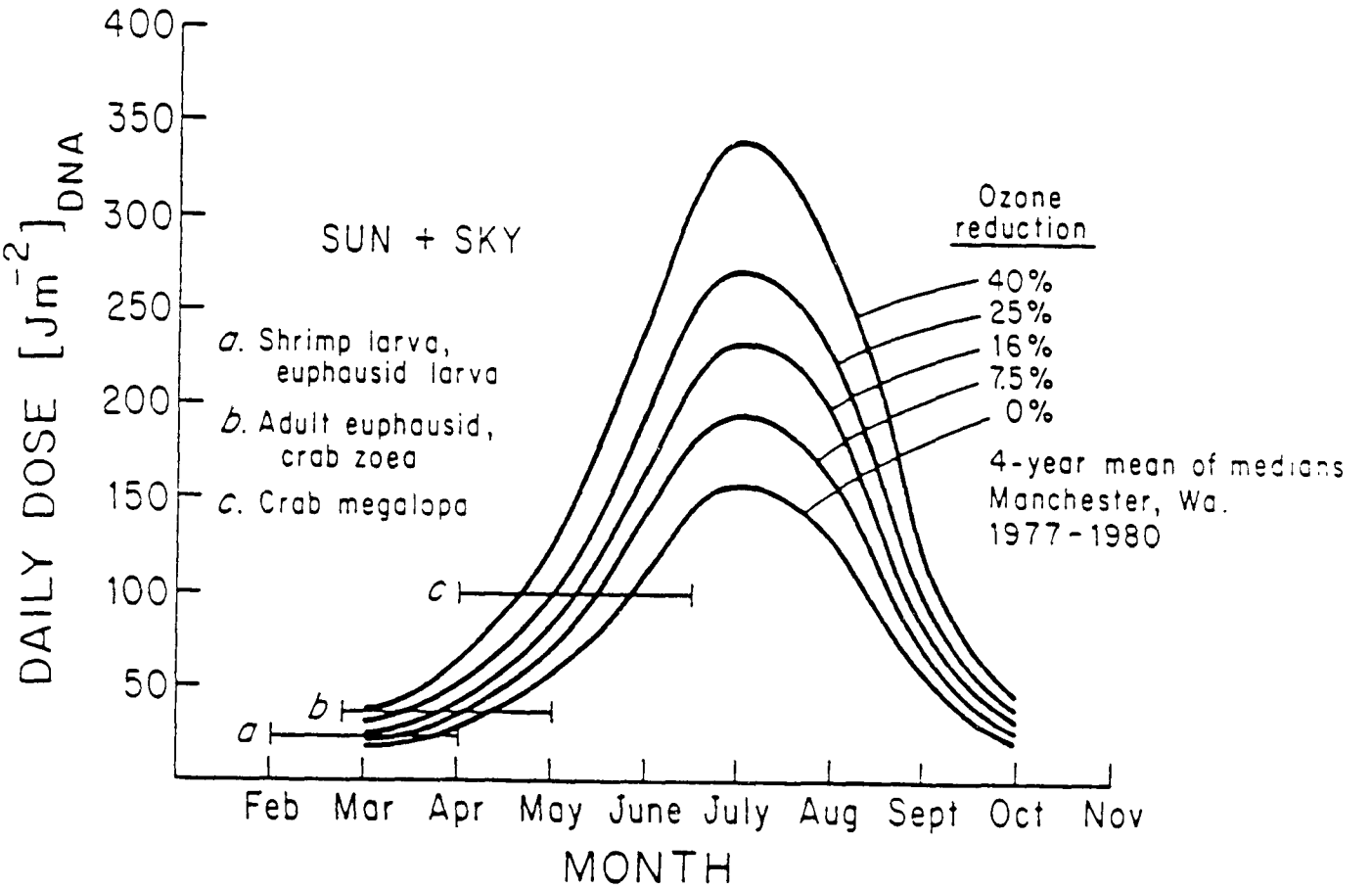

Dose increments are from Gerstl, Zardeki, and Wiser 1986. Also shown are approximate thresholds of UV-B daily dose for principal experimental zooplankton groups, in natural seasonal position (adapted from Damkaer et al. 1981).

The degree to which other zooplankton groups would be affected by these levels of UV-B irradiation cannot be predicted, although in crustaceans, the same basic tissues would likely be involved, and therefore, the response would be qualitatively similar. Species do vary substantially, however, in terms of their sensitivity to UV-B radiation. If the accumulated level of UV-B radiation is the most important factor in damage, then increased UV radiation through ozone depletion may significantly affect even species that are moderately resistant to short exposures of high UV intensities.

Copepods are the most important zooplankton from the perspective of ecosystems. Karanas, Van Dyke, and Worrest (1979) reported on the survival of developmental stages of the estuarine copepod Acartia clausii exposed to daily UV-B doses approaching natural (Oregon coast) daily doses. Although the total doses in this experiment were relevant, the dose-rates exceeded natural dose-rates by about a factor of two.

It is known that organisms are protected to some degree by their own pigmentation, and this suggests that organisms may have evolved pigmentation as a consequence of the damaging effects of solar radiation. Damkaer (1982) reviewed several possibilities for this in regard to zooplankton. Siebeck (1978) found a direct relationship between pigmentation in cladocerans of mountain and lowland lakes and their apparent natural UV exposure. In field and laboratory experiments, the more-pigmented cladocerans tolerated the greater exposures. Siebeck also noted a marked photorepair potential.

Hairston (1980) has drawn attention to the relationship between vertical distribution and pigmentation in some freshwater copepods. Typically, the most pigmented forms are closest to the surface. Because the pressure of predation should be against the conspicuous pigmented forms, Hairston concluded that "photodamage may be a more important selective force than previously supposed."

These kinds of copepods do have a UV-tolerance related to their pigmentation, as has been verified in laboratory experiments. Ringelberg, Keyser, and Flik (1984) studied the UV-B tolerance of a red-pigmented and a translucent variety of the same copepod species from separate, though nearby, lakes in France. The red copepod tolerated higher artificial UV-B doses. The experimental doses were obtained by exposure to a single dose-rate for varying amounts of time. Sharp mortality increases began in the translucent form at about half the total dose as for the pigmented form.

An interesting aspect of these experiments is that in all cases where death occurs, the dose-rate was equivalent to that determined to be the threshold dose-rate for shrimp (Damkaer, Dey, and Heron 1981). The total doses tolerated by the two copepod color-forms bracket the total dose threshold of shrimp larvae. The tolerance limit appears to be the same in vulnerable zooplankton, suggesting perhaps a universal tolerance limit in near-surface organisms of the structure and size of shrimp larvae and copepods. It would be useful to conduct additional experiments with such copepod color-forms and include exposures to lower and higher dose-rates at more natural periodicities. Also, Ringelberg et al. observed no photorepair, but indicated that the intensity of visible radiation in their experiments was extremely low (~ 0.4 W m^{-2}).

Thomson (personal communication) has demonstrated that current levels of UV-B radiation are of significance in the developmental life of several species of shellfish. For some species a 10% decrease in column ozone could lead to as much as an 18% increase in the number of abnormal larvae produced. Exhibit 12-6 is a compilation by Thomson of data denoting the estimated biologically effective UV-B doses leading to significant effects in major zooplankton groups.

Sublethal Effects of UV-B

There are many examples of sublethal stresses (of all kinds) that can affect natural populations. If stresses alter the reproductive capacity of organisms, effects can be significant and rapid. Karanas, Worrest, and Van Dyke (1981) reported a possible mechanism through which enhanced solar UV-B radiation could have a large impact on copepod populations without direct killing. The estuarine copepod Acartia clausii was irradiated with a UV radiation dose that was comparable to mid-summer surface irradiance at 45°N. After five days, the surviving copepods were mated. If either (but not both) parent had been irradiated, the egg production and subsequent hatch of the female was significantly reduced. If both parents had been irradiated, the production of viable larvae was halved. The subsequent survival of the hatched larvae from irradiated crosses did not appear to be significantly affected.

Even though Karanas, Worrest, and Van Dyke (1981) applied a natural-level surface dose-rate of artificial UV-B radiation, this dose-rate was still rather high and probably represents an extreme situation. To obtain reasonable total doses, the copepods were exposed for only 1-2 hours. Real dose-rates, especially at depth, would be considerably less. These copepods are found at the surface, as well as some distance below, but their distribution on the required scale of 1 m or less is not well known. Acartia clausii are taken in a wide variety of water types, but generally this is a coastal/estuarine species. Effective UV-B irradiation may not extend beyond a depth of a few meters into the usual habitat of Acartia claussi. In view of the apparently profound sublethal, reproductive response to UV-B radiation, it would be of great interest to have additional multi-generation observations.

Possible Photorepair of UV-B Damage: Implications for use of Experimental Data

The photochemistry and photobiology of UV-B-induced damage, particularly nucleic acid disruption, as well as the several molecular repair mechanisms that are consistently found in plants and animals, have been reviewed by Caldwell and Nachtwey (1975). Among the repair mechanisms, the quantitative capacity of the dark-repair systems is quite different from those systems that require light. Under typical experimental conditions, it is presumed that the dark-repair mechanisms could function freely. Dark-repair systems appear to offset a very high proportion of the damage caused by relatively low doses of irradiation. However, photorepair mechanisms often appear capable of repairing only so much damage, even over a wide UV-B dose range (Murphy 1975). Consequently, the restorative effects of photoreactivation may be regarded as particularly critical in situations where organisms are subjected to UV-B irradiation near and above tolerance limits. There has been an implication in

EXHIBIT 12-6

Estimated Biologically Effective UV-B Doses Leading to Significant Effects in Major Marine Zooplankton Groups

Zooplankton Group	Dose Rate $W\ m^{-2}$ (DNA eff)[a/]	Total Dose $J\ m^{-2}$ (DNA eff)	Time For Effect
Shrimp/Euphausiid larvae	6.0×10^{-2}	2.6×10^{3}	4 days
Euphausiid adults	9.9×10^{-2}	6.5×10^{3}	6 days
Copepod larvae	3.4×10^{-1}	1.4×10^{3}	1.0 hour
Copepod postlarvae	1.6×10^{-1}	2.7×10^{3}	4.5 hours
Copepod adults	3.4×10^{-1}	3.0×10^{3}	2.5 hours
Crab larvae	9.9×10^{-2}	6.5×10^{3}	6 days
Crab postlarvae	2.8×10^{-1}	6.0×10^{4}	20 days
Anchovy/Mackerel	6.0×10^{-2}	2.5×10^{4}	12 days
Oyster/Mussel larvae	1.2×10^{-1}	2.2×10^{3}	5.0 hours

[a/] DNA action spectrum is referenced to 300 nm = 1.00.
Compilation by Thomson.

some review papers (e.g., NAS 1984) that UV-B damage will be overcome by the maximally functioning photorepair mechanism. Up to some level (daily dose threshold) this is probably true, but beyond that threshold there will be some residual, irreversible damage.

Experiments with artificial sources of UV-B radiation usually are conducted in the laboratory under light regimes using more than an order of magnitude less visible light than found in nature. Near UV and/or visible light is needed for photoreactivation, and the accuracy of some observations may have been influenced by less-than-maximum photorepair in the laboratory. Experiments with shrimp larvae and adult euphausiids (Damkaer and Dey 1983), comparing survival at various UV-B doses and dose-rates combined with different levels of near-UV and visible irradiance, suggest that photorepair occurs in these organisms. The dramatic sensitivity of both shrimp larvae and adult euphausiids when deprived of photoreactivating light clearly demonstrates the relative importance of photorepair under UV stress. However, this apparent photorepair reaches maximum levels at relatively low levels of visible irradiance. Consequently, it is doubtful that photorepair and related survival would have been greater if experimental levels had been equal to solar levels of irradiance.

A similar relationship has been reported between survival in UV-damaged anchovy larvae and level of irradiance of photoreactivating light needed for repair (Kaupp and Hunter 1981). The level needed for maximum photorepair is far less than ambient solar irradiation. The photoreactivation experiments on shrimp larvae and euphausiids suggest that the previously derived dose/dose-rate thresholds are not altered with additional photoreactivating light. Clearly, a significant lack of photoreactivating light, which normally would be concurrent with solar UV-B irradiance, would certainly depress threshold levels. Past experiments have not approached the intensity or dose of local solar photoreactivating light. However, for UV-B exposures below threshold levels, maximum photorepair potential has been reached at the low levels (2-9 W m^{-2}) of photoreactivating light. Nearly doubling the dose-rate and dose of photoreactivating light did not increase the survival of euphausiids. With anchovy larvae, Kaupp and Hunter (1981) reported that the photorepair mechanisms appeared to be "fully activated" at a photoreactivating light (320-500 nm) irradiance of 7 W m^{-2} and a daily dose of 77.5 kJ m^{-2} available over four days. At greater irradiance levels, up to levels equivalent to solar photoreactivating light at 45°N latitude, Kaupp and Hunter observed no further increase in anchovy survival. There is extraordinary close agreement between the relatively low dose-rates and doses necessary for apparent maximum photoreactivation in anchovy larvae and euphausiids. Thus, most of the experimental data cannot be eliminated on the basis of failing to account for photorepair.

Another important point is that from these observations, it is clear that in nature there would always be sufficient photoreactivating light to provide maximum photorepair potentials in shrimp larvae and euphausiids (and also in anchovy larvae). But it must be emphasized that even maximum photorepair may not be sufficient to reverse all potential injuries caused by UV-B radiation.

Possible Vertical Distribution: Implications for Use of Experimental Data

The actual solar radiation to which surface-living zooplankton are exposed in nature is very important in assessing risks to higher ambient UV-B. Given the large effects UV radiation had on zooplankton and the apparent existence of threshold levels, understanding UV-B in the natural environment is critical to assessing risks. To assess the potential dangers to zooplankton populations from increasing solar UV-B irradiation requires consideration of the subsurface irradiance levels. The data for the shrimp larvae, Exhibit 12-4, show that the mean of the observed daily UV-B surface doses (current ozone thickness) between mid-February and mid-April is within the experimentally determined safe zone. Daily doses calculated for a 1-m depth are therefore even farther within the safe zone, so that presumably the shrimp larvae could tolerate these mean dose-rates for long periods. With a 16% or 40% ozone reduction, the total dose thresholds would be exceeded at the surface only if the mean dose-rates are attained for two or three consecutive days (two sunny days). Even then, however, the calculated mean UV-B levels at 1 m would remain in the safe zone. Understanding the implications of higher UV-B requires knowing where the shrimp larvae spend their time.

The actual vertical distributions of the shrimp in nature are not known. In the laboratory, young larvae are attracted to light and definitely prefer the near surface. The larvae do not appear to avoid high UV-B irradiance (Damkaer and Dey 1982), It is not likely they can sense this radiation in sufficient time to prevent lethal damage. Damkaer and Dey assumed that the younger shrimp larvae are constantly moving toward the surface, and that during the day the majority of the population is in the upper meter.

Vertical motion makes it difficult to determine the probability that particular shrimp larvae would receive lethal exposures of UV-B radiation; Exhibit 12-7 shows an approximate estimate. The probability is obviously time-dependent. At the surface, shrimp larvae are unlikely to encounter lethal daily or bi-daily UV-B exposures until the end of the surface season (mid-April). This is also about the time that the mean noon dose-rate exceeds the dose-rate threshold. Before then, the shrimp larvae would be exposed daily to a one-third total dose limit for three consecutive days. This level is in the safe exposure zone because the dose-rate would be low (Exhibit 12-7). At 1 m, the mean dose-rates in mid-April are still less than the shrimp's threshold dose-rates, yet the surface probabilities for lethal exposure may be sufficiently high at that time to limit the seasonal occurrence of the larvae. With a 16% ozone reduction, the current mid-April UV-B conditions would be reached near the end of March. If UV-B radiation is a contributing factor in regulating the seasonal occurrence of shrimp larvae, ozone reductions may act to shorten the surface time available to the larvae. The seasonal relationships in the UV-B tolerance of different zooplankton groups (Exhibit 12-7) suggest that UV irradiance is an important environmental factor. Hunter, Kaupp, and Taylor (1982) postulate that the surface occurrence of eggs and larvae of a number of clupeid fishes are already limited by UV-B.

EXHIBIT 12-7

Percentage of Total Dose Limit Likely to be Reached on Any Particular Day; Lethal Doses Accumulated Only After Dose-Rate Threshold is Exceeded

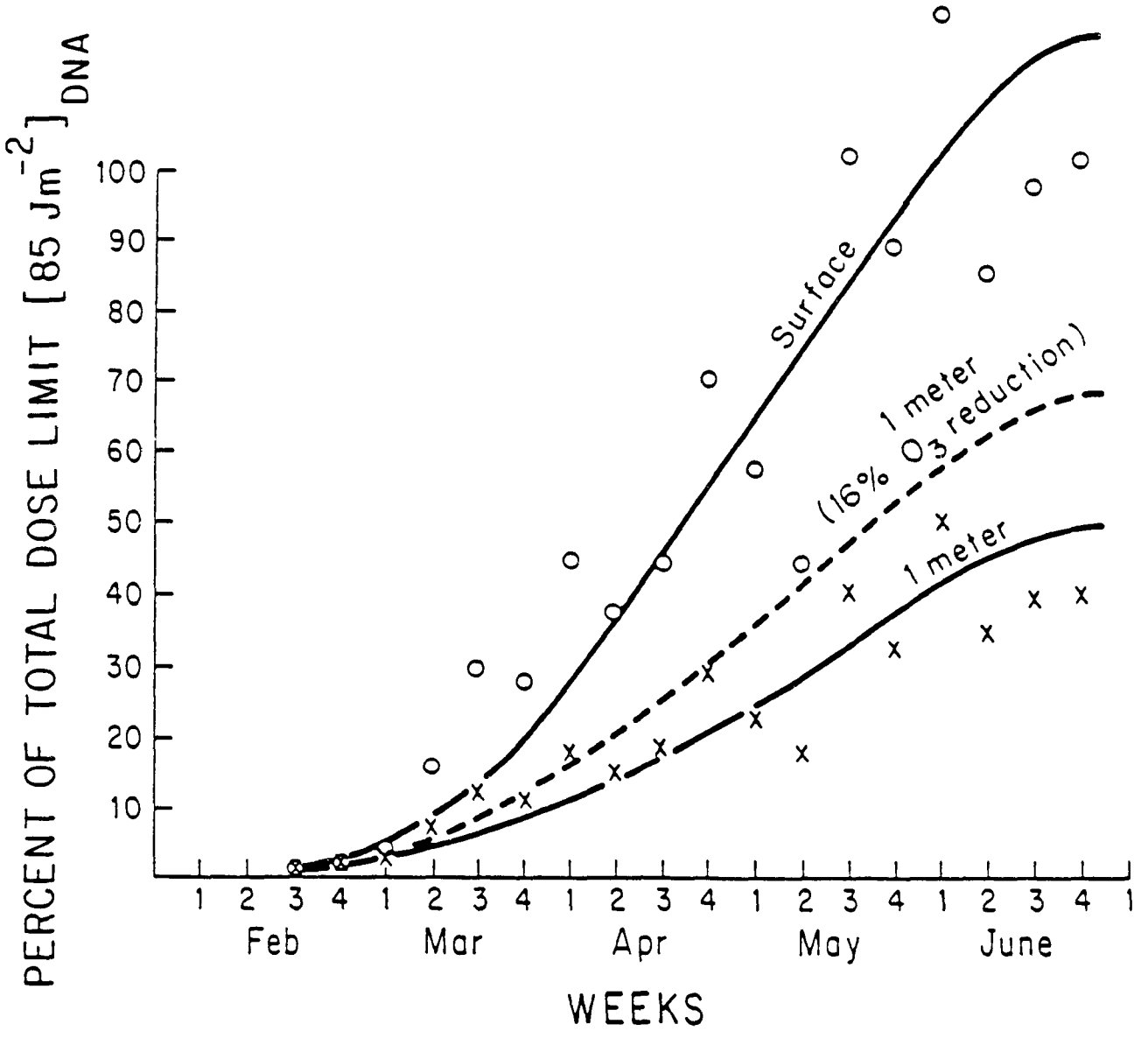

Circles are 4-year weekly means of surface daily UV-B doses; x's are these doses calculated at 1 m (adapted from Damkaer et al. 1981).

Knowing that shrimp larvae are limited by UV-B already, and could be further limited, does not provide us with an assessment of damage. Data on population dynamics and recruitment of shrimp stocks are insufficient to estimate the impacts of shortened surface seasons. It is possible that ordinarily the greatest number of successful recruits are normally derived from early-season larvae and that increased UV-B irradiance would then have no appreciable direct effect on shrimp population stability. It is also possible that late-season larvae are essential to maintaining local populations. In fact, it is possible that the situation varies from year to year with other environmental stresses, so that having a long season is critical to sustaining the population in the long term. Thus, ozone reductions may lead to no change, to a loss in productivity, or to extinction of these shrimp in particular locations.

It is clear that increases in UV radiation through depletion of ozone would create an additional stress to the seasonal near-surface stages of these species. It is quite possible that natural UV levels have already had a selective role in the seasonal adaptation of these species. The question remains: how much of their surface-living time could these species forego and still maintain survival-level populations?

Avoidance and Its Implications In Assessing Risk

Investigations of the biological effects of UV-B radiation on aquatic organisms have included a variety of approaches, ranging from histological analyses to simple survival studies. Most of this work has been concerned with the direct effects of natural or enhanced UV-B radiation. The assumption implicit in some of the conclusions is that the organisms that live in the near-surface layer will be passive recipients of ambient UV-B radiation, regardless of its irradiance level.

Because some of these near-surface organisms appear to be living near their UV tolerance limits (Damkaer et al. 1980) it is possible that they have evolved a sensitivity to fluctuations in UV-B radiation. In addition to photorepair mechanisms, they may possess an ability to avoid harmful levels of UV-B radiation by appropriate defensive behavior. In moderately productive ocean waters, the DNA-weighted irradiance at 1 m is only about 40% incident on the surface (Smith and Baker 1979). Under these conditions, the capacity to sense harmful UV-B radiation and to avoid it by simply swimming or sinking a meter below the surface would provide considerable protection.

However, even if sensory mechanisms exist to warn an organism of dangerous UV-B radiation, the particular stimulus that evokes the avoidance response may not be effective under a new spectral distribution caused by ozone depletion. A reduction in the ozone layer would not increase UV-A and visible radiation. If the avoidance response is linked to high levels of visible irradiance, for example, the avoidance response would not be activated by increased depletion. It seems likely that only a sensory system that directly detects irradiance in the UV-B range and does so before irreparable damage occurs will afford surface-living organisms a safety potential.

Experiments by Damkaer and Dey (1982) suggest that shrimp possess no organ to sense UV-B. They observed differences in behavior between irradiated and non-irradiated shrimp larvae (Pandalus platyceros) or copepods (Epilabidocera

longipedata). The irradiated specimens maintained their near-surface positions in visible light (as did the controls) until the time of decreased activity and death at about four days. Adult euphausiids, on the other hand, seemed to avoid this same level of visible light (with or without UV-B radiation) but were attracted to low levels of visible light with or without extremely high levels of UV-B radiation (Damkaer and Dey 1983). These investigators also found that the zoea stage of the shore crab (Hemigrapsus nudus) is extremely attracted to strong visible light. No difference in response-time (seconds) was noted between control larvae and larvae receiving lethal UV-B doses until decreased activity and death of the irradiated larvae at about 10 days. There was no apparent reluctance of the crab larvae to swim toward and to hold themselves within a zone producing a lethal dose of UV-B radiation.

These experiments suggested that there were no differences in behavior between UV-B irradiated organisms and the control organisms until lethal doses of radiation reduced their activity. This is not considered to be an active response to UV radiation, and it would have no value in avoidance. The apparent inability to perceive potential danger from UV-B exposure occurred at dose-rates well above established laboratory thresholds and at exposures to total doses that, in most experiments, surpassed lethal total dose thresholds for similar animals (Damkaer et al. 1980). If the animals tested in these studies pose a behavioral mechanism for protection from dangerous levels of irradiation, it seems unlikely that it could be based on the direct sensing of UV-B radiation. The zooplankton tested seemed to be attracted to wavelengths of radiation longer than those in the UV-B range, and the additional exposure to high levels of UV-B irradiance did not alter their short-term behavior. Within the limits examined, these animals generally positioned themselves as near the light source as possible. That organisms continue to seek out a strong light source even while doomed from past UV-B exposures demonstrates not only the strength of this photo-positive response but also, probably, their inability to independently discriminate between safe and dangerous levels of UV-B irradiance. Since reductions in atmospheric ozone would allow more incident UV-B (and create no change in visible irradiation), the currently evolved response of some organisms to future solar irradiation is unlikely to be optimal.

Effects of UV-B on Biological Diversity and Subsequent Impact on Food Web

Almost all life ultimately depends on plants, and in the ocean most plant life is planktonic (phytoplankton). To function, plants must receive sunlight, and plants have evolved to require (and tolerate) more or less sunlight, depending on the species. For plants, their balance with current levels of solar radiation is therefore critical. Ultimately, animal life exists because it obtains fixed chemical energy from plants. The interaction of life forms in obtaining energy makes them interdependent, forming food chains, or, more frequently, complex food webs. Animals feeding directly on plants also have evolved receptor mechanisms for solar light. These adaptations typically involved movements and secondary responses to visually feeding predators.

Even if UV-B caused an adverse effect in only a few marine organisms, others are likely to be affected. There have been several studies indicating that reduced UV irradiation leads to increased productivity in phytoplankton.

Only a very few experiments have subjected phytoplankton to reasonable enhancements of UV radiation. Some of these experiments (e.g., that by Thomson, Worrest, and Van Dyke 1980) suggest that phytoplankton have resistance to above-ambient UV levels. Also, Worrest (1982) cites a study by Wolniakowski in which growth rates of a flagellated phytoplankton, initially depressed by exposure to enhanced UV radiation, returned to the base rate after a few days. Finally, in field observations, Hobson and Hartley (1983) found that summer UV levels did not depress phytoplankton photosynthesis. This is not unexpected since it may have resulted from a combination of seasonal succession of UV-resistant species and adaptation to increased UV radiation.

The most likely direct negative effect of higher UV radiation on phytoplankton would be a change in community composition (Worrest et al. 1981); primary production may not suffer any decrease. The species composition that follows is likely to have differences in size and/or nutritional value. The impact of this kind of change, at the lowest level of the food web, could be marked and severe. One quite likely effect is a loss of diversity. Diversity is associated with stability in ecosystems, allowing alternate routes or choices within food webs. In nature, stresses are often best measured not by changes in productivity or population size, but by changes in species diversity. With loss of species, an ecosystem loses some of its natural resiliency and flexibility. Other "shocks" to the system become potentially more damaging. Unfortunately, our knowledge base is insufficient to make any definitive assessments. All that can be done is to argue by analogy. Experience has shown that a loss in diversity leads to instability in ecosystems, which can cascade to create significant change.

EFFECTS ON ICHTHYOPLANKTON (FISHERIES)

As explained with invertebrate zooplankton, regardless of the cellular-level responses to UV irradiation, it is usually noted that up to some UV level there is no apparent effect on ichthyoplankton. At greater doses either the repair systems themselves may become inactivated by the radiation, or the damage to the general tissues is beyond the capacity of the repair systems. To be effective, these threshold levels probably must be exceeded during several consecutive days. The apparent UV thresholds are near current-incident UV levels. In one experiment the thresholds for all groups appeared to be above the present median solar incident UV levels at the test location, at least until late in the time span of natural occurrence near the surface. An ozone depletion of 20% would significantly shorten this season. The effects of this shortening on annual productivity is not known. Whether or not the population could endure with a drastically reduced time of near-surface occurrence is not known. Success of any year-class depends on the timing of a great number of other events in addition to levels of exposure to UV-B radiation.

Hunter, Kaupp, and Taylor (1982) exposed anchovy eggs and larvae and mackerel larvae to high doses of UV-B radiation in small closed containers. They reported that the dose that killed one-half of the test organisms (LD_{50}) is clearly not an acceptable criterion for biological effect. They recognized that "it seems unlikely that any of the damaged survivors, regardless of

dosage, would be able to feed successfully." Hunter, Kaupp, and Taylor (1982) recognized that "none of the larvae surviving LD_{50} doses at age 4-days would survive to age 12-days."

Apart from the fact that laboratory experiments can never duplicate natural responses, the subsequent experiments on UV effects by Hunter, Kaupp, and Taylor (1981, 1982) involved some additional shortcomings that must be kept in mind while evaluating the results. First, it is often difficult to maintain test organisms in good condition. For some common animals, it is not yet possible to keep them alive in the laboratory, much less experiment meaningfully with them. For most of the other animals the laboratory conditions themselves exert a powerful negative influence, so that a true and isolated measurement of UV stress is not attainable. This can be seen in the high 12-day mortalities (average 61%) in the controls for the anchovy larvae. These larvae were kept in small closed containers, a poor but perhaps necessary approximation of the open ocean. There can be no doubt that these larvae were under significant stress even without UV radiation. Hunter et al. refer to wide fluctuations in temperature in the solar-light experiments; oxygen was probably also a limiting factor. Perhaps the use of a flow-through seawater system or another species of fish larvae would eliminate this serious problem. As in some agricultural field tests (Teramura 1986), actual field tolerance of UV radiation is greater than that determined in the laboratory.

The second confounding factor in the experimental design of Hunter, Kaupp, and Taylor is that the tests apparently ended at Day 12. Hunter, Kaupp, and Taylor (1982) reported that at age 20-days, anchovy larvae begin daily vertical migrations. This larval movement into deeper water during the day, and into shallow water at night, would coincidentally avoid significant UV-B exposure. After 20-days survival, then, the gauntlet of UV exposure would have been successfully negotiated. A more meaningful experimental criterion would have been survival to at least age 20-days. However, from the reported mortality rates, perhaps even the control larvae would not have survived this long.

Related to the test endpoint is the third major problem in the interpretation of these experiments. When experiments are conducted to an appropriate developmental endpoint (e.g., to the age when larvae avoid the daytime near-surface layer), it is usually apparent that below a certain irradiation level the organisms are not seriously affected. On the other hand, beyond that irradiation level there seems to be fairly general and irreversible damage. In experiments with planktonic invertebrates (Damkaer et al. 1980; Damkaer, Dey, and Heron 1981; Damkaer and Dey 1983), it can be seen that a very great range of UV-B dose-rates and doses could lead to the same LD_{50}; this depends solely on the time chosen for the observation. In every case, however, at the developmental endpoint, the groups that had exhibited an LD_{50} were essentially all dead.

Hunter, Kaupp, and Taylor (1982) stated that none of the larvae surviving the reported LD_{50} daily dose to age 4-days would have survived to age 12-days. The LD_{50} criterion, then, was clearly inappropriate. Hunter, Kaupp, and Taylor admit that their LD_{50} daily dose to age 12-days may also have underestimated the effect of UV on survival. In their 1981 study they predicted the effects on natural populations by assuming that all organisms receiving less that this LD_{50} value will survive, but this is not an

appropriate use of the LD_{50}. To the extent that organisms receiving just under LD_{50} doses will probably all die, and that LD_{50} values here suggest only that a lower dose might also lead to death, the lethal daily dose estimated by Hunter, Kaupp and Taylor could be an underestimate of UV effects. However, in a reinterpretation of the data considering threshold dose-rate and dose effects (Damkaer, personal communication), the critical daily dose can be estimated.

Hunter, Kaupp, and Taylor (1981) noted that the lengths of anchovy larvae in all UV treatments, even with the lowest dose, were significantly less than the length of control larvae. Length, then, could be a sensitive criterion for UV-B effects, and this, and other criteria, should be explored. A judgment would be necessary as to what diminished length the individual larvae could tolerate before there is a significant effect on survival.

Hunter, Kaupp, and Taylor (1982) realized that information is required on seasonal abundance and vertical distributions of anchovy larvae, vertical mixing, and penetration of UV-B radiation into anchovy-populated seawater before effects of current and increased levels of UV-B radiation can be predicted. There are fairly good data on seasonal abundances and vertical distributions of anchovy larvae, as well as good calculations on average UV-B penetration into known water types. To detect a mortality due to UV-B radiation, against the high natural mortality, would be a difficult problem. But this is not the same as predicting the effect due to this factor alone. For this, mortality rates from other causes are not required because we are concerned only with how UV-B radiation would act on those that survive the other perils of their existence.

Hunter, Kaupp, and Taylor assumed that all larvae at depths where UV-B exceeds the LD_{50} daily dose will die. They also assumed a static, unmixed vertical distribution. Finally, these authors provided data that indicated that anchovy larvae off southern California are typically centered in moderately productive ocean waters that have about 0.5 mg Chl-a m^{-3} (surface chlorophyll concentration). Baker, Smith, and Green (1981) calculated surface DNA-effective UV-B irradiance levels expected for this area, and Smith and Baker (1979) calculated the penetration of UV-B radiation into moderately productive ocean water.

While Hunter, Kaupp, and Taylor calculated that 13.4% of the annual larval anchovy population would die (presumably after 12-day exposures during certain critical times) in a static situation, an analysis by Damkaer (personal communication) indicates that somewhat more would die (14.7%) and in shorter times (4 to 10 days), if there were no vertical mixing. However, static situations are not probable because of physical vertical mixing of water (through the action of wind, density currents, and tides) and the active and passive movement of fish larvae. If some vertical mixing did not offer relief from the effects of UV-B radiation, it is likely that there would be no anchovy larvae above a few meters depth; this is clearly not the case. Probably the surface mixed layer extends to at least 25 m from December to February (Sverdrup, Johnson, and Fleming 1942). A mixed layer of at least 10 m can be assumed for the rest of the year.

For the mixed situation in February, the larvae would spend less than one hour each day in the surface 1-m layer, resulting in exposures where the

threshold doses would never be reached in the larval stage. In the February model, with mixing to 25 m, there would have to be a six-fold increase in incident UV-B radiation before threshold doses would be reached. For the months March-October, with mixing to 10 m, the threshold doses are also not reached within the 20 days available before the larvae become vertically migrating. Only in April and August, with the highest surface irradiances, are these doses approached within this available time (about 22 days).

For March-October, with 10-m mixing, a 10% increase in incident UV-B radiation would still not lead to threshold doses in less than 20 days. With a 20% increase in incident UV-B radiation (a result of about a 9% decrease in the atmospheric ozone column) the depth of the threshold dose-rate is increased. With the 20% increase in incident irradiance, in the dose/dose-rate threshold model, all of the anchovy larvae within the 10-m mixed layer in April and August would be killed, the threshold doses being achieved after 15 days.

Apparently, at all months about 36% of the larval anchovy population is above 10 m (Hunter, Kaupp, and Taylor 1981). The greatest numbers of anchovy larvae are found in April (20% of annual population), so that 7.2% of the annual population would be eliminated with a 9% ozone decrease. Only 1.9% of the annual population is present in August, so the loss of those above 10 m would amount to 0.7% of the annual population. The total predicted loss, then, due to a 9% decrease in total ozone column, would be about 8% of the larval anchovy population (Exhibit 12-8).

In the static model of Hunter, Kaupp, and Taylor, 13.4% of the larval anchovy population dies through the current effects of solar UV-B radiation. They predict only an additional 4.2% decrease in population if UV-B levels increase 60+%. Presumably, in that model, a 20% increase in UV-B irradiance would lead to only a 1.4% additional loss, so the total loss under a 20% increase would be 14.8%. In contrast, the dose/dose-rate threshold and vertical mixing model presented by Damkaer would predict no current solar UV-B damage, but an 8% total larval population loss at a 20% increase in UV-B irradiance (10% depletion) (Exhibit 12-8). Because of complex interactions between mixing-depths, vertical distribution of larval anchovy, seasonal changes in solar irradiance and the penetration of UV into seawater, and seasonal change in anchovy abundance, there is not a linear relationship between mixing-depth and predicted annual loss of anchovy larvae. However, within the range of values represented in Exhibit 12-8, there is a maximum predicted loss at current UV levels with a 15-m mixed layer, and a maximum predicted loss at a 60% increase in UV-B irradiance with a 10-m mixed layer.

Perhaps changes in lower levels of the food web, if they occur with higher UV-B, are likely to be more important than the direct effects upon the fisheries. Changes in the composition of primary production of organic biomass could alter the mortality experienced by larval fish, and perhaps there would be a synergistic effect on mortality. Some fish die from direct exposure, some die from lack of food, and some die from the combination of a reduction in food and the weakening from exposure (or are weakened and become outcompeted by other fauna for limited food reserves).

EXHIBIT 12-8

Effect of Increased Levels of Solar UV-B Radiation on the Predicted Loss of Larval Northern Anchovy from Annual Populations, Considering the Dose/Dose-Rate Threshold and Three Vertical Mixing Models

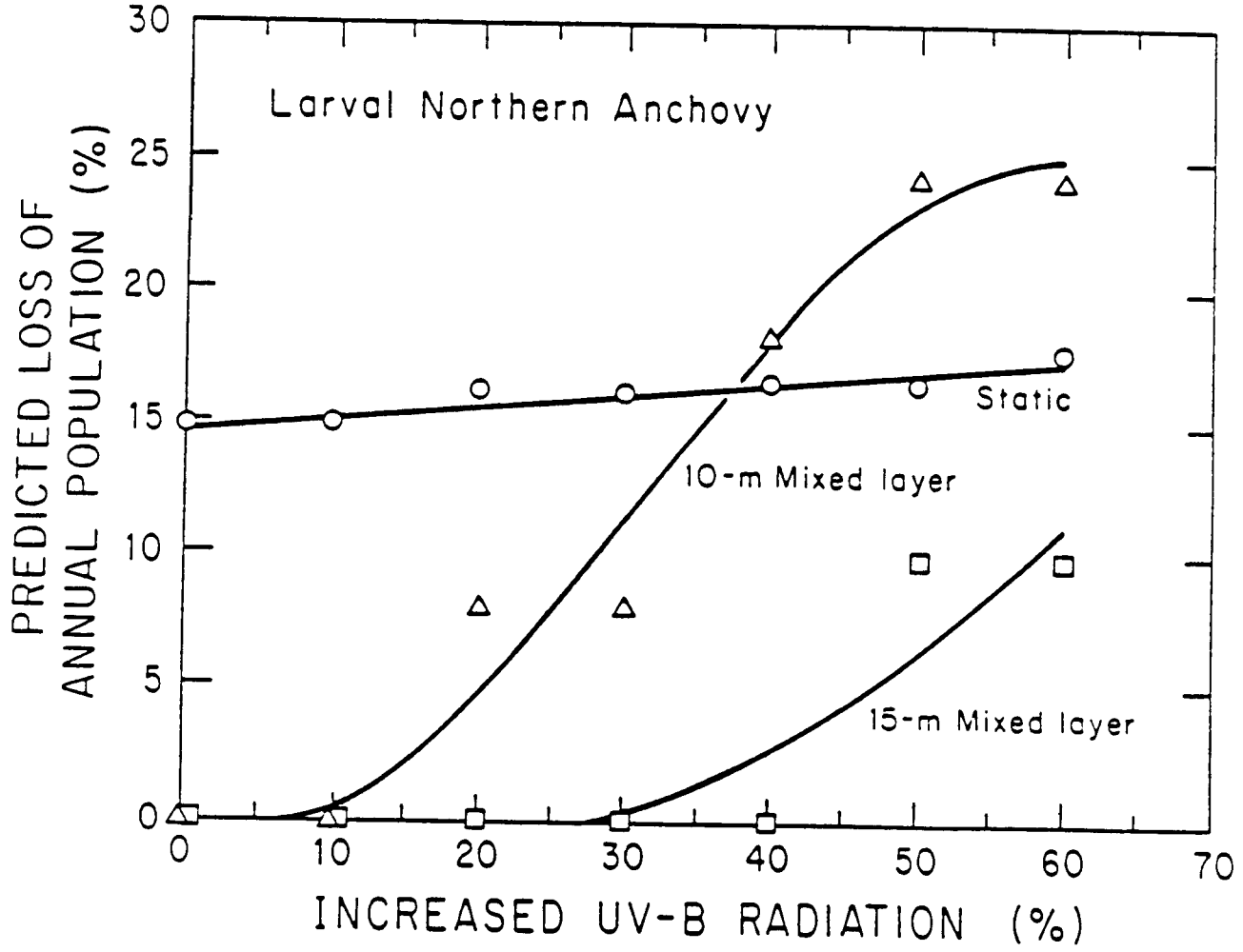

Based on data of Hunter, Kaupp, and Taylor 1982.

The impact on marine fisheries as a food supply to humans would be significant if the species of phyto- and zooplankton that adapted to enhanced UV-B radiation were of different nutritional value (i.e., if they altered growth and fecundity of the consumers or different accessibility to humans). If the indirect impact of suppression upon consumers were linear, a 5% reduction of primary production would result in a 5% reduction in fish production (Exhibit 12-2). A question still under investigation is whether the trophodynamic relationships might be nonlinear. For example, there may be an amplification factor involved that results in a relatively greater impact at higher trophic levels than at the primary-producer level.

Levels of UV-B irradiance range latitudinally, with the highest exposures in the tropics. The current difference between the extremes of exposures is about 3- to 6-fold, but biota are presently adapted to the levels that are normally experienced at their current locations. An effect of ozone depletion of ecological significance is that a 10% decrease in the ozone concentration would produce a 25% increase of biologically effective ultraviolet radiation (DNA, Plant; Exhibit 12-2), which would correspond to migrating over 30° toward the equator. Continued investigations concerning the range of natural ecological uncertainties, which are much larger than the uncertainties in the particular photobiological effects, will be required to permit assessment of the possible consequences for the many complex ecological interactions, as well as for the productivity of fisheries.

CONCLUSIONS

At a minimum, evidence exists that both small and large changes in the stratospheric ozone layer would affect aquatic ecosystems. It will be very difficult to determine the biological effects of small changes in UV-B irradiance at the ocean surface because aquatic ecosystems have a huge physical and biological "noise" level. Storms, clouds, and global currents make dramatic changes in the status of life in the ocean, which cannot at present be predicted. One should not, however, conclude that changes that are lost in the "noise" of the system are automatically insignificant simply because we cannot measure and define exactly what is taking place. Changes that occur because of small systemic events, such as higher UV-B, could accumulate in time to produce much more significant change in aquatic organisms that appear very sensitive to current UV-B radiation. The possibility exists that changes outside the historical range of UV-B could have implications far greater than we are currently able to predict with confidence. We ought not to mistake our ignorance about what will happen if UV-B increases for a conclusion that all is well. At this time we can place almost no limit on what will happen. An increase in UV-B might have small effects, or it might be much more significant.

REFERENCES

Baker K.S. (1979). Calculation of biologically effective UV-B radiation in aquatic systems. SIO Ref 79-1, Scripps Institution of Oceanography. 46 p.

Baker K.S., Smith, R.C., Green, A.E.S. (1981). Middle ultraviolet radiation reaching the ocean surface. Photochem Photobiol 32:367-374.

Banse K. (1982). Cell volumes, maximal growth rates of unicellular algae and ciliates, and the role of ciliates in the marine pelagial. Limnol Oceanogr 27:1059-1071.

Bell G.M., Hoar, W.S. (1950). Some effects of ultraviolet radiation on sockeye salmon eggs and alevins. Can J Res 28:35-43.

Caldwell, M.M. (1968). Solar ultraviolet radiation as an ecological factor for alpine plants. Ecol Monogr 38:243-268.

Caldwell, M.M. (1971). Solar UV irradiation and the growth and development of higher plants. Photophysiology 6:131-177.

Caldwell, M.M., Nachtwey, D.S. (1975). Introduction and overview. In: Nachtwey, D.S., Caldwell, M.M., Biggs, R.H. (eds.) Impacts of climatic change on the biosphere, part I - ultraviolet radiation effects, pp (1)3-(1)30, US Dept Transport, CIAP Monogr 5, NTIS, Springfield, Virginia.

Caldwell, M.M., Robberecht, R., Billings, W.D. (1980). A steep latitudinal gradient of solar ultraviolet-B radiation in the arctic-alpine life zone. Ecology 61:600-611.

Calkins, J. (1982a). Modeling light loss versus UV-B increase for organisms which control their vertical position in the water column. In: Calkins, J. (ed.) The role of solar ultraviolet radiation in marine ecosystems, pp 539-542, Plenum, New York.

Calkins, J. (1982b). Some considerations on the ecological and evolutionary effects of solar UV. In: Calkins, J. (ed.) The role of solar ultraviolet radiation in marine ecosystems, pp 685-689, Plenum, New York.

Cheng, L., Douek, M., Goring, D. (1978). UV absorption by gerrid cuticles. Limnol Oceanogr 23:554-556.

Cote, B., Platt, T. (1983). Day-to-day variation in the spring-summer photosynthetic parameters of coastal marine phytoplankton. Limnol Oceanogr 28:320-344.

Damkaer, D.M. (1982). Possible influence of solar UV radiation in the evolution of marine zooplankton. In: Calkins, J. (ed.) The role of solar ultraviolet radiation in marine ecosystems, pp 701-706, Plenum, New York.

Damkaer, D.M., Dey, D.B., and Heron, G.A. (1981). Dose/Dose-Rate Responses of Shrimp Larvae to UV-B Radiation. Ecologia (BRL) 48:178-182.

Damkaer, D.M., Dey, D.B. (1982). Short-term responses of some planktonic Crustacea exposed to enhanced UV-B radiation. In: Calkins, J. (ed.) The role of solar ultraviolet radiation in marine ecosystems, pp 417-427, Plenum, New York.

Damkaer, D.M., Dey, D.B. (1983). UV damage and photoreactivation potentials of larval shrimp, Pandalus platyceros, and adult euphausiids, Thysanoessa raschii. Oecologia 48:178-182.

Damkaer, D.M., Dey, D.B., Heron, G.A., Prentice, E.F. (1980). Effects of UV-B radiation on near-surface zooplankton of Puget Sound. Oecologia 44:149-158.

Doehler, G. 1984. Effect of UV-B radiation on biomass production, pigmentation and protein content of marine diatoms. Z Naturf 39:634-638.

Doehler, G. 1985. Effect of UV-B radiation (290-320 nm) on the nitrogen metabolism of several marine diatoms. J Plant Physiol 118:391-400.

Dunbar, C.E. (1959). Sunburn in fingerling rainbow-trout. Progr Fish Cult 21:74.

Forsythe, W.E. (1954). Smithsonian Physical Tables. Smithsonian Institution Press, Washington, D.C. pp 721-723.

Gerstl, S.A.W., Zardecki, A., Wiser, H.L. (1986). A new UV-B Handbook, Vol. 1. In: Worrest, R.C., Caldwell, M.M. (eds.) Stratospheric Ozone Reduction, Solar Ultraviolet Radiation and Plant Life, pp 87-111, Springer-Verlag, New York, Heidelberg, Berlin.

Giese, A.C. (1938). The effects of ultra-violet radiations of various wave-lengths upon cleavage of sea urchin eggs. Biol Bull 75:238-247.

Giese, A.C. (1976). Living with Our Sun's Ultraviolet Rays. Plenum Press, New York. 185 pp.

Green, A.E.S., Cross, K.R., Smith, L.A. (1980). Improved analytic characterization of ultraviolet skylight. Photochem Photobiol 31:59-65.

Haeder, D.P. (1986). The effect of enhanced UV-B radiation on motile microorganisms. In: Worrest, R.C., Caldwell, M.M. (eds.) Stratospheric Ozone Reduction, Solar Ultraviolet Radiation and Plant Life, pp 223-233, Springer-Verlag, New York, Heidelberg, Berlin.

Hairston, N. (1980) The vertical distribution of diaptomid copepods in relation to body pigmentation. In: Kerfoot, W. (ed.) Evolution and Ecology of Zooplankton Communities, pp 98-110, Univ Press New England, Hanover, New Hampshire.

Harvey, J.M. (1930). The action of light on Calanus finmarchicus (Gunner) as determined by its effect on the heart rate. Contrib Can Biol 5:85-92.

Hobson, L., Hartley, F. (1983). Ultraviolet irradiance and primary production in a Vancouver Island fjord, British Columbia, Canada. J Plankton Res 5:325-331.

Hunter, J.R., Kaupp, S.E., Taylor, J.H. (1981). Effects of solar and artificial ultraviolet-B radiation on larval northern anchovy, Engraulis mordax. Photochem Photobiol 34:477-486.

Hunter, J.R., Kaupp, S.E., Taylor, J.H. (1982). Assessment of effects of UV radiation on marine fish larvae. In: Calkins, J. (ed.) The role of solar ultraviolet radiation in marine ecosystems, pp 459-497, Plenum, New York.

Huntsman, A.G. (1925). Limiting factors for marine animals. I. The lethal effect of sunlight. Contrib Can Biol 2:83-88.

Jitts, H.R., Morel, A., and Saijo, Y. (1976). The relation of oceanic primary production to available photosynthetic irridantsm Aust J Mar Freshwater Res 27:441-454.

Jokiel, P.L., York, R.H., Jr. (1984). Importance of ultraviolet radiation in photoinhibition of microbial growth. Limnol Oceanog R 29:192-199.

Jones, L.W., Kok, B. (1966). Photoinhibition of chloroplast reactions. I. Kinetics and action spectra. Plant Physiol 41:1037-1043.

Karanas, J.J., Van Dyke, H., Worrest, R.C. (1979). Midultraviolet (UV-B) sensitivity of Acartia clausii Giesbrecht (Copepoda). Limnol Oceanogr 24:1104-1116.

Karanas, J.J., Worrest, R.C., Van Dyke, H. (1981). Impact of UV-B radiation on the fecundity of the copepod Acartia clausii. Mar Biol 65:125-133.

Kaupp, S.E., Hunter, J.R. (1981). Photorepair in larval anchovy, Engraulis mordax. Photochem Photobiol 33:253-256.

Kelly, J.R. (1986). How might enhanced levels of solar UV-B radiation affect marine ecosystems? In: Proceedings of EPA/UNEP International Conference on Health and Environmental Effects of Ozone Modification and Climate Change, July, 1986.

Klugh, A.B. (1929). The effect of the ultra-violet component of sunlight on certain marine organisms. Can J Res 1:100-109.

Klugh, A.B. (1930). The effect of ultra-violet component of the sun's radiation upon some aquatic organisms. Can J Res 2:312-317.

Lasker, R. (1975). Field criteria for survival of anchovy larvae: the relation between inshore chlorophyll maximum layers and successful first feeding. Fishery Bull 73:453-462.

Marinaro, J.Y., Bernard, M. (1966). Contribution a l'etude des oeufs et larves pelagiques de poissons mediterraneens. I. Note preliminarie sur l'influence lethale du rayonnement solaire sur les oeufs. Pelagos 6:49-55.

Murphy, T. (1975). Effects of UV radiation no nucleic acids. In: Nachtwey, D.S., Caldwell, M.M., Biggs, R.H. (eds.) Impacts of climatic change on the biosphere, part I - ultraviolet radiation effects, pp (3)21-(3)44, US Dept Transport, CIAP Monogr 5, NTIS, Springfield, Virginia.

Nachtwey, D.S., Rundel, R.D. (1982). Ozone change: biological effects. In: Bower, F.A., Ward, R.B. (eds.) Stratospheric Ozone and Man, Vol 2, pp. 81-121, CRC Press, West Palm Beach.

NAS. National Academy of Science (1984). Causes and Effects of Changes in Stratospheric Ozone: Update 1983. Natl Acad Sci, Washington, D.C. 254 pp.

Nielsen, E.S. (1964). On a complication in Maine productivity work due to the influence of ultraviolet light, J Cons Cons Int Explor Mer 20:130-135.

Pommeranz, T. (1974). Resistance of plaice eggs to mechanical stress and light. In: Blaxter, J.H.S. (ed.) The Early Life History of Fish, pp 397-416, Springer-Verlag, New York, Heidelberg, Berlin.

Ringelberg, J., Keyser, A., Flik, B. (1984). The mortality effect of ultraviolet radiation in a translucent and in a red morph of Acanthodiaptomus denticornis (Crustacea, Copepoda) and its possible ecological relevance. Hydrobiologia 112:217-222.

Russell-Hunter, W.D. (1970). Aquatic Productivity. MacMillan.

Ryther, J.H. (1969). Photosynthesis and fish production in the sea. Science 166:72-76.

Setlow, R.B. (1974). The wavelengths in sunlight effective in producing skin cancer: a theoretical analysis. Proc Natl Acad Sci (USA) 71:3363-3366.

Siebeck, O. (1978). Ultraviolet tolerance of planktonic crustaceans. Verh Intern Verein Limnol 20:2469-2473.

Smith, R.C., Baker, K.S. (1978). Optical classification of natural waters. Limnol Oceanogr 23:260-267.

Smith, R.C., Baker, K.S. (1979). Penetration of UV-B and biologically effective dose-rates in natural waters. Photochem Photobiol 29:311-323.

Smith, R.C., Baker, K.S. (1980). Stratospheric ozone, middle ultraviolet radiation and carbon-14 measurements of marine productivity. Science 208:592-593.

Smith, R.C., Baker, K.S., Holm-Hanson, O., Olson, R. (1980). Photoinhibition of photosynthesis in natural waters. Photochem Photobiol 31:585-592.

Sverdrup, H.U., Johnson, M.W., Fleming, R.H. (1942). The Oceans, Their Physics, Chemistry and General Biology. Prentice-Hall, New York. 1087 p.

Teramura, A.H. (1986). Interaction between UV-B radiation and other stresses in plants. In: Worrest, R.C., Caldwell, M.M. (eds.) Stratospheric Ozone Reduction, Solar Ultraviolet Radiation and Plant Life, pp 327-343, Springer-Verlag, New York, Heidelberg, Berlin.

Thomson, B.E., Worrest, R.C., Van Dyke, H. (1980). The growth response of an estuarine diatom (Melosira nummuloides øDillw.! Ag.) to UV-B (290-320 nm) radiation. Estuaries 3:69-72.

Worrest, R.C. (1982). Review of literature concerning the impact of UV-B radiation upon marine organisms. In: Calkins, J. (ed.) The role of solar ultraviolet radiation in marine ecosystems, pp 429-457, Plenum, New York.

Worrest, R.C. (1983). Depletion of stratospheric ozone: impact of UV-B radiation upon nonhuman organisms. In: Covello, V., et al. (eds.) The Analysis of Actual Versus Perceived Risks, pp 303-315, Plenum Press, New York.

Worrest, R.C., Wolniakowski, K.U., Scott, J.D., Brooker, D.L., Thomson, B.E., Van Dyke, H. (1981). Sensitivity of marine phytoplankton to UV-B radiation: impact upon a model ecosystem. Photochem Photobiol 33:223-227.

ZoBell, C.E., McEwen, G.F. (1935). The lethal action of sunlight upon bacteria in seawater. Biol Bull 68:93-106.

CHAPTER 13

EFFECTS OF UV-B ON POLYMERS

SUMMARY

Several polymers (and largely the impurities present in the polymers) readily absorb the ultraviolet (UV) radiation. One effect of increased UV-B radiation, resulting from possible future depletion of the ozone layer in the stratosphere, will be accelerated degradation of the polymeric materials. Energies associated with the UV radiation are large enough to initiate reactions in polymers, which lead to their degradation by affecting their mechanical and optical properties and thus reducing their service life. Several methods are used to stabilize the polymers to maintain a useful service life in their various important applications.

While much is known about the physical processes of degradation, little research has focused to date on the potential costs and responses to such degradation. Initial studies suggest that one likely response to increased UV-B induced damage is to increase the amount of light stabilizer in the polymers. Because of the lack of relevant data, only approximate estimation methods are available to determine the extent of light-induced damage and the degree of stabilization required to minimize it. The effect of increased UV-B radiation is manifested in increased costs of production, including raw material costs, energy costs, and maintenance costs.

FINDINGS

1. INCREASED UV-B RADIATION WILL ACCELERATE THE DEGRADATION OF POLYMERS.

   1a. Several commercial polymers (e.g., polyethylene, polypropylene, poly(vinylchloride)), although theoretically UV transparent, contain chromophore impurities that absorb light in the UV-B region of the spectrum. Other polymers (e.g., polycarbonate) have structural features in their molecules that result in strong UV-B light absorption.

   1b. Several polymers have important outdoor applications (e.g., used in siding and window glazing in the building industry, in film and containers in packaging, in housewares and toys, and in paints and protective coatings). Such polymers are likely to be exposed to significant amounts of UV-B radiation. Other polymers are stored outside before use and could deteriorate during these periods.

   1c. Absorption of UV-B radiation in polymers causes photo-induced reactions and alters important mechanical, physical, or optical properties of the polymers (e.g., yellowing, brittleness) and thus degrades (i.e., reduces the useful life of) the polymers.

2. INCREASED USE OF UV-STABILIZERS FOR PROTECTION OF POLYMERS AGAINST UV RADIATION WOULD HAVE NEGATIVE EFFECTS.

   2a. Increased amounts of stabilizers might adversely affect the processing and use properties of some polymers (e.g., hardness, thermal conductivity, flow characteristics). For example, increased amounts of titanium dioxide in poly(vinylchloride) might affect its processing properties, increasing its costs of production.

   2b. Changes in the amount of stabilizer (and other additives) would increase costs of products. Alternatively, manufacturers could develop new formulations to avoid or minimize impurities in production.

   2c. The addition of stabilizers to polymers may be limited by practical problems of material characteristics or manufacture. However, other responses may be possible to limit damage.

3. INCREASED UV-B RADIATION DUE TO OZONE DEPLETION COULD HAVE ADVERSE ECONOMIC EFFECTS.

   3a. Changes in polymer processing properties can result in more equipment shutdowns, higher maintenance costs, and increased utility costs.

   3b. Increased operating costs and material costs (e.g., for stabilizers, lubricants, and other additives) would have an adverse economic impact on the polymer/plastic and related industries.

   3c. In a case study using preliminary data and methods, and a given scenario of ozone depletion (26% depletion by 2075), undiscounted

cumulative (1984-2075) economic damage for poly(vinylchloride) is estimated at $4.7 billion (USA only). Due to the lack of data, possible damage to other polymers has not been assessed.

4. POTENTIAL DAMAGES TO POLYMERS RELATED TO OZONE DEPLETION AND CLIMATE CHANGE ARE DIFFICULT TO ESTIMATE.

4a. Due to lack of relevant experimental data, only approximate estimation methods are available to determine the potential extent of light-induced damage to polymers and other materials.

4b. Depending upon the chemical nature of a polymer, the components of the compound, and the weathering factors, both temperature and humidity tend to increase the rate of degradation.

4c. Research on dose-response relationships for polymers could increase our ability to project the effects of ozone depletion.

4d. Actual action spectra need to be developed for different polymers.

4e. The feasibility of different mitigation measures needs to be experimentally determined.

4f. The synergistic effects of increased humidity and temperature need to be considered.

PHOTODEGRADATION OF POLYMERS

Structure of Polymers

Macromolecules in the polymers are composed of several monomeric units joined by chemical bonds to each other. The monomeric units contain chemical bonds that are either in the main chain of the macromolecule or connect various atoms or side groups to it. Side groups, if present, contain additional chemical bonds. All of these bonds may be reaction sites in polymer degradation, and various energy sources may be effective in supplying the energy necessary to break the bonds. The dissociation energies of chemical bonds in common polymers range from about 65 kcal/mole (C-Cl) to 108 kcal/mole (C-F) with carbon-carbon bonds in the middle (75-85 kcal/mole). The most important types of energy that cause polymer degradation are heat, mechanical energy, and radiation. Thermal and mechanical degradation of polymers may occur during thermomechanical processing. The most common form of radiant energy that causes degradation is that of the UV component of sunlight; the energy of a photon with wavelength λ = 300 nm is about 95 kcal/mole, which is higher than most bond dissociation energies in polymers, and therefore capable of breaking these bonds.

Wavelengths of UV radiation at which various commercial polymers have maximum sensitivity and their corresponding photon energies are given in Exhibit 13-1.

EXHIBIT 13-1

Wavelengths of UV Radiation and Polymers With Maximum Sensitivity and Corresponding Photon Energies

Polymer	Wavelength (nm)	Energy kcal/mole
Styrene-acrylonitrile copolymer	290,325	99,88
Polycarbonate	295,345	97,83
Polyethylene	300	96
Polystyrene	318	90
Polyvinyl chloride	320	89
Polyester	325	88
Vinyl chloride-vinyl acetate copolymer	327,364	87,79
Polypropylene	370	77

Source: Kelen, T., Polymer Degradation, Van Nostrand Reinhold, New York, 1983.

Light Absorption

A prerequisite for light-induced damage in materials is their ability to absorb the radiation (this observation is sometimes referred to as the Grotthus-Draper Law of Photochemistry) (Andrady 1986). Very few materials absorb light at all wavelengths across the spectrum. Pure samples of polyethylene, polypropylene, and polyvinyl chloride, for instance, are theoretically UV transparent and are not expected to absorb light in the range 290-315 nm, the UV-B region of the spectrum. However, completely "pure" polymers do not exist. During synthesis, processing, and storage, various amounts of carbonyl and hydroperoxy groups accumulate in the commercial polymers. These chromophores readily absorb UV light in the 290-315 nm wavelengths. Initiation of degradation consists mainly of the decomposition of these chromophores.

Photophysical and Photochemical Processes

Degradation of the polymers involves a series of photophysical and photochemical processes. The physical processes involved in photodegradation include absorption of light by the material, electronic excitation of the molecules, and deactivation energy transfer to some acceptor. When the lifetime of the excited state is sufficiently long, the species can participate in various chemical transformations. This is especially true when the photoinduced degradation reactions are carried out in the presence of oxygen (see equations 1-4).

$$\text{Polymer (RH)} \xrightarrow{\text{light}} \text{polymer excited state (RH*)} \quad (1)$$

$$\text{RH*} \xrightarrow{\text{degradation}} \text{polymer radicals or broken (scission) chain end (R}\cdot\text{)} \quad (2)$$

$$\text{R}\cdot + \text{air} \longrightarrow \text{polymer peroxy radicals (RO2}\cdot\text{)} \quad (3)$$

$$\text{RO2}\cdot + \text{RH} \xrightarrow{\text{light}} \text{ROOH} + \text{R}\cdot \text{ (further polymer degradation)} \quad (4)$$

As mentioned earlier, hydroperoxy and carbonyl groups are the two most common impurities present in the polymers. In the case of hydroperoxy groups (ROOH), the energy of UV light is sufficient to cause both of the following decompositions (Kelen 1983):

$$\text{ROOH} \xrightarrow{\text{light}} \text{RO}\cdot + \cdot\text{H} \quad (\sim 42 \text{ kcal/mole}) \quad (5)$$

$$\text{ROOH} \xrightarrow{\text{light}} \text{R}\cdot + \cdot\text{OH} \quad (\sim 70 \text{ kcal/mole}) \quad (6)$$

Dissociation of the O-H bond is less facile:

$$\text{ROOH} \xrightarrow{\text{light}} \text{ROO}\cdot + \cdot\text{H} \quad (\sim 90 \text{ kcal/mole}) \tag{7}$$

Because of the low bond dissociation energy (42 kcal/mole), decomposition according to reaction (5) is predominant in photo-oxidation of polymers containing hydroperoxy groups.

The carbonyl group absorbs UV light readily and hence is easily excited. The excited carbonyl group decomposes via Norrish reactions of Types I, II, and III (Kelen 1983). The Norrish-I reaction (8) is a radical cleavage of the bond between the carbonyl group and the α-carbon atom (α-scission).

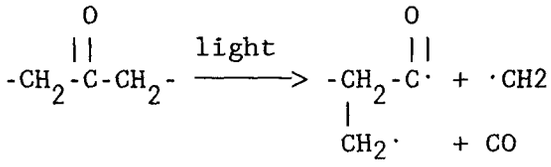

(8)

The Norrish-II reaction (9) is a nonradical scission that occurs through the formation of a six-membered cyclic intermediate to form an olefin and an alcohol or ketone.

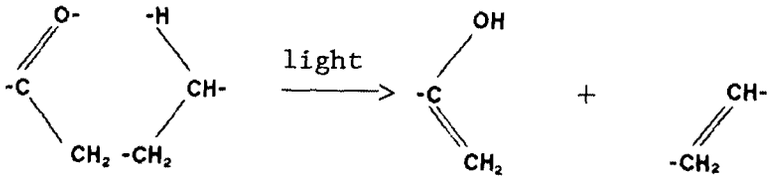

(9)

The Norrish-III reaction (10) is also a nonradical chain scission and leads to the formation of an olefin and an aldehyde.

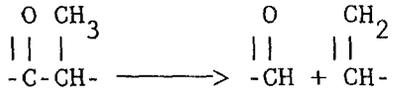

(10)

In the case of PVC, the photolytic scission takes place as follows:

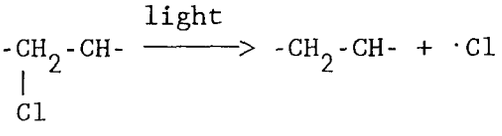

(11)

POLYMERS IN OUTDOOR USES AND POTENTIAL DEGRADATION

A variety of polymeric materials are used in applications where the material is routinely exposed to solar radiation. These include mainly the use of plastics in the building industry and in paints/coatings. In other applications such as packaging, outdoor furnishings, housewares, and toys, exposure occurs from extended to more limited, possibly intermittent, periods of time.

According to recent estimates, of the 45,506 million pounds of U.S. plastic sales in 1985, the building industry above accounted for 9,428 million pounds, 21% of the total consumption. Packaging applications were the largest market consuming 10,846 million pounds (Horst et al. 1986).

However, the bulk of the consumption is represented by a limited number of different plastics. These include the so-called "commodity" plastics and a few other types selected on the basis of their unique physical-chemical properties. Exhibit 13-2 gives a breakdown of the types of plastics used in each application along with the likelihood of exposure to sunlight in normal use. Some plastics/products, not experiencing direct sunlight, can still be exposed to UV light since the UV light is easily reflected and scattered by terrain and buildings, resulting in significant irradiation levels at surfaces illuminated only by diffused or reflected light (Andrady 1986). Thus, vulnerability to degradation is a function of a polymer's normal lifetime and the percent of time it is exposed to direct or indirect sunlight.

Light-Induced Damage

Exposure to light and several physical-chemical processes (described earlier) occurring simultaneously result in deterioration of polymeric materials.

Properties most likely to be affected by the degradation of the polymer include both mechanical and optical properties. Mechanical properties such as tensile strength, elongation, modulus, and impact strength can all be affected by UV degradation of polymeric materials. Optical properties that have been observed to change upon exposure to UV radiation include transparency, color, chalking or cracking of surfaces, and yellowing. These effects are most noticeable on the surface of plastic materials because of the limited penetration of UV light through the materials. Thus, the material may show cosmetic changes in appearance long before any degradation in its bulk mechanical property is noted.

The mechanical weakening of plastic material occurs because of a reduction in the molecular weight of the polymer. Essentially all of the mechanical properties of polymers are related to the molecular weight of the material. Thus, for every bond in the polymer molecule that breaks because of UV radiation, the average molecular weight will be reduced, and the corresponding mechanical properties will be reduced in some proportion to this molecular weight reduction (Andrady 1986).

EXHIBIT 13-2

Plastics Used in Applications Where Exposure of the Material to Sunlight Might be Expected

Type of Plastic	Application	Usage 1000 metric tons	Exposure
	Building Industry		
Polyvinyl chloride (rigid)	siding	410	high
	door/window	284	high
	other	33	high
	conduit	493	moderate
	Irrigation pipe	247	high
	other pipe	1912	low
Polyvinyl chloride (plasticized)	roofing	22	high
	liners	25	moderate
	wire-cable	410	NA*
	weatherstrip	38	moderate
	garden hose	48	high
Unsaturated Polyester	glazing	41	high
	panels/siding	122	high
	pipe	237	low
Polycarbonate	glazing	90	high
	fixtures	9	low
Acrylic	glazing	84	high
	Packaging		
Polyethylene	film	696	NA *
	containers	2990	NA
Polypropylene	film	375	NA
	containers	325	NA
Thermoplastic Polyester	containers	635	NA

EXHIBIT 13-2
(Continued)

Type of Plastic	Application	Usage 1000 metric tons	Exposure
	Housewares and Toys		
Polyethylene		954	NA
Polystyrene		378	NA
Polypropylene		176	NA

Source: Based on 1985 estimates as reported in Modern Plastics, (1986) 63(1): 69.

*NA indicates exposure information is not available. However, based on the application, it is expected to be low to moderate.

Discoloration of polymeric materials is also related to bond breaking, but in these cases, bonds that are broken may have little effect on mechanical properties. The best example of a polymer discoloring by yellowing is in transparent flexible polyvinyl chloride (PVC) window materials used for rear windows of convertible automobiles. The PVC darkens from weathering because of impurities in the resin initiating a dehydrochlorination reaction as outlined below:

$$-CH_2-\underset{Cl}{CH}- \xrightarrow[\text{impurities}]{\text{light}} -\overset{H}{C}=CH- + HCl \qquad (12)$$

The color is caused by the multiple double bonds (~9 repeat units in sequence) created between the carbon atoms, resulting in a polymer that absorbs the light in the visible region of the spectrum and thus appears yellow. Often this discoloration is evident long before mechanical properties of the polymer material begin to change. This, again, is because mechanical properties are related to the molecular weight of the polymer more than to the chemical structure.

Other changes in polymeric materials from UV exposure, similar to yellowing, also occur mostly at the surface. Such changes as surface cracking, chalking or crazing (i.e., when a clear surface becomes translucent because of formation of microcracks) are all evident in polyolefins, polycarbonates, vinyl, acrylic, and styrenic polymers when exposed to UV radiation. These surface effects drastically reduce the life expectancy of materials that require maximum transmission of visible light, such as Plexiglas and greenhouse windows, solar energy collectors, and streetlamp globes.

Several different modes of damage occur concurrently. However, depending on the application of the polymer, one or more of such properties may be important. Exhibit 13-3 gives the critical mode of damage and one or more secondary modes of damage identified for selected applications of polymers. The critical mode of damage is defined as the degree of damage that renders the material "unacceptable" at the shortest duration of exposure, thus reducing the polymer's service life.

Plastic Compounds

Polymer resins are rarely, if ever, used by themselves in any application. To optimize the properties demanded by a given application and to enable the product to be easily fabricated, a number of other "ingredients" are added to the polymer to obtain a "compound." The nature of the non-polymer ingredients in a compound and the ratio in which they are mixed will depend on the processing technique, the grade of polymer, and the desired properties in the end product.

EXHIBIT 13-3

Modes of Damage Experienced by Polymers Used in Outdoor Applications

Polymer	Application	Damage
Polyvinyl chloride	siding, window frames	[+ yellowing] + chalking - impact properties - tensile properties + surface distortion
	pipes	[- burst pressure] - impact properties + yellowing
	roofing materials	[+ brittleness]
	automobile upholstery	+ discoloration
Unsaturated polyethylene	outdoor surfaces	[+ surface erosion] + discoloration - strength
Polyethylene/polypropylene	irrigation pipe, outdoor furniture synthetic turf, stadium seats, packaging	[+ brittleness] - tensile properties - electrical properties
Polycarbonates	glazing material	[+ yellowing] + loss of transparency

\+ = increase
\- = decrease
[ ] = brackets indicate critical mode of damage

Source: Andrady, A., "Analysis of Technical Issues Related to the Effect of UV-B on Polymers," Research Triangle Institute, Research Triangle Park, N.C., March 1986.

An example of a rigid PVC siding compound is given in Exhibit 13-4.

The fabrication of the siding involves feeding the melted compound through a slit die, a process where the polymer is heated and sheared. Therefore a heat stabilizer is usually used in the compound. The lubricant prevents sticking of melt to metal parts in the processing machinery. A suitable rubber is added as an impact modifier to reduce the brittleness of PVC resin. The processing aid is added to improve the melt processing characteristics while the chalk is added to cheapen the compound. Titanium dioxide is the light stabilizer. As explained in the previous sections, several polymers when exposed to sunlight (even under current UV conditions), would degrade, some of them rapidly. Therefore, stabilizers such as titanium dioxide are used to reduce the damage from exposure to light. Any depletion in the stratospheric ozone with potential increase in the UV-B radiation would accelerate the degradation process.

Light Stabilizers in Polymer Products

Light stability in polymeric materials is achieved by the inclusion of an appropriate "light stabilizer" in a polymer compound. Light stabilizers are substances that absorb the light in the UV-B range of the spectrum very efficiently. When incorporated into a transparent polymer matrix, the stabilizer molecules compete with the polymer molecules for the available light. Light absorbed by the UV-absorber molecules is harmlessly dissipated and does not lead to any damage of the polymer matrix. For best results the light absorber should be soluble in polymer, absorb light in the UV-B range of the spectrum, and have a very high molar extinction coefficient (so that it is effective at relatively low concentrations).

Three different methods are used to achieve light stability. The first method involves use of UV-absorbing compounds such as 2-hydroxy-benzophenones, 2-hydroxyphenylbenzotriazoles, 2-hydroxyphenyl-S-triazines and derivatives of phenyl salicylates (Heller 1969). These compounds absorb and dissipate the light without degrading the polymer.

A second approach is to prevent light from reaching the bulk of the polymer (light shielding) by opacification of the matrix. Inclusion of a light absorbing (or light reflecting) insoluble pigment in the matrix prevents the light from penetrating the bulk of the polymer. However, a fraction of surface layer is unprotected and is therefore affected by light. Titanium dioxide absorbs UV-B radiation very effectively and is used in PVC compositions as a light screener. Other pigments used as light screeners include zinc oxide, magnesium oxide, lead carbonate, and barium sulfate. One of the most effective light screeners is carbon black. Used in appropriate concentrations and adequately dispersed in the matrix, the small-sized carbon black particles impart excellent light stability in polyethylene formulations. Exhibit 13-5 gives the UV screening effectiveness of several selected pigments at concentrations of 2% in polypropylene films of 10-ml thickness (Uzelmier 1970). The screening power is given as the ratio of the weathering stability (lifetime) of the pigmented to unpigmented materials (Andrady 1986). Higher

EXHIBIT 13-4

PVC Siding Compound Composition

Component	Concentration (pph)*
PVC resin	100
Heat stabilizer	1.5
Lubricant	1
Titanium dioxide	12
Impact modifier	6
Calcium carbonate	3
Processing aid	1

* pph = parts per hundred parts resin

Source: Andrady, A., "Analysis of Technical Issues Related to the Effect of UV-B on Polymers," Research Triangle Institute, Research Triangle Park, N.C., March 1986.

ratio indicates longer stability of the polymer. For example, a polymer that is compatible with carbon black would have a lifetime 12 times longer when pigmented with carbon black and exposed to sunlight than without carbon black. On the other hand, a polymer that is compatible with cadmium yellow would have a lifetime twice as long when pigmented with cadmium yellow (at the same concentration as carbon black in the previous polymer) than without cadmium yellow.

The UV absorbance at specific wavelengths is also given in Exhibit 13-5. This is an indication of how well the pigment is able to absorb the light. Higher absorbance for titanium dioxide (0.92 at 300 nm) than for iron oxide (0.29 at 300 nm) means that at the same pigment concentration (2%), titanium dioxide is able to absorb more light than iron oxide.

The third approach to achieve light stability does not prevent or control the interaction of light with the polymer. Instead, the light stabilizer additive either seeks to deactivate or quench the excited state chromophores before the degradation process occurs, or acts as a free radical scavenger, which mops up the damaging free radicals as soon as they are formed. Complex chelates of nickel, for example, have been used as light stabilizers in polyolefins and are believed to act as quenchers and peroxide decomposers.

EXHIBIT 13-5

UV Screening Effectiveness of Selected Pigments

Pigment	Screening Power	Absorbance 300nm	325nm	350nm
Titanium Dioxide	2.25	0.92	0.97	1.01
Iron Oxide	3.25	0.29	0.30	0.32
Cadmium Yellow	2.0	0.36	0.36	0.36
Chromium Oxide	2.75	0.05	0.06	0.07
Carbon Black (Channel Black)	12.0	1.56	1.56	1.56

Chemical interactions limit the use of some of the above pigments in several polymers. For instance, iron oxide can be effectively used with polypropylene but not with PVC, as it catalyzes the photo-oxidation of the latter polymer (King 1968).

In recent years the use of radical scavenger molecules, particularly the very effective Hindered Amine Light Stabilizers (HALS), has gained wide industrial acceptance. Exhibit 13-6 gives the current U.S. consumption of light stabilizers in various types of plastics.

EXHIBIT 13-6

Domestic Consumption of Light Stabilizers, 1984-85

	Domestic Consumption (1000 lb)	
	1984	1985
Plastics (UV Stabilizers)*		
Polyolefins	4290	4600
Polycarbonates	352	400
PVC and related copolymers	171	180
Acrylic	165	170
Polyester	165	171
Pigment/Colorant		
Titanium Dioxide	71	272
Carbon Black	80	85
Iron Oxide	9	10
Cadmium Compounds	5	5
Chromium Compounds	5	5

*Figures for plastics do not include light shielders such as titanium dioxide

Source: Andrady, A., "Analysis of Technical Issues Related to the Effect of UV-B on Polymers," Research Triangle Institute, Research Triangle Park, North Carolina, March 1986.

DAMAGE FUNCTIONS AND RESPONSE TO DAMAGE

Depletion of the stratospheric ozone would change the spectral distribution as well as the solar radiation pattern, with a potential increase in the UV-B radiation striking the earth's surface. The magnitude of such changes on the weathering of plastics and potential damage that might occur are difficult to assess due to lack of experimental data. However, various theoretical approaches are considered to estimate the damage.

There are three possible responses to potential damage from increased UV-B radiation:

1. Add greater amount of light stabilizers to prevent further degradation of polymers.

2. Develop new or improved performance stabilizers to absorb the additional radiation.

3. Switch from polymers to alternative materials (e.g. ceramics, metal, etc.)

Several attempts have been made to estimate the increased damage to materials from potential increase in UV-B radiation. Because of the complexity of the analysis, each approach has focused on only the first response. Each approach analyzes how much additional light stabilizer would be required for a given ozone depletion (function of UV light intensity) scenario, to maintain the current level of useful life for various polymers. Thus, each approach has attempted to relate intensity of the UV light and concentration of the light stabilizer in the polymer.

Transparent Polymers (CIAP Approach)

In a research study funded by the U.S. Department of Transportation (Climatic Impact Assessment Program (CIAP)), Schultz, Gordon, and Hawkins (1974) were the first to examine the potential adverse effects of the ozone depletion on materials. Although their concern was depletion of ozone from SST flights and not from discharge of chlorofluorocarbons, their approach appears on the basis of first principles to be correct.

The CIAP approach employed the Beer-Lambert law to calculate approximate increases in UV stabilizer required to offset the effects of increased UV light (Andrady 1986). According to this law, for a homogeneous material with no scattering losses at the surface or in the bulk of the polymer, the monochromatic light absorption by the system is described as follows:

The fraction of incident monochromatic light energy absorbed is proportional to the concentration of the chromophores and to the path length of the light within the substrate.

$$\text{Log } I_t/I_o = -ec\ell \quad (13)$$

I_t = intensity of the transmitted light

I_o = intensity of the incident light

e = molar extinction coefficient (proportionality constant)

c = molar concentration of the light absorbing moiety

ℓ = thickness of the film

An increase in the incident light intensity will result in a higher light flux in the polymer; therefore, to maintain the same level of protection, the concentration of the UV absorber has to be increased. If an increase in the light intensity by a factor x required a corresponding increase in the UV absorber concentration by a factor y, the Beer-Lambert Law for the new system gives

$$\text{Log}(I_t/I_o \cdot X) = -eyc\ell \quad (14)$$

The two above equations can be combined to give

$$y = \text{Log}(x)/H + 1 \quad (15)$$

where $H = ec\ell$, is a constant.

This simple equation predicts the variation of the factor increase in the UV absorber concentration, y, with the factor increase in the intensity of light, x. An empirical observation made is that an increase in the UV light intensity by a factor of 1.5 generally requires an increase in the UV absorber concentration by a factor of 2.0.

Based on this empirical observation and the damage function (equation 15), Schultz, Gordon, and Hawkins developed the following relationship:

$$y = 1 + (\log_{10}x)/(\log_{10}1.5) \quad (16)$$

Using the above relationship and using a brash extrapolation of the world market, Schultz, Gordon, and Hawkins developed increased stabilizer requirements for various levels of ozone depletion. A market period of 50 years (1970-2020) was considered in the CIAP study to estimate the future market of plastics. The results are summarized in Exhibit 13-7.

Battelle Study

The Battelle study (Hattery, McGinniss, and Taussig 1985) was a follow-up to the CIAP study. The basic assumptions remained the same, but all economic market data used for analysis was updated using more current information.

EXHIBIT 13-7

Increased Stabilization Market
(1970-2020)

Ozone Depletion (Percent)	By 1990	By 2020
	(millions of 1974 dollars)*	
50	1,040	5,040
20	370	1,800
10	172	840
5	84	408

* Values at zero discount rate.

Source: Schultz, A., D. Gordon, and W. Hawkins, "Economic and Social Measures of Biologic and Climatic Change," CIAP Monograph 6, September 1974.

Also, a different ozone depletion scenario was used in the Battelle study. Exhibit 13-8 below shows the ozone depletion estimates used in the study.

EXHIBIT 13-8

Ozone Depletion Estimates

Year	Ozone Depletion (percent)
1985	0.0
1995	0.15
2005	0.62
2015	1.50
2025	2.84
2035	4.66
2045	7.08
2055	10.41
2065	15.44
2075	26.08

Source: EPA estimates based on emission scenario developed by EPA and modeled by Lawrence Livermore Laboratory.

For the projection of the polymer demand to the year 2075, Battelle used a simplified assumption that the growth rate ratio of UV-stabilized plastics to GDP (Gross Domestic Product) for the United States will remain constant at 1.7 percent into the 21st century.

Historical U.S. market share of the world plastic market and projection of the U.S. plastic market were used to project the world plastic market through the year 2075.

In the Battelle study, Cutchis's formula was used to estimate the effect of ozone depletion on the average UV light intensity (Cutchis 1974):

$$\log x = 0.00954D \qquad (17)$$

where x is UV light intensity factor and D is the percentage of ozone depletion.

To describe the relationship between light intensity (x) and the stabilizer concentration (y), Battelle used a mathematical formula developed by Shultz, Gorden, and Hawkins (1974):

$$\log x = 0.176\ (y-1) \tag{18}$$

The combination of the Cutchis and Shultz formuli, gave the following relationship:

$$y-1 = 0.0542D \tag{19}$$

This combined formula was used in the economic impact model.

Exhibit 13-9 gives cumulative added cost for the United States and the world in the presence of ozone depletion.

EXHIBIT 13-9

Cumulative Added Cost

Year	Ozone Depletion (percent)	U.S. (1983 $ billion)*	World (1983 $ billion)*
1985	0.0	0.0	0.0
2015	1.50	0.13	0.60
2045	7.08	2.3	14.0
2075	26.08	19.4	120.0

* Values at zero discount rate.

Source: Hattery, G., V. McGinniss, and P. Taussig "Costs Associated with Increased Ultraviolet Degradation of Polymers." BATTELLE Columbus Laboratories, Columbus, Ohio, April 1985.

Extension to Filled Polymers (Andrady/Shultz)

While the CIAP approach is sound and simple to use, its applicability is limited to the transparent, homogeneous polymers. With the exception of window glazing, polymers used outdoors are generally opaque and are often stabilized using light screeners. Therefore a parallel model based on light stabilization, applicable to opaque materials (filled polymer), was developed by the Research Triangle Institute (Andrady 1986).

A filled polymer can be described by a homogeneous resin matrix in which essentially spherical filler particles are randomly dispersed. The filler can be a pigment with high light absorptivity, so that all the light reaching the filler particle is absorbed. For simplicity, the random distribution can be described as spheres of radius r, in two dimensions, within a series of layers of thickness 2r (see Exhibit 13-10). If the pigment volume fraction is V, the number of spherical pigment particles within a lamina volume element of $y \cdot y \cdot 2r$ cm^3 is $N = 2ry^2V/(4\pi/3)r^3$.

The fraction of light obliterated in passing through the laminar is the cumulative cross-sectional area of the spheres per unit laminar area, $N\pi r^2/y^2$, which is equal to 3V/2. The surface intensity, Io, can then be related to I_ℓ, intensity at depth ℓ, as

$$I = I_o(1-3V/2)^{\ell/2r} \tag{20}$$

For light intensity increased by a factor x and a corresponding increase in the light stabilizer by a factor y, the above equation can be modified as

$$I = x \cdot I_o(1-3Vy/2)^{\ell/2r} \tag{21}$$

Using the assumption of equal residual fractional intensity at a characteristic depth of ℓ units, it can be shown that

$$\ln x = \frac{\ell}{2r} \cdot \ln((1-3V/2)/(1-3Vy/2)) \tag{22}$$

This equation has the same predictive feature as the CIAP equation but requires a knowledge of ℓ and r for its application.

An empirical observation relating x to y is needed in this case as well; however, such experimental data are not presently available for the polymers of interest. No economic damage estimates have been developed using this approach.

Comprehensive Approach (Andrady 1986)

While the two approaches described previously can be used for clear or filled polymers to determine the amount of additional stabilizer requirements

EXHIBIT 13-10

Diagrammatic Representation of the Effect of Pigment/Fillers as Light Shield. (Monodisperse Spherical Filler)

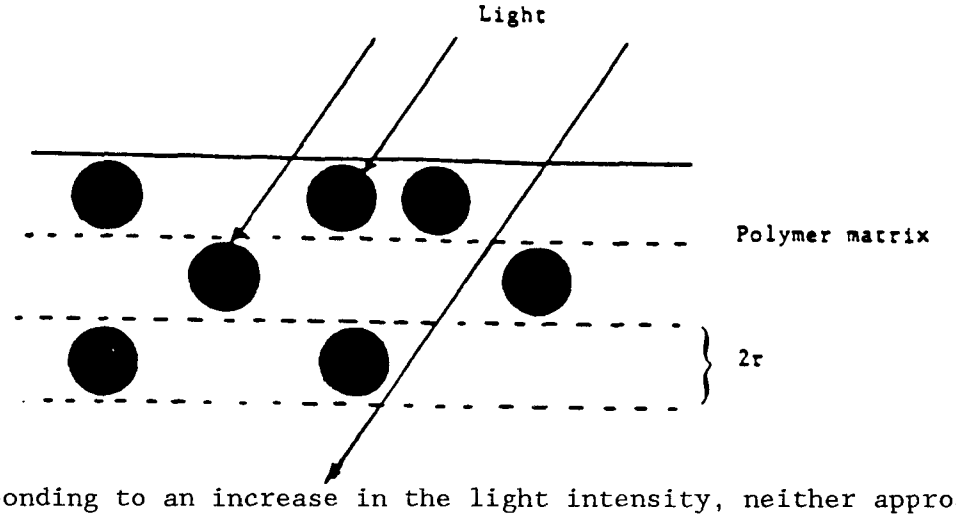

corresponding to an increase in the light intensity, neither approach takes into account the activation spectra for degradation.

The extent (and even the nature) of damage suffered by a polymer on exposure to sunlight is markedly wavelength dependent. More appropriate methodology to obtain the damage function should include (1) source spectral distribution, (2) activation spectra, and (3) the functional relationship between the ozone concentration in the stratosphere and the spectral irradiance.

Atmospheric attenuation of sunlight is a result of several processes. The following are the three main processes: (1) Rayleigh scattering -- scattering of light due to gas molecules in the atmosphere; (2) aerosol scattering or Mie scattering caused by fine particles and fluid droplets suspended in the atmosphere; and (3) absorption by ozone. These factors should be considered in calculating the spectral distribution and intensity of light at a given location.

An activation spectra should be available for each specific polymer to assess the damage. A normalized activation spectra then can be used as a continuous weighting function describing the spectral sensitivity of a specific damage process in a given polymer.

The total damage function (index), D, for a polymer exposed to sunlight can be presented as

$$D = \int_{\lambda_0}^{\lambda_1} F(\lambda)H(\lambda)d\lambda \tag{23}$$

where $F(\lambda)$ = adjusted normalized activation spectrum (ANAS)
$H(\lambda)$ = spectral distribution of sunlight for natural weathering
λ_0, λ_1 = wavelength range of the ANAS

It is assumed that the effect of each wavelength in the range is additive, with no synergism or mutual inhibition.

If $H(\lambda)$ represents an actual measured terrestrial spectrum, then D will be a measure of the damage under current ozone layer conditions, arbitrarily defined as being deteriorated to zero extent.

The above approach of using the actual measured spectrum of the solar irradiance as the source of spectral distribution limits the usefulness of the analysis to specific localities and possibly to certain times of the year (the time when $H(\lambda)$ is a fair representation of the solar spectrum). This approach avoids various scattering coefficients and their effects. If we assume that the depletion of the ozone layer has the sole effect on the spectral distribution (with other effects being small), the damage index can be modified (D*), which will relate to damage under reduced ozone level conditions.

This requires a knowledge of the absorption coefficient of ozone. Reliable data have been published for the absorption coefficient, $A(\lambda)$ (Griggs 1968):

$$A(\lambda) = \exp\ (38.54 - 0.1237\lambda) \tag{24}$$

The effect of reduced ozone concentration on the terrestrial solar irradiance at a given wavelength can be expressed as

$$I(\lambda,c',\Theta) = I_0 \exp(-A(\lambda)c'\sec\Theta - \tau(\lambda)\sec\Theta) \tag{25}$$

where

$A(\lambda)$ = ozone absorption coefficient, equation (20)

c' = ozone concentration at reduced level

$\sec\Theta$ = approximation term for path length of light through the air mass

τ = Rayleigh scattering thickness

Θ = solar zenith angle at the location

If we neglect the Rayleigh scattering, the factor increase in the UV radiation due to ozone loss can be given by

$$I(\lambda, c', \Theta)/I_o = \exp(A(\lambda)c(1-c'/c)\sec\Theta) \tag{26}$$

where (1-c'/c) is the fractional decrease (f) in the ozone concentration.

The damage index under the conditions of ozone layer deterioration can be expressed as

$$D(f,\Theta) = \int_{\lambda_0}^{\lambda_1} F(\lambda)H(\lambda)\exp(A(\lambda)\cdot c\cdot f\cdot \sec\Theta)d\lambda \tag{27}$$

The seasonal variation of ozone concentrations, the seasonal variation of the solar zenith angle and the diurnal variation of the sun angle (time angle) should be considered while estimating the damage index for different time periods (i.e., daily, annual, seasonal, etc.) For instance, the daily damage index at a given level of ozone depletion is given by

$$D(f,\Theta)_{24} = 2\ Z \iint F(\lambda)H(\lambda)\Delta(\lambda)d\lambda dt \tag{28}$$

where $\Delta(\lambda)$ is the factor increase defined in equation (26). The value of ozone concentration c is no longer a constant but is time dependent c(t). The term Z is a constant used to convert the time angle to seconds.

Illustration of Comprehensive Approach for Polyvinyl chloride: A Case Study

Using the solar spectrum as observed at Miami, Florida, on March 23, 1985, at the solar noon, spectral distribution $H(\lambda)$ was calculated for various wavelengths. An adjusted normalized action spectrum , $F(\lambda)$, was developed using the Miami sunlight spectrum. The integral in equation (28) was evaluated numerically using a computer program. Damage function and the factor increase in the damage were calculated for several solar zenith angles at different fractional ozone depletion. The results are shown in Exhibit 13-11.

As might be expected, the factor increase in damage is higher at larger solar zenith angles and hence will be greater for higher latitudes. However, the solar irradiation is also lower at these latitudes.

The value of the damage index is very sensitive to (a) the action spectra used in its calculation, (b) the zenith angle of the sun at the location in question, and (c) the thickness of the polymer used.

EXHIBIT 13-11

Relative Damage Indices for Yellowing of PVC Under Miami (March 22nd) Conditions, at Different Extents of Ozone Layer Deterioration

Fractional Loss of Ozone	Relative Damage Index at Different Solar Zenith Angles*		
	0°	30°	60°
0.0	1.00	1.00	1.00
0.05	1.01	1.01	1.02
0.10	1.02	1.02	1.04
0.15	1.03	1.03	1.06
0.20	1.04	1.05	1.09
0.25	1.05	1.06	1.13
0.30	1.06	1.08	1.18
0.35	1.08	1.09	1.25
0.40	1.09	1.11	1.36
0.45	1.11	1.14	1.55
0.50	1.13	1.17	1.93

* Relative damage index = D/D_o where D_o is the damage index calculated for current levels of ozone; solar irradiance values used were for a surface facing south at 45°.

Source: Andrady, A., "Analysis of Technical Issues Related to the Effect of UV-B on Polymers," Research Triangle Institute, Research Triangle Park, North Carolina, March 1986.

The thickness of the polymer is an important factor. In the case of a film of the material, a fraction of the incident light is transmitted through it. Often, the transmitted light is deficient in UV radiation. In the case of a thick polymer, the light is totally absorbed but the absorption is limited to a thin surface layer of the polymer. Thus in those modes of damage involving the surface integrity, thick samples undergo as much damage as the thin films. This is true, for instance, where "yellowing" is the critical mode of damage.

Mathtech Study

This is the most recent study in which the economic damage from potential depletion of ozone was estimated. The study used the comprehensive approach developed by the Research Triangle Institute (Andrady 1986).

According to the comprehensive approach, the total damage D is given by

$$D = \int \lambda H(\lambda)\, \Delta(\lambda)\, F(\lambda)\, d\lambda \qquad \text{(equation (23))}$$

The integral might be evaluated numerically with $\Delta(\lambda) = 1$ to represent current baseline conditions. However, the lack of activation spectrum for polymers limits the usefulness of the approach. The only action spectrum available in literature relates to transparent PVC films and to type of damage other than yellowing. However, a very approximate estimate might be made using the activation spectra for polyene formation based on Reinisch, Gloria, and Andros 1970. Yellowing in PVC is a direct result of the generation of long polyene sequences.

Based on the data, the damage (D) can be estimated as

$$\mathrm{Ln}(D) = a + g(S) \qquad (29)$$

where a, g = constants
S = stabilizer concentration

For reduced ozone level, this equation can be modified further to the following form:

$$\frac{S'}{S} = \left(\frac{1}{g(S)} \cdot \ln \frac{D'}{D}\right) + 1 \qquad (30)$$

where $\frac{D'}{D}$ = factor increase in damage

$\frac{S'}{S}$ = factor increase in titanium dioxide stabilizer

S',D' = stabilizer concentration and damage at reduced ozone level

This equation allows the determination of the required concentration of the stabilizer of increased extent of damage. Applying the data available for yellowing (damage) of rigid PVC versus various stabilizer concentrations to the above equation, ranges of factor increase in damage and stabilizer concentration are calculated for PVC as illustrated in Exhibit 13-12. The same approach can be extended to other polymers and stabilizers.

To calculate the economic damage, Mathtech has maintained a hypothesis similar to the other studies, which is that producers of the PVC products will change the amount of stabilizer (titanium dioxide) in the resin compound in order to maintain quality and lifetime characteristics of their products. However, the earlier studies (Schultz, Gordon, and Hawkins 1974; Hattery, McGinniss, and Taussig 1985) did not consider how changes in compound formulation would affect production costs of PVC--which can occur in several ways. First, resource costs will be increased as more titanium dioxide is used per pound of plastic produced. Second, the change in formulation will lead to more frequent replacements of screws and barrels since titanium dioxide is abrasive in nature and its higher concentration will increase wear and tear of the machinery. Third, the change in formulation will lead to increased energy requirements for PVC processing equipment since the melt viscosity of the extrudate increases with titanium dioxide increase and will require higher energy to operate the screw. Also increased viscosity may require more lubricant and processing for successful extrusion.

In order to estimate the cumulative damage, demand for PVC was estimated using historical data and related to construction activity since PVC is used heavily in several outdoor construction activities. The supply side of the market for PVC products was determined through a model plant analysis. The information from demand and supply analyses is used to determine aggregate price indices for PVC products and subsequent economic damage.

The ozone depletion estimates were the same as those shown in Exhibit 13-8. The total PVC damage associated with ozone depletion is given in Exhibit 13-13.

The results are made for the following set of circumstances: 1) All estimates are reported in millions of 1984 dollars; 2) the factor increase in titanium dioxide concentration is computed for a zenith angle of 60°; and 3) polymer producers do not respond to the hypothesized decreases in stratospheric ozone until 10 years after the impact is observed.

As indicated so far, because of the lack of data, the Mathtech analysis is limited to PVC only. In order to provide broader coverage of potential damages, it is appropriate to consider other polymers that may be adversely affected by increased UV-B radiation.

EXHIBIT 13-12

Estimated Ranges of Factor Increase in Damage and the Factor Increase in Stabilizer Needed to Counter the Change for Yellowing of Rigid PVC Compositions

Percent Loss of Ozone	Zenith Angle 30° [a] Spring ~ Noontime		Zenith Angle 60° [a] Fall ~ Noontime	
	D'/D[b]	S'/S[c]	D'/D	S'/S
0-5	~ 1.01	1.01-1.02	1.01-1.02	1.01-1.05
5-10	1.01-1.02	1.01-1.05	1.03-1.04	1.03-1.09
10-20	1.02-1.05	1.03-1.11	1.04-1.09	1.05-1.20
20-30	1.03-1.08	1.03-1.18	1.07-1.18	1.08-1.38

[a] Zenith angles selected to reflect North American locations.

[b] D'/D = factor increase in damage

[c] S'/S = factor increase in titanium dioxide stabilizer

Source: Horst, R., K. Brown, R. Black, and M. Kianka, "The Economic Impact of Increased UV-B Radiation on Polymer Materials: A Case Study of Rigid PVC," Mathtech, Inc., Princeton, New Jersey, June 1986.

EXHIBIT 13-13
PVC Damage with Ozone Depletion
(Millions of 1984 dollars)

Estimates of PVC Consumption	Discount Rate 0%	2%	5%	10%
Low	2,440	603	97	10
Middle	4,716	1,137	174	17
High	9,158	2,159	315	27

Source: Horst, R., K. Brown, R. Black, and M. Kianka, "The Economic Impact of Increased UV-B Radiation on Polymer Materials: A Case Study of Rigid PVC," Mathtech, Inc., Princeton, New Jersey, June 1986.

The following equations, developed by Mathtech, Inc., provide future demand projections for each polymer:

$$Q = A\ (1 - \exp\ (-kT)) \tag{31}$$

For small values of parameter k, the above equation can be linearized as follows:

$$Q_T = a+b\ (T-T_0) + c(T-T_0)^2 \tag{32}$$

where Q = consumption per person in year T

T_0 = year for which the projection is made

a, b, c = parameters to be estimated.

Projections of future demands for selected polymers and selected years are provided in Exhibit 13-14. Damage to these polymers is difficult to estimate without any activation spectra. However, the magnitude of the damage is expected to be similar to that for PVC.

EFFECT OF TEMPERATURE AND HUMIDITY ON PHOTODEGRADATION

A necessary element in the discussion of damage functions missing so far is the possible role of temperature and humidity. Increasing the temperature almost always results in an increase in the rate of a chemical reaction. This is certainly true of the chemical reactions responsible for photodegradation. The extent of such an increase depends upon the energy of activation for the particular reaction. The activation energy for photodegradation of

EXHIBIT 13-14

Projections of Future Demand for Selected Years
(Thousands of Metric Tons)

Year	Acrylics	Polyester
1980	75.0	644.0
2000	148.5	1130.6
2025	179.4	1400.0
2050	186.7	1472.8
2075	190.0	1504.8

Source: Horst, R., K. Brown, R. Black, and M. Kianka, "The Economic Impact of Increased UV-B Radiation on Polymer Materials: A Case Study of Rigid PVC," Mathtech, Inc., Princeton, New Jersey, June 1986.

polypropylene in air, for instance, is 77-80 kcal/mole. That for PVC (based on polyene formation) determined by Reinisch, Gloria, and Androes (1970) was 18 kcal/mole. These values allow the estimation of approximate factor increase in the weathering reaction due to increased temperature.

The general effect of humidity or water is to increase the rate of degradation of the polymer. It is generally believed to cause slight plasticization (or softening) of the polymer matrix. This is hardly likely to be the only mechanism. Several experimental studies strongly suggest water/pigment interactions. The effect of irradiation of titanium dioxide in the presence of water was shown to generate hydrogen peroxide (Hoffmann and Savacz 1971). The deleterious effect of peroxides on polymers is well known. Thus, depending upon the chemical nature of polymer, the components of the compound, and the weathering factors, both temperature and humidity tend to increase the rate of degradation. Generalized quantitative data are not available on the polymers of interest to provide potential damage estimates.

FUTURE RESEARCH

As evident in the discussion of this chapter, there are no experimental data available on several polymers of interest to provide a good estimate of damage in polymers under increased light intensity. The EPA is currently funding a research study to evaluate the available scientific and technical information and conduct experimental as well as field studies to evaluate effects of increased UV radiation on polymers.

Polyvinyl chloride (PVC) polymers are selected for the experimental study, since PVC is the most widely used thermoplastic for outdoor applications. Two main categories of PVC formulations, (a) rigid PVCs such as those used in siding and window frames and (b) plasticized PVCs such as those used in flexible roofing membranes and cable coatings, will be studied. Typical formulations and formulations with varying amounts of titanium dioxide will be evaluated in a simulated solar radiation using a Xenon lamp source.

The field research will study the question of UV-induced material damage from a global point of view. The types of UV radiation (in terms of spectral quality) that North Americans would receive at 10%-20% ozone depletion is typical of the solar flux received at some equatorial locations at current levels of ozone. Studying the material behavior at these locations would be invaluable in estimating the effects of increased UV light at northern latitudes.

The yellowing of PVC will be the main criterion used to assess damage, although other tests may be employed as necessary. Data obtained from this research will be used to assess damage to PVCs and to estimate additional costs to stabilize PVC in the event of partial ozone depletion.

REFERENCES

Andrady, A., "Analysis of Technical Issues Related to the Effect of UV-B on Polymers," Research Triangle Institute, Research Triangle Park, North Carolina, March 1986.

Cutchins, 1974 (supply missing info)

Griggs, M., "Absorption Coefficients of Ozone in the Ultraviolet and Visible Regions," Journal of Chemical Physics, Vol. 49(2), pp. 857, 1968.

Hattery, G., V. McGinniss, and P. Taussig "Costs Associated with Increased Ultraviolet Degradation of Polymers," BATTELLE Columbus Laboratories, Columbus, Ohio, April 1985.

Heller, H., "Protection of Polymers Against Light Irradiation," European Polymer Journal, Supplementary, 105, 1969.

Horst, R., K. Brown, R. Black, and M. Kianka, "The Economic Impact of Increased UV-B Radiation on Polymer Materials: A Case Study of Rigid PVC," Mathtech, Inc., Princeton, New Jersey, June 1986.

Hoffmann, E. and A. Saracz, "Weathering of Paint Films. III. Influence of Wavelength of Radiation and Temperature on the Chalking of Latex Paints," J. Oil Color Chem. Association, Vol. 54, p. 450, 1971.

Kelen, T., Polymer Degradation, Van Nostrand Reinhold, New York, 1983.

King, A., "Ultraviolet Light: Its Effects on Plastics," Plastics and Polymers, 195, 1968.

Reinisch, R., R. Gloria, and G. Androes, Photochemistry of Macromolecules, Plenum Press, New York, 1970.

Schultz, A., D. Gordon, and W. Hawkins, "Economic and Social Measures of Biologic and Climatic Change," CIAP Monograph 6, September 1974.

Uzelmier, C., "Effects of Pigments on the Heat and Light Stability of Polypropylene," Society of Plastic Engineers, Vol 26, p. 69, 1970.

CHAPTER 14

POTENTIAL EFFECTS OF STRATOSPHERIC OZONE DEPLETION ON TROPOSPHERIC OZONE

SUMMARY

Tropospheric or ground-based ozone, 03(T), is an air pollutant formed near the earth's surface as a result of photochemical reactions involving ultraviolet radiation, hydrocarbons, nitrogen oxides, oxygen, and sunlight. At high concentrations, often found during warmer months, tropospheric ozone can adversely affect human health, agricultural crops, forests, and materials. To protect public health, the U.S. Environmental Protection Agency (EPA) has established a primary standard of 0.12 ppm (one-hour average), which is not to be exceeded more than one day per year. In 1979, EPA also determined that a secondary welfare standard, more stringent than the primary standard, was unnecessary for the protection of vegetation. Currently, EPA is reviewing available scientific and technical information to determine whether these standards are adequate to protect health and welfare.

This chapter reviews preliminary scientific information that suggests that increases in UV-B radiation may affect the rate of tropospheric ozone formation in urban areas. The results from these analyses suggest that increased ultraviolet radiation increases the rate of ground-based ozone production and acid rain precursors. Moreover, global warming, associated with ozone-depleting substances, may enhance these reactions. Further analyses of additional cities are being conducted. If these analyses confirm these results, it would appear likely that in the future more cities and regions would violate the ambient air standards and that more restrictive measures to control hydrocarbons and nitrogen oxides may be required in order to comply with current standards.

FINDINGS

1. RESULTS FROM ONE MODELING STUDY AND ONE CHAMBER STUDY SUGGEST THAT INCREASED ULTRAVIOLET RADIATION FROM OZONE DEPLETION MAY INCREASE THE RATE OF TROPOSPHERIC OZONE FORMATION.

   1a. According to these studies, increases in UV-B associated with ozone depletion would increase the quantity of ground-based ozone associated with various hydrocarbon and nitrogen oxides emission levels. Results for individual cities vary, depending on the city's location and on the exact nature of the pollution.

   1b. According to these studies, global warming would enhance the effects of increased UV-B radiation on the formation of ground-based ozone.

   1c. According to these studies, ground-based ozone would form closer to urban centers. This would cause larger populations in some cities to be exposed to peak values.

   1d. More research is needed to verify and expand the results of these initial studies.

2. PRELIMINARY RESULTS FROM ONE STUDY ALSO SUGGEST THAT LARGE INCREASES IN HYDROGEN PEROXIDE WOULD RESULT FROM INCREASED UV-B RADIATION.

   2a. If hydrogen peroxide increases as predicted in this study, the oxidizing capability potential of the atmosphere, including the formation of acid rain, would be influenced.

   2b. More research, especially a chamber study, is needed to verify this effect.

3. INCREASES IN GROUND-BASED OZONE WOULD ADVERSELY AFFECT PUBLIC HEALTH AND WELFARE.

   3a. If UV-B increases enhanced ozone production, more U.S. cities would be unable to meet health-based ground-level ozone standards, and background ozone would increase.

   3b. Crops, ecosystems, and materials would be adversely affected by increased ground-level ozone.

INTRODUCTION

Tropospheric ozone (alternatively called ground-based ozone), O3(T), is an air pollutant formed in the ambient air as a result of a series of complex photochemical reactions involving ultraviolet radiation, hydrocarbons, and nitrogen oxides emitted from mobile and stationary sources, atmospheric oxygen, and sunlight. At ambient concentrations, often measured during warmer months, O3 can adversely affect human health, agricultural crops, forests, ecosystems, and materials. Interactions of O3 with nitrogen oxides and sulfur oxides may also contribute to the formation of acidic precipitation. Typical short-term (1-hour) O3 levels range from 0.01 ppm in some isolated rural areas to as high as 0.35 ppm in one of the nation's most heavily populated metropolitan areas. Daily daylight seasonal averages in some rural areas have been reported to be 0.06 ppm and higher.

Using 1982-1984 data -- the most recent available -- 216 metropolitan statistical areas (MSAs) out of 319 (68%) have enough O3 air quality data to ascertain attainment status. Of these 216 MSAs, 119 (55%) exceed the current EPA health-based O3 standard of 0.12 ppm more than once per year. Thus, more than one-half of the MSAs with sufficient data violate the standard. Approximately 115 million people (over one-half of the total U.S. population) live in areas that exceed the standard. However, this does not mean that everyone in these areas is exposed to O3 at concentrations that exceed the standard (EPA 1986).

Of MSAs with sufficient data, about 14% (34) have a characteristic highest concentrations (CHC) of 0.16 ppm O3 or higher and over 4% (11) of MSAs have a CHC above 0.20 ppm O3. There is no clear temporal trend in O3 concentration levels in MSAs around the country, although in 1982 -- and to a lesser extent, in 1981 -- levels were generally lower than in other years during the 1979-1984 time period.

Generally, the third quarter (July-September) and seasonal (April-September) averages of the 8:00 a.m. - 4:00 p.m. daily daylight values are both in the range of 0.043-0.050 ppm O3. Statistically significant, but modest, relationships exist between peak and longer-term mean indices of O3 air quality in urban areas.

Recently, EPA (1986) reviewed scientific and technical information on the known and potential health effects of ozone. The information includes respiratory tract absorption and deposition of ozone, studies of mechanisms of O3 toxicity, effects of exposure to O3 reported in controlled human exposure, field, epidemiological, and animal toxicology studies, as well as air quality information. The results of that review suggest that:

(1) The mechanisms by which inhaled O3 may pose health risks involve (a) penetration into and absorption of O3 in various regions of the respiratory tract, (b) pulmonary response resulting from chemical interactions of O3 along the respiratory tract, and (c) extrapulmonary effects caused indirectly by effects of O3 in the lungs.

(2) The risks of adverse effects associated with absorption of O3 in the tracheobronchial and alveolar regions of the

respiratory tract are much greater than for absorption in the extrathoracic region (head). Increased exercise levels are generally associated with higher ventilation rates and increased oronasal or oral (mouth) breathing. Thus, maximum penetration and exposure of sensitive lung tissue occurs when heavily exercising individuals are exposed to O3.

(3) Factors that affect susceptibility to O3 exposure are activity level and environmental stress (e.g., humidity, high temperature).

(4) The major subgroups of the population at greatest risk to the effects of O3 include: (a) individuals with pre-existing respiratory disease (e.g., asthmatics and persons with chronic obstructive lung disease or allergies), (b) "responders," who are otherwise healthy individuals, both adults and children, but experience significantly greater group mean lung function response to O3 exposure, and (c) any individual exercising heavily during exposure to O3.

(5) The major health concerns associated with exposure to O3, in approximate order of strength of the data base include:

(a) alterations in pulmonary function;

(b) symptomatic effects;

(c) effects on work performance;

(d) aggravation of pre-existing respiratory disease;

(e) morphological effects (lung structure damage);

(f) altered host defense systems (i.e., increased susceptibility to respiratory infection); and

(g) extrapulmonary effects (e.g., effects on blood enzymes, central nervous system, liver, endocrine system).

(6) The most useful exposure-response information is from controlled human exposure and field studies that provide a quantitative relationship between alterations in pulmonary function and O3 exposure concentrations.

The EPA (1986) document came to the following conclusions on vegetation impacts:

(1) The mechanisms by which O3 may injure plants and plant communities include (a) absorption of O3 into leaf through stomata followed by diffusion through the cell wall and membrane, (b) alteration of cell structure and

function, as well as critical plant processes, resulting from the chemical interaction of O3 with cellular components, and (c) occurrence of secondary effects including reduced growth and yield and altered carbon allocation;

(2) The magnitude of the O3-induced effects depends upon the physical and chemical environment of the plant, as well as various biological factors (including genetic potential, the developmental age of the plant and interaction with plant pests);

(3) Effects of O3 on vegetation and ecosystems have been demonstrated to occur from both short-term and long-term exposures. Although there are a limited number of studies in which short-term (1-2 hour) exposures have resulted in growth and yield reduction, there is a growing body of evidence that repeated peaks above a given level are important in eliciting plant response;

(4) Concerning long-term exposures, the bulk of the evidence indicates that growth and yield losses occur in several plant species exposed to seasonal concentrations of O3, typically characterized as the daily daylight mean over the growing season. In addition, evidence indicates that forests experience cumulative stress as a result of chronic exposure to O3. Exhibit 14-1 summarizes the range of O3 levels and exposure times required to induce 5% and 20% foliar injury. Exhibit 14-2 (EPA 1986) provides a more complete survey; and

(5) Damage to materials is another effect of O3. There appears to be no threshold level below which material damage will not occur; the slight acceleration of the aging processes of materials occurs at the level of the proposed standard. The materials known to be most susceptible to ozone attack are elastomers, textile fibers and dyes, and certain types of paint.

POTENTIAL EFFECTS OF ULTRAVIOLET RADIATION AND INCREASED TEMPERATURES ON GROUND-BASED OZONE

Recently, Whitten and Gery (1986) conducted a preliminary investigation into the potential changes in urban ozone levels because of an increase in solar ultraviolet (UV) radiation resulting from reductions in the stratospheric ozone layer. Estimates were also made of the effects on urban ozone chemistry resulting from a general warming of the lower atmosphere. The focus of this study was the effect of reductions in stratospheric ozone by as much as 30 percent of (1) peak ozone concentrations in urban areas and (2) the attendant control requirements predicted by a modified version of the Empirical Kinetics Modeling Approach (EKMA). The model used in this study was the simple trajectory model used in the EKMA. This model was developed by the EPA and is widely used to assess the effectiveness of emission control scenarios to abate urban ozone.

EXHIBIT 14-1

Ozone Concentrations for Short-Term Exposures That Produce 5% or 20% Injury to Vegetation Growth Under Sensitive Conditions[1]

Exposure Time, Hours	Ozone Concentrations (ppm) that may Produce 5% (20%) Injury		
	Sensitive Plants	Intermediate Plants	Less Sensitive Plants
0.5	0.35 to 0.50 (0.45 to 0.60)	0.55 to 0.70 (0.65 to 0.85)	≥0.70 (0.85)
1.0	0.15 to 0.25 (0.20 to 0.35)	0.25 to 0.40 (0.35 to 0.55)	≥0.40 (0.55)
2.0	0.09 to 0.15 (0.12 to 0.25)	0.15 to 0.25 (0.25 to 0.35)	≥0.30 (0.40)
4.0	0.04 to 0.09 (0.10 to 0.15)	0.10 to 0.15 (0.15 to 0.30)	≥0.25 (0.35)
8.0	0.02 to 0.04	0.07 to 0.12	≥0.20 (0.30)

[1] The concentrations in parentheses are for the 20% injury level.

Source: EPA (1986), p. X-4.

EXHIBIT 14-2

Ozone Concentrations at Which Significant Yield Losses Have Been Noted for a Variety of Plant Species Exposed Under Various Experimental Conditions

Plant Species	Exposure Duration	Yield Reduction, % of Control	O_3 Concentration (ppm)	Reference
Alfalfa	7 hr/day, 70 days	51, top dry wt	0.10	Neely et al., 1977
Alfalfa	2 hr/day, 21 day	16, top dry wt	0.10	Hoffman et al., 1975
Pasture grass	4 hr/day, 5 days/wk, 5 wk	20, top dry wt	0.09	Horsman et al., 1980
Ladino clover	6 hr/day, 5 days	20, shoot dry wt	0.10	Blum et al., 1982
Soybean	6 hr/day, 133 days	55, seed wt/plant	0.10	Heagle et al., 1974
Sweet corn	6 hr/day, 64 days	45, seed wt/plant	0.10	Heagle et al., 1972
Sweet corn	3 hr/day, 3 days/wk, 8 wk	13, ear fresh wt	0.20	Oshima, 1973
Wheat	4 hr/day, 7 day	30, seed yield	0.20	Shannon and Mulchi, 1974
Radish	3 hr	33, root dry wt	0.25	Adedipe and Ormrod, 1974
Beet	2 hr/day, 38 days	40, storage root dry wt	0.20	Ogata and Maas, 1973
Potato	3 hr/day, every 2 wk, 120 days	25, tuber wt	0.20	Pell et al., 1980
Pepper	3 hr/day, 3 days/wk, 11 wk	19, fruit dry wt	0.12	Bennett et al., 1979
Cotton	6 hr/day, 2 days/wk, 13 wk	62, fiber dry wt	0.25	Oshima et al., 1979
Carnation	24 hr/day, 12 days	74, no. of flower buds	0.05-0.09	Feder and Campbell, 1968
Coleus	2 hr	20, flower no.	0.20	Adedipe et al., 1972
Begonia	4 hr/day, once every 6 days for a total of 4 times	55, flower wt	0.25	Reinert and Nelson, 1979
Ponderosa pine	6 hr/day, 126 days	21, stem dry wt	0.10	Wilhour and Neely, 1977
Western white pine	6 hr/day, 126 days	9, stem dry wt	0.10	Wilhour and Neely, 1977
Loblolly pine	6 hr/day, 28 days	18, height growth	0.05	Wilhour and Neely, 1977
Pitch pine	6 hr/day, 28 days	13, height growth	0.10	Wilhour and Neely, 1977
Poplar	12 hr/day, 5 mo	+1333, leaf abscission	0.041	Wilhour and Neely, 1977
Hybrid poplar	12 hr/day, 102 days	58, height growth	0.15	Patton, 1981
Hybrid poplar	8 hr/day, 5 day/wk, 6 wk	50, shoot dry wt	0.15	Patton, 1981
Red maple	8 hr/day, 6 wk	37, height growth	0.25	Dochinger and Townsend, 1979
American sycamore	6 hr/day, 28 days	9, height growth	0.05	Kress and Skelly, 1982
Sweet gum	6 hr/day, 28 days	29, height growth	0.10	Kress and Skelly, 1982
White ash	6 hr/day, 28 days	17, total dry weight	0.15	Kress and Skelly, 1982
Green ash	6 hr/day, 28 days	24, height growth	0.10	Kress and Skelly, 1982
Willow oak	6 hr/day, 28 days	19, height growth	0.15	Kress and Skelly, 1982
Sugar maple	6 hr/day, 28 days	12, height growth	0.15	Kress and Skelly, 1982

Whitten began by investigating how the ozone formation processes in the lower troposphere would be affected by increased UV transmission through the atmosphere. From preliminary work, it became evident that the photolysis channel of formaldehyde that leads to radical products is selectively enhanced at a higher UV flux. Formaldehyde emissions are products of incomplete combustion, and formaldehyde is a major intermediate oxidation product from virtually all organic molecules. Radicals from formaldehyde photolysis provide the main source of radicals needed to drive the chain reactions that generate photochemical ground-based ozone (Whitten 1983); therefore, an increase in the rate of photolysis will have a bearing on the design of future control strategies.

The photolysis of ozone to electronically-excited oxygen atoms is thought to be the second most important source of the radicals that drive smog formation. However, the role of ozone photolysis is different from that of formaldehyde because ozone is the principal ingredient of ground-based ozone. At low levels of oxidation potential, the excited oxygen atoms tend to accelerate photochemical reactions, making the atmospheric chemistry more efficient in generating ozone from minimal precursor emissions. However, at the higher or more severe ozone levels, the excess radicals can partially suppress the ozone peak, making the precursors seem less efficient in generating ozone. Other photolysis rates can also be affected, but their contribution to smog formation is less important.

A specific increase in formaldehyde photolysis to radical products is difficult to determine accurately for a number of reasons. Atmospheric photolysis rates have often been calculated in 10-nm wavelength intervals. However, the accurate calculation of formaldehyde photolysis requires fine spectral resolution for both the formaldehyde absorption cross-section and the surface solar flux (related to the ozone absorption cross-section). Only in this manner can a comparison of the respective fine structures be performed. Near-ground solar flux data of high resolution and known stratospheric ozone abundance have not been readily available. Hence, Whitten and Gery (1986) estimated surface solar fluxes using low-resolution information provided by the National Aeronautics and Space Administration.

Using the spectral data, Whitten and Gery (1986) estimated formaldehyde and ozone photolysis rates as a function of zenith angle and ultraviolet flux changes due to stratospheric ozone depletion. The estimated photolysis rates for formaldehyde, coupled with the information compiled for surface ozone photolysis, provide the inputs needed to calculate diurnal photolysis rates for projected future ozone column densities. This information is used to evaluate the future impact of stratospheric ozone changes on near-surface ground-based ozone formation.

The preliminary results of the possible effects of increased ultraviolet radiation on urban ground-based ozone are based on simulation of atmospheric conditions for three urban cities:

(1) Nashville -- because it is nearly in compliance with the 0.12 ppm federal ozone standard.

(2) Philadelphia -- to represent cities that require moderate control (30%-50% reduction in organic precursors) to achieve the 0.12 ppm standard.

(3) Los Angeles -- because of the severity of the exceedance of the ozone standard in that region.

Present-day estimates assume a total ozone column of 300 Dobson Units (DU) and future predictions assume a total ozone column of 250 and 200 DU. A 33% decrease in total ozone column would increase ozone photolysis by approximately a factor of two, and increase formaldehyde photolysis to radical products by nearly 20%. Both of these increases are approximations because of uncertainties regarding the spectral fine structure and other factors.

The effects of these photolysis rate increases are given in Exhibit 14-3 for background temperatures of 298 and 302 Kelvin (K). For all three cities, the model predicts higher ozone concentrations resulting either from increases in temperature or decreases in the Dobson number. The magnitude of the increases in ozone is apparently a function of local hydrocarbon-to-nitrogen-oxide ratio, reactivity, meteorology, and emission distribution. The linearity of the response to stratospheric ozone depletion is not general. For the Los Angeles case, the increases in ozone are moderate and quite linear with decreasing Dobson number. For the Philadelphia case, ozone is predicted to increase progressively as the Dobson number declines; that is, only a modest increase in ozone is seen for a decline in Dobson number from 300 to 250 units, but a more dramatic increase in ozone is seen when the Dobson number declines from 250 to 200 units. For the Nashville case, the increases are all very dramatic and the linearity exists only if temperature does not increase. At the "current" temperature of 298K, the simulated urban ozone tends to increase linearly with Dobson number decrease; but at the warmer 302K temperature, the simulated ozone increases more for the first 50-unit Dobson change than for the second 50-unit change, down to the 200-unit limit of the studies. Preliminary trajectory model results suggest that peak ground-based ozone levels are reached earlier in the day, which would expose larger populations to peak values. Hydrogen peroxide increased from approximately 1.7 ppb to 3.3 ppb in Los Angeles and from 0.19 ppb to approximately 3.0 ppb in Philadelphia for a 100-unit change in Dobson. These later changes suggest significant potential impacts for ozone depletion on acid rain formation.

The effects of a 4K increase in temperature are most pronounced in the Los Angeles and Nashville simulations where 14 to 23 ppb increases in simulated ozone peaks are predicted. The effects of a combined temperature increase and reduced Dobson number appear to be additive, if not synergistic, especially for the Nashville simulations. When a 4K temperature increase is combined with only a 50-unit Dobson reduction, the simulated ozone peak jumps from a base value of 0.13 ppm to over 0.18 ppm ozone. See Exhibit 14-4.

CONCLUSIONS AND FUTURE RESEARCH DIRECTIONS

The preliminary study (Whitten and Gery 1986) was limited in several ways because the primary focus was on the atmospheric chemistry of ozone formation (e.g., potential changes in acid rain were not addressed). (Although the effects of local warming and increased ultraviolet radiation were addressed in the preliminary study, increases in air pollution such as ground-based ozone and

EXHIBIT 14-3

Ozone Concentrations Predicted for Changes in Dobson Number and Temperature for Three Cities (ppm)

City	Ozone Concentrations					
	298K			302K		
	300 DU	250 DU	200 DU	300 DU	250 DU	200 DU
Los Angeles[a/]	0.288	0.301	0.315	0.306	0.318	0.331
Philadelphia	0.112	0.127	0.149	0.122	0.134	0.159
Nashville	0.130	0.161	0.195	0.146	0.184	0.215

[a/] For Los Angeles, values under 298K used actual hourly temperatures, and values under 302K are from simulations using those temperatures increased by 4K.

Whitten began by investigating how the ozone formation processes in the lower troposphere would be affected by increased UV transmission through the atmosphere. From preliminary work, it became evident that the photolysis channel of formaldehyde that leads to radical products is selectively enhanced at a higher UV flux. Formaldehyde emissions are products of incomplete combustion, and formaldehyde is a major intermediate oxidation product from virtually all organic molecules. Radicals from formaldehyde photolysis provide the main source of radicals needed to drive the chain reactions that generate photochemical smog (Whitten 1983); therefore, an increase in the rate of photolysis will have a bearing on the design of future control strategies.

The photolysis of ozone to electronically-excited oxygen atoms is thought to be the second most important source of the radicals that drive smog formation. However, the role of ozone photolysis is different from that of formaldehyde because ozone is the principal ingredient of photochemical smog. At low levels of oxidation potential, the excited oxygen atoms tend to accelerate smog reactions, making the atmospheric chemistry more efficient in generating ozone from minimal precursor emissions. However, at the higher or more severe ozone levels, the excess radicals can partially suppress the ozone peak, making the precursors seem less efficient in generating ozone. Other photolysis rates can also be affected, but their contribution to smog formation is less important.

A specific increase in formaldehyde photolysis to radical products is difficult to determine accurately for a number of reasons. Atmospheric photolysis rates have often been calculated in 10-nm wavelength intervals. However, the accurate calculation of formaldehyde photolysis requires fine spectral resolution for both the formaldehyde absorption cross-section and the surface solar flux (related to the ozone absorption cross-section). Only in this manner can a comparison of the respective fine structures be performed. Near-ground solar flux data of high resolution and known stratospheric ozone abundance have not been readily available. Hence, Whitten and Gery (1986) estimated surface solar fluxes using low-resolution information provided by the National Aeronautics and Space Administration.

Using the spectral data, Whitten and Gery (1986) estimated formaldehyde and ozone photolysis rates as a function of zenith angle and ultraviolet flux changes due to stratospheric ozone depletion. The estimated photolysis rates for formaldehyde, coupled with the information compiled for surface ozone photolysis, provide the inputs needed to calculate diurnal photolysis rates for projected future ozone column densities. This information is used to evaluate the future impact of stratospheric ozone changes on near-surface smog formation.

The preliminary results of the possible effects of increased ultraviolet radiation on urban smog are based on simulation of atmospheric conditions for three urban cities:

(1) Nashville -- because it is nearly in compliance with the 0.12 ppm federal ozone standard.

(2) Philadelphia -- to represent cities that require moderate control (30%-50% reduction in organic precursors) to achieve the 0.12 ppm standard.

(3) Los Angeles -- because of the severity of the exceedance of the ozone standard in that region.

Present-day estimates assume a total ozone column of 300 Dobson Units (DU) and future predictions assume a total ozone column of 250 and 200 DU. A 33% decrease in total ozone column would increase ozone photolysis by approximately a factor of two, and increase formaldehyde photolysis to radical products by nearly 20%. Both of these increases are approximations because of uncertainties regarding the spectral fine structure and other factors.

The effects of these photolysis rate increases are given in Exhibit 14-3 for background temperatures of 298 and 302 Kelvin (K). For all three cities, the model predicts higher ozone concentrations resulting either from increases in temperature or decreases in the Dobson number. The magnitude of the increases in ozone is apparently a function of local hydrocarbon-to-nitrogen-oxide ratio, reactivity, meteorology, and emission distribution. The linearity of the response to stratospheric ozone depletion is not general. For the Los Angeles case, the increases in ozone are moderate and quite linear with decreasing Dobson number. For the Philadelphia case, ozone is predicted to increase progressively as the Dobson number declines; that is, only a modest increase in ozone is seen for a decline in Dobson number from 300 to 250 units, but a more dramatic increase in ozone is seen when the Dobson number declines from 250 to 200 units. For the Nashville case, the increases are all very dramatic and the linearity exists only if temperature does not increase. At the "current" temperature of 298K, the simulated urban ozone tends to increase linearly with Dobson number decrease; but at the warmer 302K temperature, the simulated ozone increases more for the first 50-unit Dobson change than for the second 50-unit change, down to the 200-unit limit of the studies. Preliminary trajectory model results suggest that peak smog levels are reached earlier in the day, which would expose larger populations to peak values. Hydrogen peroxide increased from approximately 1.7 ppb to 3.3 ppb in Los Angeles and from 0.19 ppb to approximately 3.0 ppb in Philadelphia for a 100-unit change in Dobson. These later changes suggest significant potential impacts for ozone depletion on acid rain formation.

The effects of a 4K increase in temperature are most pronounced in the Los Angeles and Nashville simulations where 14 to 23 ppb increases in simulated ozone peaks are predicted. The effects of a combined temperature increase and reduced Dobson number appear to be additive, if not synergistic, especially for the Nashville simulations. When a 4K temperature increase is combined with only a 50-unit Dobson reduction, the simulated ozone peak jumps from a base value of 0.13 ppm to over 0.18 ppm ozone. See Exhibit 14-4.

CONCLUSIONS AND FUTURE RESEARCH DIRECTIONS

The preliminary study (Whitten and Gery 1986) was limited in several ways because the primary focus was on the atmospheric chemistry of ozone formation (e.g., potential changes in acid rain were not addressed). (Although the effects of local warming and increased ultraviolet radiation were addressed in the preliminary study, increases in air pollution such as smog and acid rain can only be addressed through more extensive modeling using more complex atmospheric models). However, the simple, moving box model remains applicable in the more extensive modeling.

EXHIBIT 14-3

Ozone Concentrations Predicted for Changes in Dobson Number and Temperature for Three Cities (ppm)

City	Ozone Concentrations					
	298K			302K		
	300 DU	250 DU	200 DU	300 DU	250 DU	200 DU
Los Angeles[a/]	0.288	0.301	0.315	0.306	0.318	0.331
Philadelphia	0.112	0.127	0.149	0.122	0.134	0.159
Nashville	0.130	0.161	0.195	0.146	0.184	0.215

[a/] For Los Angeles, values under 298K used actual hourly temperatures, and values under 302K are from simulations using those temperatures increased by 4K.

EXHIBIT 14-4

Global Warming Would Exacerbate Effects of Depletion on Ground-Based Ozone in Nashville

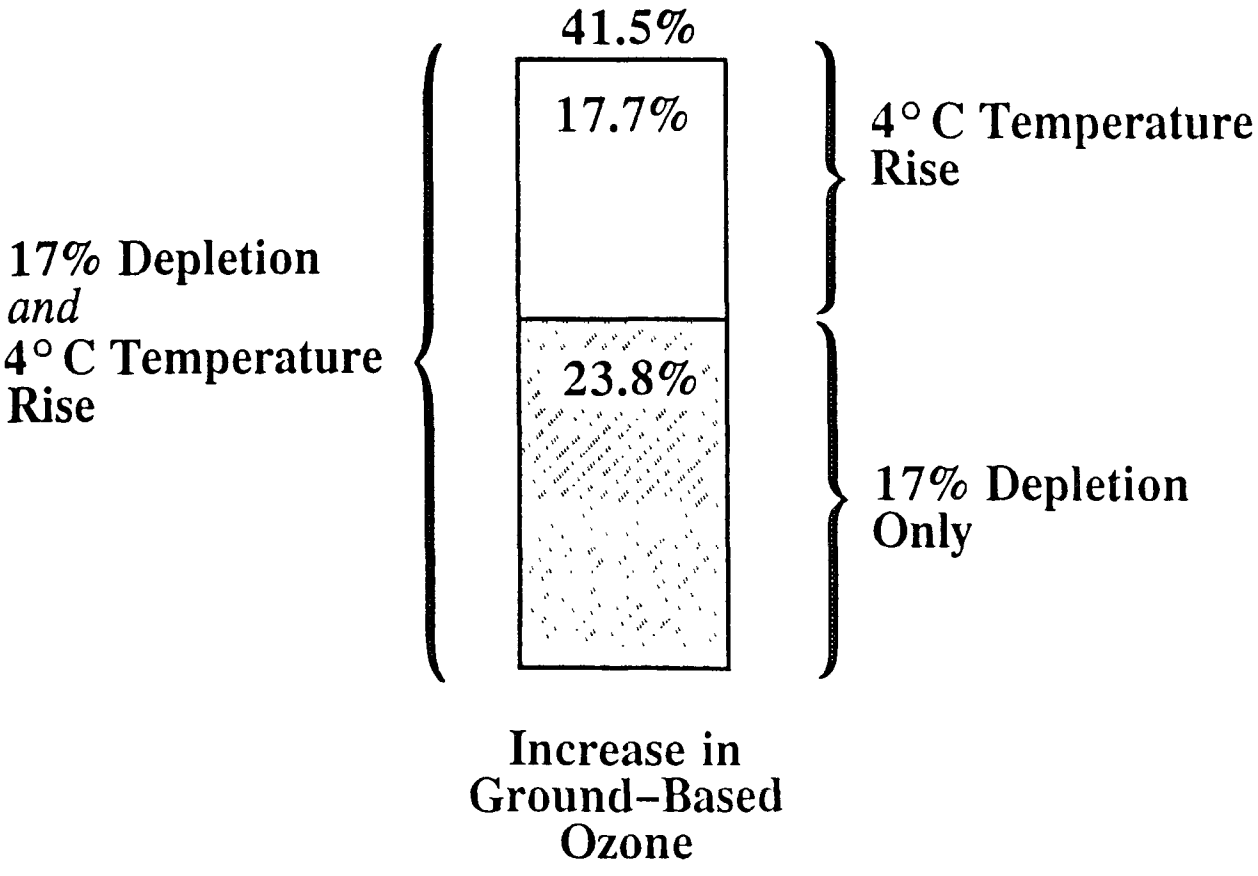

Source: Adapted from Whitten and Gery (1986).

acid rain can only be addressed through more extensive modeling using more complex atmospheric models). However, the simple, moving box model remains applicable in the more extensive modeling.

Although the initial study involved the use of only one atmospheric chemical mechanism, the Carbon Bond Mechanism (CBM), the key reactions are virtually identical in all currently-accepted atmospheric mechanisms. Hence, it can be expected that other mechanisms would show the same or similar responses to the global effects. Thus, the use of the CBM is not considered a serious limitation of the current work. However, the increased radiation effects studied could not utilize high resolution spectral data even though the preliminary study seemed to show a need to use such data.

Thus far, atmospheric modeling has addressed only three trajectories, one each in three cities. Three cities does not constitute an adequate sample size for characterizing the potential range of conditions affected by these global effects. Although the model is sensitive to initial and boundary conditions, these conditions were not varied, even though the hypothesized global effects would affect such conditions. The data for initial and boundary conditions were primarily composed of air from upwind cities or air recirculated from the day before. Emissions were not varied to account for local warming, even though many emissions increase with temperature. Climate and other meteorological changes would affect important factors such as mixing height and wind flow patterns. These possible changes were also not addressed in the preliminary study.

A very important finding of the preliminary study is the increased rate of smog formation due to increased ultraviolet radiation. Even if the peak ground-based ozone concentration is not affected, the increased rate of formation will move the high concentrations of ground-based ozone closer to the precursor emissions where the population density is invariably higher. Hence, the number of people exposed to high ground-based ozone concentrations would increase. This exposure effect is not addressed in the preliminary study. A grid type model is more appropriate for such exposure studies.

In summary, the following limitations of the preliminary study are noted:

- Effects on pollutants other than urban ozone (tropospheric ozone) were not addressed; acid rain may be affected by global effects.
- The chemical effects were calculated using low resolution spectral data; high resolution data appear to be needed.
- Since only three cities were studied, the range of conditions most affected by global effects could not be elucidated.
- Multi-day effects such as inter- or intracity carryover of pollutants were not addressed.

- Temperature effects on emission rates or changes in wind patterns, mixing heights, or frequency of episodic meteorological conditions were not addressed.

- Possible increases in population exposure due to increased smog levels and increased rates of ground-based ozone formation were not addressed.

Current studies attempt to address these limitations by (1) increasing the number of trajectory cases, (2) using high resolution spectral data, (3) studying the range of conditions that can possibly affect carryover of pollutants, (4) varying the emissions with temperature, (5) studying climate change effects, and (6) calculating population exposure changes. The use of an acid rain model and a grid model will be incorporated in the on-going investigations.

REFERENCES

Bass AM, LC Glasgow, C Miller, JP Jesson, and DL Filken. 1980. Planet. Space Sci. 28:675.

Bahe FC, WN Marx, U Schurath, and EP Roth. 1983. "Determination of the Absolute Photolysis Rate of Ozone by Sunlight, $O3 + \eta\nu \longrightarrow O(^1D) + O_2\ (^1\Delta g)$, at Ground Level." Institut fur Physikalische Chemie der Universitat Bonn. Bonn, W. Germany.

EPA 1986. "Review of the National Ambient Air Quality Standards for Ozone: Preliminary Assessment of Scientific and Technical Information," Office of Air Quality Planning and Standards Staff Paper. March 1986.

Whitten GZ 1983. "The chemistry of smog formation: A review of current knowledge." Environ. International 9:447-463.

Whitten GZ, KR Styles, and MW Gery. 1986. "Assessment of Existing Tropospheric UV-Radiation Data and the Effect of its Increase on Ozone Formation in the Troposphere." Monthly Technical Narrative No. 2 to U.S. Department of Interior, National Park Service, Washington, D.C.

Whitten GZ, and MW Gery. 1986. "Effects of Increased UV Radiation on Urban Ozone," Presented at EPA Workshop on Global Atmospheric Change and EPA Planning. Edited by Jeffries, H., EPA Report # 600/9-86016 July 1986.

CHAPTER 15

CAUSES AND EFFECTS OF SEA LEVEL RISE

SUMMARY

One of the most widely examined impacts of the projected global warming is the possible rise in sea level. Researchers have identified at least four mechanisms that might cause a significant rise: the warming and resulting expansion of the upper layers of the ocean, the melting of alpine glaciers, the melting of polar ice sheets in Greenland and Antarctica, and the disintegration of these land-based ice sheets. Estimates of the rise through the year 2100, in the absence of efforts to limit the greenhouse warming, range from 50 cm to over 2 m. Even the most conservative estimate implies a substantial acceleration over the 10-15 cm rise of the last century.

A rise in sea level in that range would permanently innundate wetlands and lowlands, accelerate coastal erosion, exacerbate coastal flooding, and increase the salinity of estuaries and aquifers. Although wetlands have kept pace with sea level rise in the last several thousand years, a 1- to 2-m rise would destroy a majority of U.S. coastal marshes and swamps. River deltas, such as those of the Mississippi, Ganges, and Nile rivers, appear to be particularly vulnerable.

Along the open coast, beach erosion could reach 1 to 2 m for every 1-cm rise in sea level, in addition to whatever erosion might be caused by other factors. Because buildings are generally found within 50 m of the shore, even the 30-cm rise projected for the next 40 years could threaten coastal property and the recreational use of beaches, unless additional remedial measures are implemented.

Sea level rise would also increase the vulnerability of coastal areas to flooding from storm surges and rainwater. In the area of Charleston, S.C., for example, the area now flooded once every 100 years would be flooded every 10 years if sea level rises 1.6 m. Protecting against increased flooding would require improvement or construction of levees, seawalls, and drainage facilities.

Higher water levels would also increase the salinity of estuaries and aquifers. For example, Philadelphia's drinking water intake on the Delaware River would be threatened by a 73-cm rise, as would adjacent aquifers in New Jersey that are recharged by the (currently) fresh part of the river. Construction of additional reservoirs might be necessary to offset salinity increases.

Few studies have estimated the economic significance of future sea level rise. One study suggests that the impacts of a 0.9- to 2.4-m rise by 2075 could be as great as 17% to 35% of total economic activity in the Charleston, South Carolina, area and 5% to 16% of the activity around Galveston, Texas. No one has yet estimated the potential nationwide cost of defending shorelines and other resources from the projected rise in sea level.

FINDINGS

1. THE PROJECTED GLOBAL WARMING WOULD ACCELERATE THE CURRENT RATE OF SEA LEVEL RISE BY EXPANDING THE DENSITY OF OCEAN WATER, MELTING ALPINE GLACIERS, AND EVENTUALLY INCREASING THE RATE AT WHICH POLAR ICE SHEETS MELT OR DISCHARGE ICE INTO THE OCEANS.

2. GLOBAL AVERAGE SEA LEVEL APPEARS TO HAVE RISEN 10 TO 15 CM OVER THE LAST CENTURY.

   2a. Studies of the possible contribution of thermal expansion and alpine meltwater to sea level rise, based on the 0.6°C warming of the past century, indicate that these two sources are insufficient to explain the estimated sea level rise that has occurred during this period. Consequently, some other source, such as melting of the polar ice caps, must be considered a possibility.

3. ESTIMATES OF THE RISE IN SEA LEVEL THAT COULD TAKE PLACE IF MEASURES TO LIMIT THE GLOBAL WARMING ARE NOT UNDERTAKEN RANGE FROM 10 TO 20 CM BY THE YEAR 2025, AND 50 TO 200 CM BY 2100.

   3a. According to published studies, thermal expansion of the oceans alone would increase sea level rise between about 30 cm and 100 cm by 2100, depending on the realized temperature change. This is the most certain contribution.

   3b. Melting of alpine glaciers and possibly of ice on Greenland could each contribute 10 to 30 cm through 2100, depending on the scenario. This contribution also has a high degree of likelihood.

   3c. The contribution of Antarctic deglaciation is more difficult to project. It has been estimated at between 0 and 100 cm; however, the possibilities cannot be ruled out that (1) increased snowfall could increase the size of the Antarctic ice sheet and thereby partially offset part of the sea level rise from other sources; or (2) meltwater and enhanced calving of the ice sheet could increase the contribution of Antarctic deglaciation to as much as 2 m. The Antarctic contribution to sea level rise may be more sensitive to time delays after certain threshold conditions are reached than to the magnitude of total warming.

4. OVER THE MUCH LONGER TERM (THE NEXT FEW CENTURIES) DISINTEGRATION OF THE WEST ANTARCTIC ICE SHEET MIGHT RAISE SEA LEVEL BY 6 METERS.

   4a. If a disintegration takes place, glaciologists generally believe that such a complete disintegration of the west Antarctic ice sheet would take at least 300 years, and probably at least 500 years.

   4b. A global warming might result in sufficient thinning of the Ross and Filcher-Ronne Ice Shelves in the next century to make the process of disintegration irreversible.

5. LOCAL TRENDS IN SUBSIDENCE AND EMERGENCE MUST BE ADDED OR SUBTRACTED TO GLOBAL RISK ESTIMATES IN ORDER TO ESTIMATE RELATIVE SEA LEVEL RISE AT PARTICULAR LOCATIONS.

5a. Most of the Atlantic and Gulf Coasts of the United States--as well as the Southern Pacific coast--are subsiding 10-20 cm per century.

5b. Louisiana is subsiding 1 m per century, while parts of Alaska are emerging 10-150 cm per century.

5c. Due to subsidence already occurring in areas such as Bangladesh, Bangkok, and the Nile delta, these areas are extremely vulnerable to sea level rise.

6. A SUBSTANTIAL RISE IN SEA LEVEL WOULD PERMANENTLY INUNDATE WETLANDS AND LOWLANDS, ACCELERATE COASTAL EROSION, EXACERBATE COASTAL FLOODING, AND INCREASE THE SALINITY OF ESTUARIES AND AQUIFERS.

6a. Louisiana is the state most vulnerable to a rise in sea level. Important impacts would also occur in Florida, Maryland, Delaware, New Jersey, and in the coastal regions of other states.

6b. A rise in sea level of 1 to 2 m by the year 2100 could destroy 50 percent to 80 percent of U.S. coastal wetlands.

6c. Limited studies predict that increased salinity from sea level rise would convert cypress swamps to open water and threaten drinking water supplies in areas such as Louisiana, Philadelphia, and New Jersey. Other areas, such as Southern Florida, may also be vulnerable but have not been investigated.

6d. Studies of Bangladesh and the Nile River Delta indicate that these river deltas, which are already subsiding, would be greatly affected by rising sea level, experiencing significant economic and environmental losses.

7. EROSION PROJECTED IN VARIOUS STUDIES TO RESULT FROM ACCELERATED SEA LEVEL RISE COULD THREATEN U.S. RECREATIONAL BEACHES

7a. Case studies of beaches in New Jersey, Maryland, California, South Carolina, and Florida have concluded that a 30-cm rise in sea level would result in beaches eroding 20-60 m or more. Major beach preservation efforts would be required if recreational beaches are to be maintained.

8. ACCELERATED SEA LEVEL RISE WOULD INCREASE THE DAMAGES FROM FLOODING IN COASTAL AREAS

8a. Flood damages would increase because higher water levels would provide a higher base for storm surges.

8b. Erosion would increase the vulnerability to storm waves, and decreased natural and artificial drainage would increase flooding during rainstorms.

9. ESTIMATES OF DAMAGE FROM SEA LEVEL RISE MUST CONSIDER POSSIBLE MITIGATION BY HUMAN RESPONSES

9a. The adverse impacts of sea level rise could be ameliorated through anticipatory land use planning and structural design changes.

9b. In a case study of two cities, Charleston, South Carolina, and Galveston, Texas, accelerated anticipatory planning was estimated to reduce net damages by 20 to 60 percent.

10. RELATED IMPACTS OF A GLOBAL WARMING WOULD ALSO AFFECT IMPACTS OF SEA LEVEL RISE

10a. Increased droughts might amplify the salinity impacts of sea level rise.

10b. Increased hurricanes and increased rainfall in coastal areas could amplify flooding from sea level rise.

10c. Warmer temperatures might impair peat formation of salt marshes and would enable mangrove swamps to take over areas that are presently salt marsh.

10d. Decreased northeasters might reduce damage.

11. RESEARCH OPPORTUNITIES EXIST TO IMPROVE SEA LEVEL RISE ESTIMATES AND IMPACTS

11a. The most critical areas of research for reducing the variation in estimates of future sea level rise are ice melting and runoff in Antarctica and Greenland and ice discharge.

11b. Research in glacial discharge in Antarctica should focus not just on West Antarctica, but on Pine Island and East Antarctica.

11c. An improved program of tidal gauge stations, especially in the southern hemisphere, and satellite altimetry should be used to measure sea level rise and the mass balance of ice sheets.

CAUSES OF SEA LEVEL RISE

The worldwide average sea level depends primarily on (1) the shape and size of ocean basins, (2) the amount of water in the oceans, and (3) the average density of seawater. Only the latter two factors are influenced by climate. Subsidence and emergence caused by natural factors such as isostatic and tectonic adjustments of the land surface, as well as human-induced factors such as oil and water extraction, can cause trends in relative sea level at particular locations to differ from trends in global sea level.

Past Trends in Sea Level

Hays and Pitman (1973) analyzed fossil records and concluded that over the last 100 million years, changes in mid-ocean ridge systems have caused the sea level to rise and fall over 300 m. However, Clark, Farrell, and Peltier (1978) have pointed out that these changes have accounted for sea level changes of less than 1 mm per century. No published study has indicated that this determinant of sea level is likely to have a significant impact in the next century.

The impact of climate on sea level has been more pronounced. During ice ages the glaciation of substantial portions of the northern hemisphere has removed enough water from the oceans to lower sea level 100 m below the present level during the last (18,000 years ago) and earlier ice ages (Donn, Farrand, and Ewing 1962; Kennett 1982; Oldale 1985).

Although the glaciers that once covered much of the northern hemisphere have retreated, the world's remaining ice cover contains enough water to raise sea level over 75 m (Hollin and Barry 1979). As Exhibit 15-1 shows, Hollin and Barry (1979) and Flint (1971) estimate that existing alpine glaciers contain enough water to raise sea level 30 cm or 60 cm, respectively. The Greenland and West Antarctic Ice Sheets each contain enough water to raise sea level about 8 m, and East Antarctica has enough ice to raise sea level over 60 m.

There is no evidence that either the Greenland or East Antarctic Ice Sheets have completely disintegrated in the last two million years. However, it is generally recognized that sea level was about 7 m higher than today during the last interglacial (Moore 1982; Mercer 1968; Hollin 1962), which was 1°-2° warmer than today. Because the West Antarctic Ice Sheet is marine-based and thought by some to be vulnerable to climatic warming, attention has focused on this source for the higher sea level. Mercer (1968) found that lake sediments and other evidence suggested that summer temperatures in Antarctica have been 7°-10°C higher than today at some point in the last two million years, probably during the last interglacial 125,000 years ago, and that such temperatures could have caused a disintegration of the West Antarctic Ice Sheet. However, others are not certain that marine-based glaciers are more vulnerable to climate change than land-based glaciers;[1] Robin (1985) suggests that the higher sea level during the last interglacial period may have resulted from changes in the East Antarctic Ice Sheet.

Tidal gauges have been available to measure the change in relative sea level at particular locations over the last century.[2] Studies combining these measurements to estimate global trends have concluded that sea level has risen 10-15 cm during the last century (Barnett 1984; Gornitz, Lebedeff, and Hansen 1982; Fairbridge and Krebs 1962; Hicks, Debaugh, and Hickman 1983 for the U.S.

EXHIBIT 15-1

Snow and Ice Components

	Area (10^6 km^2)	Ice Volume (10^6 km^3)	Sea Level Equivalent a/ (m)
Land ice:			
East Antarctica b/	9.86	25.92	64.8
West Antarctica c/	2.34	3.40	8.5
Greenland	1.7	3.0	7.6
Small ice caps and mountain glaciers d/	0.54	0.12	0.3 0.6
Permafrost (excluding Antarctica):			
Continuous	7.6	0.03 to	0.08 to
Discontinuous	17.3	0.7	0.17
Sea ice: Arctic e/			
Late February	14.0	0.05	
Late August	7.0	0.02	
Antarctic f/			
September	18.4	0.06	
February	3.6	0.01	
Land snow cover g/			
N. Hemisphere			
Early February	46.3	0.002	
Late August	3.7		
S. Hemisphere			
Late July	0.85		
Early May	0.07		

a/ 400,000 km^3 of ice is equivalent to 1 m global sea level.
b/ Grounded ice sheet, excluding peripheral, floating ice shelves (which do not affect sea level). The shelves have a total area of 1.62 x 10^6 km^2 and a volume of 0.79 x 10^6 km^3 (Dewey and Heim 1981).
c/ Including the Antarctic Peninsula.
d/ Flint (1971); Hollin and Barry (1979)
e/ Excluding the Sea of Okhotsk, the Baltic Sea, and the Gulf of St. Lawrence (Walsh and Johnson 1979). Maximum ice extents in these areas are 0.7 million, 0.4 million, and 0.2 million km^2, respectively.
f/ Actual ice area excluding open water (Zwally, Parkinson, and Comiso 1983). Ice extent ranges between 4 million and 20 million km^2.
g/ Snow cover includes land ice but excludes snow-covered sea ice (Dewey and Heim 1981).

Source: Meier et al. 1985, p. 242. Modified from Hollin and Barry 1979.

Coast); Exhibit 15-2 shows the sea level curve estimated by Gornitz, Lebedeff, and Hansen. Barnett (1984) found that the rate of sea level rise over the last 50 years had been about 2.0 mm/year, while in the previous 50 years there had been little change; however, the acceleration in the rate of sea level rise was not statistically significant. Emery and Aubrey (1985 and 1986) have accounted for estimated land surface movements in their analyses of tidal gauge records in Northern Europe and western North America and have found an acceleration in the rate of sea level rise over the last century.[3] Braatz and Aubrey (1987) have found that the rate of relative sea level rise on the east coast of North America accelerated after 1934.

Several researchers have investigated possible causes of current trends in sea level. Barnett (1984) and Gornitz, Lebedeff, and Hansen (1982) estimate that thermal expansion of the upper layers of the oceans resulting from the observed global warming of 0.4°C in the last century could be responsible for a rise of 0.4-0.5 mm/year. Recent analysis suggests that the warming has been 0.6°C, which would account for thermal expansion of 0.6-0.7 mm/year (Jones, Wigley, and Wright 1986). Roemmich and Wunsch (1984) examined temperature and salinity measurements at Bermuda and concluded that the 4°C isotherm had migrated 100 m downward, and that the resulting expansion of ocean water could be responsible for some or all of the observed rise in relative sea level. Roemmich (1985) showed that the warming trend 700 m below the surface was statistically significant. However, Barnett (1984) found no significant trend based on an examination of the upper layers of the ocean. Nevertheless, Braatz and Aubrey (n.d.) note that long-term steric changes in the ocean are not confined to the upper layers of the oceans, implying that the Barnett analysis does not necessarily contradict the Roemmich and Wunsch conclusion. Because one-dimensional models that cannot capture the complexities of the ocean have been used to estimate the past expansion of ocean water, these authors all caution that their results should be viewed as first approximations.

Meier (1984) estimates that retreat of alpine glaciers and small ice caps could currently contribute between 0.2 and 0.72 mm/year to sea level. The National Academy of Sciences Polar Research Board (Meier et al. 1985) concluded that existing information is insufficient to determine whether the impacts of Greenland and Antarctica are positive or zero. Thus, thermal expansion and alpine melting would explain a rise of 0.8-1.4 mm/yr, compared with the observed rise of 1.0-1.5 mm/yr. Although the estimated global warming of the last century appears at least partly responsible for the last century's rise in sea level, no study has demonstrated that global warming might be responsible for an acceleration in the rate of sea level rise.

Impact of Future Global Warming on Sea Level

Concern about a substantial rise in sea level as a result of the projected global warming stemmed originally from Mercer (1968), who suggested that the Ross and Filchner-Ronne ice shelves might disintegrate, causing a deglaciation of the West Antarctic Ice Sheet and a resulting 6- to 7-m rise in sea level, possibly over a period as short as 40 years (see also Mercer 1978).

Subsequent investigations have concluded that such a rapid rise is unlikely. Hughes (1983) and Bentley (1983) estimated that such a disintegration would take

EXHIBIT 15-2

Worldwide Sea Level in the Last Century

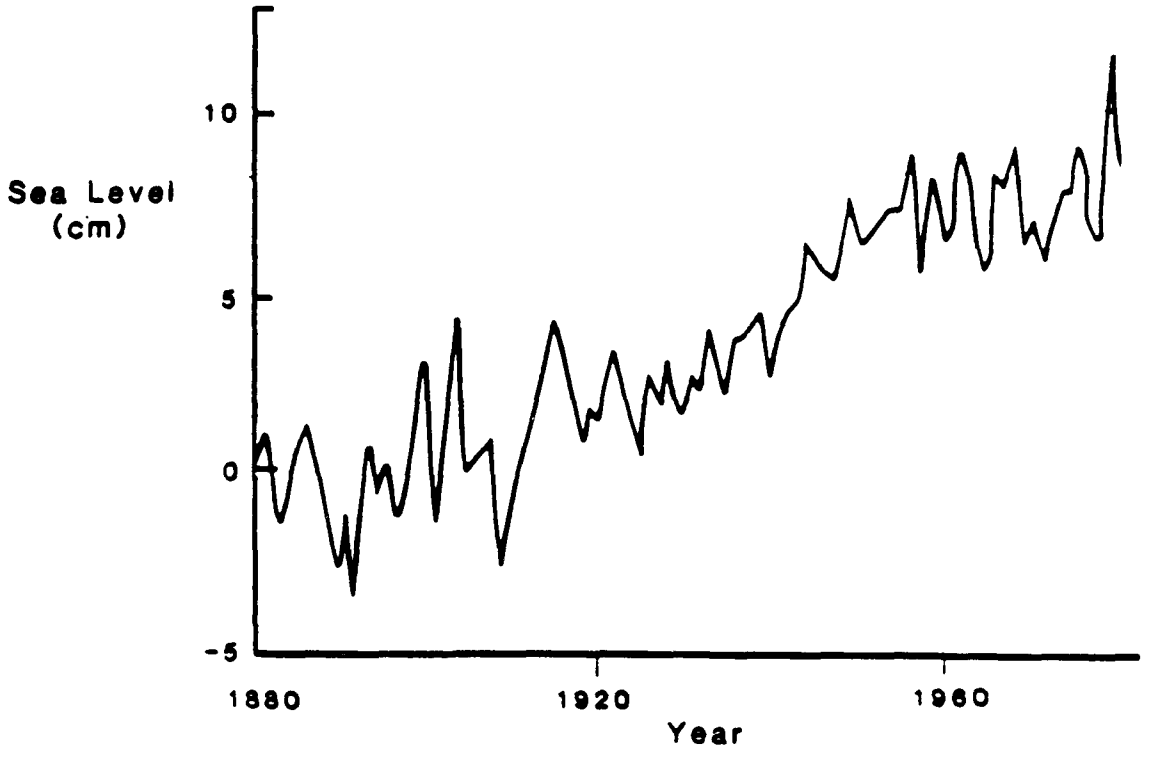

Sources: Gornitz, Lebedeff, and Hansen 1982.

at least 200 or 500 years, respectively. Other researchers have estimated that this process would take considerably longer (Fastook 1985; Lingle 1985).

Researchers have turned their attention to the magnitude of sea level rise that might occur in the next century. The best-understood factors are the thermal expansion of ocean water and the melting of alpine glaciers. In the National Academy of Sciences report Changing Climate, Revelle (1983) used the model of Cess and Goldenberg (1981) to estimate temperature increases at various depths and latitudes resulting from a 4.2°C warming by the years 2050-2060 (Exhibit 15-3). Although his assumed time constant of 33 years probably resulted in a conservatively low estimate, he estimated that thermal expansion would result in an expansion of the upper ocean sufficient to raise sea level 30 cm.

Using a model of the oceans developed by Lacis et al. (1981), Hoffman, Wells, and Titus (1986) examined a variety of possible scenarios of future emissions of greenhouse gases and global warming. They estimated that a warming of between 1° and 2.6°C could result in a thermal expansion contribution to sea level of between 12 and 26 cm by the year 2050. They also estimated that a global warming of 2.3°-7.0°C by 2100 would result in a thermal expansion of 28-83 cm.

Revelle (1983) suggested that although he could not estimate the future contribution of alpine glaciers to sea level rise, a contribution of 12 cm through 2080 would be reasonable. Meier (1984) used glacier balance and volume change data for 25 glaciers for which the available record exceeded 50 years to estimate the relationship between historical temperature increases and the resulting negative mass balances of the glaciers. He estimated that a 28-mm rise had resulted from a warming of 0.5°C and concluded that a 1.5°-4.5°C warming would result in a rise of 8-25 cm in the next century. Using these results, Meier et al. (1985) concluded that the contribution of glaciers and small ice caps to a rise in sea level through 2100 is likely to be 10-30 cm. They noted that the gradual depletion of remaining ice cover might reduce the contribution of sea level rise somewhat. However, the contribution might also be greater because the historical rise took place over a 60-year period, while the forecast period is over 100 years. Using Meier's estimated relationship between global warming and the alpine contribution, Hoffman, Wells, and Titus (1986) estimated alpine contributions through the year 2100 at 12-38 cm for a global warming of 2.3°-7.0°C.

The first published estimate of the contribution of Greenland meltwater to future sea level rise was Revelle's (1983) estimate of 12 cm through the year 2080. Using estimates by Ambach (1980 and 1982) that the equilibrium line (between snowfall accumulation and melting) rises 100 m for each 0.6°C rise in air temperature, Revelle concluded that the projected 6°C warming would be likely to raise the equilibrium line 1000 m. He estimated that such a change in the equilibrium line would result in a 12-cm contribution to sea level rise for the next century.

Meier et al. (1985) noted that the large ablation area makes Greenland a "significant potential contributor of meltwater to the ocean if climatic warming causes an increase in the rate of ablation and an upward shift of the

EXHIBIT 15-3

Temperature Increase At Various Depths and Latitudes

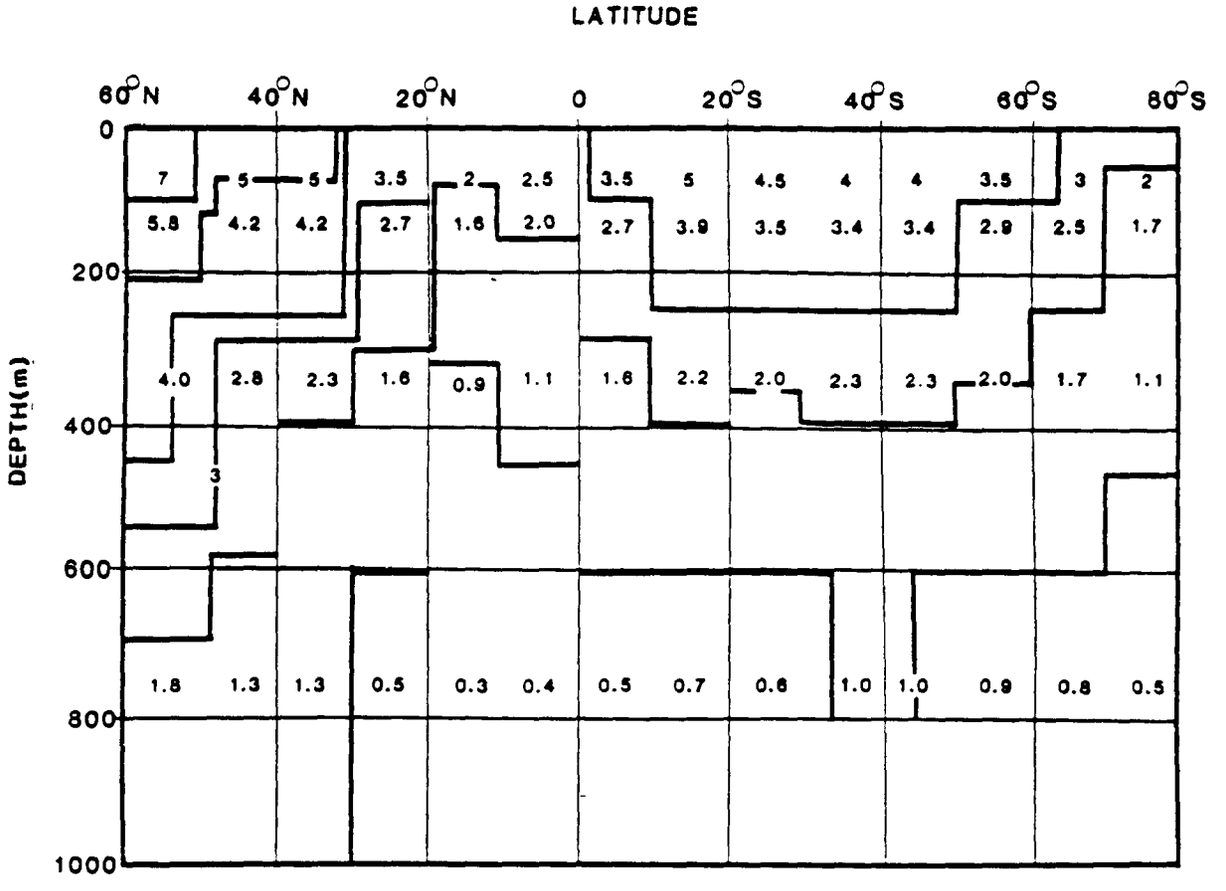

Computed average increase in ocean temperatures at particular depths and latitudes for a doubling of atmospheric carbon dioxide and probable increase in other greenhouse gases by the year 2080, based on Flohn's (1982) prognosis. Solid lines are isopleths for temperature changes. Note that the top 100 m warms 2°-7°, while at depths of 800-1000 m the warming is mostly less than 1°.

Source: Revelle (1983).

equilibrium line." They found that a 1000-m rise in the equilibrium line would result in a contribution of 30 cm through the year 2100. However, because Ambach (1985) found the relationship between the equilibrium line and temperature to be 77 m per degree (C), the panel concluded that a 500-m shift in the equilibrium line would be more likely. Based on the assumption that Greenland will warm 6.5°C by the year 2050 and that temperatures will remain constant thereafter, they estimated that such a change would contribute about 10 cm to sea level through 2100, but also noted that "for an extreme but highly unlikely case, with the equilibrium line raised 1000 m, the total rise would be 26 centimeters." Bindschadler (1985) treated the two cases as equally plausible. However, his analysis was conducted before the results of Ambach (1985) were known and he has since indicated agreement with the findings of Meier et al. (1985).[4]

Available estimates of the Greenland contribution assume that all meltwater flows into the oceans and that the ice dynamics of the glaciers do not change. Meier et al. (1985) suggested that much of the water would refreeze and therefore decrease the contribution to sea level rise. Although a change in ice dynamics might imply additional deglaciation and eventually increase the rate of sea level rise, they concluded that such changes were unlikely to occur in the next century.

The potential impact of a global warming on Antarctica in the next century is the least certain of all the factors by which a global warming might contribute to sea level rise. Meltwater from East Antarctica might make a significant contribution by the year 2100. This source could be significant since global warming is expected to be amplified in polar regions, and large parts of East Antarctica are far enough from the poles to possibly warm up such that meltwater runoff would be significant. Unfortunately, no one has estimated the likely contribution.[5] Several studies have examined "deglaciation," which also includes the contribution of ice sliding into the oceans. Bentley (1983) examined the processes by which a deglaciation of West Antarctica might occur. The first step in the process would be accelerated melting of the undersides of the Ross and Filchner-Ronne ice shelves caused by warmer water circulating underneath them. The thinning of these ice shelves could cause them to become unpinned and cause their grounding lines to retreat. Revelle (1983) concluded that the available literature suggests that the ice shelves might disappear in 100 years; the Antarctic ice streams would then flow directly into the oceans, without the back pressure of the ice shelves. Hughes (1983) and Bentley (1983) estimate that a complete disintegration of the West Antarctic Ice Sheet could take an additional 200 and 500 years, respectively.

Although a West Antarctic deglaciation would occur over a period of centuries, it is possible that an irreversible deglaciation could commence before 2050. Thomas, Sanderson, and Rose (1979) suggested that if the ice shelves thinned more than about 1 m per year, the ice would move into the sea at a sufficient speed such that even a cooling back to the temperatures of today would not be sufficient to result in a reformation of the ice shelf.

To estimate the likely Antarctic contribution for the next century, Thomas (1985) developed four scenarios of the impact of a 3°C global warming by the year 2050:

(1) For a shelf melting rate of 1 m/year with seaward ice fronts remaining at present locations--implies a rise of 28 cm by the year 2100.

(2) For a shelf melting rate of 1 m/year with ice fronts calving back to a line linking the areas where the shelf is grounded, during the 2050s--implies a rise of 1.6 m by 2100.

(3) For a scenario similar to case 1 but with a melt rate of 3 m/year--implies a rise of 1 m by 2100.

(4) For a scenario similar to case 2 but with a melt rate of 3 m/year--implies a rise of 2.2 meters by 2100.

Thomas concluded that the 28-cm rise implied by case 1 would be most likely to occur. He also stated that even if enhanced calving did occur, it would be likely to occur after 2050, "suggesting that associated sea-level rise would probably be closer to the 1 m of case 3 than the 2.2 m of case 4."

Meier et al. (1985) evaluated the Thomas study and papers by Lingle (1985) and Fastook (1985). Although Lingle estimated that the contribution to sea level rise of West Antarctica through 2100 would be 3 to 5 cm, he did not evaluate East Antarctica; Fastook made no estimate for the year 2100. Thus, the panel concluded that "imposing reasonable limits" on the Thomas model yields a range of 20 to 80 cm by the year 2100 for the Antarctic contribution. However, they also noted several factors that would reduce the amount of ice discharged into the sea: removal of the warmest ice from the ice shelves, retreat of grounding lines, and increased lateral shear stress. They also concluded that increased precipitation over Antarctica might increase the size of the polar ice sheets there. Thus, they concluded that the contribution from Antarctica could cause a rise in sea level up to 1 m or a drop of 10 cm; a rise of between 0 and 30 cm is most likely.

Exhibit 15-4 summarizes the various estimates of future global sea level rise for specific years. Revelle (1983) estimated that the rise was likely to be 70 cm, ignoring the impact of a global warming on Antarctica. He also noted that the latter contribution was likely to be 1 to 2 m per century after 2050, but declined to add that to his estimate. Meier et al. (1985) projected that the contribution of glaciers would be sufficient to raise sea level 20 to 160 cm, with a rise of "several tenths of a meter" most likely. Thus, if one extrapolates from the Revelle (1983) estimate of thermal expansion through the year 2100, the Meier et al. report predicts a rise of between 50 and 200 cm. Using a range of estimates for future concentrations of greenhouse gases, the climate's sensitivity to such increases, oceanic heat uptake, and the behavior of glaciers, Hoffman, Wells, and Titus (1986) estimated that the rise would be 10 to 21 cm by 2025 and 57 to 368 cm by 2100.

Future Trends in Local Sea Level

Although most attention has focused on projections of global sea level, impacts on particular areas would depend on local relative sea level. As Exhibit 15-5 shows, tidal gauge measurements suggest that relative sea level rises ten to twenty centimeters per century more rapidly along much of the U.S.

EXHIBIT 15-4

Estimates of Future Sea Level Rise (centimeters)

Year 2100 by Cause (Year 2085 for Revelle 1983):

	Thermal Expansion	Alpine Glaciers	Greenland	Antarctica	Total
Revelle (1983)	30	12	12	2	70
Hoffman et al. (1983)	28-115	b/	b/	b/	56-345
Meier et al. (1985) c/	-	10-30	10-30	-10-+100	50-200
Thomas (1985)	-	-	-	0-200	-
Hoffman et al. (1986)	28-83	12-37	6-27	12-220	57-368

Total Rise in Specific Years: d/

	2000	2025	2050	2075	2085	2100
Hoffman et al. (1983)						
Low	4.8	13	23	38	-	56.0
Mid-range low	8.8	26	53	91	-	144.4
Mid-range high	13.2	39	79	137	-	216.6
High	17.1	55	117	212	-	345
Hoffman et al. 1986						
Low	3.5	10	20	36	44	57
High	5.5	21	55	191	258	368

a/ Revelle attributes 16 cm to other factors.

b/ Hoffman et al. (1983) assumed that the glacial contribution would be one to two times the contribution of thermal expansion.

c/ The Meier et al. (1985) estimate includes extrapolation of thermal expansion from Revelle (1983).

d/ Only Hoffman et al. reports made year-by-year projections for the next century.

Sources: Hoffman et al. (1986); Meier et al. (1985);
Hoffman et al. (1983): Revelle (1983); Thomas (1985).

EXHIBIT 15-5

Local Sea Level Rise

Location	Historical[a/] Relative Sea Level Trend (mm/yr)	Historical[b/] Subsidence Rate (mm/yr)	Local Rise for[c/] One-Meter Global Rise by 2100 (cm)
Portland, Maine	2.3	1.1	112.6
Boston, Massachusetts	2.3	1.1	112.6
Newport, Rhode Island	2.6	1.4	116.1
New London, Connecticut	2.2	1.0	111.5
New York, New York	2.8	1.6	118.4
Sandy Hook, New Jersey	4.2	3.0	134.5
Atlantic City, New Jersey	4.0	2.8	132.2
Philadelphia, Pennsylvania	2.6	1.4	116.1
Baltimore, Maryland	3.2	2.0	123.0
Annapolis, Maryland	3.7	2.5	128.8
Hampton Roads, Virginia	4.3	3.1	135.7
Charleston, South Carolina	3.4	2.2	125.3
Fernandina, Florida	1.7	0.5	105.8
Miami Beach, Florida	2.3	1.1	112.6
Cedar Key, Florida	2.0	0.8	109.2
Pensacola, Florida	2.4	1.2	113.8
Eugene Island, Louisiana	10.0	8.8	201.2
Galveston, Texas	6.3	5.1	158.7
San Diego, California	1.9	0.7	108.0
Los Angeles, California	0.6	-0.6	93.1
San Francisco, California	1.2	0	100.0
Astoria, Oregon	-0.5	-1.7	80.5
Seattle, Washington	1.9	0.7	108.5
Juneau, Alaska	-12.9	-14.1	-62.2
Sitka, Alaska	-2.4	-3.6	58.6
Worldwide	1.2	0	100.0

a/ Based on assumed global rise of 12 cm/century. From Hicks, Debaugh, and Hickman (1983).

b/ Relative sea level trend minus consensus estimate of 12 cm/century for global sea level rise.

c/ One meter plus extrapolation of historical subsidence rate.

Source: Hicks, Debaugh, and Hickman 1983.

coast than the worldwide average (Hicks, Debaugh, and Hickman 1983). Important exceptions include Louisiana, which is subsiding close to 1 m per century, and Alaska, which is emerging 10 to 100 cm per century.

Local subsidence and emergence are caused by a variety of factors. Rebound from the retreat of glaciers after the last ice age has resulted in the uplift of northern Canada, New England, and parts of Scandinavia; emergence in Alaska is due more to tectonic adjustments. The uplift in polar latitudes has resulted in subsidence in other areas, notably the U.S. Atlantic and Gulf coasts. Groundwater pumping has caused rapid subsidence around Houston, Texas; Taipei, Taiwan; and Bangkok, Thailand, among other areas (Leatherman 1984). River deltas and other newly created lands subside as the unconsolidated materials compact. Although subsidence and emergence trends may change in the future, particularly where anthropogenic causes are curtailed, no one has linked these causes to future climate change in the next century.

However, the removal of ice from Greenland and Antarctica would deform the ocean floor. Clark and Lingle (1977) have calculated the impact of a uniform 1 m contribution from West Antarctica. They concluded that relative sea level at Hawaii would rise 125 cm, and that along much of the U.S. Atlantic and Gulf Coasts, the rise would be 15 cm. On the other hand, sea level would drop at Cape Horn by close to 10 cm, and the rise along the southern half of the Argentine and Chilean coasts would be less than 75 cm.

Other contributors to local sea level that might change as a result of a global warming include currents, winds, and freshwater flow into estuaries. None of these impacts, however, has been estimated.

EFFECTS OF SEA LEVEL RISE

A rise in sea level of 1 or 2 m would permanently inundate wetlands and lowlands, accelerate coastal erosion, exacerbate coastal flooding, threaten coastal structures, and increase the salinity of estuaries and aquifers. Substantial research has been done on the implications of sea level rise for coastal erosion and wetlands and relatively little work has been done in the other areas.

The remaining sections of this chapter summarize research on the impacts of sea level rise. The level of damage would depend in large measure on when and how people respond. Much of the research has been conducted to assist agencies that might have to respond to the impacts of sea level rise, and has attempted to estimate impacts for three alternative responses: (1) no countermeasures are taken; (2) measures are taken in response to sea level rise as it occurs; and (3) sea level rise is planned for in advance of its occurrence. We follow this convention and examine potential impacts, possible responses, and the relative merits of anticipating a rise in sea level.

Submergence of Coastal Wetlands

The most direct impact of a rise in sea level is the inundation of areas that had been just above the water level before the sea rose. Coastal wetlands are generally found at elevations below the highest tide of the year and above mean sea level. Thus, wetlands account for most of the land less than 1 m above sea level.

Because a common means of estimating past sea level rise has been the analysis of marsh peats, the impact of sea level rise on wetlands is fairly well understood. For the last several thousand years, marshes have generally kept pace with the rate of sea level rise through sedimentation and peat formation (Emery and Uchupi 1972; Redfield 1972 and 1967; Davis 1985). As sea level rose, new wetlands formed inland while the seaward boundary was maintained. Because the wetland area has expanded, Titus, Henderson, and Teal (1984) hypothesized that one would expect a concave marsh profile (i.e., there is more marsh area than area found immediately above the marsh). Thus, if sea level rose more rapidly than the marsh's ability to keep pace, there would be a net loss of wetlands. Moreover, a complete loss might occur if protection of developed areas prevented the inland formation of new wetlands (see Exhibit 15-6).

Kana et al. (1986 and 1987) surveyed marsh transects in Charleston, South Carolina, and in two sites near Long Beach Island, New Jersey, to evaluate the concavity of wetland profiles and the vulnerability of wetlands to a rise in sea level. Their data showed that in the Charleston area, all of the marsh was between 30 and 110 cm above current sea level, an elevation range of 80 cm (see Exhibit 15-7). The area with a similar elevation range just above the marsh was only 20% as large. Thus, a rise in sea level exceeding vertical marsh accretion by 80 cm would result in an 80% loss of wetlands. In the New Jersey sites, the marsh was also found within an elevation range of 80 cm; a rise in sea level 80 cm in excess of marsh accretion would result in 67%-90% losses.

The future ability of marshes to accrete vertically is uncertain. Based on field studies by Ward and Domeracki (1978), Hatton, DeLaune, and Patrick (1983), Meyerson (1972), Stearns and MacCreary (1957), Kana, Baca, and Williams (1986) concluded that current vertical accretion rates are approximately 4-6 mm/year in the two case study areas, greater than the current rate of sea level rise but less than the rates of rise projected for the next century. If current accretion trends continue, rises of 87 and 160 cm by 2075 would imply 50% and 80% losses of wetlands, respectively, in the Charleston area. Kana et al. (1987) also estimated 80% losses in the New Jersey sites for a 160-cm rise through 2075. However, because the high marsh dominates in that area, they concluded that the principal impact of an 87-cm rise by 2075 would be the conversion of high to low marsh.

In both cases, the losses of marsh could be greater if inland areas are developed and protected with bulkheads or levees. Because there is a buffer zone between developed areas and the marsh in South Carolina, protecting development from a 160-cm rise would increase the loss from 80% to 90%. Without the buffer, the loss would be close to 100%.

The marshes and swamps of Louisiana, which account for 40% of the coastal wetlands in the United States (excluding Alaska), would be particularly vulnerable to an accelerated rise in sea level. The wetlands in this state are mostly less than 1 m above sea level, and are generally subsiding approximately 1 m per century as its deltaic sediments compact (Boesch 1982). Until the last century, the wetlands were able to keep pace with this rate of relative sea level rise because of the sediment conveyed to the wetlands by the Mississippi River.

EXHIBIT 15-6

Evolution of Marsh as Sea Level Rises

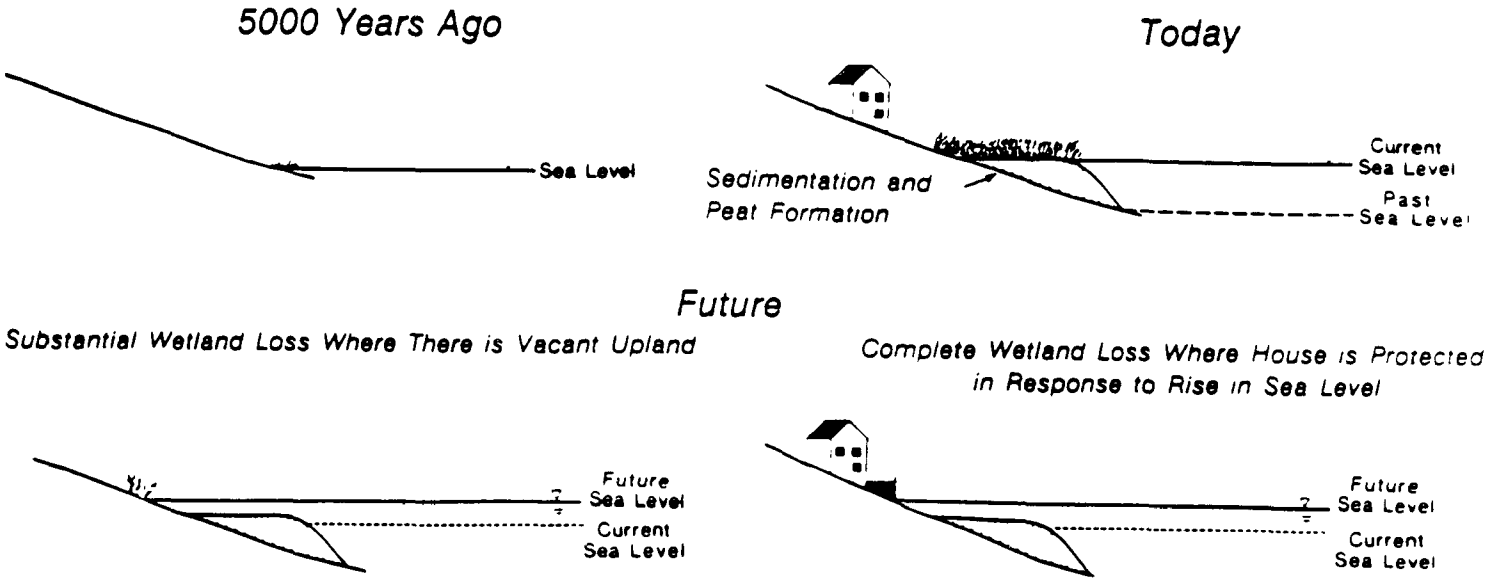

Coastal marshes have kept pace with the slow rate of sea level rise that has characterized the last several thousand years. Thus, the area of marsh has expanded over time as new lands were inundated. If in the future, sea level rises faster than the ability of the marsh to keep pace, the marsh area will contract. Construction of bulkheads to protect economic development may prevent new marsh from forming and result in a total loss of marsh in some areas.

Source: Titus 1986.

EXHIBIT 15-7

Composite Transect -- Charleston, S.C.

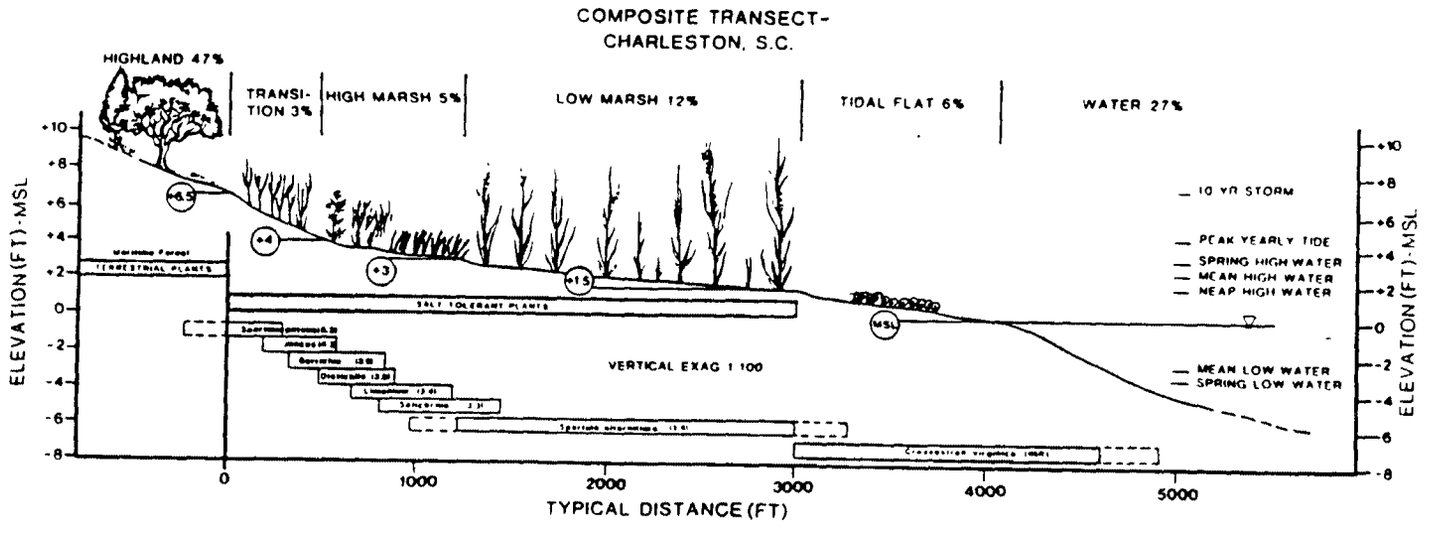

Composite wetlands transect for Charleston area. Area above the marsh is much steeper than the marsh.

Source: Kana, Baca, and William 1986.

Human activities, however, have largely disabled the natural processes by which coastal Louisiana might keep pace with sea level rise. Dams, navigation channels, canals, and flood protection levees have interrupted the flow of sediment, freshwater, and nutrients to the wetlands. As a result, over 100 square kilometers of wetlands convert to open water every year (Gagliano, Meyer-Arendt, and Wicker 1981). A substantial rise in sea level would further accelerate the process of wetland loss in Louisiana (see Exhibit 15-8).

Throughout the world, people have dammed, leveed, and channelized major rivers, curtailing the amount of sediment that reaches river deltas. Even at today's rate of sea level rise, substantial amounts of land are converting to open water in Egypt and Mexico (Milliman and Meade 1983). Other deltas, such as the Ganges in Bangladesh and India, are currently expanding seaward. These areas would require increased sediment, however, to keep pace with an accelerated rise in sea level. Additional projects to divert the natural flow of river water would increase the vulnerability of these areas to a rise in sea level.

Broadhus et al. (1986) examined the possible impacts of future sea level rise on Egypt and Bangladesh, the inhabited areas of which are in the deltas of the Nile and Ganges Rivers. They estimated that 50- and 200-cm rises by 2100 would flood 0.35% and 0.7%, respectively, of Egypt's land area. However, because the nation's population is concentrated in the low-lying areas, 16% and 21% of the people currently reside in the areas that would be lost. Broadhus et al. (1986) also estimate that Bangladesh could lose 12% and 28% of its land, which currently houses 9% and 27% of its population (see Exhibit 15-9).

To develop an understanding of the potential nationwide impact of sea level rise on coastal wetlands in the United States, Park, Armentano, and Cloonan (1986) used topographic maps to characterize wetland elevations at 52 sites comprising 4800 square kilometers (1.2 million acres) of wetlands, over 17% of all U.S. coastal wetlands. Using published vertical accretion rates, they estimated the impact of 1.4 m and 2.1 m rises in sea level through the year 2100 for each of the sites. Weighing their results according to the coastal wetland inventory by Alexander, Broutman, and Field (1986), Titus (1987) estimated a loss of wetlands between 47% and 82%, which could be reduced to between 31% and 70% if new wetlands are not prevented from forming inland.

Inundation

Although coastal wetlands are found at the lowest elevations, inundation of lowlands could also be important in some areas, particularly if sea level rises at least 1 m. Unfortunately, the convention of 10-ft contours in the mapping of most coastal areas has prevented a general assessment of land loss. Nevertheless, a few case studies have been conducted.

Kana et al. (1984) used data from aerial photographs to assess elevations in the area around Charleston. They concluded that 160- and 230-cm rises would result in 30% and 46% losses, respectively, of the area's dry land. Leatherman (1984) estimated that such rises would result in 9% and 12% losses, respectively, of the land in the area of Galveston and Texas City, Texas, assuming that the elaborate network of seawalls and levees was maintained.

EXHIBIT 15-8

Louisiana Shoreline in the Year 2030

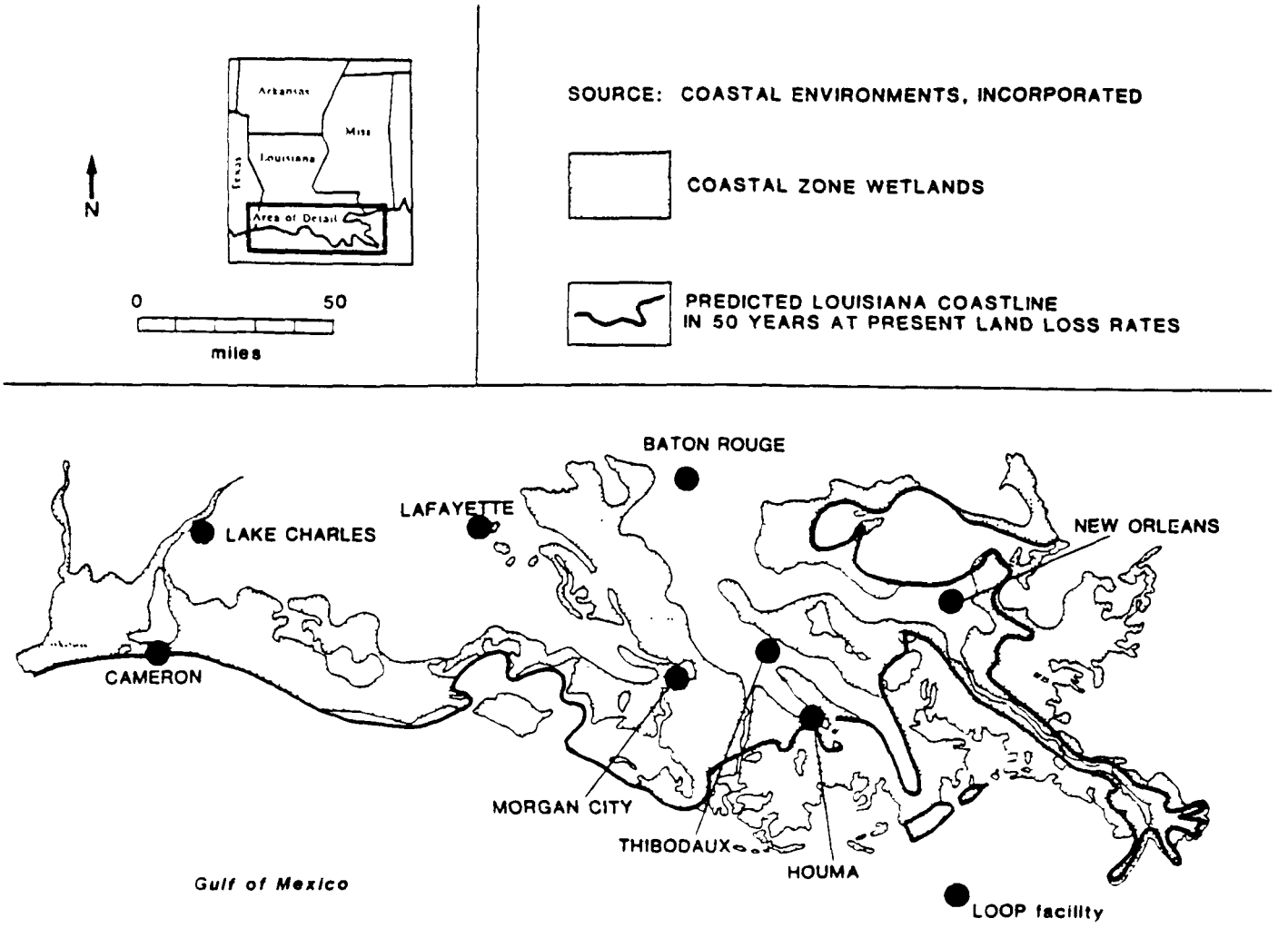

The solid line shows the predicted shoreline for 2030 if current trends continue. The entire shaded area could be lost by 2085 if sea level rises 1 m. However, a 20-cm rise by 2020 would result in the shore retreating to this point by 2020 or sooner.

Source: Coastal Environments, Incorporated.

EXHIBIT 15-9

Distribution of Population in Bangladesh

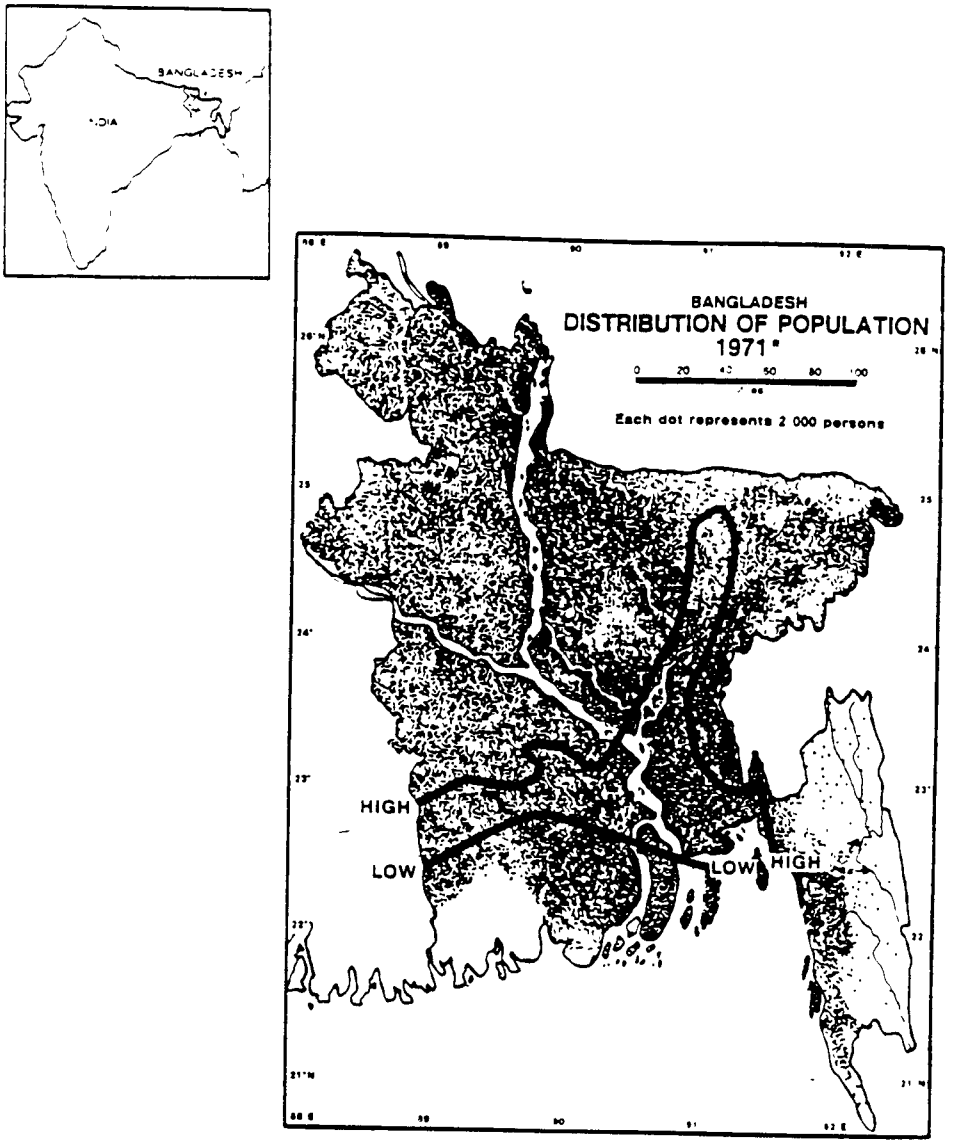

The high scenario represents a 2- to 2.5-m rise with sedimentation disrupted by human activities. The low scenario represents a 50-cm rise and natural sedimentation maintained.

Source: Broadhus et al. (1986).

The only nationwide assessment of the inundation from projected sea level rise was conducted by Schneider and Chen (1980). Unfortunately, the smallest rise in sea level they considered was a 4.5-m (15-ft) rise, in part because smaller contours are not generally available in topographic maps. Nevertheless, their findings suggest which coastal states would be most vulnerable: Louisiana (which would lose 28% of its land and 51% of its assets); Florida (24% and 52%); Delaware (16% and 18%); Washington, D.C. (15% and 15%); Maryland (12% and 5%); and New Jersey (10% and 9%).

As with wetland loss, the responses to inundation broadly fall into the categories of retreat and holding back the sea. Levees are used extensively in the Netherlands and New Orleans to prevent areas that are below sea level from being flooded and could be similarly constructed around other major cities. In lightly developed areas, however, the cost of a levee might be greater than the value of the property being protected. Moreover, even where levees prove to be cost-effective, the environmental implications of replacing natural shorelines with manmade structures would need to be considered.

Coastal Erosion

Sea level rise can also result in the loss of land above sea level through erosion. Bruun (1962) showed that the erosion resulting from a rise in sea level would depend upon the average slope of the entire beach profile extending from the dunes out to the point where the water is too deep for waves to have a significant impact on the bottom, generally a depth of about 10 m (see Exhibit 15-10):

$$r = s * p/(h + d)$$

where r = shoreline retreat; s = sea level rise; p = horizontal length of the beach profile from dune to the offshore limit of significant wave action; h = height of the dune crest; and d = depth of the offshore limit of the beach profile. By comparison, inundation depends only on the slope immediately above the original sea level. Because beach profiles are generally flatter than the portion of the beach just above sea level, the "Bruun Rule" generally implies that the erosion from a rise in sea level is several times greater than the amount of land directly inundated.

Processes other than sea level rise also contribute to erosion. These include storms, structures, currents, and alongshore transport. Because sea level has risen slowly in recent centuries, verification of the Bruun Rule on the open coast has been difficult; it has been difficult to distinguish erosion due to sea level rise from erosion caused by other processes. However, water levels along the Great Lakes can fluctuate over 1 m in a decade. Hands (1976, 1979, and 1980) and Weishar and Wood (1983) have demonstrated that the Bruun Rule generally predicts the erosion resulting from rises in water levels there.

The Bruun Rule has been applied to project erosion due to sea level rise for several areas. Bruun (1962) found that a 1-cm rise in sea level would generally result in a 1-m shoreline retreat, but that the retreat could be as great as 10 m along some parts of the Florida coast. Everts (1985) and Kyper and Sorensen (1985) however, found that along the coasts of Ocean City, Maryland, and Sandy Hook, New Jersey, respectively, the shoreline retreat implied by the Bruun Rule would be only about 75 cm. Kana et al. (1984) found that along the coast of South Carolina, the retreat could be 2 m. The U.S.

EXHIBIT 15-10

The Bruun Rule

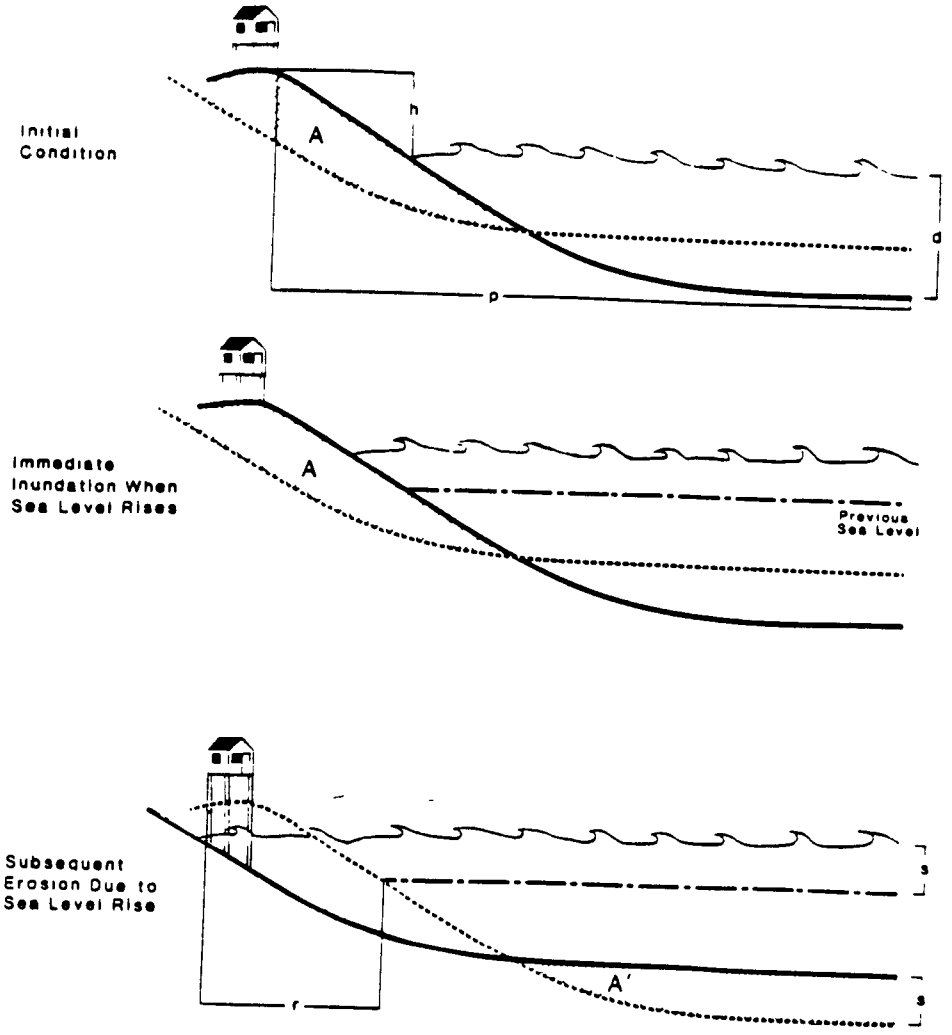

A rise in sea level of s causes immediate inundation. However, it would eventually require the offshore bottom to rise by s. The necessary s and A' would be supplied from the upper part of the beach A. Total shoreline retreat r is equal to s * p/(h + d).

Army Corps of Engineers (1979) indicated that along the coast of San Francisco, where waves are generally larger than those found along the Atlantic Coast, the shore might retreat 2-4 m for a 1-cm rise in sea level.

Dean and Maurmeyer (1983) generalized the "Bruun Rule" approach to consider the "overwash" of barrier islands. Coastal geologists generally believe that coastal barriers can maintain themselves in the face of slowly rising sea level through the landward transport of sand, which washes over the island during storms, building the island upward and landward. Because this formulation of the Bruun Rule extends the beach profile horizontally to include the entire islands as well as the active surf zone, it always predicts greater erosion than the Bruun Rule. However, the formulation may not be applicable to developed barrier islands, where the common practice of public officials is to bulldoze sand back onto the beach after a major storm.

The potential erosion from a rise in sea level could be particularly important to recreational beach resorts, which include some of the nation's most economically valuable and intensely used land. Although nationwide statistics are not available, information on particular locations is instructive. Every weekend in the summer, approximately 250,000 people visit Ocean City, Maryland, to sunbathe on its 15-km (9-mile) beach.[6] Along most of the Ocean City shoreline, the beach is less than 15 m wide during high tide--a width that is typical of the most extensively used beach resorts. Relatively few of the most intensely developed resorts along the Atlantic Coast have beaches wider than about 30 m at high tide. Thus, the rise in relative sea level that is projected to occur in the next 40 to 50 years (30 cm) could erode most recreational beaches in developed areas, unless additional erosion response measures are taken.

Flooding and Storm Damage

A rise in sea level could increase flooding and storm damages in coastal areas for three reasons: Erosion caused by sea level rise would increase the vulnerability of communities; because of higher water levels, storm surges would have a higher base on which to build; and higher water levels would decrease natural and artificial drainage.

The impact of erosion on vulnerability to storms is generally a major consideration in proposed projects to control erosion, most of which have historically been funded through the U.S. Army Corps of Engineers. The impact of sea level rise, however, has not generally been considered separately from other causes of erosion.

The impact of higher base water levels on flooding has been investigated for the areas around Charleston, South Carolina, and Galveston, Texas (Barth and Titus 1984). Kana et al. (1984) found that around Charleston, the area within the 10-year flood plain would increase from 33% in 1980, to 48%, 62%, and 74% for rises in sea level of 88, 160, and 230 cm, respectively, and that the area within the 100-year flood plain would increase from 63% to 76%, 84%, and 90%, respectively, for the three scenarios.[7] Gibbs (1984) estimated that a rise of about 90 cm would double the average annual flood damages in the Charleston area (but that flood losses would not increase substantially for higher rises in sea level because shoreline retreat would result in a large part of the community being completely abandoned).[8]

Leatherman (1984) conducted a similar analysis of Galveston Island, Texas. He estimated that the area within the 100-year flood plain would increase from 58% to 94% for an 88-cm rise in sea level,[9] and that for a rise greater than 1 m, the Galveston seawall would be overtopped during a 100-year storm. Gibbs estimated that the damage from a 100-year storm would be tripled for a rise of about 90 cm.[10]

A wide variety of shore-protection measures would be available for communities to protect themselves from increased storm surge and wave damage due to sea level rise (Sorensen, Weisman, and Lennon 1984). Many of the measures used to address erosion and inundation, including construction of seawalls, breakwaters, and levees, and rebuilding beaches, also provide protection against storms. In Galveston, which is already protected on the ocean side by the seawall, Gibbs hypothesized that it might be necessary to completely encircle the developed areas with a levee to prevent flooding from the bay side; upgrading the existing seawall might also be necessary.

Kyper and Sorensen (1985 and 1987) examined the implications of sea level rise for the design of coastal protection works at Sea Bright, New Jersey, a coastal community that is currently protected by a seawall and has no beach. Because the seawall is vulnerable to even a 10-year storm, the Corps of Engineers and the State of New Jersey have been considering a possible upgrade. Kyper and Sorensen estimated that the cost of upgrading the seawall for current conditions would be $3.5-6.0 million per kilometer of shoreline, noting that if designed properly, the seawall would be useful throughout the next century. However, they estimated that a rise in relative sea level of 30-40 cm would be likely to result in serious damage to the seawall during a major storm because of higher water levels and the increased wave heights resulting from the erosion of submerged sand in front of the seawall. To upgrade the seawall to withstand a 1-m rise in relative sea level would cost $5.7-9.0 million per kilometer (50% more). They concluded that policymakers would have to weigh the tradeoff between the cost of designing the wall to withstand projected sea level rise and the cost of subsequent repairs and a second overhaul.

In addition to community-wide engineering approaches, measures can also be taken by individual property owners to prevent damages from increased flooding. In 1968, the U.S. Congress created the National Flood Insurance Program to encourage communities to avoid risky construction in flood-prone areas. In return for requiring new construction to be elevated above expected flood levels, the federal government provides flood insurance, which is not available from the private sector. If sea level rises, flood risks will increase. In response, local ordinances will automatically require new construction to be further elevated, and insurance rates on existing properties will rise unless those properties are further elevated. As currently organized, the National Flood Insurance Program would react to sea level rise as it occurred. Various measures that would ensure the continued viability of the program if the sea level were to rise substantially have been proposed, including warning policyholders that rates may increase in the future if sea level rises, denying coverage to new construction in areas that are expected to be lost to erosion within the next 30 years, and setting premiums according to the average risk expected over the lifetime of the mortgage (Howard, Pilkey, and Kaufman 1985; Titus 1984).

Case studies in Charleston, South Carolina, and Fort Walton Beach, Florida, have examined the implications of sea level rise for rainwater flooding and the design of coastal drainage systems. Waddell and Blaylock (n.d.) estimated that a 25-year rainstorm (with no storm surge) would result in no damage for the Gap Creek watershed in Fort Walton Beach. However, a rise in sea level of 30-45 cm would result in damages of $1.1-1.3 million in this community of 4,000 residents during a 25-year storm. An upgrade costing $550,000, however, would prevent such damages.

LaRoche and Webb (n.d.) had previously developed the master drainage plan for Charleston, South Carolina, and later evaluated the implications of sea level rise for the Grove Street watershed in that community. They estimated that the cost of upgrading the system for current conditions would be $4.8 million and the cost of upgrading the system for a 30-cm rise would be $5.1 million. If the system is designed for current conditions and sea level rises, the system would be deficient and the city would face a retrofit cost of $2.4 million. Thus, for the additional $300,000 necessary to upgrade for a 30-cm rise, the city could ensure that it would not have to spend an additional $2.4 million later. Noting that the decision whether to design now for a rise in sea level depends on the probability that sea level would rise, they concluded that a 3% real social discount rate would imply that designing for sea level rise is worthwhile if the probability of a 30-cm rise by 2025 is greater than 30%. At a discount rate of 10%, they concluded, designing for future conditions is not worthwhile.

Increased Salinity in Estuaries and Aquifers

Although most researchers and the general public have focused on the increased flooding and shoreline retreat associated with a rise in sea level, the inland penetration of salt water could be important in some areas.

A rise in sea level increases the salinity of an estuary by altering the balance between freshwater and saltwater forces. The salinity of an estuary represents the outcome of (1) the tendency for the ocean salt water to completely mix with the estuarine water and (2) the tendency of fresh water flowing into the estuary to dilute the saline water and push it back toward the ocean. During droughts, the salt water penetrates upstream; during the rainy season, low salinity levels prevail. A rise in sea level has an impact similar to decreasing the freshwater inflow. By widening and deepening the estuary, sea level rise increases the ability of salt water to penetrate upstream.

The implications of sea level rise for increased salinity have only been examined in detail for Louisiana and the Delaware Estuary. In Louisiana, saltwater intrusion is currently resulting in the conversion of cypress swamps--which cannot tolerate salt water--to openwater lakes, as well as the conversion of fresh marsh and intermediate marsh to marsh with higher salinity levels. In response to these trends, numerous projects have been proposed to divert fresh water from the Mississippi River to these wetlands (Roberts et al. 1983; U.S. Army Corps of Engineers 1982; van Beek et al. 1982). Although the cause of the saltwater intrusion has been primarily the dredging of canals and the sealing off of river tributaries that once provided the wetlands with fresh water, relative sea level rise is gradually increasing the saltwater force in Louisiana's wetlands; a further rise in sea level would accelerate this process. Haydl (1984) also concluded that subsidence may be resulting in

increased salinity of drinking and irrigation water supplies in some parts of Louisiana.

The impact of current sea level trends on salinity has been considered in the long-range plan of the Delaware River Basin Commission since 1981 (DRBC 1981). The drought of the 1960s resulted in salinity levels that almost contaminated the water supply of Philadelphia and surrounding areas. Hull and Tortoriello (1979) found that the 13-cm rise projected between 1965 and 2000 would result in the "salt front" migrating 2-4 km farther upstream during a similar drought. They found that a moderately sized reservoir (57 million cubic meters) to augment river flows would be needed to offset the resulting salinity increases.

Hull, Thatcher, and Tortoriello (1986) examined the potential impacts of an accelerated rise in sea level due to the greenhouse warming. They estimated that 73-cm and 250-cm rises would result in the salt front migrating an additional 15 and 40 kilometers, respectively, during a repeat of the 1960s drought. They also found that the health-based, 50-ppm sodium standard (equivalent to 73 ppm chloride) adopted by New Jersey would be exceeded 15% and 50% of the time, respectively, and that the EPA drinking water 250-ppm chloride standard would be exceeded over 35% of the time in the high scenario (see Exhibit 15-11).

Lennon, Wisniewski, and Yoshioka (1986) examined the implications of increased estuarine salinity for the Potomac-Raritan-Magothy aquifer system, which is recharged by the (currently fresh) Delaware River and serves the New Jersey suburbs of Philadelphia. During the 1960s drought, river water with chloride concentrations as high as 150 ppm recharged these aquifers. Lennon et al. estimated that a repeat of the 1960s drought with a 73-cm rise in sea level would result in river water with chloride concentrations as high as 350 ppm recharging the aquifer, and that during the worst month of the drought, over one-half of the water recharging the aquifer system would have chloride concentrations greater than 250 ppm. With a 250-cm rise, 98% of the recharge during the worst month of the drought would exceed 250 ppm chloride, and 75% of the recharge would be greater than 1000 ppm.

Hull and Titus (1986) examined the options by which various agencies might respond to increased salinity in the Delaware estuary. They concluded that planned but unscheduled reservoirs would be more than enough to offset the salinity increase from a 30-cm rise in sea level, although those reservoirs had originally been intended to meet increased consumption. They noted that construction of the reservoirs would not be necessary until the rise became more imminent. However, they also suggested that, given the uncertainties, it might be advisable today to identify additional reservoir sites to ensure that future generations retain the option of building additional reservoirs if necessary.

A rise in sea level could increase salinities in other areas, although the importance of those impacts has not been investigated. Kana et al. (1984) and Leatherman (1984) made preliminary inquiries into the potential impacts on coastal aquifers around Charleston and Galveston, respectively. However, they concluded that in-depth assessments were not worthwhile because the aquifers around Charleston are already salt-contaminated because of overpumping, and pumping of ground water has been prohibited in the Galveston area due to the

EXHIBIT 15-11

Percent of Tidal Cycles in Which Specified Concentration is Exceeded at Torresdale During a Recurrence of the 1960s Drought for Three Sea Level Scenarios

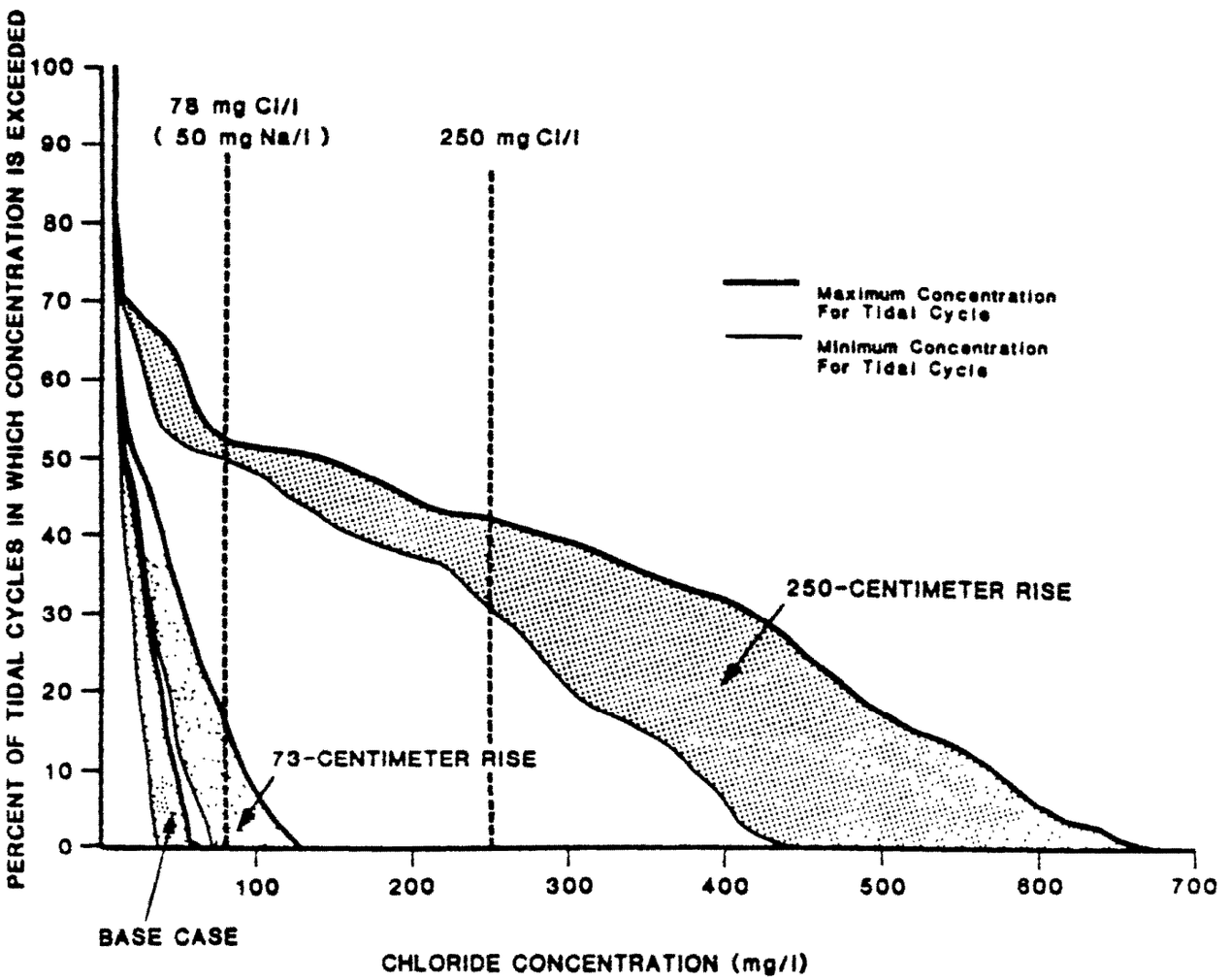

The 250 mg Cl/l level is the EPA drinking water standard for chloride. The 50 mg/l Na level is the New Jersey sodium standard.

Source: Hull et al. 1986.

resulting land subsidence. The potential impacts on Florida's Everglades and the shallow aquifers around Miami might be significant, but they have not been investigated.

Economic Significance of Sea Level Rise

No one has estimated a dollar value of the likely impacts of sea level rise for the nation or any coastal state. Schneider and Chen (1980) estimated the economic impact of what was once (but is no longer) thought to be a plausible scenario: rises of 4.6-7.6 m (15-25 ft) occurring with little or no warning during the early part of the twenty-first century. They estimated that this scenario would result in real property losses of $100-150 billion, representing 6.2% to 8.4% of all real property in the nation.

The only comprehensive attempt to place a dollar value on the impacts of sea level rise for particular communities was the study by Gibbs (1984) of the Charleston and Galveston areas. In addition to considering more realistic scenarios ranging from 0.9 to 2.4 m through 2075, Gibbs made several improvements on the approach of Schneider and Chen: Gibbs' approach (1) differentiated between the economic impact if preventive measures are taken in anticipation of sea level rise and the economic impact if such measures are not taken (with and without anticipation; see Exhibit 15-12), (2) modeled how investment decisions might respond to floods and erosion, and (3) explicitly considered community-wide strategies to limit losses, including shore protection and abandonment.

In the Charleston study, Gibbs evaluated the implications of (1) efforts to avoid development of some vacant suburban areas likely to be flooded in the future, (2) a partial abandonment, and (3) elevating the existing seawalls protecting Charleston to provide additional protection. For a rise of 28-64 cm through 2025, Gibbs estimated that present value of the cumulative impact would be $280-1065 million (5% to 19% of economic activity in the area for the period), which could be reduced to $160-420 million if sea level rise was anticipated. Most of this impact would result from a 10% to 100% increase in expected storm damages, although Gibbs also estimated losses to erosion at $7-35 million. For the period between 1980 and 2075, Gibbs estimated that the economic impacts would be $1250-2510 million (17% to 35%) and could be reduced to $440-1100 million through anticipatory measures. If accurate, these estimates suggest that Charleston would be extremely vulnerable to a rise in sea level. However, these estimates were necessarily based on a number of simplifying assumptions regarding storm damage and current elevation of structures.

Gibbs performed a similar analysis of the Galveston area and concluded that the economic impacts of sea level rise through 2025 would amount to $115-360 million (1.1%-3.6%) if a rise in sea level is not anticipated, and $90-140 million if a rise is anticipated. The impacts through 2075 were estimated at $555-1840 million (4.9%-16%) if not anticipated, and $310-730 million if a rise is anticipated. The assumptions Gibbs used suggest that a 100-year storm today would result in damages equal to the value of about 7% of the property in the area, and that average annual storm damages are equal to $6 million, slightly less than 0.2% of the value of property in the study area.

EXHIBIT 15-12

Estimates of Flood Damages for Charleston and Galveston Resulting from Sea Level Rise[a/]

Scenario	Global Sea Level Rise by 2075 (cm)	Charleston Impact b/ With Anticipation	Charleston Impact b/ Without Anticipation	Galveston Impact b/ With Anticipation	Galveston Impact b/ Without Anticipation
Trend	11.4	c/	c/	c/	c/
Low	75.2	440	1250	310	555
Medium	146.8	730	1910	415	965
High	219.2	1100	2510	730	1890

a/ The damage estimates consist of a low estimate and a high estimate. The low estimate is derived by linearly interpolating the "with anticipation" estimates for Charleston and Galveston according to the amount of global sea level rise. The high estimates are derived by linearly interpolating the "without anticipation" estimates.

b/ Through 2075 in millions of 1980 dollars discounted at 3%.

c/ All estimates are relative to the trend scenario.

Source: Gibbs 1984.

Other studies can be used to gain an understanding of the economic significance of particular classes of impacts. As discussed above, a 30-cm rise in sea level would erode most recreational beaches back to the first row of houses. The studies cited in the section on erosion indicate that the typical beach profile extends out about 1000 m, which suggests that 300,000 cubic yards of sand per kilometer of shoreline are required to raise the beach profile 30 cm. If sand costs are typically $3-10/cubic meter, the beach rebuilding costs of a 30-cm rise in sea level would be $1-3 million per kilometer. If the United States has a few thousand kilometers of recreational beaches, it would cost billions and perhaps tens of billions of dollars to rebuild beaches if the sea rises 30 cm. This estimate considers only the beaches themselves; raising people's lots to prevent property inundation would further increase the costs.

The U.S. Army Corps of Engineers (1971) estimated that in 1971, 25,000 km of shoreline (exclusive of Alaska, Great Lakes, and Hawaii) were eroding, of which 17% were "critically eroding," and would require engineering solutions. If 17% of all shorelines require erosion control, that would imply protection of close to 10,000 km of shoreline. Sorensen, Weisman, and Lennon (1984) describes dozens of engineering options for preventing erosion, the least expensive of which costs $300,000 per kilometer, which would imply a cost of at least $3 billion for protecting all shorelines.

Relationship to Other Impacts of the Greenhouse Warming

The impacts of sea level rise on coastal areas, as well as their importance, is likely to depend in part on other impacts of the greenhouse warming. Although future sea level is uncertain, there is a general consensus that a global warming would cause sea level to rise; by contrast, the direction of most hydrological and storm event changes at particular locations is unknown.

Warmer temperatures might change the ability of wetlands to keep pace with sea level rise. Mangrove swamps would replace salt marshes in some areas that are currently too cold for mangroves. No one has assessed the impact of this vegetation change on vertical accretion. Peat formation is generally greater in New England marshes than at lower latitudes. Warmer temperatures might reduce that rate of vertical accretion for these wetlands.

Changing climate could alter the frequency and tracks of storms. Because hurricane formation requires water temperatures of 27°C or higher (Wendland 1977), a global warming might result in a longer hurricane season and in the formation of hurricanes at higher latitudes. Besides increasing the amount of storm damage, increased frequency of severe storms would tend to flatten the typical beach profile, causing substantial shoreline retreat unless additional sand was placed on the beach. A decreased frequency of severe winter storms might have the opposite impact at higher latitudes.

Changes in precipitation could also affect the impacts of sea level rise. Because warmer temperatures would intensify the hydrologic cycle, it is generally recognized that a global warming would increase rainfall worldwide. If rainfall in maritime environments increases, rainwater flooding could be increased because of decreased drainage and increased precipitation. The impact of sea level rise on saltwater intrusion could be offset by decreased

drought frequency or exacerbated by increased drought frequency (Rind and Lebedeff 1984).

CONCLUSION

Researchers have identified a wide variety of impacts that could result from a 50- to 200-cm rise in sea level. These impacts include both economic losses resulting from land loss, flooding, shore protection, and increased costs for drinking water, as well as environmental costs such as the disruption of coastal ecosystems resulting from wetland loss and increased salinity. Although there are substantial uncertainties regarding the magnitude of both the causes and effects of future sea level rise, even conservative estimates suggest that important impacts are likely to result.

A high priority for future research should be the use of existing case studies to derive estimates of the nationwide and worldwide magnitude of the various impacts that have been identified. Although preliminary estimates of the potential loss of U.S. coastal wetlands exist, the implications of those losses have not been assessed. For most other impacts, no nationwide estimates are available. That type of information will be important for evaluating the benefits of possible actions to mitigate the greenhouse warming and resulting rise in sea level.

NOTES

1. Mark Meier, University of Colorado, Boulder (personal communication).

2. The only true measure of absolute sea level would be the rise of sea level relative to the center of the earth. Unfortunately, no such measurements are yet available. Therefore, researchers have had to combine tidal gauge measurements of relative sea level trends at various locations, filter out known movements of the land surface, and take weighted averages to arrive at estimates of global sea level trends.

3. This result was reported in the North America study. The data also show this to be true in the Northern Europe study, but the result was not reported. David Aubrey, Woods Hole Oceanographic Institute, Woods Hole, Massachusetts (personal communication).

4. Robert Bindschadler, Goddard Space Flight Center, Greenbelt, Maryland (personal communication).

5. James Hansen, Goddard Institute for Space Studies, New York (personal communication).

6. Sandy Coyman, Department of Planning and Community Development, Town of Ocean City, Maryland (personal communication).

7. Results of the Charleston and Galveston case studies have been reported in J.G. Titus and Michael C. Barth, 1984, "An Overview of the Causes and Effects of Sea Level Rise," Appendix, In Greenhouse Effect and Sea Level Rise: A Challenge for This Generation, New York: Van Nostrand Reinhold, 1984.

8. See Note 7.

9. See Note 7.

10. See Note 7.

REFERENCES

Alexander, C.E., M.A. Broutman, and D.W. Field. 1986. An Inventory of Coastal Wetlands of the USA. Rockville, MD.: National Oceanic and Atmospheric Administration (NOAA), National Ocean Service (NOS).

Ambach, W. 1985. "Climatic Shift of the Equilibrium Line--Kuhn's Concept Applied to the Greenland Ice Cap." Annals of Glaciology 6:76-78.

Ambach, W. 1980 (translated by G.P. Weidhaas). "Increased CO2 Concentration in the Atmosphere and Climate Change: Potential Effects on the Greenland Ice Sheet." Wetter und Leben 32:135-142, Vienna. (Available as Lawrence Livermore National Laboratory Report UCRL-TRANS-11767, April 1982.)

Associated Press. 1985. "Doubled Erosion Seen for Ocean City." The Washington Post, November 14th, (Maryland Section).

Barnett, T.P. 1984. "The Estimation of 'Global' Sea Level Change: A Problem of Uniqueness." Journal of Geophysical Research 89(C5):7980-7988.

Barth, M.C. and J.G. Titus (eds.) 1984. Greenhouse Effect and Sea Level Rise: A Challenge for this Generation. New York: Van Nostrand Reinhold.

Bentley, C.R. 1983. "West Antarctic Ice Sheet: Diagnosis and Prognosis." In Proceedings: Carbon Dioxide Research Conference: Carbon Dioxide, Science, and Consensus, Conference 820970. Washington, D.C.: Department of Energy.

Bindschadler, R.A. 1985. "Contribution of the Greenland Ice Cap to Changing Sea Level: Present and Future." In Meier et al. 1985. op. cit.

Boesch, D.F. (ed.) 1982. Proceedings of the Conference of Coastal Erosion and Wetland Modification in Louisiana: Causes, Consequences, and Options, FWS-OBS-82/59. Slidell, Louisiana: National Coastal Ecosystems Team, U.S. Fish and Wildlife Service.

Braatz, B.V. and D.G. Aubrey. 1987. "Recent Relative Sea-Level Movement Along the Eastern Coastline of North America." Journal of Sedimentary Petrology, in press.

Broadhus, J., et al. 1986. "Sea Level Rise and the Damming of Rivers." In Titus, J.G. (ed.) Effects of Changes in Stratospheric Ozone and Global Climate. Washington, D.C.: United Nations Environment Programme and U.S. Environmental Protection Agency.

Bruun, P. 1962. "Sea Level Rise as a Cause of Shore Erosion." Journal of Waterways and Harbors Division (ASCE) 1:116-130.

Cess, R.D., and S.D. Goldenberg. 1981. "The Effect of Ocean Heat Capacity Upon Global Warming Due to Increasing Atmospheric Carbon Dioxide." Journal of Geophysical Research 86:498-502.

Clark, J.A., and C.S. Lingle. 1977. "Future Sea-Level Changes Due to West Antarctic Ice Sheet Fluctuations." Nature 269(5625):206-209.

Clark, J.A., W.E. Farrell, and W.R. Peltier. 1978. "Global Changes in Postglacial Sea Level: A Numerical Calculation." Quarternary Research 9:265-87.

Davis, R.A. 1985. Coastal Sedimentary Environments. New York: Springer Verlag.

Dean, R.G., and E.M. Maurmeyer. 1983. "Models for Beach Profile Response." In Handbook of Coastal Processes and Erosion. Fort Belvoir: U.S. Army Corps of Engineers, Coastal Engineering Research Center.

Delaware River Basin Commission (DRBC). 1981. The Delaware River Basin Comprehensive (Level B) Study: Final Report and Environmental Impact Statement. West Trenton, New Jersey: Delaware River Basin Commission.

Dewey, K.F., and R.J. Heim. 1981. Satellite Observations of Variations in Northern Hemisphere Seasonal Snow Cover. NOAA Technical Report, NESS 87, Washington, D.C.

Donn, W.L., W.R. Farrand, and M. Ewing. 1962. "Pleistocene Ice Volumes and Sea-Level Lowering." Journal of Geology 70:206-214.

Edmonson, J., and R. Jones. 1985. Terreboone Parish Barrier Island and Marsh Management Program. Houma, Louisiana: Terrebonne Parish Council.

Emery, K.O., and D.G. Aubrey. 1986. "Relative Sea Level Change from Tide Gauge Records of Western North America." Journal of Geophysical Research 91(14):914-953.

Emery, K.O., and D.G. Aubrey. 1985. "Glacial Rebound and Relative Sea Levels in Europe From Tide-Gauge Records." Tectonophysics 120:239-255.

Emery, K.O., and E. Uchupi. 1972. Western North Atlantic Ocean Memoir 17. Tulsa, Oklahoma: American Association of Petroleum Geologists.

Everts, C.H. 1985. "Effect of Sea Level Rise and Net Sand Volume Change on Shoreline Position at Ocean City, Maryland." In Potential Impacts of Sea Level Rise on the Beach at Ocean City, Maryland. Washington, D.C.: U.S. Environmental Protection Agency.

Fairbridge, R.W., and W.S. Krebs, Jr. 1962. "Sea Level and the Southern Oscillation." Geophysical Journal 6:532-545.

Fastook, J.L. 1985. "Ice Shelves and Ice Streams: Three Modeling Experiments." In Meier et al. 1985, op. cit.

Flint, R.F. 1971. Glacial and Quarternary Geology. New York: John Wiley and Sons.

Flohn, H. 1982. "Climate change and An Ice-Free Arctic Ocean". In Carbon Dioxide Review: 1982, W.C. Clark, ed. New York: Oxford University Press, pp.145-199.

Gagliano, S.M., K.J. Meyer-Arendt, and K.M. Wicker. 1981. "Land Loss in the Mississippi Deltaic Plain." In Transactions of the 31st Annual Meeting of the Gulf Coast Association of Geological Societies. Corpus Christi, Texas, p. 293-300.

Gibbs, M. "Economic Analysis of Sea Level Rise: Methods and Results." In Barth and Titus (eds.) 1984, op. cit.

Gornitz, V., S. Lebedeff, and J. Hansen. 1982. "Global Sea Level Trend in the Past Century." Science 215:1611-1614.

Hands, E.G. 1980. Prediction of Shore Retreat and Nearshore Profile Adjustments to Rising Water Levels on the Great Lakes, Tech. Paper 870-7. Fort Belvoir: U.S. Army Corps of Engineers.

Hands, E.G. 1979. Changes in Rates of Offshore Retreat: Lake Michigan. Fort Belvoir: U.S. Army Corps of Engineers Coastal Engineering Research Center Publication TP79-4.

Hands, E.G. 1976. Observations of Barred Coastal Profiles Under Influence of Rising Water Levels: Eastern Lake Michigan, CERC Publication TR76-1. Fort Belvoir: U.S. Army Corps of Engineers.

Hatton, R.S., R.D. DeLaune, and W.H. Patrick. 1983. "Sedimentation, Accretion and Subsidence in Marshes of Barataria Basin, Louisiana." Limnology and Oceanography 28:494-502.

Haydl, N.C. 1984. Louisiana Coastal Area, Louisiana: Water Supply, Initial Evaluation Study. New Orleans: U.S. Army Corps of Engineers.

Hays, J.D., and W.C. Pitman III. 1973. "Lithospheric Plate Motion, Sea Level Changes, and Climatic and Ecological Consequences." Nature 246:18-22.

Hicks, S.D., H.A. Debaugh, and L.H. Hickman. 1983. Sea Level Variations for the United States 1855-1980. Rockville, Maryland: U.S. Department of Commerce, NOAA-NOS.

Hoffman, J.S., D. Keyes, and J.G. Titus. 1983. Projecting Future Sea Level Rise. Washington, D.C.: Government Printing Office.

Hoffman, J.S., J. Wells, and J.G. Titus. 1986. "Future Global Warming and Sea Level Rise." In Bruun, P. (ed.), Iceland Symposium '85. Reykjavik: National Energy Authority.

Hollin, J.T., 1962. "On the Glacial History of Antarctica." Journal of Glaciology 4:273-295.

Hollin, J.T., and R.G. Barry. 1979. "Empirical and Theoretical Evidence Concerning the Response of the Earth's Ice and Snow Cover to a Global Temperature Increase." Environment International 2:437-444.

Howard, J.D., O.H. Pilkey, and A. Kaufman. 1985. "Strategy for Beach Preservation Proposed." Geotimes 30:12:15-19.

Hughes, T. 1983. "The Stability of the West Antarctic Ice Sheet: What Has Happened and What Will Happen." In Proceedings: Carbon Dioxide Research Conference: Carbon Dioxide, Science, and Consensus, Conference 820970. Washington, D.C.: Department of Energy.

Hull, C.H.J. and J.G. Titus (eds). 1986. "Responses to Salinity Increases." In Greenhouse Effect, Sea Level Rise, and Salinity in the Delaware Estuary. Washington, D.C.: Environmental Protection Agency and Delaware River Basin Commission.

Hull, C.H.J., M.L. Thatcher, and R.C. Tortoriello. 1986. "Salinity in the Delaware Estuary." In Hull and Titus (eds.) 1986, op. cit.

Hull, C.H.J. and R.C. Tortoriello. 1979. Sea Level Trend and Salinity in the Delaware Estuary. West Trenton, N.J.: Delaware River Basin Commission.

Jones, P.D., T.M.L. Wigley, and P.B. Wright. 1986. "Global Temperature Variations between 1861 and 1984." Nature 322:430-434.

Kana, T.W., J. Michel, M.O. Hayes, and J.R. Jensen. 1984. "The Physical Impact of Sea Level Rise in the Area of Charleston, South Carolina." In Barth and Titus (eds.) 1984, op. cit.

Kana, T.W., B.J. Baca, and M.L. Williams. 1986. Potential Impacts of Sea Level Rise on Wetlands Around Charleston, South Carolina. Washington, D.C.: U.S. Environmental Protection Agency.

Kana, T.W., W.C. Eiser, B.J. Baca, and M.L. Williams. 1987 "Potential Impacts of Sea Level Rise on Wetlands Around Little Egg Harbor, New Jersey." In Greenhouse Effect, Sea Level Rise and Coastal Wetlands. Washington, D.C.: U.S. Environmental Protection Agency.

Kennett, J. 1982. Marine Geology. Englewood Cliffs, New Jersey: Prentice-Hall.

Kuo, C. n.d. Sea Level Rise, Climate Change and Coastal Drainage Systems. Washington, D.C.: U.S. Environmental Protection Agency, (in press)

Kyper, T., and R. Sorensen. 1985. "Potential Impacts of Selected Sea Level Rise Scenarios on the Beach and Coastal Works at Sea Bright, New Jersey." In O.T. Magoon et al. (eds.), Coastal Zone '85. New York: American Society of Civil Engineers.

Kyper, T. and R. Sorensen. 1987. Potential Impacts of Sea Level Rise on the Beach and Coastal Structures at Sea Bright, New Jersey. Washington, D.C.: U.S. Environmental Protection Agency and U.S. Army Corps of Engineers (in press).

Lacis, A., J.E. Hansen, P. Lee, T. Mitchell, and S. Lebedeff. 1981. "Greenhouse Effect of Trace Gases, 1970-1980." Geophysical Research Letters 8:(10):1035-1038.

LaRoche, T.B., and M.K. Webb. n.d. "Impact of Sea Level Rise on Stormwater Drainage Systems in the Charleston, South Carolina, Area." In Kuo, C. (ed.), Sea Level Rise, Climate Change and Coastal Drainage Systems. Washington, D.C.: U.S. Environmental Protection Agency (in press).

Leatherman, S.P. 1984. "Coastal Geomorphic Responses to Sea Level Rise: Galveston Bay, Texas." In Barth and Titus (eds.) 1984, op. cit.

Lennon, G.P., G.M. Wisniewski, and G.A. Yoshioka. 1986. "Impact of Increased River Salinity On New Jersey Aquifers." In Hull and Titus (eds.) 1986, op. cit.

Lingle, C.S. 1985. "A Model of a Polar Ice Stream and Future Sea-Level Rise Due to Possible Drastic Retreat of the West Antarctic Ice Sheet." In Meier et al. 1985, op. cit.

Meier, M.F. 1984. "Contribution of Small Glaciers to Global Sea Level." Science 226:1418-1421.

Meier, M.F., et al. 1985. Glaciers, Ice Sheets, and Sea Level: Effect of a CO2-Induced Climatic Change. Washington, D.C.: National Academy Press.

Mercer, J.H. 1978. "West Antarctic Ice Sheet and CO2 Greenhouse Effect: A Threat of Disaster?" Nature 271:321-325.

Mercer, J.H. 1968. "Antarctic Ice and Sangamon Sea Level." Geological Society of America Bulletin 79:471.

Meyerson, A.L. 1987. "Pollen and Paleosalinity Analyses from a Holocene Tidal Marsh Sequence." Marine Geology 12:335-357.

Milliman, J.D., and R.H. Meade. 1983. Worldwide Delivery of River Sediment to the Oceans. Journal of Geology 91(1):1-21.

Moore, W.S. 1982. Late Pleistocene Sea-Level History. In Uranium Series Disequilibrium: Applications to Environmental Problems, M. Ivanovich and R.S. Harmon (eds.). Clarendon, Oxford, p. 41.

Oldale, R. 1985. "Late Quarternary Sea Level History of New England: A Review of Published Sea Level Data." Northeastern Geology 7:192-200.

Park, R.A., T.R. Armentano, and C.L. Cloonan. 1986. "Predicting the Effects of Sea Level Rise on Coastal Wetlands." In J.G. Titus (ed.), 1986. Effects of Changes in Stratospheric Ozone and Global Climate. Washington, D.C.: U.S. Environmental Protection Agency and United Nations Environment Programme.

Redfield, A.C. 1972. "Development of a New England Salt Marsh." Ecological Monograph 42:201-237.

Redfield, A.C. 1967. "Postglacial Change in Sea Level in the Western North Atlantic Ocean." Science 157:687-692.

Revelle, R. 1983. "Probable Future Changes in Sea Level Resulting from Increased Atmospheric Carbon Dioxide." In Changing Climate. Washington, D.C.: National Academy Press.

Rind, D., and S. Lebedeff. 1984. Potential Climate Impacts of Increasing Atmospheric CO2 with Emphasis on Water Availability and Hydrology in the United States. Washington, D.C.: Government Printing Office.

Roberts, D., D. Davis, K.L. Meyer-Arendt, and K.M. Wicker. 1983. Recommendations for Freshwater Diversion to Barataria Basin, Louisiana. Baton Rouge: Coastal Management Section, Louisiana Department of Natural Resources.

Robin, G. 1985. "Contrast in Core: Changes in Climate or Ice Volumes?" Nature 316:578-589.

Roemmich, D. 1985. "Sea Level and Thermal Variability of the Ocean." In Meier et al., Glaciers, Ice Sheets, and Sea Level. Washington, D.C.: National Academy Press.

Roemmich, D., and C. Wunsch. 1984. "Apparent Changes in the Climatic State of the Deep North Atlantic Ocean." Nature 307:447-450.

Schneider, S.H., and R.S. Chen. 1980. "Carbon Dioxide Flooding: Physical Factors and Climatic Impact." Annual Review of Energy 5:107-140.

Sorensen, R.M., R.N. Weisman, and G.P. Lennon. 1984. "Control of Erosion, Inundation, and Salinity Intrusion." In Barth and Titus (eds.) 1984, op. cit.

Stearns, L.A., and B. MacCreary. 1957. "The Case of the Vanishing Brick Dust." Mosquito News 17:303-304.

Thomas, R.H. 1985. "Responses of the Polar Ice Sheets to Climatic Warming." In Meier et al. 1985, op. cit.

Thomas, R.H., T.J.O. Sanderson, and K.E. Rose. 1979. "Effect of Climatic Warming on the West Antarctic Ice Sheet." Nature 227:355-358.

Titus, J.G. 1984. "Planning for Sea Level Rise Before and After a Coastal Disaster." In Barth and Titus (eds.) 1984, op. cit.

Titus, J.G. 1985. "Sea Level Rise and the Maryland Coast." In Potential Impacts of Sea Level Rise on the Beach at Ocean City, Maryland. Washington, D.C.: U.S. Environmental Protection Agency.

Titus, J.G. n.d. "Greenhouse Effect, Sea Level Rise, and Society's Response." In Devoy, R.J., Sea Surface Studies. Cork, Ireland: University College.

Titus, J.G. 1986. "Greenhouse Effect, Sea Level Rise, and Coastal Zone Management." In Coastal Zone Management Journal, Volume 14, Number 3.

Titus, J.G. 1987. "Greenhouse Effect, Sea Level Rise, and Wetland Loss." In Greenhouse Effect, Sea Level Rise, and Coastal Wetlands. Washington, D.C." U.S. Environmental Protection Agency.

Titus, J.G., T. Henderson, and J.M. Teal. 1984. "Sea Level Rise and Wetlands Loss in the United States." National Wetlands Newsletter 6:4.

U.S. Army Corps of Engineers. 1982. Louisiana Coastal Area, Louisiana: Freshwater Diversion to Barataria and Breton Sound Basins. New Orleans: U.S. Army Corps of Engineers.

U.S. Army Corps of Engineers. 1980. Feasibility Report and Final Environmental Impact Statement: Atlantic Coast of Maryland and Assateague Island, Virginia. Baltimore: U.S. Army Corps of Engineers.

U.S. Army Corps of Engineers. 1979. Ocean Beach Study: Feasibility Report. San Francisco: U.S. Army Corps of Engineers.

U.S. Army Corps of Engineers, 1977. Shore Protection Manual. Fort Belvoir, Virginia: Coastal Engineering Research Center.

U.S. Army Corps of Engineers. 1971. National Shoreline Study. Washington, D.C.: U.S. Army Corps of Engineers.

Van Beek, J.L., D. Roberts, D. Davis, D. Sabins, and S.M. Gagliano. 1982. Recommendations for Freshwater Diversion to Louisiana Estuaries East of the Mississippi River. Baton Rouge: Coastal Management Section, Louisiana Department of Natural Resources.

Waddell, J.O., and R.A. Blaylock. n.d. "Impact of Sea Level Rise on Gap Creek Watershed in the Fort Walton Beach, Florida Area." In Kuo, C.Y. (ed.), op. cit.

Walsh, J.E., and C.M. Johnson. 1979. "Interannual Atmospheric Variability and Associated Fluctuations in Arctic Sea-Ice Extent." Journal of Geophysical Research 84:6915-6928.

Ward, L.G., and D.D. Domeracki. 1978. "The Stratographic Significance of Back-Barrier Tidal Channel Migration." Geological Society of America 10(4):201.

Weishar, L.L., and W.L. Wood. 1983. "An Evaluation of Offshore and Beach Changes on a Tideless Coast." Journal of Sedimentary Petrology 53(3):847-858.

Wendland, W.M. 1977. "Tropical Storm Frequencies Related to Sea Surface Temperatures." Journal of Applied Meteorology 16:480.

Zwally, H.J., C.L. Parkinson, and J.C. Comiso. 1983. "Variability of Antarctic Sea Ice and Changes in Carbon Dioxide." Science 220:1005-1012.

CHAPTER 16

POTENTIAL EFFECTS OF FUTURE CLIMATE CHANGES ON FORESTS AND VEGETATION, AGRICULTURE, WATER RESOURCES, AND HUMAN HEALTH

SUMMARY

The greenhouse effect resulting from increased levels of CO2, chlorofluorocarbons, methane, N2O, and other trace gases in the atmosphere has been recognized by the scientific community for several decades as a potential cause of future climate change. In the last few years, estimates of the rate of change of these gases in the atmosphere has heightened concern about global warming and associated climate and environmental change. Chapter 6 -- Global Warming--presents a review of recent chemical and physical evidence supporting the greenhouse phenomenon. From this evidence it is generally concluded that in the relatively short period of time of the next 50-100 years the earth's climate will undergo significant changes. These include potential increases in temperatures, and changes in precipitation, humidity, windfields, ocean currents, and in the frequency of extreme events such as hurricanes. Furthermore, these climate parameters will induce still other shifts in sea levels, ice margins, the hydrologic cycle, air pollution episodes and other phenomena.

Recently (1986) the World Meterological Organization (WMO), the United Nations Environment Program (UNEP), and the International Council of Scientific Unions (ICSU) summarized current scientific data on global climate change. These findings are presented in Exhibit 16-1. Similar findings have been reported by NAS (1979 and 1982).

EXHIBIT 16-1

Summary of Findings from the WMO/UNEP/ICSU Conference on Global Climate Held in Villach, Austria, October 1985

- Many important economic and social decisions are being made today on long-term projects -- major water resource management activities such as irrigation and hydro-power, drought relief, agricultural land use, structural designs and coastal engineering projects, and energy planning -- all based on the assumption that past climatic data, without modification, are a reliable guide to future climate conditions. This is no longer a valid assumption, since the increasing concentrations of greenhouse gases are expected to cause a significant warming of the global climate in the next century. It is a matter of urgency to refine estimates of future climate conditions to improve these decisions.

- The amounts of some trace gases in the troposhere, notably carbon dioxide (CO2), nitrous oxide (N2O), methane (CH4), ozone (O3), and chlorofluorocarbons (CFCs), are increasing. These

EXHIBIT 16-1
(continued)

gases are essentially transparent to incoming short-wave solar radiation, but absorb and emit long-wave radiation and are thus able to influence the earth's climate.

- The role of greenhouse gases other than CO2 in changing the climate is already about as important as that of CO2. If present trends continue, the combined concentrations of atmospheric CO2 and other greenhouse gases would be (radiatively) equivalent to a doubling of CO2 from pre-industrial levels, possibly as early as the 2030's.

- The most advanced experiments with general circulation models of the climatic system show increases of the global mean equilibrium surface temperature of between 1.5°C and 4.5°C for a doubling of the atmospheric CO2 concentration or the equivalent. Because of the complexity of the climatic system and the imperfections of the models, particularly with respect to ocean-atmosphere interactions and clouds, values outside of this range cannot be excluded. The realization of such changes will be slowed by the inertia of the oceans; the delay in reaching the mean equilibrium temperatures corresponding to doubled greenhouse gas concentrations is expected to be a matter of decades.

- While other factors such as aerosol concentrations, changes in solar energy input, and changes in vegetation may also influence climate, the increased amounts of greenhouse gases are likely to be the most important cause of climate change over the next century.

- Regional scale changes in climate have not yet been modeled with confidence. However, regional differences from the global averages show that warming may be greater in high latitudes during late autumn and winter than in the tropics; annual mean runoff may increase in high latitudes, and summer dryness may become more frequent over the continents at middle latitudes in the Northern Hemisphere. In tropical regions, temperature increases are expected to be smaller than the average global rise, but the effects on ecosystems and humans could have far-reaching consequences. Potential evapotranspiration probably will increase throughout the tropics, whereas in moist, tropical regions, convective rainfall could increase.

- Based on the observed changes since the beginning of this century, it is estimated that global warming of 1.5°-4.5°C would lead to a sea-level rise of 20-140 cm. A sea-level rise in the upper portion of this range would have major direct effects on coastal areas and estuaries. A significant melting of the West Antarctic ice sheet leading to a much larger rise in

EXHIBIT 16-1
(continued)

sea level, although possible at some future date, is not expected during the next century.

- Based on analyses of observational data, the estimated increase in global mean temperature of between 0.3°C and 0.7°C during the last 100 years is consistent with the projected temperature increase attributable to the observed increase in CO2 and other greenhouse gases, although it cannot be ascribed in a scientifically rigorous manner to these factors alone.

- Based on evidence of the effects of past climate changes, there is little doubt that a future change in climate of the magnitude obtained from climate models could have a profound effect on global ecosystems, agriculture, water resources, and sea ice.

As noted in the WMO/UNEP/ICSU report, the projected changes in climate will have important impacts on all aspects of society. Agriculture, forests, human health, water resources, wildlife, energy planning, and recreation are among the sectors likely to be affected. Moreover, all these sectors are likely to be affected simultaneously throughout the world, but to different extents. Today we know a great deal from paleoclimatic records about how past shifts in climate affected the growth and development of forest systems, the location of lakes, and the development of agriculture. But the changes that occurred to these systems in the past took 18 to 20 thousand years to unfold as the earth warmed approximately 4°-5°C. During that time, forest composition shifted, some lake systems were lost and new ones were formed. Most important, the changes took place during a period when the earth's population was small and civilizations were in formative stages.

Today modern society is much more complex, but still vulnerable to climatic changes. Our industrial society relies on a sustained climate to replenish natural resources as a source of raw materials, for transport of goods, and for the food we eat. We assume that the climate that supports our society, while variable and difficult to predict over short periods, will not shift appreciably. Indeed, most decisions made by farmers, forest managers, state and local water management officials, utility executives and government policy makers are based on the assumption that climate will be constant. However, if current predictions from global climate models prove to be correct, some increase in global temperatures may be inevitable simply because of the presence of trace gases that have already been emitted to the atmosphere.

Our current understanding of the effects of global climate change on the environment is incomplete. Moreover, several features of the greenhouse phenomenon make it unique, different from other environmental issues and difficult to analyze. Among these features are the following:

- The effects will not take place immediately, but over many decades.

- The effects will be virtually irreversible over several centuries.

- All nations of the world will experience the effects at the same time.

- There is no historical analog for the amount of global warming likely to occur in the relatively short period of the next 50-100 years.

Scientists have only begun to analyze the potential impacts from global warming and changes in other climate variables. Insights are available from historical data and from the application of predictive models. In most cases, however, our understanding of the consequences, both beneficial and detrimental, is in a formative stage. Historical analogs provide qualitative information about likely effects, but they cannot predict the future because the anticipated rate and increase in temperature are beyond the range of previous warm periods. Predictive models of both the climate system and potential effects often do not include complete parameterizations of important system variables. Thus, more advanced global climate models capable of providing regional predictions are needed, and more comprehensive and sophisticated analyses of environmental effects are necessary to understand fully the implications throughout the world.

Recognizing these limitations, the following section summarizes what is known about climate impacts on the environment with emphasis on forests, agriculture, water resources, and human health. Perhaps of equal importance are potential impacts that have not been reported or analyzed, including potential impacts on ports, electricity demand and supply, population shifts, hurricane frequency, air pollution emissions, wildlife management, and the U.S.' competitive position in the world. These potential impact areas and many others represent the challenges to be investigated as the science supporting predictions of global climate change improves.

FINDINGS

The following findings are summarized from Appendix B of the Risk Assessment, which provides a comprehensive review of potential impacts of global climate change.

1. CLIMATE CHANGE HAS HAD A SIGNIFICANT IMPACT ON FORESTS IN THE PAST. IF CURRENT PREDICTIONS PROVE ACCURATE, THERE IS A POTENTIAL FOR DRAMATIC SHIFTS IN FORESTS AND VEGETATION OVER THE NEXT 100 YEARS.

   1a. Climate models predict that a global warming of approximately 1.5°C to 4.5°C will be induced by a doubling of atmospheric CO2 and other trace gases during the next 50 to 100 years. The period 18,000 to 0 years B.P. is the only general analog for a global climate change of this magnitude. The geological record from this glacial to inter-glacial interval provides a basis for qualitatively understanding how vegetation may change in response to large climatic change.

   1b. The paleovegetational record shows that climatic change as large as that expected to occur in response to CO2 doubling is likely to induce significant changes in the composition and patterns of the world's biomes. Changes of 2°C to 4°C have been significant enough to alter the composition of biomes, and to cause new biomes to appear and others to disappear. At 18,000 B.P., the vegetation in eastern North America was quite distinct from that of the present day. The cold, dry climate of that time seems to have precluded the widespread growth of birch, hemlock, beech, alder, hornbeam, ash, elm, and chestnut, all of which are fairly abundant in present-day deciduous forest. Southern pines were limited to grow with oak and hickory in Florida.

   1c. Available paleoecological and paleoclimatological records do not provide an analog for the high rate of climate change and unprecedented global warming predicted to occur over the next century. Previous changes in vegetation have been associated with climates that were nearly 5°C to 7°C cooler and took thousands of years to evolve rather than decades, the time during which such changes are now predicted to occur. Insufficient temporal resolution (e.g., via radiocarbon dates) limits our ability to analyze the decadal-scale rates of change that occurred prior to the present millennium.

   1d. Limited experiments conducted with dynamic vegetation models for North America suggest that decreases in net biomass may occur and that significant changes in species composition are likely. Experiments with one model suggest that eastern North American biomass may be reduced by 11 megagrams per hectare (10% of live biomass) given the equivalent of a doubled CO2 environment. Plant taxa will respond individualistically rather than as whole communities to regional changes in climate variables. At this time such analyses must be treated as only suggestive of the kinds of change that could occur. Many critical processes are simplified or omitted and the actual situation could be worse or better.

1e. Future forest management decisions in major timber-growing regions are likely to be affected by changes in natural growing conditions. For example, one study suggests that loblolly pine populations are likely to move north and northeast into Pennsylvania and New Jersey, while its range shrinks in the west. The total geographic range of the species may increase, but a net loss in productivity may result because of shifts to less accessible and less productive sites. While the extent of such changes is unclear, adjustments will be needed in forest technology, resource allocation, planning, tree breeding programs, and decision-making to maintain and increase productivity.

1f. Dynamic vegetation models based on theoretical descriptions of all factors that could influence plant growth must be improved and/or developed for all major kinds of vegetation. In order to make more accurate future predictions, these models must be validated using the geological record and empirical ecological response surfaces. In particular, the geological record can be used to test the ability of vegetation models to simulate vegetation that grew under climate conditions unlike any of the modern day conditions.

1g. Dynamic vegetation models should incorporate direct effects of atmospheric CO2 increases on plant growth and other air pollution effects. Improved estimates of future regional climates are also required in order to make accurate predictions of future vegetation changes.

2. LIMITED ASSESSMENTS SUGGEST THAT IMPORTANT CHANGES IN AGRICULTURE AND FARM PRODUCTIVITY ARE LIKELY THROUGHOUT THE WORLD IF CLIMATE CHANGE OCCURS AS PREDICTED. ESTIMATES OF IMPACTS ON SPECIFIC REGIONS ARE DIFFICULT TO MAKE BECAUSE REGIONAL PROJECTIONS OF CHANGE CANNOT BE RELIABLY MADE. CURRENT CLIMATIC KNOWLEDGE IS ONLY SUFFICIENT TO SUPPORT VULNERABILITY STUDIES FOR ALTERNATIVE SCENARIOS.

2a. Climate has had a significant impact on farm productivity and geographical distribution of crops. Examples include the 1983 drought, which contributed to a nearly 30 percent reduction in corn yields in the U.S.; the persistent Great Plains drought between 1932-1937, which contributed to nearly 200,000 farm bankruptcies; and the climate shift of the Little Ice Age (1500-1800), which led to the abandonment of agricultural settlements in Scotland and Norway.

2b. World agriculture is likely to undergo significant shifts if trace-gas-induced climate warming in the range of 1.5°C to 4.5°C occurs over the next 50 to 100 years. Climatic effects on agriculture will extend from local to regional and international levels. However, modern agriculture is very dynamic and is constantly responding to changes in production, marketing, and government programs.

2c. The main effects likely to occur at the field level will be physical impacts of changes in thermal regimes, water conditions, and pest infestations. High temperatures have caused direct damage to crops such as wheat and corn; moisture stress, often associated with elevated temperatures, is harmful to corn, soybean, and wheat during

flowering and grain fill; and increased pests are associated with higher, more favorable temperatures.

2d. Even relatively small increases in the mean temperature can increase the probability of harmful effects in some regions. Analysis of historical data has shown that an increase of 1.7°C (3°F) in mean temperature changes by about a factor of three the likelihood of a five-consecutive-day maximum temperature event of at least 35°C (95°F) occurring in a city like Des Moines. In regions where crops are grown close to their maximum tolerance limits, extreme temperature events may have significant harmful effects on crop growth and yield.

2e. Limited experiments using climate scenarios and agricultural productivity models have demonstrated the sensitivity of agricultural systems to climate change. Future farm yields are likely to be affected by climate because of changes in the length of the growing season, heating units, extreme winter temperatures, precipitation, and evaporative demand. In addition, field evaluations show that total productivity is a function of the drought tolerance of the land and the moisture reserve, the availability of land, the ability of farmers to shift to different crops, and other factors.

2f. The transition costs associated with adjusting to global climatic change are not easily calculated, but are likely to be very large. Accommodating to climate change may require shifting to new lands and crops, creating support services and industries, improving and relocating irrigation systems, developing new soil management and pest control programs, and breeding and introducing new heat- or drought-tolerant species. The consequences of these decisions on the total quantity, quality, and cost of food are difficult to predict.

2g. Current projections of the effects of climate change on agriculture are limited because of uncertainties in predicting local temperature and precipitation patterns using global climate models, and because of the need for improved research studies using controlled atmospheres, statistical regression models, dynamic crop models and integrated modeling approaches.

3. WATER RESOURCE SYSTEMS HAVE UNDERGONE IMPORTANT CHANGES AS THE EARTH'S CLIMATE HAS SHIFTED IN THE PAST. CURRENT ANALYSES SUGGEST AN INTENSIFIED HYDROLOGIC CYCLE, IF CLIMATE CHANGE OCCURS AS PREDICTED.

3a. There is evidence that climate change since the last ice age (18,000 years B.P.) has significantly altered the location of lakes -- although the extent of present day lakes is broadly comparable with 18,000 years B.P. For example, there is evidence indicating the existence of many tropical lakes and swamps in the Sahara, Arabian, and Thor Deserts around 9,000 to 8,000 years B.P.

3b. The inextricable linkages between the water cycle and climate ensure that potential future climate change will significantly alter hydrologic processes throughout the world. All natural hydrologic processes--precipitation, infiltration, storage and movement of soil

moisture, surface and subsurface runoff, recharge of groundwater, and evapotranspiration--will be affected if climate changes.

3c. As a result of changes in key hydrologic variables such as precipitation, evaporation, soil moisture, and runoff, climate change is expected to have significant effects on water availability. Early hydrologic impact studies provide evidence that relatively small changes in precipitation and evaporation patterns might result in significant, perhaps critical, changes in water availability. For many aspects of water resources, including human consumption, agricultural water supply, flooding and drought management, groundwater use and recharge, and reservoir design and operation, these hydrologic changes will have serious implications.

3d. Despite significant differences among climate change scenarios, a consistent finding among hydrologic impact studies is the prediction of a reduction in summer soil moisture and changes in the timing and magnitude of runoff. Winter runoff is expected to increase and summer runoff to decrease. These results appear to be robust across a range of climate change scenarios.

3e. Future directions for research and analyses suggest that improved estimates of climate variables are needed from large-scale climate models; innovative techniques are needed for regional assessments; increased numbers of assessments are necessary to broaden our knowledge of effects on different users; and increased analyses of the impacts of changes in water resources on the economy and society are necessary.

4. MORBIDITY AND MORTALITY RATES ARE ASSOCIATED WITH WEATHER EXTREMES IN OUR SOCIETY (chapter 16).

4a. Weather has a profound effect on human health and well being. It has been demonstrated that weather is associated with changes in birth rates, outbreaks of pneumonia, influenza, and bronchitis, and related to other morbidity effects, and is linked to pollen concentrations and high pollution levels.

4b. Large increases in mortality have occurred during previous heat and cold waves. It is estimated that 1,327 fatalities occurred in the United States as a result of the 1980 heat wave, and Missouri alone accounted for over 25 percent of that total.

4c. Hot weather extremes appear to have a more substantial impact on mortality than cold wave episodes.

4d. Threshold temperatures, which represent maximum and minimum temperatures associated with increases in total mortality, have been determined for various cities. These threshold temperatures vary regionally; for example, the threshold temperature for winter mortality in mild southern cities such as Atlanta is $0^{o}C$ and for more northerly cities such as Philadelphia, threshold temperature is $-5^{o}C$.

4e. If future global warming induced by increased concentrations of trace gases does occur, it has the potential to affect human mortality significantly. In one study, total summertime mortality in New York City was estimated to increase by over 3,200 deaths per year for a 7°F trace-gas-induced warming without acclimatization. If New Yorkers fully acclimatize, the number of additional deaths is estimated to be no different than today. It is hypothesized that if climate warming occurs, some additional deaths are likely to occur because economic conditions and the basic infrastructure of the city will prohibit full acclimatization even if behavior changes.

REFERENCES

National Academy of Sciences (1979), Carbon Dioxide and Climate: A Scientific Assessment, National Academy Press, Washington, D.C.

National Academy of Sciences (1982), Carbon Dioxide and Climate: A Second Assessment, National Academy Press, Washington, D.C.

World Meterological Organization, United Nations Environment Programme, and International Council of Scientific Unions (1986), Report of the International Conference on the Assessment of the Role of Carbon Dioxide and of Other Greenhouse Gases in Climate Variations and Associated Impacts, Villach Austria, 9-15 October 1985, WMO No. 661.

CHAPTER 17

MODELS FOR INTEGRATING THE ANALYSES OF HEALTH AND ENVIRONMENTAL RISKS ASSOCIATED WITH OZONE MODIFICATION

SUMMARY

Analyses of the potential risks due to emissions of ozone-modifying substances and greenhouse gases must assess a variety of effects on human health and the environment. To assess risks numerous factors must be examined together, including: economic and population growth; chemical use and emissions; ozone modification; changes in ultraviolet (UV) radiation flux; climate change; and effects on human health and the environment.

To evaluate risks the Integrating Analysis Model has been developed to provide a framework for systematically evaluating the risks and costs associated with alternative assumptions about the ozone modification issue and policies for limiting the emissions of ozone-modifying substances. This chapter describes the manner in which the Integrating Analysis Model (the model) draws from the analyses described in earlier chapters.

The model begins with assumptions about the potential future use of ozone-modifying substances and concentrations of other trace gases, including chlorofluorocarbons, methyl chloroform, carbon tetrachloride, Halons (bromine-containing compounds), carbon dioxide, methane, and nitrous oxide. This potential future use and emissions may be modified by control strategies. The resulting global emissions of the substances are computed, followed by the atmospheric science module, which assesses the impacts of these emissions on ozone. The risks of ozone modification for human health and the environment are evaluated using specified dose-response relationships where available for each of the areas of interest.

Using this overall framework, the model can reflect a wide range of assumptions and the joint implications of all the assumptions can be identified. Of note is that the model is not a substitute for choosing the assumptions, relationships, and data to describe the system being modeled. It merely reflects these assumptions and data in a consistent framework.[1]

---

[1] When used for performing policy analysis, the model does not make decisions, for example, about which, if any, control strategies are preferred or about which, if any, ozone depletion estimates are correct. Decisions about the need to protect stratospheric ozone or the best way to do so must be based not only on model results, but also on considerations and judgments either not reflected in the model or reflected implicitly in the assumptions provided as inputs to the model.

INTRODUCTION

Analyses of the potential risks due to emissions of ozone-modifying substances and greenhouse gases must assess a variety of effects on human health and the environment. As described earlier in this document, numerous factors influence ozone modification and its effects. To assess risks, the following must be characterized, and their joint implications (including their uncertainties) examined together: economic and population growth; chemical use and emissions; ozone modification; changes in ultraviolet (UV) radiation flux; climate change; and effects on human health and the environment.

Analyzing and combining these factors is a complex task. To make this task tractable, two models have been developed:

1. Integrating Analysis Model. The primary role of the Integrating Analysis Model is to provide a framework for systematically evaluating the risks and costs associated with alternative assumptions about the ozone modification issue and policies for limiting the emissions of ozone-modifying substances.

2. Transient Temperature and Sea Level Rise Model. The primary role of this model is to assess the implications of emissions of greenhouse gases in terms of increases in global average temperature and sea level over time.

Together, these two models provide a comprehensive framework for evaluating the potential risks of emissions of ozone-modifying substances and greenhouse gases. This chapter describes the manner in which the Integrating Analysis Model (the model) draws from the analyses described in earlier chapters.[2] The Transient Temperature and Sea Level Rise Model is described in Appendix A of Chapter 6.

This chapter first describes the framework that the model provides for the analysis. Then, an overview of the model's analytic procedure is presented. The third section of this chapter presents the major limitations of the model. The chapter concludes with a series of appendices that describe the model's design and operation in detail.

THE MODEL AS A FRAMEWORK

The objective of the model is to provide a framework within which the implications of alternative assumptions and policies can be identified. The framework reflects the order and structure of the analysis, and the user may define the assumptions and data to be used in the model for any given run. Exhibit 17-1 displays the major parts or "modules" of the model. The model begins with assumptions about the potential future use of ozone-modifying substances and concentrations of other trace gases, including chlorofluorocarbons, methyl chloroform, carbon tetrachloride, Halons (bromine-containing

---

[2] The Integrating Analysis Model was originally described in Gibbs and Hoffman (1986).

EXHIBIT 17-1

Modular Structure

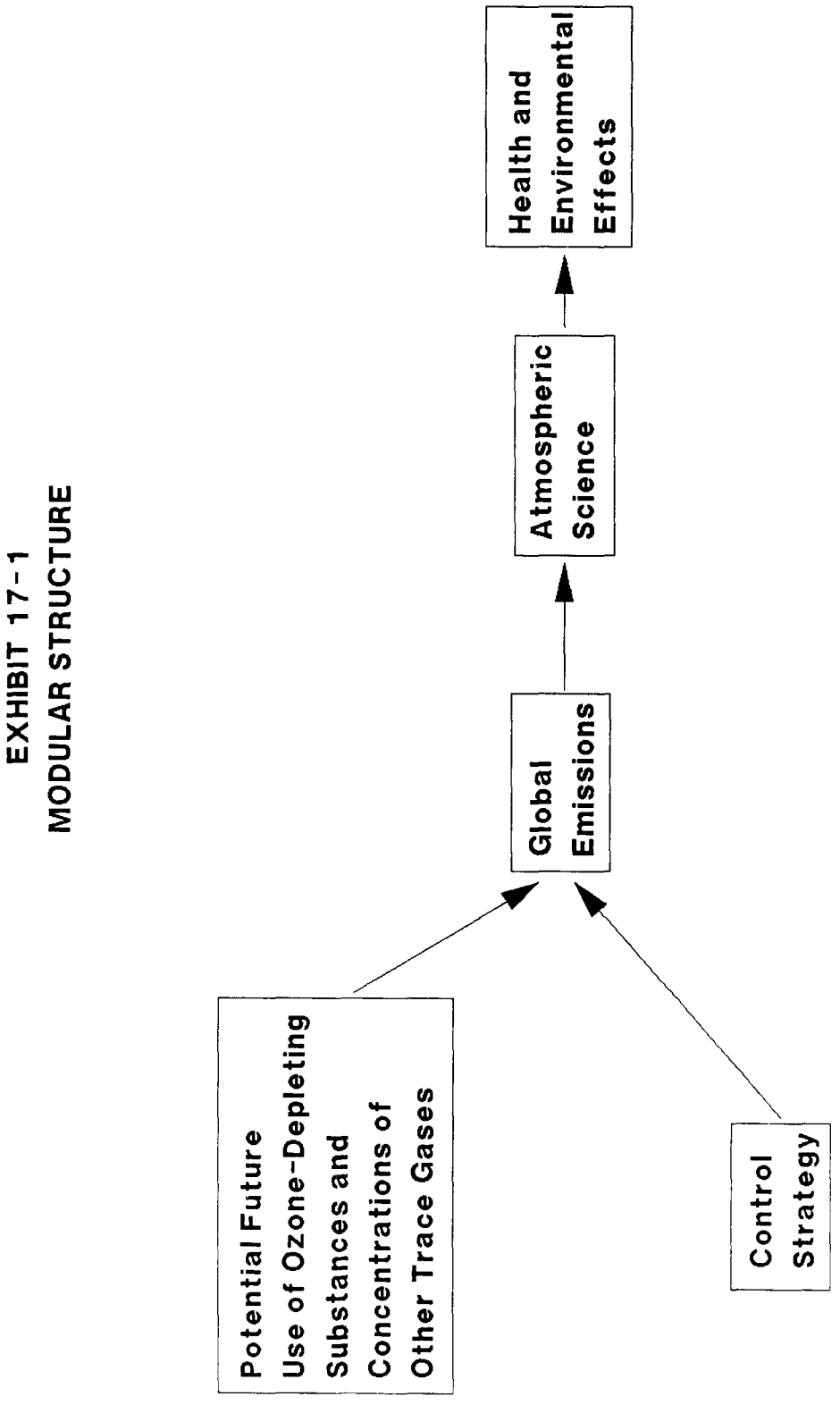

compounds), carbon dioxide, methane, and nitrous oxide. This potential future use and emissions may be modified by control strategies. The resulting global emissions of the substances are computed, followed by the atmospheric science module, which assesses the impacts of these emissions on ozone.[3] The risks of ozone modification for human health and the environment are evaluated using specified dose-response relationships where available for each of the areas of interest.

Using this overall framework, the model can reflect a wide range of assumptions within each of the modules. When the model is run, the joint implications of all the assumptions are identified. Of note is that the model is not a substitute for choosing the assumptions, relationships, and data to describe the system being modeled. It merely reflects these assumptions and data in a consistent framework. In its simplest terms, the model is a calculator that is needed to assist in computing multiple estimates of possible values. Decisions about best assumptions or the need to protect stratospheric ozone or the best way to do so may be made using the model and its results, but must also be based on considerations and judgments either not reflected in the model or reflected implicitly in the assumptions provided as inputs to the model.

ANALYSIS PROCEDURE

A model "run" is comprised of:

- o inputs provided by the user that define the data and assumptions to use in the analysis;
- o algorithms that are carried out according to the user's inputs and instructions contained within the model; and
- o outputs prepared by the model that describe the results of the algorithms that are carried out.

The model is "deterministic," meaning that a unique output or result is produced by a specified input; there are no random (i.e., stochastic) elements within the model.

To initiate a model run, the user must specify inputs for each module he wishes to use. (The user may choose to run only a portion of the model.) Exhibit 17-2 provides an overview of the input choices for each of the following modules:

- o Potential Use. The user may choose one of the six scenarios of future use that have been incorporated into the model. The compounds included are: chlorofluorocarbons (CFC-11; CFC-12; HCFC-22; CFC-113); carbon-tetrachloride (CCL4); methyl chloroform (CH3CCL3); Halon-1211; and Halon-1301. Each compound can be

---

[3] These emission rates are also used in the Transient Temperature and Sea Level Rise Model to evaluate climate change effects.

EXHIBIT 17-2

Major Model Input Choices

MODULE	CHOICES	COMMENTS	SOURCES
Potential Future Use of Ozone-Modifying Substances	Future Use: -- Scenarios based on studies of historical trends and projections of economic growth and population growth -- Any user-supplied estimates of future use can be incorporated	Future Use: -- Scenarios reflect a wide range of potential future use.	Based on: UNEP (1986).
Control Strategies	Strategies can be defined in terms of limits to production in various ways, including: -- limits in kilograms; -- limits in kilograms per capita; -- bans of specified uses; -- requirements to implement specified technologies; and -- fees or taxes.	Data on control options are based on U.S. data.	Estimates of the costs and effectiveness of controls are based on data developed in EPA (1987).
Global Emissions	Several estimates of the rate of release after use have been developed based on analyses of historical data. Emissions reflect the effectiveness of the control strategy in limiting emissions. The user may choose several scenarios of effectiveness, which reflects the level of reductions expected to occur as the result of the control strategy identified.	Data on the effectiveness of control options are based on U.S. data. Information on other parts of the world may be entered by the user.	The rates of emissions following use are based on data presented in Quinn (1986).

EXHIBIT 17-2 (continued)

MAJOR MODEL INPUT CHOICES

MODULE	CHOICES	COMMENTS	SOURCES
Atmospheric Science	Ozone Modification: -- Parameterized relationship between global emissions and global ozone depletion. -- The user may specify his own estimate of ozone depletion for use in the model. If this choice is made, the global emissions estimate is not used.	Ozone Modification: Global estimates based on analysis of a one-dimensional atmospheric model.	Based on Connell (1986).
Health and Environmental Effects	Ranges of relationships with UV radiation are developed for each effect. The user may specify for each effect low, medium, or high estimates.	Ranges based on published estimates.	Based on analyses by: Scotto, Fears, and Fraumeni (1981), Scotto and Fears (in press), Hiller, Sperduto, and Ederer (1983), Horst (1986), Andrady (1986), and Pitcher (in press).

analyzed for up to six end uses, in 10 regions of the world. The six scenarios reflect a wide range of potential future use, and are based on historical trends and projections.[4] Alternatively, the user may specify his own scenario of future use.

- o Control Strategy. The user may specify a variety of controls on future use, such as kilogram limits, use limits, technology requirements, or fees. The potential costs and benefits of controls are not evaluated in this document because the objective of this risk assessment is to evaluate risks in the absence of regulation.

- o Global Emissions. Emissions of the chlorofluorocarbons, CCL4, CH3CCL3, Halon-1211 and Halon-1301 are computed from the production and use estimates based on release rates that reflect the fact that these chemicals are stored in certain products for various periods of time. The effects of control strategies are reflected in the release estimates, and the user may specify alternative release rates as desired. Scenarios of atmospheric concentrations are also specified for carbon dioxide (CO2), methane (CH4) and nitrous oxide (N2O).

- o Atmospheric Science. A parameterized numerical fit to a one-dimensional (1-D) atmospheric model is used to compute global ozone depletion as a function of global emissions of chlorofluorocarbons, CCl4, CH3CCl3, and Halons, and concentrations of CO2, N2O and CH4.[5] The uncertainty in the estimates of global depletion may be modeled.[6] Alternatively, the user may bypass this algorithm and use a different relationship or independent estimates of global ozone depletion.

- o Health and Environmental Effects. The association between ozone depletion, ultraviolet (UV) radiation, and effects may be specified by the user. Ranges of dose-response relationships may be identified for melanoma and nonmelanoma skin cancers, and cataracts. Population projections (by race, age, and sex) are incorporated into the model for purposes of computing future incidence of human health effects. Alternative population estimates may be identified by the model user. The effects on PVC polymers are also reported. Potential impacts on aquatic organisms, plants, ground-based ozone, and coastal areas are also identified based on existing case study data. Estimates of effects are made for the U.S. only.

---

[4] These six scenarios are described in Chapter 18.

[5] See Connell (1986) for a description of this method.

[6] The range of uncertainty identified in Stolarski and Douglass (1985) is currently incorporated into the model. These uncertainties reflect the results of a Monte Carlo analysis in which kinetic rate coefficients and cross sections are varied according to the JPL 85-37 panel. Consequently, not all uncertainties are included. The user may provide alternative uncertainty estimates.

Based on these inputs, the model performs calculations on a year-by-year basis. For example, at the beginning of year t, the model first computes the potential use of each of the ozone-modifying substances in each of its applications in each portion of the world being analyzed. This estimate of use reflects the user's choice of scenario (for the first module) as well as the effects of any controls initiated according to the user's instructions prior to and including year t. Based on this estimate of use in year t, and estimates for all years prior to year t, the global emissions in year t are computed for each potential ozone-depleting substance.

The atmospheric science module computes an estimate of global ozone depletion for year t based on the emission estimates for year t, atmospheric conditions due to emissions prior to year t, and user-specified assumptions regarding the concentrations of carbon dioxide, methane, and nitrous oxide.[7] Global ozone depletion is computed and then translated into associated changes in UV flux, using three action spectra for weighting the different UV wavelengths: DNA damage; Robertson-Berger Meter (RB-Meter), and erythema. The changes in UV flux in year t (and prior years) are used in dose-response relationships to estimate increased risks of melanoma and nonmelanoma skin cancers and cataracts. Other impacts, such as polymer degradation, are also computed.

After the computations for year t are performed, the model repeats the computations for year t+1. This annual series of computations is consequently repeated for each year of the model run. After all the years have been analyzed, the following summary outputs are produced:

- future production of ozone-depleting substances;
- future emissions of ozone-depleting substances;
- future global ozone depletion;
- future ozone depletion by latitude;
- future increases in UV flux; and
- estimates of effects, including:
  - -- melanoma skin cancers (incidence and mortality);
  - -- nonmelanoma skin cancers (incidence and mortality);
  - -- cataracts (incidence);
  - -- costs of damages to polymers (PVC used outdoors); and
  - -- potential impacts on ground-based ozone, plants, aquatic organisms, and coastal areas.

The effects estimates are currently based primarily on data that describe the U.S. Consequently, only U.S. effects estimates are currently produced.

---

[7] Ranges of assumptions for these gases are described in Chapter 4.

MODEL LIMITATIONS

In using any model, it is important to understand its limitations. The model is being developed in a neutral fashion. Its flexible design allows users to evaluate wide ranges of inputs and assumptions. The model cannot incorporate, however, numerous factors that are as yet undefined or poorly understood. Consequently, the model excludes a variety of potential factors and analyses that may be important for making decisions regarding stratospheric ozone protection.

The most important exclusions from the model are a variety of effects of ozone modification. Many effects that increased UV radiation will have on human health and the environment are not well quantified. For example, only limited data are available that describe the effects of UV radiation on plants and aquatic organisms. These data cannot necessarily be extrapolated to all crops and ecosystems to evaluate the net effects of ozone modification and global warming; actual damages could be higher or lower. The potential for effects is substantial, but current data do not allow reliable quantitative estimates at this time. Similarly, the effects of UV radiation on ground oxidants are not well quantified at this time for most cities or rural areas (see Whitten (1986) for case studies of effects on oxidants).

Similarly, too little knowledge currently exists to allow immune suppression effects of increased UV radiation to be quantified. These effects may be particularly important because they may affect all individuals in the world in important ways that are not currently anticipated.

Exhibit 17-3 summarizes the effects for which reliable projections are not yet possible. The omission of these known effects would be a clear bias reflected in the estimates of the risks associated with ozone depletion. In addition, there may be other links among UV radiation, global warming, and human health and the environment that have not yet been identified. The potential bias of omitting the results of these latter areas due to lack of information on these effects is unknown.

The model could be used to address issues related to risk management and policy analysis.[8] However, this document does not address these issues because it is focused on risk assessment.

---

[8] The model could be used to address a variety of risk management issues, including: (1) the feasibility of alternative control strategies; and (2) the number of countries likely to participate in international agreements to limit the use and emissions of ozone-depleting substances. It does not have the capability, however, to evaluate potential trade of ozone-modifying substances among regions of the world.

Decision makers must use their own judgments regarding these factors. The model may be used to test the implications of these judgments (e.g., the implications of only half the countries participating in a control strategy may be identified by specifying the expected participation as a model input). However, the model is not meant to be used in place of these types of judgments, or any others, that are required of decision makers.

Similarly, extrapolation of case study results to a wider scope is unlikely to yield reliable estimates of damages: they may be too high or too low. Nonetheless, it is a question of judgment whether examination of such output adds information to the decision-making process.

EXHIBIT 17-3

Effects Not Quantified

Effect	Comments
Impact on plants	Preliminary experiment data indicate risks of decreased yields. See Chapter 11.
Impact on aquatic organisms	Laboratory data indicate increase UV radiation may adversely affect survivability and breeding. See Chapter 12.
National impact on urban and rural ground-based ozone formation (smog)	Case studies of three cities indicate potential increases in smog formation, and formation earlier in the day. See Chapter 14.
Increased incidence of cutaneous diseases as a result of immune suppression	See Chapter 9.
Impacts of climate change on human health, water resources, forestry, and agriculture	See Chapter 16.
Impacts of sea level rise on wetlands	See Chapter 15.
Impacts on polymers other than PVC	See Chapter 13.

REFERENCES

Andrady, A. (1986), "Analysis of Technical Issues Related to the Effect of UV-B on Polymers," prepared for the U.S. Environmental Protection Agency, Washington, D.C.

Camm, F. et al. (1986), "Social Cost of Technical Control Option to Reduce Emissions of Potential Ozone Depleters in the United States: An Update," The RAND Corporation, prepared for the U.S. Environmental Protection Agency, Washington, D.C.

Connell, Peter S. (1986), "A Parameterized Numerical Fit to Total Column Ozone Changes Calculated by the LLNL 1-D Model of the Troposphere and Stratosphere," Lawrence Livermore National Laboratory, Livermore, California.

EPA (1987). Draft Regulatory Impact Analysis: Protection of Stratospheric Ozone, Office of Air and Radiation, U.S. Environmental Protection Agency, Washington, D.C.

Gibbs, M.J. and J.H. Hoffman (1986), "STRATO: A Model for Analyzing the Implications of Control Strategies for Protecting Stratospheric Ozone," presented at the EPA Workshop on CFCs, March 1986.

Hiller, R., R. Sperduto, and F. Ederer (1983), "Epidemiologic Associations with Cataract in the 1971-1972 National Health and Nutrition Examination Survey," American Journal of Epidemiology, Vol. 118, No. 2, pp. 239-248.

Horst, R.L. (1986), "The Economic Impacts of Increased UV-B Radiation on Polymer Materials: A Case Study of Rigid PVC," prepared for the U.S. Environmental Protection Agency, Washington, D.C.

Isaksen, I.S.A. (1986), "Ozone Perturbations Studies in a Two-Dimensional Model with Temperature Feedback in the Stratosphere Included," presented at UNEP Workshop on the Control of Chlorofluorocarbons, Leesburg, Virginia, September 1986.

Pitcher, H. (1986), "Melanoma Death Rates and Ultraviolet Radiation in the United States," U.S. Environmental Protection Agency, Washington, D.C.

Quinn, T.H., et al. (1986), "Projected Use, Emissions, and Banks of Potential Ozone-depleting Substances," The RAND Corporation, prepared for the U.S. Environmental Protection Agency, Washington, D.C.

Scotto, J., T.R. Fears, and J.F. Fraumeni, Jr. (1981), "Incidence of Nonmelanoma Skin Cancer in the United States," U.S. Department of Health and Human Services, (NIH) 82-2433, Bethesda, Maryland.

Scotto, J., and T. Fears (in press), "The Association of Solar Ultraviolet Radiation and Skin Melanoma Among Caucasians in the United States," Cancer Investigations.

Stolarski, R.S., and A.R. Douglas. (1985), "Sensitivity of an Atmospheric Photochemistry Model to Chlorine Perturbations Including Consideration of Uncertainty Propagation," NASA/Goddard Space Flight Center, Greenbelt, Maryland, and Applied Research Corporation, Landover, Maryland.

UNEP (1986), "Summary Paper for Topic #2: Projections of Future Demand," presented at the UNEP Workshop on the Control of Chlorofluorocarbons, Rome, Italy, May 1986.

APPENDIX A

MODEL DESIGN AND MODEL FLOW

INTRODUCTION

This appendix describes the design and flow of the CFC Policy Model (the model). The model is deterministic -- it computes a series of outputs from data supplied by the model user and from data that reside in files associated with the model. A model "run" is comprised of (1) a set of instructions (i.e., inputs) supplied by the model user; (2) a set of computations performed within the model; and (3) a set of output tables that present the results of the computations performed by the model. The model is designed with a modular structure, with each "module" performing a designated function. The modules are independent entities that communicate with each other.

The modular structure facilitates the maintenance and development of the model by:

- allowing desired modifications to the model to be localized to individual modules;
- allowing communication among modules to be identified easily (communication among modules is particularly important for modeling feedbacks from one portion of the model to another portion); and
- minimizing memory requirements and execution time.

The remainder of this appendix is divided into the following sections:

- Level of Aggregation;
- Model Flow;
- Specifying a Model Run; and
- Limitations.

LEVEL OF AGGREGATION

The smallest unit of analysis in the model includes compound, region, end use, and time, as follows:

- Compound -- Up to ten compounds may be analyzed separately:
  - -- CFC-11;
  - -- CFC-12;
  - -- HCFC-22;
  - -- CFC-113;
  - -- CFC-114;

-- CFC-115;
-- Carbon tetrachloride (CCl_4);
-- Methyl chloroform (CH_3CCl_3);
-- Halon-1211; and
-- Halon-1301.

Data are currently not analyzed for CFC-114 and CFC-115.

- Region -- The world is divided into 10 separate regions (the regions can be analyzed individually or in groups):

  -- USA;
  -- Canada;
  -- Western Europe;
  -- Japan, Australia, and New Zealand;
  -- USSR and East Bloc;
  -- Centrally Planned Asia;
  -- Middle East;
  -- Africa;
  -- Latin America; and
  -- South and East Asia.

- End Use -- Each compound may be identified with up to six applications or "end uses." Each end use can be analyzed separately. End uses currently incorporated into the model include:

  -- aerosol propellant;
  -- flexible foam;
  -- rigid polyurethane foam;
  -- rigid nonurethane foam;
  -- refrigeration;
  -- solvent;
  -- fire extinguisher; and
  -- miscellaneous.

- Time -- a year is the smallest unit of time in this model. The current range is 1931-2165.

Analysis is performed at these levels of information. Major revisions to the model are required to modify this level of disaggregation.

MODEL FLOW

The model is divided into two main parts: (1) the Analysis Program reads input data, performs computations, and creates output files; (2) the Report Writer Program reads output files from the Analysis Program, and creates formatted reports as specified by the user. This section discusses each part of the model in turn.

Analysis Program

The Analysis Program begins by reading an input file that describes the configuration of the model run desired by the user, including:

- o which years will be analyzed;
- o the portions of the model (i.e., modules) that will be used in the analysis;
- o the data files that will be used as inputs;
- o the years for which output values should be computed; and
- o the discount rates used for estimating the present value of costs and benefits.

Based on these user-supplied data, a series of variables are initialized and the model run specified by the user then proceeds.

The flow of a model run can be described in terms of the following five primary parts or "modules" of the Analysis Program:

1. Production Scenarios Module;
2. Policy Alternatives Module;
3. Emissions Module;
4. Atmospheric Science Module; and
5. Effects Module.

As shown in Exhibit A-1, these five modules are all executed within a "year loop," i.e., all the information from all the modules is computed for one year, then the model moves on to the next year. This structure has several benefits, including:

- o the results of year "t" can be used to indicate what would happen in year "t+1" (in other words, feedbacks between modules and across years can be modeled);
- o the information required to be stored is limited to the current year being analyzed.

Appendices B through F describe each of the modules in turn. Briefly, each module performs the following computations:

- o Appendix B: Production Scenarios Module -- This module computes a scenario of production over time for each compound. The scenario for each compound is disaggregated by region and end use.
- o Appendix C: Policy Alternatives Module -- This module identifies the implications of alternative control policies specified by the user. The module's inputs include policy specifications (from the user), production scenarios (from the previous module), and candidate

EXHIBIT A-1

Flow of Analysis Program

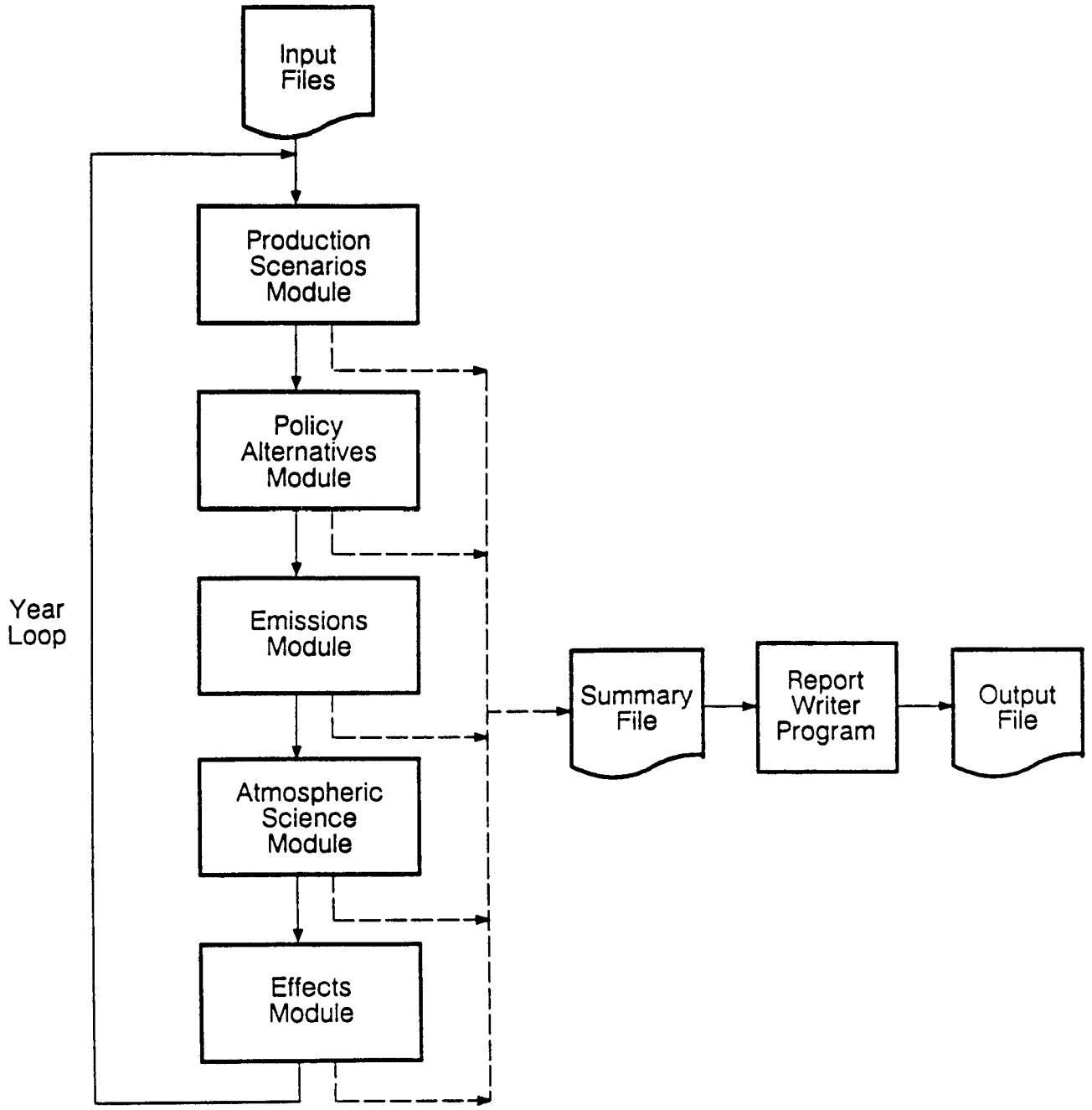

technical options for controlling the use of potential ozone-depleting substances (identified in an input file). The final results of this module are (1) the incurred costs of control attributable to the policy; and (2) the reductions in production realized as a consequence of control.

- Appendix D: Emissions Module -- This module calculates global emissions of each compound by applying a release algorithm to the production scenarios (which have been modified by the Policy Alternatives Module). The release algorithm specifies the time it takes (after production) for the compound to be released for each end use of each compound. The algorithm reflects the fact that the chemicals are stored in products for many years.

- Appendix E: Atmospheric Science Module -- This module uses the global emissions estimates from the Emissions Module and estimates of atmospheric concentrations of carbon dioxide (CO2), methane (CH4) and nitrous oxide (N2O) to calculate global and latitudinal ozone depletion. Ozone depletion is calculated using parameterized equations that represent a one-dimensional model. Uncertainty is also modeled based on investigations of uncertainty propagation through an atmospheric model.

- Appendix F: Effects Module -- This module projects the effects that ozone depletion may have on human health and the environment. Human health effects are focused on melanoma and nonmelanoma skin cancers and cataracts. Other effects include degradation of materials, soybean yield impacts based on the Essex and Williams soybean cultivars, and ground-based ozone levels in three cities (which are used to estimate a 'national' average).

The results of each module are written to a "Summary File." This Summary File is used by the Report Writer Program to create detailed tables as specified by the user.

Report Writer Program

The Report Writer Program reads in the data stored in the Summary File and creates reports for the model run as specified by the user. The reports for a given model run may show results disaggregated by region, compound, end use, and time. Results across runs may also be displayed and compared. Of note is that once a Summary File is created by the Analysis Program, the Report Writer Program can be run several times to generate reports at various levels of aggregation without re-running the Analysis Program.

SPECIFYING A MODEL RUN

To specify a model run the user fills out a set of data files that describe the assumptions and data to be used. The names of these data files, and their purposes, are listed in Exhibit A-2. Each is described in turn.

EXHIBIT A-2

Files Required to Specify a Run

File Name	Purpose
Run File	To identify modules included in the run and data files to be used, specify years for which outputs are desired, and define the discount rates used to calculate costs and benefits.
Production Scenarios File	To choose a scenario of future production for each compound and of future population and economic growth.
Policy Alternatives File	To define the control strategy to be evaluated and the scenario of available technical controls.
Atmospheric Science File	To choose a method for estimating ozone depletion and specify a range of uncertainty surrounding the method. Also to specify scenarios of concentrations of other trace gases.
Effects File	To specify the dose-response coefficients for each human health effect, the action spectrum to be used for each human health effect, and the economic value to be placed on each human health effect. Also, to specify the values used to estimate polymer degradation.
Report Writer File	To identify runs for which reports are to be written and the reports desired.

- The Run File identifies the overall model flow, including which modules are to be executed. This file includes:
  - -- the range of years for the model run;
  - -- the names of modules to be executed;
  - -- the names of the data files to be used;
  - -- the years for which summary results will be retained; and
  - -- the discount rates for cost/benefit analysis.
- The Production Scenarios File specifies the scenario of future production of potential ozone-depleting compounds to use in the analysis. The user may choose one of a set of defined scenarios, or may create his own. The user also chooses (or creates) a scenario of population and economic growth.
- The Policy Alternatives File defines the control strategy (if any) that the user is evaluating. In addition to defining the level of controls or the policy objective, the user must choose among alternative scenarios that define the technical options available for reducing the use of potential ozone-depleting compounds.
- The Atmospheric Science File allows the user to choose among alternative methods for computing ozone depletion. The user may specify a range of uncertainty surrounding the ozone depletion estimate. The assumptions regarding the concentrations of other trace gases (carbon dioxide, methane, and nitrous oxide) are also specified in this file.
- The Effects File identifies the assumptions used to (1) estimate effects (in their natural units); and (2) evaluate the effects in monetary terms. The user chooses (or supplies) dose-response coefficients for each effect. The value (in dollars) of each effect may also be specified.
- The Report Writer File identifies the runs for which reports are to be written and the reports desired.

Of note is that once these files have been specified, and the model is run, the entire model need not be re-run to perform additional analyses. For example, to analyze an alternative set of effects assumptions, only the Effects File needs to be filled out, and only the Effects Module needs to be executed. The results from the previous modules can be stored for future use. This flexibility in the modular design of the model helps to facilitate numerous comparison runs and reduces the time and expense of the analysis.

LIMITATIONS

Although the model was implemented in a modular fashion to allow for flexibility in development and use, it has several important limitations.

- o Size. The size of the model was kept manageable by limiting the units of analysis to 10 regions, 10 compounds, and six end uses per compound. More regions (e.g., for analyses of individual countries) cannot be accommodated easily. The number of compounds and end uses per compound are also fixed.

- o Feedback between compounds. Each compound is analyzed independently. The control of one compound (e.g., CFC-12) does not influence the use of other compounds. (This aspect of the model is under revision so that it will be possible to consider, for example, how HCFC-22 and methyl chloroform emissions increase as they substitute for CFC-11, 12, 113 etc.) These feedbacks may be analyzed by specifying alternative production scenarios that reflect the expected substitutions.

- o Feedback between years. Each year is analyzed independently, and feedbacks are handled by making previous years' data available through special data structures. To minimize memory requirements, special data structures are established only for those data needed to model feedbacks. Consequently, the addition of new feedbacks between years would likely require modifications to the data structure.

APPENDIX B

SCENARIOS OF CHEMICAL PRODUCTION, POPULATION, AND GNP

INTRODUCTION

This portion of the model generates scenarios of (1) historical and future production of potential ozone-depleting substances, (2) population, and (3) economic activity (i.e., gross national product, or GNP). Ten potential ozone-depleting compounds may be specified for analysis: CFC-11; CFC-12; HCFC-22; CFC-113; CFC-114; CFC-115; Carbon Tetrachloride (CCl4); Methyl Chloroform (CH3CCl3); Halon-1211; and Halon-1301. The production of each compound is disaggregated by up to 10 regions of the world, and up to six different end uses or applications. The population and GNP scenarios may also be disaggregated by up to 10 regions of the world.

The remainder of this appendix is organized as follows:

- o Production Scenarios describes the standard procedure for specifying scenarios of production (historical and future);
- o Population and GNP Scenarios describes the specification of these scenarios;
- o User-Modified Scenarios describes how the user may override portions of the standard procedures for specifying the production, population, and GNP scenarios; and
- o Limitations presents the limitations of this portion of the model.

PRODUCTION SCENARIOS

Production scenarios may cover any period from 1931 to 2100. Historical data are used through 1984, and a variety of scenarios are specified to reflect potential future production from 1985 onward. To run the model, the user may (1) choose an existing scenario included in the Production Scenario File,[1] (2) create a new scenario in the Production Scenario File, (3) modify an existing scenario using the procedure outlined below in the section on user-modified scenarios, or (4) omit the specification of production from the model by specifying emissions directly (see Appendix D) or ozone depletion directly (see Appendix E). This section describes the format of the existing scenarios specified in the Production Scenarios File. These scenarios are defined in three parts: global production; regional shares; and end use shares. Each part is described in turn.

---

[1] The six scenarios included in the Production Scenario File are described in Chapter 18.

Global Production

World production for each of the 10 potential ozone-depleting compounds is reported in units of millions of kilograms per year. Exhibit B-1 shows an example production scenario for all eight compounds currently analyzed. Intermediate values between the years reported are calculated by the model (using either linear or exponential interpolation, as specified by the user). Production is assumed to be constant following 2050.

Regional Shares

Regional shares are used to divide global production into the following 10 regions:

- o U.S.;
- o Canada (CAN);
- o Western Europe (WEUR);
- o Japan, Australia, and New Zealand (JANZ);
- o USSR and East Bloc (EUSSR);
- o Centrally Planned Asia (ASCEN);
- o Middle East (MIDE);
- o Africa (AFR);
- o Latin America (LA); and
- o South and East Asia (SEASIA).

Exhibit B-2 shows a scenario of regional shares for CFC-11. The regional shares are multiplied by the global production to produce regional production estimates. For example, to compute 2000 U.S. CFC-11 production, the model multiplies CFC-11 global production for that year, 543.0 million kg, by the regional share for the U.S. for that year, 0.212, to calculate 115.1 million kg of production. For each year, the shares add to one, indicating that all global production is accounted for when disaggregating across regions. Also notice that the regional shares may change over time (e.g., in this scenario the U.S. share of world CFC-11 production shrinks from 73.7 percent [0.737] in 1958 to 19.9 percent [0.199] by 1980).

End Use Shares

An "end use share" is the fraction of regional production that is allocated to a particular application or end use. Each compound may have up to six different end uses. End use shares may vary by the 10 regions of the world and may change over time. The model currently includes the following end uses:

- o aerosol propellant;
- o flexible urethane foam;
- o rigid polyurethane foam;
- o rigid nonurethane foam;
- o refrigeration;
- o solvent;
- o fire extinguisher; and
- o miscellaneous.

EXHIBIT B-1

Example Global Production Scenario
(millions of kilograms)

	CFC-11	CFC-12	HCFC-22	CFC-113	CCl4	CH3CCl3	Halon-1211	Halon-1301
1985	375.0	475.0	111.0	163.0	71.2	545.0	10.8	10.8
2000	543.0	688.0	161.0	283.0	103.0	848.0	19.7	19.7
2025	1,006.9	1,275.6	298.1	525.0	191.0	1,534.6	36.5	32.3
2050	1,867.0	2,365.0	552.0	974.0	354.2	2,777.0	67.8	53.1
2075	1,867.0	2,365.0	552.0	974.0	354.2	2,777.0	67.8	53.1

EXHIBIT B-2

Regional Use Shares for CFC-11

Year	U.S.	CAN	WEUR	JANZ	EUSSR	ASCEN	MIDE	AFR	LA	SEASIA	TOTAL
Historical Data											
1931	1.000	0.000	0.000	0.000	0.000	0.000	0.000	0.000	0.000	0.000	1.000
1958	0.737	0.023	0.165	0.075	0.000	0.000	0.000	0.000	0.000	0.000	1.000
1965	0.577	0.037	0.263	0.120	0.001	0.000	0.000	0.000	0.000	0.000	1.000
1970	0.410	0.052	0.364	0.166	0.003	0.001	0.001	0.001	0.001	0.001	1.000
1975	0.333	0.057	0.406	0.185	0.007	0.003	0.002	0.002	0.003	0.002	1.000
1980	0.199	0.067	0.470	0.215	0.019	0.007	0.004	0.004	0.009	0.006	1.000
Scenario Of Future Regional Shares											
1985	0.211	0.035	0.251	0.114	0.149	0.057	0.034	0.034	0.069	0.046	1.000
2000	0.212	0.033	0.231	0.118	0.133	0.066	0.037	0.037	0.081	0.052	1.000
2025	0.212	0.030	0.214	0.116	0.113	0.069	0.046	0.042	0.097	0.061	1.000
2050	0.212	0.028	0.197	0.115	0.093	0.072	0.054	0.046	0.113	0.070	1.000
2100	0.212	0.028	0.197	0.115	0.093	0.072	0.054	0.046	0.113	0.070	1.000

Exhibit B-3 shows an example of end use shares for CFC-11 in the U.S. All end use shares for a year add to one (i.e., all production is assigned to some type of end use). In the module, end use shares are multiplied by estimated regional production to estimate the amount of production going into each end use. For example, U.S. CFC-11 production, used to make rigid polyurethane foam, would be calculated for the year 2000 as follows:

543.0 (2000 CFC-11 Global Production)	x	0.212 (2000 CFC-11 U.S. Regional Share)	x	0.588 (2000 CFC-11 U.S. Rigid Polyurethane Foam Share)	=	67.7 million kg (2000 CFC-11 U.S. Rigid Polyurethane Foam Use)

Using these three factors (global production, regional shares, and end use shares), the historical and potential future production of each of the 10 compounds can be specified in detail. For ease of use, the model incorporates a range of scenarios that reflect a large range of potential future growth in production (80 percent reduction in use to 5 percent annual growth). The user may choose one of these scenarios, create a new scenario, or modify an existing scenario as described below in the section entitled User-Modified Scenarios.

POPULATION AND GNP SCENARIOS

A series of population and GNP scenarios are provided in the model.[2] The user has the option of choosing one of these scenarios, or creating his own scenario. Existing scenarios reflect a wide range of projected growth, ranging from 0.5 percent to 1.1 percent growth per year (population from 1985 to 2075) and 1.0 percent to 3.6 percent growth per year for GNP (1985 to 2075).

The population scenario is specified for each of 10 regions in terms of a base year value (1975) and a list of growth indices. Each index value is multiplied by the base year value to produce a population projection for a given year for a region. Exhibit B-4 presents the scenario for the U.S. population. To compute the U.S. population projection for 2050, the base year population for the U.S. (213,925,000) is multiplied by the index for 2050 (1.447) which results in a U.S. population projection of 309,488,000 in 2050. This method allows for the rates of growth of population to vary by region, and to change over time.

Regional GNP scenarios are specified in a similar manner. Exhibit B-5 shows the scenario for U.S. GNP. The base GNP in 1975 is in 1975 U.S. dollars and the indices correspond to projected years. For example, the model would calculate projected GNP for the U.S. in 2050 by multiplying the base year GNP, $1,519,890 million, by the corresponding index for the U.S. in the year 2050, 4.899. This computation results in a projected 2050 GNP for the U.S. of $7,445,941 million (in 1975 dollars). GNP for other regions is also calculated in 1975 U.S. dollars.

---

[2] These scenarios can be varied by the user if desired.

EXHIBIT B-3

U.S. End Use Shares for CFC-11

	Year	Aerosol Propellant	Flexible Urethane Foam	Rigid Polyurethane Foam	Rigid Nonurethane Foam	Refrigeration	Miscellaneous	Total
HISTORICAL DATA	1931	0.000	0.000	0.000	0.000	1.000	0.000	1.000
	1958	0.869	0.045	0.046	0.003	0.011	0.026	1.000
	1970	0.542	0.157	0.162	0.009	0.037	0.093	1.000
	1980	0.132	0.284	0.371	0.020	0.064	0.129	1.000
SCENARIO OF FUTURE END USE SHARES	1985	0.055	0.290	0.490	0.026	0.061	0.078	1.000
	2000	0.038	0.275	0.588	0.031	0.053	0.015	1.000
	2050	0.011	0.283	0.604	0.031	0.055	0.016	1.000

EXHIBIT B-4

U.S. Population Scenario

Year	Population Index	Population (thousands)
1975	1.000	213,925
1985	1.115	238,631
2000	1.253	267,955
2025	1.409	301,394
2050	1.447	309,488
2075	1.452	310,639

EXHIBIT B-5

U.S. GNP Scenario

Year	GNP Index	GNP (millions of (1975 U.S.$)
1975	1.000	1,519,890
1985	1.348	2,048,812
2000	2.040	3,100,576
2025	3.242	4,927,483
2050	4.899	7,445,941
2075	7.830	11,900,739

USER-MODIFIED SCENARIOS

The user has the option of overriding portions of the scenarios described in the previous sections. This capability expands flexibility by allowing modified scenarios to be analyzed without creating complete scenario data files for each. This option is especially useful for performing sensitivity analysis. There are six options for modifying the scenarios:

- Population -- The user may specify population projections over time for individual regions. The specified production(s) override(s) the appropriate portion(s) of the standard scenario without changing the projections for other regions.

- GNP -- The user may specify GNP projections over time for individual regions, thereby overriding the projections from the standard scenario without changing the projections for other regions.

- Production by End Use -- The user may specify production (by end use) over time for individual regions. Projections for end uses and regions not explicitly specified are drawn from one of the standard production scenarios.

- Production as a Function of Population -- The user may specify the production of each compound as a function of population for individual regions.

- Production as a Function of GNP -- The user may specify the production of each compound in each region as a function of GNP.

- Production as a Function of GNP per Capita -- The user may specify the production of each compound in each region as a function of GNP per capita. GNP per capita is calculated within the model from the GNP and population scenarios for each region.

For each user-modified scenario, the user must specify in a table the type of projection (population, GNP, etc.), the applicable region, the compound (if appropriate), and the end use (if appropriate). For example, to specify 2.0 percent annual growth in the production of CFC-11 in the U.S. from 1985 to 2050, and zero growth thereafter, the user would fill out the table shown in Exhibit B-6. The values in this table would override the values for CFC-11 in the U.S. reported in the standard scenarios.

Another example of a user-specified projection type would be to have U.S. CFC-11 production vary with U.S. population. Exhibit B-7 shows an example of how to specify this production versus population information. The model utilizes this information by (1) determining the level of population for that region, and (2) identifying (by interpolation) the associated production for that population. Because the information specifying the user-modified scenarios

EXHIBIT B-6

User-Modified Scenario Specifying a Growth Rate of 2 Percent Annually for CFC-11 in the U.S.

Year	Millions of kg of CFC-11
1985	78
2000	105
2025	172
2050	283
2075	283

EXHIBIT B-7

A User-Modified Scenario: Production as a Function of Population

Population Millions of People	Production Millions of kg of CFC-11
200	50
250	100
300	200

is entered in the form of tables, the user is free to adopt any arbitrary function or "shape" for his data. This capability enhances the ability to use the model for sensitivity analysis.

LIMITATIONS

The primary limitations of this scenarios module are described below.

- Range of Standard Scenarios. A set of standard (i.e., pre-defined) scenarios are included in the module, and the user may choose among them. To perform an analysis with scenarios outside the range reflected by the standard scenarios, the user must define his own scenario or modify a standard scenario. The limitation of this approach is that the scenarios are comprised of a significant amount of data, thereby making the establishment of an additional scenario somewhat cumbersome. This limitation is alleviated to some extent by allowing the user to make selective modification to standard scenarios to allow sensitivity analysis.

- Sub-regional Scenarios. Scenarios for areas other than the 10 regions in the model cannot be specified.

- Consistency. The user is free to choose or create individual production, population, and GNP scenarios. In fact, the future production of the different compounds was generally projected under various assumptions regarding population and GNP growth. Therefore, the user should be careful to choose scenarios that are consistent with each other. The model does not check for consistency among the scenarios chosen by the user (e.g., the user may choose a high production scenario and a low population scenario simultaneously).

REFERENCES

Gibbs, Michael J. (1986), "Scenarios of CFC Use: 1985 to 2075," prepared for the U.S. Environmental Protection Agency, Washington, D.C.

APPENDIX C

EVALUATION OF POLICY ALTERNATIVES

This module evaluates control policy alternatives. If a policy specified by the model user requires reductions in the production of potential ozone-depleting substances, the model simulates these reductions by choosing from a list of possible technical control options. Each technical control is defined by its cost and the percentage reduction that it can achieve.

Because this risk assessment is focused on evaluating risks in the absence of regulation, this module is not employed in the analysis at this time. Therefore, this module is not described here. For discussion of control policy alternatives, the interested reader is referred to Regulatory Impact Analysis: Protection of Stratospheric Ozone, U.S. Environmental Protection Agency.

APPENDIX D

EMISSIONS OF POTENTIAL OZONE-DEPLETING COMPOUNDS

INTRODUCTION

Emissions are estimated on a global basis for each compound analyzed. Two approaches are available for modeling emissions:

- Internal estimates -- Emissions are modeled based on the production scenarios described in Appendix B and modified through the implementation of policies described in Appendix C. A release algorithm is used to describe how fast the compounds are released into the atmosphere after production. This algorithm is based on "release tables" that are specific for each compound and end use. Each release table shows the annual fraction of the chemical that is released over time.

- Exogenous specification -- Emission scenarios may be defined directly by the user.

INTERNAL ESTIMATES OF EMISSIONS

The model calculates emissions from release tables and estimates of production developed by the Production Scenario Module (Appendix B) and modified by the Policy Alternatives Module (Appendix C). This section first defines a release table, then describes how releases are estimated from one year's production, and, finally, presents how emissions are calculated from production over a series of years.

Release Tables

Compounds are released into the atmosphere at different rates following production, depending on their uses. Some uses (such as aerosol propellants) release compounds into the atmosphere very soon after production. However, some uses (such as refrigeration and rigid foam production) store compounds for many years, releasing them gradually over time. This storage is called a "bank."

A release table represents the fraction of production emitted over time for a particular compound and end use. Release tables have been defined for each of the end uses in the model based on Quinn (1986), and the user may specify alternative release tables as desired. Exhibit D-1 presents the release tables for CFC-11 in its end uses. A total of 20 years is shown, and the fraction of the production from year 1 released into the atmosphere in the following years is listed. For example, during the year of production of refrigeration uses, 19.0 percent of the compound is released. By the end of the second year, a total of 27.1 percent of the production from year 1 is released. Releases continue through the fourth year, after which all of the production from year 1 is released. Annual release rates may be calculated by subtracting each year's cumulative fraction from the previous year's cumulative fraction. For example, 8.1 percent (0.271 minus 0.190) is released in year 2, 7.3 percent (0.344 minus 0.271) is released in year 3.

EXHIBIT D-1

Release Tables for CFC-11

Year	Aerosol Propellant		Flexible Foam		Rigid Polyurethane Foam		Rigid Nonurethane Foam		Refrigeration		Miscellaneous	
	Cumulative Fraction Released	Annual Fraction Released	Cumulative Fraction Released	Annual Fraction Released	Cumulative Fraction Released	Annual Fraction Released	Cumulative Fraction Released	Annual Fraction Released	Cumulative Fraction Released	Annual Fraction Released	Cumulative Fraction Released	Annual Fraction Released
1	1.000	1.000	1.000	1.000	0.145	0.145	0.600	0.600	0.190	0.190	1.000	1.000
2					0.190	0.045	1.000	0.400	0.271	0.081		
3					0.235	0.045			0.344	0.073		
4					0.280	0.045			1.000	0.656		
5					0.325	0.045						
6					0.370	0.045						
7					0.415	0.045						
8					0.460	0.045						
9					0.505	0.045						
10					0.550	0.045						
11					0.595	0.045						
12					0.640	0.045						
13					0.685	0.045						
14					0.730	0.045						
15					0.775	0.045						
16					0.820	0.045						
17					0 865	0.045						
18					0.910	0.045						
19					0 955	0.045						
20					1.000	0.045						

Source: Quinn, T., et al. (1980), "Projected Use, Emissions, and Bank of Potential Ozone Depleting Substances," The RAND Corporation, prepared for the U.S. Environmental Protection Agency, Washington, D.C.

The release tables vary in length (some end uses store their compounds for many years). Also, the release table need not reflect complete emissions. If the cumulative release fraction in the table reaches 1.0, then all of the compound that is produced is eventually released into the atmosphere. If some of the compound is expected to be retained forever within a product, or destroyed, the release table would have as its highest value a number less than 1.0. The difference between the reported value and 1.0 would be the portion of the compound that is never emitted.

Estimating Emissions From One Year's Production

Exhibit D-2 shows the emissions from the hypothetical production of 100 million kg in 1985. The cumulative fraction of production released over time is presented in column 2. The annual fraction of production released is shown in column 3. The model calculates annual emissions by multiplying the annual fraction by the amount of production in the initial year (100 million kg in this example). The projected emissions per year are shown in column 4. In this example the total emissions sum to the initial production amount, indicating that all of the production is eventually emitted into the atmosphere.

Estimating Emissions From Production Over a Series of Years

Exhibit D-3 presents how the model calculates emissions from production over a series of years. Columns 1 and 2 show years and production in that year, respectively. In this example, production grows by 10 million kg per year, and, for simplicity, emissions from production before 1985 are omitted (emissions from past production are not omitted in the model). Columns 3 through 8 show emissions over time due to the production shown in column 2, each row showing how releases of its production are spread over the course of years.

The first row shows the emissions from 1985 production. The second row shows emissions from the 1986 production, and so on. The total emissions for a year are calculated by summing emissions values in the columns to compute a total. For example, emissions in 1985 are 19.0, emissions in 1986 are 29.0, emissions in 1987 are 39.0, and so on. By 1990, a total of 441.1 million kg has been emitted, and a total of 750 million kg has been produced. Therefore, 750 - 441.1, or 308.9 million kg, remains to be emitted after 1990.

This method of estimating emissions reflects the delays between the production and release of many potential ozone-depleting substances. The implications of the method are that releases in a given year are caused not only by production in that year, but also by production and use in previous years.

EXOGENOUS SPECIFICATION OF EMISSIONS

The user has the option of directly specifying the level of emissions over time. This is accomplished by filling out an emissions table; a sample table is presented in Exhibit D-4. This table shows emissions estimates for eight chemical compounds over a time period of 65 years. The module can interpolate intermediate emissions values by either linear or exponential interpolation. These specified emissions override the estimates of emissions that the model would have generated from production data as discussed in the previous section. This ability to specify emissions directly to the model allows the flexibility

EXHIBIT D-2

Emissions from a Hypothetical
100 Million Kilograms of Production in 1985

1 Year	2 Cumulative Fraction Released	3 Annual Fraction Released	4 Annual Emissions (millions of kg)
1985	0.190	0.190	19.0
1986	0.271	0.081	8.1
1987	0.344	0.073	7.3
1988	1.000	0.656	65.6
TOTAL		1.000	100.0

EXHIBIT D-3

Emissions from Production Over a Series of Years (millions of kilograms)

Year	Production	1985	1986	1987	1988	1989	1990
1985	100	19.0	8.1	7.3	65.6	--	--
1986	110	--	20.9	8.9	8.0	72.2	--
1987	120	--	--	22.8	9.7	8.8	78.7
1988	130	--	--	--	24.7	10.5	9.5
1989	140	--	--	--	--	26.6	11.3
1990	150	--	--	--	--	--	28.5
TOTAL EMISSIONS PER YEAR		19.0	29.0	39.0	108.0	118.1	128.0

EXHIBIT D-4

Sample Table of Exogenously Specified Emissions
(millions of kilograms)

Year	CFC-11	CFC-12	HCFC-22	CFC-113	CCl4	CH3CCl3	Halon-1211	Halon-1301
1985	298	438	81	138	71	500	3	3
2000	462	668	151	240	103	721	9	9
2025	897	1,237	279	446	191	1,303	25	22
2050	1,650	2,281	516	828	355	2,356	48	38

to evaluate the ozone depletion and other effects that may be associated with given emission levels, without having to specify a policy that would result in such emissions.

LIMITATIONS

The primary limitation of this module is that the emission tables are not designed to change over time. Therefore, changes in technology that influence emissions rates of existing end use products cannot be modeled.

REFERENCES

Quinn, T., et al. (1986), "Projected Use, Emissions, and Bank of Potential Ozone-Depleting Substances," The RAND Corporation, prepared for the U.S. Environmental Protection Agency, Washington, D.C.

APPENDIX E

ATMOSPHERIC SCIENCE MODULE

INTRODUCTION

This portion of the model computes the level of global average ozone depletion as a function of the emissions of the 10 potential ozone-depleting substances. The emissions are computed in the previous module (presented in Appendix D). The user has three options for estimating ozone depletion:

- Use a relationship between emissions and ozone depletion developed to reflect the results of a one-dimensional (1-D) atmospheric model;
- Specify his own relationship; and
- Specify the level of ozone depletion directly.

Each of these options is described in turn. Then, the method used to reflect uncertainty is presented. Finally, the limitations of the atmospheric science module are presented.

PARAMETERIZED RELATIONSHIP

The module incorporates a series of equations that describe the change in total column ozone as a function of:

- emissions of potential ozone-depleting substances; and
- abundances of three trace gases (CO2 in ppm, N2O in ppb, and CH4 in ppm).

This relationship was developed by Connell (1986), and it computes global total column ozone change (in percent) relative to 1985.

To use this relationship, the user must specify scenarios of trace gas abundances to use in conjunction with the emissions of potential ozone-depleting substances. A range of scenarios has been developed from which the user may choose, or the user may specify his own scenarios. The reference case set of assumptions used in the development of the relationship is shown in Exhibit E-1. Exhibit E-2 compares the results of the LLNL 1-D model to the relationship developed by Connell for the base case of emissions of ozone-depleting substances.

The following six steps are performed to compute global ozone depletion in year t using the parameterization:

1. Compute the change in the chlorine concentration in year t relative to 1985 as:

EXHIBIT E-1

Trace Gas Assumptions Used To Develop the Ozone-Depletion Relationship[a/]

Year	Carbon Dioxide (ppm)	Nitrous Oxide (ppb)	Methane (ppm)
1985	350.2	303.1	1.756
1995	361.3	309.2	1.926
2005	377.2	315.5	2.096
2015	399.6	321.8	2.266
2025	422.0	328.3	2.436
2035	456.4	334.9	2.606
2045	490.8	341.7	2.776
2055	531.4	348.6	2.946
2065	578.2	355.6	3.116
2075	625.0	362.8	3.286

[a/] This base case set of assumptions was one of several used to develop the relationship between emissions of ozone-depleting substances and ozone depletion.

Source: Connell, Peter S. (1986), "A Parameterized Numerical Fit to Total Column Ozone Changes Calculated by the LLNL 1-D Model of the Troposphere and Stratosphere," Lawrence Livermore National Laboratory, Livermore, California.

EXHIBIT E-2

Comparison of Total Column Ozone Depletion Results from the 1-D Model and the Parameterized Numerical Fit[a/]

Year	Ozone Depletion (percent) Numerical Fit	1-D Model	Difference
1985	0.0	0.0	0.00
1995	-0.18	-0.18	0.00
2005	-0.74	-0.61	0.13
2015	-1.64	-1.42	0.22
2025	-2.86	-2.65	0.21
2035	-4.48	-4.30	0.18
2045	-6.63	-6.41	0.22
2055	-9.60	-9.10	0.50
2065	-14.0	-12.9	1.10
2075	-21.6	-19.9	1.70

[a/] This base case was one of many cases used to develop the relationship between emissions of ozone-depleting substances and ozone depletion. This result does not necessarily reflect the base case estimates from this model.

Source: Connell, Peter S. (1986), "A Parameterized Numerical Fit to Total Column Ozone Changes Calculated by the LLNL 1-D Model of the Troposphere and Stratosphere," Lawrence Livermore National Laboratory, Livermore, California.

$$dCl(t) = dCl(o) + \Sigma\,[CF(j)\Sigma emissions(i,j) * \exp(-(t-i)/lifetime(j)) * (1-\exp(-(-t-i)/mixing\ time))]$$

where: dCl(t) equals the change in chlorine concentrations in year t;

dCl(o) equals the change in chlorine concentration in year t due to emissions prior to 1985;

CF equals a conversion factor for each compound j;

emissions are the annual emissions for compound j for years 1985 to year t;

lifetime equals the average atmospheric lifetime for each compound j; and

mixing time equals the time it takes for source emissions to become well mixed.

2. Compute the changes in CO2, N2O and CH4 for year t as follows:

$dCO2 = CO2(t)/CO2(1985)$;
$dN2O = N2O(t)/N2O(1985)$; and
$dCH4 = CH4(t)/CH4(1985)$,

where the values for CO2, N2O and CH4 over time are model inputs as discussed above.

3. Compute ozone depletion due to CFCs as:

$$dO3(t) = 14.58[\text{asinh}(.332(21.05(1+(dN2O-1)/(dCH4)^2) - dCl(t)*\exp(-.15(dCH4-1)))) - \text{asinh}(.332*21.05(1+(dN2O-1)/(dCH4)^2))]$$

where dO3(t) equals the ozone depletion in year t (in percent).

4. Compute ozone depletion (in percent) from CO2, N2O, and CH4 as follows:

$dO3(t) = 3.6\ln(dCO2)$;
$dO3(t) = 3.75(dCH4-1)$; and
$dO3(t) = -7.0(dN2O-1)$.

5. Compute ozone depletion (in percent) from Halons as follows:

$dO3(t) = -0.0302$[concentration of Halon-1301]
-0.0618[concentration of Halon 1211]

6. Compute total ozone depletion (in percent) as the sum of the individual estimates computed in Steps 3, 4, and 5.

These equations are used to represent the potential for ozone depletion as a function of emissions and concentrations of the various substances analyzed. The details of this method are described in Connell (1986).

USER-SPECIFIED RELATIONSHIP

The user has the option of specifying his own relationship between emissions and ozone depletion. For each substance, the user specifies a "conversion factor" and a "lifetime." These values are used in the following equation to compute an atmospheric abundance for each compound over time:

$$\text{Abundance (T)} = \text{Conversion Factor} \sum_{t=t_o}^{T} [\text{emissions (t)} e^{-(T-t)/\text{lifetime}}].$$

The abundances are summed across the compounds to create a total abundance. The amount of ozone depletion associated with each level of abundance is then specified by the user in a table.

This formulation of the user-specified ozone-depletion relationship is similar to the parameterized numerical fit developed by Connell (1986). It can produce abundances of the different compounds that exhibit behavior similar to the results produced by 1-D models. The value of this option is that the user may identify, in tabular form, his best understanding of the manner in which ozone depletion will vary with the abundances of the compounds in the atmosphere.

USER-SPECIFIED OZONE DEPLETION

The user has the option of bypassing the computation of ozone depletion based on emissions of potential ozone-depleting substances. Instead, the user may provide estimates of global ozone depletion directly to the model. This option allows the user to evaluate the impacts of such a level of depletion (possibly computed via other means) without identifying a level of emissions or a control policy that would produce such depletion.

To specify levels of ozone depletion, the user fills out the table shown in Exhibit E-3. For each year, a level of total column ozone depletion (or increase) is identified. The model interpolates between the values supplied in the table.

UNCERTAINTY

The user has the option of recognizing the uncertainty inherent in current models of ozone depletion by specifying a range within which the "true" level of ozone depletion is expected to fall. This range is specified using multiplicative scaling factors, as shown in Exhibit E-4. The scaling factors are multiplied by the estimate of ozone depletion produced within the

EXHIBIT E-3

HYPOTHETICAL TABLE OF USER-SPECIFIED OZONE DEPLETION*

Year	Total Column Global Ozone Depletion (percent)
1985	0.00
1990	0.01
2000	0.10
2025	1.00
2050	5.00
2075	10.00
2100	20.00

* Values are illustrative only.

EXHIBIT E-4

EXAMPLE OZONE-DEPLETION SCALING FACTORS*

Ozone Depletion (percent)	Scaling Factors Low	High
≤15.0	0.4	2.0
≥20.0	0.5	1.8

*These factors represent the 10th and 90th fractile estimates from a lognormal distribution of uncertainty developed from values reported in: Stolarski, R.S., and A.R. Douglass (1986), Sensitivity of an Atmospheric Photochemistry Model to Chlorine Perturbation Including Consideration of Uncertainty Propagation, Draft Report to the U.S. Environmental Protection Agency, Washington, D.C.

model.[3] These multiplications produce a range of ozone depletion values for each year; the end points of the range (as well as the middle value estimated within the model) are passed to the effects module for evaluation.

As shown in Exhibit E-4, the scaling factors may change at different levels of ozone depletion. The values shown in the exhibit are based on a Monte Carlo uncertainty analysis performed by Stolarski and Douglass (1985). Each Monte Carlo iteration draws from a distribution of estimated reaction rates and cross sections to generate predictions of atmospheric abundances. These predicted abundances can be compared to actual measurements in the atmosphere; those iterations that do not compare favorably with actual measurements can be screened out. The values reported in Exhibit E-4 are based on those iterations that compared favorably with actual measurements and were not screened out.

Because the ozone-depletion models are not considered reliable at high levels of ozone depletion, the user may also specify a "cap" on ozone depletion. If the computed level of ozone depletion (after scaling) exceeds the user specified cap, then the ozone depletion used to evaluate effects (in the next module) is reduced to the level of the cap.

LIMITATIONS

The Atmospheric Science Module is a simplified representation of a complex set of atmospheric reactions. In using the module, the user should become aware of the range of emissions and trace gas values for which the parameterized relationship is considered valid. Outside this range, the equations do not necessarily reflect current estimates from 1-D models of the atmosphere. The range of production scenarios discussed in Appendix B to this chapter and Chapter 18 are generally well within the range for which these equations are valid. In those few instances when they are not within the range, the allowable values are capped to avoid extrapolating beyond the bounds of the analyses from which the equations were developed.

---

[3] The scaling factors are not used when ozone depletion is specified directly by the user.

REFERENCES

Connell, Peter S. (1986), "A Parameterized Numerical Fit to Total Column Ozone Changes Calculated by the LLNL 1-D Model of the Troposphere and Stratosphere," Lawrence Livermore National Laboratory, Livermore, California.

Stolarski, R.S., and A.R. Douglass (1985), "Sensitivity of an Atmospheric Photochemistry Model to Chlorine Perturbation Including Consideration of Uncertainty Propagation," Draft Report to the U.S. Environmental Protection Agency, Washington, D.C.

APPENDIX F

HEALTH AND ENVIRONMENTAL IMPACTS OF OZONE DEPLETION

INTRODUCTION

This appendix presents the methods used to model the health and environmental effects of ozone depletion in the CFC Policy Model. This module incorporates analyses performed by a variety of researchers, including analyses of:

- the relationship between global ozone depletion and latitudinal-dependent ozone depletion (Isaksen 1986);
- the relationship between ozone depletion and ultraviolet radiation (UV);[1]
- the relationship between UV and the incidence (and mortality) of nonmelanoma skin cancers;[2]
- the relationship between UV and the incidence (and mortality) of melanoma skin cancers;[3]
- the relationship between UV and the prevalence (and incidence) of senile cataracts;[4] and
- the relationship between ozone depletion and the costs of modifying polymers to prevent degradation of polymer appearance and/or performance due to increased UV.[5]

These analyses pertain primarily to the U.S., consequently, this module focuses on the risks in the U.S. associated with ozone depletion. The module is designed to allow risk estimates to be performed for other portions of the world if: (1) the model user supplies data needed to quantify effects in these other regions; or (2) the model user assumes that the data for the U.S apply to other portions of the world. The descriptions below relate exclusively to the analysis of impacts in the U.S.

---

[1] See Serafino and Frederick (1986) for a description of the model used to estimate the relationship between ozone depletion and UV flux.

[2] See Chapter 7 for a discussion of the relationship between nonmelanoma skin cancer and UV.

[3] See Chapter 8 for a discussion of the relationship between melanoma skin cancer and UV.

[4] See Chapter 10 for a discussion of the relationship between senile cataracts and UV.

[5] See Chapter 13 for a discussion of the relationship between polymer degradation and UV.

This appendix is divided into the following sections:

- Changes in UV Flux presents the method used to estimate changes in the flux of UV for given levels of ozone depletion;
- Skin Cancers and Cataracts presents the methods used to model melanoma and nonmelanoma skin cancers and cataracts;
- Materials presents the methods used to model the costs associated with the degradation of polymers; and
- Limitations summarizes the major limitations of the methods used, including the risks believed to be associated with increases in ambient levels of UV that are not modeled at this time in the CFC Policy Model.

CHANGES IN UV FLUX

This portion of the module evaluates the expected changes in UV flux associated with changes in total column ozone. The estimates of changes in UV flux vary by latitude because the change in UV flux (measured in percent) for a given change in total column ozone (also measured in percent) varies as a function of the initial total abundance of ozone (i.e., the level of ozone abundance in the absence of ozone depletion).

The relationship between ozone change and UV flux will also vary for different measures of UV energy. Three measures of UV, also referred to as action spectra, are currently incorporated into the model: Robertson-Berger Meter (RB-Meter); DNA Action Spectrum; and Erythema Action Spectrum. Each measure has a unique weighting of the wavelengths in the UV spectrum. Because ozone selectively screens out radiation at given wavelengths, the different weighting schemes will produce different estimates of increased radiation levels when total column ozone abundance changes.

The UV Model developed by Serafino and Frederick (1986) was used to evaluate the expected changes in UV flux for given levels of total column ozone change. Pitcher (1986) performed a validation of the UV model, comparing monthly model estimates to monthly field instrumentation readings for three cities: El Paso, San Francisco, and Minneapolis. Although the model was found to overestimate UV flux in the months of September through March, and underestimate UV flux in May, June, and July, the annual estimates are generally within 10 percent of the RB-meter readings in the field (differences are probably attributable to errors in input data about clouds from real world situations, in which that data base is weak).

Changes in UV flux (as measured by the three action spectra) as a function of changes in ozone abundance were evaluated using the UV model for 24 cities across the U.S. These cities are divided into three regions of the U.S.: north, middle, and south (see Exhibit F-1). These three regions are used to evaluate potential changes in the incidence and mortality due to skin cancers.

EXHIBIT F-1

Cities Used to Evaluate Changes in UV Flux for the Three Regions of the U.S.

REGION 1: NORTH	REGION 2: MIDDLE	REGION 3: SOUTH
New York	Chicago	Los Angeles
Detroit	Philadelphia	San Diego
Milwaukee	Baltimore	Houston
Boston	San Francisco	Dallas/Fort Worth
Seattle	Washington	Phoenix
Minneapolis	Denver	New Orleans
Portland	Salt Lake City	Miami
Buffalo	Kansas City	Atlanta

The states included in each region are shown in Exhibit F-2. The population weighted average latitudes for the three regions are also shown.

Exhibit F-3 shows the percent change in UV (measured with the DNA action spectrum) in the three regions of the U.S. associated with a range of percent changes in total column ozone (from a 10 percent increase in ozone (listed as a -10 percent ozone depletion) to a 30 percent ozone depletion). As expected, the change in UV for a given level of ozone change is not constant across the three regions of the U.S., although they are very similar. Statistical analysis indicates that the estimates for the three regions are statistically different from each other.

Similar tables have been developed for the RB-Meter and the Erythema action spectra. The values for the Erythema Action Spectrum are approximately 80 to 85 percent of the DNA Action Spectrum values; the RB-Meter values are 35 to 45 percent. The user may define additional action spectra and prepare additional tables that relate changes in UV flux to changes in ozone depletion if he wishes to evaluate effects as a function of different action spectra.

SKIN CANCERS AND CATARACTS

The objective of this portion of the module is to evaluate the potential changes in risks of melanoma and nonmelanoma skin cancers and cataracts associated with changes in total column ozone abundance over time. The purpose of the evaluation is to provide information for assessing the implications of alternative emission rates of potential ozone-modifying substances. The inputs to this portion of the module include estimates of changes in UV flux associated with changes in total column ozone abundance. The output of this portion of the module includes estimates of the increased number of cases and deaths associated with skin cancers over time and an estimate of the increased number of cases of cataracts.

This analysis is organized into four parts as follows:

1. characterize the population at risk;

2. estimate the baseline incidence of the conditions being evaluated;

3. apply dose-response relationships to estimate the change in the risk of the conditions as a function of changes in ozone abundance over time; and

4. summarize the results.

Data have been developed primarily for the three regions of the U.S. for purposes of evaluating these skin cancer and cataract risks (see above for the definition of the three regions in the U.S.). The risks of these cancers in other portions of the world can be evaluated by the model user if: (1) the user supplies data to characterize the populations at risk in the other regions, the baseline incidence in the other regions, and the dose-response relationships

EXHIBIT F-2

States Included in the Three Regions of the U.S.

REGION 1: NORTH	REGION 2: MIDDLE	REGION 3: SOUTH
Alaska	California (N) a/	Alabama
Connecticut	Colorado	Arizona
Idaho	Delaware	Arkansas
Maine	District of Columbia	California (S) a/
Massachusetts	Illinois	Florida
Michigan	Indiana	Georgia
Minnesota	Iowa	Hawaii
Montana	Kansas	Louisiana
New Hampshire	Kentucky	Mississippi
New York	Maryland	New Mexico
North Dakota	Missouri	South Carolina
Oregon	Nebraska	Texas
Rhode Island	Nevada	
South Dakota	New Jersey	
Vermont	North Carolina	
Washington	Ohio	
Wisconsin	Oklahoma	
	Pennsylvania	
	Tennessee	
	Utah	
	Virginia	
	West Virginia	
	Wyoming	
Latitude = 43.3 N	Latitude = 39.1 N	Latitude = 31.8 N

a/ California is divided in half, one half included in the Middle Region, and one half included in the South Region.

Source: Latitude estimates based on population centroids for each state from the 1980 U.S. census, Master Area Reference File #2, Geography Section, U.S. Bureau of Census, Department of Commerce.

EXHIBIT F-3

Percent Change in UV as a Function of Change in Ozone Abundance for Three U.S. Regions (DNA Action Spectrum)

OZONE DEPLETION (%)	CHANGE IN UV (%) North	Middle	South
-10	-17.3	-17.2	-16.7
-5	-9.3	-9.1	-8.9
-2	-3.8	-3.8	-3.8
0	0.0	0.0	0.0
2	4.2	4.3	4.2
5	10.8	10.6	10.5
10	22.9	22.8	22.2
20	53.8	53.2	51.0
30	96.0	94.8	90.4

Source: Based on analyses using the UV Model developed by Serafino and Frederick (1986).

that apply to the other regions; or (2) the user assumes that the information provided for the U.S. applies to the other regions. Each of the four steps discussed below is presented for the U.S.

Step 1 -- Characterize the Population at Risk

The incidence of skin cancers and cataracts has been found to vary by race, age, sex, and the ambient level of UV in the area of residence of the individual.[6] The population in the U.S. is characterized by age, sex, and race using data from the U.S. Bureau of the Census.[7] Each of the three regions in the U.S. are characterized separately.

For each region, the current and expected age distribution of the population is defined in a series of tables as shown in Exhibit F-4. These age distributions were obtained by taking age distributions for the United States and assuming the age distribution for each region (in this case the north region) were identical.

The age distribution of the U.S. population is expected to change over time due to changing survival and birth rates. These changes in the distribution through 2080 are included in the characterization of the population, as shown in Exhibit F-4. Changes beyond 2080 have not been estimated, and consequently, the age distribution is assumed to remain fixed beyond 2080. If the U.S. population becomes older (younger) on average after 2080, this fixed population distribution underestimates (overestimates) the population of older individuals, and may consequently underestimate (overestimate) risks of ozone depletion. The user may relax this assumption by inserting alternative data for years beyond 2080 as appropriate.

The regional distribution of the U.S. population is assumed to remain unchanged over time. Recent trends do not indicate a definite shift from one region to another. If the U.S. population distribution were to shift toward the south (north), the risks of ozone depletion would be underestimated (overestimated) by this assumption. The user may alter this assumption by inserting alternative data on regional distribution patterns.

The portions of the population in each region that are male and female, black and white are also defined. These portions could be changed over time within the model to reflect changing demographic patterns; however, in this analysis these population variables were assumed to be equal across regions and over time.

From these data the fraction of the U.S. population is characterized by age, race, and sex for each of the three regions of the country. The total U.S. population over time is provided as an input to the Scenarios Module (see

---

[6] See Chapter 7 for a discussion of nonmelanoma skin cancer, Chapter 8 for a discussion of melanoma skin cancer, and Chapter 10 for a discussion of cataracts.

[7] The Census Data were obtained directly from the U.S. Bureau of the Census.

EXHIBIT F-4

Age Distribution of the U.S. Population Over Time in the North Region (fraction of total population in the region)

YEAR	AGE GROUP									FRACTION OF TOTAL U.S. POP.*
	0-14	15-24	25-34	35-44	45-54	55-64	65-74	75-84	85+	
1985	.2074	.1619	.1739	.1360	.0961	.0973	.0748	.0404	.0122	.2486
2000	.1990	.1303	.1329	.1633	.1422	.0925	.0700	.0498	.0200	.2486
2025	.1752	.1168	.1240	.1310	.1162	.1282	.1166	.0651	.0269	.2486
2050	.1692	.1151	.1214	.1235	.1190	.1229	.1005	.0723	.0561	.2486
2080	.1665	.1146	.1186	.1219	.1196	.1174	.1040	.0757	.0617	.2486

* The fraction of the total U.S. population represents the portion of the U.S. population that is estimated to reside in this region (in this case the North region). This fraction does not change over time, thereby reflecting stable regional distribution patterns.

Source: Age distribution from: U. S. Bureau of Census, Current Population Reports, series P-25, No. 952, Projections of the Population of the United States, by Age, Sex and Race: 1983 to 2080, U.S. Government Printing Office, Washington, D.C., 1984.

Appendix B), and is used as the basis of estimating the number of people in each age, race, and sex grouping.

Step 2 -- Baseline Incidence

To evaluate the potential future risk of skin cancers in the U.S., the baseline risk (i.e., the risk in the absence of changes in the level of total column ozone) is required. Incidence of melanoma and nonmelanoma skin cancers has been found to vary by latitude. Therefore, baseline incidence values have been developed for each of the three U.S. regions separately. The age-sex specific baseline rates used for melanoma and nonmelanoma are described separately. The baseline data for cataracts follow.

Nonmelanoma Skin Cancer

There are two major types of nonmelanoma skin cancers: basal cell and squamous cell (Scotto, Fears, and Fraumeni 1981; and see Chapter 7). Because the two types may respond differently to changes in UV, their baseline incidences are estimated separately (Scotto, Fears, and Fraumeni 1981). Data describing the age-sex specific incidence for whites are available for 10 locations from Scotto, Fears, and Fraumeni (1981). The incidence rates by age and sex were estimated for each of the three U.S. regions by taking the population-weighted averages of the rates for the cities reported in Scotto, Fears, and Fraumeni (1981) that are in each of the regions. The locations in each region are:

North: Seattle, Minneapolis-St. Paul, Detroit;
Middle: Utah, San Francisco, Iowa; and
South: Atlanta, New Orleans, New Mexico, Dallas-Fort Worth.

Exhibit F-5 displays an example of the age-specific incidence rates for basal and squamous cell skin cancers in the North region of the U.S. These data apply only to whites.

The baseline incidence rates for blacks and members of other races are not well characterized. The rates are believed to be approximately one order of magnitude or more below the rates for whites, and are consequently not expected to play a major role in evaluating risks of skin cancers in the U.S. (they may play a more important role in the risks in other countries). For purposes of this analysis, risks for blacks and members of other races are not evaluated.

The mortality associated with each of these cancers is believed to be quite low. Approximately 1.0 percent of all cases of nonmelanoma skin cancer result in death (Scotto, Fears, and Fraumeni 1981). The rates for basal and squamous cell cancer differ, and have been estimated from data in Scotto, Fears and Fraumeni to be: basal cell -- 0.3 percent; and squamous cell -- 3.75 percent. These percentages are multiplied by the baseline incidence rates to estimate the baseline rates of death associated with each cancer type over time.

EXHIBIT F-5

Baseline Incidence for Nonmelanoma Skin Cancers (North Region of the U.S. -- White Population Only) (Rate per 100,000)

	AGE GROUP								
	15	15-24	25-34	35-44	45-54	55-64	65-74	75-84	85+
NONMELANOMA SKIN CANCER									
Basal Cell Skin Cancer									
Male	0.1	2.9	22.1	91.1	259.2	465.8	761.0	1162.8	1311.3
Female	0.5	5.6	22.2	91.0	201.8	287.4	465.9	638.2	754.1
Squamous Cell Skin Cancer									
Male	0.2	0.3	1.6	7.4	32.6	87.4	147.4	349.7	431.8
Female	0.0	0.1	1.4	4.1	10.5	27.5	54.8	112.5	167.7

Source: Derived from Scotto, Fears, and Fraumeni (1981).

The model user may also specify that the baseline incidence and mortality ratio may change over time (increase or decrease). The purpose of this specification is to allow the user to include the implications of potential changes in the baseline incidence of these skin cancers that are not related to changes in UV flux.

Melanoma Skin Cancer

There are four principal classes of melanoma skin cancers: Hutchinson's melanotic freckle, superficial spreading melanoma, nodular melanoma, and unclassifiable melanoma (Elder et al. 1980). For purposes of modeling the baseline incidence of these cancers, two groups are defined that are based on the location of the cancer on the body:

- Group 1: Face, Head, Neck, and Upper extremities; and
- Group 2: Trunk and Lower Extremities.

These groups have been defined by Scotto and Fears (in press), and incidence data have been collected for seven U.S. cities that divide the occurrence of melanoma skin cancers into these groups. The division of these cancers into these groups appears to be warranted because Scotto and Fears have identified different correlations with UV for each of the two groups.

The incidence data for these groups of melanoma skin cancer were developed for the three regions of the U.S. by taking population-weighted averages of the incidence data reported for the following seven locations in the three regions:[8]

- North: Seattle, Detroit;
- Middle: Utah, San Francisco, Iowa; and
- South: Atlanta, New Mexico.

The incidence data were taken from the National Cancer Institute, Cancer Incidence and Mortality in the United States: SEER Report (1984), and the data apply to whites only. Because the SEER data do not divide the incidence by the two groups of melanoma skin cancer defined above, the fractions of age-specific incidence associated with each type of cancer were taken from Scotto and Fears (in press).

Exhibit F-6 displays sample baseline incidence data for melanoma skin cancer by sex and age for whites in the North U.S. region. As shown in the exhibit, the incidence rates for the two types of melanoma were estimated separately.

Mortality data were taken from the SEER Report (1984) for whites only. Because the SEER data do not divide the mortality rates by the two groups of

---

[8] Although the National Cancer Institute SEER Report (1984) reports data for ten locations, incidence data for only seven locations were used. These seven locations correspond to the locations for which Scotto and Fears (in press) reported body site percentages (face, head, neck, and upper extremities vs. trunk and lower extremities) for melanoma incidence. The three locations that were not included in this analysis are: Connecticut, Hawaii, and Puerto Rico.

EXHIBIT F-6

Baseline Incidence for Melanoma Skin Cancers
(North Region of the U.S. -- White Population Only)
(Rate per 100,000)

Melanoma Skin Cancer	Age Group 10-14	15-24	25-34	35-44	45-54	55-64	65-74	75-84	85+
Face, Head, Neck and Upper Extremities									
Males	0.0	0.8	2.4	5.3	5.5	8.4	10.4	9.2	9.1
Females	0.1	0.9	3.2	4.2	5.3	5.4	4.5	4.6	4.9
Trunk and Lower Extremities									
Males	0.0	1.2	3.4	7.5	7.9	12.0	14.9	13.2	13.0
Females	0.1	1.4	5.3	6.9	8.6	8.9	7.4	7.4	8.0

Source: Derived from Scotto and Fears (in press) and National Cancer Institute SEER Report (1984).

melanoma skin cancer defined above, mortality is modeled without dividing the data into the two cancer types. Exhibit F-7 displays the mortality rates currently used in the model.

The incidence and mortality associated with melanoma skin cancers in nonwhite populations in the U.S. are less well defined. The rates for nonwhites are much lower than the rates for whites, and are consequently not modeled.

The model user may also specify that the baseline incidence rates may change over time (increase or decrease). The purpose of this specification is to allow the user to include the implications of potential changes in the baseline incidence of melanoma skin cancer that are not related to changes in UV flux.

Senile Cataracts

Epidemiological studies have identified a correlation between the prevalence of various types of cataracts in humans and the flux of sunlight or ultraviolet radiation reaching the earth's surface (Hiller, Giacometti and Yuen 1977; Zigman, Datiler, and Torczynski 1979; Taylor 1980; Hollows and Moran 1981). Hiller, Sperduto and Ederer (1983) developed a multivariate logistic risk function that describes the correlation found between the prevalence of senile cataracts and the flux of UV-B and other risk factors. The results of this study were used to indicate the magnitude of change in the prevalence of senile cataracts that could be associated with changes in UV-B flux due to ozone depletion.

The study by Hiller, Sperduto, and Ederer included HANES data on a total of 2,225 persons between the ages of 45 and 74 years who had resided in the state where the HANES examination took place for at least one-half of their lives. Of these 2,225 people, 413 (18.6 percent) were placed in the cataract or aphakia outcome category.

UV-B flux data were developed by NOAA for the 35 HANES locations used in the study based on a statistical analysis of UV-B data collected at 10 locations using Robertson-Berger meters. The statistical analysis incorporates season, latitude, elevation, weather (clouds), and haze. Subsequent validation of the estimates at six locations indicated that the differences between the estimated and observed mean daily flux average about seven percent.

These data on UV-B and outcome (i.e., cataract) were used by Hiller, Sperduto, and Ederer in conjunction with demographic and medical history data to estimate the following multivariate logistic risk function:

$$P = \frac{1}{1 + \exp(-a - b_i X_i - \ldots - b_k X_k)}$$

where P is the probability (or risk) of having a cataract, and X_i are risk factors. In addition to UV-B, the following risk factors were analyzed: age; race; sex; education; diabetes; systolic blood pressure; and residence (urban, rural).

EXHIBIT F-7

Mortality Rates for Melanoma Skin Cancers
(White Population Only)
(Rate per 100,000)

	Age Group								
	10-14	15-24	25-34	35-44	45-54	55-64	65-74	75-84	85+
Male	0.0	0.5	1.0	2.9	4.6	5.5	8.0	7.7	10.3
Female	0.0	0.0	0.8	1.6	2.8	2.9	3.3	5.3	5.5

Source: Derived from Scotto and Fears (in press) and National Cancer Institute SEER Report (1984).

Exhibit F-8 displays the standardized regression coefficients estimated for each of the risk factors. Positive coefficients indicate factors that are correlated with increased risk; negative coefficients indicate factors that are correlated with decreased risk. The coefficients presented in the exhibit are "standardized," meaning that they represent the expected change in the logit of P (equal to ln (P/1-P)) for a one standard deviation change in the risk factor. Standardization of the coefficients allows the relative importance of the risk factors to be identified by the relative size of the standardized coefficients.

As shown in Exhibit F-8, three risk functions were estimated: (1) univariate (outcomes as a function of the risk factor); (2) bivariate (outcome as a function of the risk factor and age); and (3) outcome as a function of all the risk factors simultaneously. For all three formulations, UV-B is statistically significant, and positively correlated with the increased risk of being in the cataract outcome category.

Using the multivariate risk function coefficients, and the mean values for all the risk factors other than UV-B, the change in the prevalence of cataract for each 1.0 percent change in UV-B is estimated to be approximately 0.5 percent. This relationship holds for changes in UV-B as large as minus 20 percent to plus 30 percent. Outside of this range, reductions in UV-B are associated with less of a reduction in cataract prevalence, and increases in UV-B are associated with larger increases.

Of note is that this estimated relationship between UV-B and cataract prevalence varies with age; UV-B has a larger effect on prevalence (on a percentage basis) among younger individuals. Exhibit F-9 displays the percent increase in cataract prevalence due to increases in UV-B for persons of different ages. As shown in the exhibit, the percentage increase in prevalence due to changes in UV-B are estimated to be larger for 50 year olds than for 70 year olds.

Although the effect of UV-B on prevalence is estimated to be larger at younger ages (on a percentage basis) using the multivariate risk function, the prevalence of senile cataracts is known to increase substantially with age. Leske and Sperduto (1983) report the prevalence of senile cataracts in both sexes found in the Framingham Eye Study to be as follows: 52 to 64 years old -- 4.5 percent; 65 to 74 years old -- 18.0 percent; 75 to 85 years old -- 45.9 percent. These prevalence estimates use the same definition of cataracts as used by Hiller, Sperduto, and Ederer. Because cataracts are more prevalent in older individuals, increases in the actual number of cases of cataracts would likely be larger for older individuals, even though the percentage increase in risk has been estimated to be larger for younger individuals.

Step 3 -- Apply Dose-Response Relationships

The purpose of applying the dose-response relationships is to estimate how the risks of melanoma and nonmelanoma skin cancers and cataracts may change as the flux of UV reaching the earth's surface changes due to changes in total column ozone abundance. Two factors are required to apply dose-response relationships: (1) a measure of exposure; and (2) a dose-response equation. Each is described in turn.

EXHIBIT F-8

STANDARDIZED REGRESSION COEFFICIENTS FOR CATARACTS

Risk Factor a/	Mean b/	Univariate c/	Bivariate d/	Multivariate e/
Age	61.97	1.22 f/		1.20 f/
Race	1.22	0.18 f/	0.20	0.13 g/
Sex	1.52	0.07	0.08	0.08
Education	2.87	-0.43 f/	-0.25 f/	-0.14 g/
Diabetes	0.08	0.25 f/	0.23 f/	0.21 f/
Systolic Blood Pressure	146.3	0.33 f/	0.15 g/	0.08
UV-B	3.59	0.19 f/	0.20 f/	0.13 g/
Residence	1.37	0.18 f/	0.21 f/	0.19 f/

a/ Values for categorical risk factors: race: 1 = white, 2 = black; sex: 1 = male, 2 = female; education 1 = <5 grades, 2 = 5-8 grades, 3 = 9-11 grades, 4 = 12 grades, 5 = college; diabetes: 0 = absent, 1 = present; residence: 1 = urban, 2 = rural.

b/ Mean value for the risk factor in the 2,225 persons in the study.

c/ Each risk factor analyzed separately.

d/ Each risk factor analyzed with age only.

e/ All risk factors analyzed simultaneously.

f/ p(two sided) <0.005.

g/ p(two sided) <0.05.

Source: Hiller, R., R. Sperduto, and F. Ederer, "Epidemiologic Associations with Cataract in the 1971-1972 National Health and Nutrition Examination Survey," American Journal of Epidemiology, Vol. 118, No. 2, pp. 239-249, 1983.

EXHIBIT F-9

ESTIMATED RELATIONSHIP BETWEEN RISK OF CATARACT AND UV-B FLUX

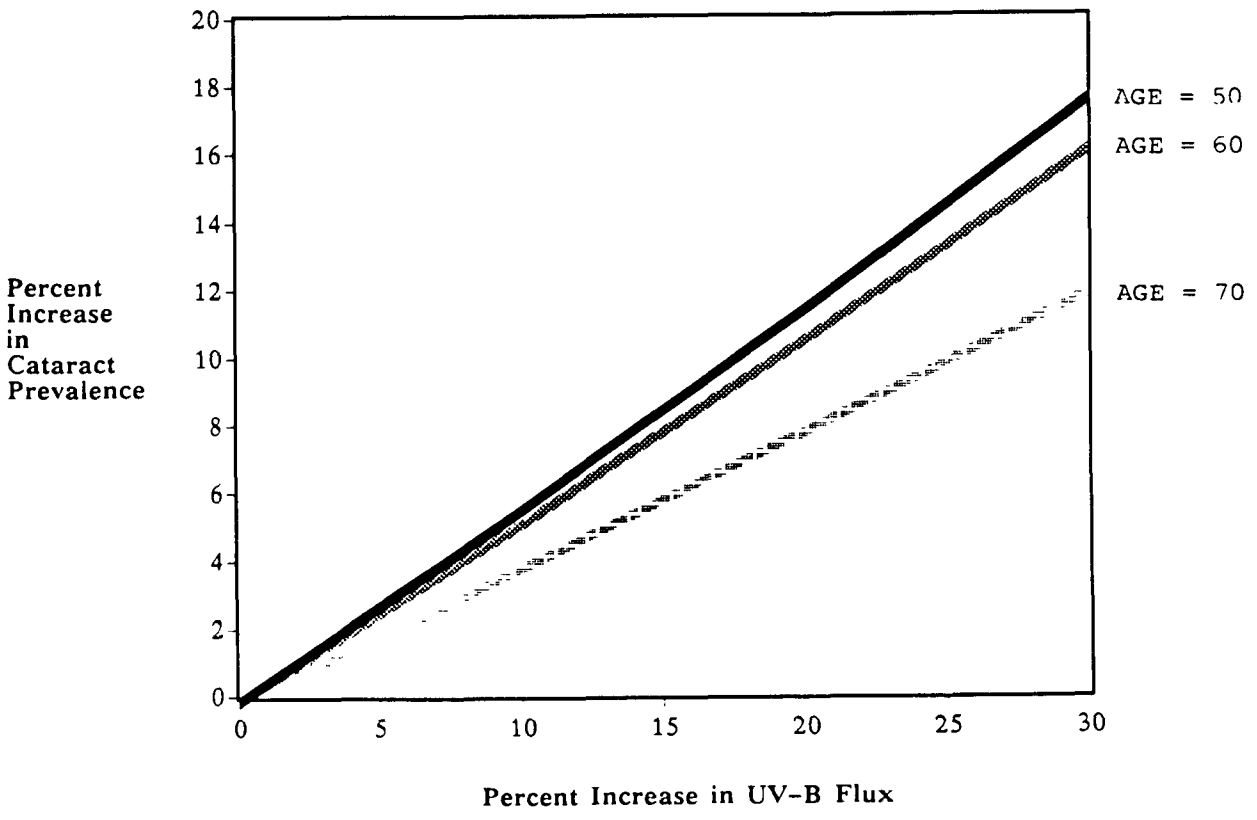

Increased UV-B flux (measured with an RB-meter) is associated with increased prevalence of cataract. The percent change in prevalence varies by age.

Source: Developed from data presented in R. Hiller, R. Sperduto, and F. Ederer, "Epidemiologic Associations with Cataract in the 1971-1972 National Health and Nutrition Examination Survey," American Journal of Epidemiology, Vol. 118, No. 2, pp. 239-249, 1983.

The measure of exposure used to model skin cancers and cataracts is related to the level of ambient UV flux estimated to reach the earth's surface in the three regions of the U.S. To use the dose-response relationships incorporated into the model, the change in UV flux (in percent) associated with changes in ozone abundance is used -- the change in the absolute level of UV energy reaching the earth's surface (in units such as millijoules per meter squared) is not used. (The method used to estimate changes in UV flux (in percent) along several scales of UV measurement was described above.)

Given these estimates of percent changes in UV over time for given locations in the U.S. (i.e., the three regions), the change in exposure for individuals estimated to live in those areas is estimated on an age-specific basis. In year T of the analysis, the change in UV flux for a person who is 40 years old is a function of the change in UV estimated from years T-40 to year T. Changes in UV for years prior to 1985 are assumed to be zero.

The current understanding for nonmelanoma skin cancer is that the cumulative exposure received during a person's life is the appropriate measure to use for modeling the dose-response relationship. Insufficient evidence exists to define the appropriate measure of exposure for purposes of modeling cataract prevalence. Similarly, a major question remains regarding the most appropriate measure of exposure for modeling the incidence and mortality of melanoma skin cancer. Recent analyses of melanoma incidence by Scotto and Fears (in press) have used annual RB-meter values as estimates of exposure. Pitcher (1986) used peak values to model mortality. Although some evidence indicates that peak or intermittent exposures to UV may best explain melanoma incidence patterns (see Chapter 8), significant research remains to be done on this issue. Of note is that the UV Model indicates that changes in UV flux (in percent) as a function of changes in ozone levels are about the same for the annual values and peak values for a given action spectrum. However, the choice of peak UV flux versus annual UV flux (or flux measured over some other time period) influences the estimate of the relationship between mortality risks and UV significantly (by as much as 60 percent). Therefore, the choice of annual or peak UV flux as an exposure estimate for purposes of modeling risk influences the risk estimates substantially.

A related issue regarding modeling exposure for purposes of estimating melanoma risks is the relative weight to put on exposures (annual or peak) experienced throughout a person's life. Migration studies indicate that exposure before the age of 15 may be most important and should be given more weight than subsequent exposures (see Chapter 8). These relative weights have yet to be quantified, however. To allow alternative assumptions regarding the relative importance of exposure during a person's life to be modeled, relative weights can be assigned to different ages during a person's life for purposes of estimating changes in exposure. Exhibit F-10 presents a simplified version of the tables that the user can use to define these weights.

As shown in the exhibit, for a person who is currently 40 years old, the relative weight to give to the exposure that a person of that age has received during his life is: 2.0 times the exposure received from ages zero to 10, 2.0 times the exposure received from ages 10 to 20; 1.0 times the exposure received from ages 20 to 30; and 1.0 times the exposure received from ages 30 to 40. With these assumptions, the childhood exposures of individuals that are currently 40 years old are weighted twice as heavily as subsequent exposures.

EXHIBIT F-10

Sample Table for Specifying Relative Weights for Exposure During a Person's Lifetime

Current Age (years)	Age During Exposure (years)					
	0-10	10-20	20-30	30-40	40-50	50-60
10	2.0	-	-	-	-	-
20	2.0	2.0	-	-	-	-
30	2.0	2.0	1.0	-	-	-
40	2.0	2.0	1.0	1.0	-	-
50	2.0	2.0	1.0	1.0	1.0	-
60	2.0	2.0	1.0	1.0	1.0	1.0

All values are illustrative.

The assumptions used in the model for both melanoma skin cancers and cataracts are equal weights across all ages. The user may modify these assumptions as desired to evaluate alternative formulations.

The dose-response relationships currently included in the model are called "power functions" and are generally of the form:

$$\ln(\text{incidence}) = a + b * \ln(E),$$

where:

incidence = the age-specific incidence for a given race and sex;

a = a constant that varies by age, race, and sex;

b = a constant that varies by age, race and sex; and

E = measure of lifetime exposure to ultraviolet radiation.

Using this equation, the fractional change in incidence as a function of the fractional change in UV can be expressed as:

$$\text{fractional change in incidence} = (\text{fractional change in exposure} + 1)^{b} - 1$$

The value of this formulation is that:

- the change in incidence is expressed as a fractional change that can be multiplied by the baseline incidence to compute the increased age-specific incidence; and
- the change in exposure can be expressed as a fractional change, thereby avoiding potential difficulties in specifying the absolute levels of changes in exposure to UV (see Serafino and Frederick (1986) for a description of these potential difficulties).

To specify the dose-response relationship, the user must choose a measure of UV (e.g., RB-Meter, DNA, or Erythema action spectrum) and provide estimates of b in the above equations. Scotto, Fears, and Fraumeni (1981) present a range of estimates of b for white males and females for use with the RB-Meter action spectrum.[9] Their analysis indicates that these coefficients do not vary by age, indicating that the incidence at each age is correlated to changes in exposure to UV in the same manner.

---

[9] The coefficients for nonmelanoma were derived from the regression coefficients presented in Scotto, Fears, and Fraumeni (1981, p. 10). The values reported were for an exponential formulation of the risk model. To translate the coefficients into the power formulation, the coefficients were multiplied by 135 UV units, the ambient UV exposure level at which the power function and exponential function models predict equal incidence results.

As described in Chapter 7, an analysis of the data in Scotto, Fears, and Fraumeni (1981) was performed using the DNA action spectrum. The estimated coefficients did not differ significantly from the coefficients reported by Scotto, Fears and Fraumeni for the RB-Meter action spectrum. This result is expected because at current ozone levels the RB-Meter and DNA UV flux values are highly correlated. Exhibit F-11 displays the estimated coefficients for the incidence of basal and squamous cell nonmelanoma skin cancer used with the DNA action spectrum. The risk estimates in Chapter 18 are based on the DNA Action Spectrum, with a sensitivity analysis to evaluate the implications of using the Erythema Action Spectrum in its place.

The coefficients for the dose-response relationships for each of the types of melanoma were derived from data presented in Scotto and Fears (in press).[10] These coefficients vary by type of melanoma and sex. As with the coefficients for nonmelanoma, the values do not vary by age, and are for whites only. These values are also presented in Exhibit F-11. These coefficients are assumed to be applicable for the DNA action spectrum.

A dose-response relationship for nonmelanoma mortality has not been estimated. For purposes of modeling, the relationships for nonmelanoma incidence (basal and squamous) are assumed to apply.

A separate analysis of melanoma mortality has been performed by Pitcher (1986). The coefficients estimated as the result of that investigation are used to model the potential increase in mortality due to melanoma skin cancer. The coefficients estimated using peak UV flux values (weighted using the DNA action spectrum) as the measure of exposure are reported in Exhibit F-12. Analysis is continuing on alternative measures of exposure. Preliminary results indicate that using annual UV flux as the exposure measure would result in coefficients that are as much as 60 percent smaller.

---

[10] The information reported in Scotto (in press) reported the percent increase in the incidence in each of the different types of melanoma for a 10 percent increase in UV. To translate these data into coefficients in the power formulation of the risk model, the power function was rearranged to solve for the coefficient (b) as follows:

$$b = \frac{\ln\left(1 + \frac{\text{Change in incidence}}{\text{incidence}}\right)}{\ln\left(1 + \frac{\text{Change in UV}}{\text{UV}}\right)}$$

For example, an 8 percent increase in incidence resulting from a 10 percent increase in UV yields the following coefficient: $\ln(1.08)/\ln(1.1) = 0.807$.

EXHIBIT F-11

Coefficients Relating Percent Change in UV to Percent Change in Skin Cancer Incidence (For use with the DNA Action Spectrum -- Whites only)

	Low [a/]	Middle	High [b/]
NONMELANOMA SKIN CANCER			
Squamous			
Male	1.42	2.03	2.64
Female	1.47	2.22	2.98
Basal			
Male	0.932	1.29	1.65
Female	0.316	0.739	1.16
MELANOMA SKIN CANCER			
Face, Head and Neck			
Male	0.661	0.846	1.029
Female	0.798	1.019	1.236
Trunk and Lower Extremities			
Male	0.421	0.651	0.875
Female	0.341	0.522	0.700

a/ Middle value minus one standard error.

b/ Middle value plus one standard error.

Sources: Melanoma coefficients derived from Scotto and Fears (in press). Nonmelanoma coefficients presented in Chapter 7.

EXHIBIT F-12

Coefficients Relating Percent Change in UV to Percent Change in Melanoma Mortality (For Use with DNA Action Spectrum -- Whites Only)

	Low [a/]	Middle	High [b/]
Males	0.78	0.85	0.92
Females	0.50	0.58	0.66

a/ Middle estimate minus one standard error.

b/ Middle estimate plus one standard error.

Source: Pitcher (1986).

Coefficients for dose-response relationships for blacks and members of other races have not been developed. Skin cancer risks for blacks and members of other races are not modeled.

The correlation between UV-B and cataract prevalence estimated by Hiller, Sperduto and Ederer (1983) is used to model the potential changes in the incidence of cataracts as a function of changes in UV-exposure These prevalence values were used to compute incidence estimates (again, in the absence of ozone depletion) under the assumption that mortality and cataract prevalence are not related, and that the people in each age group (e.g., 55 to 64 year olds) are distributed uniformly across the ages. Based on these assumptions, the incidence rates assuming zero ozone depletion are as follows: 55 to 64 years old -- 450 per 100,000; 65 to 74 years old -- 1,350 per 100,000; 75 to 85 years old -- 2,750 per 100,000. Because (in the absence of ozone depletion) prevalence of cataracts in those 85+ years old is assumed to be equal to the prevalence in those 75 to 85 years old, there is no incidence among those over 85.

To evaluate the impact of ozone depletion on cataract incidence, a "power model" was used to relate increases in prevalence to changes in lifetime UV radiation exposure. The use of the power model is justified because the percent change in prevalence divided by the percent change in UV radiation is fairly constant over a wide range of changes in UV. Exhibit F-13 displays the age-weighted coefficients used in the analysis. The age-weighting was performed because the dose-response coefficient varies by age.

Of note is that these coefficients were developed using Robertson-Berger (R-B) meter measures of annual UV radiation flux as the surrogate measure of exposure, and that the coefficients were then used with the DNA-damage action spectrum and erythema action spectrum estimates of changes in UV flux due to ozone depletion. Use of R-B meter-derived coefficients for the dose-response relationship coupled with estimates of changes in DNA-damage-weighted and erythema-weighted UV radiation flux in response to ozone depletion may result in <u>overestimating</u> the increase in cataract incidence in response to ozone depletion.

There are various important limitations in the use of these estimates and data. The correlation between UV-B and cataracts reported by Hiller, Sperduto, and Ederer does not prove a causal connection -- other (unknown) factors could be playing a role. These (unknown) factors would have to be correlated with UV-B flux. Also, the study does not have estimates of individual lifetime UV-B exposure, thereby limiting the strength of the evidence for the association between UV-B exposure and cataracts. Additionally, the sample population analyzed may not be representative of the entire U.S. population. Finally, the outcome category used in the study does not differentiate between different types of cataracts, some of which may be more strongly related than others to UV-B exposure.

Confidence in the estimates developed here are strengthened by several considerations. The correlation between UV-B flux and sunlight flux is high, and a correlation between sunlight and cataracts has also been found in Australia (Taylor 1980) and in China (Mao and Hu 1982). An association between UV-B exposure and cataracts has also been demonstrated in laboratory animals.

EXHIBIT F-13

DOSE-RESPONSE COEFFICIENTS -- CATARACTS

Low a/	Middle	High b/
0.127	0.225	0.296

a/ Middle minus one standard error.

b/ Middle plus one standard error.

Source: Derived from data presented in: Hiller, Sperduto, and Ederer, "Epidemiologic Associations with Cataract in 1971-1972 National Health and Nutrition Examination Survey, "American Journal of Epidemiology, Vol. 118, No. 2, pp. 239-249, 1983.

Therefore, although considerable investigation remains to be performed, indications are that the association between UV-B and cataracts is a reasonable basis for evaluating potential impacts due to increased UV-B flux associated with ozone depletion.

Step 4 -- Summarize the Results

The dose-response relationships are applied to each of the age groups of the population over time using estimated changes in UV exposure as outlined above. The results of the method include:

- changes in the total population incidence rates (e.g., per 100,000 people) for a standard population age, sex, and race distribution;
- the total number of cases of each type of cancer over time, and the change in the number of cases from the number that would exist in the absence of changes in UV flux associated with changes on total column ozone; and
- the total number of deaths due to each type of cancer over time, and the change in the number of deaths from the number that would exist in the absence of changes in UV flux associated with changes on total column ozone.

These results are reported for the U.S. as a whole (the calculations are performed separately for each of the three U.S. regions). The increased number of cases and deaths are reported separately for those individuals that are alive today and for those individuals who are born in the future.

DEGRADATION OF POLYMERS

The purpose of this portion of the module is to evaluate the potential damages and costs associated with polymer degradation that may be caused by increases in the flux of ultraviolet radiation (UV) reaching the earth's surface. As described in Chapter 13, UV can degrade the physical and appearance characteristics of polymers. This module evaluates the economic impacts that increased UV flux may have on polymer performance based on studies by Andrady (1986) and Horst (1986).

There are several types of polymers that may be adversely affected by increases in UV, including: polyvinylchloride (PVC); acrylics; polycarbonate; polypropylene; and polyester (Andrady 1986, p. 22). To date, data for assessing the potential future markets and potential damages due to UV have only been developed for the portion of the PVC market used in construction (siding, window profiles, rainwater systems, and pipe and conduit). This PVC market accounts for about 26 percent of all polymers subject to exposure to UV (measured by production volume), and consequently, the estimates from this module are underestimates of the potential risks of polymer degradation due to ozone depletion.

Recognizing that the current data only account for a portion of the polymer market, the module is designed to evaluate up to five different types of polymers using the method outlined for PVC. As data for other polymers become available, it will be integrated into the module as appropriate.

The effects of UV on polymers are evaluated in three steps:

1. Project the size of the market for polymers that may be subject to degradation due to UV.

2. Assess the damage that increases in UV (due to ozone depletion) may have on the polymers.

3. Assess the costs of the damage to the polymers.

Each step is described in turn for evaluating PVC in construction applications.

Step 1 -- Market for Polymers

The future market for PVC polymers in construction will be influenced by construction activity and the costs and performance of substitute materials. Horst (1986) developed several approaches for projecting the expected production and use of PVC through 2075. The approach used here reflects expected market saturation and is of the following form:

$$Q = A \left(1 - \exp \left(-k(T - T_o)\right)\right)$$

where:

Q = quantity per person per year in pounds;
A = a constant;
k = a constant;
T = the current year of the projection; and
T_o = a base year identified for the polymer type.

The constants and base year computed for PVC by Horst (1986, p. 4A-3) using statistical analyses of historical data are as follows: A = 63.0308; k = 0.01265; and T_o = 1966. These values are used along with the U.S. population scenario (see Appendix B) to compute a middle estimate of the size of the future market for PVC in pounds. By using the population scenario from the scenarios module, the estimates of the PVC market will be consistent with the values used to develop the scenarios of production of CFCs and the other trace gases and the evaluation of human health effects.

Because there is uncertainty in the expected future market for PVC, the module also produces low and high estimates of future demand. The low and high estimates are based on the statistical uncertainty in the estimates of A and k. By approximating the future demand, Q, with the first three terms of its expansion series, Horst (1986) showed that the variance of Q could be estimated from the covariance matrix of A and k. Specifically,

$$\text{Var}(Q) = \text{Var}(Ak)\ (T-T_o)^2 . - \text{Covar}(Ak, Ak^2)\ (T-T_o)^3 + \text{Var}(Ak^2/4)\ (T-T_o)^4 .$$

The model computes the variance of demand in each year. The low estimate is set at one standard deviation below the middle estimate; the high estimate is set at one standard deviation above. These low and high values (along with the middle value described above) are used in step 3 to evaluate the costs associated with the degradation of these polymers.

Step 2 -- Polymer Damage

A damage index that indicates the level of degradation of polymer characteristics was developed by Andrady (1986). When there is no degradation, the index value equals 1.0. Degradation is indicated by increasing values of the index, such as 1.1. This index is used here to describe the potential damage to polymers due to increased UV flux associated with ozone depletion.

Andrady (1986) also developed an estimate of how the damage index may vary as a function of ozone depletion. Due to uncertainties in the relationship between ozone depletion and UV, and UV and polymer characteristics, the relationship between ozone depletion and the damage index is represented as a range. These ranges are displayed in Exhibit F-14.

To evaluate the damage index in each year, the ozone depletion estimate for that year is used get a range of values in the damage index table. The ozone depletion estimate for the U.S. is taken as the estimate for the middle U.S. region. The result of this method is a range of damage index values for each year (low, middle, and high).

Step 3 -- Assess Damage Costs

The costs of polymer degradation depend on the manner in which the characteristics of the polymers degrade, and the steps that are taken in response to the degradation. Horst (1986) developed an approach for evaluating the costs associated with the production of new PVC each year. These costs represent the implications of changing the formulation of PVC during manufacture in order to maintain its characteristics in light of increased UV exposure. These costs do not include the potential damages to PVC already in place. Additionally, these estimates do not reflect the losses that may be associated with polymer degradation in the absence of changes in the polymer formulation. Therefore, these estimates are an underestimate.

Horst (1986) identified the costs of changing the formulation of PVC as a function of the increased amount of stabilizer that needs to be added to the polymer to maintain its characteristics. A 25 percent increase in stabilizer was estimated to lead to a 1.86 percent increase in the price of PVC, from its current cost of $0.604 per pound (Horst 1986, p. 5-16 and 6-8). The increased amount of stabilizer required as a function of ozone depletion was identified by Andrady (1986) and is presented in Exhibit F-14.

EXHIBIT F-14

Damage Index and Increase in Stabilizer For Ranges of Ozone Depletion

Ozone Depletion (percent)	Damage Index			Stabilizer Increase (%)		
	Low	Middle	High	Low	Middle	High
0-5	1.01	1.015	1.02	1.0	3.0	5.0
5-10	1.01	1.025	1.04	1.0	5.0	9.0
10-15	1.02	1.055	1.09	3.0	11.5	20.0
15-20	1.03	1.105	1.18	3.0	20.5	38.0

Source: Derived from Horst (1986), p, 6-10.

To estimate the costs of increasing the amount of stabilizer in response to ozone depletion, Horst recommends using a ten year lag between the increase in stabilizer required and the increase in the price of PVC. This lag reflects the time needed for the industry to respond to changing environmental conditions and the fact that the current stabilizer concentrations include a margin of safety. This ten year lag is used in the module, although the model user may override it with an alternative assumption.

To compute the costs in year T, the following computations are performed:

- compute the increased amount of stabilizer required, based on the ozone depletion in year T - 10;
- compute the increase in price by interpolating between no increase in price, and a 1.86 percent increase in price for a 25 percent increase in stabilizer;
- given the increase in price, compute the cost as follows:

$$C(T) = (D(T)/P_o^{\,b})/(1+b) * [P_o^{\,(1+b)} - P_1^{\,(1+b)}]$$

where:

$C(T)$ = cost in year T;

$D(T)$ = demand in year T;

P_o = price of PVC in the absence of changes in the formulation of the polymer;

b = price elasticity of demand for PVC;

P_1 = the new price for PVC given the change in the formulation of the polymer.

This equation represents the annual loss in consumer surplus associated with the estimated changes in price. The price elasticity of demand estimated by Horst (1986) is -1.956. This value represents (in part) the estimated availability of appropriate substitutes for PVC.

This equation can be evaluated three times each year to generate low, medium, and high estimates of the costs. The low estimate uses the low demand value (from step 1) and the estimate of the change in price associated with the low estimate of the increase in stabilizer associated with ozone depletion. The middle and high estimates use the middle and high values for these components, respectively. If there is an increase in ozone abundance, the damage index is set to 1.0 and there are no estimated costs. The maximum price increase (1.86 percent) estimated by Horst is associated with a 25 percent increase in stabilizer. Price increases are capped at this value (1.86 percent) even when an increase in stabilizer exceeding 25 percent may be indicated as being required. The present value of the costs over time can be evaluated by discounting these annual costs at user-supplied discount rates.

LIMITATIONS

The Effects Module draws together a diverse set of analyses and applies these analyses to estimates of global ozone depletion (from the Atmospheric Science Module) to evaluate potential risks to human health. The analyses require that a chain of events from ozone depletion to health outcomes be modeled. There are limitations in each link of this chain, creating uncertainties in the estimates of the outcomes.

The estimates of changes in UV as a function of changes in the ozone level are based on a model. The model is in its early stages of field validation, and additional analyses remain to be performed.

The dose-response relationships for skin cancers and cataracts all depend on epidemiologic studies of humans in the U.S. Because the studies are based on humans in the U.S., there are no extrapolation problems (e.g., from animals to humans, or from one population of humans to the U.S. population). However, the epidemiologic studies are generally limited by their measures of environmental exposure to UV, as opposed to individual lifetime exposures. In addition to the limitations of the estimates of the dose-response relationship themselves, the characterization of baseline evidence (in the absence of ozone depletion) and baseline population characteristics are subject to uncertainty.

In addition to uncertainties and limitations in the estimates produced by the module, the module is limited because there are a variety of important effects that are not evaluated. These omitted effects include:

- o polymers other than PVC;
- o impacts on plants;
- o impacts on aquatic organisms;
- o impacts on urban smog formation;
- o potential immune suppression in humans; and
- o possible other diseases.

The omission of these effects biases the estimates downward. In Chapter 18, qualitative estimates of some of these effects are presented based on interpolations and extrapolations from case studies and research in early stages. Data used to prepare these estimates include:

- o Impacts on soybeans. For depletion of 25 percent, a 7.5 percent reduction in yield is used (average of statistically-significant results reported in Chapter 11 for Essex and Williams cultivars). For depletion between zero and 25 percent, a value is interpolated between zero and 7.5 percent. Values are not extrapolated outside this range.

- Impacts on Ground-Based Ozone (Smog). Estimates of increased smog levels are interpolated from case study estimates (Chapter 14) as follows:

  -- Los Angeles: 16.6% depletion yields a 4.5 percent increase;
  33.3% depletion yields a 9.4 percent increase;

  -- Philadelphia: 16.6% depletion yields a 13.4 percent increase;
  33.3% depletion yields a 33.0 percent increase;

  -- Nashville: 16.6% depletion yields a 23.8 percent increase; and
  33.3% depletion yields a 50.0 percent increase.

- Impacts on Aquatic Organisms. Estimates for reduced anchovy populations are interpolated from laboratory tank experiments (described in Chapter 12) as follows:

Percent Change in UV-B	Percent Annual Population Death
0%	0%
10%	0%
20%	0% to 4.8%
30%	0% to 11.5%
40%	2.5% to 18.0%
50%	6.0% to 23.0%
60%	11.0% to 25.0%

Because these data are based on case studies and research in early stages, all the estimates of these effects are very preliminary and should be viewed with caution.

REFERENCES

Andrady, A. (1986), "Analysis of Technical Issues Related to the Effect of UV-B on Polymers," prepared for the U.S. Environmental Protection Agency, Washington, D.C.

Cole, C.A., P.D. Forbes, and R.E. Davies (1986), "An Action Spectrum for UV Photocarcinogenesis," Photochemistry and Photobiology, pp. 275-284.

Connell, P.S. (1986), "A Parameterized Numerical Fit to Total Column Ozone Changes Calculated by the LLNL I-D Model of the Troposphere and Stratosphere," Lawrence Liverpool National Laboratory, Livermore, California.

Elder, D.E., Jacoby P.M., Tuthill, R.J. and Clark W.H. Jr. (1980), "The Classification of Malignant Melanoma," American Journal of Dermatopathology, Vol. 2, pp. 315-320.

Hiller, R., R. Sperduto and F. Ederer (1981), "Epidemiologic Association with Cataract in the 1971-1972 National Health and Nutrition Examination Survey," American Journal of Epidemiology, Vol. 118, No. 2, pp. 239-298.

Horst, R.L. (1986), "The Economic Impacts of Increased UV-B Radiation on Polymer Materials: A Case Study of Rigid PVC," prepared for the U.S. Environmental Protection Agency, Washington, D.C.

Isaksen, I.S.A. (1986), "Ozone Perturbations Studies in a Two Dimensional Model with Temperature Feedbacks in the Stratosphere Included," presented at UNEP Workshop on the Control of Chlorofluorocarbons, Leesburg, Virginia, September 1986.

Leske, C.L., and R.D. Sperduto (1983), "The Epidemiology of Senile Cataracts: A Review," American Journal of Epidemiology, Vol. 118, No. 2, pp. 152-165.

Pitcher, H. (1986), "Melanoma Death Rates and Ultraviolet Radiation in the United States 1950-1979," U.S. Environmental Protection Agency, Washington, D.C. This paper has been revised and submitted for publication as: Pitcher, H. (1987), "Examination of the Empirical Relationships Between Melanoma Death Rates in the United States 1950-1979 and Satellite-based Estimates of Exposure to Ultraviolet Radiation."

Scotto, Fears, and Fraumeni (1981), "Incidence of Nonmelanoma Skin Cancer in the United States," U.S. Department of Health and Human Services, (NIH) 82-2433, Bethesda, Maryland.

Scotto J. and T. Fears (in press), "The Association of Solar Ultraviolet Radiation and Skin Melanoma Among Caucasians in the United States," Cancer Investigation.

Serafino, G. and J. Frederick (1986), "Global Modeling of the Ultraviolet Solar Flux Incident on the Biosphere," prepared for the U.S. Environmental Protection Agency, Washington, D.C.

U.S. Bureau of Census. (1984), Projections of the Population of the United States by Age, Sex, Race: 1983 to 2080, Current Population Reports, series P-25, No. 952, Washington, D.C.

CHAPTER 18

HUMAN HEALTH AND ENVIRONMENTAL EFFECTS

SUMMARY

Future damage to human health and the environment depends on the magnitude of future emissions of ozone depleters and of greenhouse gases into the atmosphere. This chapter presents a range of quantitative estimates of the potential risks to human health and the environment arising from various scenarios of production and emissions of ozone-modifying substances.

The risk estimates draw on the data and methods described in earlier chapters. These chapters describe: (1) potential future emissions and concentrations of ozone-modifying substances; (2) the effects that these substances may have on stratospheric ozone and global climate; (3) the potential damage to human health and the environment arising from ozone modification and climate change; and (4) a comprehensive modeling framework for estimating these risks.

The major types of effects for which quantitative estimates are provided include: ozone depletion; additional cases and deaths related to skin cancers; additional cases of senile cataract; damage to polyvinyl chloride materials; rise in global equilibrium temperature; sea level rise; cost of sea level rise; reduction in soybean yield; increases in ground-based ozone; and effects on the survivability of a selected aquatic organism. Certain important risks discussed in earlier chapters are not evaluated because of data limitations and the absence of relevant scientific information. In most instances, the estimates cover the U.S. only.

Estimates of the potential risks due to emissions of ozone-modifying substances are necessarily uncertain for two reasons. First, estimating future risks requires projections of key factors, such as population and economic growth. Second, the many relationships that define how emissions result in risks are themselves uncertain.

To investigate the significance of key assumptions and data used to model risks, the chapter presents a range of risk estimates by varying the most important assumptions one at a time. The range of results obtained by varying each assumption is used to determine which factors used to model risks are most important.

FINDINGS

1. MODIFICATION OF THE TRACE GAS COMPOSITION OF THE ATMOSPHERE CAN BE EXPECTED TO ALTER COLUMN OZONE ABUNDANCE.

   1a. The range of global average total column ozone change projected for the year 2075 based on a parameterized representation of a one-dimensional model could vary from as high as over 50 percent depletion, for a case where global use of chlorine and bromine bearing substances grows at an average annual rate of 2.8 percent from 1985 to 2100 (5.0 percent per year from 1985 to 2050, followed by no growth through 2100), to increased abundance of ozone of approximately 3 percent, for a case where global use of chlorine and bromine bearing substances declines to 20 percent of its 1985 value by 2010. The six "what if" scenarios examined include:

   - o 80% Reduction: Use of chlorine and bromine bearing substances declines to 20 percent of its 1985 value by 2010, and remains constant thereafter, yielding approximately 3.0 percent increased ozone abundance by 2075;
   - o No Growth: no growth in use of chlorine and bromine-bearing substances from 1985 to 2100, yielding approximately 0.3 percent increased ozone abundance by 2075;
   - o 1.2% Growth: 1.2 percent growth from 1985 to 2050, followed by no growth, yielding approximately 4.5 percent depletion by 2075;
   - o 2.5% Growth: 2.5 percent growth from 1985 to 2050, followed by no growth, yielding approximately 25 percent depletion by 2075;
   - o 3.8% Growth: 3.8 percent growth from 1985 to 2050, followed by no growth, yielding over 50 percent depletion by 2075;
   - o 5.0% Growth: 5.0 percent growth from 1985 to 2050, followed by no growth, yielding over 50 percent depletion by 2075.

   The trace gas concentration assumptions used in these six cases are: CO2 -- NAS 50th percentile; CH4 -- 0.017 ppm per year (approximately 1 percent of current CH4 concentration); and N2O -- 0.20 percent per year.

   1b. Current data are not sufficient for distinguishing whether CH4 concentrations are likely to increase in a linear manner (e.g, at 0.017 ppm per year, or approximately 1 percent of current concentrations) or in a compound manner (e.g., at 1 percent per year, compounded annually). The sensitivity of the ozone change estimates in 2075 was evaluated for the following six assumptions regarding future CH4 concentrations:

   - o Scenario A: compound annual growth of 1 percent from 1985 to 2010, followed by constant concentrations at 2.23 ppm; and

- o Scenario B: linear growth at 0.01275 ppm per year (75 percent of the 0.017 ppm growth);

- o Scenario C: linear growth of 0.017 ppm per year (approximately 1 percent of current concentrations);

- o Scenario D: linear growth at 0.02125 ppm per year (125 percent of the 0.017 ppm growth);

- o Scenario E: compound annual growth of 1 percent;

- o Scenario F: compound annual growth of 1 percent from 1985 to 2020, growing to 1.5 percent compound annual growth by 2050 and thereafter.

For the 2.5% Growth scenario, the estimate of ozone depletion by 2075 ranges from about 14 percent (Scenario F) to 30 percent (Scenario A) across these six CH4 assumptions evaluated. The difference between the 1 percent linear (0.017 ppm per year) and 1 percent compounded assumptions (Scenarios C and E) is approximately 6 percent depletion. This sensitivity of the ozone depletion estimates to the assumption about linear versus compound growth of CH4 concentrations is much larger than the sensitivity to the range of assumptions examined regarding future CO2 concentrations (from the 25th to the 75th percentile NAS estimates) and regarding future N2O concentrations (from 0.15 percent annual compound growth to 0.25 percent annual compound growth).

2. TWO-DIMENSIONAL (2-D) MODELS PREDICT GREATER AVERAGE GLOBAL DEPLETION THAN ONE-DIMENSIONAL (1-D) MODELS. 2-D MODELS ALSO PREDICT THAT OZONE DEPLETION WILL EXCEED THE GLOBAL AVERAGE AT HIGH LATITUDES AND BE LESS THAN THE GLOBAL AVERAGE AT THE EQUATOR.

2a. For a case of 3 percent annual growth in emissions of CFCs, no emissions of Halons, and increases in trace gases of: CO2 -- approximately 0.6 percent per year; CH4 -- 1 percent per year; and N2O -- 0.25 percent per year, a 2-D model estimates approximately 5.4 percent global average depletion by 2030. For the same scenario of emissions and trace gas concentrations, the parameterized representation of a 1-D model estimates only 3.0 percent depletion by 2030.

2b. For this same case of emissions and trace gas concentrations, the 2-D model estimates of ozone depletion in 2030 at high latitudes are approximately: 60^{o}N -- 8.7 percent; and 50^{o}N -- 7.0 percent.

3. ESTIMATES OF ATMOSPHERIC MODIFICATION, SKIN CANCER CASES AND DEATHS, CATARACT CASES, MATERIALS DAMAGE, GLOBAL TEMPERATURE, AND SEA LEVEL DEPEND ON THE RATE AT WHICH OZONE-DEPLETING GASES GROW, ATMOSPHERIC RESPONSE, DOSE RESPONSE, AND WHETHER GREENHOUSE GASES THAT COUNTER OZONE DEPLETION GROW INDEFINITELY. THE ASSUMPTIONS BEHIND QUANTITATIVE PROJECTIONS MUST BE NOTED CAREFULLY.

3a. The models used in this risk assessment assume that Antarctic ozone depletion has no global implications and that global trends do not invalidate estimates of current models.

3b. Except as noted, projected effects assume that: greenhouse gases grow at historical rates indefinitely; current one-dimensional models accurately project depletion; production of ozone depleters does not grow after 2050; ozone depletion is limited to 50 percent; the action spectrum causing skin cancers is DNA; and the temperature sensitivity of the earth to doubled CO2 is 3°C.

3c. In 2100, projections of ozone depletion range from over 50 percent for the 5% Growth scenario (ozone depletion is constrained at 50 percent in this analysis) to 47 percent for the 2.5% Growth scenario to an increase in column ozone abundance of nearly 5 percent for the 80% Reduction scenario.

3d. For cohorts born before 2075, the number of nonmelanoma skin cancers projected ranges from a 261.5 million increase for the 5% Growth scenario to a 115 million increase for the 2.5% Growth scenario to a reduction of 6.5 million skin cancers for the scenario of 80% Reduction in all ozone depleters.

3e. For cohorts born before 2075, total melanoma cases ranges from a 1.3 million case increase for the 5% Growth scenario to a 609,000 increase for the 2.5% Growth scenario to 54,000 fewer cases for the scenario of an 80% Reduction in all ozone depleters.

3f. For cohorts born before 2075, total mortality from melanoma and nonmelanoma ranges from a 5.6 million increase for the 5% Growth scenario to a 2.4 million increase for the 2.5% Growth scenario to 115,000 fewer cases for the scenario of 80% Reduction in all ozone depleters.

3g. For cohorts born before 2075, the increase in total cataract cases ranges from 26 million for the 5% Growth scenario to 15.1 million for the 2.5% Growth scenario to 9,500 for the scenario of 80% Reduction in ozone depleters.

3h. The rise in global temperature by 2075 ranges from 11.6°C in the 5% Growth scenario to 5.6°C in the 2.5% Growth scenario to 4°C in the scenario of 80% Reduction in all ozone depleters.

3i. Impacts are also projected for other areas such as sea level rise, ground-based ozone, materials, aquatics, and soybean yield.

4. <u>QUANTITATIVE ESTIMATES OF RISKS VARY WITH ASSUMPTIONS ABOUT FUTURE EMISSIONS OF GREENHOUSE GASES THAT WILL CONTRIBUTE TO GLOBAL WARMING</u>.

4a. Model projections that extrapolate historical growth rates of greenhouse gases, which tend to counter ozone depletion, into the indefinite future assume certain policy decisions from future decisionmakers; alternative assumptions are possible.

4b. If future decisionmakers limit the concentrations of CO2, N2O, and CH4 to prevent global warming from exceeding 2°C (±50%) in 2075, they

would by necessity have to limit growth of ozone depleters to the No Growth case; for other cases increases in ozone depleters would be too large to achieve that objective.

4c. Ozone depletion associated with the No Growth or 1.2% Growth scenarios increases nearly 3 to 5 percent if global warming is limited to $3^{o}C$ ($\pm$50%); skin cancer deaths would increase 43 percent for people alive today.

4d. Estimates of methane emissions are inherently uncertain even without consideration of future policy decisions and could affect quantitative risk estimates.

5. QUANTITATIVE ESTIMATES OF RISK VARY WITH UNCERTAINTY ABOUT DOSE-RESPONSE COEFFICIENTS, ACTION SPECTRUM, LIMITS OF OZONE DEPLETION, AND RESPONSIVENESS OF MODELS TO ATMOSPHERIC DEPLETION.

5a. For people alive today and born before 2075, additional skin cancer cases would be reduced 45 percent if one assumes the lower dose-response coefficients that are one standard error below the best estimate and 66 percent higher if one assumes the higher coefficients that are one standard error above the best estimate.

5b. For people alive today and born before 2075, additional skin cancer cases would be reduced 11 percent if the Erythema action spectrum, rather than the DNA action spectrum, were used to measure health effects.

5c. Limiting projected depletion to 50 percent from what the parameterized 1-D model would project reduces projected deaths for later cohorts. For people born from 2030 to 2074, limiting depletion to 50 percent reduces deaths by 13 percent for the 2.5% Growth scenario and 66 percent for the 5% Growth scenario.

5d. For people alive today and born before 2075, skin cancer cases would be reduced 62 percent in the 2.5% Growth scenario if the atmosphere were less sensitive to potential ozone depleters (using the 10th percentile), and increased 54 percent if the atmosphere were more sensitive (using the 90th percentile).

6. WHILE NATIONAL QUANTITATIVE ESTIMATES OF AQUATIC, CROP, GROUND-BASED OZONE, AND SEA LEVEL RISE DAMAGE CANNOT BE MADE AT THIS TIME, CASE STUDY RESULTS INDICATE THAT SIGNIFICANT INCREASES IN GROUND-BASED OZONE, LOSS OF AQUATIC LIFE, SEA LEVEL RISE DAMAGE, AND LOSS OF CROP YIELD ARE POSSIBLE.

INTRODUCTION

The previous chapters of this document have described: (1) best estimates of the future production, emission, and concentrations of ozone-modifying substances; (2) the likely effects that these emissions and concentrations may have on stratospheric ozone and global climate; (3) the potential risks to human health and the environment arising from ozone-modification and global climate change; and (4) a comprehensive modeling framework for estimating these risks. This chapter integrates the data and methods presented in earlier chapters to develop quantitative estimates of risks for human health and the environment due to ozone modification and climate change.

Quantitative risk estimates are made for six different "what if" scenarios of emissions of ozone-depleting substances. The scenarios have been designed to cover a larger range of emissions than would be likely to occur either in the absence of regulations or with very stringent regulations, thereby providing a comprehensive assessment of risks of possible trajectories of future emissions. In general, the scenarios of ozone-depleting substances are run through models in conjunction with scenarios of greenhouse gas emissions that assume that historical rates of growth for these trace species continue indefinitely. Sensitivity analysis is performed, however, to assess the potential consequences of limits to greenhouse gas emissions taken in order to reduce global warming. With the exceptions of global sea level rise, global ozone depletion, and change in global equilibrium temperature, all effects are estimated for the U.S. only.[1]

The following ozone-depleting substances are considered in estimating risks:[2]

- o CFC-11, CFC-12, HCFC-22, and CFC-113;
- o methyl chloroform (CH3CCl3);
- o carbon tetrachloride (CCL4); and
- o Halon-1211 and 1301.

The following trace gases that add ozone or counter ozone depletion are considered:[3]

- o carbon dioxide (CO2);
- o methane (CH4); and
- o nitrous oxide (N2O).

Exhibit 18-1 displays the types of effects that are estimated in this

---

[1] The estimates presented in this chapter are for the entire U.S. As described in Chapter 17, the U.S. estimates combine analyses of three geographic regions (by latitude): north, middle, and south.

[2] See Chapter 3 for a description of the available estimates of future production and emissions.

[3] See Chapter 4 for a discussion of the future concentrations of these greenhouse gases. These greenhouse gases also counter ozone depletion in high chlorine cases. CO_2 is thought to increase ozone by cooling the stratosphere; CH4 adds ozone to the troposphere and counters chlorine-induced depletion in the stratosphere; nitrous oxide increases depletion in the stratosphere if chlorine levels are high.

chapter along with the chapter that describes the data and methods used to derive the effects. The effects are divided into two sets: (1) effects that can be estimated quantitatively for the U.S.; and (2) effects estimated on the basis of case studies and research in early stages. The first set is estimated using detailed epidemiologic, economic, demographic, and other scientific information within the modeling framework described in Chapter 17. Effects estimated in this first set are representative of risks to the entire U.S., and include:

- o global average ozone depletion;
- o nonmelanoma skin cancer (cases and deaths);
- o melanoma skin cancer (cases and deaths);
- o senile cataracts (cases);
- o damage to polyvinyl chloride (PVC) materials;
- o increased global average temperature; and
- o global sea level rise.

The second set of estimates is based either on research in early stages or on a small number of case studies, the results of which are more difficult to generalize to the entire U.S. Effects estimates included in the second set should be considered preliminary and are included here to indicate the potential order of magnitude of these effects. The second set of estimates includes the following types of effects:

- o costs of sea level rise;
- o reductions in soybean yields (for two cultivars; 2 out of 3 cultivars appear sensitive);
- o increases in ground-based ozone (smog); and
- o effects on the survivability of a selected aquatic organism (the Northern Anchovy population).

Because of data limitations and the absence of relevant scientific information, certain important effects discussed in earlier chapters were not evaluated. The major effects not analyzed in this chapter are:

- o overall impacts on agricultural and natural plants (Chapter 11);
- o impacts of climate change on human health, water resources, forestry, and wetlands (Chapter 16);
- o increased incidence of cutaneous diseases from immune suppression (Chapter 9);

EXHIBIT 18-1

Types of Human Health and Environmental Effects Estimated

TYPE OF EFFECT (Reference Chapter)	UNITS
Effects Estimated Quantitatively for the U.S.	
Ozone Depletion (Chapter 5)	Percentage Depletion from 1985 to 2075
Nonmelanoma Skin Cancer (Chapter 7)	Additional Cases and Deaths for People Alive Today; People Born 1986-2029; and People Born 2030-2074.
Melanoma Skin Cancer (Chapter 8)	Additional Cases and Deaths for People Alive Today; People Born 1986-2029; and People Born 2030-2074.
Senile Cataracts (Chapter 10)	Additional Cases for People Alive Today; People Born 1986-2029; and People Born 2030-2074.
Damage to Polyvinyl Chloride Materials (Chapter 13)	Present Value Costs in 1985 U.S. Dollars
Rise in Equilibrium Temperature from 1985 to 2075 (Chapter 6)	Degrees Centigrade
Sea Level Rise from 1985 to 2075 (Chapter 15)	Centimeters

EXHIBIT 18-1
(Continued)

Types of Human Health and Environmental Effects Estimated

TYPE OF EFFECT (Reference Chapter)	UNITS
Effects Based on Case Studies and Research in Early Stages:	
Reduction in Soybean Yield (Chapter 11)	Percent in 2075
Increase in Fatality Rate of Northern Anchovy Population (Chapter 12)	Percent in 2075
Increase in Ground-Based Ozone (Chapter 14)	Percent in 2075
Cost of Sea Level Rise in Charleston, SC and Galveston, TX (Chapter 15)	Present Value Costs in 1985 U.S. Dollars

- impacts of sea level rise on wetlands (Chapter 15); and
- impacts on materials other than polyvinyl chloride (Chapter 13).

Estimates of human health and environmental effects are necessarily uncertain for two reasons. Effects are estimated into the future, requiring projections of such factors as population growth; economic growth; and production, use, and emissions of ozone-modifying substances and greenhouse gases. Furthermore the linkages from emissions to risks are themselves uncertain. For example, the models and analyses used to evaluate ozone modification and global warming continue to be developed and may undergo change.

In order to understand the significance of uncertainties in the numerous factors and assumptions used to model the chain of events that starts with emissions and results in risks, following the presentation of the quantitative risk estimates for six scenarios, the implications of various uncertainties systematically explored so that a quantitative assessment of their relative importance can be made.

The remainder of this chapter is organized as follows:

- Methods for Estimating Health and Environmental Risks summarizes the major steps used to estimate risks.
- Description of Range of Production, Emissions, and Concentrations Scenarios For Evaluating Risks describes the key scenarios discussed throughout this chapter.
- Sensitivity of Health and Environmental Effects to Differences in Emissions of Ozone Depleters assesses the sensitivity of potential risks to assumptions about the growth in production and emissions of ozone-depleting gases, assuming greenhouse gases that counter ozone depletion grow at historical rates.
- Sensitivity of Results To Alternative Atmospheric Assumptions explores the relationships of potential risks to assumptions about: (1) the ozone-depletion model used; (2) sensitivity of global warming to concentrations of greenhouse gases; (3) future concentrations of greenhouse gases (4) ozone level response to emissions; and (5) the maximum level of ozone depletion allowed in modeling.
- Sensitivity of Effects to Uncertainty in Dose Response identifies how the risk estimates are influenced by uncertainty in estimates of: (1) dose-response coefficients; and (2) choice of action spectrum (i.e., the weighting of wavelengths in the increased flux of UV that would be associated with various levels of ozone depletion).

- Relative Importance of Key Uncertainties summarizes the results of previous sections and compares the significance of the different uncertainties analyzed in this chapter.

METHODS FOR ESTIMATING HEALTH AND ENVIRONMENTAL RISKS

A complete description of these methods is given in Chapter 17. Briefly, emissions of ozone-modifying substances and greenhouse gases lead to effects on human health and the environment by means of the following principal mechanisms:

1. Production leads to emissions of ozone depleters and greenhouse gases, which in turn result in a time stream of ozone depletion.

2. Ozone depletion produces increases in ultraviolet radiation reaching the earth's surface.

3. Ultraviolet radiation increases have health impacts, including melanoma skin cancer, nonmelanoma skin cancer, and cataracts.

4. Changes in concentrations of ozone depleters and trace gases that counter ozone depletion directly cause global warming.

5. Changes in global temperature and ultraviolet radiation have other environmental impacts on sea level, aquatic organisms, agricultural yields, energy demand, and other concerns.

As discussed in chapters 7, 8, 9 and 17, to quantify risks for human health and the environment, each of these mechanisms was evaluated using mathematical relationships. For example, estimates of additional cases of melanoma skin cancers rely on mathematical relationships between: (1) emissions and ozone depletion, (2) ozone depletion and UV, and (3) UV and cancer incidence. The sources and derivation of the mathematical relationships are described in earlier chapters.

The mathematical relationships were integrated in the modeling framework described in Chapter 17. The framework provides a method of estimating expected risks as well as analyzing the joint implications of key assumptions and uncertainties in each mathematical relationship. The primary period of analysis used in the models is 1985 to 2075. Emissions of ozone-modifying substances and concentrations of greenhouse gases are analyzed during this period. Risks to human health are evaluated for individuals born before 2075, in three discrete cohorts (i.e., groups):

- those individuals alive today (i.e., 1985);

- those individuals born between now and 2029; and

- o those individuals born between 2030 and 2074 (the end of the analysis period).

Risk estimates for these individuals are based on simulated lifetime exposures to increased UV. For example, a 50 year old person who is alive today is assumed to experience no increase in UV prior to 1986.[4] During his remaining life, however, this 50 year old may experience increased exposure to UV as total column ozone depletes. Exposure histories for each population cohort are analyzed separately as a basis for estimating risks.

All the risk estimates presented below assume constant baseline incidence and mortality rates; recent secular trends of increasing incidence are not extrapolated into the future.

Of note is that some of the individuals in the second and third cohorts (born after 1985) will live beyond the end of the primary period of analysis (2075). To estimate the lifetime risk for these individuals, the time horizon was extended to 2165 (i.e., a 90-year lifetime was assumed), holding emissions constant after 2075. Risk estimates for the second two population cohorts are affected by the assumption that emissions are constant after 2075. In most of the scenarios investigated, depletion, UV radiation, and temperature are still increasing in 2075.

Environmental risks (e.g., global warming, sea level rise, and PVC damages) are reported for 2075. Risk estimates based on preliminary research and case studies (aquatics, food, and ground-based ozone) are also reported for 2075.

It is important to note that the models used to estimate risks do not include feedbacks among factors. For example, the economic production used to generate an emissions growth rate (2.5 percent for CFC emissions, for example) is assumed not to be affected by the rate of global warming (5.6°C for the 2.5% Growth scenario). To the extent that there are feedbacks from effects to subsequent economic growth, that is, to the extent that effects may reduce economic growth, the earth will be somewhat self-limiting in the growth of CFCs. As now conceived, the risk models implicitly assume that the damage from effects is not large enough to alter the economic growth of society.

DESCRIPTION OF RANGE OF PRODUCTION, EMISSIONS, AND CONCENTRATIONS SCENARIOS FOR EVALUATING RISKS

For purposes of evaluating the risks of emitting ozone-modifying substances and greenhouse gases, scenarios of future production, emissions, and concentrations of ozone depleters are required. The purpose of the scenarios chosen here is to cover the complete range of possible futures--that is, the largest rate of growth in the absence of regulation to the greatest reduction in growth in the case of unanticipated technological breakthroughs or stringent regulation. It is unnecessary to decide on a single reference case for evaluating risks -- all quantitative estimates will be given in terms of additional (i.e., incremental) effects.

---

[4] This assumption of no prior increase in UVB is based on the conclusion in Chapter 5 that it is premature for this risk assessment to conclude that global ozone has decreased. If it turns out later that global ozone has already begun to decrease, then the risk estimates presented herein will be too low.

As described above, the key substances of concern are the major ozone-depleting substances: CFCs; chlorocarbons; and Halons (see Chapter 3). In addition, for the first set of runs we will assume that the greenhouse gases that counter ozone depletion -- carbon dioxide (CO2), nitrous oxide (N2O), and methane (CH4) -- grow at historical rates into the definite future.

In order to evaluate the risks of stratospheric changes due to these substances, the scenarios of emissions and concentrations must extend over very long periods of time because the impacts of the compounds are long-lived. The lifetimes of the key CFCs are on the order of 100 or more years. Therefore, to assess properly the implications of current and future emissions of these substances, long-term scenarios are required.

Scenarios for Ozone-modifying Substances

Although Chapter 3 summarized the best available estimates from a variety of authors of future production and emissions of the CFCs, chlorocarbons, and Halons, use of those estimates is unnecessary at this juncture. As discussed in the chapter, the global production and emissions of these compounds is expected to increase in the near term (e.g., through the year 2000) in the absence of regulatory intervention due to factors such as economic growth, population growth, the development of new applications for the compounds, and increases in the saturation of existing applications.

For purposes of assessing the full range of potential risks, however, we will expand the production emission, and concentration scenarios far beyond the best estimates made in Chapter 3, using six "what if" scenarios of global production. Through out this chapter, these six scenarios of future production and emissions will be referred to as:

- 80% Reduction Scenario--80% reduction in ozone-depleting substances by 2010, constant production thereafter.
- No Growth Scenario--0.0% annual growth through 2050, constant production thereafter.
- 1.2% Growth Scenario--1.2% annual growth through 2050, constant production thereafter.
- 2.5% Growth Scenario--2.5% annual growth through 2050, constant production thereafter.
- 3.8% Growth Scenario--3.8% annual growth through 2050, constant production thereafter.
- 5.0% Growth Scenario--5.0% annual growth through 2050, constant production thereafter.

For each of these scenarios, CFC-11, CFC-12, HCFC-22, and carbon tetrachloride (CCL4) all grow at the specified rates. The following compounds grow at slightly different rates:

- o CFC-113 is assumed to grow at 1.5 times the growth rates in the 1.2%, 2.5%, 3.8%, and 5.0% scenarios from 1985 to 2000.

- o Methyl chloroform is assumed to grow slightly slower in the 1.2%, 3.8% and 5.0% scenarios.

- o Halons are assumed to grow as projected by Camm and Hammitt (1986).

The production and emissions for each scenario result in simulated changes in atmospheric chlorine concentrations (Clx), which drive stratospheric ozone depletion. To assist readers in translating these scenarios tc various "real world" situations, Exhibit 18-2 shows, for two of the scenarios, alternative ways in which emissions could grow in the real world and achieve essentially the same Clx levels.

In Exhibit 18-2a the simulated Clx concentration in the No Growth case is shown to increase to 5.0 ppbv by 2075. Approximately equal future Clx values could be achieved if the underlying growth rate is assumed to be the same as shown in the 2.5% Growth scenario, but global limitations are placed on the growth of a subset of the chemicals, with 10 percent of the world's producing countries not complying. Of course, the real growth rate could be 1.2 percent or 3.8 percent, which would require lesser or greater stringency and coverage to achieve equivalent Clx concentrations.

Exhibit 18-2b provides another example of how various scenarios are equivalent. The 1.2% Growth scenario in the risk assessment leads to a Clx concentration of 9.9 ppbv by 2075. This would be similar to the 3.8% Growth scenario if global limitations led to a 50 percent reduction. That is, if world growth actually were 3.8 percent, to achieve 1.2 percent would require a 50 percent cutback for CFC-11, -12, -113, and CCl4 in nations with 90 percent of the world's CFC production.

The scenarios in Exhibit 18-2a and 2b demonstrate that there are a variety of ways in which the Clx levels associated with individual scenarios can be achieved. A global policy of reductions in use for a subset of the compounds, assuming less than 100 percent participation, could result in the same Clx values as the assumed No Growth scenario (which assumes 100 percent compliance across all the compounds).

Given these examples, therefore, it is clear that the six "what if" scenarios used here to assess risks reflect a great diversity of potential future outcomes. Furthermore, interpreting real world options does not require these scenarios to be exactly as simulated vis a vis specific substances since the same Clx growth paths can be achieved by many difficult scenarios.

Scenarios of future production and emissions of other CFCs, including CFC-13, CFC-14, CFC-21, CFC-23, CFC-114, CFC-115, CFC-142b, and CFC-152a are not presented here because these chemicals are only produced in limited quantities.

Representatives from DuPont, Allied, and Imperial Chemical Industries have reported that they had investigated chemical substitutes beginning a decade ago. HCFC-123 and FC-134a were identified as attractive candidates for replacing

EXHIBIT 18-2A

Real World Equivalent to the No Growth Scenario in Risk Assessment

Risk Assessment No Growth Scenario	Equivalent Real World Case
Chemical Coverage:	Chemical Coverage[a/]
o CFCs: 11, 12, 113, 22 o Methyl chloroform o Carbon tetrachloride o Halons: 1211, 1301 o Other ozone depleters assumed to have zero emissions	o CFCs: 11, 12, 113 o Carbon tetrachloride
Stringency:	Stringency:
o Freeze at 1985 levels	o 70 percent reduction from 1985 levels by 1990
Compliance:	Compliance:[b/]
o 100 percent of global production	o Nations representing 90 percent of global production

Resulting Increases in Clx Concentrations (ppbv)

1985	0.0
2000	1.3
2025	2.9
2050	4.1
2075	5.0

Resulting Increases in Clx Concentrations (ppbv)

1985	0.0
2000	1.2
2025	2.2
2050	3.7
2075	5.1

a/ Chemicals not covered grow as follows: HCFC-22: 2.5%/yr through 2050; methyl chloroform: 2.5%/yr through 2050; Halon-1211: 2.9%/yr through 2050; Halon-1301: 2.5%/yr.

b/ Non-compliers are assumed to grow at 2.5%/yr through 2050 for CFC-11 and CFC-12, and 2.8%/yr for CFC-113.

EXHIBIT 18-2B

Real World Equivalent to the 1.2% Growth Scenario in Risk Assessment

Risk Assessment No Growth Scenario	Equivalent Real World Case
Chemical Coverage:	Chemical Coverage[a/]
o CFCs: 11, 12, 113, 22 o Methyl chloroform o Carbon tetrachloride o Halons: 1211, 1301 o Other ozone depleters assumed to have zero emissions	o CFCs: 11, 12, 113 o Carbon tetrachloride
Stringency:	Stringency:
o Limited to 1.2% Growth	o 50 percent reduction from 1985 levels by 1990
Compliance:	Compliance:[b/]
o 100 percent of global production	o Nations representing 90 percent of global production

Resulting Increases in Clx Concentrations (ppbv)		Resulting Increases in Clx Concentrations (ppbv)	
1985	0.0	1985	0.0
2000	1.5	2000	1.4
2025	4.0	2025	3.3
2050	6.9	2050	6.6
2075	9.9	2075	10.3

a/ Chemicals not covered grow as follows: HCFC-22: 3.8%/yr through 2050; methyl chloroform: 3.4%/yr through 2050; Halon-1211: 4.2%/yr through 2050; Halon-1301: 3.8%/yr.

b/ Non-compliers are assumed to grow at 3.8%/yr through 2050 for CFC-11 and CFC-12, and 4.3%/yr for CFC-113.

CFC-11 and CFC-12. HCFC-123 has a hydrogen atom and would probably have a short atmospheric lifetime. FC-134a has no chlorine and thus no depletion potential. HCFC-123 and FC-134a are not now commercially produced. At the current time it is believed that producers will not produce these chemicals unless environmental controls lead to increases in the prices of existing CFCs, unless there is an improvement in the technology of producing these chemicals.

Greenhouse Gas Scenarios

Chapter 4 summarizes the data available on the potential future levels of emissions and concentrations of three key greenhouse gases: CO2, CH4, and N2O. All three gases also influence stratospheric ozone. Because stratospheric ozone is most sensitive to the uncertainty surrounding the potential future levels of CH4 concentrations, many CH4 scenarios are examined, including:

- linear growth of 0.017 ppm/yr (about 1.0 percent of current concentrations);
- compounded annual growth of 1.0 percent per year;
- linear growth of 0.01275 ppm/yr (75 percent of the 0.017 ppm/yr growth);
- linear growth of 0.02125 ppm/yr (125 percent of the 0.017 ppm/yr growth);
- compounded annual growth of 1.0 percent per year from 1985 to 2010, followed by no growth thereafter; and
- compounded annual growth of 1.0 percent per year from 1985 to 2020, growing to 1.5 percent per year by 2050 and thereafter.

These six scenarios reflect the potential consequences of the diverse set of factors affecting CH4 concentrations discussed in Chapter 4.

The levels of CO2 and N2O concentrations, although important for evaluating stratospheric ozone, have less of an impact than the CH4 concentrations. Initial assumptions for these two gases are:

- CO2: 50th percentile estimate reported by NAS (1984), which implies an annual rate of growth in concentrations of about 0.7 percent over the period of the analysis; and
- N2O: compounded annual growth of 0.2 percent per year.

Because CO2, N2O and CH4 are radiatively active gases that may contribute to future global warming, governments may take action to limit future increases in their concentrations if they become concerned about global warming. The potential influence of such government actions could be significant over the time period used to assess risks of stratospheric modification. Rather than assume that future decision makers choose to never control these gases to limit warming, a range of scenarios of greenhouse gas growth is presented in order to explore the eventuality of limiting global warming to various levels.

SENSITIVITY OF HEALTH AND ENVIRONMENTAL EFFECTS TO DIFFERENCES IN EMISSIONS OF OZONE DEPLETERS[5]

Using the six scenarios presented in the previous section, this section identifies the potential risks to assumptions regarding the future production, use, and emissions of ozone-modifying substances.

Exhibit 18-3 displays estimates of ozone depletion for the six scenarios. The 80% Reduction scenario shows a slight decline in ozone levels until 2010, after which ozone levels increase. The 2.5%, 3.8%, and 5.0% Growth scenarios result in greatly accelerated ozone depletion. Ozone depletion reaches nearly 50 percent on or before 2100 in these scenarios.

For purposes of evaluating potential health effects, the maximum ozone depletion was (arbitrarily) set to 50 percent. Depletion exceeding 50 percent was considered to be outside the range for which the atmospheric models used here was tested. This arbitrary cutoff affected ozone depletion estimates in the 2.5%, 3.8%, and 5.0% Growth scenarios only. Once 50 percent depletion is reached, depletion is held constant for the remainder of the analysis period. (The implications of relaxing this assumption are explored below.)

Exhibits 18-4 to 18-8 present estimates of the health risks across the emissions scenarios for the three population cohorts. All of the estimates reflect human health impacts due to ozone depletion:

- Exhibit 18-4 shows the additional cases of nonmelanoma by type of nonmelanoma (basal or squamous).
- Exhibit 18-5 shows the additional mortality from nonmelanoma by type of nonmelanoma.
- Exhibit 18-6 shows the additional cases of melanoma.

---

[5] Many of the estimates of ozone depletion and health risks presented in this section show increases relative to the estimates in the previous draft of this document. Modification to the analyses that resulted in increased estimates of risks include: (1) inclusion of the expected increases in the average age of the U.S. population through the year 2080, rather than assuming the population profile does not age as expected (as had been assumed for purposes of simplification in the draft); (2) use of 0.017 ppm/yr. growth rate for methane and 0.20 percent/yr for nitrous oxide concentrations, as opposed to earlier larger estimates; (3) use of estimates of global ozone depletion for purposes of estimating risks rather than relying on a single 2-D model result; and (4) inclusion of simulated changes in chlorine concentrations through 2165 for estimating ozone depletion through 2165 (previous analysis held ozone depletion constant after 2100, implying constant atmospheric concentrations after 2100).

EXHIBIT 18-3

Global Average Ozone Depletion: Emission Scenarios

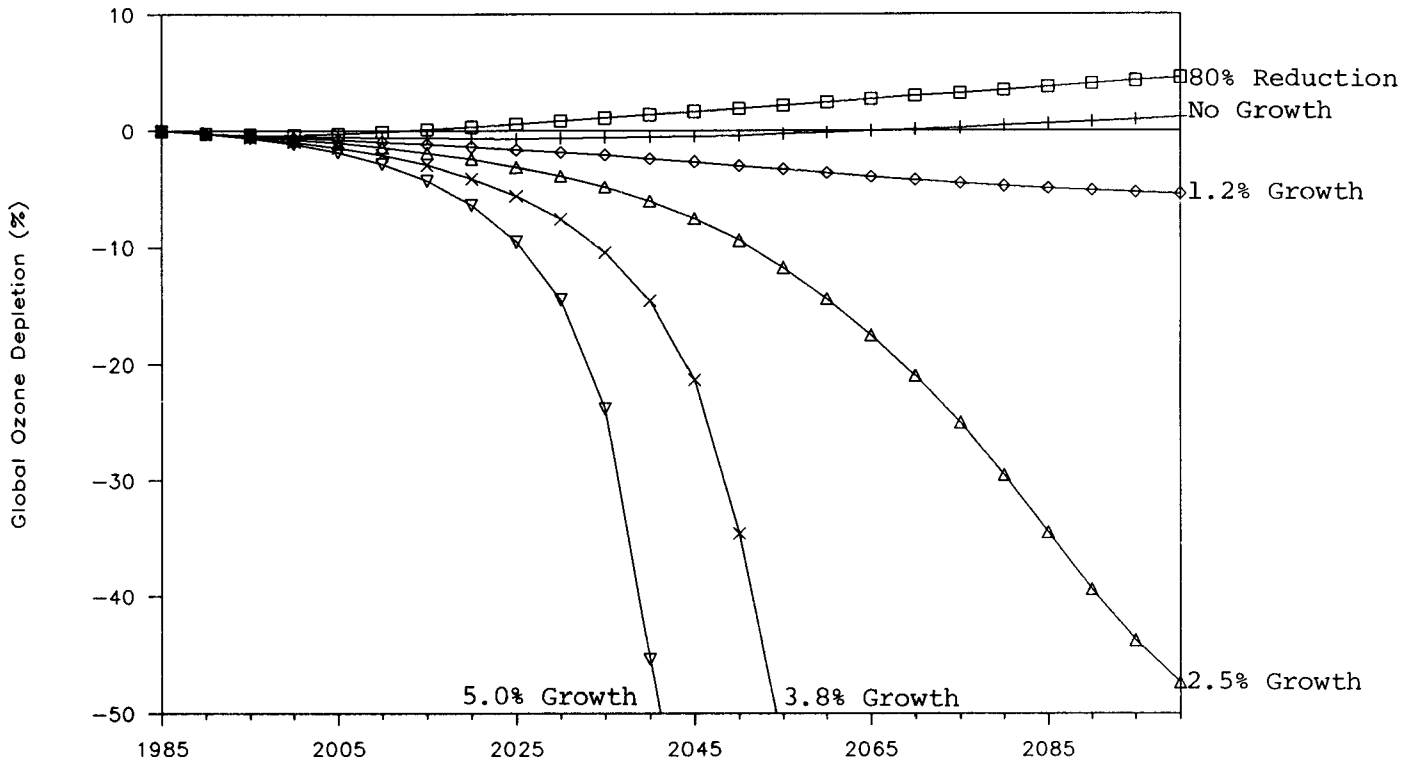

Assumptions:

-- Current 1-D models accurately reflect global depletion; Antarctic ozone hole has no impact on global ozone levels.

-- Greenhouse gases that counter depletion grow at historically-extrapolated rates.

-- Growth rates for ozone depleters are for global emissions; it is assumed that emissions do not increase after 2050.

-- Ozone depletion limited to 50 percent.

EXHIBIT 18-4

Additional Cases of Nonmelanoma Skin Cancer
By type of Nonmelanoma
(Whites only)

Scenario	People Alive Today	People Born 1986-2029	People Born 2030-2074	Total
5.0% Growth				
Basal	6,882,800	46,429,300	78,600,200	131,912,300
Squamous	5,431,800	42,922,400	81,244,300	129,598,500
Total	12,314,600	89,351,700	159,844,500	261,510,800
3.8% Growth				
Basal	3,481,500	34,272,500	74,802,800	112,556,800
Squamous	2,587,200	30,330,000	76,314,500	109,231,700
Total	6,068,700	64,602,500	151,117,300	221,788,500
2.5% Growth				
Basal	1,289,300	11,998,800	47,744,000	61,032,100
Squamous	846,500	9,091,300	44,078,600	54,016,400
Total	2,135,800	21,090,100	91,822,600	115,048,500
1.2% Growth				
Basal	623,700	2,301,600	4,191,800	7,117,100
Squamous	390,800	1,411,900	2,564,500	4,367,200
Total	1,014,500	3,713,500	6,756,300	11,484,300
No Growth				
Basal	284,200	288,000	-572,900	-700
Squamous	169,900	150,500	-354,400	-34,000
Total	454,100	438,500	-927,300	-34,700
80% Reduction				
Basal	-74,400	-1,164,800	-2,853,400	-4,092,600
Squamous	-57,300	-698,100	-1,622,200	-2,377,600
Total	-131,700	-1,862,900	-4,475,600	-6,470,200

Assumptions:

-- Current 1-D models accurately reflect global depletion; Antarctic ozone hole has no impact on global ozone levels.
-- Greenhouse gases that counter depletion grow at historical rates.
-- Growth rates for ozone depleters are for global emissions; it is assumed that emissions do not increase after 2050.
-- Ozone depletion limited to 50 percent.

EXHIBIT 18-5

Additional Mortality From Nonmelanoma Skin Cancer
By Type of Nonmelanoma
(Whites only)

Scenario	People Alive Today	People Born 1986-2029	People Born 2030-2074	Total
5.0% Growth				
Basal	21,300	143,900	243,700	408,900
Squamous	203,700	1,609,600	3,046,700	4,860,000
Total	225,000	1,753,500	3,290,400	5,268,900
3.8% Growth				
Basal	10,800	106,200	231,900	348,900
Squamous	97,000	1,137,400	2,861,800	4,096,200
Total	107,800	1,243,600	3,093,700	4,445,100
2.5% Growth				
Basal	4,000	37,200	148,000	189,200
Squamous	31,700	340,900	1,652,900	2,025,500
Total	35,700	378,100	1,800,900	2,214,700
1.2% Growth				
Basal	1,900	7,100	13,000	22,000
Squamous	14,700	52,900	96,200	163,800
Total	16,600	60,000	109,200	185,800
No Growth				
Basal	900	900	-1,700	100
Squamous	6,400	5,600	-13,200	-1,200
Total	7,300	6,500	-14,900	-1,100
80% Reduction				
Basal	-100	-3,500	-8,700	-12,300
Squamous	-2,100	-26,100	-60,700	-88,900
Total	-2,200	-29,600	-69,400	-101,200

Assumptions:

-- Current 1-D models accurately reflect global depletion; Antarctic ozone hole has no impact on global ozone levels.
-- Greenhouse gases that counter depletion grow at historical rates.
-- Growth rates for ozone depleters are for global emissions; it is assumed that emissions do not increase after 2050.
-- Ozone depletion limited to 50 percent.

EXHIBIT 18-6

Additional Cases of Melanoma Skin Cancer By Cohort (Whites only)

Scenario	People Alive Today	People Born 1986-2029	People Born 2030-2074	Total
5.0% Growth	62,500	445,900	771,500	1,279,900
3.8% Growth	33,700	324,400	734,300	1,092,400
2.5% Growth	13,900	124,400	470,400	608,700
1.2% Growth	7,100	29,800	56,800	93,700
No Growth	3,500	5,200	-6,400	2,300
80% Reduction	-300	-14,300	-39,800	-54,400

Assumptions:

-- Current 1-D models accurately reflect global depletion; Antarctic ozone hole has no impact on global ozone levels.

-- Greenhouse gases that counter depletion grow at historical rates.

-- Growth rates for ozone depleters are for global emissions; it is assumed that emissions do not increase after 2050.

-- Ozone depletion limited to 50 percent.

- Exhibit 18-7 shows the additional mortality from melanoma.
- Exhibit 18-8 shows the additional senile cataract cases.

The exhibits provide a range of risk estimates and illustrate how risk estimates respond to assumptions about emissions.

The 80% Reduction and No Growth scenarios result in the fewest additional cumulative cases and deaths related to nonmelanoma skin cancer, melanoma skin cancer, and senile cataract. The reduction in risk results from lower ozone depletion (and UV radiation) in these scenarios. For example, in the 80% Reduction scenario in Exhibit 18-4, it is estimated that people alive today would actually experience fewer cases of basal cell skin cancer than in the absence of ozone depletion due to an increase in ozone abundance.

The 3.8% and 5.0% Growth scenarios produce the largest increases in cases and deaths. The large increases in cases and deaths in the higher emission scenarios can lead to estimates of total cases that exceed the size of the population. For example, in Exhibit 18-4 the total number of nonmelanoma cases in the 3.8% and 5.0% Growth scenarios among people born from 2030 to 2074 exceeds the total size of the population. This level of increase in risk is possible since many people often develop two or more cases of nonmelanoma in their lives, while other people may not develop nonmelanoma at all. In general, however, the risk estimates for the higher emission scenarios should be treated with caution because the dose-response coefficients used to derive risk estimates were estimated over a limited range of UV radiation levels. The dose-response parameters may not be valid for the extreme changes in UV radiation expected in these scenarios (it is possible they overestimate or underestimate total changes).

The risk estimates shown in Exhibit 18-4 to 18-8 are incremental to the risks that can be expected in the absence of depletion. If current levels of skin cancer and cataracts are extrapolated into the future (without changing their baseline incidence and mortality rates), there would be 160 million nonmelanoma skin cancer cases for the three cohorts, 1.77 million deaths from nonmelanoma, 4.2 million melanoma cases, 1.2 million melanoma deaths, and 182 million cataract cases.

Exhibit 18-9 displays estimates of environmental risks for those effects that could be estimated quantitatively. Exhibit 18-10 displays estimates for environmental effects that were estimated based on other case studies or research in its early stages (these effects are more difficult to quantify). As with the health risks, the range of environmental effects is very large. Of note is that the global warming estimates for 2075 range from 4.0°C in the 80% Reduction scenario to 11.6°C in the 5.0% Growth scenario. Exhibit 18-11 shows the greenhouse equilibrium temperature increase over time for the six scenarios.

SENSITIVITY OF RESULTS TO ALTERNATIVE ATMOSPHERIC ASSUMPTIONS

This section identifies the sensitivity of potential risks to assumptions regarding: (1) the type of model used to characterize ozone depletion; (2) the sensitivity of the global climate to greenhouse gas forcings; (3) the concentration of greenhouse gas emissions; (4) ozone level response to

EXHIBIT 18-7

Additional Mortality From Melanoma Skin Cancer By Cohort (Whites only)

Scenario	People Alive Today	People Born 1986-2029	People Born 2030-2074	Total
5.0% Growth	17,800	107,900	170,300	296,000
3.8% Growth	9,500	81,900	163,500	254,900
2.5% Growth	3,800	32,500	111,900	148,200
1.2% Growth	1,900	7,300	13,400	22,600
No Growth	900	1,100	-1,700	300
80% Reduction	-100	-3,600	-9,600	-13,300

Assumptions:

-- Current 1-D models accurately reflect global depletion; Antarctic ozone hole has no impact on global ozone levels.

-- Greenhouse gases that counter depletion grow at historical rates.

-- Growth rates for ozone depleters are for global emissions; it is assumed that emissions do not increase after 2050.

-- Ozone depletion limited to 50 percent.

EXHIBIT 18-8

Additional Senile Cataract Cases By Cohort

Scenario	People Alive Today	People Born 1986-2029	People Born 2030-2074	Total
5.0% Growth	3,238,700	10,361,300	12,405,300	26,005,300
3.8% Growth	1,829,400	8,928,100	12,333,500	23,091,000
2.5% Growth	613,900	4,311,900	10,214,500	15,140,300
1.2% Growth	267,400	752,000	1,157,600	217,700
No Growth	102,800	49,100	0	151,900
80% Reduction	9,500	0	0	9,500

Assumptions:

-- Current 1-D models accurately reflect global depletion; Antarctic ozone hole has no impact on global ozone levels.

-- Greenhouse gases that counter depletion grow at historical rates.

-- Growth rates for ozone depleters are for global emissions; it is assumed that emissions do not increase after 2050.

-- Ozone depletion limited to 50 percent.

EXHIBIT 18-9

Environmental Effects Estimated Quantitatively for the U.S.

Scenario	Materials Damage[a] (10^6 1985 $)	Rise In Equilibrium Temperature by 2075[b] (°C)	Sea Level Rise by 2075 (cm)
5.0% Growth	971	11.6	134.3
3.8% Growth	829	7.6	108.8
2.5% Growth	606	5.6	95.1
1.2% Growth	305	4.7	88.6
No Growth	272	4.3	85.3
80% Reduction	131	4.0	82.2

---

a/ Present value, discounted over 1985-2075 using a real discount rate of 3 percent.

b/ Assuming a climate sensitivity of 3°C for doubled CO_2. A range of climate sensitivity from 1.5 to 4.5°C could be used based on NAS (1979). Recent climate model developments indicate that 4.0°C may be the most likely estimate. Estimates of equilibrium warming that would occur if one chose 1.5°C and 4.5°C can be made by multiplying the values shown by 50 percent and 150 percent, respectively.

Assumptions:

-- Current 1-D models accurately reflect global depletion; Antarctic ozone hole has no impact on global ozone levels.

-- Greenhouse gases that counter depletion grow at historical rates.

-- Growth rates for ozone depleters are for global emissions; it is assumed that emissions do not increase after 2050.

-- Ozone depletion limited to 50 percent.

EXHIBIT 18-10

Environmental Effects Based On Case Studies and Research in Early Stages

Scenario	Cost of Sea Level Rise In Charleston and Galveston[a] (10^6 1985 $)	Reduction for Soybean Yield by 2075[b] (%)	Increase In Ground-Based Ozone by 2075[c] (%)	Loss of Northern Anchovy Population By 2075[d] (%)
5.0% Growth	1,403-3,507	>7.5	>9.4 - >50.0	>11.0 - >25.0
3.8% Growth	1,221-3,013	>7.5	>9.4 - >50.0	>11.0 - >25.0
2.5% Growth	1,123-2,748	>7.5	7.0 - 36.9	>11.0 - >25.0
1.2% Growth	1,076-2,622	1.4	1.2 - 6.5	0.0 - 3.3
No Growth	1,053-2,558	e/	e/	e/
80% Reduction	1,031-2,498	e/	e/	e/

a/ Lowest estimate based on anticipation of sea level rise; highest estimate without anticipation. Present value discounted using a real discount rate of 3 percent.

b/ Based on statistically significant results developed by Teramura (1986, 1987) for two soybean cultivars -- Essex and Williams -- as reported in Rowe, et al. (1987). Maximum value reported is 7.5 percent.

c/ Lowest estimate is for Los Angeles, California; (9.4 percent is maximum value reported) highest estimate is for Nashville, Tennessee (50.0 percent is maximum value reported).

d/ Lowest estimate assumes 15-meter vertical mixing of the top ocean layer (11 percent is maximum value reported); highest estimate assumes 10-meter vertical mixing if ozone depletion is above 11.2 percent, no vertical mixing if below 11.2 percent (25 percent is maximum value reported).

e/ Impacts were not evaluated because ozone levels are estimated to increase, not decrease, by 2075 in these scenarios.

Assumptions:

-- Current 1-D models accurately reflect global depletion; Antarctic ozone hole has no impact on global ozone levels.
-- Greenhouse gases that counter depletion grow at historical rates.
-- Growth rates for ozone depleters are for global emissions; it is assumed that emissions do not increase after 2050.
-- Ozone depletion limited to 50 percent.

EXHIBIT 18-11

Equilibrium Temperature Change for the Six Emission Scenarios Assuming 3.0°C Warming for Doubled CO2*

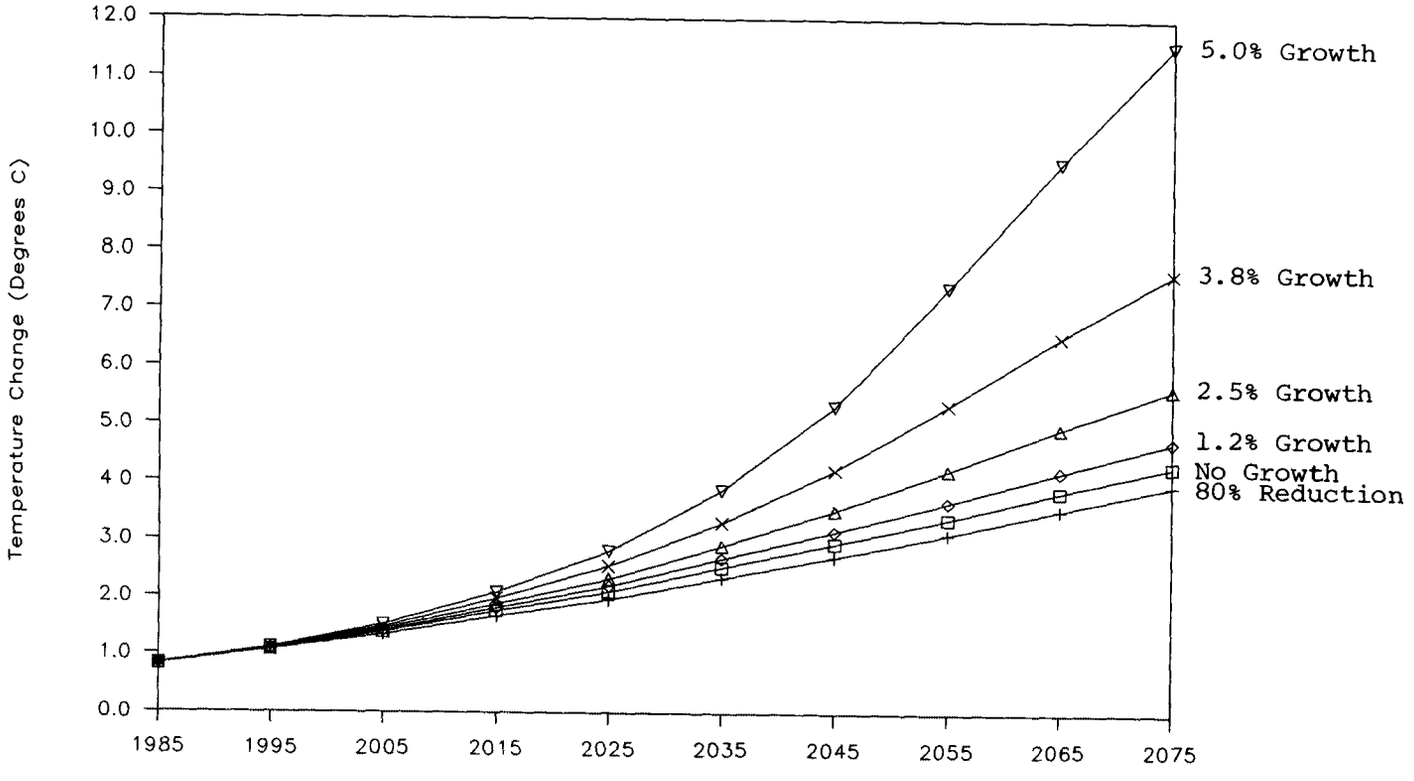

* Computed assuming that the climate sensitivity to a doubling of carbon dioxide is 3°C. This assumption is in the middle of the NAS range of 1.5°C to 4.5°C (see Chapter 6). Note that the actual warming that may be realized will lag by several decades or more. To compute the equilibrium warming associated with high or low NAS estimates multiply the y axis "temperature change" by 1.5 or 0.5.

Growth levels refer to global estimates of production of all ozone depleters.

emissions; and (5) the maximum level of ozone depletion simulated to occur. For purposes of comparison, the results of these sensitivity analyses are shown for the 2.5% Growth scenario only (unless indicated otherwise). Information is presented for one scenario to avoid complicating the presentation of results unnecessarily. The selection of the 2.5% Growth scenario case should not be interpreted as other than a presentational device; comparison could have been made with any of the six scenarios to demonstrate the impact of the alternative assumptions.

Comparison with Results from a 2-Dimensional Atmospheric Model

A variety of models have been developed to assess potential changes in the stratosphere due to emissions of CFCs and other ozone-modifying substances (see Chapter 5). The various scenario risk estimates rely on a parameterized representation of a one-dimensional model of the atmosphere (see Chapter 17). For comparison purposes, the results of a time-dependent two-dimensional model developed by Isaksen (1986) are presented here. Two-dimensional models are believed to be preferable for risk assessment (see Chapter 5).

The results of Isaksen's analysis are currently only available beyond 2030. Therefore, a complete comparison of risks is not possible at this time (as additional data become available, a full comparison of risks will be performed).

Exhibit 18-12 displays estimates of ozone depletion from the one- and two-dimensional atmospheric models for two scenarios of emissions. The first scenario is a 3.0 percent growth rate of CFCs-11, 12, and 22, methyl chloroform, and carbon tetrachloride. This scenario is not directly comparable to any of the scenarios described above. The exhibit shows that the two-dimensional model results in larger estimates of ozone depletion than does the parameterized representation of the one-dimensional model for this scenario.

The second scenario shown in the exhibit is a 0.0 percent per year growth scenario. Comparing the one-and two-dimensional model estimates, the results from Isaksen's two-dimensional model show more depletion. In general, two-dimensional models appear to produce larger estimates of ozone depletion than do one-dimensional models (see Chapter 5).

Alternative Assumptions about Sensitivity of Atmosphere to Greenhouse Gases

The 2.5% Growth scenario (as well as the other five scenarios) assumes that the sensitivity of the global climate system is such that a doubling of atmospheric CO2 would result in a 3°C increase in the average global temperature. This climate sensitivity is the middle of a range published by the NAS in 1983 of 1.5°C to 4.5°C. Exhibit 18-13 displays estimates of temperature-sensitive effects for the limits of this NAS range. As expected, the warming and sea level rise estimates are lower for the 1.5°C sensitivity and higher for the 4.5°C sensitivity.

EXHIBIT 18-12

Global Average Ozone Depletion:
Comparison to Results with a 2-Dimensional Atmospheric Model

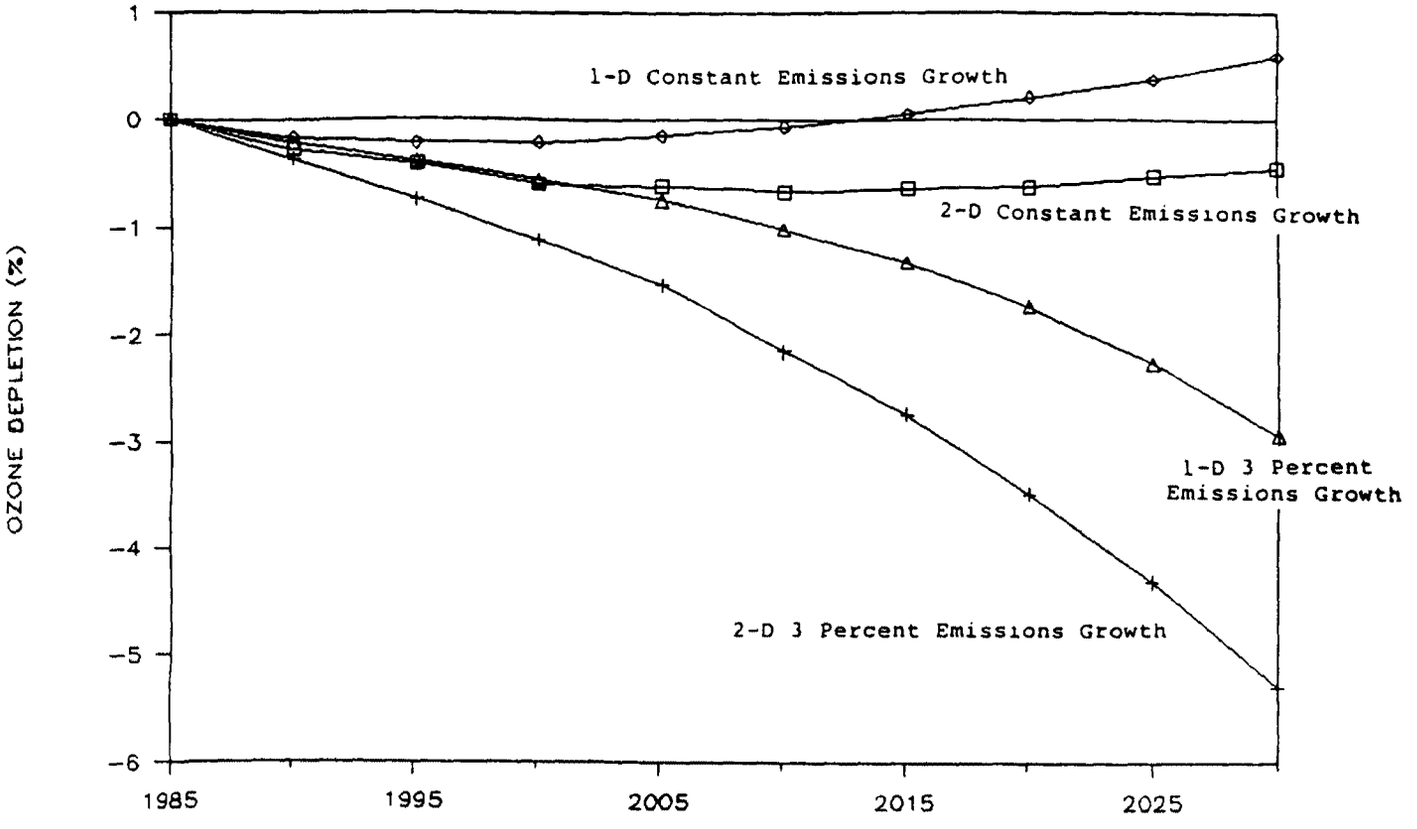

EXHIBIT 18-13

Climate and Other Effects:
Sensitivity to Relationship Between Climate Change and CO2 Concentrations
(Figures in Parentheses are Percentage Changes from 2.5% Growth Scenario)

Type of Effect	DOUBLED CO2 CLIMATE SENSITIVITY 1.5°C	3°C	4°C	4.5°C	UNITS
Effects Estimated Quantitatively for the U.S.					
Rise in Equilibrium Temperature by 2075	2.7 (-52)	5.6	7.6 (36)	8.7 (55)	Degrees Centigrade
Sea Level Rise by 2075	76 (-20)	95	104	107 (9)	Centimeters (13)
Effects Based on Case Studies and Research In Early Stages					
Cost of Sea Level Rise in Charleston and Galveston a/	977-2,188	1,123-2,748	1,177-2,897	1,199-2,955	Present Value (millions of 1985 dollars)

a/ Lowest estimate with anticipation of sea level rise; highest estimate without anticipation.

Also shown in the exhibit are estimates for a 4°C sensitivity. Recent model runs from the major general circulation models in the U.S. produced a warming of 4°C for a doubling of CO2 (see Chapter 6).

Alternative Assumptions about Emissions of Trace Gases

Uncertainty exists about potential future changes in atmospheric concentrations of the greenhouse gases: carbon dioxide (CO2); methane (CH4); and nitrous oxide (N2O). This uncertainty arises from at least two sources. First, to limit the potential for future global warming, governments may agree to take steps to limit growth in the concentrations of these gases. However, the timing and stringencies of such potential steps are not known. Second, future concentrations of methane are influenced by numerous natural as well as anthropogenic factors that have not been well characterized to date (see Chapter 4). Therefore, the rate of future increases in methane concentrations is particularly uncertain even in the absence of potential government regulations to limit global warming.

Through their roles in chemical reactions in the stratosphere, trace gases affect both total column ozone and the potential for future global warming. Exhibit 18-14 summarizes the implications of changes in concentrations of the gases for ozone depletion and global warming. In general, each greenhouse gas <u>increases</u> global temperature but <u>counters</u> ozone depletion.

Any risk assessment requires an assumption about future global warming and whether governments take actions to limit warming. The "standard assumption" generally has been that warming is never limited. To examine the sensitivity of the risk estimates to this issue, the implications of reducing the growth in concentrations of the trace gases to limit warming was examined for all six scenarios for two different limits: (1) 2°C by 2075 and (2) 3°C by 2075. In some scenarios, it may not be possible to limit warming to these levels by reducing the growth in concentrations of trace gases because even if no growth in these gases occurs, the limit will still be exceeded due to emissions from other CFCs. In fact, the only scenarios for which a limit of 2°C can be examined are the 80% Reduction and No Growth scenarios, since the 2°C limit cannot be achieved because of CFC growth in the other scenarios even if there is no growth in the concentrations of other trace gases; with a limit of 3°C, only the 80% Reduction, No Growth, 1.2% Growth, and 2.5% Growth scenarios can be estimated.

Exhibits 18-15 to 18-19 compare the results from the 80% Reduction, No Growth, 1.2% Growth and 2.5% Growth scenarios without limiting warming to the situation in which global warming is limited to 2°C and 3°C for those scenarios. As shown in Exhibit 18-15, the increase in ozone depletion can be significant; e.g., by 2050 in the 2.5% Growth scenario with a 3°C limit the difference is about 4 percent depletion. Exhibits 18-16 to 18-18 show the increased health risks expected for the three population cohorts. In general, the latter cohorts are affected more. For example, in the 2.5% Growth scenario, the people alive today may experience an increase in health risks on the order of 40 percent relative to the No Limits value. People born from 2030 to 2074 experience an increase in health risks up to 90 percent.

EXHIBIT 18-14

Summary of Effects of Greenhouse Gases on Ozone Depletion and Global Equilibrium Temperature

GREENHOUSE GAS	STRATOSPHERIC OZONE	GLOBAL TEMPERATURE
Methane (CH_4)	Counters Depletion	Increases
Nitrous Oxide (N_2O)	Counters Depletion in High Chlorine Cases	Increases
Carbon Dioxide (CO_2)	Adds Ozone	Increases

EXHIBIT 18-15

Global Average Ozone Depletion: Scenarios of Limits to Future Global Warming

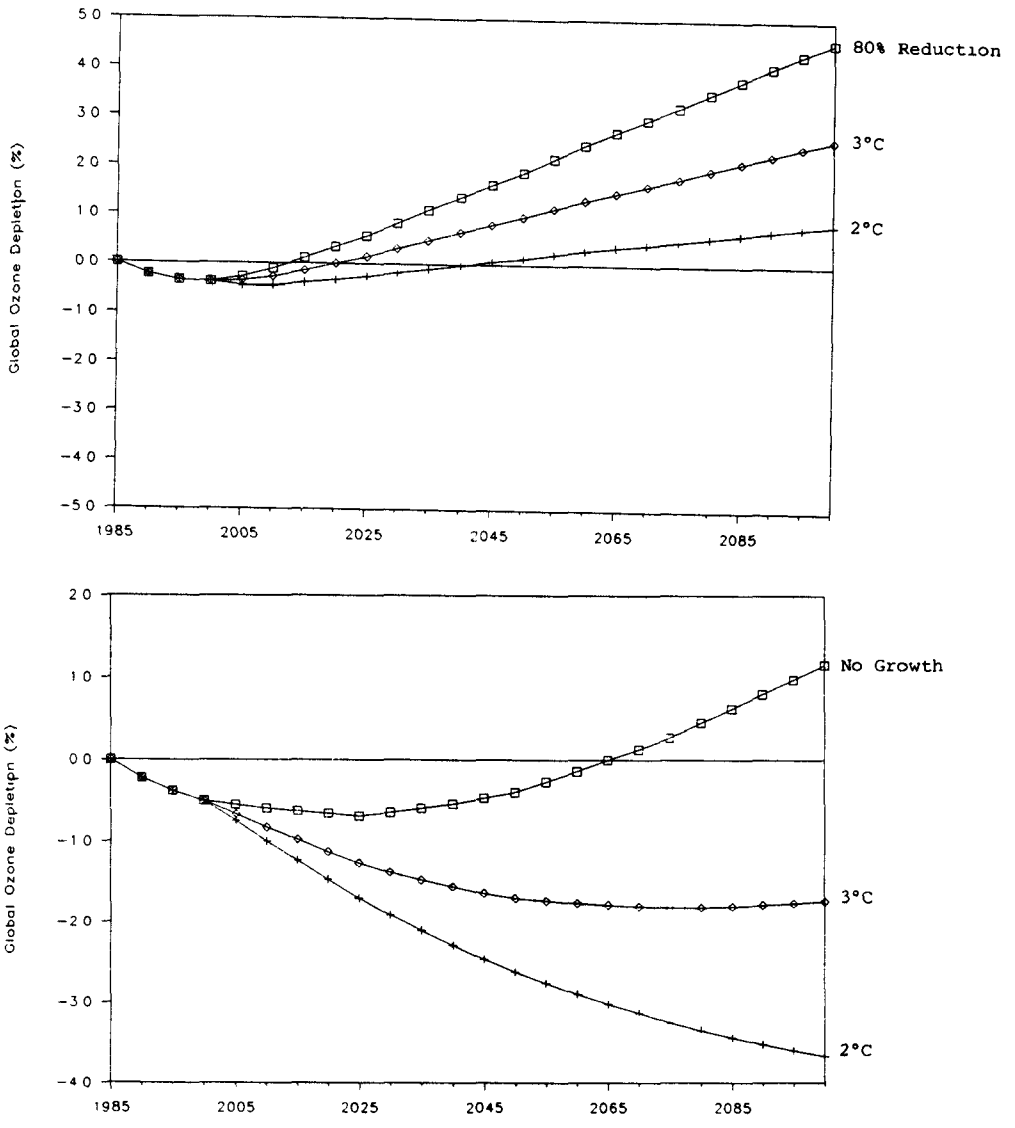

Assumptions:

- Current 1-D models accurately reflect global depletion; Antarctic ozone hole has no impact on global ozone levels.

- Greenhouse gases other than ozone depleters are limited sufficiently so that total equilibrium warming does not exceed 2°C or 3°C in 2075.

- A doubling of CO2 would ultimately warm the earth 3°C. (Thus, if the sensitivity were 4°C, the two limits would be 4°C and 2.67°C, respectively.)

EXHIBIT 18-15
(Continued)

Global Average Ozone Depletion: Scenarios of Limits to Future Global Warming

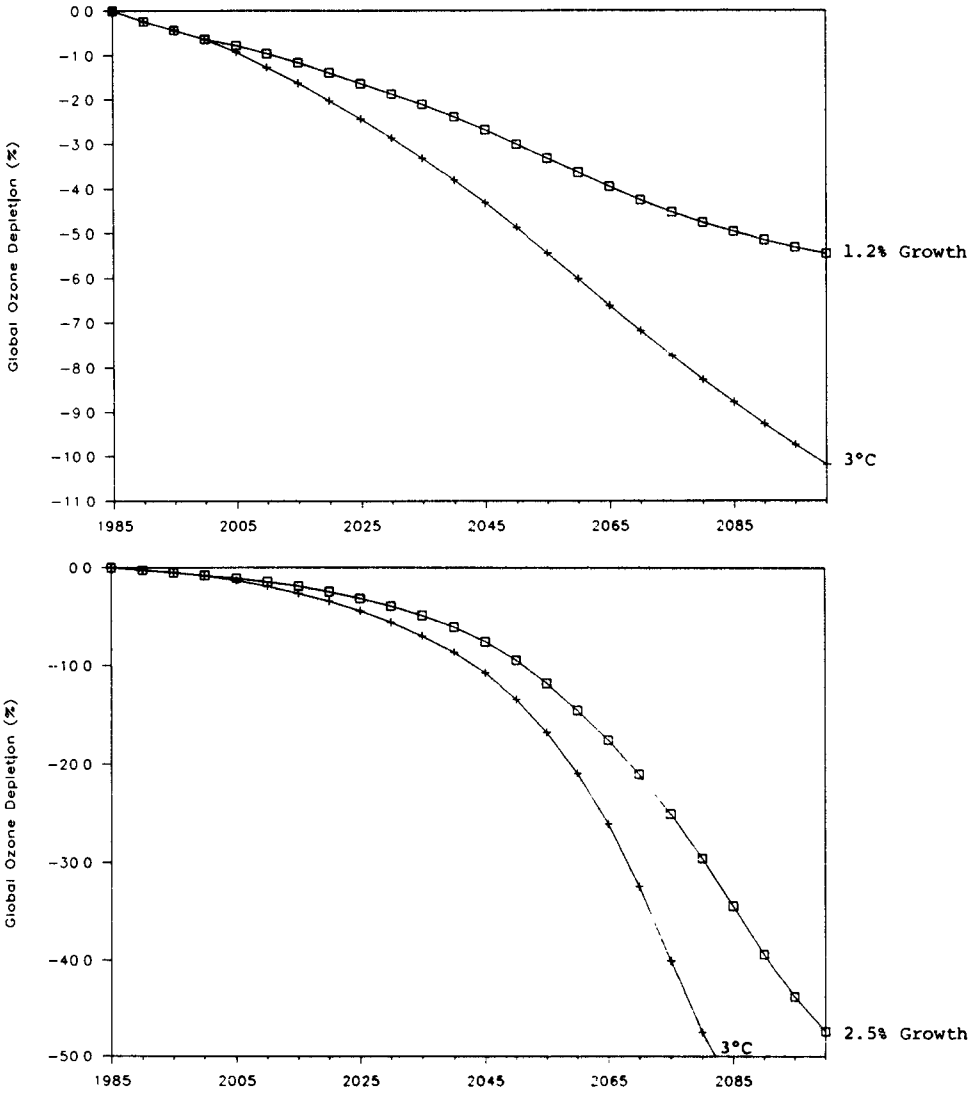

Assumptions:

- Current 1-D models accurately reflect global depletion; Antarctic ozone hole has no impact on global ozone levels.

- Greenhouse gases other than ozone depleters are limited sufficiently so that total equilibrium warming does not exceed 2°C or 3°C in 2075.

- A doubling of CO2 would ultimately warm the earth 3°C. (Thus, if the sensitivity were 4°C, the two limits would be 4°C and 2.67°C, respectively.)

EXHIBIT 18-16

Human Health Effects: Scenarios of Limits to Future Global Warming
Additional Cumulative Cases and Deaths Over Lifetimes of People Alive Today
(Figures in Parentheses are Percentage Changes from No Limit Case)

	80% Reduction			No Growth			1.2% Growth		2.5% Growth	
	2°C	3°C	No Limit	2°C	3°C	No Limit	3°C	No Limit	3°C	No Limit
Nonmelanoma Skin Tumors										
Additional Basal Cases	166,800 a/	47,400 a/	-74,400	607,000 (114)	471,400 (66)	284,200	883,500 (42)	623,700	1,925,600 (42)	1,289,300
Additional Squamous Cases	96,100 a/	20,100 a/	-57,300	379,300 (123)	291,100 (71)	169,900	561,700 (44)	390,800	1,224,000 (45)	846,500
Additional Deaths	4,100 a/	900 a/	-2,200	16,100 (121)	12,400 (70)	7,300	23,800 (43)	16,600	51,600 (44)	35,700
Melanoma Skin Tumors										
Additional Cases	2,200 a/	900 a/	-300	6,900 (97)	5,500 (57)	3,500	9,800 (38)	7,100	19,200 (38)	13,900
Additional Deaths	500 a/	200 a/	-100	1,800 (100)	1,500 (67)	900	2,700 (42)	1,900	5,300 (39)	3,800
Senile Cataract										
Additional Cases	51,400 (441)	17,900 (88)	9,500	257,100 (150)	192,800 (88)	102,800	391,400 (46)	267,400	878,700 (43)	613,900

a/ Percentage changes are not computed from negative to positive values.

Assumptions:

- Temperature limits shown assumed that a doubling of CO2 ultimately warms earth 3°C; numbers could be larger or smaller if doubling warms earth 1.5°C or 4.5°C.
- Assumes 1-D models results are accurate; Antarctic ozone hole has no relevance to global ozone.
- Emissions growth estimates refer to 1985 to 2050; held constant thereafter.

EXHIBIT 18-17

Human Health Effects: Scenarios of Limits to Future Global Warming
Additional Cumulative Cases and Deaths Over Lifetimes of People Born 1986-2029
(Figures in Parentheses are Percentage Changes from No Limit Case)

	80% Reduction			No Growth			1.2% Growth		2.5% Growth	
	2°C	3°C	No Limit	2°C	3°C	No Limit	3°C	No Limit	3°C	No Limit
Nonmelanoma Skin Tumors										
Additional Basal Cases	-6,300	-570,500	-1,164,800	1,949,300	1,260,700	288,000	3,840,200	2,301,600	19,746,400	11,998,800
	(99)	(51)		(577)	(338)		(67)		(65)	
Additional Squamous Cases	-15,500	-350,600	-698,100	1,175,900	746,500	150,500	2,421,500	1,411,900	16,527,400	9,091,300
	(98)	(50)		(681)	(396)		(72)		(82)	
Additional Deaths	-500	-14,800	-29,600	50,100	31,900	6,500	102,700	60,000	681,000	378,100
	(98)	(50)		(671)	(391)		(71)		(80)	
Melanoma Skin Tumors										
Additional Cases	800	-6.500	-14,300	26,100	17,500	5,200	48,100	29,800	191,200	124,400
	a/	(54)		(402)	(237)		(61)		(54)	
Additional Deaths	100	-1,700	-3,600	6,300	4,200	1,100	11,900	7,300	49,800	32,500
	a/	(53)		(473)	(282)		(63)		(53)	
Senile Cataract										
Additional Cases	6,000	0	0	604,100	371,300	49,100	1,277,700	752,000	6,476,200	4,311,900
				(1,130)	(656)		(70)		(50)	

a/ Percentage changes are not computed from negative to positive values.

Assumptions:

- Temperature limits shown assumed that a doubling of CO2 ultimately warms earth 3°C; numbers could be larger or smaller if doubling warms earth 1.5°C or 4.5°C.
- Assumes 1-D models results are accurate; Antarctic ozone hole has no relevance to global ozone.
- Emissions growth estimates refer to 1985 to 2050; held constant thereafter.

EXHIBIT 18-18

Human Health Effects: Scenarios of Limits to Future Global Warming
Additional Cumulative Cases and Deaths Over Lifetimes of People Born 2030-2074
(Figures in Parentheses are Percentage Changes from No Limit Case)

	80% Reduction			No Growth			1.2% Growth		2.5% Growth	
	2°C	3°C	No Limit	2°C	3°C	No Limit	3°C	No Limit	3°C	No Limit
Nonmelanoma Skin Tumors										
Additional Basal Cases	-514,300 (82)	-1,637,500 (43)	-2,853,400	2,949,200 (515)	1,498,100 (261)	-572,900	8,243,500 (97)	4,191,800	76,861,100 (61)	47,744,000
Additional Squamous Cases	-305,800 (81)	-947,700 (42)	-1,622,200	1,772,400 (500)	876,600 (247)	-354,400	5,326,400 (108)	2,564,500	84,308,400 (91)	44,078,600
Additional Deaths	-12,900 (81)	-40,400 (42)	-69,400	75,600 (507)	37,500 (252)	-14,900	225,300 (106)	109,200	3,399,900 (89)	1,800,900
Melanoma Skin Tumors										
Additional Cases	-6,600 (83)	-22,400 (44)	-39,800	41,000 (641)	21,800 (341)	-6,400	106,100 (87)	56,800	685,600 (46)	470,400
Additional Deaths	-1,600 (83)	-5,400 (44)	-9,600	9,600 (565)	5,000 (294)	-1,700	25,300 (89)	13,400	159,600 (43)	111,900
Senile Cataract										
Additional Cases	0 (0)	0 (0)	0	799,400 a/	379,900 a/	0	2,297,300 (98)	1,157,600	13,901,600 (36)	10,214,500

a/ No percentage estimated.

Assumptions:

- Temperature limits shown assumed that a doubling of CO2 ultimately warms earth 3°C; numbers could be larger or smaller if doubling warms earth 1.5°C or 4.5°C.
- Assumes 1-D models results are accurate; Antarctic ozone hole has no relevance to global ozone.
- Emissions growth estimates refer to 1985 to 2050; held constant thereafter.

EXHIBIT 18-19

Materials, Climate, and Other Effects: Scenarios of Limits to Future Global Warming
(Figures in Parentheses are Percentage Changes from No Limit Case)

Type of Effect	80% Reduction			No Growth			1.2% Growth		2.5% Growth		
	2°C	3°C	No Limit	2°C	3°C	No Limit	3°C	No Limit	3°C	No Limit	
Effects Estimated Quantitatively for the U.S.											
Materials Damage a/	228 (74)	163 (24)	131	301 (11)	272 g/ (0)	272	397 (30)	305	739 (22)	606	Present Value (millions of 1985 dollars)
Rise in Equilibrium Temperature by 2075	2.0	3.0	4.0	2.0	3.0	4.3	3.0	4.7	3.0	5.6	Degrees Centigrade
Sea Level Rise by 2075	67	75	82	67	75	85	75	89	75	95	Centimeters
Effects Based on Case Studies and Research in Early Stages											
Cost of Sea Level Rise in Charleston and Galveston b/	913-2,180	971-2,335	1,031-2,498	913-2,180	971-2,335	1,053-2,558	971-2,335	1,076-2,622	971-2,335	1,123-2,748	Present Value (millions of 1985 dollars)
Reduction in Soybean Seed Yield c/	f/	f/	f/	1.0	0.5	f/	2.3	1.4	>7.5	>7.5	Percent in Year 2075
Increase in Ground-Based Ozone d/	f/	f/	f/	0.9-4.6	0.5-2.6	f/	2.1-11.1	1.2-6.5	>9.4->50.0	7.0-36.9	Percent in Year 2075
Loss of Northern Anchovy Population e/	f/	f/	f/	0.0-2.4	0.0-1.3	f/	0-5.9	0.0-3.3	>11.0->25.0	>11.0->25.0	Percent in Year 2075

a/ Discounted over 1985-2075 using a real discount rate of 3 percent.
b/ Lowest estimate with anticipation of sea level rise; highest estimate without anticipation.
c/ Essex and Williams cultivars; statistically-significant results only.
d/ Lowest estimate is for Los Angeles, California; highest estimate is for Nashville, Tennessee.
e/ Lowest estimate 15-meter vertical mixing of the top ocean layer; highest estimate 10-meter vertical mixing if ozone depletion is greater than 11.2 percent, while ozone depletion less than 11.2 percent assumes no vertical mixing.
f/ Impacts were not evaluated because ozone levels are estimated to increase, not decrease, by 2075 in these scenarios.
g/ Value of materials damage for this case does not differ from the No Limit case because the difference in ozone depletion between the two cases is too small, i.e., the damage function from which the damage estimates are computed is a step function that defines materials damage for various ranges of ozone depletion.

Assumptions:
- Temperature limits shown assumed that a doubling of CO2 ultimately warms earth 3°C; numbers could be larger or smaller if doubling warms earth 1.5°C or 4.5°C.
- Assumes 1-D models results are accurate; Antarctic ozone hole has no relevance to global ozone.
- Emissions growth estimates refer to 1985 to 2050; held constant thereafter.

Exhibit 18-19 displays environmental risks. As shown in the exhibit, warming and its impacts are reduced from 5.6°C in the 2.5% Growth scenario to 3°C. As a result, sea level rise impacts are also reduced. The ozone-sensitive risks are increased, however. If global warming were held to less than 3°C by 2075 the risks from ozone depletion would be even greater.

A second sensitivity case is examined in which several alternative scenarios of methane concentrations are examined. To evaluate the sensitivity of the results to the methane growth rates, five methane scenarios were examined in addition to the assumption of 0.017 ppm/yr used above. Other trace gas assumptions were not changed. The six methane scenarios examined are:

- Scenario A -- compound annual growth of 1 percent from 1985 to 2010, followed by constant concentrations at 2.23 ppm;
- Scenario B -- linear growth at 0.01275 ppm per year (75 percent of the 0.017 ppm/yr growth);
- Scenario C -- linear growth at 0.017 ppm per year;
- Scenario D -- linear growth at 0.02125 ppm per year (125 percent of the 0.017 ppm/yr growth);
- Scenario E -- compound annual growth of 1 percent; and
- Scenario F -- compound annual growth of 1 percent from 1985 to 2020, growing to 1.5 percent compound annual growth by 2050 and thereafter.

Exhibit 18-20 shows that higher concentrations of atmospheric methane would reduce ozone depletion, while lower concentrations result in more depletion. Contrasting the highest methane scenario (Scenario F) to the assumption used above (0.017 ppm/yr - Scenario C), ozone depletion is roughly equal until 2025, when the contributions to ozone from increased methane concentrations begin to dampen depletion. The influence of increased methane concentrations becomes more pronounced after 2025, and depletion reaches an inflection point in 2085, after which ozone levels rise. The lower methane scenarios (i.e., Scenarios A and B) cause the ozone depletion estimates to increase compared to Scenario C.

The implications of the resulting differences in ozone depletion for the risk estimates from the six methane scenarios are shown in Exhibits 18-21 through 18-24. Of note in Exhibit 18-24 is that the lower methane scenarios reduce the estimate of global warming, while the higher scenarios increase it.

Effects at High and Low Sensitivities of Ozone Depletion to Emissions

A previous section analyzed the sensitivity of risk estimates to assumptions about the levels of emissions of ozone-modifying substances. This section explores another source of uncertainty in the risk estimates: the relationship between emissions (and their resulting chlorine concentrations) and ozone depletion. This uncertainty was quantified using Monte Carlo modeling techniques to reflect the implications of the convolution of the individual

EXHIBIT 18-20

Global Average Ozone Depletion: Methane Scenarios

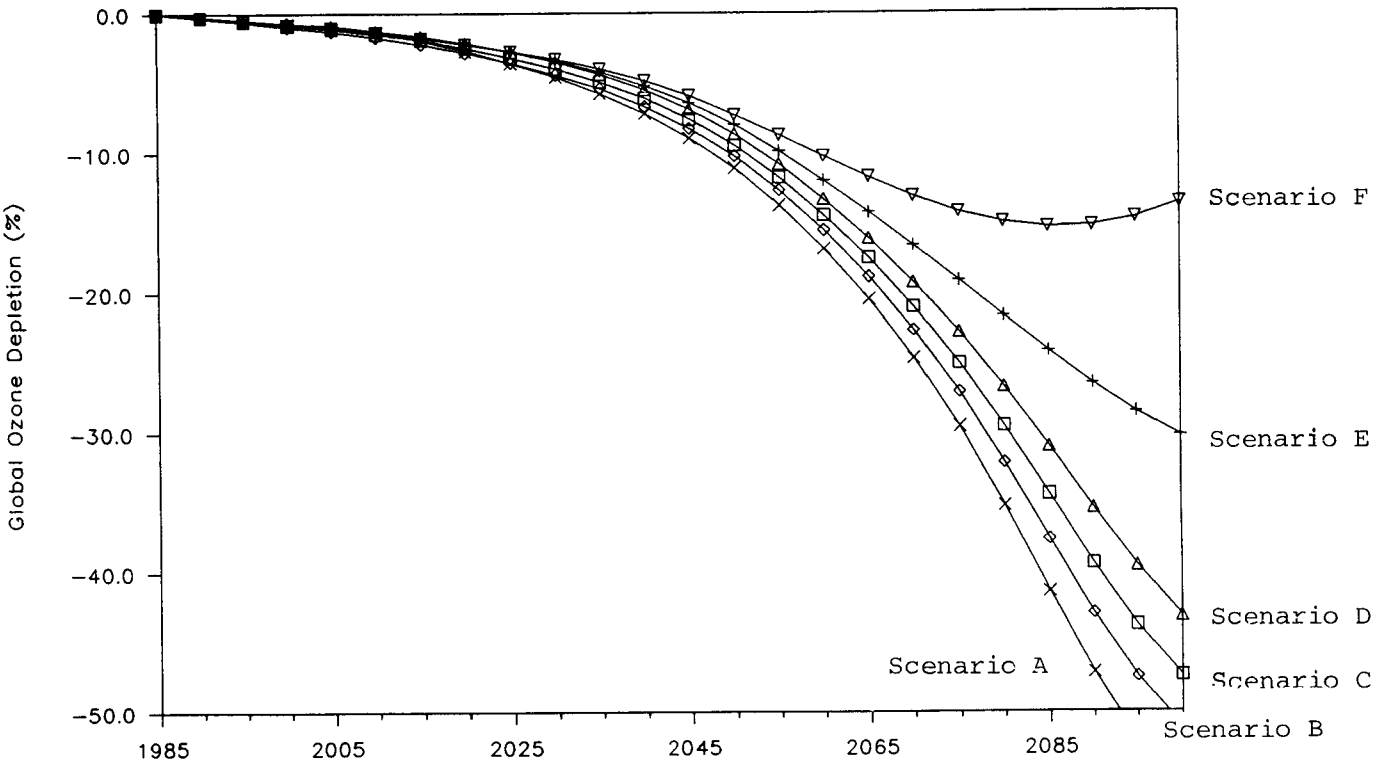

Scenario A = Compound annual growth of 1 percent from 1985 to 2010, followed by constant concentrations at 2.23 ppm.

Scenario B = Linear growth at 0.01275 ppm per year.

Scenario C = Linear growth at 0.017 ppm per year.

Scenario D = Linear growth at 0.02125 ppm per year.

Scenario E = Compound annual growth of 1 percent per year.

Scenario F = Compound annual growth of 1 percent from 1985 to 2020, growing to 1.5 percent compound annual growth by 2050 and thereafter.

Assumptions:

- Current 1-D models accurately reflect global depletion; Antarctic ozone hole has no impact on global ozone levels.
- Greenhouse gases that counter depletion (other than CH4) grow at historical rates.
- Growth rates for ozone depleters are for global emissions; it is assumed that emissions do not increase after 2050.
- Ozone depletion limited to 50 percent.

EXHIBIT 18-21

Human Health Effects: Methane Scenarios
Additional Cumulative Cases and Deaths Over Lifetimes of People Alive Today
(Figures in Parentheses are Percentage Changes from Scenario C)*

	METHANE SCENARIOS					
HEALTH EFFECT	Scenario A	Scenario B	Scenario C	Scenario D	Scenario E	Scenario F
Nonmelanoma Skin Tumors						
Additional Basal Cases	1,434,100 (11)	1,455,300 (13)	1,289,300	1,122,200 (-13)	1,104,200 (-14)	1,071,700 (-17)
Additional Squamous Cases	953,200 (13)	956,100 (13)	846,500	736,600 (-13)	719,100 (-15)	692,200 (-18)
Additional Deaths	40,100 (12)	40,400 (13)	35,700	31,100 (-13)	30,400 (-15)	29,300 (-18)
Melanoma Skin Tumors						
Additional Cases	15,200 (9)	15,700 (13)	13,900	12,000 (-14)	12,000 (-14)	11,700 (-16)
Additional Deaths	4,200 (11)	4,300 (13)	3,800	3,300 (-13)	3,300 (-13)	3,200 (-16)
Senile Cataract						
Additional Cases	698,300 (14)	685,300 (12)	613,900	541,500 (-12)	521,400 (-15)	494,700 (-19)

* All estimates from 2.5% Growth Scenario.

Scenario A = Compound annual growth of 1 percent from 1985 to 2010, followed by constant concentrations at 2.23 ppm.
Scenario B = Linear growth at 0.01275 ppm per year.
Scenario C = Linear growth at 0.017 ppm per year.
Scenario D = Linear growth at 0.02125 ppm per year.
Scenario E = Compound annual growth rate of 1 percent per year.
Scenario F = Compound annual growth of 1 percent from 1985 to 2020, growing to 1.5 percent compound annual growth by 2050 and thereafter.

Assumptions:

- Current 1-D models accurately reflect global depletion; Antarctic ozone hole has no impact on global ozone levels.
- Greenhouse gases (other than CH4) that counter depletion grow at historical rates.
- Growth rates for ozone depleters are for global emissions; it is assumed that emissions do not increase after 2050.
- Ozone depletion limited to 50 percent.

EXHIBIT 18-22

Human Health Effects: Methane Scenarios
Additional Cumulative Cases and Deaths Over Lifetimes of People Born 1986-2029
(Figures in Parentheses are Percentage Changes from Scenario C)*

	METHANE SCENARIOS					
HEALTH EFFECT	Scenario A	Scenario B	Scenario C	Scenario D	Scenario E	Scenario F
Nonmelanoma Skin Tumors						
Additional Basal Cases	14,520,400	13,277,100	11,998,800	10,619,500	8,539,000	6,186,600
	(21)	(11)		(-11)	(-29)	(-48)
Additional Squamous Cases	11,352,200	10,210,300	9,091,300	7,896,700	6,021,700	4,075,100
	(25)	(12)		(-13)	(-34)	(-55)
Additional Deaths	470,700	424,100	378,100	329,000	252,300	172,000
	(24)	(12)		(-13)	(-33)	(-55)
Melanoma Skin Tumors						
Additional Cases	147,000	136,500	124,400	111,300	93,800	72,900
	(18)	(10)		(-11)	(-25)	(-41)
Additional Deaths	38,400	35,600	32,500	29,100	24,300	18,500
	(18)	(10)		(-10)	(-25)	(-43)
Senile Cataract						
Additional Cases	5,044,100	4,678,800	4,311,900	3,887,600	3,085,700	2,098,100
	(17)	(9)		(-10)	(-28)	(-51)

* All estimates for 2.5% Growth Scenario.

Scenario A = Compound annual growth of 1 percent from 1985 to 2010, followed by constant concentrations at 2.23 ppm.
Scenario B = Linear growth at 0.01275 ppm per year.
Scenario C = Linear growth at 0.017 ppm per year.
Scenario D = Linear growth at 0.02125 ppm per year.
Scenario E = Compound annual growth rate of 1 percent per year.
Scenario F = Compound annual growth of 1 percent from 1985 to 2020, growing to 1.5 percent compound annual growth by 2050 and thereafter.

Assumptions:

- Current 1-D models accurately reflect global depletion; Antarctic ozone hole has no impact on global ozone levels.
- Greenhouse gases (other than CH4) that counter depletion grow at historical rates.
- Growth rates for ozone depleters are for global emissions; it is assumed that emissions do not increase after 2050.
- Ozone depletion limited to 50 percent.

EXHIBIT 18-23

Human Health Effects: Methane Scenarios
Additional Cumulative Cases and Deaths Over Lifetimes of People Born 2030-2074
(Figures in Parentheses are Percentage Changes from Scenario C)*

	METHANE SCENARIOS					
HEALTH EFFECT	Scenario A	Scenario B	Scenario C	Scenario D	Scenario E	Scenario F
Nonmelanoma Skin Tumors						
Additional Basal Cases	53,384,400 (12)	50,593,800 (6)	47,744,000	43,994,600 (-8)	28,059,300 (-41)	10,538,800 (-78)
Additional Squamous Cases	50,458,200 (14)	47,282,900 (7)	44,078,600	39,902,600 (-9)	21,938,900 (-50)	6,596,600 (-85)
Additional Deaths	2,057,700 (14)	1,929,900 (7)	1,800,900	1,632,700 (-9)	909,700 (-49)	280,100 (-84)
Melanoma Skin Tumors						
Additional Cases	523,600 (11)	497,100 (6)	470,400	436,400 (-7)	311,200 (-34)	147,300 (-69)
Additional Deaths	123,000 (10)	117,500 (5)	111,900	104,500 (-7)	74,100 (-34)	33,100 (-70)
Senile Cataract						
Additional Cases	10,785,600 (6)	10,512,300 (3)	10,214,500	9,779,800 (-4)	6,673,500 (-35)	2,145,900 (-79)

* All estimates for 2.5% Growth Scenario.

Scenario A = Compound annual growth of 1 percent from 1985 to 2010, followed by constant concentrations at 2.23 ppm.
Scenario B = Linear growth at 0.01275 ppm per year.
Scenario C = Linear growth at 0.017 ppm per year.
Scenario D = Linear growth at 0.02125 ppm per year.
Scenario E = Compound annual growth of 1 percent per year.
Scenario F = Compound annual growth of 1 percent from 1985 to 2020, growing to 1.5 percent compound annual growth by 2050 and thereafter.

Assumptions:

- Current 1-D models accurately reflect global depletion; Antarctic ozone hole has no impact on global ozone levels.
- Greenhouse gases (other than CH4) that counter depletion grow at historical rates.
- Growth rates for ozone depleters are for global emissions; it is assumed that emissions do not increase after 2050.
- Ozone depletion limited to 50 percent.

EXHIBIT 18-24

Materials, Climate, and Other Effects: Methane Scenarios
(Figures in Parentheses are Percentage Changes from Scenario C)[g/]

TYPE OF EFFECT	METHANE SCENARIOS						Units
	Scenario A	Scenario B	Scenario C	Scenario D	Scenario E	Scenario F	
Effects Estimated Quantitatively for the U.S.							
Materials Damage a/	662 (9)	646 (7)	606	570 (-6)	553 (-9)	532 (-12)	Present Value (millions of 1985 dollars)
Rise in Equilibrium Temperature by 2075 b/	5.4 (-4)	5.6 (0)	5.6	5.7 (2)	5.8 (4)	5.9 (5)	Degrees Centigrade
Sea Level Rise by 2075	93 (-2)	94 (-1)	95	96 (1)	96 (1)	97 (2)	Centimeters
Effects Based on Case Studies and Research in Early Stages							
Cost of Sea Level Rise in Charleston and Galveston c/	1100-2684	1106-2703	1123-2748	1120-2742	1120-2742	1128-2761	Present Value (millions of 1985 dollars)
Reduction in Soybean Seed Yield d/	>7.5	>7.5	>7.5	6.8	5.7	4.3	
Increase in Ground-Based Ozone e/	8.3-44.1	7.6-40.2	7.0-36.9	6.3-33.4	5.2-27.7	3.8-20.3	Percent in Year 2075
Loss of Northern Anchovy Population f/	>11.0->25.0	>11.0->25.0	>11.0->25.0	>11.0->25.0	6.3-17.4	1.4-12.3	Percent in Year 2075

a/ Discounted over 1985-2075 using a real discount rate of 3 percent.
b/ Estimates of the rise in equilibrium temperature neglect increases and decreases in tropospheric that would occur with deviations from the 2.5% Growth case of methane growth (1%) and changes in stratospheric water vapor.
c/ Lowest estimate with anticipation of sea level rise; highest estimate without anticipation.
d/ Essex and Williams cultivars; statistically significant results only.
e/ Lowest estimate is for Los Angeles, California; highest estimate is for Nashville, Tennessee.
f/ Lowest estimate 15-meter vertical mixing of top ocean layer; highest estimate 10-meter vertical mixing if ozone depletion is greater than 11.2 percent and no mixing if ozone depletion is less than 11.2 percent.
g/ All estimates for 2.5% Growth Scenario.

Assumptions:

- Current 1-D models accurately reflect global depletion; Antarctic ozone hole has no impact on global ozone levels.
- Greenhouse gases (other than CH4) that counter depletion grow at historical rates.
- Growth rates for ozone depletion are for global emissions; it is assumed that emissions do not increase after 2050.
- Ozone depletion limited to 50 percent.

See text for definition of methane cases.

EXHIBIT 18-25

Global Average Ozone Depletion: Sensitivity to Relationship Between Ozone Depletion and Emissions (Based on 10th and 90th percentiles of Monte Carlo Analysis of Rate Constants and Cross-Sections

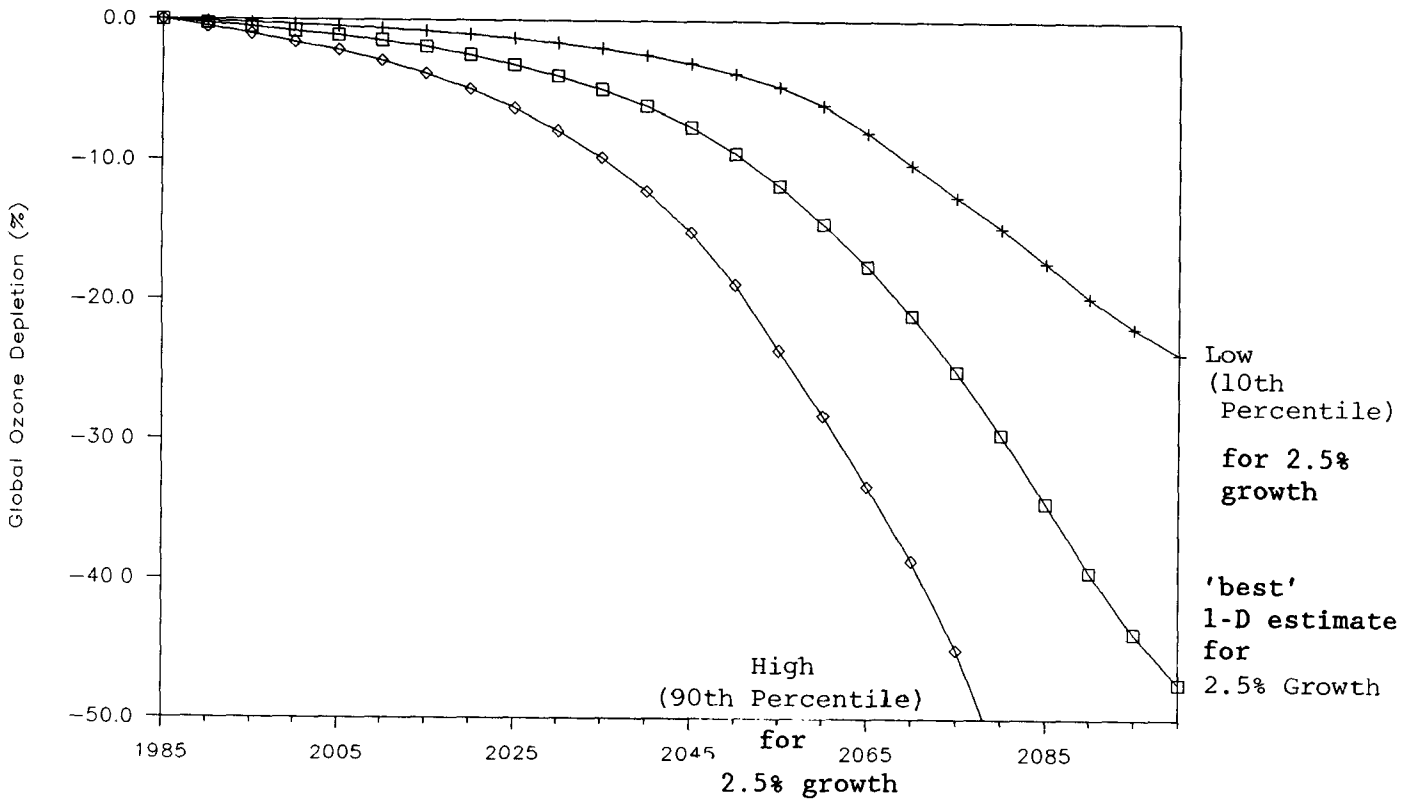

Assumptions:

- Scenario is 2.5% Growth scenario.
- Global depletion varies from best 1-D estimates.
- Greenhouse gases that counter depletion grow at historical rates.
- Growth rates for ozone depleters are for global emissions; it is assumed that emissions do not increase after 2050.
- Ozone depletion limited to 50 percent.

ranges of uncertainty that surround estimates of rate constants for atmospheric reactions. The range analyzed here is the tenth and ninetieth percentile estimates.

The effect of varying the sensitivity of ozone depletion to emissions is illustrated in Exhibit 18-25. The exhibit shows that the tenth percentile estimate of ozone depletion is about one half of the 2.5% Growth scenario value. The ninetieth percentile estimate is about twice the 2.5% Growth scenario value and reaches 50 percent depletion in approximately 2078.

The implications for health risks are displayed in Exhibits 18-26 to 18-28 for each of the three population cohorts. In general, increased health risks would be about 50 to 65 percent lower than the 2.5% Growth in the tenth percentile case, and roughly double the increased risks in the ninetieth percentile case for the first two cohorts and about 30 to 45 percent higher for people born from 2030 to 2074. The differences are not as high for the third cohort because ozone depletion was arbitrarily limited to 50 percent; the 50 percent depletion level is reached just after 2100 in the 2.5% Growth scenario and about 2078 in the ninetieth percentile case, implying that for the period during which the third cohort is alive, the amount of ozone depletion between the 2.5% Growth scenario and the High (90th percentile) case is very similar.

Alternative Maximum Ozone Depletion Assumption

Throughout this Risk Assessment, the maximum level of ozone depletion allowed was 50 percent. This arbitrary limit was applied to avoid extrapolating beyond the bounds of the atmospheric model upon which the parameterized quantitative risk estimates have been based. In instances where the 50 percent limit is reached, this assumption underestimates the risks posed by ozone depletion. To evaluate the potential impact of this assumption, the sensitivity of the risk estimates was analyzed assuming a maximum level of ozone depletion of 95 percent.[6]

The health risks estimated with the 95 percent ozone depletion limit are shown in Exhibits 18-29 to 18-31 for the 2.5% and 5.0% Growth scenarios. These health risk estimates tend to increase significantly (1) as the rate of growth in emissions increases, which increases the rate of ozone depletion and hence, the likelihood that the 50% limit will become binding; and (2) for the later cohorts, since ozone depletion is more likely to reach the 50% limit as time goes on. For example, for all cohorts a 95 percent limit has a higher percentage impact on the risk estimates in the 5.0% Growth scenario compared to the 2.5% Growth scenario. This impact is also greater on people born later, since in the 2.5% Growth scenario there is no increase in risk for people alive today since 50% depletion is not reached in their lifetimes (see Exhibit 18-29), while people born from 2030 to 2074 will have about a 5 to 10 percent increase in risk (see Exhibit 18-31).

---

[6] This level of depletion is projected using the parameterized model. Two questions arise: (1) would the 1-D model project the same depletion level for the same emissions scenario, and (2) would real world depletion occur the way the model projects. We do not know the answer to these questions, so caution must be used in interpreting these results.

EXHIBIT 18-26

Human Health Effects:
Sensitivity to Relationship Between Ozone Depletion and Emissions
Additional Cumulative Cases and Deaths Over Lifetimes of People Alive Today
(Figures in Parentheses are Percentage Changes from Current Model)

	SENSITIVITY OF OZONE DEPLETION TO EMISSIONS[1]		
HEALTH EFFECT	Low[2]	Current Model	High[3]
Nonmelanoma Skin Tumors			
Additional Basal Cases	503,300 (-61)	1,289,300	2,772,600 (115)
Additional Squamous Cases	324,400 (-62)	846,500	1,891,900 (123)
Additional Deaths	13,800 (-61)	35,700	79,500 (123)
Melanoma Skin Tumors			
Additional Cases	5,500 (-60)	13,900	29,000 (109)
Additional Deaths	1,500 (-61)	3,800	8,000 (111)
Senile Cataract			
Additional Cases	240,500 (-61)	613,900	1,307,100 (113)

1/ Emissions of ozone depleters are from the 2.5% Growth scenario.
2/ 10% percentile of Monte Carlo runs of rate constants and cross-sections.
3/ 90% percentile of Monte Carlo runs of rate constants and cross-sections.

Assumptions

-- Current 1-D models accurately reflect global depletion; Antarctic ozone hole has no impact on global ozone levels.
-- Greenhouse gases that counter depletion grow at historical rates.
-- Growth rates for ozone depleters are for global emissions; it is assumed that emissions do not increase after 2050.
-- Ozone depletion limited to 50 percent.

EXHIBIT 18-27

Human Health Effects:
Sensitivity to Relationship Between Ozone Depletion and Emissions
Additional Cumulative Cases and Deaths Over Lifetimes of People Born 1986-2029
(Figures in Parentheses are Percentage Changes from Current Model)[1/]

	SENSITIVITY OF OZONE DEPLETION TO EMISSIONS		
HEALTH EFFECT	Low[2/]	Current Model	High[3/]
Nonmelanoma Skin Tumors			
Additional Basal Cases	4,665,600 (-61)	11,998,800	23,670,800 (97)
Additional Squamous Cases	3,185,400 (-65)	9,091,300	19,638,900 (116)
Additional Deaths	134,000 (-65)	378,100	809,900 (114)
Melanoma Skin Tumors			
Additional Cases	51,300 (-59)	124,400	234,500 (89)
Additional Deaths	13,600 (-58)	32,500	59,800 (84)
Senile Cataract			
Additional Cases	1,884,300 (-56)	4,311,900	7,046,300 (63)

1/ Emissions of ozone depleters are from the 2.5% Growth scenario.
2/ 10% percentile of Monte Carlo runs of rate constants and cross-sections.
3/ 90% percentile of Monte Carlo runs of rate constants and cross-sections.

Assumptions

-- Current 1-D models accurately reflect global depletion; Antarctic ozone hole has no impact on global ozone levels.
-- Greenhouse gases that counter depletion grow at historical rates.
-- Growth rates for ozone depleters are for global emissions; it is assumed that emissions do not increase after 2050.
-- Ozone depletion limited to 50 percent.

EXHIBIT 18-28

Human Health Effects:
Sensitivity to Relationship Between Ozone Depletion and Emissions
Additional Cumulative Cases and Deaths Over Lifetimes of People Born 2030-2074
(Figures in Parentheses are Percentage Changes from Current Model)[1/]

HEALTH EFFECT	SENSITIVITY OF OZONE DEPLETION TO EMISSIONS: Low[2/]	Current Model	High[3/]
Nonmelanoma Skin Tumors			
Additional Basal Cases	19,949,600 (-58)	47,744,000	64,862,800 (36)
Additional Squamous Cases	14,947,400 (-66)	44,078,600	63,901,200 (45)
Additional Deaths	622,300 (-65)	1,800,900	2,597,400 (44)
Melanoma Skin Tumors			
Additional Cases	221,900 (-53)	470,400	637,200 (35)
Additional Deaths	54,400 (-51)	111,900	145,300 (30)
Senile Cataract			
Additional Cases	5,444,800 (-47)	10,214,500	11,717,700 (15)

1/ Emissions of ozone depleters are from the 2.5% Growth scenario.
2/ 10% percentile of Monte Carlo runs of rate constants and cross-sections.
3/ 90% percentile of Monte Carlo runs of rate constants and cross-sections.

Assumptions

-- Current 1-D models accurately reflect global depletion; Antarctic ozone hole has no impact on global ozone levels.
-- Greenhouse gases that counter depletion grow at historical rates.
-- Growth rates for ozone depleters are for global emissions; it is assumed that emissions do not increase after 2050.
-- Ozone depletion limited to 50 percent.

EXHIBIT 18-29

Human Health Effects: Maximum Depletion of 95 Percent
Additional Cumulative Cases and Deaths Over Lifetimes of People Alive Today
(Figures in Parentheses are Percentage Changes from 50% Limit Scenario)

HEALTH EFFECT	EMISSIONS SCENARIOS			
	2.5% Growth		5.0% Growth	
	50% Limit	95% Limit	50% Limit	95% Limit
Nonmelanoma Skin Tumors				
Additional Basal Cases	1,289,300	1,289,300 (0)	6,882,800	8,780,400 (28)
Additional Squamous Cases	846,500	846,500 (0)	5,431,800	7,624,500 (40)
Additional Deaths	35,700	35,700 (0)	225,000	313,100 (39)
Melanoma Skin Tumors				
Additional Cases	13,900	13,900 (0)	62,500	75,300 (20)
Additional Deaths	3,800	3,800 (0)	17,800	21,500 (21)
Senile Cataract				
Additional Cases	613,900	613,900 (0)	3,238,700	4,094,600 (26)

Assumptions:

- Current 1-D models accurately reflect global depletion; Antarctic ozone hole has no impact on global ozone levels.
- Greenhouse gases that counter depletion grow at historical rates.
- Growth rates for ozone depleters are for global emissions; it is assumed that emissions do not increase after 2050.
- Ozone depletion limited to 50 percent.

EXHIBIT 18-30

Human Health Effects: Maximum Depletion of 95 Percent
Additional Cumulative Cases and Deaths Over Lifetimes of People Born 1986-2029
(Figures in Parentheses are Percentage Changes from 50% Limit Scenario)

HEALTH EFFECT	EMISSIONS SCENARIOS			
	2.5% Growth		5.0% Growth	
	50% Limit	95% Limit	50% Limit	95% Limit
Nonmelanoma Skin Tumors				
Additional Basal Cases	11,998,800	12,011,300 (1)	46,429,300	81,851,800 (76)
Additional Squamous Cases	9,091,300	9,107,600 (2)	42,922,400	97,750,000 (128)
Additional Deaths	378,100	378,700 (2)	1,753,500	3,919,300 (224)
Melanoma Skin Tumors				
Additional Cases	124,400	124,500 (0.1)	445,900	653,000 (46)
Additional Deaths	32,500	32,500 (0)	107,900	158,700 (47)
Senile Cataract				
Additional Cases	4,311,900	4,315,600 (0.1)	10,361,300	15,627,400 (51)

Assumptions:

- Current 1-D models accurately reflect global depletion; Antarctic ozone hole has no impact on global ozone levels.
- Greenhouse gases that counter depletion grow at historical rates.
- Growth rates for ozone depleters are for global emissions; it is assumed that emissions do not increase after 2050.
- Ozone depletion limited to 50 percent.

EXHIBIT 18-31

Human Health Effects: Maximum Depletion of 95 Percent
Additional Cumulative Cases and Deaths Over Lifetimes of People Born 2030-2074
(Figures in Parentheses are Percentage Changes from 50% Limit Scenario)

HEALTH EFFECT	EMISSIONS SCENARIOS			
	2.5% Growth		5.0% Growth	
	50% Limit	95% Limit	50% Limit	95% Limit
Nonmelanoma Skin Tumors				
Additional Basal Cases	47,744,000	50,452,800 (6)	78,600,200	167,287,400 (113)
Additional Squamous Cases	44,078,600	48,085,800 (9)	81,244,300	246,526,800 (203)
Additional Deaths	1,800,900	1,959,600 (9)	3,290,400	9,763,400 (297)
Melanoma Skin Tumors				
Additional Cases	470,400	485,400 (3)	771,500	1,293,100 (68)
Additional Deaths	111,900	115,900 (4)	170,300	278,700 (64)
Senile Cataract				
Additional Cases	10,214,500	10,818,100 (6)	12,405,300	19,740,300 (59)

Assumptions:

- Current 1-D models accurately reflect global depletion; Antarctic ozone hole has no impact on global ozone levels.
- Greenhouse gases that counter depletion grow at historical rates.
- Growth rates for ozone depleters are for global emissions; it is assumed that emissions do not increase after 2050.
- Ozone depletion limited to 50 percent.

SENSITIVITY OF EFFECTS TO UNCERTAINTY IN DOSE RESPONSE

This section analyzes the sensitivity of risk estimates to uncertainties in two areas: (1) estimates of dose-response between UV radiation and health effects, and (2) the choice of action spectrum.

The statistical uncertainty in the dose-response relationships reported here does not reflect uncertainties in the underlying specifications of the dose-response relationships. For example, as described in Chapter 8, there remains a major question regarding the appropriate measure of exposure to use for modeling melanoma skin cancer risks. The uncertainty estimates reported below reflect the implications of the statistical variation reported using one particular measure of exposure. Using alternative exposure measures would increase the range of risk estimates.

Effects at High and Low Estimates of UV Radiation Impact on Human Health

The dose-response relationships between increases in UV radiation and associated health risks were obtained using a variety of statistical techniques (see Chapters 7, 8, 10 and 17). In these studies, the responsiveness of health effects to changes in UV radiation were characterized by dose-response parameters estimated using mathematical functions fitted statistically to detailed epidemiologic data. The results of the statistical analysis included estimates of the standard errors of dose-response parameters.

The standard errors of the dose-response parameters were used to develop high and low estimates of health risks. Low risk estimates were calculated by using the 2.5% Growth scenario dose-response coefficients minus one standard error; high risk estimates use the 2.5% Growth scenario use coefficients plus one standard error. All other assumptions are held fixed.

Health risks estimated using the low, middle and high coefficients are presented in Exhibits 18-32 through 18-34 for the 2.5% Growth scenario. The low dose-response coefficients produced an approximately 10 to 50 percent reduction in health effects, while the high dose-response coefficients produced about a 10 to 85 percent increase. The magnitude of the differences with the 2.5% Growth scenario tend to increase as time goes on.

Choice of Action Spectrum

This section analyzes the sensitivity of risk estimates to the action spectrum that is specified to determine the relationship between ozone abundance and UV flux. In the 2.5% Growth scenario, the DNA-damage action spectrum developed by Setlow was used to derive biologically effective UV radiation fluxes for changes in ozone levels. The sensitivity of the risk estimates to the erythema action spectrum was investigated. Health risks estimated using the DNA action spectrum (which was used in the 2.5% Growth scenario) and the erythema action spectrum are presented in Exhibits 18-35 to 18-37 for each of the population cohorts. On average, health risks using the erythema action spectrum are about 10-15 percent lower than risks estimated with the DNA-action spectrum due to the lower levels of weighted UV flux derived with the erythema action spectrum.

EXHIBIT 18-32

Human Health Effects: Sensitivity to Dose-Response Relationship
Additional Cumulative Cases and Deaths Over Lifetimes of People Alive Today
(Figures in Parentheses are Percentage Changes from 2.5% Growth Scenario)

HEALTH EFFECT	SENSITIVITY OF EFFECT TO UV DOSE		
	Low	Standard Coefficient	High
Nonmelanoma Skin Tumors			
Additional Basal Cases	831,400 (-36)	1,289,300	1,757,300 (36)
Additional Squamous Cases	570,900 (-33)	846,500	1,134,100 (34)
Additional Deaths	24,000 (-33)	35,700	47,900 (34)
Melanoma Skin Tumors			
Additional Cases	10,000 (-28)	13,900	17,700 (27)
Additional Deaths	3,400 (-11)	3,800	4,200 (11)
Senile Cataract			
Additional Cases	345,800 (-44)	613,900	810,100 (32)

Assumptions:

- Current 1-D models accurately reflect global depletion; Antarctic ozone hole has no impact on global ozone levels.
- Greenhouse gases that counter depletion grow at historical rates.
- Growth rates for ozone depleters are for global emissions; it is assumed that emissions do not increase after 2050.
- Ozone depletion limited to 50 percent.

EXHIBIT 18-33

Human Health Effects: Sensitivity to Dose-Response Relationship
Additional Cumulative Cases and Deaths Over Lifetimes of People Born 1986-2029
(Figures in Parentheses are Percentage Changes from 2.5% Growth Scenario)

HEALTH EFFECT	SENSITIVITY OF EFFECT TO UV DOSE		
	Low	Standard Coefficient	High
Nonmelanoma Skin Tumors			
Additional Basal Cases	7,360,900 (-39)	11,998,800	17,296,900 (44)
Additional Squamous Cases	5,476,200 (-40)	9,091,300	13,771,600 (51)
Additional Deaths	228,200 (-40)	378,100	570,000 (51)
Melanoma Skin Tumors			
Additional Cases	88,100 (-29)	124,400	161,600 (30)
Additional Deaths	29,200 (-10)	32,500	35,800 (10)
Senile Cataract			
Additional Cases	2,387,400 (-45)	4,311,900	5,761,300 (34)

Assumptions:

- Current 1-D models accurately reflect global depletion; Antarctic ozone hole has no impact on global ozone levels.
- Greenhouse gases that counter depletion grow at historical rates.
- Growth rates for ozone depleters are for global emissions; it is assumed that emissions do not increase after 2050.
- Ozone depletion limited to 50 percent.

EXHIBIT 18-34

Human Health Effects: Sensitivity to Dose-Response Relationship
Additional Cumulative Cases and Deaths Over Lifetimes of People Born 2030-2074
(Figures in Parentheses are Percentage Changes from 2.5% Growth Scenario)

HEALTH EFFECT	SENSITIVITY OF EFFECT TO UV DOSE		
	Low	Standard Coefficient	High
Nonmelanoma Skin Tumors			
Additional Basal Cases	26,911,600 (-44)	47,744,000	75,759,400 (59)
Additional Squamous Cases	22,076,300 (-50)	44,078,600	81,760,300 (85)
Additional Deaths	911,300 (-49)	1,800,900	3,300,900 (83)
Melanoma Skin Tumors			
Additional Cases	324,400 (-31)	470,400	628,600 (34)
Additional Deaths	99,600 (-11)	111,900	124,200 (11)
Senile Cataract			
Additional Cases	5,529,300 (-46)	10,214,500	13,877,300 (36)

Assumptions:

- Current 1-D models accurately reflect global depletion; Antarctic ozone hole has no impact on global ozone levels.
- Greenhouse gases that counter depletion grow at historical rates.
- Growth rates for ozone depleters are for global emissions; it is assumed that emissions do not increase after 2050.
- Ozone depletion limited to 50 percent.

EXHIBIT 18-35

Human Health Effects:
Sensitivity to Relationship Between Ozone Depletion and Action Spectrum
Additional Cumulative Cases and Deaths Over Lifetimes of People Alive Today
(Figures in Parentheses are Percentage Changes from 2.5% Growth Scenario)

HEALTH EFFECT	SENSITIVITY OF OZONE DEPLETION TO ACTION SPECTRUM	
	Erythema (2.5% Growth Scenario)	DNA (2.5% Growth Scenario)
Nonmelanoma Skin Tumors		
Additional Basal Cases	1,170,300 (-9)	1,289,300
Additional Squamous Cases	763,300 (-10)	846,500
Additional Deaths	32,200 (-10)	35,700
Melanoma Skin Tumors		
Additional Cases	11,500 (-17)	13,900
Additional Deaths	3,500 (-8)	3,800
Senile Cataract		
Additional Cases	509,800 (-17)	613,900

Assumptions:

- Current 1-D models accurately reflect global depletion; Antarctic ozone hole has no impact on global ozone levels.
- Greenhouse gases that counter depletion grow at historical rates.
- Growth rates for ozone depleters are for global emissions; it is assumed that emissions do not increase after 2050.
- Ozone depletion limited to 50 percent.

EXHIBIT 18-36

Human Health Effects:
Sensitivity to Relationship Between Ozone Depletion and Action Spectrum
Additional Cumulative Cases and Deaths Over Lifetimes of People Born 1986-2029
(Figures in Parentheses are Percentage Changes from 2.5% Growth Scenario)

HEALTH EFFECT	SENSITIVITY OF OZONE DEPLETION TO ACTION SPECTRUM	
	Erythema (2.5% Growth Scenario)	DNA (2.5% Growth Scenario)
Nonmelanoma Skin Tumors		
Additional Basal Cases	10,800,800 (-10)	11,998,800
Additional Squamous Cases	8,004,100 (-12)	9,091,300
Additional Deaths	333,700 (-12)	378,100
Melanoma Skin Tumors		
Additional Cases	102,800 (-17)	124,400
Additional Deaths	29,600 (-9)	32,500
Senile Cataract		
Additional Cases	3,583,400 (-17)	4,311,900

Assumptions:

- Current 1-D models accurately reflect global depletion; Antarctic ozone hole has no impact on global ozone levels.
- Greenhouse gases that counter depletion grow at historical rates.
- Growth rates for ozone depleters are for global emissions; it is assumed that emissions do not increase after 2050.
- Ozone depletion limited to 50 percent.

EXHIBIT 18-37

Human Health Effects:
Sensitivity to Relationship Between Ozone Depletion and Action Spectrum
Additional Cumulative Cases and Deaths Over Lifetimes of People Born 2030-2074
(Figures in Parentheses are Percentage Changes from 2.5% Growth Scenario)

HEALTH EFFECT	SENSITIVITY OF OZONE DEPLETION TO ACTION SPECTRUM	
	Erythema (2.5% Growth Scenario)	DNA (2.5% Growth Scenario)
Nonmelanoma Skin Tumors		
Additional Basal Cases	43,173,200 (-10)	47,744,000
Additional Squamous Cases	38,368,300 (-13)	44,078,600
Additional Deaths	1,572,600 (-13)	1,800,900
Melanoma Skin Tumors		
Additional Cases	390,500 (-17)	470,400
Additional Deaths	103,200 (-8)	111,900
Senile Cataract		
Additional Cases	8,631,500 (-15)	10,214,500

Assumptions:

- Current 1-D models accurately reflect global depletion; Antarctic ozone hole has no impact on global ozone levels.
- Greenhouse gases that counter depletion grow at historical rates.
- Growth rates for ozone depleters are for global emissions; it is assumed that emissions do not increase after 2050.
- Ozone depletion limited to 50 percent.

RELATIVE IMPORTANCE OF KEY UNCERTAINTIES

As expected, quantitative estimates of risks to human health and the environment are sensitive to the assumptions, methods, and data used to model risks. It appears that the 1-D parameterization underestimates ozone depletion compared to 2-D models.

The largest range of risk estimates was produced by varying assumptions about future production, use, and emissions of ozone-modifying substances. Estimates of ozone depletion were particularly sensitive to these assumptions. The 80% Reduction scenario leads to a projected increase in ozone levels; the highest case scenario (i.e., the 5.0% Growth scenario) results in extremely rapid depletion. In addition, the 3.8% Growth and 5.0% Growth scenarios caused ozone depletion estimates by 2100 to reach an amount believed to be outside the valid range of the atmospheric models used to analyze changes in total column ozone (in the 2.5% Growth scenario, this amount of depletion was reached just after 2100).

Because estimates of human health effects are driven by projections of ozone depletion, health risks were similarly affected by this range of emissions assumptions. Increased risks to people alive today were found to vary by as much as 500 percent. The sensitivity of health risks to emissions is greater in future generations; individuals yet to be borne were simulated to experience greater changes in exposure to UV radiation over a larger fraction of their lives. Environmental effects were also shown to be most sensitive to emissions assumptions; however, compared to health effects, the range of results was narrower.

The health risk estimates were also sensitive to variations in the relationship between ozone depletion and emissions. Changing the responsiveness of ozone depletion to emissions in the 2.5% Growth scenario resulted in up to 65 percent fewer additional cases of skin cancers and senile cataract among people alive today (low sensitivity) and up to 120 percent more additional cases for these individuals (high sensitivity).

Assumptions about potential actions taken to limit global warming were also found to be important for estimating health risks. Actions aimed at limiting future warming to 2°C or 3°C would reduce future potential concentrations of greenhouse gases. Because these gases also counter ozone depletion, an increase in ozone depletion and associated UV exposure would accompany such actions. For example, in the 2.5% Growth scenario where global warming is limited to 3°C, people alive today would experience about 45 percent more cases of skin cancer and senile cataract compared to the number of cases estimated to occur in the absence of actions to limit warming. The sensitivity of health risks to assumptions about potential limits to global warming is greater for future generations; in the 2.5% Growth scenario up to 90 percent more cases of skin cancer are estimated for people born during 2030 through 2074 if global warming is limited to 3°C.

Health risk estimates also were sensitive to assumptions about future concentrations of methane, but to a lesser extent. The analysis suggests that for the 2.5% Growth scenario people alive today will contract about 10 to 15 percent more cases of skin cancer and senile cataract if lowest methane growth assumptions are used. Note that lowering methane concentrations increases ozone depletion and hence increases UV radiation damaging to human health.

Health risks were also sensitive to the uncertainty of the parameters used to characterize dose-response. However, low and high estimates of cases and deaths associated with low and high dose-response coefficients (plus and minus one standard error) fell well within the ranges of risk estimates produced by varying assumptions about emissions and other factors. Nonetheless, health risks were found to decrease by as much as 50 percent for low dose-response coefficients and increase up to 85 percent for high dose-response coefficients.

The choice of action spectrum could also affect the health risk estimates, although the variation between the DNA action spectrum and the Erythema action spectrum is unlikely to exceed 10 to 15 percent (the Erythema action spectrum has lower impacts).

Health risks were also sensitive to the assumption that ozone depletion could not exceed 50 percent. For example, in the 2.5% Growth scenario, risk estimates could increase up to 10 percent if ozone depletion exceeds 50 percent; for higher emission scenarios, the increase in risk could be significantly greater.

Exhibit 18-38 shows the comparative impact of these uncertainties, using mortality among people born before 2075 as an indicator of the sensitivity of the risk estimates to each factor. Clearly, for current models, the emission of ozone depleting substances is the most sensitive variable, although future greenhouse policies, dose-response coefficients, and model response all are about half as important in explaining differences in estimates of mortality as production estimates.

SUMMARY

The risk of stratospheric modification on human health and the environment depends on the level of future emissions of ozone depleters. Lower levels of emissions always reduces risks, with smaller increments of risk reduction achieved for greater percentage reductions in emissions. The benefits of lower emissions of ozone depleters could substantially increase if reductions are made in greenhouse gases (evaluated within this Risk Assessment) and if the Antarctic ozone hole is found to have global implications (assumed herein not to be relevant). While uncertainly in many factors makes risk estimates quantitatively variable, the range of uncertainty does not alter the fundamental conclusion that risks are significant.

EXHIBIT 18-38

Comparative Sensitivity of Mortality From Skin Cancer to Various Factors[a/]

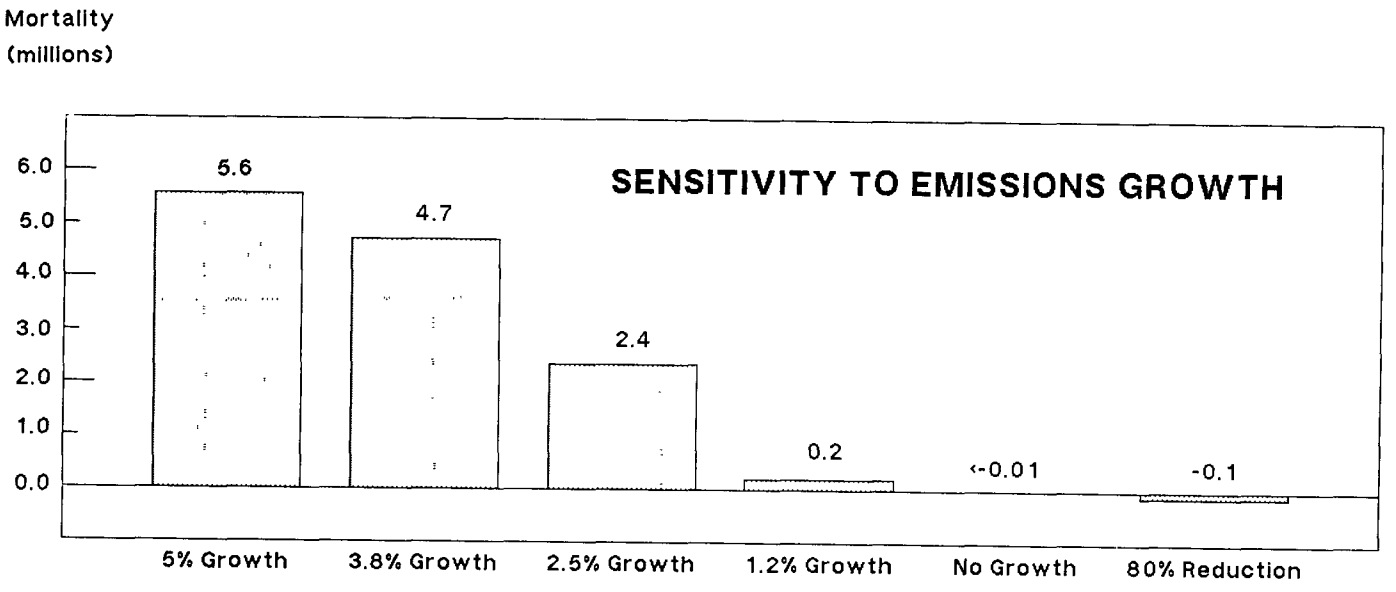

Growth rates refer to global production of chlorine and bromine bearing compounds.

---

a/ Estimate of additional mortality from skin cancer for all people born before 2075.

Assumptions:

-- Current 1-D models accurately reflect global depletion; Antarctic ozone hole has no impact on global ozone levels.

-- Greenhouse gases that counter depletion grow at historically-extrapolated rates.

-- Growth rates for ozone depleters are for global emissions; it is assumed that emissions do not increase after 2050.

-- Ozone depletion limited to 50 percent.

EXHIBIT 18-38
(Continued)

Comparative Sensitivity of Mortality From Skin Cancer to Various Factors[a/]

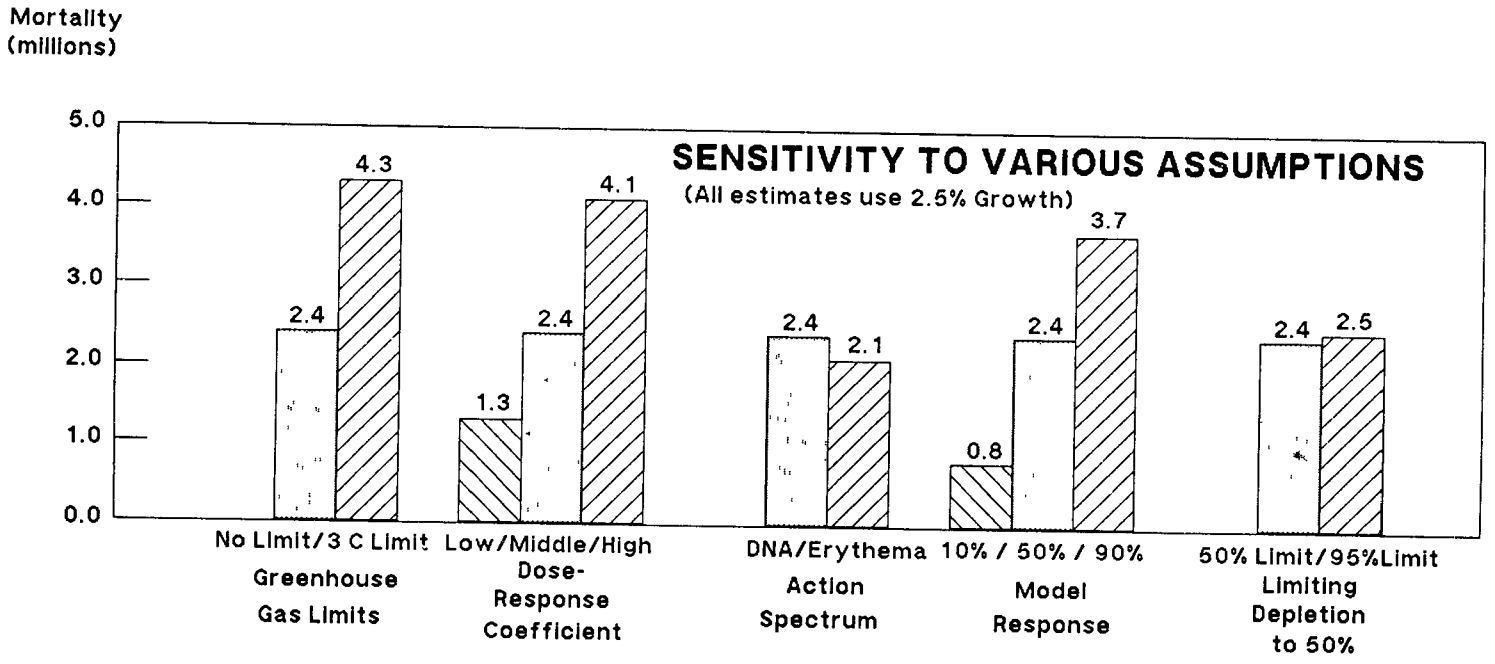

a/ Estimate of additional mortality from skin cancer for all people born before 2075.

Assumptions:

-- Current 1-D models accurately reflect global depletion; Antarctic ozone hole has no impact on global ozone levels.

-- Greenhouse gases that counter depletion grow at historically-extrapolated rates (except in the scenario of greenhouse gas limits).

-- Growth rates for ozone depleters are for global emissions; it is assumed that emissions do not increase after 2050.

-- Ozone depletion limited to 50 percent (except in the sensitivity scenario in which the limit is increased to 95 percent).

REFERENCES

Camm, F. and J.K. Hammitt (1986). "An Analytic Method for Constructing Scenarios From a Subjective Joint Probability Distribution," The RAND Corporation, Santa Monica, California.

Hansen, J., A. Lacis, D. Rind, G. Russell, P. Stone, I. Fung, R. Ruedy, and J. Lerner (1984), "Climate Sensitivity: Analysis of Feedback Mechanisms," in Hansen, J.E., and T. Takahashi, (eds.), Climate Processes and Climate Sensitivity, Geophysical Monograph 29, Maurice Ewing Volume 5, American Geophysical Union, Washington, DC.

Isaksen, I.S.A., and F. Stordal, (1986), "Ozone Perturbations by Enhanced Levels of CFCs, N2O, and CH4: A Two-Dimensional Diabatic Circulation Study Including Uncertainty Estimates," Journal of Geophysical Research, 91(D4): 5249-5263.

Manabe, S., and R.T. Wetherald (1986), "Reduction in Summer Soil Wetness Induced by an Increase in Atmospheric Carbon Dioxide," Science, 232: 626-628.

Ramanathan, V., R.J. Cicerone, H.B. Singh, and J.T. Kiehl (1985), "Trace Gases and Their Potential Role in Climate Change," National Center for Atmospheric Research, NCAR/0304/84-9, Boulder, Colorado.

Rowe, R.D., and R.M. Adams (1987), Analysis of Economic Impacts Of Lower Crop Yields Due To Stratospheric Ozone, Draft Report, prepared for U.S. Environmental Protection Agency, No. 68-01-7033.

Washington, W.M., and G.A. Meehl (1984), "Seasonal Cycle Experiment on the Climate Sensitivity Due to a Doubling of CO2 With an Atmospheric General Circulation Model Coupled to a Simple Mixed-Layer Ocean Model," Journal of Geophysical Research, 89(D6): 9475-9503.

☆U.S. GOVERNMENT PRINTING OFFICE:1988-516-002:80035